

**A PHYLOGENETIC APPROACH TO THE CLASSIFICATION OF
MACROSTYLID ISOPODS**

**AND
FAUNAL LINKAGES BETWEEN THE DEEP SEA AND SHALLOW-WATER ENVIRONMENTS**

Dissertation

zur Erlangung des Doktorgrades
im Department Biologie,
der Fakultät für Mathematik, Informatik und Naturwissenschaften
der Universität Hamburg

vorgelegt von
Torben Riehl
aus Geesthacht

Hamburg, 2014

Genehmigt vom Fachbereich Biologie
der Fakultät für Mathematik, Informatik und Naturwissenschaften
an der Universität Hamburg

auf Antrag von Frau Professor Dr. A. BRANDT

Weiterer Gutachter der Dissertation:
Professor Dr. P. MARTINEZ ARBIZU

Tag der Disputation: 05. Juni 2014



Professor Dr. C. Lohr
Vorsitzender des
Fach-Promotionsausschusses Biologie

Acknowledgements

It is one of the enjoyments in the final period of writing up a thesis to look back over the past years and remember all the colleagues, friends and family who have helped and supported me along this road. It was long and tedious, but exceptionally enjoyable thanks to them! I would like to express my gratitude to everyone who has supported, encouraged and inspired me whether on expeditions, and excursions, in meetings, at coffee and lunch breaks, conferences, over a pint in a pub, or at the Kicker table, and thus made this period.

More specifically, my thanks begin with my main supervisor, Angelika Brandt (University of Hamburg), for her support, and for the “long lead” that she used to guide me – no matter on which continent or ocean I was. Thanks for introducing me to the world of science and inspiring me with the seemingly endless energy you spawn and invest in order to achieve what you aim for. I would like to express my heartfelt gratitude especially for your trust in me as well as your patience.

Furthermore, I am very grateful to Pedro Martínez Arbizu (Senckenberg, German Center for Marine Biodiversity Research – DZMB) for taking on the second supervision, for providing advice, support and constructive criticism, whenever needed. You gave me the great opportunities, for example to participate in the DIVA 3 cruise, and to study isopod DNA at the Smithsonian National Museum of Natural History, and I am much appreciative for this.

Exceptional gratitude is owed to George D. F. (Buz) Wilson (Australian Museum) for great collaboration and hospitality at the Australian Museum in Sydney. I undoubtedly have benefited hugely from his effort getting me Downunder to work with him, and his enthusiasm introducing me to numerous researchers and even more isopods, which has resulted in some great ideas, discussions and opportunities! You inspired me to always delve a bit deeper and the barbies at your place were brilliant. Thanks, mate!

Special thanks is due to Stefanie Kaiser. For several years, she was a fantastic lab mate and has become a true friend. She participated significantly in organizing my sometimes confused ideas about this thesis. She has greatly assisted me in writing up and helped me focus. I am grateful this and for your thoughtful and detailed comments.

This thesis was made possible with the support of many colleagues, friend, and family members and funding from the German National Academic Foundation (Studienstiftung des deutschen Volkes) for which I am most thankful. The CeDAMar taxonomic exchange program, Foundation of the University

of Hamburg, the Geddes Fellowship of the Australian Museum, as well as the Studienstiftung helped me fund several inter-continental trips to participate in conferences or visit laboratories and natural-history collections. I appreciate the “pharmacological“ support by Marina Malyutina and Simon Bober that kept me alive during these last days. Thanks to Jörundur Svavarsson (University of Iceland), T. Chat Walther and Amy Driskell (Smithsonian) for generous hospitality, extraordinary samples, recommendations and discussions as well as friendliness and good mood. Without Nils Brenke, none of our joint expeditions would have been half as amusing. Without the gorgeous crews of the research vessels Polarstern, Meteor, and Sonne, I would not have accomplished any of my work. All the collection managers and peers that contributed to my thesis and papers are kindly acknowledged.

During the last three years, I was affiliated with three laboratories: “Niedere Tiere II” at the Zoological Museum Hamburg, the German Center for Marine Biodiversity Research (Senckenberg) and the Marine Invertebrates at the Australian Museum. All colleagues I have been involved with have been inviting and supportive in allowing me to participate in lab activities whilst pursuing my PhD studies. And thanks to you I never ran out of coffee. In this context, it is my pleasure to emphasize the contributions of Saskia Brix-Elsig, Karen Jeskulke, Martina Vortkamp, Sarah Schnurr, Sabine Holst, Antje Fischer, Sven Hoffmann, Karin Meißner, Jasmin Renz, Petra Wagner, and Kathrin Philipps Bussau in Hamburg, Anna Murray, Steven Keable, Shane Ahyong, Frank Köhler, Eunice Wong, and Francesco Criscione in Sydney.

A warm thank you to my friends Arne, Philipp, Steffi and Steffi, Jörg and Julia, Maria, Tim, Gerald, Stefan and Benjamin for their invaluable friendship, patience with my enduring absence and help with difficult decisions.

I would not have attempted this road if not for my parents, Monika and Peter, my granddad Otto, as well as my sister Annika who implanted within me a love of creative pursuits and scientific endeavor and technical understanding, which drove me into becoming a biologist.

Last but not least, I owe my current sanity, health and happiness to the caring support of my partner, Jasmin. She was key witness to the buzzing brain and immense time and energy that I invested in to completing this thesis. Her love, humor and wisdom, have taught me to see the wider picture and what life really is about; taught me about confidence and being content. I don't want to miss one day! For sharing passions with me, kindling dreams and encouraging me to keep going, I thank you.

TABLE OF CONTENTS

Summary	11
Zusammenfassung	13
Chapter 1: General Introduction	15
The deep-sea environment	16
The deep sea and the importance of alpha taxonomy and phylogeny	17
Age and origin of the deep-sea fauna	17
Isopod crustaceans and deep-sea colonizations	18
Deep-sea asellote isopods	18
Macrostylidae	19
Origin and colonization of the continental shelves	19
Aims	20
Content.	20
References	21
Chapter 2: New Macrostylidae Hansen, 1916 (Crustacea: Isopoda) from the Gay Head-Bermuda transect with special consideration of sexual dimorphism . .	27
Abstract	28
Introduction	29
Material and Methods	29
Implicit Attributes	30
Systematics	35
<i>Macrostylis dorsaetosa</i> n. sp.	35
<i>Macrostylis papillata</i> n. sp.	42
Discussion	51
Sexual dimorphism and terminal male stages	51
Ecological and evolutionary implications	52
Implications for future systematic work	54
Acknowledgements	54
References	55
Author contributions.	57

Chapter 3: Conquered from the Deep Sea? A New Deep-Sea Isopod Species from the Antarctic Shelf Shows Pattern of Recent Colonization 59

Abstract 60

Introduction 61

Material and Methods 62

Systematics 69

Macrostyliis roaldi n. sp. 70

 Development 83

 Molecular Results 83

Discussion 84

 Morphological Affinities 84

 Developmental and Reproductive Notes 84

 Distribution. 85

 Genetic Structure. 86

 Evidence for Shelf Refuges? 87

Conclusions 89

Acknowledgements 89

References 89

Author contributions 94

Chapter 4: Southern Ocean Macrostyliidae reviewed with a key to the species and new descriptions from Maud Rise 97

Abstract 98

Introduction 99

Material and methods 100

Systematics 104

Macrostyliis scotti n. sp. 108

Macrostyliis matildae n. sp. 118

Macrostyliis antennamagna Riehl & Brandt, 2010 131

Macrostyliis cerrita Vey & Brix, 2009 131

 Key to the Southern-Ocean species of *Macrostyliis* 132

Macrostyliis gerdesi (Brandt, 2002) 135

Macrostyliis obscura (Brandt, 1992) nom. dub. 135

Macrostyliis sarsi Brandt, 1992 nom. dub. 136

Macrostyliis setulosa Mezhov, 1992 136

Macrostyliis uniformis Riehl & Brandt, 2010 138

Macrostyliis vinogradovae Mezhov, 1992 138

 Molecular results 140

Discussion	140
Characters used to distinguish species in the key	141
Development and sexual dimorphism	142
Molecular phylogeny.	142
Acknowledgements	143
References	144
Author contributions.	147

Chapter 5: Urstylidae – a new family of abyssal isopods (Crustacea: Asellota) and its phylogenetic implications 149

Abstract	150
Introduction	151
Material and Methods	151
Results	154
Character Conceptualization	154
Systematics.	163
Urstylidae Fam. Nov.	163
<i>Urstylis</i> gen nov.	165
<i>Urstylis zapiola</i> gen. et sp. nov.	166
<i>Urstylis solicopia</i> sp. et gen. nov.	173
<i>Urstylis thiotyntlus</i> gen. et sp. nov.	183
Phylogenetic Results	193
Discussion	194
The Phylogenetic Relationship between Urstylidae and Macrostylidae	196
New Insights on the Evolution of the Highly Derived Macrostylidae	198
Classificatory Consequences	201
Key to the species of Urstylidae	205
Biogeographic Considerations	206
Acknowledgements.	206
References	206
Supporting Information	209
Author contributions.	210

Chapter 6: A comparative review of the morphology of Macrostylidae (Isopoda) from the phylogenetic perspective 211

Abstract	212
Introduction	213
Material and methods	216

Polymerase-chain reaction (PCR) at LAB	339
Results	341
Discussion	343
Recommended next steps.	345
References	345
Acknowledgements	349

Summary

The aim of this thesis is to explore phylogenetic relationships in the isopod family Macrostylidae and to gain insights from these data on faunal connections between the deep-sea and shallow-water biota as well as the origin of Macrostylidae. Applying a combination of taxonomic and phylogenetic approaches, DNA data and morphology, I studied macrostylid characters, developed homology concepts for morphological traits and inferred both the position of Macrostylidae amongst Janiroidea as well as within-family relationships.

Macrostylid isopods are a common and ubiquitous component of the deep-sea benthos (i.e. fauna living on the bottom of the sea below the continental shelf break), yet they are poorly studied to date. However, macrostylids are not restricted to the deep sea since some species have been found in relatively shallow waters on the continental shelves of the cold Antarctic, Arctic as well as Boreal regions. Macrostylids are considered an old group with their origin lying more than 250 million years in the past. They are amongst the descendants of the first isopod lineage to colonize the deep sea and still having modern-day representatives; their morphology is remarkably homogeneous though. While invasions from the shelf into the deep sea, especially in the Antarctic, are an increasingly well-understood phenomenon, offshore-onshore colonizations remain a rarely discussed topic.

With the intention to tackle the apparent

morphological conformity, I produced new species descriptions and taxonomic revisions (Chapters 2–5, and 7). Investigations of stage development and DNA data led to the discovery of astonishing sexual dimorphisms in some macrostylid species (Chapter 2). Sexual dimorphisms were identified to be amongst the causes for descriptions of conspecific adult males and females as separate taxa. Despite its obviously hampering nature for taxonomic allocation, this phenomenon has been revealed to hold valuable information for phylogenetic inference and providing a first clue for sexual selection to be amongst the driving factors of evolution in a deep-sea isopod family.

Furthermore, an astounding contrast between strong morphological conformity and high molecular divergence in macrostylids could be revealed when mitochondrial markers of Antarctic Macrostylidae were analyzed (Chapter 4). This observation indicates an old age of this taxon and contradicts the perceived interspecific conformity in the morphology.

Building upon the new insights on macrostylid morphology, a broad survey across the whole superfamily Janiroidea allowed a new phylogenetic approach to the origin of Macrostylidae (Chapter 6). The description and phylogenetic classification of the new isopod family Urstylidae with the genus *Urstylis* provided interesting new insights to the evolution of the specialized morphology

of macrostylids. Urstylidae is the sister taxon to Macrostylidae supporting an abyssal origin of the latter.

Finally, combining data on within-family variation and the macrostylid origin, phylogenetic inference of shelf-deep-sea colonization was conducted on two contrasting levels. On the one hand, I described a new species from the Amundsen Sea in the Southern Ocean that interestingly showed almost zero variation across hundreds of kilometers distance and roughly 1,000 m depth (Chapter 3). On the background of the local climatic history, that is dominated by glacial coverage of the whole shelf around 14,000 years ago, these findings suggest recent colonization of the Amundsen Sea continental shelf, likely from deeper waters. On the other hand, the origin of shallow-water macrostylids from the Antarctic, off the coasts of Western Australia, and from the North Atlantic is studied

in a phylogenetic context. This suggests that the shelves have been colonized from the deep oceans multiple times independently and do not have a common origin in a single emergence event that would have had to take place before the disintegration of Pangaea (Chapter 7).

In this thesis, I could show that the deep sea seems to be an important source of biodiversity for continental-shelf environments. On the other hand, considering severe environmental changes that have made parts of the deep sea uninhabitable especially in the Jurassic (~200–145 million years ago (Ma)) and Cretaceous (~145–66 Ma), besides the abyss the continental shelves might have also acted as refuges for deep-sea fauna. Repeated shelf-deep-sea and opposite colonization processes might have played an important role in shaping biodiversity not only on the shelves but in the deep-sea as well.

Zusammenfassung

Ziel dieser Dissertation ist es, die phylogenetischen Verwandtschaftsverhältnisse der marinen Isopodenfamilie Macrostylidae zu erforschen und daraus Erkenntnisse über mögliche evolutionsgeschichtliche Verbindungen zwischen der Tiefseefauna und der Fauna der Kontinentalschelfe zu gewinnen. Darüber hinaus liegt ein Schwerpunkt dieser Arbeit auf der Ergründung des Ursprunges der Macrostylidae.

Macrostylidae gehören der Krebsgruppe der Isopoda an und sind häufige Vertreter des Tiefseebenthos. Während die meisten Macrostyliden-Arten aus dem Abyssal (i.e. 3000–6000 m Tiefe) beschrieben wurden, konnten auch einige in relativ flachen Gewässern Kontinentalschelfe der kalten antarktischen, arktischen sowie borealen Regionen nachgewiesen werden. Diese Tiergruppe eignet sich daher ausgezeichnet, um Theorien der Schelf- und Tiefseebesiedlung zu testen. Macrostyliden werden als Nachfahren der ersten Isopodenstammeslinie angesehen, welche die Tiefsee besiedelt hat. Dieses Ereignis wurde auf mehr als 250 Millionen Jahre vor unserer Zeit datiert. Obwohl solch lange Zeiträume in den meisten Taxa zu einer hohen Diversifizierung führen, ist die morphologische Vielfalt innerhalb der Macrostyliden überraschend gering. Dies ist vermutlich der Grund dafür, dass innerhalb der Macrostyliden bisher nur eine einzige Gattung beschrieben wurde.

Unter Verwendung von sowohl genetischen

als auch morphologischen Merkmalen habe ich in meiner Arbeit eine Kombination von taxonomischen und phylogenetischen Verfahren benutzt, um Homologiekonzepte zu erstellen und so sowohl die systematische Stellung der Macrostylidae innerhalb der Janiroidea zu ergründen, als auch die Verwandtschaften innerhalb der Macrostylidae herzuleiten.

Als Grundlage für die Auflösung der morphologischen Übereinstimmungen innerhalb der Macrostyliden diente die Beschreibung neuer Arten sowie Erstellung biologisch-systematischer Revisionen (Kapitel 2–5, 7). Untersuchungen von Entwicklungsstadien und genetischer Daten führten zur Aufdeckung eines bemerkenswerten Sexualdimorphismus, der in einigen Arten der Macrostylidae vorkommt (Kapitel 2). Dieser starke Unterschied in der Ausprägung bestimmter morphologischer Merkmale zwischen Männchen und Weibchen innerhalb der Macrostylidae führte in der Vergangenheit dazu, dass die unterschiedlichen Geschlechter einer Art als zwei verschiedene Arten beschrieben wurden.

Diese morphologische Diskrepanz zwischen den unterschiedlichen Geschlechtern stellt einerseits sowohl für die Taxonomie also auch Erfassung von Biodiversität und Biogeographie eine große Herausforderung dar. Andererseits konnte ich in diesem stark ausgeprägtem Sexualdimorphismus wertvolle phylogenetische Informationen finden, welche zur Erforschung der Stammesgeschichte

dieser Krebsgruppe beitragen konnten. Außerdem lässt dieses Ergebnis erstmalig die Vermutung zu, dass sexuelle Selektion eine wichtige Rolle in der Evolution von Tiefseeisopoden spielt.

Darüber hinaus zeigten genetische Analysen anhand von mitochondrieller DNA antarktischer Macrostyliden einen erstaunlichen Gegensatz zwischen morphologischer Ähnlichkeit und genetischer Distanz auf (Kapitel 4). Dieses Ergebnis verdeutlicht das hohe Alter der Macrostyliden.

Die Funde aus den taxonomischen und phylogenetischen Vorarbeiten innerhalb der Macrostylidae nutzte ich für die breiter angelegte Studie über die Variabilität innerhalb der Überfamilie Janiroidea, um den stammesgeschichtlichen Ursprung der Macrostyliden zu ergründen (Kapitel 6). Die Familie Urstylidae wurde mit der Gattung *Urstylis* neu beschrieben. Phylogenetisch wurde sie als Schwestergruppe der Macrostylidae erkannt und ließ aufgrund ihrer ausschließlich abyssalen Verbreitung den Schluss zu, dass auch für Macrostylidae ein abyssaler Ursprung wahrscheinlich ist.

Abschließend wurden Besiedlungsmuster auf Populations- und Familienebene betrachtet. Zunächst wurde bei einer neu beschriebenen Art aus der Amundsensee im Südpolarmeer überraschenderweise festgestellt, dass über das gesamte untersuchte Verbreitungsgebiet dieser Art (d.h. > 300 km geographische Distanz und ca. 1000 m Tiefenunterschied) praktisch keine genetische Variation vorliegt (Kapitel 3). Wenn man die jüngere Klimageschichte der Antarktis in Betracht zieht, die von einer kompletten Eisbedeckung des untersuchten Kontinentalschelfs vor ca. 14.000 Jahren ausgeht, liegt der Schluss nahe, dass mit deren

Rückzug eine Neubesiedlung des Schelfs stattgefunden haben muss. Es liegt nahe, dass diese Pionierfauna aus größeren Tiefen heraus den Schelf besiedelt hat, aber ein Überleben der Fauna in eisfreien Refugien auf dem Schelf kann ebenfalls nicht ausgeschlossen werden.

In einer phylogenetischen Analyse von Flachwasser-Macrostyliden, die vor der Küste Westaustraliens, der Antarktis und Europas vorkommen, wurde erkannt, dass diese Arten nur entfernt miteinander verwandt sind. Daraus lässt sich ableiten, dass die unterschiedlichen Kontinentalschelfe mehrmals und unabhängig voneinander besiedelt wurden und nicht von einer einmaligen Besiedlung des Schelfs vor dem Auseinanderbrechen des Superkontinents Pangäa auszugehen ist (Kapitel 7).

Mit den Ergebnissen dieser Dissertation konnte ich zeigen, dass wiederholte Besiedlungen aus der Tiefsee auf die Schelfe eine wichtige Quelle für die Vielfalt des Lebens auf den Kontinentalschelfen sein kann. Darüber hinaus ergab meine Arbeit, dass neben dem Abyssal die Kontinentalschelfe auch die Funktion von Refugien für Teile der Tiefseefauna übernommen haben könnten, als während des Jura (vor ca. 200–145 Millionen Jahren) und der Kreidezeit (ca. 145–66 Millionen Jahre) Sauerstoffmangel weite Teile der Tiefsee unbewohnbar gemacht hat. Wiederholte Besiedlungen aus der Tiefsee auf die Schelfe, sowie in die entgegengesetzte Richtung, könnten schlussfolgernd nicht nur eine wichtige Rolle bei der Entstehung der Vielfalt des Lebens auf den Kontinentalschelfen, sondern auch in der Tiefsee gespielt haben.

Chapter 1

General Introduction

The deep-sea environment

Despite its enormous size and importance for the global climate system as well as a potential source for e.g., food and seafloor minerals (Eppley and Peterson 1979; Harrison 1980; Snelgrove 1999), the deep sea still represents one of the least understood ecosystems of our planet (Ramirez-Llodra *et al.* 2010). It is by far the largest environment on earth, covering roughly 60% of the planet's surface. It comprises the bathyal (~200–3,000 m), abyssal (3,000–6,000 m) and hadal (6,000–11,000 m) depth zones.

Bathyal and hadal are the structurally most diverse regions, for instance due to strong depth gradients and related habitat heterogeneity (in e.g. changing hydrostatic pressure, oxygen concentrations and sediment structure). The abyss, with its vast rolling plains of soft sediments, dominates the deep sea and is (with the exception of seamounts, submarine volcanoes and mid-ocean ridges interrupting these plains (Rogers 1993)) rather homogeneous. Physical restrictions for light penetration to the upper 100–200 m of the water column are the reason for the absence of energy fixation through photosynthesis in the deep sea and a progressively limited food supply with increasing depth. Yet, life in the deep ocean largely depends on photosynthetic products that sink to the bottom (Thiel 1979; Smith *et al.* 2008). There is hardly any primary production within the deep sea apart from chemosynthetic systems such as hydrothermal vents and seeps which are rather localized and uncommon when compared to the flat soft-sediment plains (Tyler *et al.* 2002; Baker *et al.* 2010). Therefore, the deep sea is often considered poor in food supply (Gage and Tyler 1992; Snelgrove 1999; Smith *et al.* 2008; McClain *et al.* 2012).

Due to the constancy in several physical-environmental parameters that are physiologi-

cally important, such as pressure and temperature (Mantyla and Reid 1983; Etter and Rex 1990; France and Kocher 1996; Zardus *et al.* 2006; Smith and Thatje 2012), the abyss stands out from most shallow marine, terrestrial and fresh-water environments (Mantyla and Reid 1983). Solar light is generally absent, hydrostatic pressure is high, while the water temperature is low (~ +2°C; with exceptions, for instance, in the Mediterranean, Red Sea, Sea of Japan and around hydrothermally active areas). This lack of significant environmental variability or major topographic obstacles across large areas in the abyss can be interpreted as absence of dispersal barriers (Etter *et al.* 2005; Zardus *et al.* 2006) and some abyssal species seem to have extremely wide geographic distributions (Brandt *et al.* 2007b; Pawlowski *et al.* 2007; Havermans *et al.* 2013).

The time stability hypothesis argued that these apparently stable conditions in the deep sea were the main engine generating the high observed biodiversity across larger spatial and temporal scales (Sanders 1968). It stated that unstressed and old environments maintained higher diversity than young and stressed environments through specialized competitive niche diversification over evolutionary time (Sanders 1968).

However, today we know that the seeming stability in the deep sea is frequently interrupted at ecological as well as evolutionary time scales. Thus, high local and regional diversity in the deep sea seems to be driven by intercorrelation of factors and processes acting at different scales in space and time. (Dayton 1971; Dayton and Hessler 1972; Kaiser *et al.* 2007). For example, at small spatial scales, nutrient enrichments through food falls cause patches of high food availability on the seafloor (Wolff 1976; Stockton and DeLaca 1982; Smith 1985; Amon *et al.* 2013). Furthermore, sea-bed currents, lunar tides and deep-water

formation as well as periodical benthic storms are considered as important forms of disturbance in the abyss, leading to sediment turbulence and also dislocation of food items or even species (Thistle 1983; Gage 1997, 2003; Ramirez-Llodra *et al.* 2010). Variation of surface productivity and sediment heterogeneity may as well contribute to a complex regime of environmental gradients promoting high diversity on a landscape scale (Levin *et al.* 2001). Another cause of habitat heterogeneity in the abyss is thought to be biology-dependent, such as bioturbation (Dayton and Hessler 1972; Gage 1996).

Across geological or evolutionary time scales, climate-induced changes had substantial effects on the environmental conditions of the deep sea, such as recurring events during the Phanerozoic eon, with major impacts on the deep sea and its inhabitants. Especially changes in temperature and oxygen concentration are thought to have had strong effects on the fauna (Kennett and Stott 1991), whether promoting or depleting biodiversity is still under discussion and might depend on the strength and scale of disturbance and may vary from taxon to taxon (Jacobs and Lindberg 1998; Wilson 1999; Rogers 2000; Diaz and Rosenberg 2008). Looking into the evolutionary history of deep-sea taxa thus seems a pivotal strategy for understanding deep-sea biodiversity.

The deep sea and the importance of alpha taxonomy and phylogeny

Currently, the deep sea is under pressure due to its rich hydrocarbon, mineral and seafood resources (Roberts 1997, 2002; Glover and Smith 2003; Barbier *et al.* 2014). Deep-sea mining, for instance, is on the brink of becoming a major industry; and to minimize the damage, environmental-impact as-

sessments are required (Markussen 1994; ISA 2008, 2012; Collins *et al.* 2013). Yet, large fractions of the deep-sea fauna are hardly known (Glover and Smith 2003; Danovaro *et al.* 2008); new species, genera and even families continue to emerge with increasing sampling effort and often beyond expectations (Rouse *et al.* 2004; Johnson *et al.* 2009; Osborn *et al.* 2011; Kaiser *et al.* 2013; Riehl *et al.* 2014) and knowledge about species or individual ranges, colonization patterns or even fundamental clues about behavior and ecology are largely rudimentary. It thus seems of great urgency to learn about the status quo of the deep-sea environment, catalogue its inhabitants, assess its natural variation across time and space and investigate their relationships to generate fundamental baseline knowledge necessary for impact assessments.

Unravelling the effects that major disturbance events in the deep-sea environment had in the past and still have today may help predicting the response of the deep-sea fauna to future anthropogenic impacts. One way to look at this is studying past colonization and biodiversity patterns in a phylogenetic framework (Wilson and Hessler 1987).

Age and origin of the deep-sea fauna

Since the beginning of deep-sea exploration, starting with the HMS Challenger expeditions 1872–1876 (Beddard 1886), the age and origin of the inhabitants of the deep sea, and especially of the vast abyss, have become an increasingly debated and controversial topic (Moseley 1880; Menzies and Imbrie 1958; Zenkevitch and Birstein 1960; Wilson 1999; Rex *et al.* 2005).

It is generally assumed that the origin of deep-sea taxa can be found in shallow waters (Moseley

1880; Jablonski *et al.* 1983). An 'onshore-offshore' colonization pattern was hypothesized to have occurred during the Phanerozoic era for abyssal lineages in general (Jacobs and Lindberg 1998) but also for hadal taxa (Wolff 1959) and hydrothermal-vent fauna (Little and Vrijenhoek 2003). Evidence was presented for various animal taxa including bivalves (Hessler and Wilson 1983; Etter *et al.* 2011), crustaceans (Schultz 1979; Raupach *et al.* 2004, 2009), echinoderms (Smith and Stockley 2005), and cephalopods (Strugnell *et al.* 2008).

The age of deep-sea lineages seems to vary dramatically with taxon (Wilson 1998, 1999; Thuy *et al.* 2012). Large-scale anoxia/dysoxia events in the deep sea, for example during the Turonian stage of the Cretaceous, are held accountable for mass extinctions in the abyssal and bathyal benthos and the present-day fauna is thought to have reinvaded the deep sea repeatedly after such events since after the Paleozoic (Menzies and Imbrie 1958; Menzies *et al.* 1961; Jacobs and Lindberg 1998).

Isopod crustaceans and deep-sea colonizations

To date, Isopoda Latreille, 1817 (Peracarida) comprises more than 10,300 species, most of which dwell in the marine realm (Wilson 2008a). Occurring from deepest hadal depths (Wolff 1956; Birstein 1970; Mezhov 1993) to mountain ranges (Hegna and Lazo-Wasem 2010), in marine, fresh-water and terrestrial environments and across all climatic regions, isopods can be considered a both ecologically and evolutionary successful and widely-distributed taxon. They inhabit wet tropical environments, but also deserts (Linsenmair 1975), include members of the subterrestrial stygofauna (Stock and Vonk 1990; Asmyhr and Cooper 2012), the zooplankton (Van der Baan and Holthuis 1969;

Schultz 1978; Grutter *et al.* 2000), as well as the marine benthos (bottom-dwelling organisms).

Several invasions of the deep sea are evident for this group. While the Flabellifera *sensu lato* (Wilson 1998) comprises several rather young deep-sea lineages, some Asellota may have immigrated into abyssal depths no later than before the Permo-Triassic boundary and thus must have survived adverse conditions that occurred in the Cretaceous (Wilson 1999; Lins *et al.* 2012).

The ultimate source of the abyssal fauna was hypothesized to be Antarctica (Kussakin 1973), or other areas of deep-water formation where a lack of a thermocline and thermohaline circulation is thought to promote vertical transmigration (Hessler and Wilson 1983; Strugnell *et al.* 2008). The occurrence of eye-bearing (isopod) taxa in the deep sea indicates that faunal invasion into the deep ocean is an ongoing process (Wilson 1980, 1998, 1999; Held 2000).

Contrastingly, the great diversity of asellote isopods existing in the deep sea (Sanders *et al.* 1965; Hessler and Sanders 1967; Brandt *et al.* 2007b) is thought to have evolved *in situ* (Hessler and Thistle 1975).

Deep-sea asellote isopods

Several lineages of Asellota have colonized the deep sea independently (Raupach *et al.* 2004, 2009) throughout the late Paleozoic and Mesozoic eras (Lins *et al.* 2012). Today, asellote isopods are a numerically important group of the deep-sea benthos (Sanders *et al.* 1965; Hessler and Sanders 1967; Brandt *et al.* 2007a, 2013; Kaiser *et al.* 2007).

The superfamily Janiroidea represents the most diverse isopod group in the deep sea with several families endemic to the deep sea (Hessler and Wilson 1983; Wilson 1997, 1999). The

feeding modes dominant for asellotes are thought to be amongst the primary pre-adaptations which allowed for their successful colonizations and diversifications in the generally nutrient-poor deep sea (Wilson 1998). Janiroidea are thought to be predominantly ‘cropping’ (Dayton and Hessler 1972), i.e. they feed on detritus (Wolff 1976; Elsner *et al.* 2013) or are ‘micro-predators’ preying on hard- and soft-walled foraminiferans (Wolff 1962; Svavarsson *et al.* 1993; Brandt 1997; Gudmundsson *et al.* 2000; Brökeland *et al.* 2010). In situ observations at baited traps and biochemical analyses suggest that facultative necrophagy may be also present amongst multiple abyssal and hadal isopod groups, such as Haploniscidae Hansen, 1916 and Munnopsidae Lilljeborg, 1864 (Würzberg *et al.* 2011; Jamieson *et al.* 2012).

Aside from the characteristic flat-oval isopod morphology dominant across terrestrial and freshwater isopods as well as for several marine groups (e.g. Aegidae, Cirolanidae), major adaptive radiations in the marine environment have led to a great morphological diversity, especially by the Asellota in the deep sea (Wolff 1962; Hessler *et al.* 1979).

Macrostylidae

The janiroidean family Macrostylidae Hansen, 1916 is amongst these specialized soft-bottom dwellers of the deep oceans (Hessler and Wilson 1983). The only observation of a living macrostylid published to date suggests a burrowing lifestyle (Hessler and Strömberg 1989). Considering a strong link between the general morphology and main behavioral attributes, burrowing habits could possibly be generally assumed for this group since their morphology is remarkably consistent (Wägele 1989). This assumption is supported by sampling evidence as well because macrostylids

are commonly encountered few centimeters below the ocean-floor surface in collection gear rather than on top (Thistle and Wilson 1987, 1996).

Macrostylids occur rather commonly in soft-sediment samples (Thistle and Wilson 1987; Brandt *et al.* 2004; Wilson 2008b; Kaiser *et al.* 2009) and have been reported from all ocean depths (Hessler *et al.* 1979; Brandt *et al.* 2009; Riehl and Brandt 2010). From the shallow sublittoral, for instance *Macrostylis spinifera* Sars, 1864 has been collected between about 30–1,761 m depth along the coast of Norway and is thus one of the shallowest-occurring species known to date. *Macrostylis mariana* Mezhov, 1993 on the other hand, holds the record for the deepest-living isopod species at 10,223–10,730 m depth in the tropical western Pacific Mariana Trench (Riehl and Brandt 2010). The majority of species, however, has been collected from abyssal depth between 3,000 m and 6,000 m. This core distribution in the deep sea (Hessler *et al.* 1979; Brandt *et al.* 2009; Riehl and Brandt 2010) as well as the absence of eyes and phylogenetic evidence suggest a likely deep-sea origin for Macrostylidae (Wägele 1989).

Origin and colonization of the continental shelves

Molecular phylogenetic inference suggests that macrostylids are amongst the descendants of the first isopod lineage to colonize the abyss that has modern-day representatives (Lins *et al.* 2012). A bathyal or abyssal origin of macrostylids is thus possible. Yet, how does the occurrence of shallow-water macrostylids fit into this picture?

Little is known about the existence of deep-sea-shelf colonization. Aside from corals (Lindner *et al.* 2008; Pante *et al.* 2012), and some molluscs (Berkman *et al.* 2004), isopods are amongst the few

taxa for which such a pattern has been inferred from phylogenetic reasoning (Hessler 1970; Hessler and Thistle 1975; Thistle and Hessler 1976). For these macrofaunal crustaceans, the Antarctic, Arctic and high latitude boreal region seem to be preferential regions for colonizing continental shelves from the deep sea and the lack of a thermocline was hypothesized to promote such polar emergence (Brandt 1992; Wilson 1998; Thatje *et al.* 2005).

Aims

In this thesis, the isopod family Macrostylidae is reviewed. As a group, they are considered to be old, with their origin lying more than 250 million years in the past. Yet interestingly, research has revealed only a single genus (*Macrostylis*) and the morphology of macrostylids is remarkably consistent. Occurring at all ocean depths, macrostylids make a suitable model for analyzing the direction of colonization events across depth zones and regions.

- Thorough morphological character analysis is applied to tackle this seeming lack of morphological variability.
- The origin of Macrostylidae is investigated by determination of their phylogenetic position amongst Janiroidea.
- In combination with molecular data, morphological characters are used to infer within-family relationships.
- Based upon the phylogeny of Macrostylidae, the ancestry of shallow-water macrostylids is explored.

Content

This thesis comprises six data chapters (Chapters 2–7). As a first step to better conceive Macrostyli-

dae, a baseline for understanding the fundamental units of biodiversity research, the species, is set through new species descriptions and taxonomic revisions (Chapters 2–5).

In Chapter 2, I revealed that for about half of all described species of macrostylids only one gender had been examined. However, thorough investigations of stage development in two new species, *Macrostylis dorsaetosa* Riehl, Wilson and Hessler, 2012 and *M. papillata* Riehl, Wilson and Hessler, 2012, lead to the discovery of astonishing sexual dimorphisms in some macrostylid species (later supported by means of DNA data; Chapter 7). In this study, sexual dimorphisms are identified to be amongst the causes for descriptions of conspecific adult males and females as separate taxa. Despite its hampering nature for taxonomic allocation, this phenomenon is hypothesized to hold valuable information for phylogenetic deduction. It provides a first clue for sexual selection to be amongst the driving factors of evolution in an environment that is generally scarce in isolation factors triggering allopatric speciation.

Macrostylid evolution is viewed from the population angle in Chapter 3. I was able to demonstrate that despite the apparent lack of swimming abilities throughout their lifecycle, macrostylid isopods are capable of maintaining gene flow across significant distances and depths. *Macrostylis roaldi* Riehl and Kaiser, 2012, a newly described species from the Amundsen Sea in the Southern Ocean, is the first that allowed studying morphological and genetic variation within one species of this family across hundreds of kilometers distance and roughly 1,000 m depth. Astoundingly, the observed genetic and morphological variation is close to zero. It is thus indicating ongoing genetic exchange across the whole area studied. On the background of the local climatic history, which is dominated by glacial coverage of the whole shelf around

14,000 years ago, these findings suggest recent colonization of the Amundsen Sea continental shelf, likely from deeper waters. This example demonstrates that the deep-sea fauna is an important source for the Antarctic shelf fauna.

The present knowledge of Antarctic Macrostylidae is reviewed in Chapter 4. Two new species are described, *M. matildae* Riehl and Brandt, 2013 as well as *M. scotti* Riehl and Brandt, 2013. Furthermore, an identification key to the Southern-Ocean macrostylids is presented and the first preliminary molecular phylogeny of internal macrostylid relationships reveals a surprising contrast between strong morphological conformity and high molecular divergence.

In Chapter 5, a new phylogenetic approach to macrostylid evolution revealed the phylogenetic origin of this family. The description and phylogenetic classification of the new isopod family Urstylidae with the genus *Urstylis* Riehl, Wilson and Maljutina, 2014 provide interesting new insights to the evolution of the specialized morphology of Macrostylidae. Analysis of character evolution is applied across macrostylids, urstylids and their potential relatives. The apparent retention of morphology that is in large parts plesiomorphic, and several distinctly derived evolutionary states in the three *Urstylis* species are discussed in the light of macrostylid evolution. Possible explanations for the origin, for instance, of the macrostylid statocysts are brought to light.

Going from the broader context into detail, in Chapter 6 macrostylid evolution was reviewed in a comparative context through a scanning-electron-microscopic study addressing the seeming morphological uniformity. New homology concepts are established building a foundation for a family phylogeny (Riehl and Brandt in prep.).

In Chapter 7, these data were then applied for the reconstruction of macrostylid evolution in a

parsimony context. In parallel, a multi-locus molecular dataset was analyzed based on new methods to gain high-quality DNA in a broad scale (Appendix 1). Clades consistently retrieved from the individual and combined molecular datasets as well as the morphology are the foundation for erecting new subtaxa (i.e. genera) within the so far monotypic (monogeneric) family Macrostylidae.

It was revealed that shallow-water representatives from the Antarctic, off the coasts of Western Australia, and the North Atlantic are not particularly closely related but are likely descendants of independent deep-sea representatives. This is in contrast to an alternative possibility that those species are remnants of an old Pangaeian continental-shelf fauna. Once more, it is illustrated that the deep sea seems to be a source of biodiversity for continental-shelf environments.

References

- Amon, D. J., Glover, A. G., Wiklund, H., Marsh, L., Linse, K., Rogers, A. D. and Copley, J. T. (2013) The discovery of a natural whale fall in the Antarctic deep sea. *Deep Sea Research Part II: Topical Studies in Oceanography*, 92, 87–96.
- Asmyhr, M. G. and Cooper, S. J. B. (2012) Difficulties barcoding in the dark: the case of crustacean stygofauna from eastern Australia. *Invertebrate Systematics*, 26(6), 583–591.
- Van der Baan, S. M. and Holthuis, L. B. (1969) On the occurrence of Isopoda in the surface plankton in the North Sea near the lightship “Texel”. *Netherlands Journal of Sea Research*, 4(3), 354–363.
- Baker, M. C., Ramirez-Llodra, E. Z., Tyler, P. A., German, C. R., Boetius, A., Cordes, E. E., Dubilier, N., Fisher, C. R., Levin, L. A. and Metaxas, A. (2010) Biogeography, ecology and vulnerability of chemosynthetic ecosystems in the deep sea. *Life in the World's Oceans: Diversity, Distribution, and Abundance*, edited by: McIntyre, A, 161–183.
- Barbier, E. B., Moreno-Mateos, D., Rogers, A. D., Aronson, J., Pendleton, L., Danovaro, R., Henry, L. A., Morato, T., Ardron, J. and Van Dover, C. L. (2014) Protect the deep sea. *Nature*, 505(7484), 475–477.
- Beddard, F. E. (1886) Report on the Isopoda collected by HMS Challenger during the years 1873–76. Part 2. *Report of the*

Voyage of HMS Challenger, 17, 1–178.

Berkman, P. A., Cattaneo-Vietti, R., Chiantore, M. and Howard-Williams, C. (2004) Polar emergence and the influence of increased sea-ice extent on the Cenozoic biogeography of pectinid molluscs in Antarctic coastal areas. *Deep Sea Research Part II: Topical Studies in Oceanography*, 51(14–16), 1839–1855.

Birstein, Y. A. (1970) New Crustacea Isopoda from the Kurile-Kamchatka Trench area. In: Bogorov, V. G. (Ed.) *Fauna of the Kurile-Kamchatka Trench and its environment*. pp 308–356. Moscow: Academy of Sciences of the USSR. (Proceedings of the Shirshov Institute of Oceanology; 86).

Brandt, A. (1992) Origin of Antarctic Isopoda (Crustacea, Malacostraca). *Marine Biology*, 113, 415–423.

Brandt, A. (1997) Redescription of *Munnopsurus giganteus* (Sars, 1879) (Isopoda, Asellota, Eurycopidae). *Crustaceana*, 70(3), 288–303.

Brandt, A., De Broyer, C., De Mesel, I., Ellingsen, K. E., Gooday, A. J., Hilbig, B., Linse, K., Thomson, M. R. A. and Tyler, P. A. (2007a) The biodiversity of the deep Southern Ocean benthos. *Philosophical Transactions of the Royal Society B: Biological Sciences*, 362(1477), 39–66.

Brandt, A., Brökeland, W., Brix, S. and Malyutina, M. V. (2004) Diversity of Southern Ocean deep-sea Isopoda (Crustacea, Malacostraca)—a comparison with shelf data. *Deep-Sea Research Part II*, 51(14–16), 1753–1768.

Brandt, A., Elsner, N., Brenke, N., Golovan, O., Malyutina, M. V., Riehl, T., Schwabe, E. and Würzberg, L. (2013) Epifauna of the Sea of Japan collected via a new epibenthic sledge equipped with camera and environmental sensor systems. *Deep Sea Research Part II: Topical Studies in Oceanography*, 86–87, 43–55.

Brandt, A., Gooday, A. J., Brandao, S. N., Brix, S., Brökeland, W., Cedhagen, T., Choudhury, M., Cornelius, N., Danis, B., de Mesel, I., Diaz, R. J., Gillan, D. C., Ebbe, B., Howe, J. A., Janussen, D., Kaiser, S., Linse, K., Malyutina, M. V., Pawlowski, J., Raupach, M. J. and Vanreusel, A. (2007b) First insights into the biodiversity and biogeography of the Southern Ocean deep sea. *Nature*, 447(7142), 307–311.

Brandt, A., Linse, K. and Schüller, M. (2009) Bathymetric distribution patterns of Southern Ocean macrofaunal taxa: Bivalvia, Gastropoda, Isopoda and Polychaeta. *Deep Sea Research Part I: Oceanographic Research Papers*, 56(11), 2013–2025.

Brökeland, W., Guðmundsson, G. and Svavarsson, J. (2010) Diet of four species of deep-sea isopods (Crustacea: Malacostraca: Peracarida) in the South Atlantic and the Southern Ocean. *Marine Biology*, 157(1), 177–178.

Collins, P. C., Croot, P., Carlsson, J., Colaço, A., Grehan, A., Hyeong, K., Kennedy, R., Mohn, C., Smith, S., Yamamoto, H.

and Rowden, A. (2013) A primer for the environmental impact assessment of mining at seafloor massive sulfide deposits. *Marine Policy*, 42, 198–209.

Danovaro, R., Gambi, C., Dell’Anno, A., Corinaldesi, C., Frascchetti, S., Vanreusel, A., Vincx, M. and Gooday, A. J. (2008) Exponential decline of deep-sea ecosystem functioning linked to benthic biodiversity loss. *Current Biology: CB*, 18(1), 1–8.

Dayton, P. K. (1971) Competition, disturbance, and community organization: the provision and subsequent utilization of space in a rocky intertidal community. *Ecological Monographs*, 41(4), 351.

Dayton, P. K. and Hessler, R. R. (1972) Role of biological disturbance in maintaining diversity in the deep sea. *Deep Sea Research and Oceanographic Abstracts*, 19(3), 199–208.

Diaz, R. J. and Rosenberg, R. (2008) Spreading dead zones and consequences for marine ecosystems. *Science*, 321(5891), 926–929.

Elsner, N. O., Golovan, O. A., Malyutina, M. V. and Brandt, A. (2013) Alone in the dark: Distribution, population structure and reproductive mode of the dominant isopod *Eurycope spinifrons* Gurjanova, 1933 (Isopoda: Asellota: Munnopsidae) from bathyal and abyssal depths of the Sea of Japan. *Deep Sea Research Part II: Topical Studies in Oceanography*, 86–87(0), 103–110.

Eppley, R. W. and Peterson, B. J. (1979) Particulate organic matter flux and planktonic new production in the deep ocean. *Nature*, 282(67), 7–680.

Etter, R. J., Boyle, E. E., Glazier, A., Jennings, R. M., Dutra, E. and Chase, M. R. (2011) Phylogeography of a pan-Atlantic abyssal protobranch bivalve: implications for evolution in the Deep Atlantic. *Molecular Ecology*, no–no.

Etter, R. J. and Rex, M. A. (1990) Population differentiation decreases with depth in deep-sea gastropods. *Deep Sea Research Part I: Oceanographic Research*, 37(8), 1251–1261.

Etter, R. J., Rex, M. A., Chase, M. R. and Quattro, J. M. (2005) Population differentiation decreases with depth in deep-sea bivalves. *Evolution; International Journal of Organic Evolution*, 59(7), 1479–1491.

France, S. C. and Kocher, T. D. (1996) Geographic and bathymetric patterns of mitochondrial 16S rRNA sequence divergence among deep-sea amphipods, *Eurythenes gryllus*. *Marine Biology*, 126(4), 633–643.

Gage, J. (1996) Why are there so many species in deep-sea sediments? *Journal of Experimental Marine Biology and Ecology*, 200(1–2), 257–286.

Gage, J. D. (1997) High benthic species diversity in deep-sea sediments: the importance of hydrodynamics. In: Ormond, R. P. G., Gage, J. D., and Angel, M. V. (Eds.) *Marine Biodiversity:*

- Patterns and Processes*. pp 148–177. Cambridge: Cambridge University Press.
- Gage, J. D. (2003) Food inputs, utilisation, carbon flow and energetics. In: Tyler, P. A. (Ed.) *Ecosystems of the Deep Ocean*. pp 313–426. Amsterdam: Elsevier. (Ecosystems of the World).
- Gage, J. D. and Tyler, P. A. (1992) *Deep-sea biology: a natural history of organisms at the deep-sea floor*. Cambridge University Press.
- Glover, A. G. and Smith, C. R. (2003) The deep-sea floor ecosystem: current status and prospects of anthropogenic change by the year 2025. *Environmental Conservation*, 30(3), 219–241.
- Grutter, A. S., Lester, R. J. and Greenwood, J. (2000) Emergence rates from the benthos of the parasitic juveniles of gnathiid isopods. *Marine Ecology Progress Series*, 207, 123–127.
- Gudmundsson, G., von Schmalensee, M. and Svavarsson, J. (2000) Are foraminifers (Protozoa) important food for small isopods (Crustacea) in the deep sea? *Deep Sea Research Part I: Oceanographic Research Papers*, 47(11), 2093–2109.
- Hansen, H. J. (1916) Crustacea Malacostraca: The order Isopoda. *Danish Ingolf Expedition*, 3(5), 1–262.
- Harrison, W. G. (1980) Nutrient Regeneration and Primary Production in the Sea. In: Falkowski, P. G. (Ed.) *Primary Productivity in the Sea*. pp 433–460. Springer US. (19). ISBN 978-1-4684-3892-5, 978-1-4684-3890-1.
- Havermans, C., Sonet, G., d'Udekem d'Acoz, C., Nagy, Z. T., Martin, P., Brix, S., Riehl, T., Agrawal, S. and Held, C. (2013) Genetic and morphological divergences in the cosmopolitan deep-sea amphipod *Eurythenes gryllus* reveal a diverse abyss and a bipolar species. *PLoS ONE*, 8(9), e74218.
- Hegna, T. A. and Lazo-Wasem, E. A. (2010) *Branchinecta brushi* n. sp. (Branchiopoda: Anostraca: Branchinectidae) from a volcanic crater in northern Chile (Antofagasta Province): a new altitude record for crustaceans. *Journal of Crustacean Biology*, 30(3), 445–464.
- Held, C. (2000) Phylogeny and biogeography of serolid isopods (Crustacea, Isopoda, Serolidae) and the use of ribosomal expansion segments in molecular systematics. *Molecular Phylogenetics and Evolution*, 15(2), 165–178.
- Hessler, R. R. (1970) *The Desmosomatidae (Isopoda, Asellota) of the Gay Head-Bermuda Transect* [online]. (Arrhebus, G. O. S., Cox, C. S., Fager, E. W., Hand, C. H., Newberry, T., and Schaefer, M. B., Eds.) Berkeley, Los Angeles, London: University of California Press. Available from: <http://escholarship.org/uc/item/1mn198vx>.
- Hessler, R. R. and Sanders, H. L. (1967) Faunal diversity in the deep sea. *Deep Sea Research and Oceanographic Abstracts*, 14(1), 65–70.
- Hessler, R. R. and Strömberg, J. O. (1989) Behavior of janiroidean isopods (Asellota), with special reference to deep sea genera. *Sarsia*, 74(3), 145–159.
- Hessler, R. R. and Thistle, D. (1975) On the place of origin of deep-sea isopods. *Marine Biology*, 32(2), 155–165.
- Hessler, R. R. and Wilson, G. D. F. (1983) The origin and biogeography of malacostracan crustaceans in the deep sea. In: Sims, R. W., Price, J. H., and Whalley, P. E. S. (Eds.) *Evolution, time, and space: the emergence of the biosphere*. pp 227–254. London: Academic Press. (Systematics Association Special Publication; 23).
- Hessler, R. R., Wilson, G. D. F. and Thistle, D. (1979) The deep-sea isopods: a biogeographic and phylogenetic overview. *Sarsia*, 64(1-2), 67–75.
- ISA (2008) *Biodiversity, species ranges, and gene flow in the abyssal Pacific nodule province: predicting and managing the impacts of deep seabed mining* [online]. Kingston, Jamaica: International Seabed Authority. (ISA Technical Study; 3).
- ISA (2012) *Environmental Management Needs for Exploration and Exploitation of Deep Sea Minerals* [online]. Kingston, Jamaica: International Seabed Authority. (ISA Technical Study; 10).
- Jablonski, D., Sepkoski, J. J., Bottjer, D. J. and Sheehan, P. M. (1983) Onshore-Offshore Patterns in the Evolution of Phanerozoic Shelf Communities. *Science*, 222(4628), 1123–1125.
- Jacobs, D. K. and Lindberg, D. R. (1998) Oxygen and evolutionary patterns in the sea: Onshore/offshore trends and recent recruitment of deep-sea faunas. *Proceedings of the National Academy of Sciences*, 95(16), 9396–9401.
- Jamieson, A. J., Fujii, T. and Priede, I. G. (2012) Locomotory activity and feeding strategy of the hadal munnopsid isopod *Rectisura* cf. *herculea* (Crustacea: Asellota) in the Japan Trench. *The Journal of Experimental Biology*, 215(17), 3010–3017.
- Johnson, G. D., Paxton, J. R., Sutton, T. T., Satoh, T. P., Sado, T., Nishida, M. and Miya, M. (2009) Deep-sea mystery solved: astonishing larval transformations and extreme sexual dimorphism unite three fish families. *Biology Letters*, 5(2), 235–239.
- Kaiser, S., Barnes, D. K. A. and Brandt, A. (2007) Slope and deep-sea abundance across scales: Southern Ocean isopods show how complex the deep sea can be. *Deep-Sea Research Part II: Topological Studies in Oceanography*, 54(16-17), 1776–1789.
- Kaiser, S., Barnes, D. K. A., Sands, C. J. and Brandt, A. (2009) Biodiversity of an unknown Antarctic Sea: assessing isopod richness and abundance in the first benthic survey of the Amundsen continental shelf. *Marine Biodiversity*, 39(1), 27–43.

- Kaiser, S., Brandão, S. N., Brix, S., Barnes, D. K. A., Bowden, D. A., Ingels, J., Leese, F., Schiaparelli, S., Arango, C. P., Badhe, R., Bax, N., Blazewicz-Paszkwycz, M., Brandt, A., Brenke, N., Catarino, A. I., David, B., Ridder, C. D., Dubois, P., Ellingsen, K. E., Glover, A. G., Griffiths, H. J., Gutt, J., Halanych, K. M., Havermans, C., Held, C., Janussen, D., Lörz, A.-N., Pearce, D. A., Pierrat, B., Riehl, T., Rose, A., Sands, C. J., Soler-Membrives, A., Schüller, M., Strugnell, J. M., Vanreusel, A., Veit-Köhler, G., Wilson, N. G. and Yasuhara, M. (2013) Patterns, processes and vulnerability of Southern Ocean benthos: a decadal leap in knowledge and understanding. *Marine Biology*, 160(9), 2295–2317.
- Kennett, J. P. and Stott, L. D. (1991) Abrupt deep sea warming, paleoceanographic changes and benthic extinctions at the end of the Paleocene. *Nature*, 353, 225–229.
- Kussakin, O. G. (1973) Peculiarities of the geographical and vertical distribution of marine isopods and the problem of deep-sea fauna origin. *Marine Biology*, 23(1), 19–34.
- Latreille, P. A. (1817) Les Crustacés, les Arachnides, et les Insectes. In: *Le Règne Animal, distribué d'après son organisation, pour servir de base à l'histoire naturelle des animaux et d'introduction à l'anatomie comparée*. Paris.
- Levin, L. A., Etter, R. J., Rex, M. A., Gooday, A. J., Smith, C. R., Pineda, J., Stuart, C. T., Hessler, R. R. and Pawson, D. (2001) Environmental influences on regional deep-sea species diversity. *Annual Review of Ecology and Systematics*, 32(1), 51–93.
- Lilljeborg, W. (1864) Bidrag til kännedommen om de inom Sverige och Norrige förekommande Crustaceer af Isopodernas underordning och Tanaidernas familj. *Inbjudningsskrift till Åhörande af de Offentliga Föreläsningar. C. A. Leffler, Kongl. Acad. Boktryckare, Upsala.*, 31 pp.
- Lindner, A., Cairns, S. D. and Cunningham, C. W. (2008) From offshore to onshore: multiple origins of shallow-water corals from deep-sea ancestors. *PLoS One*, 3(6), e2429.
- Lins, L. S. F., Ho, S. Y. W., Wilson, G. D. F. and Lo, N. (2012) Evidence for Permo-Triassic colonization of the deep sea by isopods. *Biology Letters*, 8(6), 979–982.
- Linsenmair, K. E. (1975) Some Adaptations of the desert woodlouse *Hemilepistus reaumuri* (Isopoda, Oniscoidea) to desert environment. *Verhandlungen der Gesellschaft für Ökologie Erlangen 1974*. pp 183–185. Springer.
- Little, C. T. S. and Vrijenhoek, R. C. (2003) Are hydrothermal vent animals living fossils? *Trends in Ecology and Evolution*, 18(11), 582–588.
- Mantyla, A. W. and Reid, J. L. (1983) Abyssal characteristics of the World Ocean waters. *Deep Sea Research Part A. Oceanographic Research Papers*, 30(8), 805–833.
- Markussen, J. M. (1994) Deep seabed mining and the environment: consequences, perceptions, and regulations. *HO Bergesen and G. Parmann, Green Globe Yearbook of International Co-operation on Environment and Development*, 1994, 31–39.
- McClain, C. R., Allen, A. P., Tittensor, D. P. and Rex, M. A. (2012) Energetics of life on the deep seafloor. *Proceedings of the National Academy of Sciences*, 109(38), 15366–15371.
- Menzies, R. J. and Imbrie, J. (1958) On the Antiquity of the Deep Sea Bottom Fauna. *Oikos*, 9(2), 192.
- Menzies, R. J., Imbrie, J. and Heezen, B. C. (1961) Further considerations regarding the antiquity of the abyssal fauna with evidence for a changing abyssal environment. *Deep Sea Research (1953)*, 8(2), 79–90, IN1, 91–94.
- Mezhov, B. V. (1993) Three new species of *Macrostylis* G.O. Sars, 1864 (Crustacea Isopoda Asellota Macrostylidae) from the Pacific Ocean. *Arthropoda Selecta*, 2(3), 3–9.
- Moseley, H. N. (1880) Deep-sea dredging and life in the deep sea. *Nature*, 21, 591–593.
- Osborn, K. J., Madin, L. P. and Rouse, G. W. (2011) The remarkable squid worm is an example of discoveries that await in deep-pelagic habitats. *Biology Letters*, 7(3), 449–453.
- Pante, E., France, S. C., Couloux, A., Cruaud, C., McFadden, C. S., Samadi, S. and Watling, L. (2012) Deep-sea origin and in-situ diversification of chrysogorgiid octocorals. *PLoS ONE*, 7(6), e38357.
- Pawlowski, J., Fahrni, J., Lecroq, B., Longet, D., Cornelius, N., Excoffier, L., Cedhagen, T. and Gooday, A. J. (2007) Bipolar gene flow in deep-sea benthic foraminifera. *Molecular Ecology*, 16(19), 4089–4096.
- Ramirez-Llodra, E., Brandt, A., Danovaro, R., De Mol, B., Escobar, E., German, C. R., Levin, L. A., Martinez Arbizu, P., Menot, L., Buhl-Mortensen, P., Narayanaswamy, B. E., Smith, C. R., Tittensor, D. P., Tyler, P. A., Vanreusel, A. and Vecchione, M. (2010) Deep, diverse and definitely different: unique attributes of the world's largest ecosystem. *Biogeosciences*, 7(9), 2851–2899.
- Raupach, M. J., Held, C. and Wägele, J.-W. (2004) Multiple colonization of the deep sea by the Asellota (Crustacea: Peracarida: Isopoda). *Deep Sea Research Part II: Topical Studies in Oceanography*, 51, 1787–1795.
- Raupach, M. J., Mayer, C., Malyutina, M. V. and Wägele, J.-W. (2009) Multiple origins of deep-sea Asellota (Crustacea: Isopoda) from shallow waters revealed by molecular data. *Proceedings of the Royal Society B: Biological Sciences*, 276, 799–808.
- Rex, M. A. and Etter, R. J. (2010) *Deep-sea Biodiversity: Pattern and Scale*. Harvard University Press. ISBN 0674036077.
- Rex, M. A., McClain, C. R., Johnson, N. A., Etter, R. J.,

- Allen, J. A., Bouchet, P. and Warén, A. (2005) A source-sink hypothesis for abyssal biodiversity. *The American Naturalist*, 165(2), 163–178.
- Riehl, T. and Brandt, A. (in prep.) A comparative review of the morphology of Macrostylidae (Isopoda) from the phylogenetic perspective.
- Riehl, T. and Brandt, A. (2010) Descriptions of two new species in the genus *Macrostylis* Sars, 1864 (Isopoda, Asellota, Macrostylidae) from the Weddell Sea (Southern Ocean), with a synonymisation of the genus *Desmostylis* Brandt, 1992 with *Macrostylis*. *Zookeys*, 57, 9–49.
- Riehl, T., Wilson, G. D. F. and Malyutina, M. V. (2014) Urstylidae – A new family of deep-sea isopods and its phylogenetic implications. *Zoological Journal of the Linnean Society*, 170, 245–296.
- Roberts, C. M. (1997) Connectivity and management of Caribbean coral reefs. *Science*, 278(5342), 1454.
- Roberts, C. M. (2002) Deep impact: the rising toll of fishing in the deep sea. *Trends in Ecology and Evolution*, 17(5), 242–245.
- Rogers, A. D. (1993) The biology of seamounts. *Advances in marine biology*, 30, 305–305.
- Rogers, A. D. (2000) The role of the oceanic oxygen minima in generating biodiversity in the deep sea. *Deep Sea Research Part II: Topical Studies in Oceanography*, 47(1–2), 119–148.
- Rouse, G. W., Goffredi, S. K. and Vrijenhoek, R. C. (2004) *Osedax*: bone-eating marine worms with dwarf males. *Science*, 305(5684), 668–671.
- Sanders, H. L. (1968) Marine benthic diversity: a comparative study. *American naturalist*, 243–282.
- Sanders, H. L., Hessler, R. R. and Hampson, G. R. (1965) An introduction to the study of deep-sea benthic faunal assemblages along the Gay Head-Bermuda transect. *Deep Sea Research and Oceanographic Abstracts*, 12(6), 845–867.
- Sars, G. O. (1864) Om en anomal Gruppe af Isopoder. *Forhandlinger Videnskaps-Selskapet, Anar 1863 in Christiania*, 205–221.
- Schultz, G. A. (1978) *More planktonic isopod crustaceans from subantarctic and antarctic seas*. Biology of the Antarctic Seas VII, 27, 69–89.
- Schultz, G. A. (1979) Aspects of the evolution and origin of the deep-sea isopod crustaceans. *Sarsia*, 64(1–2), 77–83.
- Smith, A. B. and Stockley, B. (2005) The geological history of deep-sea colonization by echinoids: roles of surface productivity and deep-water ventilation. *Proceedings of the Royal Society B: Biological Sciences*, 272(1565), 865–869.
- Smith, C. R. (1985) Food for the deep sea: utilization, dispersal, and flux of nekton falls at the Santa Catalina Basin floor. *Deep Sea Research Part A. Oceanographic Research Papers*, 32(4), 417–442.
- Smith, C. R., De Leo, F. C., Bernardino, A. F., Sweetman, A. K. and Martínez Arbizu, P. (2008) Abyssal food limitation, ecosystem structure and climate change. *Trends in Ecology and Evolution*, 23(9), 518–528.
- Smith, K. E. and Thatje, S. (2012) The secret to successful deep-sea invasion: does low temperature hold the key? *PLoS ONE*, 7(12), e51219.
- Snelgrove, P. V. R. (1999) Getting to the bottom of marine biodiversity: sedimentary habitats: ocean bottoms are the most widespread habitat on Earth and support high biodiversity and key ecosystem services. *BioScience*, 49(2), 129–138.
- Stock, J. H. and Vonk, R. (1990) Stygofauna of the Canary Islands. 15. Marine interstitial Isopoda Asellota of the superfamily Gnathostenetroidoidea. *Cahiers de Biologie marine*, [online], 31(1). Available from: <http://www.vliz.be/en/imis?refid=65125>. [Accessed 2014-03-22].
- Stockton, W. L. and DeLaca, T. E. (1982) Food falls in the deep sea: occurrence, quality, and significance. *Deep Sea Research Part A. Oceanographic Research Papers*, 29(2), 157–169.
- Strugnell, J. M., Rogers, A. D., Prodöhl, P. A., Collins, M. A. and Allcock, A. L. (2008) The thermohaline expressway: the Southern Ocean as a centre of origin for deep-sea octopuses. *Cladistics*, 24(6), 853–860.
- Svavarsson, J., Gudmundsson, G. and Brattegard, T. (1993) Feeding by asellote isopods (Crustacea) on foraminifers (Protozoa) in the deep sea. *Deep Sea Research Part I: Oceanographic Research*, 40(6), 1225–1239.
- Thatje, S., Hillenbrand, C.-D. and Larter, R. (2005) On the origin of Antarctic marine benthic community structure. *Trends in Ecology and Evolution*, 20(10), 534–540.
- Thiel, H. (1979) Structural aspects of the deep-sea benthos. *Ambio Special Report*, (6), 25–31.
- Thistle, D. (1983) The stability-time hypothesis as a predictor of diversity in deep-sea soft-bottom communities: a test. *Deep Sea Research Part A. Oceanographic Research Papers*, 30(3), 267–277.
- Thistle, D. and Hessler, R. R. (1976) Origin of a Deep-Sea Family, the Ilyarachnidae (Crustacea: Isopoda). *Systematic Biology*, 25(2), 110–116.
- Thistle, D. and Wilson, G. D. F. (1987) A hydrodynamically modified, abyssal isopod fauna. *Deep-Sea Research. Part A. Oceanographic Research Papers*, 34(1), 73–87.
- Thistle, D. and Wilson, G. D. F. (1996) Is the HEBBLE isopod fauna hydrodynamically modified? A second test. *Deep-Sea*

- Research Part I*, 43(4), 545–554.
- Thuy, B., Gale, A. S., Kroh, A., Kucera, M., Numberger-Thuy, L. D., Reich, M. and Stöhr, S. (2012) Ancient origin of the modern deep-sea fauna. *PLoS one*, 7(10), e46913.
- Tyler, P. A., German, C. R., Ramirez-Llodra, E. and Van Dover, C. L. (2002) Understanding the biogeography of chemosynthetic ecosystems. *Oceanologica Acta*, 25(5), 227–241.
- Wilson, G. D. (2008a) Global diversity of Isopod crustaceans (Crustacea; Isopoda) in freshwater. *Hydrobiologia*, 595(1), 231–240.
- Wilson, G. D. F. (1980) New insights into the colonization of the deep sea: Systematics and zoogeography of the Munnidae and the Pleurogoniidae comb. nov. (Isopoda; Janiroidea). *Journal of Natural History*, 14(2), 215–236.
- Wilson, G. D. F. (1997) The Suborder Asellota. In: Scott, P. (Ed.) *Atlas of the Fauna of the Santa Maria Basin*. pp 59–120. Santa Barbara, California: Santa Barbara Museum of Natural History.
- Wilson, G. D. F. (1998) Historical influences on deep-sea isopod diversity in the Atlantic Ocean. *Deep Sea Research Part II: Topical Studies in Oceanography*, 45, 279–301.
- Wilson, G. D. F. (1999) Some of the deep-sea fauna is ancient. *Crustaceana*, 72(8), 1019–1030.
- Wilson, G. D. F. (2008b) Local and regional species diversity of benthic Isopoda (Crustacea) in the deep Gulf of Mexico. *Deep-Sea Research Part II: Topological Studies in Oceanography*, 55(24-26), 2634–2649.
- Wilson, G. D. F. and Hessler, R. R. (1987) Speciation in the Deep Sea. *Annual Reviews in Ecology and Systematics*, 18(1), 185–207.
- Wolff, T. (1956) Isopoda from depths exceeding 6000 meters. *Galathea Report*, 2, 85–157.
- Wolff, T. (1959) The hadal community, an introduction. *Deep Sea Research (1953)*, 6, 95–124.
- Wolff, T. (1962) The systematics and biology of bathyal and abyssal Isopoda Asellota. *Galathea Report*, 6(3), 1–320.
- Wolff, T. (1976) Utilization of seagrass in the deep sea. *Aquatic Botany*, 2(0), 161–174.
- Würzberg, L., Peters, J. and Brandt, A. (2011) Fatty acid patterns of Southern Ocean shelf and deep sea peracarid crustaceans and a possible food source, foraminiferans. *Deep Sea Research Part II: Topical Studies in Oceanography*, 58(19–20), 2027–2035.
- Wägele, J.-W. (1989) *Evolution und phylogenetisches System der Isopoda: Stand der Forschung und neue Erkenntnisse [Evolution and phylogeny of isopods. New data and the state of affairs]*. Stuttgart: E. Schweizerbart'sche Verlagsbuchhandlung. (Zoologica). ISBN 978-3-510-55026-5.
- Zardus, J. D., Etter, R. J., Chase, M. R., Rex, M. A. and Boyle, E. E. (2006) Bathymetric and geographic population structure in the pan-Atlantic deep-sea bivalve *Deminucula atacellana* (Schenck, 1939). *Molecular Ecology*, 15(3), 639–651.
- Zenkevitch, L. A. and Birstein, J. A. (1960) On the problem of the antiquity of the deep-sea fauna. *Deep-Sea Research (1953)*, 7(1), 10–23.

Chapter 2

New Macrostylidae Hansen, 1916 (Crustacea: Isopoda) from the Gay Head-Bermuda transect with special consideration of sexual dimorphism

Published as: Riehl T, Wilson GDF, Hessler RR (2012) New Macrostylidae Hansen, 1916 (Crustacea: Isopoda) from the Gay Head-Bermuda transect with special consideration of sexual dimorphism. *Zootaxa* 3277:1–26.

Abstract

In the Asellota, sexual dimorphism is often characterized by males that show pronounced morphological differences after the final moult compared to females but also to subadult males. Such a sexual dimorphism may strongly complicate allocation of these terminal males to conspecifics. Consequently, we regard it to be a likely explanation for why in 50% of the described species of the family Macrostylidae Hansen, 1916, only one sex is known. Based on detailed description of two previously unknown species of the isopod genus *Macrostylis* Sars, 1864, the changes in the morphology that can occur during the final moult of the males are highlighted. *M. dorsaetosa* n. sp. is unlike any other species owing to the row of spine-like setae on the posterior margins of pereonites 5–6. *M. strigosa* Mezhov, 1999 shows remarkable similarity but lacks these setae. In *M. papillata* n. sp., cuticular ridges overlap posteriorly with the margin of the pereonites 1–4 and head forming a warty appearance. This species is easily identifiable and unlike any previously described macrostylid owing to the presence of the tergal articulation between pleonite 1 and pleotelson. Information for the identification of terminal males is provided and implications of our results for future taxonomic and systematic work on this isopod family are discussed.

Key words: Janiroidea, deep sea, benthos, bathyal, abyssal, North Atlantic, DELTA, SEM, new species

Introduction

The phenomenon of sexual dimorphism occurs widely among the animal kingdom. Its evolution is driven by both sexual selection due to mating preferences or competition for mates and natural selection (Darwin 1874; Lande 1980). Sexual dimorphism is common among isopod crustaceans (Veuille 1980; Jormalainen and Merilaita 1995; Lefebvre *et al.* 2000) and also among deep-sea asellotes (Svavarsson 1984; Wilson 2008a; Brökeland 2010; Riehl and Brandt 2010). In Asellota, sexual dimorphism is often characterized by mature males showing strong morphological differences when compared to subadult males and females only after the final moult. Since the first description of a species belonging to the deep-sea isopod family Macrostylidae by G.O. Sars (1864), 80 species have been formally described (Riehl and Brandt 2010). 50% of these have been based on only one sex and often (22 species, i.e., 17.6%) only on a single specimen.

Observations of behavior (Hessler and Strömberg 1989), morphological characteristics (Thistle and Wilson 1987), as well as sampling evidence (Hessler and Sanders 1967; Wilson 2008b) suggest an infaunal lifestyle for macrostylids. Therefore, macrostylids have probably been undersampled by epibenthic apparatus often used in deep-sea research. Low numbers of specimens available in the samples have been a frequent impediment to their description. Males tend to be especially rare compared to females (personal observation) and this might explain the above mentioned numbers. The morphological evidence presented here suggests that another explanation for descriptions based on only one sex (at least in some cases) can be found in a pronounced sexual dimorphism. Substantial morphological differences may strongly complicate allocation of conspecifics. The

terminal-male concept will be introduced to macrostylid taxonomy in this article. Based on two new species, *Macrostylis dorsaetosa* n. sp. and *M. papillata* n. sp., the changes in the morphology that occur during final moult of the males, especially of the antennulae, are described. Implications for future taxonomic and systematic work on this isopod family and the potential meaning of the sexual dimorphism for the ecology and evolution of Macrostylidae are discussed.

Material and Methods

Specimens were collected during the Gay Head–Bermuda transect project (Sanders and Hessler 1969) of the Woods Hole Oceanographic Institution by two different types of gear. Station GH#1 and GH#4 were sampled during the cruise RV Atlantis 273 by means of an Anchor Dredge (Sanders *et al.* 1965). An epibenthic sled (Hessler and Sanders 1967) was deployed at stations WHOI 62 (RV Atlantis II cruise 12), WHOI 121 and WHOI 122 (both RV Atlantis II cruise 24). Specimens were originally fixed in formaldehyde, then preserved and sorted in 70% ethanol. For habitus drawings and dissections of limbs, specimens were transferred into a glycerine-70% ethanol solution (approximately 1:1), and subsequently transferred into glycerine. For illustrations, temporary slides were used following Wilson (2008a). Line drawings were made using an Olympus BH-2 compound microscope fitted with interference-contrast optics and camera lucida. Vector-graphics software was applied (Inkscape ver. 0.48 and Adobe Illustrator ver. CS4) according to the methods described by Coleman (2003; 2009).

Figures were prepared either using GIMP 2 or Adobe Photoshop (ver. CS4). A stage micrometer was used for calibration. Measurements were made

from line drawings and are presented as ratios to normalize differences in body size. Where several specimens were used for measurement, ranges are displayed. Measurements were made following Hessler (1970) and using the distance measurement tool imbedded in Adobe Acrobat Professional. We use the term subequal to mean ‘within 5% of a measurement’ as described by Kavanagh and Wilson (2007). All appendages article-length ratios are given in proximal to distal order, excluding setae. Descriptions of pereopodal setae (e.g., type, shape and location) are listed in proximal-to-distal and lateral-to-medial order. Body lengths are given excluding appendages, appendage lengths excluding setae.

Terminology is based on Hessler (1970) and Wilson (1989). Setal nomenclature follows Hessler (1970) and Riehl and Brandt (2010) with some modifications for reasons of style and consistency with other sources. The body region ‘fossosome’ is defined as a hardening and fusion of the anterior pereonites 1–3 with a spade-like head inserting into the first pereonite; this apomorphy of the Macrostyliidae is presumed to be an adaptation for burrowing (Thistle and Wilson 1987; Hessler and Strömberg 1989). One- and two-sided serrate setae (Riehl and Brandt 2010) are called here mono- and biserrate, unequally bifid setae are simplified as bifid and the setal type bisetulate is introduced for Macrostyliidae for the first time. The latter setal type bears two rows of setules apically on opposite sides of the setal shaft. It can be found on all pereopods (Figs 9–10). The terms ‘antennula’ and ‘maxilla 1’ are preferred over but synonymous to ‘antenna 1’ and ‘maxilla 2’ (Wilson 2009). We introduce a new term, the ‘pereonal collum’, to describe the shape of the pereonites of macrostyliid species. The *collum*, a Latin term meaning ‘neck’, refers to a constricted region anterior to the widest section of the pereonite where the preceding segment over-

rides the narrowed anterior region of a segment. Although the collum is present to a degree on pereonites 4–7 posterior to the fossosome, it is most strongly developed on pereonite 4, and is referred to in the descriptions. Final permanent slides were assembled using Euparal.

For SEM of whole specimens and fragments methods according to Cunha and Wilson (2006) were applied. An Evo LS15 Carl Zeiss microscope was used. The SEM stubs are retained at the Australian Museum (see Materials Examined below). Accession numbers begin with “AM P” and SEM stub numbers have a “MI” prefix. Descriptions were generated using the taxonomic database system DELTA (Dallwitz 1980). For holotypes, female specimens were chosen and the descriptions are mainly based upon female characters for reasons of applicability (females are more abundant and therefore more easily accessible). Nevertheless, subadult and terminal male specimens were studied extensively. Terminal male characters are described where character states differ from those of the female.

Through the description of the latter, a more complex (but also more complete) description could be achieved. In the following descriptions, a great deal of space is devoted to the description of setae on the limbs. The distribution of setae in the Macrostyliidae has been found to be essential for identifying species. As a result of our findings, the setal details are a central component of macrostyliid descriptions.

Implicit Attributes

Unless indicated otherwise, the following attributes are implicit throughout the descriptions, except where the characters concerned are inapplicable.

Female

Body. Elongate. **Ventral spines.** Pereonite 1 spine present. Pereonite 2 spine absent. Pereonite 3 spine directed posteriorly. Pereonite 4 spine present. Pereonite 5–7 spine present. Marsupium with 2 pairs of oostegites. Developing oostegites in preparatory stage absent. **Cephalothorax.** Articulation with pereonite 1 present. Posterolateral setae simple. Posterior margins papillae absent, setae absent.

Pereonite 1–2. Posterolateral setae not on pedestals, posterior tergite margin papillae absent.

Pereonite 3. Posterolateral margin not produced posteriorly; setae not on pedestals, posterior tergite margin papillae absent. **Pereonite 4.** Subequal to pereonite 5 width. Tergal plates laterally not projecting below coxal articulation and not obscuring view on coxae. Posterior tergite margin papillae absent, setae absent. Posterolateral margin not produced posteriorly. Posterolateral setae absent, not articulating on pedestals.

Pereonite 5. Posterior tergite margin setulose. Posterolateral margin produced posteriorly. Tergite posterolateral setae present, flexibly articulated, not on pedestals. Coxae posterolateral setae absent, flexibly articulated, not on pedestals.

Pereonite 6. Posterior tergite margin setae absent. Posterolateral margin similar in shape to pereonite 5. Tergite posterolateral setae present, not articulating on pedestals. Coxae posterolateral setae absent, not articulating on pedestals. **Pereonite 7.** Without posterolateral protrusions, similar to pereonites 5–6. Posterior tergite margin setae absent. Tergite posterolateral setae present, not on pedestals. Coxae posterolateral setae absent, not on pedestals. **Pleonite 1.** Tergal articulation with pleotelson absent.

Antennula. Of 5 articles. All articles cylindrical. Article 2 present, shorter than article 1. Article 3 present, shorter than article 1. Article 4 present, shorter than article 1. Article 5 present,

shorter than article 1. Article 6–9 absent. Terminal article aesthetascs present, penultimate and antepenultimate articles aesthetascs absent. **Antenna.** Of 5 podomeres. Article 3 squat, globular. Scale absent. **Mandibles.** Palp absent. **Maxilliped.** With 2 receptaculi.

Pereopod I. Ischium dorsal margin with row of setae along dorsal ridge. Merus with dorsal row of setae along dorsal ridge. Articular plate on propodus present. **Pereopod II.** Ischium with dorsal row of setae along dorsal margin. Merus with dorsal row of setae along dorsal margin. Articular plate present. **Pereopod III.** Ischium with small simple seta proximodorsally, dorsal lobe present; proximally with setae; apex with prominent apical setae. Articular plate on propodus present. **Pereopod IV.** Dactylus present. **Pereopod VII.** Fully developed, all segments present. **Operculum.** With pappose setae terminally. **Pleopod III.** Exopod with plumose seta absent. **Uropod.** Uniramous. Endopod of 1 article.

Terminal male

Body. Similar to female. **Ventral spines.** Similar to female on all pereonites. **Imbricate ornamentation (IO).** Cephalothorax, pereonites 1–7 and pleotelson IO as in female. **Cephalothorax.** Dorsal setation as in female, posterior margins papillae absent, setae absent. **Fossosome.** Lateral tergite margins in dorsal view as in female, tergal plates laterally as in female. Ventrally as in female, sternite articulations as in female.

Pereonite 1–2. Posterolateral setae as in female, without pedestals. **Pereonite 3.** Posterolateral margins as in female, not produced posteriorly; setae as in female, without pedestals. **Pereonite 4.** Width/pereonite 5 width subequal to female, about as wide as pereonite 5, length/width ratio subequal in female and male. Lateral margins as in female; tergal plates laterally as in female; poste-

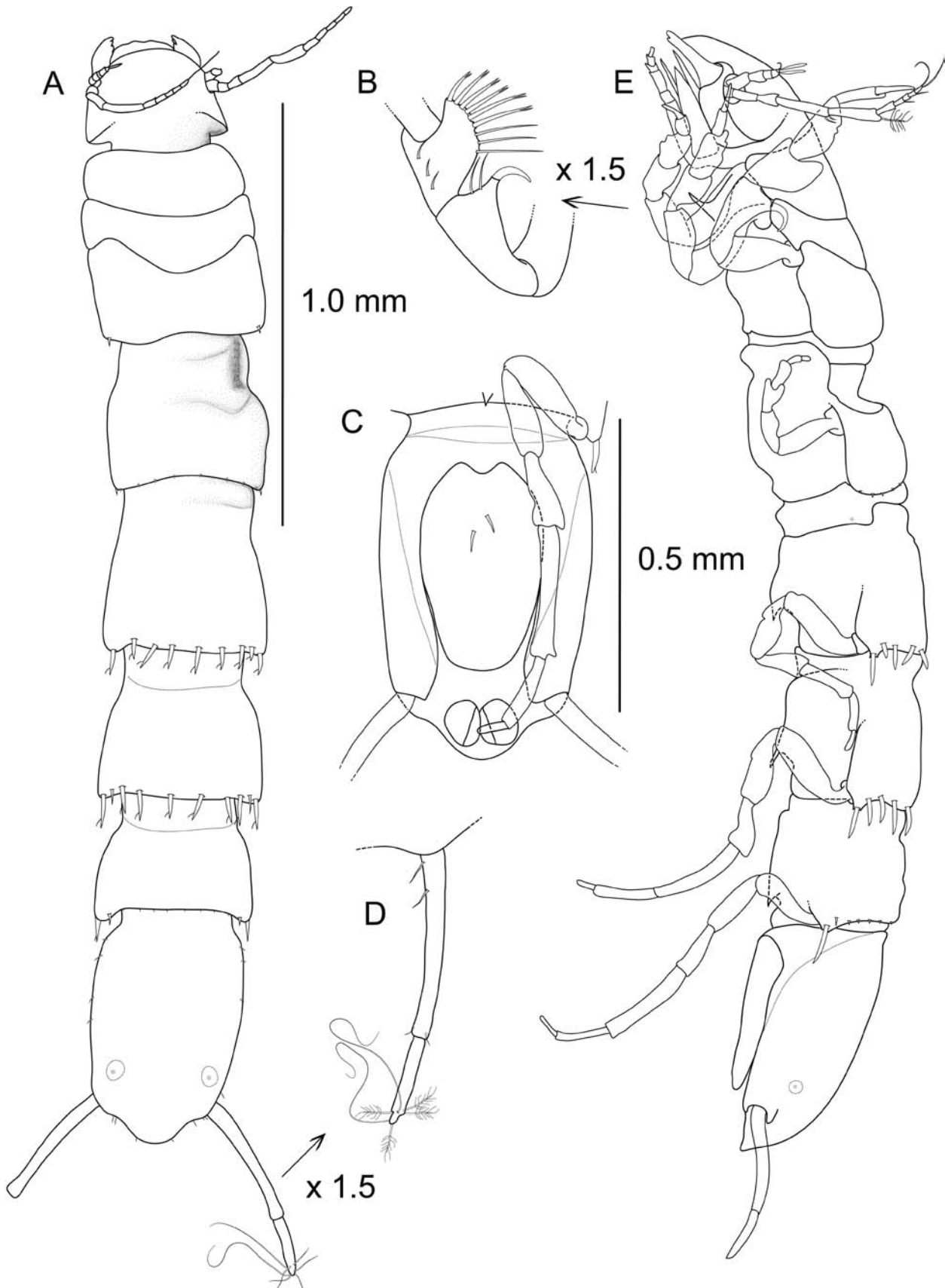


Figure 1. *Macrostylys dorsaetosa* n. sp. A–E, holotype male (AM P86000). A, dorsal habitus, imbricate ornamentation and fine setation omitted. B, left pereopod III ischium, close-up. C, pleotelson, ventral. D, right uropod, close-up. E, lateral habitus. Scales: A, D–E = 1 mm, B–C = 0.5 mm.

rolateral margins rounded. Posterior tergite margin as in female, with setae absent. Posterolateral setae

as in female, absent, without pedestals.

Pereonite 5. Posterior tergite margin as in

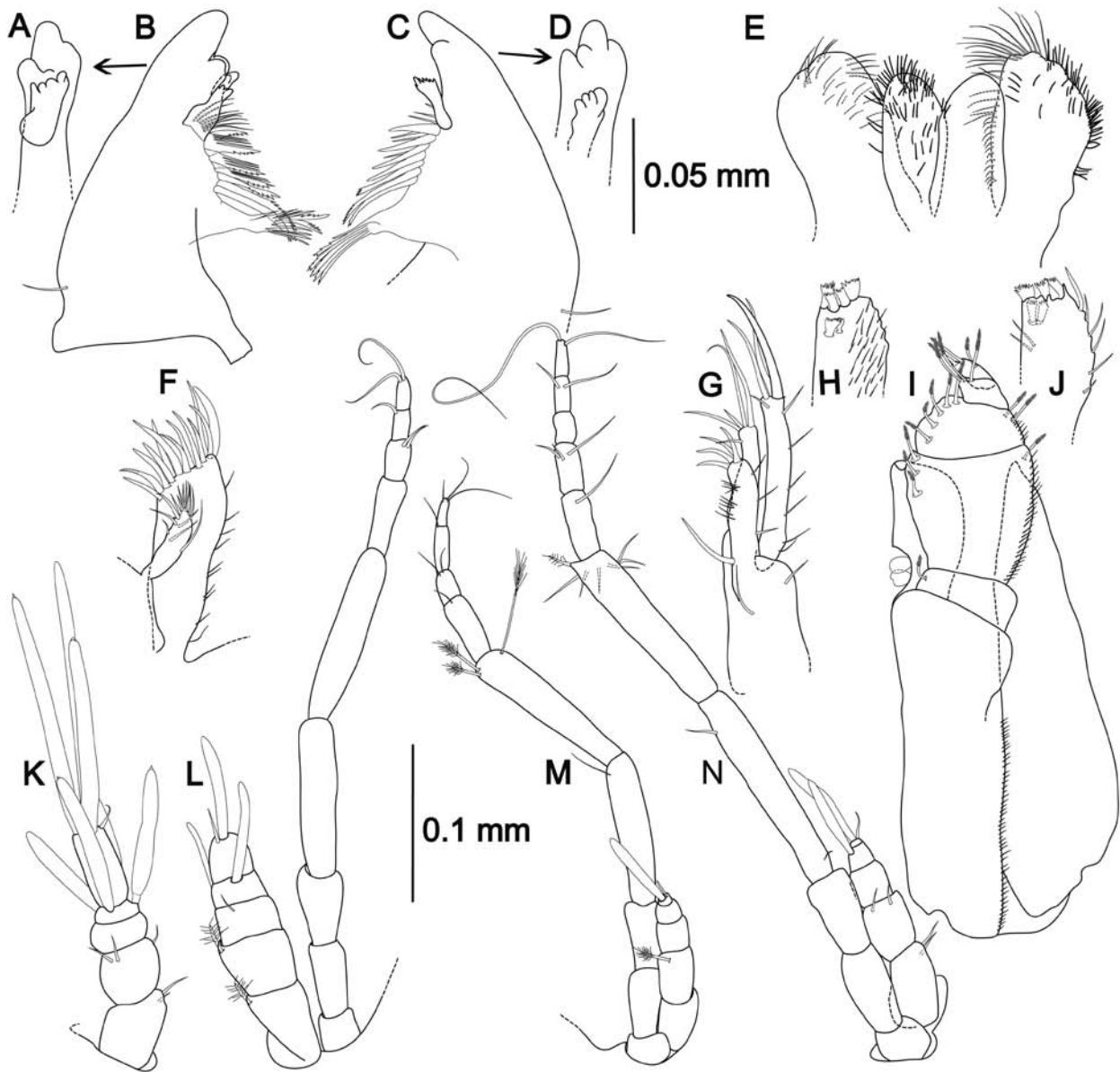


Figure 2. *Macrostylis dorsaetosa* n. sp. A–C, E, N, paratype adult (non-ovigerous) female (AM P86002). M, paratype juvenile female (AM P86006). D, F–G, K, paratype terminal male (AM P86003). L, paratype juvenile male (AM P86005). A, left mandible, medial view of incisor process and *lacinia mobilis*. B, left mandible, dorsal. C, right mandible, dorsal. D, right mandible, incisor process and *lacinia mobilis*, medial view. E, paragnaths, ventral view, ventral setae omitted in right lateral lobe, all setae omitted in left medial lobe, dorsal setae omitted in left lateral lobe. F, right maxillula, dorsal. G, left maxilla, ventral. H, left maxilliped, endite setation, ventral. I, left maxilliped, ventral. J, right maxilliped, endite setation, dorsal. K, right antennula, lateral. L, left antennula and antenna, lateral. M, right antennula and antenna, lateral. N, right antennula and antenna, lateral. Scales: A–J = 0.05 mm, K–N = 0.1 mm.

female, setae absent. Posterolateral margins as in female. Posterolateral setae on tergite as in female, present, without pedestals. Posterolateral setae on coxae absent. **Pereonite 6.** Posterior tergite margin as in female, setae absent. Posterolateral margins as in female, similar in shape to pereonite 5. Posterolateral setae on tergite as in female, present, fle-

xibly articulating, without pedestals. Posterolateral setae on coxae absent, without pedestals. **Pereonite 7.** Similar in shape to pereonites 5–6. Posterior tergite margin as in female, setae absent. Posterolateral margins similar to female. Posterolateral setae on tergite as in female, present, without pedestals. Posterolateral setae on coxae absent, without pe-

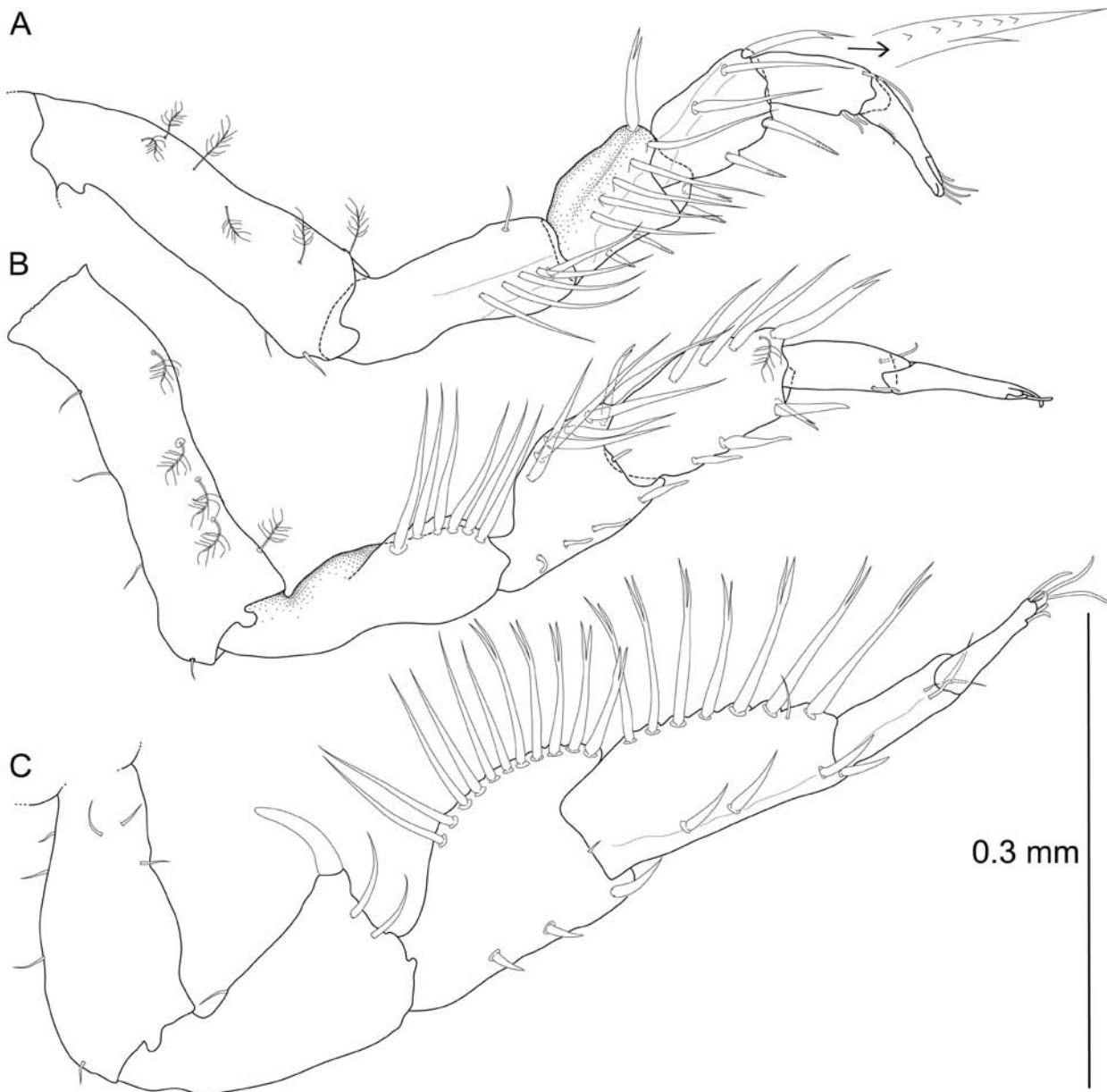


Figure 3. *Macrostylis dorsaetosa* n. sp. A–C, paratype female (AM P86002). A, pereopod I, lateral, close-up of split and monoserrate seta. B, pereopod II, lateral. C, pereopod III, lateral. Scale = 0.3 mm.

destals.

Pleonite 1. Tergal articulation with pleotelson absent. **Pleotelson.** Tergite dorsal surface in posterior view uniformly convex. Posterior apex as in female, setation as in female. **Antennula.** Of 5 articles, with articles cylindrical, articles decreasing in size; terminal article with several aesthetascs, penultimate article with several aesthetascs, antepenultimate article with no aesthetascs.

Pereopod I. Length/body-length ratio similar female. Ischium with dorsal row of setae in normal position on dorsal ridge. **Pereopod II.**

Length/body-length ratio as in female. Ischium with dorsal row of setae along dorsal margin. **Pereopod III.** Length/body-length ratio as in female. Ischium similar to female, with small simple seta proximodorsally, dorsal lobe present, proximally with row of setae; with one or two prominent apical setae. Merus setation and carpus setation as in female. **Pereopod IV.** Length/body-length ratio as in female. **Pereopod V.** Length/body-length ratio as in female; ischium setation as in female. **Pereopod VI.** Length/body-length ratio as in female. **Pleopod I.** Distally with lateral horns.

Systematics

Asellota Latreille, 1802

Macrostylidae Hansen, 1916

Macrostylis Sars, 1864 (Monotypic)

Desmosomidae Sars, 1899 Macrostylini Hansen, 1916, p. 74; Wolff, 1956, p. 99 Macrostylinae Birstein, 1973 Macrostylidae Gurjanova, 1933, p. 411; Menzies, 1962, p. 28, p. 127; Wolff, 1962; Birstein, 1970; Menzies and George, 1972, p. 79–81; Mezhov, 1988, p. 983–994; 1992, p. 69; Brandt, 1992; 2002; 2004; Kussakin, 1999, p. 336; Riehl and Brandt, 2010

Type genus. *Macrostylis* Sars, 1864

Vana Meinert, 1890 *Desmostylis* Brandt, 1992

Type species. *Macrostylis spinifera* Sars, 1864

Gender. Female

Composition. See Riehl and Brandt (2010).

Macrostylis dorsaetosa n. sp.

(Figs 1–7)

Etymology

The species name '*dorsaetosa*' is feminine and a shortened composition of three words: The first part is the prefix 'dors-' derived from the Latin word 'dorsum'. The prefix is meant to provide position information regarding the second part, 'setae', owing to the presence of conspicuous setae dorsally on the posterior tergites. Finally, the greek suffix '-osis' indicates the condition 'dorsally setose', which is the literal translation of the name.

Type fixation

Holotype: adult female, 2.6 mm, AM P.86000, designated here.

Type material examined

Holotype: non-ovigerous female, 2.6 mm, AM P.86000, used for the illustration of the habitus, WHOI 62. Paratypes: subadult male, 1.9 mm, AM P.86001, partly dissected for illustration of appendages, WHOI GH1; nonovigerous female, 2.6 mm, AM P.86002, dissected for illustration of appendages and habitus, WHOI GH1; terminal male, 2.2 mm, AM P.86003, dissected for illustration of appendages, WHOI GH1; terminal male, 2.2 mm, AM P.86004, used for habitus illustration, WHOI 62; subadult male, 2.0 mm, AM P.86005, MI 633, gold-coated for SEM, WHOI 62; juvenile female, 1.9 mm, AM P.86006, MI 639, gold-coated for SEM, WHOI 62; 14 specimens, AM P.86021, male and female, WHOI 62; 4 specimens, AM P.86025, male and female, WHOI GH4.

Type locality

Western North Atlantic off Long Island: 39°25.5'N; 70°35.0'W; 2500 m (WHOI GH #1); 39°28.8'N, 70°34.2'W; 2469 m (WHOI GH#4); 39°26'N; 70°33'W–39°27.2'N; 70°33.2'W; 2496 m (WHOI 62).

Type material — Remarks.

Collected on North American slope off Long Island during cruise R/V Atlantis- 273, stations WHOI GH1 (27. September 1961) and WHOI GH4 (30. October 1961) and R/V Atlantis II-12, station WHOI 62 (21 August 1964), about 3.4 km apart.

Further records

WHOI G#1, 1 juvenile male (AM P86024); WHOI HH#3, 1 terminal male, AM P86026; WHOI 66, 1 nonovigerous female, 1 manca, AM P98019;

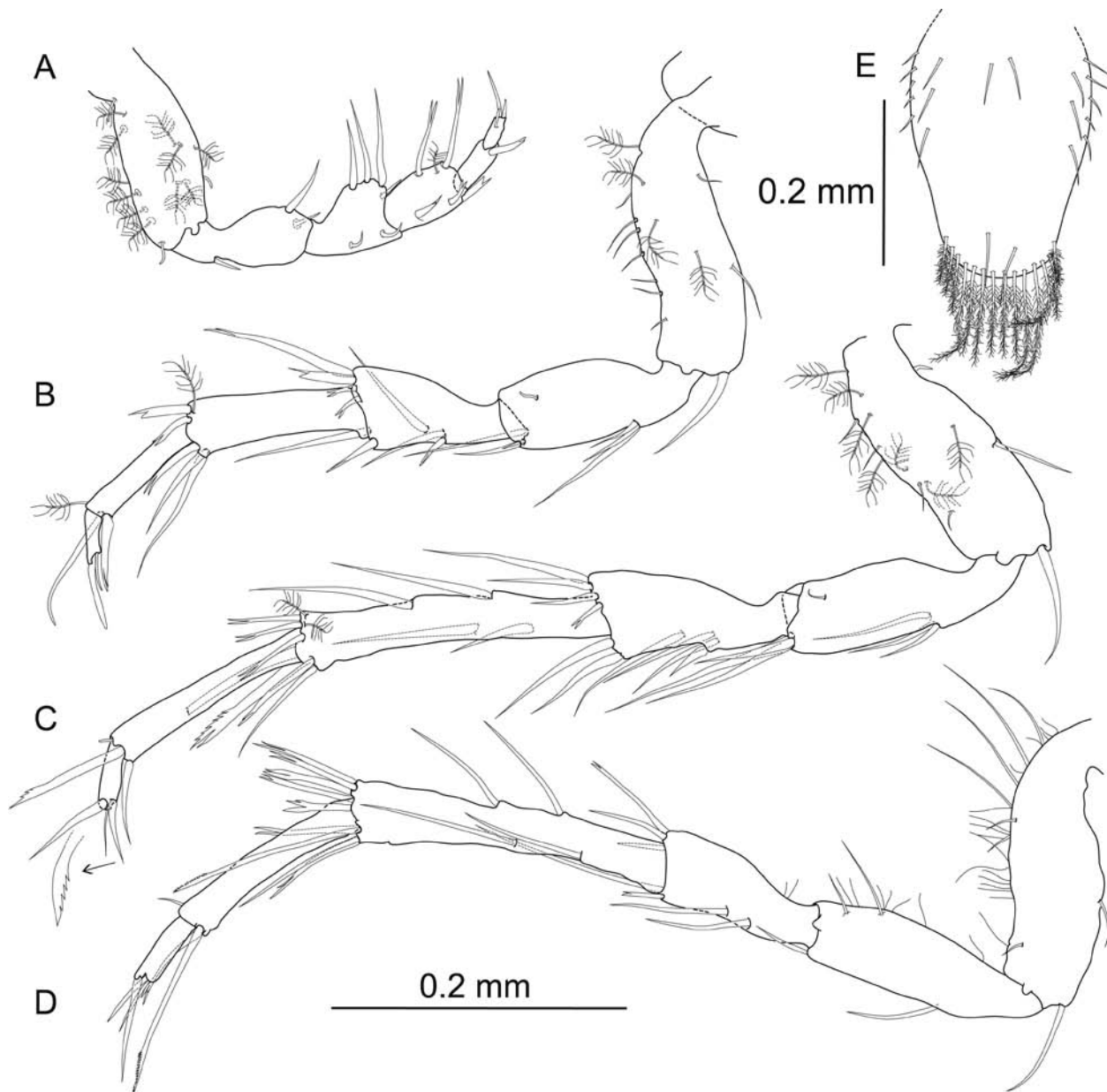


Figure 4. *Macrostylis dorsaetosa* n. sp. A–E, paratype female (AM P86002). A, pereopod IV, posterior. B, pereopod V, lateral. C, pereopod VI, lateral. D, pereopod VII, lateral. E, operculum, ventral. Scales = 0.2 mm.

WHOI 128, 7 nonovigerous females, AM P86007; WHOI 131, 12 specimen, male and female, AM P67257.

Description, female.

Body (Figs 1A, C, E, 6D, 7B). Length 2.6 mm, 6.5–6.9 width, subcylindrical, tergite surfaces with scattered setae. **Ventral spines.** Pereonite 1 spine acute, prominent. Pereonite 3–4 spine absent. Pereonite 5 spine acute, small, closer to posterior segment border. Pereonite 6 spine acute, prominent, closer to posterior segment border. Pereonite

7 spine small. **Imbricate ornamentation (IO).** Pereonite 4 IO in anterior region of tergite and sternite; pereonite 5–6 IO in anterior dorsal pereonal collum regions.

Cephalothorax. Length 0.82–0.90 width, 0.10–0.11 body length; frons in dorsal view straight, frontal ridge present, straight. Posterolateral setae present. Posterolateral margins blunt.

Fossosome. Length 1.1–1.2 width, 0.16–0.18 body length. Lateral tergite margins in dorsal view forming almost uninterrupted line, ventral surface with keel, sternite articulations present.

Figure 6 (opposite page top). *Macrostylis dorsaetosa* n. sp. **A–H, paratype juvenile male (AM P86005).** **A,** cephalothorax, dorsal. **B,** antennula close-up, dorsal. **C,** pereonites 5–6, dorsal. **D,** habitus, lateral. **E,** cephalothorax close-up, lateral. **F,** pereopod I, lateral. **G,** pereopod III, lateral. **H,** posterior apex of pleotelson and uropods, dorsal. Scales: A–B, F–H = 0.1 mm, D = 1 mm.

Figure 7 (opposite page bottom). *Macrostylis dorsaetosa* n. sp. **A–B, paratype non-ovigerous female (AM P86006; MI 639).** **A,** pereopod III, lateral. **B,** pleotelson and uropods, dorsal. Needle-like objects are crystalline artifacts. Scales = 0.1 mm.

simple, not robust, flexibly articulated.

Pereonite 5. Length 0.95–1.1 width. Posterior tergite margin setae 8 altogether, bifid, robust, flexibly articulating, long, extending beyond posterolateral margin. Posterolateral margins rounded. Tergite posterolateral setae bifid, robust. **Pereonite 6.** Length 0.90–0.97 width. Posterior tergite margin setae 8–9 altogether, bifid, robust, flexibly articulating, long, extending beyond posterolateral margin. Posterolateral margin produced posteriorly, rounded. Tergite posterolateral setae bifid, robust, flexibly articulated. **Pereonite 7.** Length 0.67–0.73 width. Posterior tergite margin setae 10–12 altogether, bifid, short, not extending beyond posterolateral margin. Posterolateral margin produced posteriorly. Tergite posterolateral setae bifid, robust, flexibly articulated.

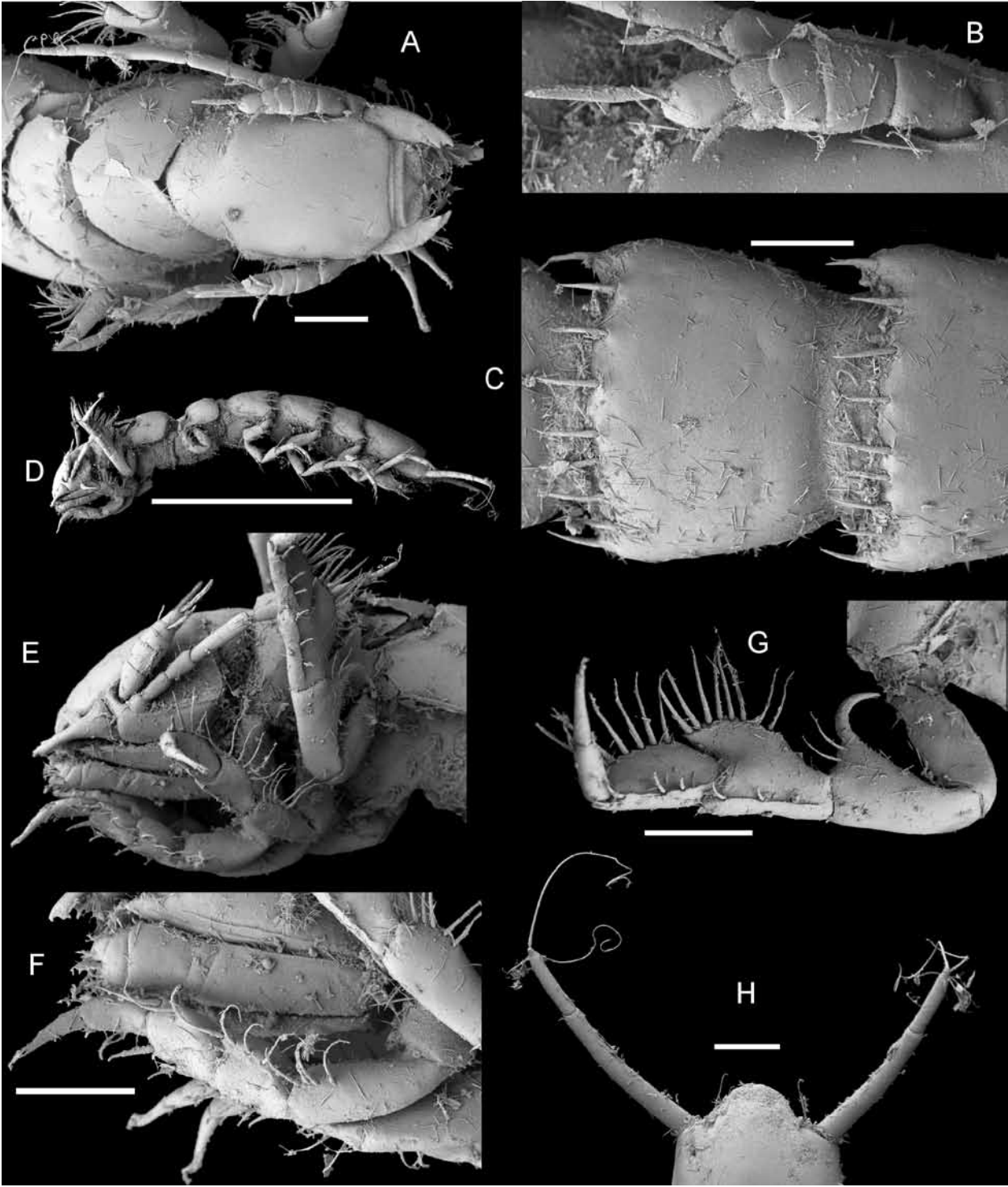
Pleonite 1. Sternal articulation with pleotelson absent. **Pleotelson.** Ovoid, length 0.21 body length, 1.6 width, narrower than pereonite 7; statocysts present, dorsal slot-like apertures absent. Posterior apex convex, bluntly rounded. Posterior apex setae 2 altogether, simple, positioned lateral to apex. Pleopodal cavity width 0.58 pleotelson width, preanal ridge width 0.42 pleotelson width. Anal opening subterminal, tilted posteriorly relative to frontal plane.

Labrum. Anterior margin in dorsal view concave. **Antennula (Fig. 2K–L).** Length 0.41 head width, 0.25 antenna length, width 1.0 antenna width. Articles decreasing in size from proximal to distal. Article 1 distinctly longer than wide, longest

and widest, with 2 simple setae. Article 2 distinctly longer than wide, tubular, with 2 simple setae. Article 3 squat, globular. Article 4 squat, globular. Article 5 minute, squat, globular, with 1 simple seta. Terminal article with 1 aesthetasc, penultimate article with 1 aesthetasc, aesthetascs simple, tubular. **Antenna (Fig. 2M–N).** Length 0.2 body length. Article 1 squat, globular. Article 2 elongate, longer than article 1. Article 3 elongate, longer than article 1. Article 4 longer than articles 1–3 together, distally with 1 simple seta. Article 5 shorter than article 4, distally with 6 simple setae, distally with 1 broom seta. Flagellum with 5 articles.

Mandibles (Fig. 2A–D). In medial view strongly narrowing from proximal to distal, subtriangular, with lateral setae; left mandible incisor process distal margin flattened and curved (shovel-like), with 3 cusps, *lacinia mobilis* grinding, with 4 cusps; right mandible incisor process with shovel-like appearance, with 3 cusps, *lacinia mobilis* grinding, clearly smaller than left lacinia, with 8 cusps. **Maxillula (Fig. 2F).** Lateral lobe with 14 robust setae Lateral lobe with 4 setae terminally; middle endite with 3 setae terminally; inner endite with 8 setae terminally. **Maxilliped (Fig. 2H–J).** Basis endite length 4.2 width; epipod length 4 width, 1.0 basis-endite length; palp wider than endite, article 2 wider than articles 1 and 3, article 1 shorter than article 3.

Pereopod I (Fig. 3A). Length 0.25 body length. Ischium dorsal margin with 5 setae, simple, in row, row of setae laterally to margin. Merus dorsal margin with 6 setae, 5 simple, 1 promi-



ment, split, ventral margin with 4 setae, 3 biserrate, 1 split, with dorsal row of setae laterally to margin. Carpus dorsally with 3 setae, 2 simple, 1 prominent, split. Dactylus distally with 3 sensillae.

Pereopod II (Fig. 3B). Longer than pereopod I, length 0.29 body length. Ischium dorsally with 6 setae, simple, with dorsal row of setae laterally to margin. Merus dorsally with 8 setae, 6 simple in row, 2 split distomedially, with dorsal row of setae laterally to margin, ventrally with 4 setae, biserrate. Carpus dorsally with 5 setae, 3 simple, 1 broom, 1 prominent split, serrate, ventrally with 4 setae, 3 biserrate, 1 split. Dactylus distally with 3 sensillae. **Pereopod III (Fig. 3C).** Length 0.26 body length. Ischium dorsal lobe tapering; proximally with no setae; apex with 1 prominent seta; apical seta robust, robust sensillate, bent towards proximal, spine-like; distally with 2 simple setae. Merus dorsally with 11 setae, 6 simple, 5 split, serrate, ventrally with 3 setae, biserrate. Carpus dorsally with 7 setae, split, serrate, ventrally with 4 setae, 3 biserrate, 1 split. Dactylus with 3 sensillae.

Pereopod IV (Fig. 4A). Length 0.15 body length, carpus laterally flattened. **Pereopod V (Fig. 4B).** Length 0.25 body length. Ischium midventrally with 3 setae, simple, distoventrally with 3 setae, simple. Merus distodorsally with 4 setae, split, midventrally with 3 setae, 1 split, 2 simple, distoventrally with 2 setae, 1 short, split, serrate, 1 long, simple. Carpus distodorsally with 3 setae, 1 split, 1 broom, 1 split, serrate, distoventrally with 3 setae, split. **Pereopod VI (Fig. 4C).** Length 0.32 body length; ischium midventrally with 3 setae, simple, distoventrally with 3 setae, all simple; merus distodorsally with 4 setae, 2 short, split, 1 simple, 1 long split, midventrally with 4 setae, simple, distoventrally with 2 setae; carpus middorsally with 2 setae, simple, distodorsally with 5 setae, 1 split, 2 broom, 1 split, serrate, 1 split, midventrally with 2 setae, simple, distoventrally with 4 setae, 2 split, 2

prominent, split, serrate. **Pereopod VII (Fig. 5D).** Length less than pereopod VI length, 0.33 body length. Basis length 2.7 width; with row of elongate setae on posterior margin. Ischium length 3 width, middorsally with 2 setae, simple, midventrally with 1 seta, simple, distoventrally with 1 seta, simple. Merus length 2.2 width, distodorsally with 3 setae, 1 split, 2 simple, midventrally with 2 setae, simple, distoventrally with 2, 1 simple, long, 1 split, short. Carpus length 5.5 width, middorsally with 2 setae, simple, distodorsally with 5 setae, all split, possibly all serrate or biserrate, midventrally with 2 setae, simple, distoventrally with 4 setae, 1 long, split, serrate, 1 simple, 2 split. Propodus length 4.3 width. Dactylus length 2.5 width.

Operculum (female pleopod II; Fig. 4E).

Elongate, length 1.6 width, 0.60 pleotelson length, distally tapering, without keel, with 14 pappose setae on apex, completely covering anal opening.

Pleopod III (Fig. 5D). Length 2.5 width, protopod length 1.6 width, 0.46 pleopod III length; exopod with fringe of fine setae, about as long as pleopod III exopod width, with simple seta subterminally, exopod length 0.77 pleopod III length. **Pleopod V (Fig. 5F).** Present. **Uropod (Figs 1A, D, 7B).** Length 0.79–0.82 pleotelson length; protopod length 0.55–0.56 pleotelson length, inserting on pleotelson ventrally on posterior margin. Protopod distal margin blunt, endopod insertion terminal, length 7.5–8.1 width; endopod length 4.7–6.1 width, 0.46–0.47 protopod length, endopod width subequal protopod width.

Description, terminal male

Body. Length 2.2 mm, 6.6 width. **Cephalothorax.** Frons smooth, frontal ridge present, straight; length/width ratio greater than in female, length 0.96 width, 0.12 body length; with conspicuous dorsal array of setae, posterolateral corners rounded, posterolateral setae absent. **Fossosome.**

Length/width ratio greater than in female, length 1.4 width, length/body-length ratio greater than in female, length 0.21 body length.

Pereonite 4. Lateral margins in dorsal view convex; posterolateral margin not produced posteriorly. Pereonal collum present, medially convex.

Pleonite 1. Sternal articulation with pleotelson present. **Pleotelson.** In dorsal view approximately rectangular, length/width ratio in male greater than in female, length 1.8–2.1 width, 0.23 body length, width less than pereonite 7 width. Pleopodal cavity width 0.69 pleotelson width, preanal ridge width 0.37 pleotelson width.

Antennula (Figs 2K–L, 6A–B, E). Length 0.52 head width, 0.33 antenna length, width 2.0 antenna width, articles 1, 2 and 5 elongate, tubular; articles 3–4 squat or noticeably shorter; terminal article with 3 aesthetascs, penultimate article with 4 aesthetascs, aesthetascs simple, tubular. Article 1 elongate, subequal in width and length compared to more distal articles, with 1 simple seta and 1 broom seta. Article 2 squat, globular, shorter than article 1, with 1 simple seta and 2 broom setae. Article 3 squat, globular, shorter than article 1, article 4 squat, globular, shorter than article 1. Article 5 elongate, longer than article 1, with 2 simple setae.

Antenna (Figs 2L, 6A, E). Length 0.2 body length, flagellum of 4 articles. Article 1 squat, globular. Article 2 elongate, longer than article 1. Article 3 elongate, longer than article 1. Article 4 shorter than articles 1–3 together, distally with 1 simple seta. Article 5 longer than article 4, with 3 broom setae.

Pereopod I (Fig. 6F). Ischium dorsally with 4 setae, all simple, with dorsal row of setae shifted laterally. Merus dorsally with 5 setae, 4 simple in row, 1 split distally, ventrally with 3 setae, 2 biserrate, 1 split seta distally. Carpus dorsally with 2 setae, 1 simple, 1 split distally, ventrally with 2 setae, biserrate. **Pereopod II.** Ischium dorsally

with 5 setae, all simple, with dorsal row of setae shifted laterally. Merus dorsally with 8 setae, 6 simple in row, 2 split distomedially, ventrally with 3 setae, all two-sided serrate. Carpus setation as in female.

Pereopod V. Merus distodorsally with 3 setae, split, midventrally with 2 setae, simple; distoventrally with 2 setae. Carpus distodorsally with 4 setae, 1 small, split, 1 broom, 2 serrate, split. **Pereopod VI.** Ischium setation as in female. Merus

distodorsally with 4 setae, 2 short, split, 1 simple, 1 long split, midventrally with 2 setae, simple, distoventrally with 1 seta, split. Carpus middorsally with 2 setae, simple, distodorsally with 3 setae, 1 split, serrate, 1 broom, 1 split; midventrally with 2 setae, simple, distoventrally with 4 setae, 3 split, 1 long, split, serrate. **Pereopod VII.** Length/body-length ratio as in female, segment L/W ratios sexually dimorphic; basis length 2.6–2.8 width; ischium length 2.6 width, middorsally with 2 setae, simple, midventrally with 1 seta, simple, distoventrally with 2 setae, simple; merus length 2.2–2.8 width, merus setation as in female; carpus length 4.8–5 width, carpus middorsally with 2 setae, simple, distodorsally with 5 setae, split, midventrally with 2 setae, simple, distoventrally with 3 setae, split; propodus length 7 width; dactylus length 4 width.

Pleopod I (Fig. 5A–B). Length 0.64 pleotelson length, with simple setae ventrally. **Pleopod II (Fig. 5C).** Protopod apex rounded, with setae on proximal lateral margin, 3 pappose setae altogether, with 6 pappose setae distally. Endopod distance of insertion from protopod distal margin 0.54 protopod length. Stylet sinuous, extending near to distal margin of protopod, length 0.84 protopod length.

Uropod (Figs 5B, 6H). Length 0.88–1.1 pleotelson length; protopod length/width ratio greater than in female, 9.6–10.3 width, with endopod inserting terminally; endopod/protopod length ratio less than in female, endopod length 0.29–0.3 pro-

topod length, length 5.4–6 width, width less than protopod.

Remarks

Macrostylis dorsaetosa n. sp. is unlike any other species in the genus owing to the row of bifid setae on the posterior margins of pereonites 5–6 (Figs 1A, E, 6C). *M. strigosa* Mezhov, 1999 shows remarkable similarity in important characters such as the ischium setation of pereopod III, a character often applied for differentiation of macrostylid species, and body shape. This latter species could therefore be regarded as closely related to *M. dorsaetosa* n. sp. However, the above mentioned dorsomarginal setae are missing in *M. strigosa*. *M. grandis* Birstein, 1970 has smaller marginal setae on pereonites 4–6 and the pleotelson, but this latter species is also unusual in having pereonite 6 laterally overlapping pereonite 7. The chaetotaxy of the pereopod III ischium is substantially different in the two species as well, with *M. dorsaetosa* having one robust proximally curving seta on the apex and 2 simple setae on the distal slope of the dorsal projection (Figs 3C, 6G, 7A).

Macrostylis papillata n. sp.

(Figs 12–15)

Etymology

The name ‘*papillata*’ is derived from the Latin word ‘*papilla*’, meaning ‘wart’ because this species is characterized by warty posterior margins of the cephalothorax’ and the anterior four pereonites’ tergites.

Type fixation

Holotype: ovigerous female, 1.5 mm, AM P.86009, designated here.

Type material examined

Holotype: ovigerous female, 1.5 mm, AM P.86009, used for habitus illustrations, WHOI 121. Paratypes: juvenile female, 1.3 mm, AM P.86008, partly used for illustration of habitus and antennae, WHOI 121; nonovigerous female, 1.5 mm, AM P.86010, used for habitus illustrations and dissected for illustration of appendages, WHOI 121; terminal male, 1.3 mm, AM P.86011, used for habitus illustrations and dissected for illustration of appendages, WHOI 121; ovigerous female, 1.5 mm, AM P.86013, MI 638, gold-coated for SEM, WHOI 121; terminal male, AM P.86014, MI 635–MI 637, dissected and gold-coated for SEM, WHOI 121; immature male, 1.3 mm, AM P.86015, partly used for illustration of habitus and antennae, WHOI 121.

Type locality

Western North Atlantic abyssal plain between Long Island and Bermuda: 35°50.0’N; 65°11.0’W; 4800 m (WHOI 121), 35°51.0’N; 64°58.2’W; 4833 m (WHOI 122). Type material – Remarks. Collected during cruise R/V Atlantis II-24 (21 August 1966).

Further records

1 terminal male, AM P.86016, WHOI LL1; 4 specimen, female and male, AM P.67254, WHOI 58; 1 terminal male, AM P.83030, WHOI 83; 1 nonovigerous female, AM P.86028, WHOI 85; 8 specimen, female and male, AM P.86029, WHOI 95; 2 ovigerous female, AM P.86055, WHOI 120; 1 terminal male, AM P.86012, WHOI 125; terminal male, 1.3 mm, AM P.86012, MI 630, gold-coated for SEM, WHOI 125.

Description, female

Body (Figs 8A–D, 15A–E). Length 1.5 mm, 4.5 width, subcylindrical, without setation. **Ventral spines.** Pereonite 1 spine acute, prominent. Pereonite 3 spine blunt, small, closer to anterior segment

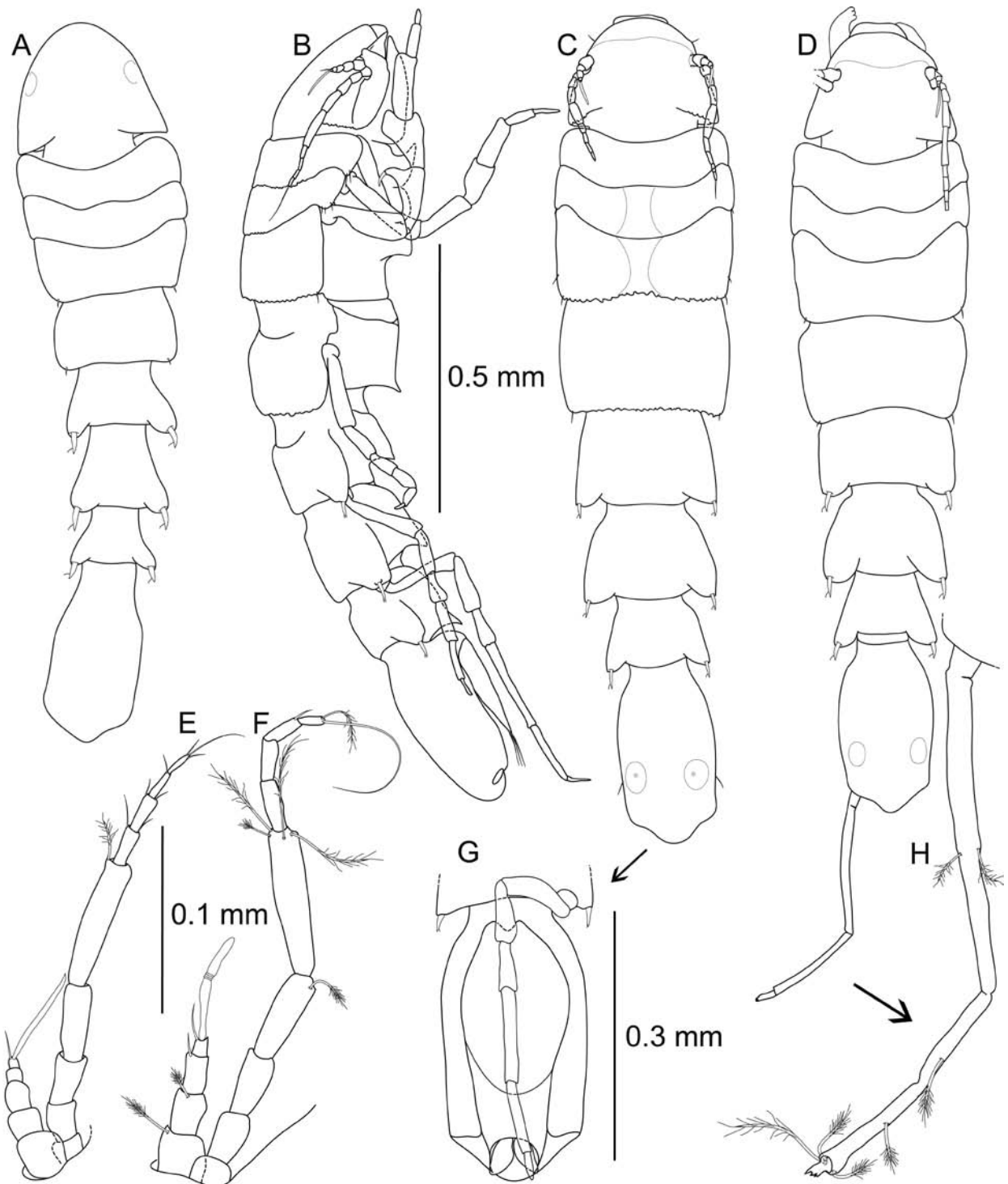


Figure 8. *Macrostylis papillata* n. sp. **A, E,** paratype juvenile female (AM P86008). **B–C, F–G,** paratype adult, non-ovigerous female (AM P860010). **D, H,** holotype ovigerous female (AM P86009). **A–D,** dorsal and lateral habitus, cuticle ornamentation and appendages mostly omitted, uropods missing where not illustrated. **D,** uropod endopod, damaged. **E–F,** left antennula and antenna, *in situ*, lateral. **G,** pleotelson, ventral. **H,** uropod, close-up, endopod damaged. Scales: A–D = 0.5 mm, E–F = 0.1 mm, G = 0.3 mm.

border. Pereonite 4 spine directed posteriorly, acute, small, closer to posterior segment border. Pereonite 5 spine blunt, closer to posterior segment border. Pereonite 6 spine acute, prominent, closer to posterior segment border. Pereonite 7 spine

small. **Imbricate ornamentation (IO).** Pereonite 1 IO along anterior tergite margin and medially on tergite from anterior to posterior, covering whole sternite; pereonites 2 and 3 IO in an hourglass-shaped band medially on tergite, wider in pereonite

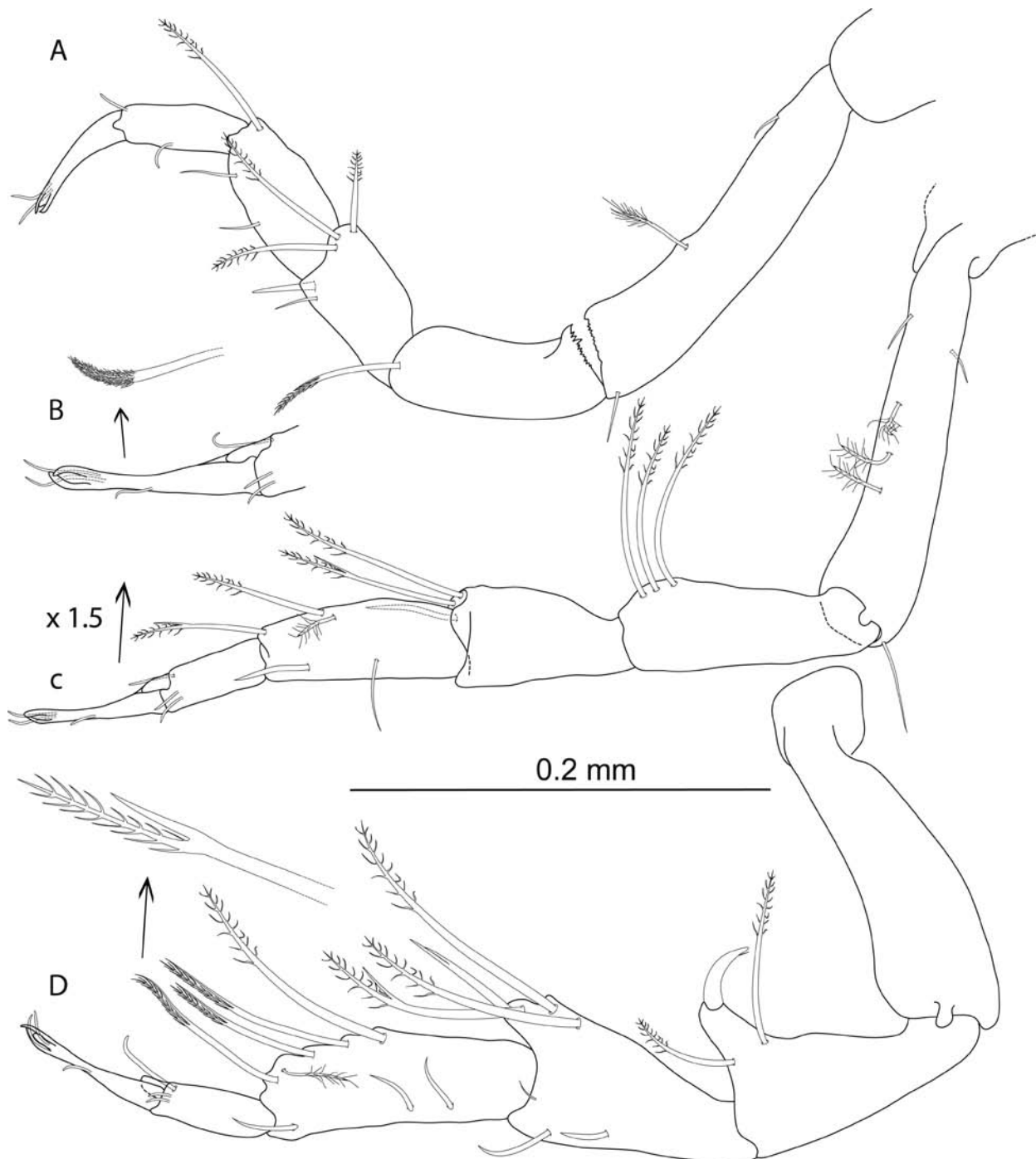


Figure 9. *Macrostylis papillata* n. sp. A–D, paratype non-ovigerous female (AM P860010). A, pereopod I, lateral, baso-ischial articulation damaged. B, pereopod II dactylus, lateral with close up of distally papillose fringe-like sensilla. C, pereopod II, lateral. D, pereopod III, lateral with close up of bisetulate split seta. Scale = 0.2 mm.

3 than in pereonite 2, covering whole sternite; pereonite 4–7 and pleotelson IO covering all tergites, sternites and operculum.

Cephalothorax. Length 0.82 width, 0.15 body length; frons in dorsal view convex, with wrinkles, frontal ridge absent; dorsal surface with array of setae, 1 pair on frons between anterior rims of antennulae articulations, 1 pair dorsally

and 1 pair at back of cephalothorax. Posterolateral setae absent. Posterolateral corners acute. Posterior margin papillose. **Fossosome.** Length 0.85 width, 0.19 body length. Lateral tergite margins in dorsal view forming almost uninterrupted line, ventral surface without keel.

Pereonite 1. Anterior margin concave; posterolateral setae simple, posterior tergite margin

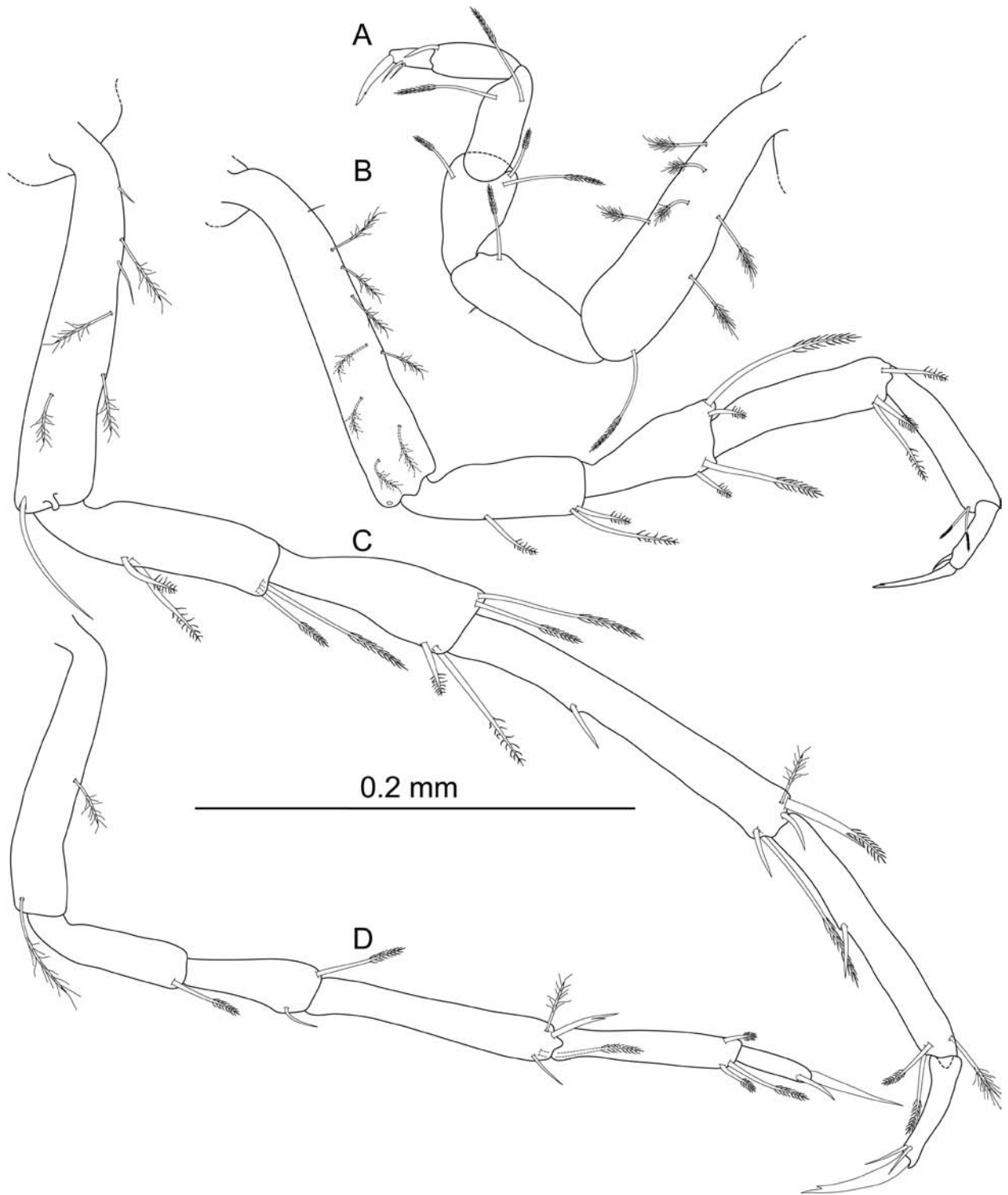


Figure 10. *Macrostylis papillata* n. sp. A–D, paratype non-ovigerous female (AM P860010). A, pereopod IV, posterior. B, pereopod V, lateral. C, pereopod VI, lateral. D, pereopod VII, lateral. Scale = 0.2 mm.

papillose. **Pereonite 2.** Posterolateral setae simple, posterior tergite margin papillose. **Pereonite 3.** Posterolateral setae simple, flexibly articulated, posterior tergite margin papillose. **Pereonite 4.** Width 1.2 pereonite 5 width, length 0.66 width; pereonal collum present. Lateral margins in dorsal view simple convex. Posterior tergite margin papil-

lose. Posterolateral margin rounded. Posterolateral setae simple, not robust, flexibly articulated.

Pereonite 5. Length 0.69 width. Posterolateral margin rounded. Tergite posterolateral setae bifid, robust. **Pereonite 6.** Length 0.72 width. Posterolateral margin produced posteriorly, rounded. Tergite posterolateral setae bifid, robust, flexibly

articulated. **Pereonite 7.** Length 0.63 width. Posterolateral margin produced posteriorly, rounded. Tergite posterolateral setae bifid, robust, flexibly articulated.

Pleonite 1. Tergal articulation with pleotelson present. **Pleotelson (Figs 8D, G, 15C).** Ovoid, constricted anteriorly to uropod articulations, length 0.22 body length, 1.8 width, narrower than pereonite 7; statocysts present, dorsal slot-like apertures absent. Posterior apex convex, bluntly rounded. Posterior apex setae absent. Pleopodal cavity width 0.72 pleotelson width, preanal ridge width 0.44 pleotelson width. Anal opening terminal, tilted posteriorly relative to frontal plane.

Labrum (Fig. 14F). Anterior margin in dorsal view concave. **Antennula (Fig. 8E–F).** Length 0.25 head width, 0.25 antenna length, width 1.5 antenna width. Articles decreasing in size from proximal to distal. Article 1 squat, globular, widest but not longest, with 1 broom seta. Article 2 distinctly longer than wide, tubular, subequal article 1 length, with 1 broom seta. Article 3 distinctly longer than wide, tubular, length subequal article 1 length, with 1 simple seta. Article 4 squat, globular. Article 5 minute, squat, globular, with 1 simple seta. Terminal article with 1 aesthetasc, aesthetasc with intermediate belt of constrictions.

Antenna (Fig. 8E–F). Length 0.18 body length. Article 1 squat, globular. Article 2 squat, globular, longer than article 1. Article 3 elongate, longer than article 1. Article 4 shorter than articles 1–3 together, distally with 1 broom seta. Article 5 longer than article 4, distally with 4 broom setae. Flagellum with 4 articles. **Mandibles (Fig. 11A–D).** In medial view dorsoventrally flattened, with lateral setae; left mandible incisor process distal margin flattened and curved (shovel-like), with 4 cusps, *lacinia mobilis* grinding, with 4 cusps; right mandible incisor process with shovel-like appearance, with 3 cusps, *lacinia mobilis* grin-

ding, clearly smaller than left lacinia, with 6 cusps.

Maxillula (Fig. 11E). Lateral lobe with 13 robust setae. **Maxilla (Fig. 11H, 15F–G).** Lateral lobe with 4 setae terminally, simple; middle endite with 5 setae terminally, simple; inner endite with 9 setae terminally, 4 monoserrate, 5 slim, simple. **Maxilliped (Figs 11F–G, 15F).** Basis endite length 3.5 width; epipod length 3.5 width, 1.2 basis-endite length; palp width subequal endite width, article 2 wider than article 1, article 2 wider than article 3, article 1 shorter than article 3.

Pereopod I (Fig. 9A). Length 0.33 body length. Ischium dorsal margin with 1 seta, split, bisetulate, laterodistally. Merus dorsal margin with 3 setae, bisetulate, distally, ventral margin with 2 setae, bisetulate, placed distally. Carpus dorsally with 1 seta, bisetulate, placed distally. Dactylus distally with 2 sensillae. **Pereopod II (Fig. 9B–C).** Longer than pereopod I, length 0.39 body length. Ischium dorsally with 3 setae, bisetulate, placed distally. Merus dorsally with 3 setae, bisetulate, placed distally. Carpus dorsally with 3 setae, 1 bisetulate and 1 broom medially, 1 split distally, ventrally with 2 setae, 1 medially, 1 distally. Dactylus distally with 2 sensillae. **Pereopod III (Fig. 9D).** Length 0.41 body length. Ischium with no seta proximodorsally, dorsal lobe tapering; proximally with 1 bisetulate seta; apex with 1 prominent seta; apical seta robust, bifid, bent towards proximal, spine-like; distally with 1 bisetulate seta. Merus dorsally with 4 setae, 2 bisetulate, 2 split, bisetulate, ventrally with 2 setae, simple. Carpus dorsally with 5 setae, 1 bisetulate, 2 split, bisetulate, 1 broom, 1 split, bisetulate, ventrally with 3 setae, simple. Dactylus with 2 sensillae.

Pereopod IV (Fig. 10A). Length 0.24 body length. **Pereopod V (Fig. 10B).** Length 0.33 body length. Ischium midventrally with 1 seta, bisetulate, distoventrally with 2 setae, bisetulate. Merus distodorsally with 2 setae, 1 short, bisetulate, 1

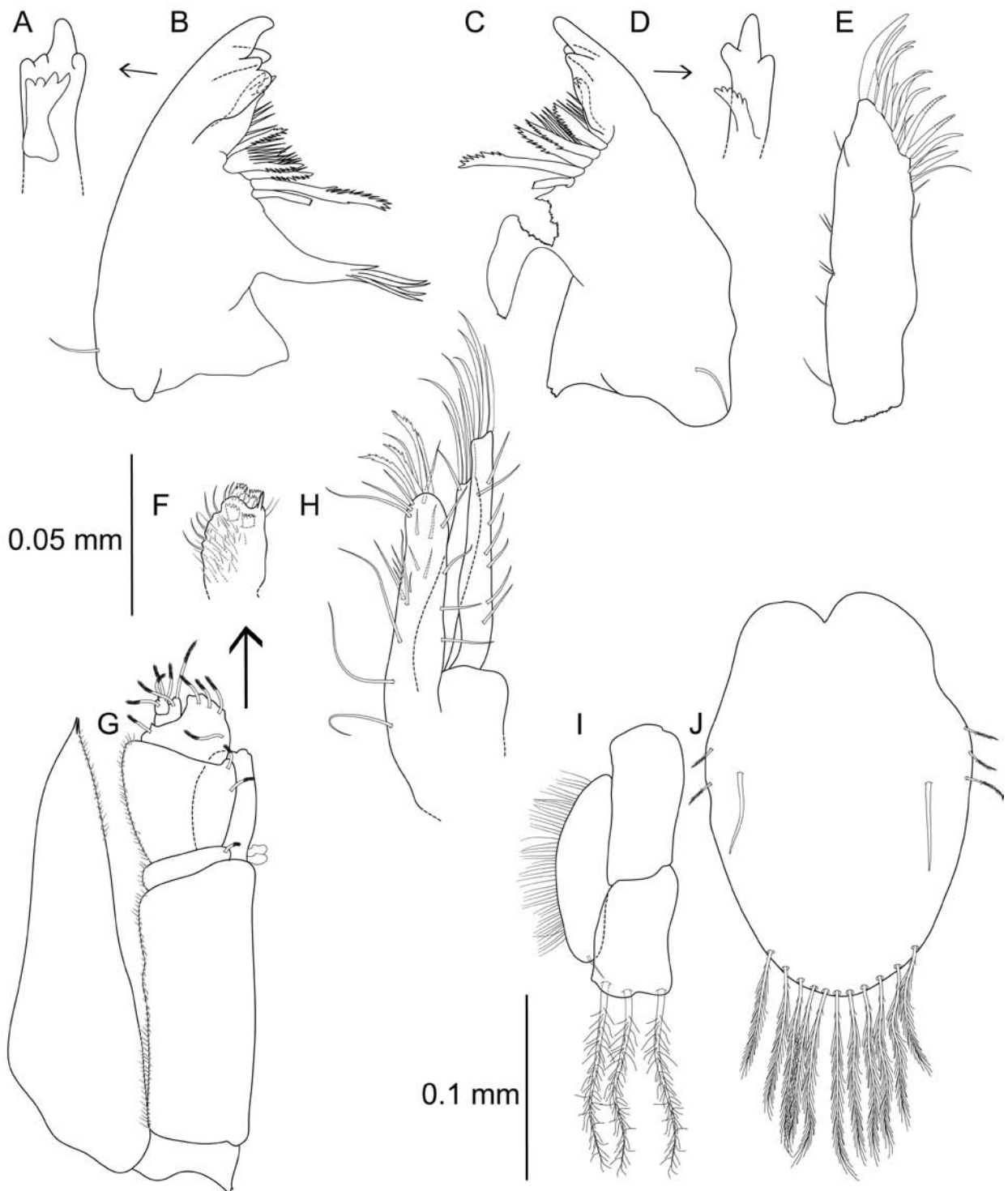


Figure 11. *Macrostylis papillata* n. sp. A–J, paratype non-ovigerous female (AM P860010). **A**, left mandible, medial view of incisor process and *lacinia mobilis*. **B**, left mandible, dorsal, setal row damaged. **C**, right mandible, dorsal, setal row and molar process damaged. **D**, right mandible, incisor process and *lacinia mobilis*, medial view. **E**, right maxillula, ventral, inner lobe broken off. **F**, right maxilliped, endite setation, ventral. **G**, right maxilliped, ventral. **H**, left maxilla, ventral. **I**, right pleopod III, ventral. **J**, operculum, ventral. Scales: A–H = 0.05 mm, I–J = 0.1 mm.

long, bisetulate, distoventrally with 2 setae, 1 long, bisetulate, 1 short, bisetulate. Carpus distodorsally with 1 seta, bisetulate, distoventrally with 2 setae, bisetulate. **Pereopod VI** (Fig. 10C). Length 0.41 body length; ischium midventrally with 2 setae,

bisetulate, distoventrally with 2 setae, bisetulate; merus distodorsally with 2 setae, bisetulate, distoventrally with 2 setae, bisetulate; distodorsally with 3 setae, 1 broom, 1 prominent, split, bisetulate, 1 small, bisetulate, midventrally with 1 seta, bi-

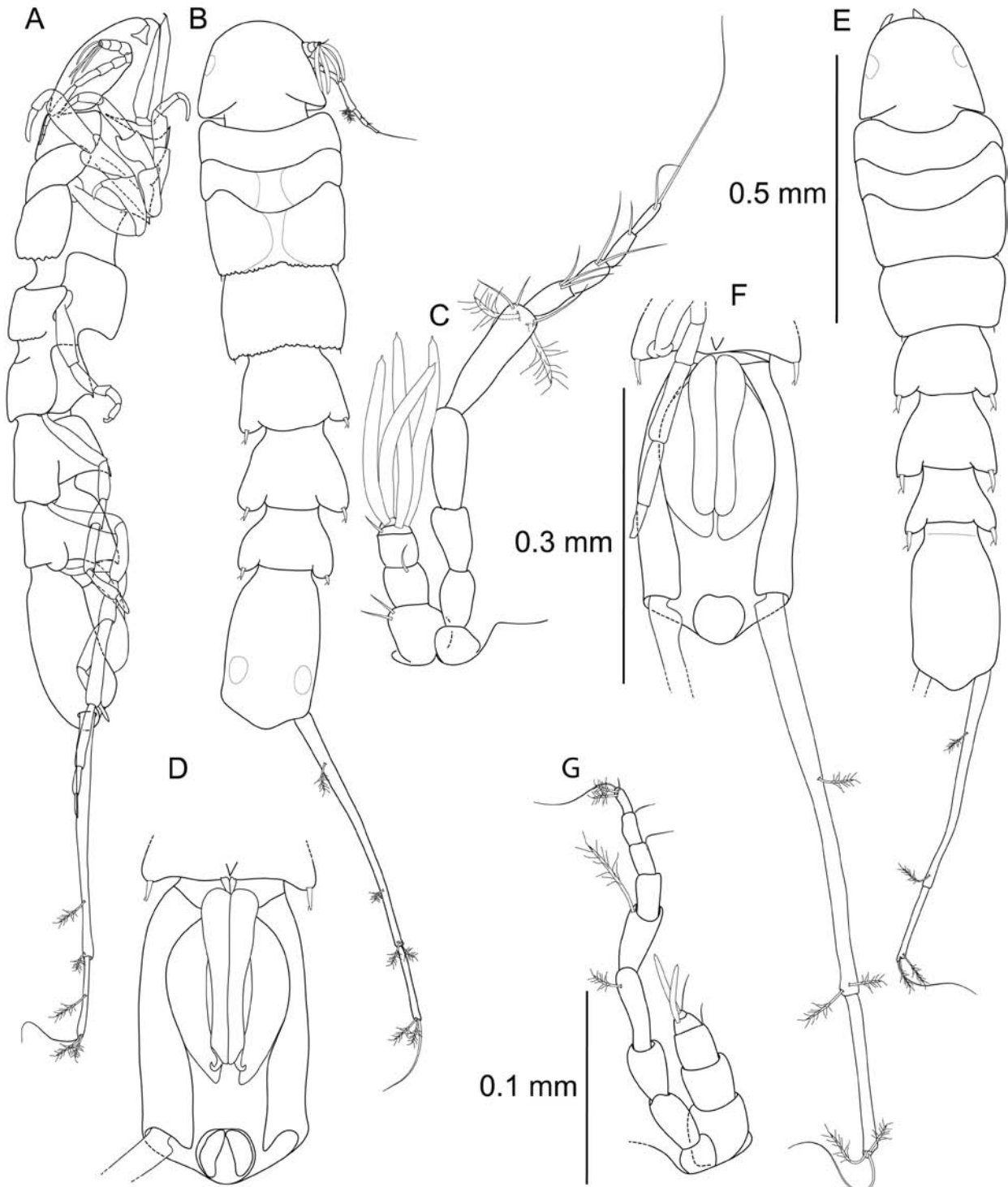


Figure 12. *Macrostylyis papillata* n. sp. **A–D**, paratype terminal male (AM P860011). **E–G**, paratype subadult male (AM P860015). **A–B, E**, dorsal and lateral habitus, cuticle ornamentation and appendages mostly omitted, uropods missing where not illustrated. **C, G**, antennula and antenna, *in situ*, lateral. **D, F**, pleotelson, ventral. Scales: **A–B, E** = 0.5 mm, **C, G** = 0.1 mm, **D, F** = 0.3 mm.

setulate, distoventrally with 2 setae, 1 short, bisetulate, 1 long, bisetulate. **Pereopod VII (Fig. 10D)**. Length less than pereopod VI length, 0.33 body length. Basis length 4.3 width; with no elongate setae. Ischium length 3.5 width, distoventrally with 1 seta, bisetulate. Merus length 3.0 width, disto-

dorsally with 1 seta, bisetulate, distoventrally with 1 seta, short, bisetulate. Carpus length 6.0 width, distodorsally with 2 setae, 1 broom, 1 split, bisetulate, distoventrally with 2 setae, 1 short, bisetulate, 1 long bisetulate. Propodus length 4.0 width. Dactylus length 4.0 width.

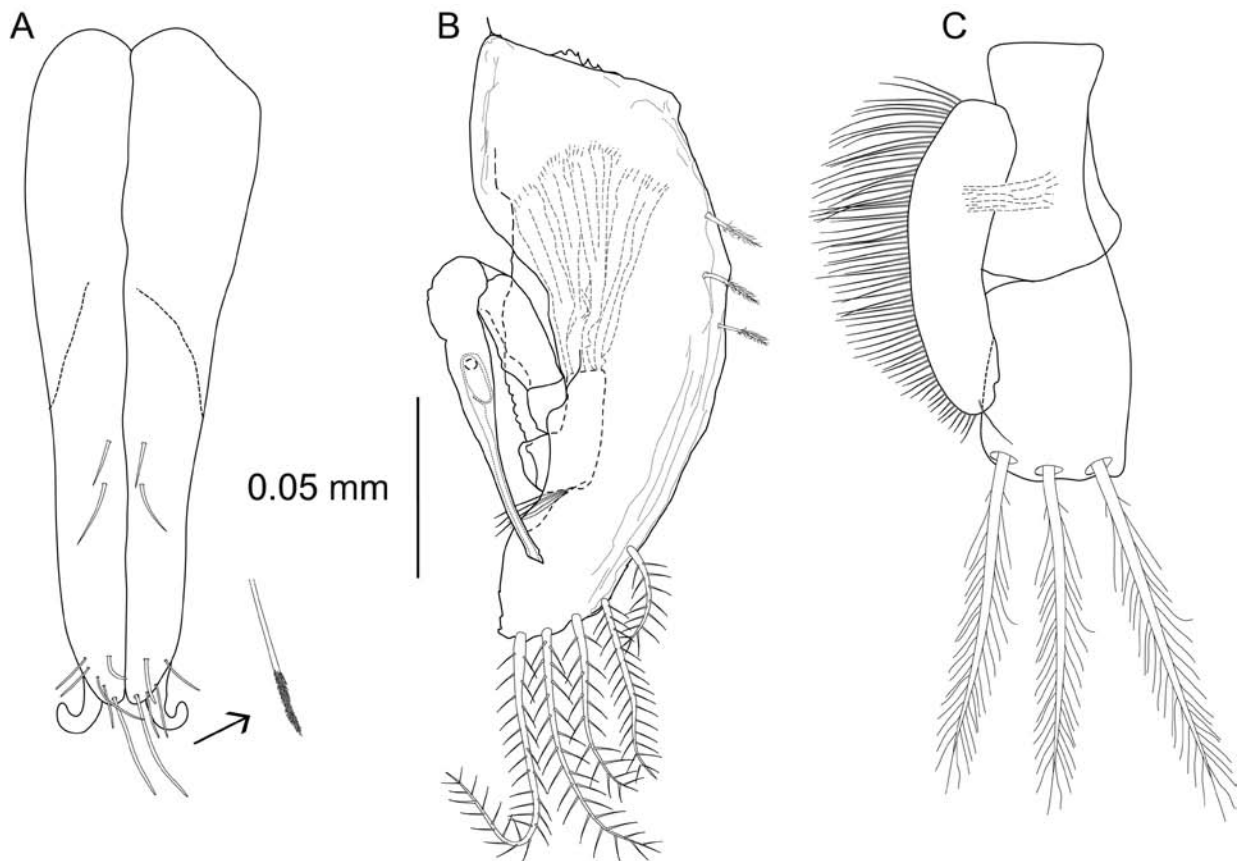


Figure 13. *Macrostylys papillata* n. sp. A–C, paratype terminal male (AM P860011). A, pleopods I, ventral. B, right pleopod II, dorsal, with indicated endopod musculature and sperm duct. C, left pleopod III, dorsal. Scale = 0.05 mm.

Operculum (Figs 8G, 11J). Stout, length 1.5 width, 0.48 pleotelson length, ovoid, without keel, with 10 pappose setae on apex, extending to anal opening. **Pleopod III (Fig. 11I).** Length 2.2 width, protopod length 2.0 width, 0.55 pleopod III length; exopod with fringe of fine setae, about as long as pleopod III exopod width, with simple seta subterminally, exopod length 0.73 pleopod III length. **Uropod (Fig. 8D, H).** Protopod length 1.3 pleotelson length; inserting on pleotelson on posterior margin. Protopod distal margin blunt, endopod insertion terminal, length 24.0 width.

Description, terminal male

Body (Figs 12A–B, E, 14A–B, D). Length 1.3 mm, 5.0 width. **Ventral spines.** Pereonite 3 spine acute, prominent, located closer to anterior segment border. Pereonite 4 spine directed ventrally and posteriorly, blunt, prominent, located closer to

posterior segment border. **Cephalothorax.** Frons with wrinkles, frontal ridge present, as cluster of slight transversal scratches between antennulae articulations; length/width ratio subequal to female, 0.16 body length; with conspicuous array of setae, posterolateral corners acute, posterolateral setae absent, posterior margins papillose.

Fossosome. Length/width ratio greater than in female, length 0.94 width, length/body-length ratio subequal to female; keeled. **Pereonite 4.** Narrower than pereonite 5, length/width ratio subequal to female; pereonal collum present. Lateral margins in dorsal view medially convex. Posterolateral margin not produced posteriorly.

Pleonite 1 (Fig. 14B). Tergal and sternal articulations with pleotelson present. **Pleotelson (Figs 12B, D–F, 14A–B).** In dorsal view, approximately rectangular, length/width ratio in male subequal to female, 0.23 body length, width subequal

pereonite 7 width. Posterior apex convex, more obtusely-angled compared to female, without setae on margin, pleopodal cavity width 0.75 pleotelson width, preanal ridge width 0.43 pleotelson width.

Antennula (Figs 12C, G, 14C). Length 0.35 head width, 0.27 antenna length, width 1.2 antenna width; terminal article with 2 aesthetascs, penultimate article with 2 aesthetascs, aesthetascs with intermediate belt of constrictions; article 1 squat, globular, longest and widest, 1 broom seta, article 2 squat, globular, shorter than article 1, 2 broom setae, article 3 squat, globular, shorter than article 1, 1 broom seta, article 4 squat, globular, minute, article 5 squat, globular, minute, with 1 simple seta. **Antenna (Figs 12C, G, 14C).** Length 0.22 body length, flagellum of 4 articles, article 1 elongate, article 2 elongate, longer than article 1, article 3 elongate, longer than article 1, article 4 shorter than articles 1–3 together, 1 broom seta, article 5 longer than article 4, distally with 1 simple seta, 4 broom setae.

Pereopod I. Length 0.37 body length. Merus setation as in female. Carpus dorsally with 2 setae, 1 broom, 1 bisetulate, carpus ventrally with 3 setae, 1 simple, 2 split. **Pereopod II.** Ischium setation as in female. Merus dorsally with 4 setae, dorso-distally, bisetulate, ventrally with 2 setae, along margin, distally, bisetulate. Carpus dorsally with 4 setae, 2 bisetulate along margin, 2 split distally, bisetulate, ventrally with 3 setae, 1 bisetulate, 1 broom, 1 split, bisetulate. **Pereopod III.** Length 0.44 body length. Pereopod V. Length 0.35 body length. Merus distodorsally with 2 setae; 1 short, bisetulate, 1 long, bisetulate; midventrally with 1 seta; bisetulate; distoventrally with 2 setae; 1 short, bisetulate, 1 long, bisetulate. Carpus distoventrally with 2 setae, 1 short, bisetulate, 1 long, bisetulate.

Pereopod VI. Length 0.51 body length; ischium, merus and carpus setation as in female.

Pereopod VII. Length 0.35 body length, less than

pereopod VI length, segment L/W ratios sexually dimorphic; basis length 4.3 width; ischium length 2.8 width, setation as in female; merus length 1.7 width, distodorsally with 1 seta, bisetulate, distoventrally with 2 setae, 1 short, bisetulate, 1 long, bisetulate; carpus length 5 width, carpus setation as in female; propodus length 4.0 width; dactylus length 3.0 width.

Pleopod I (Fig. 13A). Length 0.58 pleotelson length, distally with fringe-like sensillae. **Pleopod II (Fig. 13B).** Protopod apex tapering, with setae on proximal lateral margin, 3 pappose setae altogether, with 5 pappose setae distally. Endopod distance of insertion from protopod distal margin 0.38 protopod length. Stylet weakly curved, not extending to distal margin of protopod, length 0.52 protopod length. **Uropod (Fig. 12F).** Length 2.0 pleotelson length; protopod length/width ratio greater than in female, length 1.5 width, with endopod inserting terminally; endopod length 0.31 protopod length, 11.5 width, width less than protopod.

Remarks

M. papillata differs from any previously described macrostyloid owing to the presence of a tergal pleonite 1 articulation with the pleotelson. Furthermore, the ridges that create the imbricate ornamentation in this species overlap posteriorly with the margin of the pereonites 1–4 and head. As a result, the margins of these somites have a warty appearance that is most evident in the SEM images (Figs 14–15), but can be seen in the light microscope (Fig. 12B). Although this subtlety of the imbricate ornamentation may not have been fully noted by other authors, *M. reticulata* Birstein, 1963 has strongly developed imbricate ornamentation and could thus potentially show marginal wartyness as well. This latter species is substantially different from *M. papillata* n. sp. because it has the ornamentation on all somites. Both species differ in

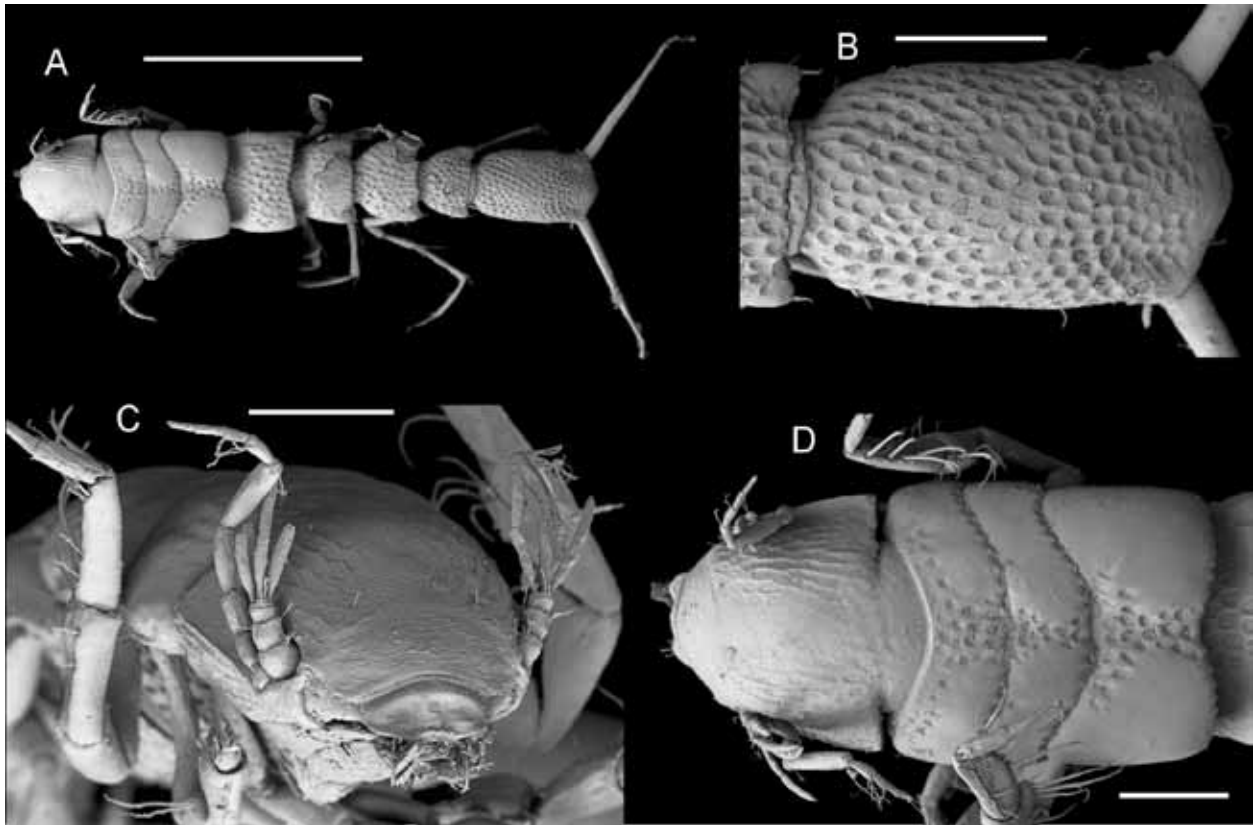


Figure 14. *Macrostylys papillata* n. sp. A–D, paratype terminal male (AM P860012, MI630). A, habitus dorsal. B, pleotelson, dorsal. C, cephalothorax, antero-lateral view. D, anterior habitus. Scales: A = 0.5 mm, B–D = 0.1 mm.

the shape of their pereopod III ischium, in that *M. papillata* has a narrow dorsal projection bearing a robust proximally curved seta with two flanking bisetulate setae, whereas *M. reticulata* has a more rounded projection with only 3 straight non-robust setae.

Discussion

Sexual dimorphism and terminal male stages

Sexual dimorphism has led (and still leads) to significant taxonomic problems across a wide range of taxa (Sibley 1957; Kelley 1993; Brökeland 2010). Morphological differences between

conspecific males and females vary between and within species during ontogeny. In macrostyloid isopods, juvenile stages typically show high similarity to adult females except from developing first pleopods and enlarged antennulae in males.

Although so far discussed only for the Macrostyliidae (discussion below) and the Paramunniidae (Just and Wilson 2004), a male that transforms substantially to the last instar occurs frequently among the Asellota. In the Ischnomesidae, the males can have substantially more elongate pereonites 4 and 5 (e.g., *Heteromesus calcar* Cunha and Wilson, 2006) and often have distinctly different spination patterns from the females (e.g., *Cornuamesus longiramus* (Kavanagh and Sorbe 2006)). Some Desmosomatidae and Nannoniscidae show important transformations of the head (e.g., *Pseudomesus pitombo* Kaiser and Brix, 2007; *Nannoniscoides latediffusus* Siebenaller and Hessler,

1977. Among common shallow water taxa such as Janiridae (species of *Ianiropsis*, see Doti and Wilson (2010)) and Munnidae (e.g., *Munna spicata* Teodorczyk and Wägele, 1994) a transformation in the last instar of the male is characterized by the male pereopod I changing substantially, being typically longer and more robust, with corresponding changes in pereonite 1.

Such transformations of the male can result in wrong identification; i.e., females and males are classified as different species, or at least not associated in ecological studies. This transformation in *Macrostylis* is parallel to the “terminal-male” stage (T male) in *Paramunna* Sars (compare Just and Wilson 2004) and hence this term will be applied to the Macrostylidae, too. As we show below, one is still able to place males with females of the same species by using other characters that may not be related to the male transformation. In adults of *Macrostylis*, the antennulae bear more aesthetascs in males (three in *Macrostylis dorsaetosa* n. sp., two in *M. papillata* n. sp.). The available dataset was not sufficient to reconstruct the whole development trajectory for these species. The largest size class of males in the samples, however, shares important characters with females, providing good support for the males and females to be conspecific.

Nevertheless, a transformation affecting large parts of the male anatomy can be observed. The collections at hand (Riehl, unpublished data) suggest that those changes appear during the final moult, as intermediate stages are generally missing. In detail, T male appear to be more slender (larger length-width ratio). In *M. dorsaetosa* and *M. papillata*, the pleotelson shows differences in shape: while the pleotelson in the female and juvenile male is widest in the anterior half and rather rounded, the pleotelson in T male appears almost parallel or trapezoidal with the greatest width just anterior to the uropod articulations (Fig. 14). In the

antennulae of the males, the transformation can be dramatic. Length-width ratios and length ratios of subsequent articles in T male of *M. dorsaetosa* are much unlike those found in juvenile males and all female instars. Antennular articles 3 and 4 are short and article 5 elongated and narrow. This is not a general pattern for Macrostylidae, as in (e.g.) *M. papillata* only the number of aesthetascs is increased, while the relative article sizes show no change. Thus, the high number of aesthetascs relative to the female condition is probably the most reliable indication for the T male stage. Uropods in T males in relation to the pleotelson are longer than in the female. A similar pattern has been described for *M. spinifera* Sars, 1864.

Because the uropods in macrostylids are often broken and missing, generality of this pattern cannot be tested at the moment. In the species described here, characters that are not affected by the sexual dimorphism and useful for allocation of conspecifics (without dissection of appendages) include: ventral spination; shape of pleotelson posterior apex; setation on posterolateral angles of pereonites; setation of the anterior pereopods; especially the ischium of pereopod III (not only number but especially arrangement and type of setae). Studies on intraspecific variability and allometry of these characters would further support these results.

Ecological and evolutionary implications

Sexually dimorphic sensory systems can be found across various Arthropoda (Schafer and Sanchez 1976; Martens 1987; Koh *et al.* 1995; Jourdan *et al.* 1995; Fernandes *et al.* 2004). In most of these cases, males show an increased size of sensory organs (e.g., antennae) and number of olfactory sensillae (i.e. chemoreceptors), which has been at-

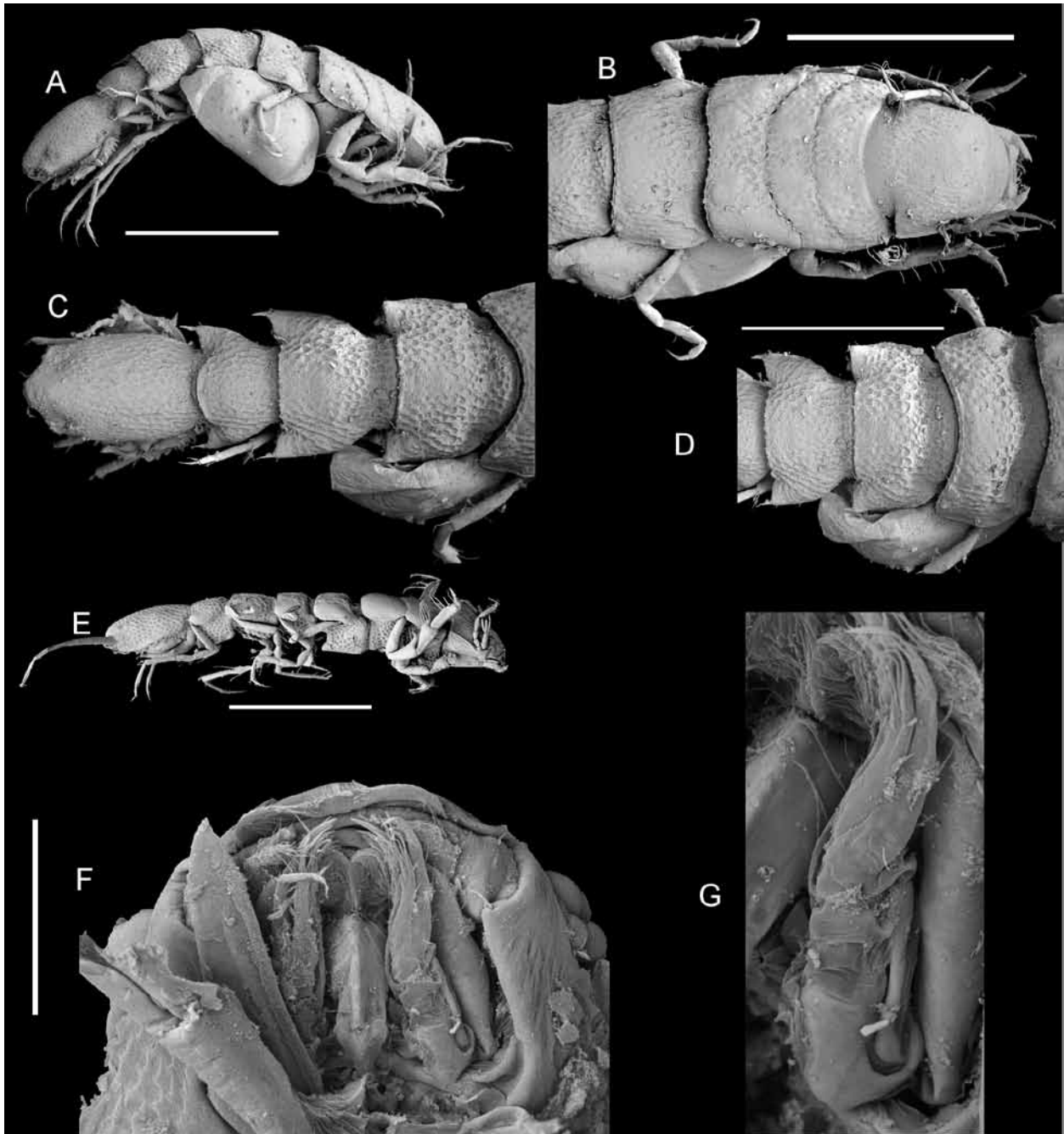


Figure 15. *Macrostyliis papillata* n. sp. A–D, paratype ovigerous female (AM P860013, MI638). E, paratype terminal male (AM P860012, MI630). F–G, paratype subadult male (AM P860014, MI635). A, habitus, lateral. B–D, habitus, dorsal. E, habitus, lateral. F, mouthparts, ventral. G, maxilla, ventral, close up. Scales: A–E = 0.5 mm, F–G = 0.1 mm.

tributed to the search for and location of (receptive) females. As an example, for several species of oniscid isopods, Lefebvre *et al.* (2000) found evidence for scramble-competition polygyny (Alcock 1980) as the prevalent mating system. Males compete indirectly by fertilizing as many mates as they can find in their fertile period. They bear longer antennae compared to the females that they

apply to compete intensively in searching and locating receptive females (Lefebvre *et al.* 2000).

Mating strategies for Macrostyliidae cannot be inferred from morphological data only. Because of the unavailability of genetic data (as discussed below) and the difficulties associated with keeping live specimens, morphology and collection data make our primary sources for ecological and evo-

lutionary implications. However, given low densities in the deep-sea benthic environment (Sanders and Hessler 1969), the search for a mating partner itself is likely to be among the dominating forces for the evolution of sexually dimorphic traits in olfactory organs. The evolution of the dimorphism found in the males' enlarged antennulae and increased number of aesthetascs implies importance of this chemosensory organ for mating in general and would hence be driven by sexually selective pressure (Lande 1980). Other than that, dimorphic body measures can be interpreted as consequence of the different reproductive roles: i.e., ovigerous females with relatively wider bodies due to resource storage and breeding. Experimental tests would be required to verify these hypotheses. However, due to their remote habitats and infaunal lifestyle (Hessler and Strömberg 1989), detailed observations on living macrostylids remain difficult.

Implications for future systematic work

Some evidence (Riehl, unpublished data) suggests that in other species the sexual dimorphism is even more developed than in *Macrostylis dorsetosa* n. sp. and *M. papillata* n. sp. Furthermore, in those species characters other than those mentioned above are affected. Herein, the reason might be found that some species, such as *M. longipes* Hansen, 1916 or *M. longipedis* Brandt, 2004, have been described without recognition of females. Genetic data would be helpful in such cases, as demonstrated by Brix *et al.* (2011), and allow reciprocal illumination *sensu* Hennig (1965). DNA studies on decades old, formaldehyde-fixed deep-sea samples, though, can be accomplished only with difficulty (France and Kocher 1996; Boyle *et al.* 2004; Skage and Schander 2007). Consequently, careful examination of the morphology remains to

date the best way to deal with sexual dimorphism. On the other hand, Brökeland (2010) and Riehl and Brandt (2010) pointed out that, while females of haploniscid and macrostyloid isopods are difficult to distinguish in some cases using morphology, the adult males usually are distinguishable. Consequently, the various characters affected by the expression of dimorphisms may hold valuable information for systematic research. We recommend the use of integrative approaches to the taxonomy including morphology as well as DNA data where possible for multiple-evidence based allocation of sexually dimorphic conspecifics (Pilgrim and Pitts 2006; Brix *et al.* 2011). Once the expression of dimorphism has been described, the characters involved will hold valuable information for inferring the lifestyle and evolution of those taxa. The above mentioned characters also should be evaluated for species that show stronger dimorphism. We argue that the inclusion of sexually dimorphic characters will most likely result in improved phylogenetic and taxonomic resolution.

Acknowledgements

We thank the Isopod Group 2011 at the Australian Museum (Luana Lins, Tae-Yoon Park and Tim Lee) for helpful discussions and Sue Lindsey for her assistance in the SEM lab. We also thank the crews involved in taking samples on research vessels of Woods Hole Oceanographic Institution. Open-access fees were covered by the Australian Museum.

TR thanks all colleagues at the ZMH NTII and the DZMB, especially Angelika Brandt, Pedro Martínez Arbizu and Stefanie Kaiser, for their support and help with travel-fund applications. S. Kaiser, Jörundur Svavarsson and Sigurður Þórðarson gave valuable comments for the improvement of the manuscript. A special word of thanks is owed

to Jasmin Ruch, who gave invaluable moral support and provided valuable suggestions to improve the manuscript.

Comments and suggestions of two anonymous reviewers led to an improved manuscript and are thankfully appreciated. The German National Academic Foundation (Studienstiftung des deutschen Volkes), Stiftung Universität Hamburg and Census of the Diversity of Abyssal Marine Life (CeDAMar) have partly funded this project. The collection of the Gay–Head Bermuda deep sea samples were funded by USA National Science Foundation grants to RRH and colleagues.

References

- Alcock, J. (1980) Natural selection and the mating systems of solitary bees. *American Scientist*, 68(2), 146–153.
- Birstein, Y.A. (1963) Deep Sea Isopod Crustaceans of the Northwestern Part of the Pacific Ocean. Institute of Oceanology, Academy of Sciences, USSR: Moscow. (In Russian with English summary).
- Birstein, Y.A. (1970) New Crustacea Isopoda from the Kurile-Kamchatka Trench area. In: V. G. Bogorov (Ed), Fauna of the Kurile-Kamchatka Trench and its environment. Proceedings of the Shirshov Institute of Oceanology. Academy of Sciences of the USSR, Moscow, pp. 308–356. (In Russian)
- Birstein, Y.A. (1973) Deep water isopods (Crustacea. Isopoda) of the north-western part of the Pacific Ocean. *Akademiya Nauk, SSSR: Moscow*, 1–213. (In Russian).
- Boyle, E.E., Zardus, J.D., Chase, M.R., Etter, R.J. and Rex, M.A. (2004) Strategies for molecular genetic studies of preserved deep-sea macrofauna. *Deep-Sea Research I*, 51(10), 1319–1336.
- Brandt, A. (1992) New Asellota from the Antarctic deep sea (Crustacea, Isopoda, Asellota), with descriptions of two new genera. *Zoologica Scripta*, 21(1), 57–78.
- Brandt, A. (2002) *Desmostylis gerdesi*, a new species (Isopoda: Malacostraca) from Kapp Norvegia, Weddell Sea, Antarctica. *Proceedings of the Biological Society of Washington*, 115(3), 616–627.
- Brandt, A. (2004) New deep-sea species of Macrostylidae (Asellota: Isopoda: Malacostraca) from the Angola Basin off Namibia, South West Africa. *Zootaxa*, 448, 1–35.
- Brix, S., Riehl, T. and Leese, F. (2011) First genetic data for *Haploniscus rostratus* and *Haploniscus unicornis* from neighbouring deep-sea basins in the South Atlantic. *Zootaxa*, 2838, 79–84.
- Brökeland, W. (2010) Description of four new species from the *Haploniscus unicornis* Menzies, 1956 complex (Isopoda: Asellota: Haploniscidae). *Zootaxa*, 2536, 1–35.
- Coleman, C.O. (2003) "Digital inking": how to make perfect line drawings on computers. *Organisms Diversity & Evolution*, 3(4), 303–304.
- Coleman, C.O. (2009) Drawing setae the digital way. *Zoosystematics and Evolution*, 85(2), 305–310.
- Cunha, M.R. and Wilson, G.D.F. (2006) The North Atlantic genus *Heteromesus* (Crustacea: Isopoda: Asellota: Ischnomesidae). *Zootaxa*, 1192, 1–76.
- Dallwitz, M.J. (1980) A general system for coding taxonomic descriptions. *Taxon*, 29(1), 41–46.
- Darwin, C. (1874) *The descent of man, and selection in relation to sex*. Second Edition. John Murray, London, 797 pp.
- Doti, B.L. and Wilson, G.D.F. (2010) The genera *Carpis* Richardson, *Ianiropsis* Sars and *Janaira* Moreira and Pires (Isopoda: Asellota: Janiridae) from Australia, with description of three new species. *Zootaxa*, 2625, 1–39.
- Fernandes, F. de F., Pimenta, P.F.P. and Linardi, P.M. (2004) Antennal sensilla of the New World screwworm fly, *Cochliomyia hominivorax* (Diptera: Calliphoridae). *Journal of Medical Entomology*, 41(4), 545–551.
- France, S.C. and Kocher, T.D. (1996) DNA sequencing of formalin-fixed crustaceans from archival research collections. *Molecular Marine Biology and Biotechnology*, 5(4), 304–313.
- Gandon, S. (1999) Kin competition, the cost of inbreeding and the evolution of dispersal. *Journal of Theoretical Biology*, 200(4), 345–364.
- Gurjanova, E. (1933) Die marinen Isopoden der Arktis. *Fauna Arctica*, 6(5), 391–470.
- Hansen, H.J. (1916) Crustacea Malacostraca: The order Isopoda. *Danish Ingolf Expedition*, 3(5), 1–262.
- Hennig, W. (1965) Phylogenetic systematics. *Annual Review of Entomology*, 10(1), 97–116.
- Hessler, R.R. (1970) The Desmosomatidae (Isopoda, Asellota) of the Gay Head–Bermuda Transect. *Bulletin of the Scripps Institution of Oceanography*, 15, 1–185.
- Hessler, R.R. and Sanders, H.L. (1967) Faunal diversity in the deep sea. *Deep-Sea Research*, 14, 65–78.

- Hessler, R.R. and Strömberg, J.O. (1989) Behavior of janiroidean isopods (Asellota), with special reference to deep sea genera. *Sarsia*, 74(3), 145–159.
- Jormalainen, V. (1998) Precopulatory mate guarding in crustaceans: male competitive strategy and intersexual conflict. *The Quarterly Review of Biology*, 73(3), 275–304.
- Jormalainen, V. and Merilaita, S. (1995) Female resistance and duration of mate-guarding in three aquatic peracarids (Crustacea). *Behavioral Ecology and Sociobiology*, 36(1), 43–48.
- Jourdan, H., Barbier, R., Bernard, J. and Ferran, A. (1995) Antennal sensilla and sexual dimorphism of the adult ladybird beetle *Semiadalia undecimnotata* Schn. (Coleoptera: Coccinellidae). *International Journal of Insect Morphology and Embryology*, 24(3), 307–322.
- Just, J. and Wilson, G.D.F. (2004) Revision of the *Paramunna* complex (Isopoda: Asellota: Paramunnidae). *Invertebrate Systematics*, 18(4), 377–466.
- Kaiser, S. and Brix, S. (2007) Two new species of the genus *Pseudomesus* Hansen, 1916 (Isopoda, Asellota) from the southern hemisphere: *Pseudomesus pitombo* sp. nov. and *Pseudomesus satanus* sp. nov. *Zootaxa*, 1658, 21–38.
- Kaiser, S., Barnes, D.K.A. and Brandt, A. (2007) Slope and deep-sea abundance across scales: Southern Ocean isopods show how complex the deep sea can be. *Deep-Sea Research Part II*, 54(16–17), 1776–1789.
- Kavanagh, F.A. and Sorbe, J.-C. (2006) *Haplomesus longiramus* sp. nov. (Crustacea: Isopoda: Asellota), a new ischnomesid species from the Bay of Biscay, North East Atlantic Ocean. *Zootaxa*, 1300, 51–68.
- Kavanagh, F.A. and Wilson, G.D.F. (2007) Revision of the genus *Haplomesus* (Isopoda: Asellota: Ischnomesidae) with erection of four new genera. *Invertebrate Systematics*, 21(5), 487–535.
- Kelley, J. (1993) Taxonomic implications of sexual dimorphism in *Lufengpithecus*. In: Kimbel, W. H. and Martin, L. B. (Eds), *Species, Species Concepts, and Primate Evolution*, Plenum Press, New York, pp. 429–458.
- Koh, Y.H., Park, K.C. and Boo, K.S. (1995) Antennal sensilla in adult *Helicoverpa assulta* (Lepidoptera: Noctuidae): morphology, distribution, and ultrastructure. *Annals of the Entomological Society of America*, 88(4), 519–530.
- Kussakin, O.G. (1999) Morskiye I solonovatovodnye ravnogie rakoobrasnye (Isopoda) chlodnix I umerennix vod severnogo polushariya [Marine and brackishwater likefooted Crustacea (Isopoda) from the cold and temperate waters of the Northern Hemisphere] Suborder Asellota. Part 2. Families Joeropsidae, Nannoniscidae, Desmosomatidae, Macrostylidae. (Alimov, A. F., Ed.), *Izdavaemye Zoologicheskimi Institutom Rossiiskiyi Akademiya Nauk, St. Petersburg*, 383 pp.
- Lande, R. (1980) Sexual dimorphism, sexual selection, and adaptation in polygenic characters. *Evolution*, 34(2), 292–305.
- Latreille, P.A. (1802) Histoire naturelle générale et particulière des Crustacés et des Insectes. In: de Buffon, G. L. L. (Ed.), *Histoire Naturelle, nouvelle édition, accompagnée des notes*. Paris, 467 pp.
- Lefebvre, F., Limousin, M. and Caubet, Y. (2000) Sexual dimorphism in the antennae of terrestrial isopods: a result of male contests or scramble competition? *Canadian Journal of Zoology*, 78(11), 1987–1993.
- Martens, K. (1987) Homology and functional morphology of the sexual dimorphism in the antenna of *Sclerocypris* Sars, 1924 (Crustacea, Ostracoda, Megalocypridinae). *Bijdragen tot de Dierkunde*, 57(2), 183–190.
- Meinert, F.V.A. (1890) Crustacea malacostraca. Videnskabelige udbytte af kanonbaden “Hauchs Dogter” pp. 147–230.
- Menzies, R.J. (1962) The isopods of abyssal depths in the Atlantic Ocean. In: Barnard, J. L., Menzies, R. J., and Bacescu, M. C. (Eds), *Abyssal Crustacea*. pp 79–206. Columbia University Press, New York.
- Menzies, R.J. and George, R. Y. (1972) Isopod Crustacea of the Peru–Chile Trench. *Anton Bruun Report*, 9, 1–124.
- Mezhov, B.V. (1988) The first findings of Macrostylidae (Isopoda, Asellota) in the Indian Ocean. *Zoologicheskii Zhurnal*, 67(7), 983–994. (In Russian).
- Mezhov, B.V. (1992) Two new species of the genus *Macrostylis* G.O.Sars, 1864 (Crustacea Isopoda Asellota Macrostylidae) from the Antarctic. *Arthropoda Selecta*, 1(2), 83–87. (In Russian with English summary).
- Mezhov, B.V. (1999) Four new species of the genus *Macrostylis* (Crustacea, Isopoda, Macrostylidae) from the Atlantic Ocean abyssal zone. *Zoologicheskii Zhurnal*, 78(12), 1417–1423. (In Russian with English summary).
- Pilgrim, E.M. and Pitts, J.P. (2006) A molecular method for associating the dimorphic sexes of velvet ants (Hymenoptera: Mutillidae). *Journal of the Kansas Entomological Society*, 79, 222–230.
- Riehl, T. and Brandt, A. (2010) Descriptions of two new species in the genus *Macrostylis* Sars, 1864 (Isopoda, Asellota, Macrostylidae) from the Weddell Sea (Southern Ocean), with a synonymisation of the genus *Desmostylis* Brandt, 1992 with *Macrostylis*. *ZooKeys*, 57, 9–49.
- Sanders, H.L. and Hessler, R.R. (1969) Ecology of the deep-sea benthos. *Science*, 163(874), 1419.
- Sanders, H.L., Hessler, R.R. and Hampson, G. R. (1965) An introduction to the study of deep-sea benthic faunal

- assemblages along the Gay Head–Bermuda transect. *Deep Sea Research and Oceanographic Abstracts*, 12(6), 845–867.
- Sars, G.O. (1864) Om en anomal Gruppe af Isopoder. In: *Forhandlinger Videnskapselskapet I Kristiania, Anar 1863*, pp. 205–221.
- Sars, G.O. (1899) An account of the Crustacea of Norway: with short descriptions and figures of all the species: Vol. 2, Isopoda. Bergen Museum, Bergen, Norway, 270 pp.
- Schafer, R. and Sanchez, T.V. (1976) The nature and development of sex attractant specificity in cockroaches of the genus *Periplaneta*. I. Sexual dimorphism in the distribution of antennal sense organs in five species. *Journal of Morphology*, 149(2), 139–157.
- Shuster, S.M. (2008) The expression of crustacean mating strategies. In: Brockmann, H. J. and Oliveira, R. F. (Eds), *Alternative reproductive tactics: an integrative approach*, Cambridge University Press, Cambridge, pp. 224–250.
- Sibley, C.G. (1957) The evolutionary and taxonomic significance of sexual dimorphism and hybridization in birds. *The Condor*, 59(3), 166–191.
- Siebenaller, J. and Hessler, R.R. (1977) The Nannoniscidae (Isopoda, Asellota): *Hebefustis* n. gen. and *Nannoniscoides* Hansen. *Transactions of the San Diego Society of Natural History*, 19(2), 17–43.
- Skage, M. and Schander, C. (2007) DNA from formalin-fixed tissue: extraction or repair? That is the question. *Marine Biology Research*, 3(5), 289–295.
- Svavarsson, J. (1984) Ischnomesidae (Isopoda: Asellota) from bathyal and abyssal depths in the Norwegian and North Polar Seas. *Sarsia*, 69(1), 25–36.
- Teodorczyk, W. and Wägele, J. (1994) On Antarctic species of the genus *Munna* Kroeyer, 1839 (Crustacea, Isopoda, Asellota, Munnidae). *Bulletin of the National Museum of Natural History, Paris*, 16, 111–201.
- Thistle, D. and Wilson, G.D.F. (1987) A hydrodynamically modified, abyssal isopod fauna. *Deep-Sea Research. Part A. Oceanographic Research Papers*, 34(1), 73–87.
- Veuille, M. (1980) Sexual behaviour and evolution of sexual dimorphism in body size in *Jaera* (Isopoda Asellota). *Biological Journal of the Linnean Society*, 13(1), 89–100.
- Wilson, G.D.F. (1989) A systematic revision of the deep-sea subfamily Lipomerinae of the isopod crustacean family Munnopsidae. *Bulletin of the Scripps Institution of Oceanography*, 27, 1–138.
- Wilson, G.D.F. (1991) Functional morphology and evolution of isopod genitalia. *Crustacean Sexual Biology*. Columbia University Press, New York, 228–245.
- Wilson, G.D.F. (2008a) A review of taxonomic concepts in the Nannoniscidae (Isopoda, Asellota), with a key to the genera and a description of *Nannoniscus oblongus* Sars. *Zootaxa*, 1680, 1–24.
- Wilson, G.D.F. (2008b) Local and regional species diversity of benthic Isopoda (Crustacea) in the deep Gulf of Mexico. *Deep-Sea Research Part II*, 55, 2634–2649.
- Wilson, G.D.F. (2009) The phylogenetic position of the Isopoda in the Peracarida (Crustacea: Malacostraca). *Arthropod Systematics & Phylogeny*, 67(2), 159–198.
- Wolff, T. (1956) Isopoda from depths exceeding 6000 meters. *Galathea Report*, 2, 85–157.
- Wolff, T. (1962) The systematics and biology of bathyal and abyssal Isopoda Asellota. *Galathea Report*, 6(3), 1–320.

Author contributions

The study was designed by myself. I created the pencil as well as digital drawings, built the fundamental DELTA database, and wrote the paper with contributions from G.D.F. Wilson. R.R. Hessler conducted the sampling and preliminary species identification as well as some pencil drawings. Sue Lindsay assisted with SEM.

Chapter 3

Conquered from the Deep Sea?

A New Deep-Sea Isopod Species from the Antarctic Shelf Shows Pattern of Recent Colonization

Published as: Riehl T, Kaiser S (2012) Conquered from the deep sea? A new deep-sea isopod species from the Antarctic shelf shows pattern of recent colonization. PLoS ONE 7:e49354. doi: 10.1371/journal.pone.0049354

Abstract

The Amundsen Sea, Antarctica, is amongst the most rapidly changing environments of the world. Its benthic inhabitants are barely known and the BIOPEARL 2 project was one of the first to biologically explore this region. Collected during this expedition, *Macrostyliis roaldi* n. sp. is described as the first isopod discovered on the Amundsen-Sea shelf. Amongst many characteristic features, the most obvious characters unique for *M. roaldi* are the rather short pleotelson and short operculum as well as the trapezoid shape of the pleotelson in adult males. We used DNA barcodes (COI) and additional mitochondrial markers (12S, 16S) to reciprocally illuminate morphological results and nucleotide variability. In contrast to many other deep-sea isopods, this species is common and shows a wide distribution. Its range spreads from Pine Island Bay at inner shelf right to the shelf break and across 1,000 m bathymetrically. Its gene pool is homogenized across space and depth. This is indicative for a genetic bottleneck or a recent colonization history. Our results suggest further that migratory or dispersal capabilities of some species of brooding macrobenthos have been underestimated. This might be relevant for the species' potential to cope with effects of climate change. To determine where this species could have survived the last glacial period, alternative refuge possibilities are discussed.

Key words: Janiroidea, deep sea, benthos, bathyal, abyssal, North Atlantic, DELTA, SEM, new species

Introduction

The Southern-Ocean benthos has been shaped by unique historical and environmental settings. The origin of the shelf fauna has been partly attributed to evolutionary polar emergence from the deep (Menzies *et al.* 1973; Brandt 1992b) and to shelf connections with other continents that existed in times before the opening of the Drake Passage for deep-water currents about 33–34 mya (Lawver *et al.* 2011). Long-term isolation and *in situ* speciation have led to a highly endemic fauna on the shelf and slope surrounding Antarctica (Brey *et al.* 1994). While homogenous abiotic conditions and circumpolar currents are likely explanations for the wide geographic and depth distributions of many taxa (Brey *et al.* 1996; Jarman *et al.* 2002; Clarke & Johnston 2003), there is evidence for geographic or bathymetric differentiation in others. Recently, several closely-related lineages, previously overlooked due to morphological similarity ('cryptic species') have been discovered by means of molecular-genetic methods (Held 2003; Held & Wägele 2005; Raupach & Wägele 2006; Brandão *et al.* 2010; Krabbe *et al.* 2010; Allcock *et al.* 2011; Arango *et al.* 2011; Havermans *et al.* 2011). These suggest largely overestimated species' distribution ranges but also underestimated diversity.

The high diversity of the fauna has been attributed to Antarctica's glaciological history (Clarke *et al.* 2004). A glacial diversity pump (Clarke & Crame 2010; O'Loughlin *et al.* 2011) featuring repetitive expansions and subsequent retreats of glacial shields has possibly wiped out large proportions of the shelf fauna. It would have led to local extinctions, changes in population genetic structure (Clarke & Crame 2010) such as founder effects or bottlenecks and temporal isolation of remaining populations (Thatje *et al.* 2008). In addition, depth-related physiological barriers could play

a role in their evolution as well (France & Kocher 1996; Etter *et al.* 2005; Brandão *et al.* 2010). The steep slopes as found in the bathyal region (i.e. between continental shelf break and continental rise) are characterized by strong abiotic and biotic gradients and habitat heterogeneity, thus facilitating population differentiation and ultimately speciation (i.e. depth-differentiation hypothesis) (Etter *et al.* 2005).

On the contrary, deep-water formation in some regions, upwelling in others and the absence of a thermocline might have facilitated polar emergence and submergence (Brey *et al.* 1996), i.e. the colonization processes from deep to shallow and vice versa (Hessler & Wilson 1983; Brandt 1992b; Raupach *et al.* 2004, 2009). In support of this theory, typical elements of slope and abyssal communities can be encountered on the Antarctic continental shelf (Held 2000; Clarke 2003; Clarke *et al.* 2005; Brandt *et al.* 2007a; Strugnell *et al.* 2008), such as deep-sea isopods. Abyssal and bathyal fauna might thus have emerged (Menzies *et al.* 1973; Brandt 1992b, 1999; Brandt *et al.* 2007b; Strugnell *et al.* 2011) and provided source populations for (re-) colonization of the shelf during interglacial periods (Brey *et al.* 1996; Thatje *et al.* 2005), although Barnes & Kuklinski (2010) argue against this hypothesis, at least for bryozoans. Isopods with a likely deep-sea origin have been frequently encountered around Antarctica (Brandt 1999). One taxon for which the emergence scenario from the deep sea seems highly probable is the family Macrostylidae Hansen, 1916 (Hessler & Thistle 1975; Brandt 1991; Raupach *et al.* 2004). Macrostylids are a taxonomically well-defined and highly derived group. Currently, it is comprised of 82 described species with the majority of species recorded from abyssal depths in all oceans (Riehl & Brandt 2010), many of which remain undescribed (Riehl, unpublished data). They have been de-

scribed as a specialized endobenthic component of deep-sea macrofauna (Thistle & Wilson 1987; Harrison 1989; Hessler & Strömberg 1989). While the depth distribution of the family Macrostylidae has been found (uniquely) wide, between the shallow subtidal of 4 m (*Macrostylis spinifera* Sars, 1864) and hadal depths of almost 11,000 m (*M. mariana* Mezhev, 1993), almost no data are available to date on individual species' spatial or depth distributions.

However, the brooding mode of reproduction (direct development) and an infaunal or tubicolous lifestyle (i.e. digging or tube-dwelling) (Harrison 1989; Hessler & Strömberg 1989; Wägele 1989) are likely to lead to a very limited range of distribution. This is expected to promote genetic differentiation and allopatric fragmentation in populations, and finally speciation due to isolation by distance (Wright 1938, 1946; Teske *et al.* 2007) (but see Wilson *et al.* 2009; Leese *et al.* 2010; Brix *et al.* 2011; Menzel *et al.* 2011). Prior to recent expeditions where macrostylids regularly occurred in samples from the Antarctic continental shelf (Kaiser *et al.* 2009) and a shallow seamount (Brandt *et al.* 2011) they had rarely been reported from shallow depths (Riehl & Brandt 2010). The Amundsen Sea in the Southern Ocean is among the most rapidly changing regions on earth with unparalleled ice-sheet loss (Rignot *et al.* 2008), due to warm-water advection (Thoma *et al.* 2008). Its fauna, though, has so far been barely studied. For the first time the benthic fauna of the Amundsen Sea was explored in detail in 2008 during the BIOPEARL 2 (Biodiversity, Phylogeny, Evolution and Adaptive Radiation of Life in Antarctica) cruise (Kaiser *et al.* 2009).

During this expedition, an isopod species of the family Macrostylidae was collected. It was identified as new to science and is described in this article. We furthermore assessed the genetic diversity in this species across sites differing in depth,

spatial distribution and topography. According to the isolation-by-distance and depth-differentiation hypotheses, our assumption was that molecular data would reveal divergent lineages or potentially cryptic species.

We hypothesized that the distribution of the haplotypes would be in congruence with topographic barriers and bathymetry. Finally, we intended to test our data for any indications for the presence of refuges and potential mechanisms where and how the species might have survived the Last Glacial Maximum (Clark *et al.* 2009). A high level of nucleotide variability in sympatric specimens or across space and depth would indicate diversification, an old age of the population and in-situ survival. On the contrary, little variation would indicate a recent colonization from a refuge. The possible existence of cryptic species within the samples could be ruled out. Instead, we found evidence for the presence of only one population with almost no nucleotide variability. Our data suggest that it is capable to maintain connectivity across space, depth and barriers. The observed pattern requires the assumption of a higher mobility than expected from Macrostylidae. The lack of nucleotide variability indicates further that the whole population is originating from a very small source population (bottle neck) and a recent colonization event can be hypothesized. Whether the species colonized the shelf from the slope, abyss or an ice-free refuge on the shelf could ultimately not be clarified.

Material and Methods

Study Area

The study area (Pine Island Bay, eastern Amundsen Sea, Fig. 1) is approximately 450 km wide, reaching from the tip of the Pine Island Glacier

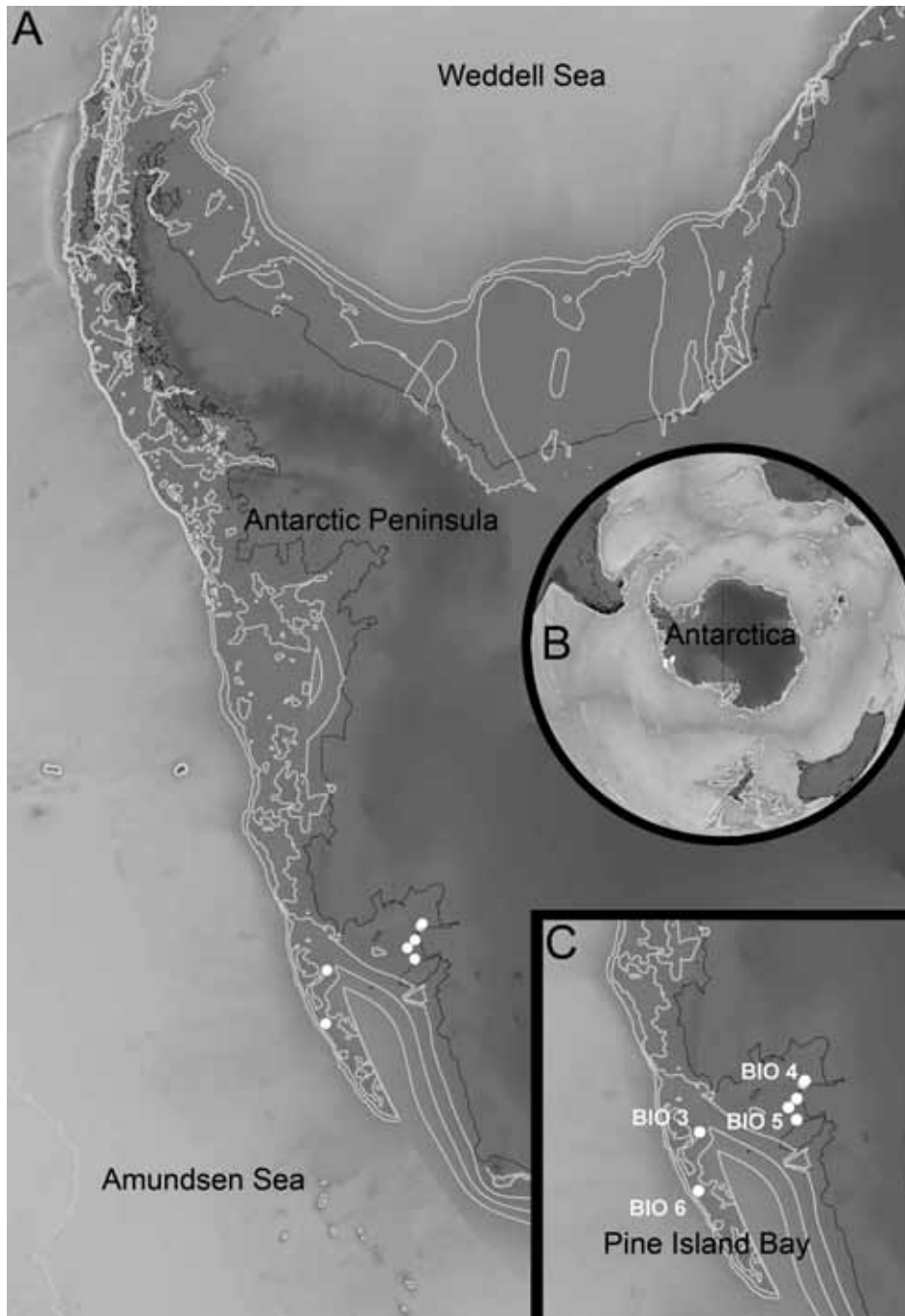


Figure 1. Type locality of *Macrostyliis roaldi* n. sp. **A**, Antarctic Peninsula with Amundsen Sea and Pine Island Bay. **B**, Antarctica, overview. **C**, Pine Island Bay, detail, with stations marked as white dots, grey dotted line marks the Polar Front, black contour lines indicate land mass boundaries, grey lines indicate 500 m depth contours. doi:10.1371/journal.pone.0049354.g001

to the shelf break. The inner shelf at Pine Island Bay is extremely rugged and characterized by deep channels and furrows shaped by previous glaciations and deglaciations; the topography smoothens towards the outer shelf. It is further characterized by an average depth of 500 m, with some deep inner shelf troughs at about 1700 m depth. There is some geophysical evidence that during past glacial maxima ice sheets expanded to the shelf break and grounded there (Kellogg & Kellogg 1987; Lowe & Anderson 2002). The Amundsen shelf is periodi-

cally flooded by relatively warm Circumpolar Deep Water (Thoma *et al.* 2008) that is one main reason for the dramatic ice loss of the Pine Island Glacier (Shepherd *et al.* 2004). The topography, physical conditions and hydrography of this area have been discussed in detail elsewhere (Lowe & Anderson 2002; Nitsche *et al.* 2007; Thoma *et al.* 2008). The continental slope, or bathyal, we define here as the benthic environment between the shelf break and the continental rise. The depths along the continental shelf break of the Amundsen Sea is on average

Table 1. Type material and further material examined for the description of *Macrostylys roadi* sp. nov. with Process IDs of the “Barcode of Live Database” (BoLD) and GenBank accession numbers.

Stage	Sex	Collection no	Station no	Process ID			GenBank accession no	Condition
		[ZMH-K]						
				COI	12S	16S		
Holotype								
Subadult, non-ovigerous	F	42994	BIO4-EBS-1A	TRII015-12	N/A	JX260302	JX260337	Partly dissected for DNA extraction, habitus and few appendages illustrated <i>in situ</i>
Paratypes measured and illustrated in this study								
Adult, non-ovigerous	F	42995	BIO04-EBS-1A	TRII014-12	N/A	JX260303	JX260338	Dissected for DNA extraction and illustration of appendages
Terminal	M	42993	BIO04-EBS-1A	TRII016-12	JX260269	JX260301	JX260336	Dissected for DNA extraction and illustration of appendages
Juvenile	M	42997	BIO04-EBS-3B	TRII034-12	JX260258	JX260284	N/A	Partly dissected for DNA extraction and illustration of appendages
Adult, ovigerous	F	42998	BIO04-EBS-3B	TRII043-12	N/A	JX260275	JX260314	Partly dissected for DNA extraction and illustration of appendages
Terminal	M	42999	BIO04-EBS-1A	TRII029-12	JX260259	N/A	JX260324	Partly dissected for DNA extraction, sputter-coated with carbon for SEM
Juvenile	M	43047	BIO04-EBS-1A	TRII017-12	JX260268	JX260300	JX260335	Partly dissected for DNA extraction
Adult, non-ovigerous	F	42999	BIO04-EBS-1A	TRII030-12	N/A	JX260288	JX260323	Partly dissected for DNA extraction, sputter-coated with carbon for SEM
Type material used only for molecular analyses								
Terminal	M	43048	BIO04-EBS-3A	TRII010-12	JX260270	JX260304	JX260339	Partly dissected for DNA extraction
Terminal	M	43049	BIO04-EBS-1B	TRII011-12	N/A	N/A	N/A	Partly dissected for DNA extraction
Adult, ovigerous and mancae	F	42996	BIO04-EBS-1A	TRII012-12	N/A	N/A	N/A	Partly dissected for DNA extraction
				TRII018-12	N/A	JX260299	JX260334	Partly dissected for DNA extraction; mancae used completely for DNA extraction, no voucher remains
					JX260267	JX260298	JX260333	
					JX260266	JX260297	JX260332	
					N/A	JX260296	JX260331	
					JX260265	JX260295	JX260330	
					JX260264	JX260294	JX260329	
					JX260263	JX260293	JX260328	
					JX260262	JX260292	JX260337	
					JX260261	JX260291	JX260336	
Diverse	F	43050	BIO04-EBS-1A	TRII028-12	JX260260	JX260289	JX260325	Partly dissected for DNA extraction
				TRII032-12	N/A	JX260286	JX260322	
				TRII033-12	N/A	JX260285	JX260321	

Continuation of Table 1. Type material and further material examined for the description of *Macrosyllis roaldi* sp. nov. with Process IDs of the “Barcode of Live Database” (BoLD) and GenBank accession numbers.

Diverse	F+M	43051	BIO04-EBS-3B	TRII035-12	JX260257	JX260283	JX260320	Partly dissected for DNA extraction	
				TRII036-12	JX260256	JX260282	JX260319		
				TRII037-12	N/A	JX260281	N/A		
				TRII038-12	N/A	JX260280	JX260318		
				TRII039-12	JX260255	JX260279	N/A		
				TRII040-12	JX260254	JX260278	JX260317		
				TRII041-12	N/A	JX260277	JX260316		
				TRII042-12	N/A	JX260276	JX260315		
	Further records								
	Non-ovigerous	F	42985	BIO05-EBS-2A	TRII001-12	JX260274	JX260313	JX260348	Partly dissected for DNA extraction
Adult	F+M	42986	BIO05-EBS-1A	TRII002-12	JX260273	JX260312	JX260347	Partly dissected for DNA extraction	
				TRII003-12	N/A	JX260311	JX260346		
				TRII004-12	N/A	JX260310	JX260345		
Terminal + juvenile	M	42987	BIO05-EBS-3B	TRII005-12	JX260272	JX260309	JX260344	Partly dissected for DNA extraction	
Adult + juvenile				TRII006-12	N/A	JX260308	JX260343		
	F	42988	BIO03-EBS-1B	TRII007-12	N/A	JX260307	JX260342	Partly dissected for DNA extraction	
				TRII008-12	N/A	JX260306	JX260341		
Adult, non-ovigerous				TRII009-12	JX260271	JX260305	JX260340		
	F	42989	BIO06-EBS-3A	TRII013-12	N/A	N/A	N/A	Partly dissected for DNA extraction	

doi:10.1371/journal.pone.0049354.t001

Table 2. Coordinates and sampling information for the type locality and further records of *Macrostyliis roaldi* sp. nov. doi:10.1371/journal.pone.0049354.t002

Station name	Start trawl [decimal degrees]		Start trawl depth [m]	End trawl [decimal degrees]		End trawl depth [m]	Sampling date [d/m/y]
	latitude	longitude		latitude	longitude		
Type locality							
BIO03-EBS-1B	-71.79152	-106.21.94	577.67	-71.78885	-106.21531	577.67	3/4/2008
BIO04-EBS-1A	-74.35975	-104.74595	1414.29	-74.36108	-104.73653	1413.5	3/6/2008
BIO04-EBS-1B	-74.35721	-104.752	1415.86	-74.358	-104.74252	1415.58	3/6/2008
BIO04-EBS-3A	-74.39845	-104.63.215	504.29	-74.40009	-104.62462	489.65	3/7/2008
BIO04-EBS-3B	-74.40232	-104.61.505	495.97	-74.40409	-104.6077	508.53	3/7/2008
Further records							
BIO05-EBS-1A	-74.11822	-105.83776	1478.92	-74.11962	-105.82882	1486.13	3/9/2008

500 m, but varies from 400 m to 600 m (Nitsche *et al.* 2007). At the continental rise around 3,000 m depth, the slope levels off down to the abyss.

Sampling and Fixation

This study is based on benthic samples collected during the BIOPEARL 2 (BIOdiversity, Phylogeny, Evolution and Adaptive Radiation of Life in Antarctica) project of the British Antarctic Survey with R/V James Clark Ross (JR 179) to the Amundsen Sea in 2008. In total, 36 samples were taken on the inner and outer shelf of Pine Island Bay, at the continental shelf break, slope and in abyssal depth. An epibenthic sledge *sensu* Brenke (2005) was applied between 480 and 3,500 m depth. From eight of these stations (Fig. 1), *Macrostyliis roaldi* n. sp. could be reported. Samples were fixed in cooled (-20°C) 96% ethanol and preserved in the same medium.

Taxonomy

Specimens were transferred to a glycerine-96% ethanol solution (1:1) and subsequently to pure glycerin in order to prepare habitus illustrations and for dissections. Methylene blue and Chlorazol

black were used for staining: from a highly concentrated solution of the respective stain in 96% ethanol, a small droplet was added to the specimen embedded in glycerin. The viscosity of the glycerin allows control over the staining process to avoid over staining. Once the preferred stain intensity was reached, the specimens were transferred to pure glycerin. Temporary slides after Wilson (Wilson 2008a) were used for habitus illustrations.

Line drawings were made using a Leica DM2500 compound microscope with camera lucida and contrast interference and calibrated using a stage micrometer. To trace line drawings, vector graphics software (Adobe® Illustrator®, ver. CS4–5) was applied following the methods described by Coleman (2003, 2009). All plates were prepared using Adobe® Photoshop® (ver. CS4). Measurements are presented as ratios (to normalize differences in body size) and were prepared from line drawings following Hessler (1970) and Riehl *et al.* (2012) using the distance-measurement tool in Adobe® Acrobat® Professional. Ranges are provided where several specimens were measured. Terminology, measures, description with DELTA [122,123] follow Hessler (1970), Wilson (1989),

Table 3. Material of previously described Antarctic and South Atlantic Macrostylidae studied for comparison with *Macrostylis roaldi* sp. nov. BM(NH) = British Museum of Natural History, London, UK; ZMH = Zoological Museum, University of Hamburg, Germany. doi:10.1371/journal.pone.0049354.t003

Species	Museum accession no	Type status
<i>M. abyssalis</i> Brandt, 2004	ZMH K-40284, ZMH K-40285	Holo- and paratypes
<i>M. angolensis</i> Brandt, 2004	ZMH K-40280, ZMH K-40281	Holo- and paratypes
<i>M. antennamagna</i> Riehl & Brandt 2010	ZMH (K-42168), ZMH (K-42169), ZMH (K-42171), ZMH (K-42172)	Holo- and paratypes
<i>M. cerritus</i> Vey & Brix, 2009	ZMH K-41431, ZMH K-41432, ZMH K-41433, ZMH K-41434	Holo- and paratypes
<i>M. gerdesi</i> (Brandt, 2002)	ZMH 39915, ZMH 39916	Holo- and paratypes
<i>M. longipedis</i> Brandt, 2004	ZMH 40278	Holotype
<i>M. longispinis</i> Brandt, 2004	ZMH K-40286	Holotype
<i>M. meteorae</i> Brandt, 2004	ZMH K-40282, ZMH K-40283, ZMH K-40698	Holo- and paratypes
<i>M. obscurus</i> (Brandt, 1992)	BM(NH) 1990:39:1	Holotype
<i>M. robusta</i> Brandt, 2004	ZMH K-40276, ZMH K-40277, ZMH K-40295, ZMH K-40296, ZMH K-40297	Holo- and paratypes
<i>M. sarsi</i> Brandt, 1992	BM(NH) 1990:40:1	Holotype
<i>M. uniformis</i> Riehl & Brandt 2010	ZMH (K-42172), ZMH (K-42173), ZMH (K-42174)	Holo- and paratypes

Kavanagh and Wilson (2007), Riehl & Brandt (2010) and Riehl *et al.* (2012). Characters were coded in DELTA following Sereno (2007) with some modifications for improved readability.

The list of implicit characters was slightly modified from Riehl *et al.* (2012) and can be obtained from the first author upon request. Appendages embedded in glycerin were not directly transferred to Euparal because these do not mix, but permanent slides were prepared with Euparal using the following method: Dissected parts were first transferred from glycerin to 70% denatured ethanol then to 96% denatured ethanol and then to a mixture of Euparal and 96% denatured ethanol (approximately 1:1). Depending on the size of the fragments, parts were kept in the respective media for up to 30 minutes to ensure sufficient penetration. Finally, parts could be transferred easily to Euparal. A Carl Zeiss Leo 1525 microscope was used for SEM. SEM stubs, whole specimens and slides were de-

posited at the Zoological Museum, University of Hamburg, Germany, accession numbers have a ZMH-K prefix. Type material analyzed for comparison is listed in Table 3.

The distribution map was produced using GIS software ArcView 10.0 (ESRI, USA). All specimens were analyzed for developmental stage, body size, and setal counts on the pereopod III ischium dorsal lobe to test for allometric relationships in these characters. Statistical correlations were tested with JMP 9.0 (SAS Institute Inc., USA). Specimens with damaged left or right pereopod III were excluded from the analyses.

Molecular Methods

Samples were kept in cold conditions whenever possible. For DNA extraction, 2–3 pereopods were removed from one side of the body. The phenol-chloroform extraction method was applied. Three

Table 4. 12S, 16S and COI primers. doi:10.1371/journal.pone.0049354.t004

Primer name	Sequence [5' – 3']	Reference
16S SF	GACCGTGCTAAGGTAGCATAATC	(L. M. Tsang, pers. comm.)
16S SR	CCGGTCTGAACTCAAATCGTG	(Tsang <i>et al.</i> , 2009)
L13337-12S	YCTWTGYTACGACTTATCTC	(Machida <i>et al.</i> , 2002; 2004)
H13842-12S	TGTGCCAGCASCTGCGGTTAKAC	(Machida <i>et al.</i> , 2002; 2004)
dgLCO1490 (COI)	GGTCAACAAATCATAAAGAYATYGG	(Meyer <i>et al.</i> , 2005)
dgHCO2198 (COI)	TAAACTTCAGGGTGACCAAARAAYCA	(Meyer <i>et al.</i> , 2005)

mitochondrial markers, cytochrome-c-oxidase subunit 1 (COI) as well as the ribosomal RNA small and large subunits (12S, 16S) were chosen because 1) they find applicability in the DNA barcode of Life program, 2) they have been widely applied in deep-sea isopod research and hence allow certain comparability and, 3) they have been found to be appropriate markers to infer phylogenetic relationships of isopods from the population to the genus level.

All three markers were amplified in a 10 μ L reaction volume containing 0.25 μ L BSA, 0.5 μ L dNTP [2.5 mM each], 1 μ L Bioline 10xNH₄ reaction buffer, 0.3 μ L of each primer [10 μ M], 0.5 μ L Biolase MgCl₂ [50 mM], 0.1 mL Biolase DNA Pol [5 u/ μ L], 2 μ L of template DNA and nuclease-free H₂O. The same primer pairs (Table 4) were used for PCR and cycle sequencing (CS) respectively in 16S and 12S. For amplification of COI, M13-tailed primers based on dgLCO1490/dgHCO2198 were used. Here, for cycle sequencing M13 primers (Messing 1983) were used. PCR and CS primers are listed in Tab. 4. The PCR temperature profile consisted of an initial denaturation at 95°C (5 min), followed by 34–36 cycles of denaturation at 95°C (30 s), annealing at 48°C (30 s) and extension at 72°C (45 s) followed by a final extension at 72°C (5 min). For CS, 30 cycles of 95°C (30 s), 48°C (30 s) and 60°C (4 min) were applied. 2 μ L of PCR product was analyzed for purity and size confor-

mity by electrophoresis in a 1.5% agarose gel with ethidium bromide.

Remaining PCR product was purified applying ExoSap-IT (USB). A 5x dilution of the enzyme was used and 2 μ L of that solution were added to 8 μ L PCR product (or 4 μ L were added to 18 μ L PCR product). Samples were incubated for cleanup at 37°C (30 min) and the enzyme was deactivated at 80°C (20 min). Cycle sequencing was performed in 10 μ L volume containing 1 μ L purified PCR product, 0.5 μ L BigDye Terminator, 1.75 μ L Big Dye Terminator reaction buffer, 0.5 μ L primer and nuclease-free water. Cycle sequencing products were cleaned up with the Sephadex G-50 (Sigma S-5897) method, dried and stored at -20°C until sequencing.

Sequences were managed, processed and quality-checked with the software Geneious (Drummond *et al.* 2011). Sequence alignment was performed with MAFFT (v6.717b) (Katoh *et al.* 2002) implemented in Geneious. The alignment of COI was additionally optimized manually using MEGA 4 (Tamura *et al.* 2007) with consideration of the amino-acid translation to check for pseudogenes (Bensasson *et al.* 2001; Buhay 2009). Alignments were checked for mutations by eye. Because of the absence of nucleotide variation among the specimens analyzed, no further analyses were conducted.

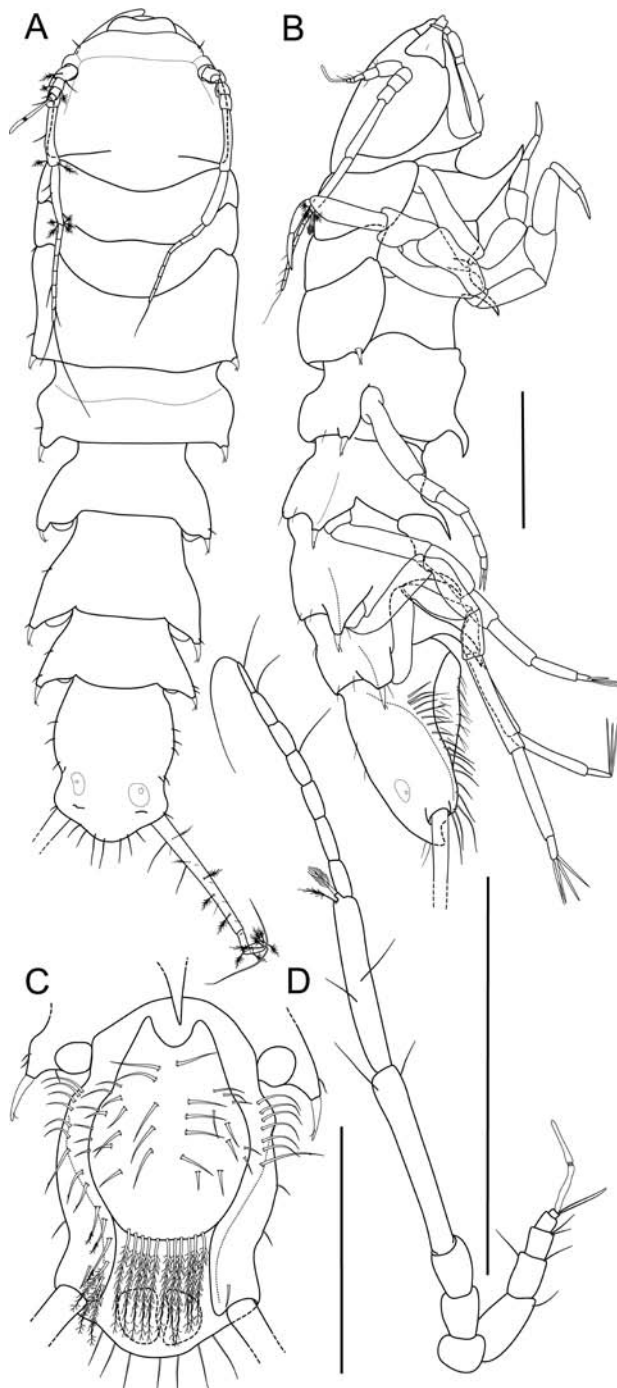


Figure 2. *Macrostyliis roaldi* sp. nov., holotype female (ZMHK42994). A, habitus, dorsal. B, habitus, lateral. C, pleotelson, ventral. D, antennula and antenna, lateral view, *in situ*. Scale bars = 0.5 mm.

doi:10.1371/journal.pone.0049354.g002

Digital Archiving

This article is deposited at PubMedCentral and LOCKSS. Molecular sequences are deposited in GenBank and BoLD (Ratnasingham & Hebert 2007) and access numbers are provided in Table 1.

Nomenclatural Acts

The electronic version of this document does not represent a published work according to the International Code of Zoological Nomenclature (ICZN), and hence the nomenclatural acts contained in the electronic version are not available under that Code from the electronic edition. Therefore, a separate edition of this document was produced by a method that assures numerous identical and durable copies, and those copies were simultaneously obtainable (from the publication date noted on the first page of this article) for the purpose of providing a public and permanent scientific record, in accordance with Article 8.1 of the Code. The separate print only edition is available on request from PLoS by sending a request to PLoS ONE, Public Library of Science, 1160 Battery Street, Suite 100, San Francisco, CA 94111, USA along with a check for \$10 (to cover printing and postage) payable to “Public Library of Science”. In addition, this published work and the nomenclatural acts it contains have been registered in ZooBank, the proposed online registration system for the ICZN. The ZooBank LSIDs (Life Science Identifiers) can be resolved and the associated information viewed through any standard web browser by appending the LSID to the prefix “<http://zoobank.org/>”. The LSID for this publication is: urn:lsid:zoobank.org:pub:1113243A-0A9F-4FBF-8739-BF255C4C8C8B.

Systematics

Asellota Latreille, 1802

Macrostylidae Hansen, 1916

Desmosomidae Sars, 1899; Macrostylini Hansen, 1916, p. 74; Wolff, 1956, p. 99; Macrostylinae Birstein, 1973; Macrostylidae Gurjanova, 1933,

p. 411; Menzies, 1962, p. 28, p. 127; Wolff, 1962; Birstein, 1970; Menzies & George, 1972, p. 79–81; Mezhev, 1988, p. 983–994; 1992, p. 69; Brandt 1992a, 2002, 2004; Kussakin, 1999, p. 336; Riehl and Brandt, 2010; Riehl *et al.*, 2012

Type genus. *Macrostylis* Sars, 1864

Macrostylis Sars, 1964 (*monotypic*); Vana Meinert, 1890; *Desmostylis* Brandt, 1992

Type species. *Macrostylis spinifera* Sars, 1864

Gender. Female

Composition. See Riehl & Brandt, 2010

***Macrostylis roaldi* n. sp.**

Etymology

Roaldi is dedicated to the Norwegian explorer Roald Amundsen, eponym of the type locality, in order to mark the 100th anniversary of Amundsen as the first person to reach the geographic South Pole on December 14th 1911.

Type material examined

See Table 1.

Type locality

Pine Island Bay, Amundsen Sea, Southern Ocean (Fig. 1); for a complete list of records see Table 2. Abiotic data, such as sediment or bottom-water characteristics, are not available.

Type fixation

Holotype: non-ovigerous female, 3.0 mm, ZMH-K 42994, designated here (Fig. 2).

Type material — Remarks.

For DNA analyses, from all specimens 2–3 posteri-

or pereopods were removed. See also Table 1.

Further records

WHOI G#1, 1 juvenile male (AM P86024); WHOI HH#3, 1 terminal male, AM P86026; WHOI 66, 1 nonovigerous female, 1 manca, AM P98019; WHOI 128, 7 nonovigerous females, AM P86007; WHOI 131, 12 specimen, male and female, AM P67257.

Material examined for comparison

See Table 3.

Description, female.

Body (Figs 2A–C, 3A–B, G, 4A–B 5A–B, D).

Length 3.0–3.6 mm, 3.9–4.1 width, subcylindrical, tergite surfaces with scattered setae. **Ventral spines.** Pereonite 1 spine acute, prominent. Pereonite 3–6 spine acute, prominent, closer to posterior segment border. Pereonite 7 spine prominent. **Imbricate ornamentation (IO).** Cephalothorax-pleotelson IO weakly expressed, covering whole tergites, sternites and operculum.

Cephalothorax. Length 0.88–0.90 width, 0.19–0.20 body length; frons in dorsal view concave, frontal ridge present, straight. Posterolateral setae present. Posterolateral margins blunt. **Fossosome.** Length 0.85–0.91 width, 0.22 body length. Lateral tergite margins in dorsal view forming almost uninterrupted line, ventral surface without keel; sternite articulations present, not fully expressed.

Pereonite 1. Anterior margin concave; posterolateral setae simple. **Pereonite 2.** Posterolateral setae simple. **Pereonite 3.** Posterolateral margin produced posteriorly, tapering, culminating in articulation of posterolateral setae; setae bifid, robust, spine-like. **Pereonite 4.** Width 1.1–1.2 pereonite 5 width, length 0.35–0.39 width; pereonal collum present. Lateral margins in dorsal view curved,

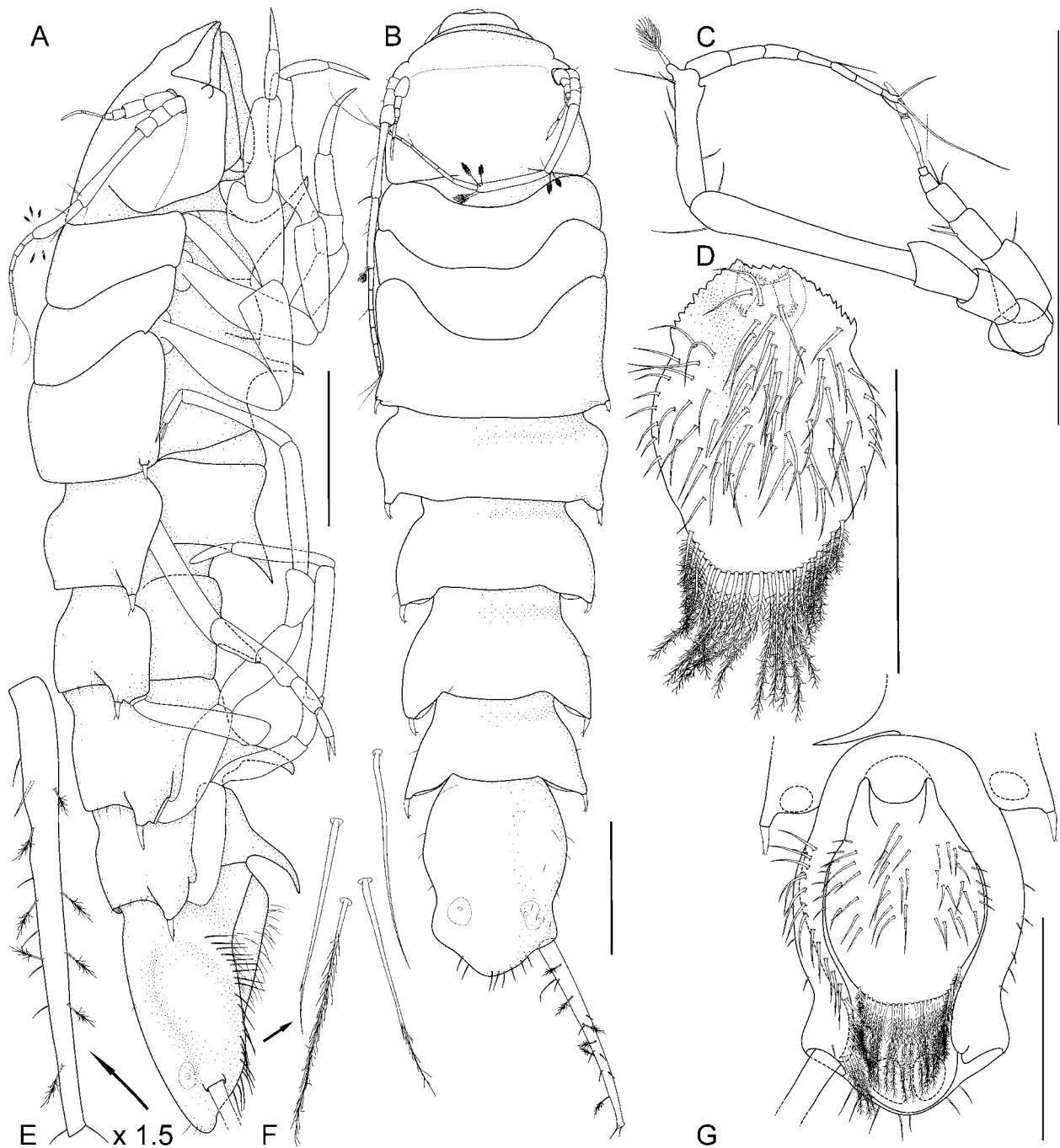


Figure 3. *Macrostylis roaldi* sp. nov., paratype female (ZMH-K42995). **A**, habitus, lateral. **B**, habitus, dorsal. **C**, antennula and antenna, lateral, *in situ*. **D**, operculum, ventral. **E**, uropod protopod (endopod broken, missing), enlarged. **F**, setae from setal ridge, latero-ventrally on pleotelson in top-to-bottom order: simple, split, split and pappose, pappose. **G**, pleotelson, ventral. Scale bars = 0.5 mm. doi:10.1371/journal.pone.0049354.g003

concave in collum region, medially convex with greatest width, constricted anterior to posterolateral margin. Posterior tergite margin with 2 simple, not robust, flexibly articulating setae; setae short, not extending beyond posterolateral margin. Posterolateral margins produced posteriorly, tapering. Posterolateral setae bifid, robust, spine-like, articulating on pedestals (Fig. 4 A–C).

Pereonite 5. Length 0.41–0.46 width. Posterior tergite margin with 4–6 simple, not robust, flexibly articulating setae; setae short, not extending beyond posterolateral margin. Posterolateral margins tapering. Tergite posterolateral setae bifid, robust, spine-like. **Pereonite 6.** Length 0.58–0.59 width. Posterior tergite margin with simple, not robust, flexibly articulating 4–8 setae; setae short, not ex-

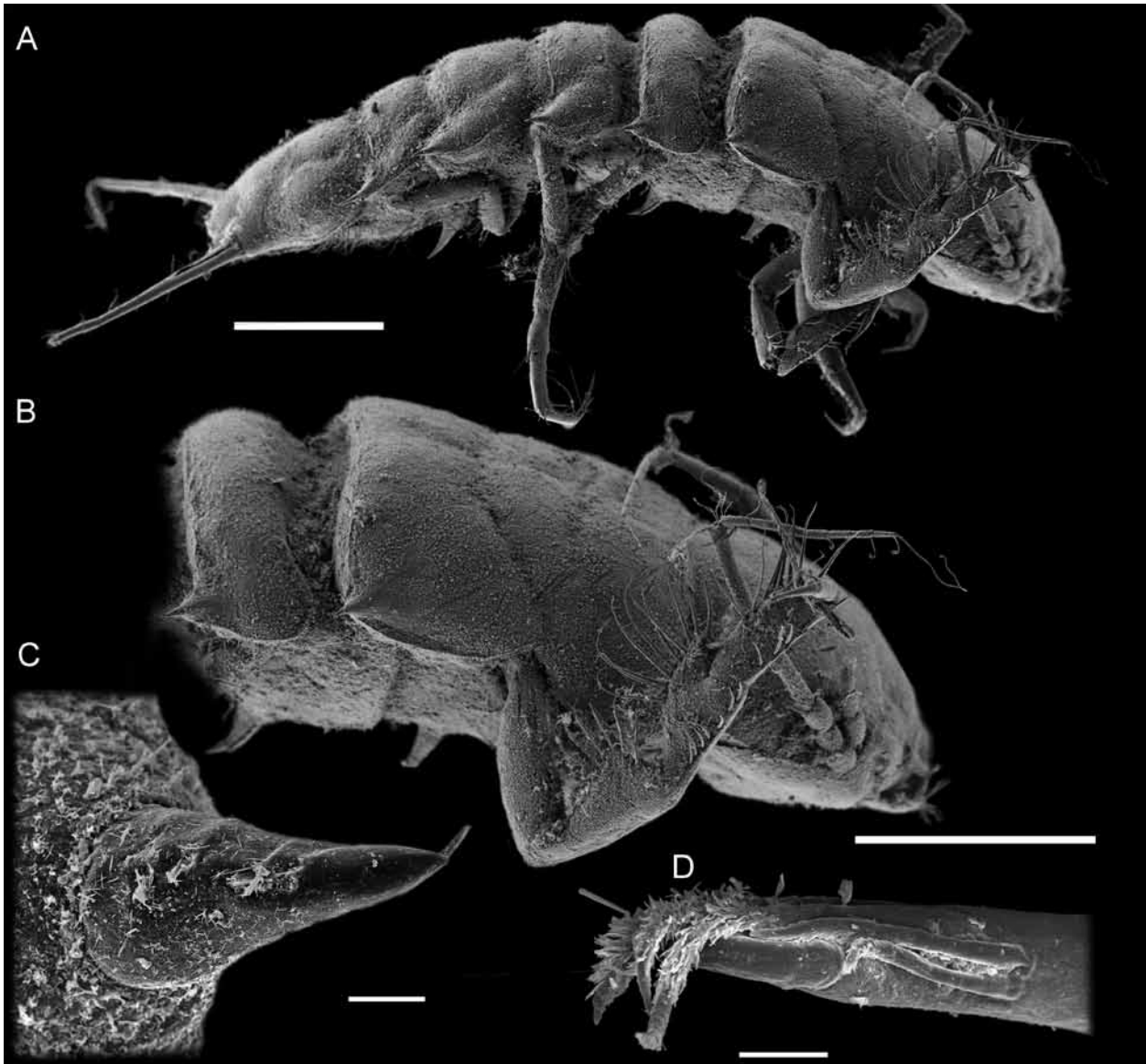


Figure 4. *Macrostylis roaldi* sp. nov., paratypes (ZMH-K42999), non-ovigerous female, SEM. **A**, habitus, dorsolateral. **B**, anterior habitus, pereopod III, enlarged. **C**, robust, bifid, spine-like seta as on posterolateral corners of posterior tergites. **D**, pereopod III dactylus with claws and fringed sensillae, dorsolateral view when pereopod III in natural position. Scales: A, B = 0.5 mm, C, D = 0.01 mm. doi:10.1371/journal.pone.0049354.g004

tending beyond posterolateral angles. Posterolateral margin produced posteriorly, tapering. Tergite posterolateral setae bifid, robust, spine-like, articulating on pedestals. **Pereonite 7.** Length 0.45–0.46 width. Posterior tergite margin with 7–8 simple, not robust, flexibly articulating setae; setae short, not extending beyond posterolateral angles. Posterolateral margin produced posteriorly, tapering and subangular. Tergite posterolateral setae bifid, robust, spine-like, on pedestals.

Pleotelson (Figs 2C, 3G, 5D). Constricted anteriorly to uropod articulations, ovoid, lateral

margins convex, setal ridges visible in dorsal view, length 0.19–0.20 body length, 1.3–1.4 width, narrower than pereonite 7; statocysts present, dorsal slot-like apertures present, transverse across longitudinal axis, concave. Posterior apex convex, bluntly triangular. Posterior apex with 6–7 simple setae positioned on and around apex. Pleopodal cavity width 0.73 pleotelson width, preanal ridge width 0.43 pleotelson width. Anal opening terminal.

Antennula (Figs 2D, 3C, 5C). Length 0.32 head width, 0.22 antenna length, width 1.0 antenna

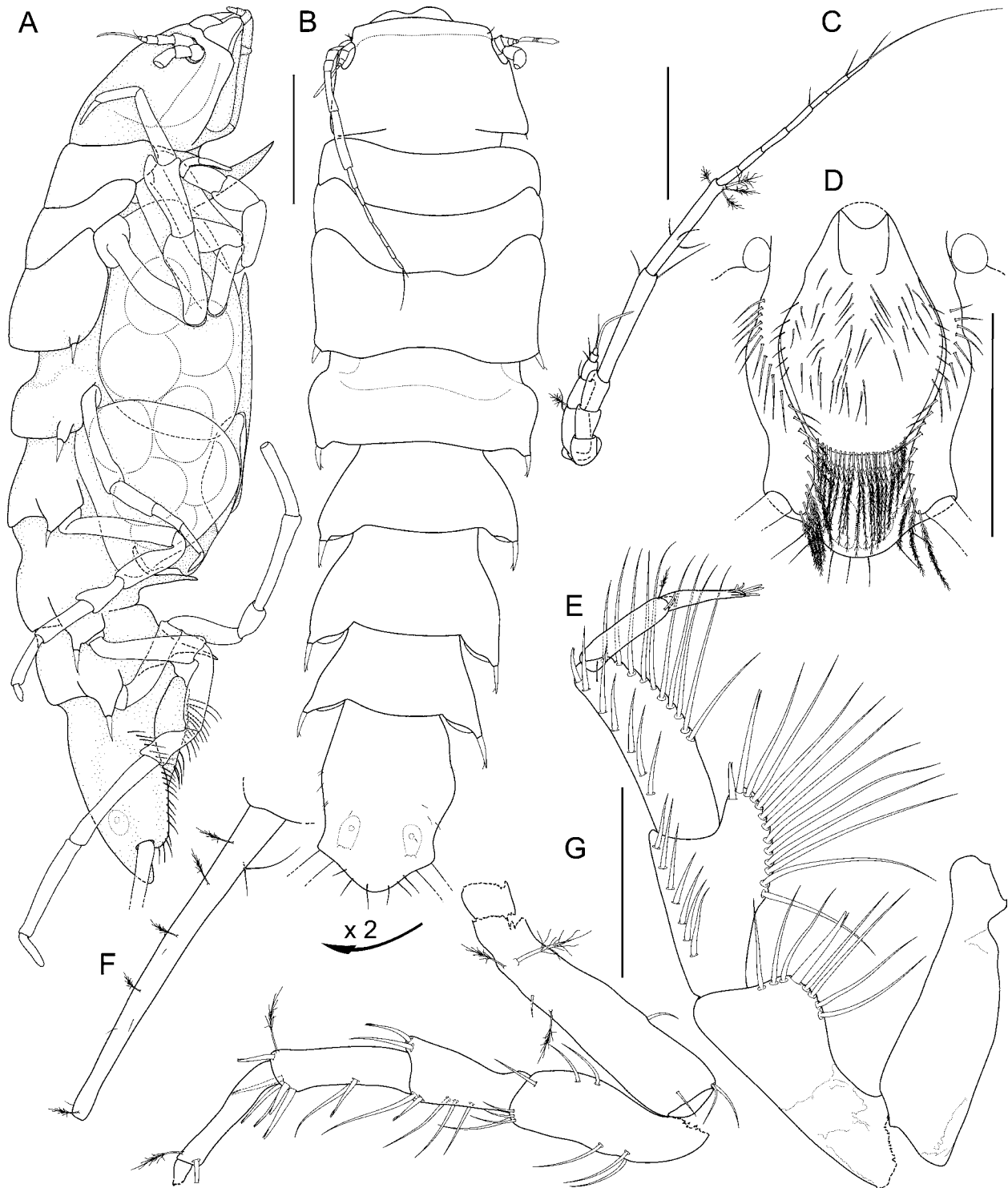


Figure 5. *Macrostylis roaldi* sp. nov., paratype ovigerous female (ZMH-K42998). A, habitus, lateral. B, habitus, dorsal. C, antennula and antenna, lateral, *in situ*. D, pleotelson, ventral. E, pereopod III. F, uropod, enlarged, endopod broken, missing. G, pereopod V, basis, baso-ischial articulation and dactylus damaged. Scales A–B, D= 0.5 mm, C, E, G = 0.3 mm. doi:10.1371/journal.pone.0049354.g005

width. Articles decreasing in size from proximal to distal. Article 1 distinctly longer than wide, longest and widest, with 1 simple seta. Article 2 distinctly longer than wide, tubular, with 2 simple setae. Article 3 distinctly longer than wide, tubular, with 2 simple setae. Article 4 length subequal

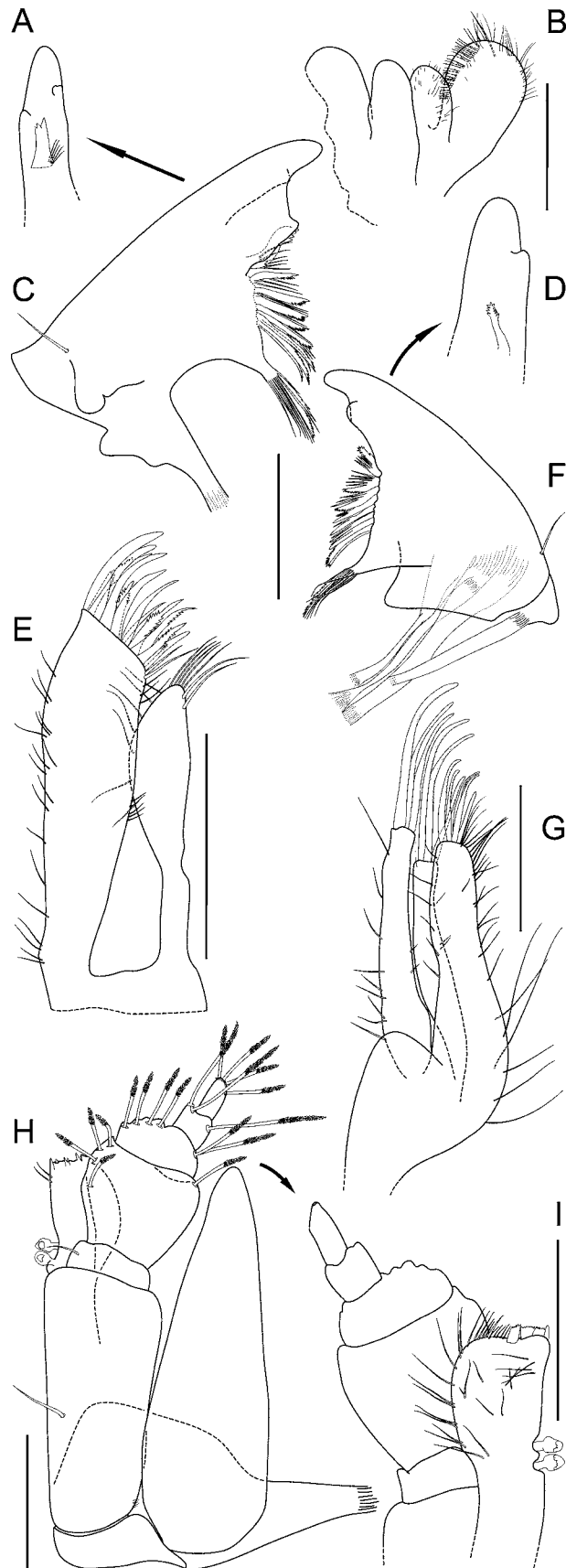
width, tubular. Article 5 squat, globular, with 2 simple setae. Terminal article with 1 aesthetasc, aesthetascs with intermediate belt of constrictions. **Antenna (Figs 2D, 3C, 5C).** Length 0.30 body length. Article 1 squat, globular. Article 2 squat, globular, longer than article 1. Article 3 elongate,

Figure 6. *Macrostylis roaldi* sp. nov., mouthparts: paratype adult male (ZMH-K42993, A-C, E-F, H-I), paratype female (ZMHK42995, D, G). **A**, left mandible incisive process and *lacinia mobilis*, medial. **B**, paragnaths. **C**, left mandible. **D**, right mandible incisive process and *lacinia mobilis*, medial. **E**, maxillula, dorsal. **F**, right mandible. **G**, maxilla, dorsal. **H**, maxilliped, ventral. **I**, maxilliped endite and palp, dorsal, setae omitted. Scales = 0.1 mm. doi:10.1371/journal.pone.0049354.g006

longer than article 1. Article 4 longer than articles 1–3 together, distally with 2 simple setae. Article 5 shorter than article 4, distally with 2 broom setae. Flagellum with 7 articles.

Mandibles (Fig. 6A, C–D, F). In medial view strongly narrowing from proximal to distal, sub-triangular, with lateral setae; left mandible incisor process distal margin flattened and curved (shovel-like), with 3 cusps, *lacinia mobilis* grinding or spine-like, adjacent to spine row without separating gap, with 3–4 cusps; right mandible incisor process bluntly rounded, with 2 cusps, *lacinia mobilis* grinding or spine-like, clearly smaller than left lacinia, adjacent to spine row without gap, with 10 cusps. **Maxillula (Fig. 6E).** Lateral lobe with 10 robust setae. **Maxilla (Fig. 6G).** Lateral lobe with 3 setae terminally, serrate; middle endite with 3 setae terminally, serrate; inner endite with 5 setae terminally, mostly serrate. **Maxilliped (Fig. 6H–I).** Basis length 3.3.3 width, medioventrally with seta present; epipod length 3.0 width, 1.1 basis length; palp wider than endite, article 2 wider than article 1, article 2 wider than article 3, article 1 shorter than article 3.

Pereopod I (Fig. 7A). Length 0.42 body length. Ischium dorsal margin with 5–6 setae, simple, row of setae laterally to margin. Merus dorsal margin with 5 setae, 4 simple, 1 bifurcate, more robust, with dorsal row of setae laterally to margin; ventral margin with 5 medially biserrate, distally fringe-like sensillae. Carpus dorsally with



4 setae: 3 simple, 1 bifurcate, more robust. Dactylus distally with 3 sensillae. **Pereopod II (Fig. 7B).** Longer than pereopod I, length 0.46–0.47 body length. Ischium dorsally with 7 setae: 6 in row, simple, 1 distomedially, simple, with dorsal row

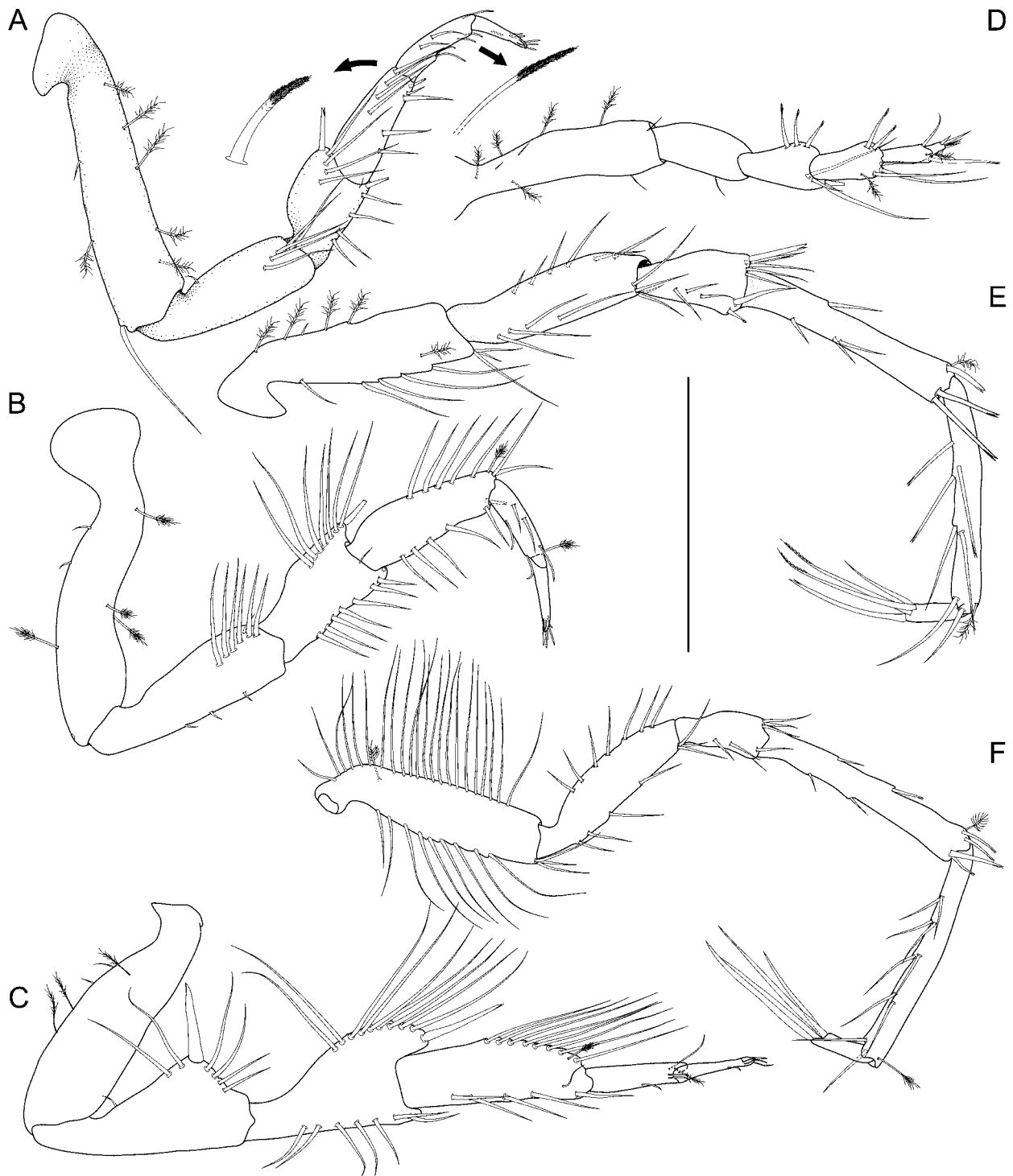


Figure 7. *Macrostyliis roaldi* sp. nov., paratype female (ZMH-K42995), pereopods. A, pereopod I, lateral, with enlarged setae (medially biserrate, distally fringe-like sensilla and distally fringe-like sensilla). **B**, pereopod II, lateral. **C**, pereopod III, lateral. **D**, pereopod IV, posterior. **E**, pereopod VI, medial. **F**, pereopod VII, medial. Pereopod V not shown, broken, missing. Scale = 0.5 mm. doi:10.1371/journal.pone.0049354.g007

of setae laterally to margin. Merus dorsally with 8 setae: 7 long, in row, simple, 1 short, more robust, split distally; ventrally with 8 distally fringe-like sensillae in row. Carpus dorsally with 8 setae: 5 medially biserrate, distally fringe-like sensillae in row, 1 broom, 2 simple distally; ventrally with

6 setae: 5 distally fringe-like sensillae in row, 1 split mediolaterally. Dactylus distally with 3 sensillae. **Pereopod III (Figs 4B, D, 6E, 7C)**. Length 0.47–0.48 body length. Ischium dorsal lobe triangular; proximally with 2–4 simple setae; apex with 1 prominent seta; apical seta robust, bifid, straight,

spine-like; distally with 3–4 simple setae. Merus dorsally with 10–13 setae in row: 9–12 simple, 1 more robust, bifid distally; ventrally with 7 distally fringe-like sensillae in row. Carpus dorsally with 9–11 setae in row: 7–9 simple, 1 broom, 1 simple; ventrally with 6–8 setae: 5–7 distally fringe-like sensillae in row, 1 laterally, minute, simple. Dactylus with 3 sensillae. **Pereopod IV (Fig. 7D)**. Length 0.26 body length, carpus laterally flattened.

Pereopod V (Fig. 5G). Ischium mid-dorsally with 2 simple setae; distodorsally with 1 short, simple seta, midventrally with 3 simple setae; distoventrally with 4 simple setae. Merus distodorsally with 2 setae: 1 simple, 1 split; midventrally with simple 3 setae; distoventrally with 2 setae: 1 short, split, 1 long, simple. Carpus distodorsally with 3 setae: 1 broom, 1 short, split, 1 long, simple; distoventrally with 5 split setae. **Pereopod VI (Fig. 7E)**. Length 0.53 body length. Ischium dorsally with 6 simple setae in row; midventrally with 4 setae in row; distoventrally with 4 simple setae; middorsally with 6 simple setae in row. Merus middorsally with setae absent; distodorsally with 6 setae: 2 simple, 1 prominent, split and more robust, 4 simple; midventrally with 3 simple setae in row; distoventrally with 2 setae: 1 simple, 1 spine-like, split. Carpus middorsally with 1 seta; distodorsally with 2 setae: 1 broom, 1 bifurcate; midventrally with 3 setae; distoventrally with 2 split setae. **Pereopod VII (Fig. 7F)**. Length subequal to pereopod VI length, 0.52 body length; basis length 3.2–4.2 width, dorsal margin row of elongate setae present, setae longer basis width, 22 altogether, ventral margin row of elongate setae present, setae longer basis width, 9–10 altogether. Ischium length 3.7 width, middorsally with 7 setae; midventrally with 4 setae in row; distoventrally with 3 setae. Merus length 2.4 width, distodorsally with 3 setae, midventrally with 2 setae, distoventrally with 2 setae. Carpus length 6.0 width, mid-dorsally with

2 bifid or split setae; distodorsally with 3 setae: 2 bifid or split, 1 broom; mid-ventrally with 2 setae; distoventrally with 2 setae: 1 short, bifid or split, 1 long, bifid or split. Propodus length 8.6 width. Dactylus length 3.3 width.

Operculum (Fig. 3D). Stout, length 1.2 width, 0.7 pleotelson dorsal length; apical width 0.69 operculum maximal width; distally not reaching anus, ovoid, ventrally keeled. With lateral fringe consisting of 6–7 setae, lateral fringe of setae distinctly separate from apical row of setae. With 22 pappose setae on apex, completely covering anal opening. **Pleopod III (Fig. 8C)**. Length 2.4 width, protopod length 2.3 width, 1.6 pleopod III length; exopod with fringe of fine setae, shorter than pleopod III exopod width, with 1 simple seta subterminally, exopod length 0.63 pleopod III length. **Pleopod V (Fig. 8F)**. Present. **Uropod (Figs 2A, 3B, E, 5F)**. Inserting on pleotelson on posterior margin; length 1.2 pleotelson length; protopod length 8.7–10.4 width, 0.93–1.0 pleotelson length, protopod distal margin blunt, endopod insertion terminal; endopod length 3.5 width, 0.27 protopod length, endopod width at articulation subsimilar protopod width.

Description, terminal male

Body (Figs 8A–B, H, 9A–B). More elongate than female, subcylindrical, elongate, length 2.4 mm, 4.4 width. **Imbricate ornamentation (IO)**. Cephalothorax IO weakly expressed, covering whole tergite and sternite, pereonite 3–pleotelson IO strongly expressed, covering whole tergite, sternite and pleopods II.

Cephalothorax. Frontal ridge present, straight between insertions of antennulae; length/width ratio subequal to female, length 0.92 width, 0.17 body length; posterolateral corners rounded. **Fossosome**. Length/width ratio greater than in female, length 1.0 width, length/body-length ratio

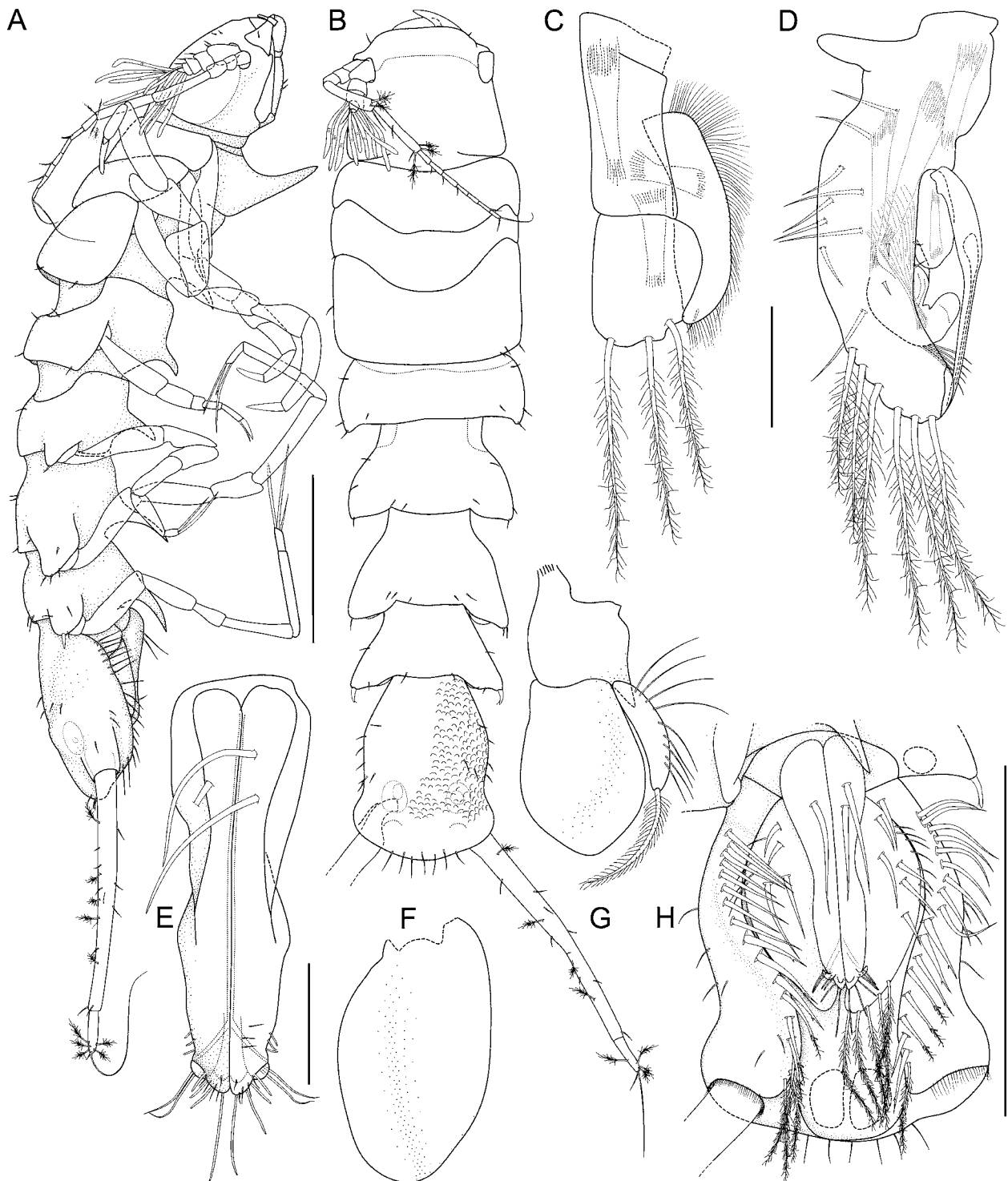


Figure 8. *Macrostylis roaldi* sp. nov., paratype adult male (ZMH-K42993), habitus and pleopods. **A**, habitus, lateral. **B**, habitus, dorsal. **C**, pleopod III, dorsal. **D**, pleopod II, dorsal. **E**, pleopod I, ventral. **F**, pleopod V, ventral. **G**, pleopod IV, ventral. **H**, pleotelson, ventral. Scales: A, B, H = 0.5 mm; C-G = 0.1 mm. doi:10.1371/journal.pone.0049354.g008

subequal to female, not keeled. **Pereonite 2.** Posterolateral setae present, simple, not robust, without pedestals. **Pereonite 3.** Posterolateral setae present, simple, not robust, flexibly articulated. Length in male 0.29 width. **Pereonite 4.** Pereonal collum present, medially straight. Lateral margins

in dorsal view convex; posterolateral margins produced posteriorly. Posterolateral setae present, not robust, simple, flexibly articulated.

Pereonite 5. Posterior tergite margin as in female. Produced posteriorly, rounded. Simple, not robust, flexibly articulated. **Pereonite 6.** Produced

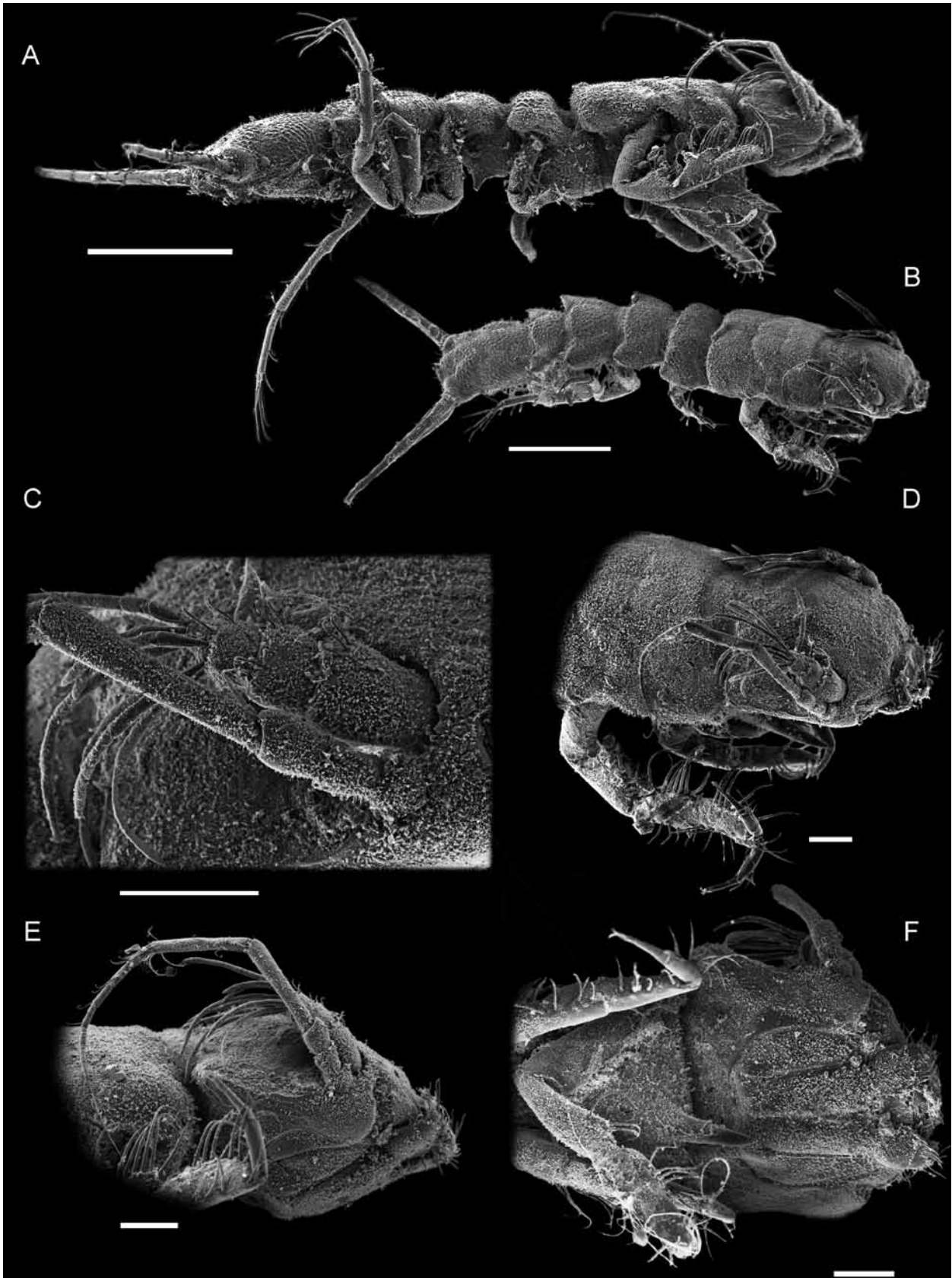


Figure 9. *Macrostylis roaldi* sp. nov., paratypes (ZMH-K42999), adult male, SEM. **A**, habitus, lateral. **B**, habitus, dorsolateral. **C**, antennula, antenna, basal segments. **D**, cephalothorax, dorsolateral. **E**, cephalothorax, antenna, lateral. **F**, cephalothorax, mouthparts, ventral. Scales: A, B = 0.5 mm, C–F = 0.1 mm. doi:10.1371/journal.pone.0049354.g009

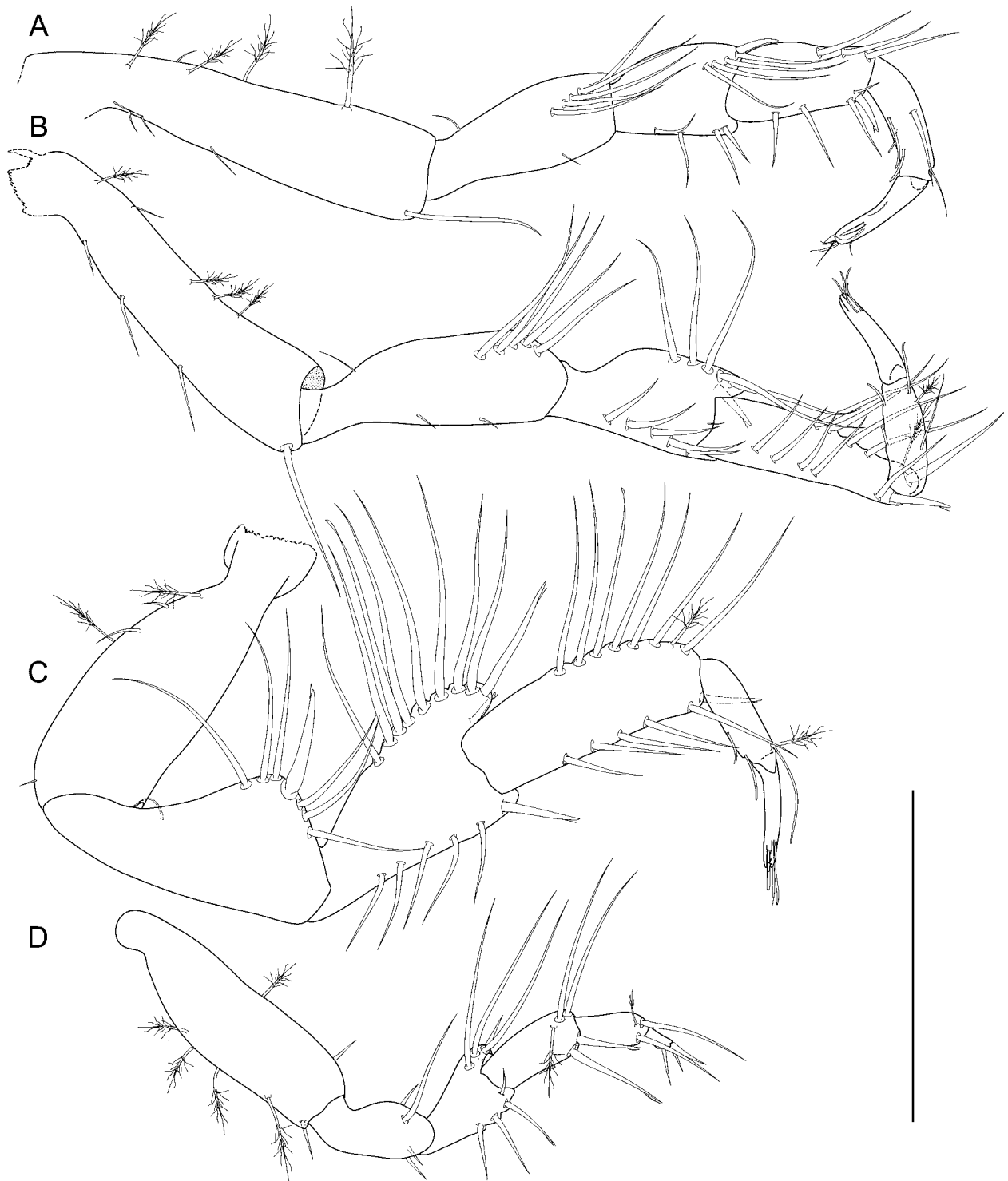


Figure 10. *Macrostylis roaldi* sp. nov., paratype adult male (ZMH-K42993), anterior pereopods. **A**, pereopod I, lateral. **B**, pereopod II, lateral, carpo-propodal articulation twisted. **C**, pereopod III, lateral. **D**, pereopod IV, posterior. Scale = 0.3 mm. doi:10.1371/journal.pone.0049354.g010

posteriorly, rounded. Simple, not robust. **Pleonite 1 (Fig. 8H)**. Sternal articulation with pleotelson present. **Pleotelson**. In dorsal view constricted anterior to uropod articulation trapezoid, widening posteriorly, lateral margins straight, length/width ratio in male subequal to female, 0.22 body length, width less than pereonite 7 width, tergite

dorsal surface in posterior view with axial ridge and 2 lateral fields. Posterior apex convex, very flat, almost straight, pleopodal cavity width 0.62 pleotelson width, preanal ridge width 0.33 pleotelson width.

Antennula (Figs 8A, B, 9C–E). Length 0.26 head width, 0.25 antenna length, width 1.75



Figure 11. *Macrostylyis roaldi* sp. nov., paratype adult male (ZMH-K42993), posterior pereopods. **A**, pereopod VI, lateral. **B**, pereopod VII, lateral. **C**, pereopod V, lateral. Scale = 0.3 mm. doi:10.1371/journal.pone.0049354.g011

antenna width; terminal article with 2–3 aesthetascs, penultimate article with 7–8 aesthetascs (Fig. 9C), aesthetascs with intermediate belt of constrictions. Article 1 elongate, longest and widest, with 3 simple setae, 1 broom seta. Article 2 squat, globular, shorter than article 1, with 4 simple setae, 1 broom seta. Article 3 squat, globular, shorter than article 1, with 2 simple setae. Article 4 squat, globular, shorter than article 1, with 1 simple seta.

Article 5 squat, globular, shorter than article 1, with 1 simple seta.

Antenna (Figs 8A–B, 9C–E). Length 0.33 body length. Flagellum of 7 articles. Article 1 squat, globular. Article 2 squat, globular, shorter than article 1. Article 3 elongate, longer than article 1. Article 4 longer than articles 1–3 together, distally with 1 simple seta, 2 broom setae. Article 5 shorter than article 4, with 4 broom setae. **Pereopod I (Fig**

10A). Length 0.39 body length. Merus setation as in female. Carpus dorsally with 3 simple setae in row; ventrally with 5 setae: 3 simple, in row, 1 small, simple, distolaterally, 1 spine-like, robust, split distoventrally. **Pereopod II (Fig. 10B).** Length/body-length ratio sexually dimorphic; length 0.44 body length. Ischium dorsally with 5 setae, simple, long, with dorsal row of setae shifted laterally. Merus dorsally with 6 setae: 5 simple, long in row, 1 spine-like, robust, bifid distomedially; ventrally with 5 simple setae. Carpus dorsally with 6 setae: 5 simple, long in row, 1 broom subdistally; ventrally with 6 setae: 5 simple in row with larger distance between setae 4 and 5, 1 spine-like, robust, bifid distomedially.

Pereopod III (Fig 10C). Ischium sexually dimorphic; triangular, proximally with 3 simple setae. Ischium apex with 1 prominent seta; apical seta robust, spine-like, straight, bifid. Distally with 3 simple setae. Merus dorsally with 10 setae: 8 long, simple in row, 1 slightly more robust, split distally, 1 short, spine-like, robust bifid seta distomedially; ventrally with 6 setae: 5 simple in row, 1 slightly more robust, split distally. Carpus dorsally with 8 setae: 7 long, simple in row, 1 broom subterminally; ventrally with 6 setae: 5 simple in row, 1 slightly more robust, split distally. **Pereopod IV (Fig. 10D).** Length 0.24 body length. **Pereopod V (Fig. 11C).** 0.39 body length. Ischium middorsally with 2 long, simple setae. Ischium distodorsally with setae absent. Ischium midventrally with 2 setae, 1 short, simple, 1 long, simple, distoventrally with 3 setae: 2 short, simple, 1 long, simple. Merus distodorsally with 3 setae: 1 split, 2 simple, long; midventrally with 2 simple setae; distoventrally with 2 setae: 1 short, split, 1 long, simple. Carpus setation as in female.

Pereopod VI (Fig. 11A). Ischium dorsally with 6 setae: 5 simple, in row, 1 short, split; midventrally with 1 simple seta; distoventrally

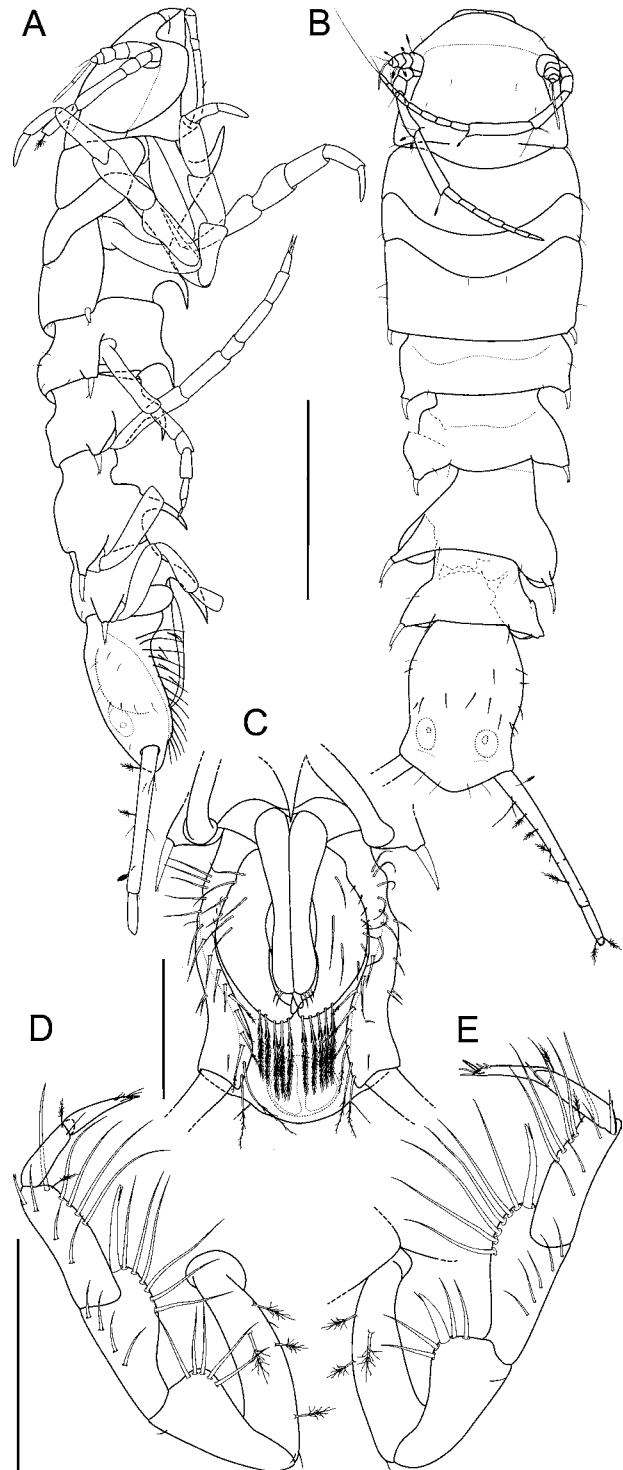


Figure 12. *Macrostylis roaldi* sp. nov., paratype juvenile male (ZMH-K42997). A, habitus, lateral. B, habitus, dorsal, posterior pereonites damaged. C, pleotelson, ventral. D, left pereopod III. E, right pereopod III. Scales: A, B = 0.5 mm; C = 0.2 mm; D, E = 0.3 mm. doi:10.1371/journal.pone.0049354.g012

with 3 setae: 2 short, simple, 1 long, simple. Merus distodorsally with 6 simple setae. Merus midventrally with setae absent. Distoventrally with 1 simple seta. Carpus middorsally with 1 split seta,

distodorsally with 2 setae: 1 short, split, 1 long, split; midventrally with 1 simple seta, distoventrally with 2 setae: 1 broom, 1 split. **Pereopod VII (Fig. 11B)**. Length 0.49 body length, length less than pereopod VI length, segment L/W ratios sexually dimorphic; basis length 3.9 width, dorsal margin row of elongate setae sexually dimorphic, setae longer basis width, 13 altogether, ventral margin row of elongate setae sexually dimorphic, setae longer basis width, 4 altogether; ischium length 3.3 width, middorsally with 3 simple, long setae; midventrally with 2 simple, long setae; distoventrally with 2 simple setae. Merus length 2.0 width; distodorsally with 3 simple setae, distoventrally with 2 simple setae; carpus length 7.3 width. Carpus mid-dorsally with 1 split seta; distodorsally with 4 setae: 1 broom, 3 split; midventrally with 1 split seta, distoventrally with 2 setae: 1 short, split, 1 long, split. Propodus length 6.5 width. Dactylus length 3.5 width.

Pleopod I (Fig. 8E, H). Length 0.63 pleotelson length, lateral horns not extending distally beyond medial lobes, distally with 9 sensillae, ventrally with setae present, 1–2 setae proximally, longer than pleopod I width, 8 minute setae distally.

Pleopod II (Fig. 8D). Protopod apex rounded, with 7 setae on proximal lateral margin; with 5 pappose setae distally. Endopod distance of insertion from protopod distal margin 0.59 protopod length. Stylet weakly curved, not extending to distal margin of protopod, length 57.9 protopod length. **Uropod (Fig. 8A–B)**. Length 1.5 pleotelson length; protopod length/width ratio subequal to female, 8.9 width, with endopod inserting terminally; endopod/protopod length ratio less than in female, endopod length 0.15 protopod length, endopod length 3.7 width, width subequal protopod width.

Remarks

The specimens included in this study were retrieved from eight stations with a minimum distance

between stations of about 0.6 km and a maximum distance of roughly 300 km (Fig. 1, Table 1). The depth range lies between 478 and 1,486 m and thus the Pine Island Bay area features potentially significant physical barriers to dispersal (see maps provided by Lowe & Anderson (2002) and Kaiser *et al.* (2009)).

The collection at hand comprises 47 specimens, 1 manca, 31 females and 15 males. The manca is 1.5 mm in length: sex indeterminable; pereonite 7 very small, posterolateral protrusions and setae both absent; antennula with 1 aesthetasc; pereopod III ischium dorsal lobe proximally with setae absent, distally 1 seta present. Pereopod VII absent.

Four male stages were identified and could be differentiated mainly based on the stage of development of the pereopod VII and pleopod I: Two specimens (1.6 and 1.8 mm length) were identified as first male stage: pereonite 7 small with posterolateral protrusions and setae both absent; antennula eutrophied, with 1 aesthetasc; pereopod III ischium dorsal lobe proximally with 1 seta, and distally with 1 seta; pereopod VII developing, shorter than pereopod VI, without setae; strongly flexed at basis-merus articulation; both pereopods VII adjoined between merus and dactylus and extending along midline of body to the distal tip of pleopod I; pleopod I posteriorly projecting about 60% of pleopod II length.

Three specimens (2.0–2.1 mm length) have been found belonging to a second male stage: pereonite 7 small, posterolateral protrusions and setae both present, disproportionally large; antennula eutrophied, with 1 aesthetasc; pereopod III ischium dorsal lobe proximally with 1–2, and distally with 2–3 setae; pereopod VII shorter (about 60%) than pereopod VI, with setae present and in normal position and orientation; pleopod I projecting posteriorly to about 80% of pleopod II length. Four

specimens could be allocated to a third male stage (1.9–2.7 mm length): pereonite 7 fully developed, little shorter than pereonite 6, with posterolateral protrusions and setae both subequal to pereonite 6; antennula eutrophied, with 1 aesthetasc; pereopod III ischium dorsal lobe proximally with 1–3, distally with 2–3 setae; pereopod VII fully developed, little shorter and more slender than pereopod VI; pleopod I projecting posteriorly to about 90% of pleopod II length (as in adult) (Fig. 12).

Six male were found in adult stage (2.1–2.5 mm length): pereonite 7 fully developed, little shorter than pereonite 6, with posterolateral protrusions and setae both subequal to pereonite 6; antennula eutrophied, with 6–9 aesthetascs; pereopod III ischium dorsal lobe proximally with 2–3, distally with 2–4 setae; pereopod VII fully developed, little shorter and more slender than pereopod VI; pleopod I distally differentiated, projecting posteriorly to about 90% of pleopod II length. Three females belong to the smallest female stage identified (2.2–2.5 mm): pereonite 7 small, posterolateral protrusions and setae both present and disproportionately large; antennula with 1 aesthetasc; pereopod III ischium dorsal lobe proximally with 1–2, and distally with 1–2 setae; pereopod VII shorter (about 60%) than pereopod VI, with setae present and in normal position and orientation. 21 females (2.2–3.7 mm length) could not clearly be allocated to a stage as developmental stages of single characters tend to overlap strongly and categories mix: pereonite 7 almost fully or fully developed, little or clearly shorter than pereonite 6, with posterolateral protrusions and setae both subequal to pereonite 6; antennula with 1 aesthetasc; pereopod III ischium dorsal lobe proximally with 2–4, distally with 2–4 setae; pereopod VII of 60% pereopod VI length or fully developed, little shorter and more slender than pereopod VI, with setae present.

Four ovigerous females were found (3.2–3.8

mm length): pereonite 7 fully developed, little shorter than pereonite 6, with posterolateral protrusions and setae both subequal to pereonite 6; antennula not eutrophied, with 1 aesthetasc; pereopod III ischium dorsal lobe proximally with 3–4, distally with 3–4 setae; pereopod VII fully developed, little shorter and more slender than pereopod VI. Female stages I and II were not found. Setal counts on the pereopod III ischium dorsal lobe often varied between left and right side of the same individual. The proximal setal row had one seta less on the right side in six specimens, and one seta more in four specimens. The distal row featured one seta more on the right side in seven cases and one less in four cases.

Development

Setal counts on the pereopod III dorsal lobe are not normally distributed. Therefore, a non-parametric spearman correlation was conducted. We found a significant correlation between body length (mm) and total number of setae of the right and left pereopods (spearman correlation right: $r_s = 0.82$, $p = 0.0001$, $n = 46$; left: $r_s = 0.83$, $p = 0.0001$, $n = 37$).

Molecular Results

Sequence fragments of the mitochondrial COI gene were obtained from 22 macrostyloid specimens resulting in a 657 bp alignment with two single variable sites occurring in a single specimen (two haplotypes are separated by two point mutations: transition (guanine – adenine) at position 244, transversion (thymine – adenine) at position 343 of the alignment; GenBank accession numbers JX260254–JX260274). On average, the sequences showed base-pair frequencies of T: 38.0%, C: 18.5%, A: 26.3%, G: 17.2% (AT rich). 16S sequences were obtained from 35 macrostyloid specimens

resulting in a 385 bp alignment, with no single variable site (GenBank accession numbers JX260314–JX260348). Here, the sequences showed average base-pair frequencies of T: 31.5%, C: 16.4%, A: 35.3%, G: 16.9% (AT rich). The 12S dataset comprises the largest dataset.

Sequences were obtained from 39 individuals resulting in a 503 bp alignment, with two closely related haplotypes (separated by two point mutations: transversion (adenine – thymine) at position 88 of the alignment; transition (cytosine – thymine) at position 244; GenBank accession numbers JX260275–JX260313). For 12S, the sequences showed average base-pair frequencies of T: 33.9%, C: 18.0%, A: 31.4%, G: 16.7% (AT rich).

Discussion

Morphological Affinities

Eight species of Macrostylidae have previously been described from the Southern Ocean (Fig. 1). *Macrostylis roaldi* n. sp. shares the general appearance with *M. vinogradovae* Mezhov, 1992 and *M. setulosa* Mezhov, 1992 with regard to the habitus, posterolateral margins and setation.

The most obvious characters unique to *M. roaldi*, however, can be found in the prominent first sternal spine in both sexes as well as the rather short pleotelson and opercular pleopods in relation to body size. Moreover, the setation of all pereopods shows considerable differences. A sexual dimorphism affecting the posterolateral setae is found in *M. roaldi* that has never been reported before. However, only for a small number of species both sexes are known (Riehl *et al.* 2012). Background knowledge about sexual dimorphism in Macrostylidae is thus still scarce.

Developmental and Reproductive Notes

For Haploniscidae, Wolff and Brökeland described the developmental trajectories of several species in detail (Wolff 1962; Brökeland 2010). They found three manca stages and three male and female stages each. In Munnopsidae and various other janiroidean families, three manca stages in which the sex is not determinable, and slightly varying numbers of female (8) and male (2–3) stages have been repeatedly reported from (Wolff 1962; Wilson 1983; Brökeland 2010). It is a rare occasion to find all stages of a deep-sea isopod species and for Macrostylidae, not a single case has been reported. Despite the great sampling effort taken during BIOPEARL 2, not all stages were collected and it is thus not possible to explore the full developmental trajectory or demography of *M. roaldi* in detail. Environmental conditions (such as depth-related factors) differ between stations and this may cause developmental differences (Wilson 1983). Size ranges amongst other characters are thus largely overlapping amongst the pooled individuals and the starting stage of the development of the males may differ. Nevertheless, among the males, four distinct stages could be identified. For the females, however, the large size range of the second identified stage suggests that several stages have been overlooked and pooled.

Developing oostegites in macrostylids are not expressed as external buds and Macrostylidae differ in this regard from their close relatives Desmosomatidae and Munnopsidae. This makes identification of preparatory females difficult. Detailed anatomical studies and dissections of the ovaries are needed but this is beyond the scope of this article. Setal counts on pereopods have been regarded as allometric, i.e. increasing with body growth

(Riehl & Brandt 2010) and this pattern was found in *M. roaldi* as well. In *M. roaldi* however, we compared the setation of the pereopod III ischium dorsal lobes on the left and right sides within individuals and found 36% (17 specimens) to be asymmetrical with this regard. This is interesting especially because this region is often used for species identification. We hence suggest that for species identification more information should be applied than setal counts. In a juvenile (Fig. 12) male, we found the prominent seta on the ischial apex of the left pereopod absent.

We assume this may be caused by a developmental error or an injury caused in an earlier stage. Analysis of more specimens is needed to solidify our speculation and elucidate the developmental trajectory of this species. Dissection of one ovigerous female did not reveal developing oocytes in the gonads which suggests semelparity in *M. roaldi*. However, the small number of ovigerous specimens at hand does not allow adequate studies or final conclusions. The size range observed here for ovigerous females (3.2–3.8 mm) would allow multiple reproductive cycles. Any size difference could also be explained by potential effects of variation in the environment as the specimens originate from different stations.

Distribution

The geographic and depth ranges recorded for *M. roaldi* (Fig. 1; Table 2) are remarkable given that a brooding mode of reproduction (Wilson & Hessler 1987) and an infaunal lifestyle (Harrison 1989; Hessler & Strömberg 1989; Wägele 1989) should limit their dispersal capabilities. It is even more surprising as macrostylids have a very limited number of offspring (Riehl, personal observation; 8–10 eggs or embryos in marsupium of the two ovigerous *M. roaldi* specimens at hand (Fig.

5). Previous studies on Southern-Ocean deep-sea isopods have shown that most species have been found at only one or a few locations; the species are regarded to be rare and endemic (Brandt *et al.* 2007b) or distributed in patches which, combined with little sampling effort at greater depth, created the illusion of rarity (Kaiser *et al.* 2007; Kaiser & Barnes 2008).

Given the regular findings of *M. roaldi* across space, a common and relatively wide or a less patchy occurrence can be assumed, probably quite different from other species of the family in deeper water or when compared to Desmosomatidae and Nannoniscidae from the same area (Kaiser *et al.* 2009) (but see Brix and Svavarsson (2010)). Sampling strategies revealing the actual distribution however, are currently lacking for *M. roaldi* as well as for most deep-sea species (Kaiser & Barnes 2008). The realization of wide and disjunct occurrences of other benthic direct-developing invertebrates in the Southern Ocean (Linse *et al.* 2007; Hunter & Halanych 2008) has been attributed to a rafting mode of long-distance dispersal. Some even outranged the distribution of *M. roaldi* by far, e.g. a doridid sea-slug species (similar 16S haplotype separated by ~6,200 km) (Wilson *et al.* 2009b) and a serolid isopod species (closely related COI haplotypes and microsatellites ~2,000 km apart) (Leese *et al.* 2010). Such dispersal events are probably rare but explainable on the background of certain attributes of lifestyle of the respective species.

Usually, rafting on preferred food items or on structures used for egg-clutch deposition that are vulnerable to drifting is assumed for explanation (Helmuth *et al.* 1994; Wilson *et al.* 2009b; Leese *et al.* 2010). Based on its morphology, we assume that *M. roaldi*, like probably all Macrostylidae, can be regarded a soft-sediment dweller that is unlikely to climb or hold on to potential rafting structures like algae or sponges. Instead, it digs in the top layer

of the sediment. Such behavior was observed only for *M. spinifera* by Hessler and Strömberg (1989).

Nevertheless, it is likely to be similar to other known species of the family on the basis of strong similarities in morphological features attributed to a burrowing or tubicolous lifestyle.

Locomotory abilities are strongly correlated with morphology (Hessler & Strömberg 1989; Wägele 1989). This assumption is further supported by other morphological (Thistle & Wilson 1987) as well as sampling evidence (Hessler & Sanders 1967; Wilson 2008b). We can hence regard rafting an implausible explanation for the wide distribution of *M. roaldi*. A drifting mode of dispersal, however, cannot generally be excluded. Brökeland (2010) as well as Brix and co-workers (2011) have shown that some janiroidean isopods must be capable to maintain connectivity between populations across long distances and physical (topographic) barriers. They found evidence for gene flow connecting two populations of a strictly non-natatory isopod from the South Atlantic abyss across a strong topographic barrier, the Walvis Ridge.

Deep-sea currents have been suggested to facilitate migration and dispersal in abyssal benthic organisms (Kaiser *et al.* 2009; Brandão *et al.* 2010; Menzel *et al.* 2011), possibly even more benthic storms (Thistle *et al.* 1985). Instead of individual movement, bottom currents and other erosion-deposition events on the shelf may be much more an important factor to realize dispersal beyond individual locomotory range by passive translocation with soft sediments (Thistle *et al.* 1985). No morphological features have been identified in *M. roaldi* that could be related to active swimming. However, the cuticle of *M. roaldi* is translucent and therefore not heavily calcified. This characteristic might facilitate passive transport in bottom-water currents. Enhanced sampling effort and standardized application of integrative taxonomy (com-

binning several sources of evidence, e.g. morphology and DNA) would help to clarify this picture.

Genetic Structure

Across many benthic taxa in Antarctica, species have a wide distribution. Re-examinations by molecular means however, have often revealed a more complex picture. Species have been found to comprise several previously unrecognized lineages, ‘cryptic’ species or species complexes (Held 2003; Held & Wägele 2005; Raupach & Wägele 2006; Brandt *et al.* 2007b; Brökeland & Raupach 2008; Brandão *et al.* 2010; Krabbe *et al.* 2010, but see Raupach *et al.* (2010)).

With two point mutations in the 12S and COI fragments and no variation at all in the 16S sequences across all *M. roaldi* samples, in our study molecular results are in accordance with morphological findings. The potential existence of cryptic species within the samples could be ruled out. The depth-differentiation hypothesis and the isolation-by-distance hypothesis could both be rejected. The homogenized gene pool across at least 1,000 m depth is an indicator for gene flow between shelf and slope. Beyond that, the lacking (mitochondrial) genetic diversity of *M. roaldi* in this area of the world cannot be explained by maintained gene flow alone.

The assumption of a bottleneck scenario (Hoelzel 1999; Weber *et al.* 2000; Wilson *et al.* 2009a), probably accompanied with slow mutation rates, and a relatively recent colonization is necessary to explain the observed pattern. The absence of nucleotide variation might thus still show the consequences of recolonization following the Last Glacial Maximum around 14,500 years ago (Clark *et al.* 2009). However, selective sweep (Amos &

Harwood 1998) cannot be ruled out as an alternative explanation. This phenomenon is driven by maternally-transferred endosymbionts (Hurst & Jiggins 2005) causing selection to favor one mitochondrial variant over another.

Evidence for Shelf Refuges?

The idea that Antarctic benthic fauna partially survived the last glacial period in refuges is now generally accepted. However, their locations are still a matter of debate and the same is true for potential mechanisms of the fauna to survive (Dayton & Oliver 1977; Brey *et al.* 1996; Thatje *et al.* 2008; Wilson *et al.* 2009b; Barnes & Hillebrand 2010; Barnes & Kuklinski 2010; Kaiser *et al.* 2011).

The data presented here allow inference of the presence of only one well-linked or recently spread population of *M. roaldi* in the sampled area, i.e. across several hundreds of kilometers from the inner to the outer shelf. Given the glaciological history of Pine Island Bay (Lowe & Anderson 2002) and current strong environmental changes that influence the study area (Thatje *et al.* 2005; Kaiser *et al.* 2009), *M. roaldi* might represent either a pioneer species which emerged from greater depth or an in-situ survivor from past major glaciations. Refuges have been mostly suggested to be located either at deeper bathyal or abyssal depth (Thatje *et al.* 2005). Yet, depth-related physiological barriers (Etter & Rex 1990; France 1994; Etter *et al.* 2005) may hinder migration across depth, especially for benthic organisms. The Antarctic, however, is known for a high degree of eurybathic taxa (Brandt *et al.* 2009), which can be interpreted as adaptation to oscillation of glacial extensions (Brey *et al.* 1996). As our data show that *M. roaldi* occurs across at least 1,000 m depth range, migratory capabilities of macrostylids amongst other deep-sea isopods (Brökeland 2010; Brix *et al.*

2011) could be underestimated. Additionally, the polar-emergence hypothesis is in concordance with a bottleneck scenario regarding a founder effect.

The fact that sampling at the shelf break and in deep bathyal depths did not yield any individuals belonging to this species does not exclude their possible existence there. Thus, *M. roaldi* might well have colonized the shelf from the abyss following the Last Glacial Maximum. However, as no abyssal material is available for this species from off Pine Island Bay and *M. roaldi* has never been reported from elsewhere, there is no evidence to either support or decline this theory. Contrastingly, slope refuges are regarded as implausible due to frequent sedimentary cascades caused by protruding glaciers. Such is theorized to have wiped out most of the fauna (Thatje *et al.* 2005; Barnes & Kuklinski 2010). This was not necessarily true all around the continent as West and East Antarctic Ice Sheets showed great differences in their maximum extent as well as diachronous expansions and retreats (Anderson *et al.* 2002, and see Kaiser *et al.* (2011)).

There is undoubtedly strong evidence for glaciers having widely bulldozed sediment to the shelf break at Pine Island Bay (Lowe & Anderson 2002; Dowdeswell *et al.* 2006) making survival for the benthos down the slope difficult. Nevertheless, mass-wasting impact was mainly localized in canyons or gullies created by and concentrating down-slope cascades of melt water, sediment and rock during maximum extent of the glaciers. Such gullies have been found at the Pine Island Bay slope (Lowe & Anderson 2002) and are characterized by valleys of 100–250 m depth with adjacent flanks and plateaus. Consequently during the Last Glacial Maximum, the slope was strongly structured featuring some areas of high and others of much lower impact, in the latter of which survival might have been easily possible (see Okey (1997)).

Furthermore, Antarctic benthic fauna shows high resilience to periodic disturbance (Kaiser *et al.* 2011) and the possibility for shelf fauna to survive major glaciations on the slope can hence not be excluded. Sediment cascades down slope would promote bottlenecks through habitat fragmentation and partial habitat destruction. Given further the close proximity of the slope to the shelf plus the observed depth distribution of *M. roaldi*, the slope-refuge scenario may seem somewhat more likely than colonization from the abyss. Alternatively, refuges may have existed in shelf pockets free from ice sheets or under the glaciers. The existence of ice-free refuges on the shelf has been repeatedly suggested (Dayton & Oliver 1977; Brandt 1991; Thatje *et al.* 2005; Barnes & Kuklinski 2010; Kaiser *et al.* 2011) but biological data supporting this theory are scarce.

Marine fauna has been found under glaciers up to hundreds of kilometers from the open sea (Lipps *et al.* 1979; Stockton & DeLaca 1982; Riddle *et al.* 2007; Gutt *et al.* 2011) so survival is possible there under certain conditions. Glaciers decoupled from the sediment are a prerequisite for this theory. Furthermore, a marine environment, i.e. supply with saline and oxygenated sea water, is a required feature of a subglacial refuge. The same holds true, but probably to a smaller extent, for the advection of food items from open water (Riddle *et al.* 2007) as macrostylids have been found to mainly rely on phytodetritus (Würzberg *et al.* 2011). Parallels between the environmental conditions in such subglacial shelf refuges with those found in the deep sea or in marine caves (Hart Jr *et al.* 1985; Wilkens *et al.* 1986) are obvious, especially with regard to limited food availability and stable abiotic conditions (Bonn *et al.* 1998).

So we even argue that in the practical absence of food influx, survival in shelf refuges under the ice would have been possible for especially un-

demanding and persistent small-sized organisms originating from deep-sea fauna, such as macrostylids. Nevertheless, either as shelf pockets or subglacial refugia, life on the shelf during the Last Glacial Maximum would have been affected by extreme conditions and great reduction of available habitats. Populations were most likely fragmented and habitat size might have been reduced strongly (Clarke & Crame 2010). In consequence, the mitochondrial genotypes could have reached fixation. Subsequent postglacial (re-) colonization of the surrounding shelf area would have happened since 14,500–10,000 years (Lowe & Anderson 2002; Clark *et al.* 2009). That might not be sufficient to re-establish (mitochondrial) genetic diversity via chance mutations or secondary colonization from elsewhere (if a second population of this species survived). This scenario would provide an alternative explanation for the observed genetic structure in *M. roaldi*. Yet, it does not provide hints about where on the Amundsen Sea shelf such refuges could have existed.

Geophysical data suggest that the troughs on the inner shelf at Pine Island Bay, though possibly free from grounded ice sheets, were uninhabitable. They were under strong influence from subglacial melt water, sedimentation, gravel deposition and sliding ice (Lowe & Anderson 2002, 2003). Regular sediment-laden plumes (Lowe & Anderson 2002) would have had catastrophic effects on marine fauna there. Consequently, *M. roaldi* has most likely colonized these troughs following the glacial retreat rather than using them as a refuge. However, more data from adjacent subtidal, shelf, shelf-break and deep-sea areas are required to identify the full range of *M. roaldi*, its source population, potential sister species and thus possible refuges.

Conclusions

Macrostylis roaldi n. sp. occurs widely in Pine Island Bay, in a geographic as well as bathymetric sense. Across its currently known distribution, this species is lacking (mitochondrial) genetic variability. This could be attributed to a bottleneck, probably caused by their emergence from bathyal or abyssal depth (founder effect) or by a catastrophic climate event such as the last glacial period that brought the ancestor population to close extinction. In the absence of nucleotide variability, we further see evidence for a colonization of the Pine Island Bay shelf by this species that must have happened relatively recently, following the Last Glacial Maximum (i.e. since 14,500–10,000 years). The lack of genetic structure and missing knowledge about closely-related species do not allow inference of a potential refuge. Assessment of the current knowledge about the glaciological history of the area plus the available evidence for life under ice sheets led to the conclusion that all three potential survival scenarios, i.e. on the shelf or polar emergence from the bathyal or abyssal provide equally plausible explanations for the observed pattern.

Acknowledgements

We are grateful to the master and crew of RV James Clark Ross. We would like to thank K. Linse, D.K.A. Barnes, H.J. Griffiths and C. Sands for their help on board sorting the samples, and making the material available. D.K.A. Barnes and W. Goodall-Copestake gave valuable comments which improved an earlier version of the manuscript. DNA was sequenced at the Smithsonian NMNH with support from K. Jeskulke, A. Driskell, A. Ormos and S. Brix. The latter kindly gave access to her micro-

scope. R. Walter provided invaluable help at the SEM. J. Ruch's constructive criticism on the original manuscript and her assistance with statistics were greatly appreciated. G.D.F. (Buz) Wilson is greatly acknowledged for many fruitful discussions during a visit at the Australian Museum which significantly improved this manuscript. He and the Marine Invertebrates Department at the Australian Museum are thanked for providing working space and support during the preparation of this article.

Funding: Two LAB visits at the National Museum of National History of Torben Riehl were partly funded by the “Census of the Diversity of Abyssal Marine Life” taxonomic exchange fellowship and the “Stiftung Universität Hamburg”. Preparation of this manuscript benefitted from a Ph.D. fellowship to the first author by the “German national academic foundation” (Studienstiftung des Deutschen Volkes) and a travel grant from the same source. Stefanie Kaiser acknowledges a grant provided by the University of Hamburg (“Innovationsfond”). The funders had no role in study design, data collection and analysis, decision to publish, or preparation of the manuscript.

Competing Interests: The authors have declared that no competing interests exist.

References

- Allcock, A.L., Barratt, I., Eléaume, M., Linse, K., Norman, M.D., Smith, P.J., Steinke, D., Stevens, D.W. & Strugnell, J.M. (2011) Cryptic speciation and the circumpolarity debate: A case study on endemic Southern Ocean octopuses using the COI barcode of life. *Deep Sea Research Part II: Topical Studies in Oceanography* 58, 242–249.
- Amos, W. & Harwood, J. (1998) Factors affecting levels of genetic diversity in natural populations. *Philosophical Transactions of the Royal Society of London. Series B: Biological Sciences* 353, 177–186.

- Anderson, J.B., Shipp, S.S., Lowe, A.L., Smith Wellner, J. & Mosola, A.B. (2002) The Antarctic Ice Sheet during the Last Glacial Maximum and its subsequent retreat history: a review. *Quaternary Science Reviews* 21, 49–70.
- Arango, C.P., Soler-Membrives, A. & Miller, K.J. (2011) Genetic differentiation in the circum-Antarctic sea spider *Nymphon australe* (Pycnogonida; Nymphonidae). *Deep-Sea Research Part II: Topical Studies in Oceanography* 58, 212–219.
- Barnes, D.K.A. & Hillebrand, C. (2010) Faunal evidence for a late quaternary trans-Antarctic seaway. *Global Change Biology* 16, 3297–3303.
- Barnes, D.K.A. & Kuklinski, P. (2010) Bryozoans of the Weddell Sea continental shelf, slope and abyss: did marine life colonize the Antarctic shelf from the deep water, outlying islands or *in situ* refugia following glaciations? *Journal of Biogeography* 37, 1648–1656.
- Bensasson, D., Zhang, D.X., Hartl, D.L. & Hewitt, G.M. (2001) Mitochondrial pseudogenes: evolution's misplaced witnesses. *Trends in Ecology & Evolution* 16, 314–321.
- Birstein, Y.A. (1970) New Crustacea Isopoda from the Kurile-Kamchatka Trench area. In: V. G. Bogorov (Ed), *Fauna of the Kurile-Kamchatka Trench and its environment*. Proceedings of the Shirshov Institute of Oceanology. Academy of Sciences of the USSR, Moscow, pp. 308–356. (In Russian)
- Birstein, Y.A. (1973) Deep water isopods (Crustacea, Isopoda) of the north-western part of the Pacific Ocean. *Akademiya Nauk, SSSR: Moscow*, 1–213. (In Russian)
- Bonn, W.J., Gingele, F.X., Grobe, H., Mackensen, A. & Fütterer, D.K. (1998) Palaeoproductivity at the Antarctic continental margin: opal and barium records for the last 400 ka. *Palaeogeography Palaeoclimatology Palaeoecology* 139, 195–211.
- Brandão, S.N., Sauer, J. & Schön, I. (2010) Circumantarctic distribution in Southern Ocean benthos? A genetic test using the genus *Macroscapha* (Crustacea, Ostracoda) as a model. *Molecular Phylogenetics and Evolution* 55, 1055–1069.
- Brandt, A. (1991) Zur Besiedlungsgeschichte des antarktischen Schelfes am Beispiel der Isopoda (Crustacea, Malacostraca) [Colonization of the Antarctic shelf by the Isopoda (Crustacea, Malacostraca)]. *Berichte zur Polarforschung [Reports on polar research]* 98, 1–240. (In German)
- Brandt, A. (1992a) New Asellota from the Antarctic deep sea (Crustacea, Isopoda, Asellota), with descriptions of two new genera. *Zoologica Scripta* 21, 57–78.
- Brandt, A. (1992b) Origin of Antarctic Isopoda (Crustacea, Malacostraca). *Marine Biology* 113, 415–423.
- Brandt, A. (1999) On the origin and evolution of Antarctic Peracarida (Crustacea, Malacostraca). *Scientia Marina* 63, 261–274.
- Brandt, A. (2002) *Desmostylis gerdesi*, a new species (Isopoda: Malacostraca) from Kapp Norvegia, Weddell Sea, Antarctica. *Proceedings of the Biological Society of Washington* 115, 616–627.
- Brandt, A. (2004) New deep-sea species of Macrostylidae (Asellota: Isopoda: Malacostraca) from the Angola Basin off Namibia, South West Africa. *Zootaxa* 448, 1–35.
- Brandt, A., Bathmann, U., Brix, S., Cisewski, B., Flores, H., Göcke, C., Janussen, D., Krägefsky, S., Kruse, S., Leach, H., Linse, K., Pakhomov, E., Peeken, I., Riehl, T., Sauter, E., Sachs, O., Schüller, M., Schrödl, M., Schwabe, E., Strass, V., van Franeker, J.A. & Wilmsen, E. (2011) Maud Rise – a snapshot through the water column. *Deep Sea Research Part II: Topical Studies in Oceanography* 58, 1962–1982.
- Brandt, A., De Broyer, C., De Mesel, I., Ellingsen, K.E., Gooday, A.J., Hilbig, B., Linse, K., Thomson, M.R.A. & Tyler, P.A. (2007a) The biodiversity of the deep Southern Ocean benthos. *Philosophical Transactions of the Royal Society B: Biological Sciences* 362, 39–66.
- Brandt, A., Gooday, A.J., Brandao, S.N., Brix, S., Brökeland, W., Cedhagen, T., Choudhury, M., Cornelius, N., Danis, B., de Mesel, I., Diaz, R.J., Gillan, D.C., Ebbe, B., Howe, J.A., Janussen, D., Kaiser, S., Linse, K., Maljutina, M.V., Pawlowski, J., Raupach, M.J. & Vanreusel, A. (2007b) First insights into the biodiversity and biogeography of the Southern Ocean deep sea. *Nature* 447, 307–311.
- Brandt, A., Linse, K. & Schüller, M. (2009) Bathymetric distribution patterns of Southern Ocean macrofaunal taxa: Bivalvia, Gastropoda, Isopoda and Polychaeta. *Deep Sea Research Part I: Oceanographic Research Papers* 56, 2013–2025.
- Brenke, N. (2005) An epibenthic sledge for operations on marine soft bottom and bedrock. *Marine Technology Society Journal* 39, 10–21.
- Brey, T., Dahm, C., Gorny, M., Klages, M., Balke, M. & Arntz, W.E. (1996) Do antarctic benthic invertebrates show an extended level of eurybathy? *Antarctic Science* 8, 3–6.
- Brey, T., Klages, M., Dahm, C., Gorny, M., Gutt, J., Hain, S., Stiller, M., Arntz, W.E., Wägele, J.-W. & Zimmermann, A. (1994) Antarctic benthic diversity. *Nature* 368, 297.
- Brix, S., Riehl, T. & Leese, F. (2011) First genetic data for *Haploniscus rostratus* and *Haploniscus unicornis* from neighbouring deep-sea basins in the South Atlantic. *Zootaxa* 2838, 79–84.
- Brix, S. & Svavarsson, J. (2010) Distribution and diversity of desmosomatid and nannoniscid isopods (Crustacea) on the Greenland–Iceland–Faeroe Ridge. *Polar biology* 33, 515–530.
- Brökeland, W. (2010) Redescription of *Haploniscus rostratus*

- (Menzies, 1962) (Crustacea: Peracarida: Isopoda) with observations on the postmarsupial development, size ranges and distribution. *Zootaxa* 2521, 1–25.
- Brökeland, W. & Raupach, M.J. (2008) A species complex within the isopod genus *Haploniscus* (Crustacea: Malacostraca: Peracarida) from the Southern Ocean deep sea: a morphological and molecular approach. *Zoological Journal of the Linnean Society* 152, 655–706.
- Buhay, J.E. (2009) “COI-like” sequences are becoming problematic in molecular systematic and DNA barcoding studies. *Journal of Crustacean Biology* 29, 96–100.
- Clark, P.U., Dyke, A.S., Shakun, J.D., Carlson, A.E., Clark, J., Wohlfarth, B., Mitrovica, J.X., Hostetler, S.W. & McCabe, A.M. (2009) The Last Glacial Maximum. *Science* 325, 710–714.
- Clarke, A. (2003) The Polar Deep Sea. In: *The Deep Seafloor. Ecosystems of the World*. Elsevier, Amsterdam, Lausanne, New York, Oxford, Shannon, Singapore, Tokyo, pp. 239–260.
- Clarke, A., Aronson, R.B., Crame, J.A., Gili, J.M. & Blake, D.B. (2004) Evolution and diversity of the benthic fauna of the Southern Ocean continental shelf. *Antarctic Science* 16, 559–568.
- Clarke, A., Barnes, D.K.A. & Hodgson, D.A. (2005) How isolated is Antarctica? *Trends in Ecology & Evolution* 20, 1–3.
- Clarke, A. & Crame, J.A. (2010) Evolutionary dynamics at high latitudes: Speciation and extinction in polar marine faunas. *Philosophical Transactions of the Royal Society B: Biological Sciences* 365, 3655–3666.
- Clarke, A. & Johnston, N.M. (2003) Antarctic marine benthic diversity. *Oceanogr Mar Biol Annu Rev* 41, 47–114.
- Coleman, C.O. (2003) “Digital inking”: how to make perfect line drawings on computers. *Organisms Diversity & Evolution* 3, 303–304.
- Coleman, C.O. (2009) Drawing setae the digital way. *Zoosystematics and Evolution* 85, 305–310.
- Dayton, P.K. & Oliver, J.S. (1977) Antarctic soft-bottom benthos in oligotrophic and eutrophic environments. *Science* 197, 55–58.
- Dowdeswell, J.A., Evans, J., Cofaigh, C.Ó. & Anderson, J.B. (2006) Morphology and sedimentary processes on the continental slope off Pine Island Bay, Amundsen Sea, West Antarctica. *Geological Society of America Bulletin* 118, 606–619.
- Drummond, A.J., Ashton, B., Buxton, S., Cheung, M., Cooper, A., Duran, C., Field, M., Heled, J., Kearse, M., Markowitz, S., Moir, R., Stones-Havas, S., Sturrock, S., Thierer, T. & Wilson, A. (2011) Geneious v5.4. Available from: <http://www.geneious.com/>.
- Etter, R.J. & Rex, M.A. (1990) Population differentiation decreases with depth in deep-sea gastropods. *Deep Sea Research Part I: Oceanographic Research* 37, 1251–1261.
- Etter, R.J., Rex, M.A., Chase, M.R. & Quattro, J.M. (2005) Population differentiation decreases with depth in deep-sea bivalves. *Evolution; International Journal of Organic Evolution* 59, 1479–1491.
- France, S.C. (1994) Genetic population structure and gene flow among deep-sea amphipods, *Abyssoorchomene* spp., from six California Continental Borderland basins. *Marine Biology* 118, 67–77.
- France, S.C. & Kocher, T.D. (1996) Geographic and bathymetric patterns of mitochondrial 16S rRNA sequence divergence among deep-sea amphipods, *Eurythenes gryllus*. *Marine Biology* 126, 633–643.
- Gurjanova, E. (1933) Die marinen Isopoden der Arktis. *Fauna Arctica* 6, 391–470. (In German)
- Gutt, J., Barratt, I., Domack, E., d’Udekem d’Acoz, C., Dimmler, W., Grémare, A., Heilmayer, O., Isla, E., Janussen, D., Jorgensen, E., Kock, K.-H., Sophia Lehnert, L., López-González, P., Langner, S., Linse, K., Eugenia Manjón-Cabeza, M., Meißner, M., Montiel, A., Raes, M., Robert, H., Rose, A., Sañé Schepisi, E., Saucède, T., Scheidat, M., Schenke, H.-W., Seiler, J. & Smith, C. (2011) Biodiversity change after climate-induced ice-shelf collapse in the Antarctic. *Deep Sea Research Part II: Topical Studies in Oceanography* 58, 74–83.
- Hansen, H.J. (1916) Crustacea Malacostraca: The order Isopoda. *Danish Ingolf Expedition* 3, 1–262.
- Harrison, K. (1989) Are deep-sea asellote isopods infaunal or epifaunal? *Crustaceana* 56, 317–319.
- Hart Jr, C.W., Manning, R.B. & Iliffe, T.M. (1985) The fauna of Atlantic marine caves: evidence of dispersal by sea floor spreading while maintaining ties to deep waters. *Proceedings of the Biological Society of Washington* 98, 288–292.
- Havermans, C., Nagy, Z.T., Sonet, G., De Broyer, C. & Martin, P. (2011) DNA barcoding reveals new insights into the diversity of Antarctic species of *Orchomene sensu lato* (Crustacea: Amphipoda: Lysianassoidea). *Deep Sea Research Part II: Topical Studies in Oceanography* 58, 230–241.
- Held, C. (2000) Phylogeny and biogeography of serolid isopods (Crustacea, Isopoda, Serolidae) and the use of ribosomal expansion segments in molecular systematics. *Molecular Phylogenetics and Evolution* 15, 165–178.
- Held, C. (2003) Molecular evidence for cryptic speciation within the widespread Antarctic crustacean *Ceratoserolis trilobitoides* (Crustacea, Isopoda). *Antarctic Biology in a Global Context*, 135–139.
- Held, C. & Wägele, J.-W. (2005) Cryptic speciation in the giant Antarctic isopod *Glyptonotus antarcticus* (Isopoda,

- Valvifera, Chaetiliidae). *Scientia Marina* 69, 175–181.
- Helmuth, B., Veit, R.R. & Holberton, R. (1994) Long-distance dispersal of a subantarctic brooding bivalve *Gaimardia trapesina* by kelp-rafting. *Marine Biology* 120, 421–426.
- Hessler, R.R. (1970) 15 The Desmosomatidae (Isopoda, Asellota) of the Gay Head-Bermuda Transect. G. O. S. Arrhebus, C. S. Cox, E. W. Fager, C. H. Hand, T. Newberry, and M. B. Schaefer (Eds). University of California Press, Berkeley, Los Angeles, London. Available from: <http://escholarship.org/uc/item/1mn198vx>.
- Hessler, R.R. & Sanders, H.L. (1967) Faunal diversity in the deep sea. *Deep Sea Research and Oceanographic Abstracts* 14, 65–70.
- Hessler, R.R. & Strömberg, J.O. (1989) Behavior of janiroidean isopods (Asellota), with special reference to deep sea genera. *Sarsia* 74, 145–159.
- Hessler, R.R. & Thistle, D. (1975) On the place of origin of deep-sea isopods. *Marine Biology* 32, 155–165.
- Hessler, R.R. & Wilson, G.D.F. (1983) The origin and biogeography of malacostracan crustaceans in the deep sea. In: R. W. Sims, J. H. Price, and P. E. S. Whalley (Eds), *Evolution, time, and space: the emergence of the biosphere*. Systematics Association Special Publication. Academic Press, London, pp. 227–254.
- Hoelzel, A. (1999) Impact of population bottlenecks on genetic variation and the importance of life-history; a case study of the northern elephant seal. *Biological Journal of the Linnean Society* 68, 23–39.
- Hunter, R.L. & Halanych, K.M. (2008) Evaluating connectivity in the brooding brittle star *Astrotoma agassizii* across the Drake Passage in the Southern Ocean. *Journal of Heredity* 99, 137–148.
- Hurst, G.D. & Jiggins, F.M. (2005) Problems with mitochondrial DNA as a marker in population, phylogeographic and phylogenetic studies: the effects of inherited symbionts. *Proceedings of the Royal Society B: Biological Sciences* 272, 1525–1534.
- Jarman, S., Elliott, N., Nicol, S. & McMinn, A. (2002) Genetic differentiation in the Antarctic coastal krill *Euphausia crystallorophias*. *Heredity* 88, 280–287.
- Kaiser, S. & Barnes, D.K.A. (2008) Southern Ocean deep-sea biodiversity: sampling strategies and predicting responses to climate change. *Climate Research* 37, 165–179.
- Kaiser, S., Barnes, D.K.A. & Brandt, A. (2007) Slope and deep-sea abundance across scales: Southern Ocean isopods show how complex the deep sea can be. *Deep-Sea Research Part II: Topological Studies in Oceanography* 54, 1776–1789.
- Kaiser, S., Barnes, D.K.A., Sands, C.J. & Brandt, A. (2009) Biodiversity of an unknown Antarctic Sea: assessing isopod richness and abundance in the first benthic survey of the Amundsen continental shelf. *Marine Biodiversity* 39, 27–43.
- Kaiser, S., Griffiths, H.J., Barnes, D.K.A., Brandão, S.N., Brandt, A. & O'Brien, P.E. (2011) Is there a distinct continental slope fauna in the Antarctic? *Deep Sea Research Part II: Topical Studies in Oceanography* 58, 91–104.
- Katoh, K., Misawa, K., Kuma, K. & Miyata, T. (2002) MAFFT: a novel method for rapid multiple sequence alignment based on fast Fourier transform. *Nucleic Acids Research* 30, 3059–3066.
- Kavanagh, F.A. & Wilson, G.D.F. (2007) Revision of the genus *Haplomesus* (Isopoda: Asellota: Ischnomesidae) with erection of four new genera. *Invertebrate Systematics* 21, 487–535.
- Kellogg, T.B. & Kellogg, D.E. (1987) Recent glacial history and rapid ice stream retreat in the Amundsen Sea. *Journal of Geophysical Research* 92, 8859–8864.
- Krabbe, K., Leese, F., Mayer, C., Tollrian, R. & Held, C. (2010) Cryptic mitochondrial lineages in the widespread pycnogonid *Colossendeis megalonyx* Hoek, 1881 from Antarctic and Subantarctic waters. *Polar Biology* 33, 281–292.
- Kussakin, O.G. (1999) 3 Marine and brackish-water isopods from cold and temperate waters of the Northern Hemisphere Suborder Asellota. Part 2. Families Joeropsididae, Nannoniscidae, Desmosomatidae, Macrostylidae. A. F. Alimov (Ed). Publication of the Zoological Institute of the Russian Academy of Sciences, St. Petersburg.
- Latreille, P.A. (1802) Histoire naturelle générale et particulière des Crustacés et des Insectes. In: G. L. L. de Buffon (Ed), *Histoire Naturelle generale et particuliere, nouvelle edition, accompagnee des notes*. Dufart, Paris, pp. 1–467. (In French)
- Lawver, L.A., Gahagan, L.M. & Dalziel, I.W.D. (2011) A different look at gateways: Drake Passage and Australia/Antarctica. In: J. B. Anderson and J. S. Wellner (Eds), *Tectonic, Climatic, and Cryospheric Evolution of the Antarctic Peninsula*. Special publication. AGU, Washington, D.C., pp. 5–33.
- Leese, F., Agrawal, S. & Held, C. (2010) Long-distance island hopping without dispersal stages: transportation across major zoogeographic barriers in a Southern Ocean isopod. *Naturwissenschaften* 97, 583–594.
- Linse, K., Cope, T., Lörz, A.-N. & Sands, C.J. (2007) Is the Scotia Sea a centre of Antarctic marine diversification? *Polar Biology* 30, 1059–1068.
- Lipps, J.H., Ronan, T.E. & Delaca, T.E. (1979) Life below the Ross Ice Shelf, Antarctica. *Science* 203, 447–449.
- Lowe, A.L. & Anderson, J.B. (2002) Reconstruction of the West Antarctic ice sheet in Pine Island Bay during the Last Glacial Maximum and its subsequent retreat history.

- Quaternary Science Reviews 21, 1879–1897.
- Lowe, A.L. & Anderson, J.B. (2003) Evidence for abundant subglacial meltwater beneath the paleo-ice sheet in Pine Island Bay, Antarctica. *Journal of Glaciology* 49, 125–138.
- Meinert, F.V.A. (1890) Crustacea malacostraca. In: *Videnskabelige udbytte af kanonbaden "Hauchs Dogter."*, pp. 147–230. (In Danish)
- Menzel, L., George, K.H. & Arbizu, P.M. (2011) Submarine ridges do not prevent large-scale dispersal of abyssal fauna: A case study of *Mesocletodes* (Crustacea, Copepoda, Harpacticoida). *Deep Sea Research Part I: Oceanographic Research Papers* 58, 839–864.
- Menzies, R.J. (1962) The isopods of abyssal depths in the Atlantic Ocean. In: J. L. Barnard, R. J. Menzies, and M. C. Bacescu (Eds), *Abyssal Crustacea*. Vema Research Series. Columbia University Press, New York, pp. 79–206.
- Menzies, R.J. & George, R.Y. (1972) Isopod Crustacea of the Peru-Chile Trench. *Anton Bruun Report* 9, 1–124.
- Menzies, R.J., George, R.Y. & Rowe, G.T. (1973) *Abyssal environment and ecology of the world oceans*. John Wiley & Sons, New York.
- Messing, J. (1983) New M13 vectors for cloning. *Methods in Enzymology* 101, 20–78.
- Mezhov, B.V. (1988) The first findings of Macrostylidae (Isopoda, Asellota) in the Indian Ocean. *Zoologicheskii Zhurnal* 67, 983–994.
- Mezhov, B.V. (1992) Two new species of the genus *Macrostylis* G.O.Sars, 1864 (Crustacea Isopoda Asellota Macrostylidae) from the Antarctic. *Arthropoda Selecta* 1, 83–87.
- Mezhov, B.V. (1993) Three new species of *Macrostylis* G.O. Sars, 1864 (Crustacea Isopoda Asellota Macrostylidae) from the Pacific Ocean. *Arthropoda Selecta* 2, 3–9.
- Nitsche, F.O., Jacobs, S.S., Larter, R.D. & Gohl, K. (2007) Bathymetry of the Amundsen Sea continental shelf: implications for geology, oceanography, and glaciology. *Geochemistry, Geophysics Geosystems* 8, Q10009.
- O'Loughlin, P.M., Paulay, G., Davey, N. & Michonneau, F. (2011) The Antarctic region as a marine biodiversity hotspot for echinoderms: Diversity and diversification of sea cucumbers. *Deep Sea Research Part II: Topical Studies in Oceanography* 58, 264–275.
- Okey, T.A. (1997) Sediment flushing observations, earthquake slumping, and benthic community changes in Monterey Canyon head. *Continental Shelf Research* 17, 877–897.
- Ratnasingham, S. & Hebert, P.D.N. (2007) bold: The Barcode of Life Data System (<http://www.barcodinglife.org>). *Molecular Ecology Notes* 7, 355–364.
- Raupach, M.J., Held, C. & Wägele, J.-W. (2004) Multiple colonization of the deep sea by the Asellota (Crustacea: Peracarida: Isopoda). *Deep Sea Research Part II: Topical Studies in Oceanography* 51, 1787–1795.
- Raupach, M.J., Mayer, C., Malyutina, M.V. & Wägele, J.-W. (2009) Multiple origins of deep-sea Asellota (Crustacea: Isopoda) from shallow waters revealed by molecular data. *Proceedings of the Royal Society B: Biological Sciences* 276, 799–808.
- Raupach, M.J., Thatje, S., Dambach, J., Rehm, P., Misof, B. & Leese, F. (2010) Genetic homogeneity and circum-Antarctic distribution of two benthic shrimp species of the Southern Ocean, *Chorismus antarcticus* and *Nematocarcinus lanceopes*. *Marine Biology* 157, 1783–1797.
- Raupach, M.J. & Wägele, J.-W. (2006) Distinguishing cryptic species in Antarctic Asellota (Crustacea: Isopoda)-a preliminary study of mitochondrial DNA in Acanthaspida drygalskii. *Antarctic Science* 18, 191–198.
- Riddle, M.J., Craven, M., Goldsworthy, P.M. & Carsey, F. (2007) A diverse benthic assemblage 100 km from open water under the Amery Ice Shelf, Antarctica. *Paleoceanography* 22, PA1204.
- Riehl, T. & Brandt, A. (2010) Descriptions of two new species in the genus *Macrostylis* Sars, 1864 (Isopoda, Asellota, Macrostylidae) from the Weddell Sea (Southern Ocean), with a synonymisation of the genus *Desmostylis* Brandt, 1992 with *Macrostylis*. *Zookeys* 57, 9–49.
- Riehl, T., Wilson, G.D.F. & Hessler, R.R. (2012) New Macrostylidae Hansen, 1916 (Crustacea: Isopoda) from the Gay Head-Bermuda transect with special consideration of sexual dimorphism. *Zootaxa* 3277, 1–26.
- Rignot, E., Bamber, J.L., Broeke, M.R. van den, Davis, C., Li, Y., Berg, W.J. van de & Meijgaard, E. van (2008) Recent Antarctic ice mass loss from radar interferometry and regional climate modelling. *Nature Geoscience* 1, 106–110.
- Sars, G.O. (1864) Om en anomal Gruppe af Isopoder. In: *Forhandlinger Videnskaps-Selskapet, Anar 1863*. Christiania, pp. 205–221.
- Sars, G.O. (1899) 2 An account of the Crustacea of Norway: with short descriptions and figures of all the species: Isopoda. A. Cammermeyer (Ed). Bergen Museum, Bergen.
- Sereno, P.C. (2007) Logical basis for morphological characters in phylogenetics. *Cladistics* 23, 565–587.
- Shepherd, A., Wingham, D. & Rignot, E. (2004) Warm ocean is eroding West Antarctic Ice Sheet. *Geophysical Research Letters* 31, L23402.
- Stockton, W.L. & DeLaca, T.E. (1982) Food falls in the deep sea: occurrence, quality, and significance. *Deep Sea Research Part A. Oceanographic Research Papers* 29, 157–169.

- Strugnell, J.M., Cherel, Y., Cooke, I.R., Gleadall, I.G., Hochberg, F.G., Ibáñez, C.M., Jorgensen, E., Laptikhovskiy, V.V., Linse, K., Norman, M., Vecchione, M., Voight, J.R. & Allcock, A.L. (2011) The Southern Ocean: Source and sink? *Deep Sea Research Part II: Topical Studies in Oceanography* 58, 196–204.
- Strugnell, J.M., Rogers, A.D., Prodöhl, P.A., Collins, M.A. & Allcock, A.L. (2008) The thermohaline expressway: the Southern Ocean as a centre of origin for deep-sea octopuses. *Cladistics* 24, 853–860.
- Tamura, K., Dudley, J., Nei, M. & Kumar, S. (2007) MEGA4: Molecular Evolutionary Genetics Analysis (MEGA) Software Version 4.0. *Molecular Biology and Evolution* 24, 1596–1599.
- Teske, P., Papadopoulos, I., Zardi, G., McQuaid, C., Edkins, M., Griffiths, C. & Barker, N. (2007) Implications of life history for genetic structure and migration rates of southern African coastal invertebrates: planktonic, abbreviated and direct development. *Marine Biology* 152, 697–711.
- Thatje, S., Hillenbrand, C.-D. & Larter, R. (2005) On the origin of Antarctic marine benthic community structure. *Trends in Ecology & Evolution* 20, 534–540.
- Thatje, S., Hillenbrand, C.-D., Mackensen, A. & Larter, R. (2008) Life hung by a thread: endurance of Antarctic fauna in glacial periods. *Ecology* 89, 682–692.
- Thistle, D. & Wilson, G.D.F. (1987) A hydrodynamically modified, abyssal isopod fauna. *Deep-Sea Research. Part A. Oceanographic Research Papers* 34, 73–87.
- Thistle, D., Yingst, J.Y. & Fauchald, K. (1985) A deep-sea benthic community exposed to strong near-bottom currents on the Scotian Rise (Western Atlantic). *Marine Geology* 66, 91–112.
- Thoma, M., Jenkins, A., Holland, D. & Jacobs, S. (2008) Modelling Circumpolar Deep Water intrusions on the Amundsen Sea continental shelf, Antarctica. *Geophysical Research Letters* 35, 1–6.
- Wägele, J.-W. (1989) 140 Evolution und phylogenetisches System der Isopoda: Stand der Forschung und neue Erkenntnisse [Evolution and phylogeny of isopods. New data and the state of affairs]. E. Schweizerbart'sche Verlagsbuchhandlung, Stuttgart. (In German)
- Weber, D.S., Stewart, B.S., Garza, J.C. & Lehman, N. (2000) An empirical genetic assessment of the severity of the northern elephant seal population bottleneck. *Current Biology* 10, 1287–1290.
- Wilkens, H., Parzefall, J. & Iliffe, T.M. (1986) Origin and age of the marine stygofauna of Lanzarote, Canary Islands. *Mitteilungen aus dem hamburgischen zoologischen Museum und Institut* 83, 223–230.
- Wilson, G.D.F. (1983) Variation in the Deep-Sea Isopod *Eurycope ipthima* (Asellota, Eurycopidae): Depth Related Clines in Rostral Morphology and in Population Structure. *Journal of Crustacean Biology* 3, 127–140.
- Wilson, G.D.F. (1989) 27 A systematic revision of the deep-sea subfamily Lipomerinae of the isopod crustacean family Munnopsidae. C. S. Cox, A. Fleminger, G. L. Kooyman, and R. H. Rosenblatt (Eds). University of California Press, Berkeley, Los Angeles, London.
- Wilson, G.D.F. (2008a) A review of taxonomic concepts in the Nannoniscidae (Isopoda, Asellota), with a key to the genera and a description of *Nannoniscus oblongus* Sars. *Zootaxa* 1680, 1–24.
- Wilson, G.D.F. (2008b) Local and regional species diversity of benthic Isopoda (Crustacea) in the deep Gulf of Mexico. *Deep-Sea Research Part II: Topological Studies in Oceanography* 55, 2634–2649.
- Wilson, G.D.F. & Hessler, R.R. (1987) Speciation in the Deep Sea. *Annual Reviews in Ecology and Systematics* 18, 185–207.
- Wilson, G.D.F., Humphrey, C.L., Colgan, D.J., Gray, K.-A. & Johnson, R.N. (2009a) Monsoon-influenced speciation patterns in a species flock of *Eophreatoicus* Nicholls (Isopoda; Crustacea). *Molecular Phylogenetics and Evolution* 51, 349–364.
- Wilson, N.G., Schrödl, M. & Halanych, K.M. (2009b) Ocean barriers and glaciation: evidence for explosive radiation of mitochondrial lineages in the Antarctic sea slug *Doris kerguelenensis* (Mollusca, Nudibranchia). *Molecular Ecology* 18, 965–984.
- Wolff, T. (1956) Isopoda from depths exceeding 6000 meters. *Galathea Report* 2, 85–157.
- Wolff, T. (1962) The systematics and biology of bathyal and abyssal Isopoda Asellota. *Galathea Report* 6, 1–320.
- Wright, S. (1938) Size of population and breeding structure in relation to evolution. *Science* 87, 430–2264.
- Wright, S. (1946) Isolation by distance under diverse systems of mating. *Genetics* 31, 39–59.
- Würzberg, L., Peters, J. & Brandt, A. (2011) Fatty acid patterns of Southern Ocean shelf and deep sea peracarid crustaceans and a possible food source, foraminiferans. *Deep Sea Research Part II: Topical Studies in Oceanography* 58, 2027–2035.

Author contributions

The study was designed and the article was written

by myself with contributions from S. Kaiser. I dissected the specimens, created the pencil drawings and descriptions; S. Kaiser transferred the drawings into digital format. Additional funding to S. Kaiser was available from the 'Innovationsfond' of the University of Hamburg through A. Brandt. The molecular part of the study was conducted by myself at the Smithsonian National Museum of Natural History with contributions from A. Driskell, A. Ormos and K. Jeskulke. Field work and preliminary species identification was conducted by S. Kaiser.

Chapter 4

Southern Ocean Macrostylidae reviewed with a key to the species and new descriptions from Maud Rise

Published as: Riehl, T. & Brandt, A. (2013) Southern Ocean Macrostylidae reviewed with a key to the species and new descriptions from Maud Rise. *Zootaxa*, 3692(1), 160–203. <http://dx.doi.org/10.11646/zootaxa.3692.1.10>; <http://zoobank.org/urn:lsid:zoobank.org:pub:256C3764-07AD-48E8-9152-B4E59DF862CB>

Abstract

The nine currently known Southern Ocean species of the asellote isopod family Macrostylidae Hansen, 1916 are reviewed. Modified diagnoses are provided. Two new species, *Macrostylis matildae* n. sp. and *M. scotti* n. sp. are formally de-scribed. *M. setulosa* Mezhov, 1992, and *M. vinogradovae* Mezhov, 1992 are redescribed. An identification key to all species is presented. Due to substantial damage and loss of type material, *M. obscura* (Brandt, 1992) and *M. sarsi* Brandt, 1992 are henceforward considered *nomina dubia*. DNA sequences were yielded for molecular characterization of both new species. A phylogenetic analysis shows, although from the same locality, both species are relatively distantly related. Huge divergence is discovered within Macrostylidae which casts doubt on the monotypy of the family.

Keywords: Janiroidea, benthos, deep sea, bathyal, abyssal, Antarctica, new species, ANDEEP-SYSTCO, Maud Rise, Southern Ocean, seamount

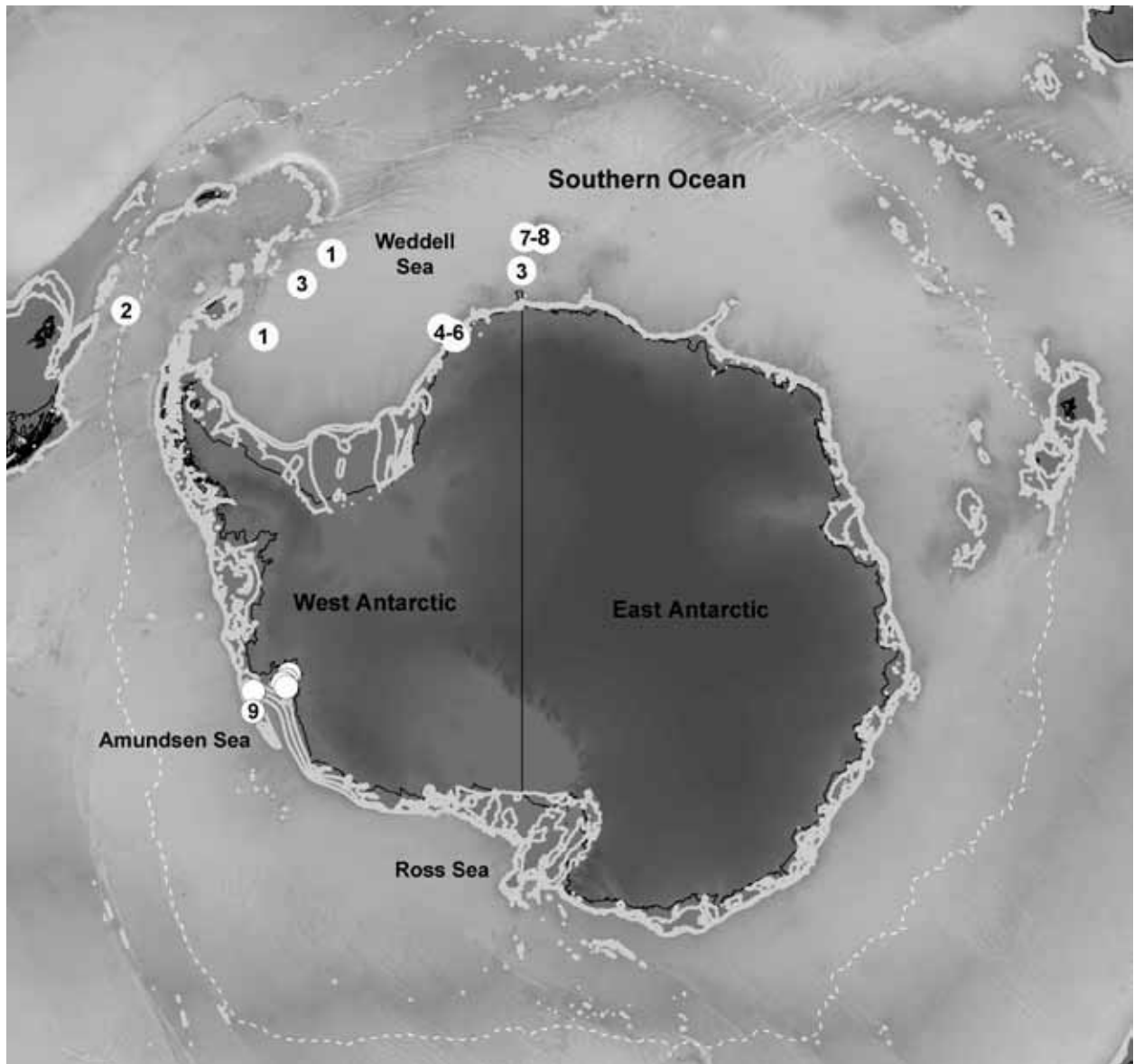


Figure 1. Type localities of Macrostyliidae from the Southern Ocean. 1) *Macrostyliis antennamagna* Riehl & Brandt, 2010. 2) *M. setulosa* Mezhov, 1992. 3) *M. uniformis* Riehl & Brandt, 2010. 4) *M. vinogradovae* Mezhov, 1992. 5) *M. cerrita* Vey & Brix, 2009. 6) *M. gerdesi* (Brandt, 2002). 7) *M. sarsi* Brandt, 1992; *M. obscura* (Brandt, 1992). 8) *M. matildae* n. sp.; *M. scotti* n. sp. 9) *M. roaldi* Riehl & Kaiser, 2012.

Introduction

Presently, nine species of the deep-sea isopod family Macrostyliidae Hansen, 1916 are formally described from the Southern Ocean (Riehl & Brandt 2010; Riehl & Kaiser 2012), almost exclusively from the Atlantic sector (Fig. 1). Many more undescribed species have been discovered, e.g. during the ANDEEP and ANDEEP-SYSTCO expeditions to the Scotia, Weddell and Lazarev Seas (Brandt *et al.* 2004, 2007a; b, 2011b; Kaiser *et al.* 2007) in the Atlantic sector, as well as in the Ross, Bellingshausen (Riehl, unpublished data)

and Amundsen Seas (Riehl & Kaiser 2012), yet most remain undescribed. That is, first of all, due to the imbalance between numbers of undescribed material and available specialized taxonomists but also because of the abundance and quality of the material available (Riehl *et al.* 2012) and a general scarcity of knowledge about this aberrant taxon.

Although Brandt *et al.* (2009) reported the bathymetric distribution of Macrostyliidae for bathyal and abyssal depths only, species of this family have been also, but less frequently, collected on the shelf (Brandt 2002; Riehl & Kaiser 2012). The currently known overall depth range of this taxon

in the Southern Ocean extends from rather shallow shelf and seamounts (239 m, *Macrostylis gerdesi* (Brandt, 2002)) to abyssal depth (4,975 m, *M. uniformis* Riehl & Brandt, 2010). The smaller number of shallow-water records might be due to sampling bias caused by rather large mesh sizes usually deployed on the Antarctic shelf. Small-meshed gear, such as the epibenthic sledge *sensu* Brenke (2005) or Brandt *et al.* (2013) more suitable for collecting benthic macrofauna, were only recently applied there (e.g. Kaiser *et al.* 2008; 2011; 2013). Findings in the Amundsen Sea, however, revealed Macrostylidae to be rather common, at least in certain shelf areas of the Antarctic (Kaiser *et al.* 2009; Riehl & Kaiser 2012). Generality of this phenomenon has yet to be shown.

The origin of Macrostylidae is likely to be located in the deep sea (Hessler & Thistle 1975; Wilson 1999; Raupach *et al.* 2004; Lins *et al.* 2012), and a polar-emergence scenario (Brandt 1992b) is hence the most plausible explanation for their occurrence on the Antarctic shelf and on seamounts. It has been hypothesized that macrostylids might have locally colonized the shelf from the abyss as recent as after the last glacial period, i.e. within the last 10,000–14,500 years, and that their actual mobility has been previously underestimated (Riehl & Kaiser 2012). Multiple independent colonization events of the shelf by several different species of this family are therefore possible. Despite the common presence of macrostylids in deep-sea sediments, intrafamilial phylogenies or family revisions are to date lacking. The family is monotypic (Riehl & Brandt 2010).

In this article, two new species of Macrostylidae, *Macrostylis scotti* n. sp. and *M. matildae* n. sp. are described from the slope of Maud Rise, a seamount in the Lazarev Sea. The first molecular inference of phylogeny for Macrostylidae based on the 16S mitochondrial DNA marker is provided in

this paper. Furthermore, all previously described species of the genus *Macrostylis* Sars, 1864 from the Southern Ocean are reviewed. Modified diagnoses of each species are provided. An illustrated key for identification is presented. *M. setulosa* Mezhov, 1992 and *M. vinogradovae* Mezhov, 1992 are redescribed. Due to substantial damage and loss of type material, *M. sarsi* Brandt, 1992 and *M. obscura* (Brandt, 1992) are henceforward considered *nomina dubia*.

Material and methods

Sampling

New species described in this study were collected during the ANDEEP-SYSTCO (Brandt *et al.* 2011b) expedition in the Lazarev Sea, Southern Ocean. The expedition was conducted with R/V Polarstern. Samples were collected by means of an epibenthic sledge *sensu* Brenke (2005). The type locality on the seamount Maud Rise was characterized by relatively high velocity, temperature, and influx of organic matter when compared to adjacent areas (Brandt *et al.* 2011a), as well as coarse, sandy sediment and low megafaunal abundances (Brenke *et al.* 2011). This region of the Southern Ocean features distinct hydrographical conditions, such as a Taylor Column. These are thought to be relevant for peculiar faunal characteristics observed there: distinct composition and strong dominance by few taxa (Brandt *et al.* 2011a). Oceanographic and topographic features of the type locality have been described and discussed in detail by Brandt *et al.* (2011a).

Next to the new descriptions, two further new species were included in the molecular analyses. These were collected in the South Polar Front during the same cruise at station PS71/13-16:

2,996–3,000 m depth; start trawl at 0° 01.12W, 52° 01.97S; end trawl at 0° 01.14 W, 52° 01.80S. A taxonomic study was not performed on these due to low numbers of specimens available. A complete station list and gear details were documented by Bathmann *et al.* (2010).

Taxonomy

Character states from all Antarctic species of Macrostyliidae were gathered from the literature and type material. The computer software DELTA (Dallwitz 1980, 1993; Dallwitz *et al.* 2010) was used to assemble data and generate descriptions. An identification key was prepared using KEY (Dallwitz 1974) as implemented in DELTA. To allow identification to species level without any dissections, easy-to-see characters such as habitus morphology were selected with priority. The maximum of four confirmatory characters in KEY was manually complemented with further characters in order to allow more exact identification.

Terminology similar to previous studies (Wilson 1989; Riehl & Brandt 2010; Riehl *et al.* 2012) was used. Additional terms are introduced here. The pereopod III ischium dorsal lobe is called “flat, rounded” in cases when the slopes are convex. When the slopes are straight, the lobe is considered “triangular”. Concave slopes indicate a “tapering” lobe. The lateral constriction anteriorly to uropod insertions are called “waist”. The operculum is stout if its length does not exceed 1.5 times its width whereas it is elongate when it does. Distal opercular setae are long if their length exceeds half the length of the operculum, short if they are shorter. A distally tapering operculum is defined by distolaterally concave margins, otherwise it is ovoid. The apical width of the operculum is defined by the most laterally articulating pappose apical setae and provides a useful measure when related to the total width of the operculum.

Setae without a distinct distally-located sensillum are called asensillate setae.

Measurements were taken from scanned line drawings applying the distance-measurement tool embedded in Adobe Acrobat Professional and in accordance with the methods described by Hessler (1970). We use the term subequal to mean ‘within 5% of a measurement’ (Kavanagh and Wilson 2007). A stage micrometer was used for calibration. All appendages article-length ratios are given in proximal to distal order, excluding setae. For habitus illustrations and dissections, whole specimens were transferred from 96% ethanol to an ethanol-glycerin solution (1:1) and subsequently to glycerin. For illustration of appendages in standard views, dissected parts were temporarily mounted on slides following Wilson (2008) and stained with methyl green or chlorazol black. Informations about features and arrangement of setae on the appendages are important components of the descriptions and their order of description follows Riehl *et al.* (2012). Finally, dissected appendages were mounted on permanent slides using either Hydromatrix or Euparal following Riehl & Kaiser (2012). A *Carl Zeiss Leo 1525* microscope was used for SEM. Photographs were taken using a Olympus SZX16 stereo microscope fitted with an Olympus SC30 microscope camera and using the corresponding software CellSense Entry 1.6. To increase focal depth, Helicon Focus 4.80 was used to merge stacks of photographs. SEM stubs, whole specimens and slides were deposited at the Zoological Museum, University of Hamburg, Germany, accession numbers have a “ZMH K-“ prefix.

Molecular laboratory methods

For DNA analyses, specimens were bulk fixed with the sediment in 96% cooled ethanol (undenatured) and kept in -30°C for the first 24 hours. Subsequently, the fixative was replaced by new

Table 1. 12S, 16S and COI primers.

Primer name	Sequence [5' – 3']	Reference
16S AR	CGCCTGTTTATCAAAAACAT	(Palumbi <i>et al.</i> 1991)
16S BR	CCGGTCTGAACTCAGATCACG	(Palumbi <i>et al.</i> 1991)
16S SF	GACCGTGCTAAGGTAGCATAATC	(L. M. Tsang, pers. comm.)
16S SR	CCGGTCTGAACTCAAATCGTG	(Tsang <i>et al.</i> 2009)
H13842-12S	TGTGCCAGCASCTGCGGTTAKAC	(Machida <i>et al.</i> 2004)
L13337-12S	YCTWTGYTACGACTTATCTC	(Machida & Tsuda 2010)
dgLCO1490 (COI)	GGTCAACAAATCATAAAGAYATYGG	(Meyer <i>et al.</i> 2005)
dgHCO2198 (COI)	TAAACTTCAGGGTGACCAARAAYCA	(Meyer <i>et al.</i> 2005)
LCO1490 (COI)	TCAACAAATCATAAAGATATTGG	(Folmer <i>et al.</i> 1994)
HCO2198 (COI)	TAAACTTCAGGGTGACCAAAAATCA	(Folmer <i>et al.</i> 1994)

ethanol of the same type and the fixation was continued for another 24 hours. During the processes of sorting, tissue dissection, and subsequent handling of the tissue, specimens were kept on ice. An AutoGenPrep 965 was used for extraction of total DNA mostly following the manufacturer's protocol for animal tissue. Tissue digestion was performed overnight in a shaking bath at 56°C and 50 rpm using the AutoGen buffers and ProtK. The suspension volume of extracted total DNA was 50 µL. Three fragments of the mitochondrial genome were amplified and sequenced. An approximately 400–500bp fragment of 16S rRNA, an about 650bp fragment of COI (DNA Barcode) and an about 550bp fragment of 12S rRNA were amplified in a 10 µL reaction volume containing 0.25 µL BSA, 0.5 µL dNTP [2.5mM each], 1 µL Bioline 10xNH4 reaction buffer, 0.3 µL of each primer [10µM], 0.5 µL Biolase MgCl₂ [50mM], 0.1 µL Biolase DNA Polymerase [5u/µL], 2 µL of template DNA and nuclease-free H₂O. The same primer pairs were used for PCR and cycle sequencing respectively in 16S and 12S. PCR primers are listed in Table 1.

16S SR/16S SF primers generally led to better amplification success than the universal primers 16S AR/BR but both were used (Table 1). For amplification of COI, M13-tailed primers based on dgLCO1490/dgHCO2198 were used (Meyer *et al.* 2005). Here, for cycle sequencing

M13 primers were used. In several cases, the use of LCO1490/HCO2198 primers would amplify COI in specimens, were dgLCO1490/dgHCO2198 did not work. Amplification and cycle sequencing reactions were carried out on Peltier Thermal Cyclers PTC200 and PTC225 (MJ Research) and 2720 Thermal Cyclers (Applied Biosystems). The PCR temperature profile consisted of an initial denaturation at 95°C (5min), followed by 34-36 cycles of denaturation at 95°C (30 s), annealing at 48°C (30 s) and extension at 72°C (45 s) followed by a final extension at 72°C (5min). Cycle sequencing was performed using the same primers as used for PCR.

2 µL of PCR product was analyzed for purity and size conformity by electrophoresis in a 1.5% agarose gel with ethidium bromide. Remaining PCR product was purified applying ExoSap-IT (USB). A 5x dilution of the enzyme was used and 2 µL of that solution were added to 8 µL PCR product. Samples were incubated for cleanup at 37°C (30min) and the enzyme was deactivated at 80°C (20min). Cycle sequencing was performed in 10 µL volume containing 1 µL purified PCR product, 0.5 µL BigDye Terminator, 1.75 µL Big Dye Terminator reaction buffer, 0.5 µL primer and nuclease-free water. Cycle-sequencing products were cleaned up with the Sephadex G-50 (Sigma S-5897) method, dried and stored at -20°C until sequencing. For cycle sequencing, 30 cycles of 95°C

Table 2. Genbank accession numbers.

Collection ID	Field ID	12S acc. no.	16S acc. no.
ZMH K-43006	SMa23	KC715784	KC715761
ZMH K-43006	SMa25	KC715785	KC715762
ZMH K-43006	SMa26	KC715786	KC715763
ZMH K-43006	SMa27	KC715787	KC715764
ZMH K-43006	SMa28	KC715788	KC715765
ZMH K-43006	SMa29	KC715789	NA
ZMH K-43003	SMa30	KC715790	KC715766
ZMH K-43002	SMa31	KC715791	NA
ZMH K-43006	SMa32	KC715792	KC715767
ZMH K-43000	SMa33	KC715793	KC715768
ZMH K-42990	SMa34	NA	KC715769
ZMH K-43006	SMa43c	NA	KC715770
ZMH K-43006	SMa44c	NA	KC715771
ZMH K-43006	SMa45c	NA	KC715772
ZMH K-43006	SMa46c	NA	KC715773
ZMH K-43006	SMa47c	NA	KC715774
ZMH K-43006	SMa48c	NA	KC715775
ZMH K-43006	SMa60c	NA	KC715776
ZMH K-43006	SMa61c	NA	KC715777
ZMH K-43006	SMa63c	NA	KC715778
ZMH K-43006	SMa65c	NA	KC715779
ZMH K-43006	SMa66c	NA	KC715780
ZMH K-43013	SMa67c	NA	KC715781
ZMH K-43007	SMa69c	NA	KC715782
ZMH K-43063	SMa70c	NA	KC715783

(30 s), 48°C (30 s) and 60°C (4min) were applied.

Phylogenetic analyses

Phylogenetic analyses were only conducted on 16S data because of the too small and incomplete datasets for COI and 12S. As outgroup taxa in the 16S tree, sequences from *Ianiropsis epilittoralis* Menzies, 1952 (Janiridae), *Betamorpha fusiformis* Barnard, 1920 (Munnopsidae), *Chelator* n. sp. and Desmosomatidae n. gen., n. sp. (Brix *et al.* submitted) were used. The ingroup consists of the macrostyliid species *Macrostyliis matildae* n. sp., *M. scotti* n. sp., *M. roaldi* Riehl & Kaiser, 2012, as well as two additional undescribed species (*M.* sp. SYSTCO #3 & #4). Sequences were aligned with MAFFT (Kato *et al.* 2002, 2009) as implemented in Geneious (Drummond *et al.* 2011) using default settings and automated model selection.

After trimming sequences, the 16S alignment comprised 412bp. A quality check of the datasets was conducted with the DAMBE package (Xia & Xie 2001), such as proportion of invariant sites and Xia-test of saturation (Xia *et al.* 2003). For phylogenetic inference, a Maximum Likelihood approach was selected and the software RAxML 7 (Stamatakis 2006) was used. For evaluation of statistical support, 10,000 bootstrap replicates were calculated.

Additionally, a Bayesian analysis was performed using MrBayes 3.2 (Huelsenbeck & Ronquist 2001; Ronquist & Huelsenbeck 2003) with parameters set to 2,000,000 generations and 4 separate chains. The first 100,000 generations were discarded as burn-in. According to the suggestion of MrModeltest (Nylander 2004), the GTR+G model was applied. Finally, using Paup 4.0beta (Swofford

2002), the most parsimonious trees were searched and a 50% Majority-rule consensus tree constructed. Statistical support was gained from 1,000 bootstrap replicates. All sequences were deposited in GenBank (Benson *et al.* 2008). Accession numbers are provided in Table 2.

Systematics

Asellota Latreille, 1802

Macrostylidae Hansen, 1916

Synonymy: Desmosomidae Sars, 1899; Macrostylini Hansen, 1916, p. 74; Wolff, 1956, p. 99 Macrostylinae Birstein, 1973 Macrostylidae Gurjanova, 1933, p. 411; Menzies, 1962, p. 28, p. 127; Wolff, 1962; Birstein, 1970; Menzies and George, 1972, p. 79–81; Mezhov, 1988, p. 983–994; 1992, p. 69; Brandt 1992a, 2002, 2004; Kussakin, 1999, p. 336; Riehl and Brandt, 2010; Riehl *et al.*, 2012

Type genus. *Macrostylis* Sars, 1864 (Monotypic)
Vana Meinert, 1890 *Desmostylis* Brandt, 1992

Macrostylis Sars, 1864

Type species. *Macrostylis spinifera* Sars, 1864

Not *M. spinifera* Sars, 1899

Gender. Female

Composition. See Riehl & Brandt (2010)

Implicit Attributes

Unless indicated otherwise, the following attributes are implicit throughout the descriptions, except where the characters concerned are inapplicable.

Female

Body. Elongate. **Ventral spines.** Pereonite 1 spine present. Pereonite 2 spine absent. Pereonite 3 spine

directed posteriorly. Pereonites 4–7 spines present. Marsupium with 2 pairs of oostegites. Developing oostegites (buds) in preparatory stage internal. **Cephalothorax.** Articulation with pereonite 1 present; rostrum absent; antennal articulations dorsolaterally. Posterolateral setae (if present) simple. Posterior margins papillae absent, setae absent. **Fossosome.** Present. **Pereonites 1–3.** Posterolateral setae (if present) not on pedestals, posterior tergite margin papillae absent.

Pereonite 4. Width subequal pereonite 5 width. Posterior tergite margin papillae absent, setae absent; posterolateral margins not produced posteriorly; posterolateral setae absent. **Pereonites 5–7.** Similar in shape. Posterior tergite margin setae absent; posterolateral margins produced posteriorly; posterolateral setae present, flexibly articulated, not on pedestals. Coxae posterolateral setae absent. **Pleonite 1.** Tergal articulation with pleotelson absent.

Pleotelson. Width maximum anterior to waist, ventrally with setal rows present, fringing pleopodal cavity and preanal trough laterally, extending posteriorly to anus. Statocysts present. Preanal ridge absent. Anal opening exposed, located in preanal trough.

Antennula. Of 5 articles. Articles 2–5 shorter than article 1. Terminal article with aesthetascs, penultimate and antepenultimate articles with no aesthetasc. **Antenna.** Of 5 podomeres. Article 3 squat. **Mandibles.** Straight, palp absent; molar process thin, triangular, setose. **Maxilliped.** With 2 receptaculi.

Anterior tagma. Dactyli with 2 claw setae. **Pereopods I–II.** Shape subsimilar. Ischium and merus with dorsal row of setae marginally. Articular plate on propodus present. **Pereopod III.** Ischium with small simple seta proximo-dorsally, dorsal lobe present; proximally with setae; apex with prominent apical seta. Articular plate on pro-

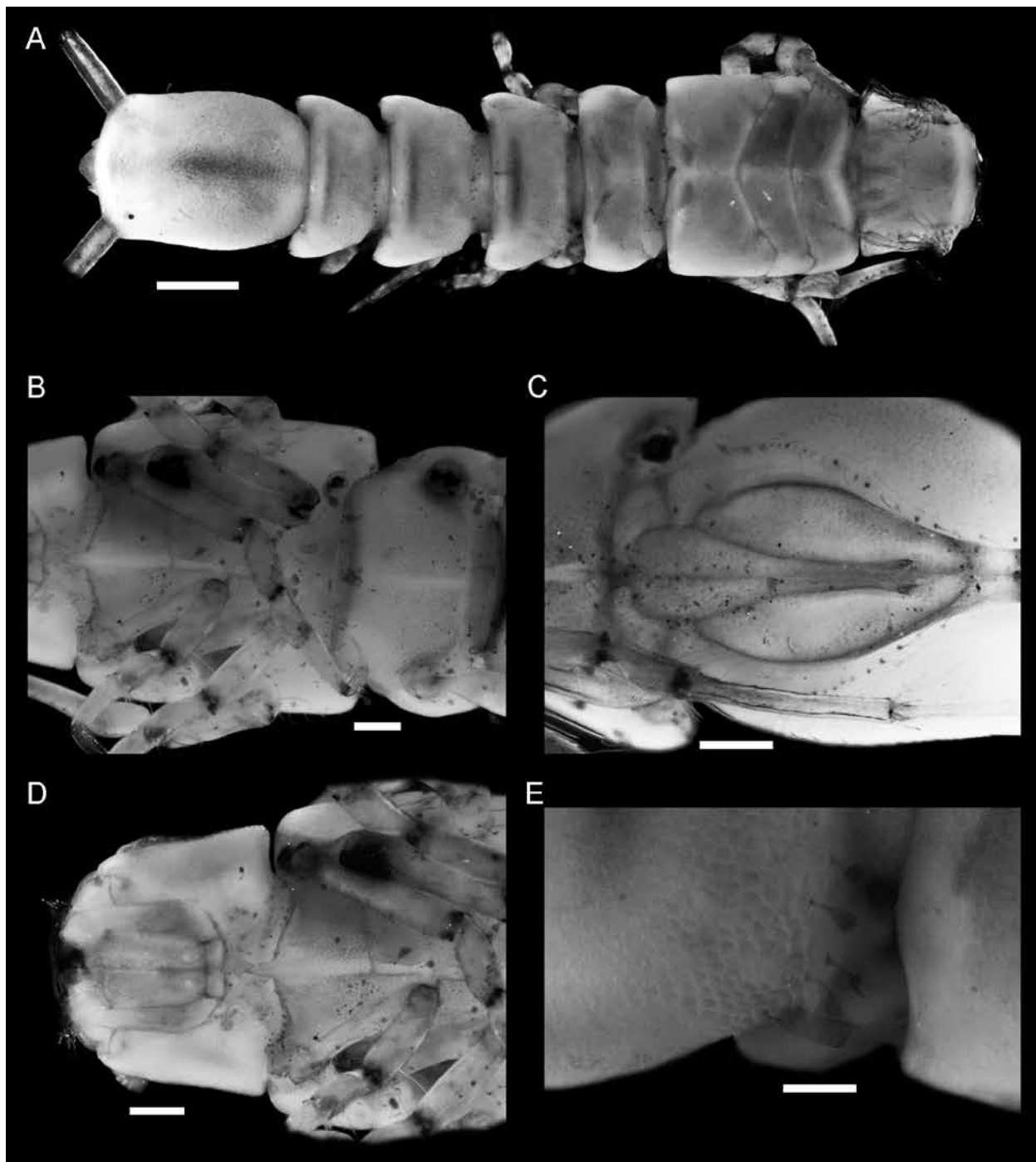


Figure 2. *Macrostylis scotti* n. sp. A–E, holotype adult male (ZMH K-42990), with ciliate epibionts, photoplate. **A**, dorsal habitus. **B**, ventral fossosoma. **C**, ventral pleotelson. **D**, ventral cephalothorax. **E**, ciliate epibionts on right lateral margins of tergites 4–5. Scales: A = 0.5 mm, B–D = 0.2 mm, E = 0.1 mm.

podus present. **Pereopod IV.** Shortest pereopod. Dactylus present. **Pereopod VII.** Fully developed, all segments present.

Operculum. With pappose setae terminally. **Pleopod III.** Exopod articles with fluent outline transition (if articulation expressed); distally with simple seta present. **Uropod.** Styliform, uniramous; endopod monoarticulate.

Adult male

Body, ventral spines and imbricate ornamentation (IO). As in female. **Cephalothorax.** Dorsal setation as in female, posterior margins papillae absent, posterior margins setae absent. **Fossosome.** Lateral tergite margins as in female, tergal plates laterally as in female; sternite articulations as in female. **Pereonites 1–4.** Posterolateral



Figure 3. *Macrostylis scotti* n. sp. A–E, holotype adult male (ZMH K-42990), with ciliate epibionts. **A**, lateral habitus, ornamentation omitted, setae simplified, uropods partially omitted. **B**, dorsal habitus, ornamentation omitted, setae simplified, areas free of imbricate ornamentation indicated by thin dashed lines on pereonites 6–7. **C**, pereopod III, ischium dorsal apex proximal prominent seta damaged. **D**, ciliate epibiont. **E**, ventral pleotelson, left setal ridge and ventral setation on left pleopod II omitted. Scales: A, B, E = 0.5 mm, C = 0.3 mm, D = 0.1 mm.

setae as in female, without pedestals. **Pereonite 3.** Posterolateral margins as in female, not produced posteriorly; posterolateral setae as in female. **Pereonite 4.** Subequal pereonite 5 width; width/pereonite 5 width, L/W ratio, lateral margins and tergal plates laterally as in female; posterolateral

margins rounded. Setae at posterior tergite margin and posterolaterally absent, as in female. **Pereonites 5–7.** Similar in shape. L/W ratios and pereonite 5 length/pereonite 4 length ratio similar to female. Posterior tergite margin setae absent, as in female. Posterolateral margins as in female. Posterolateral

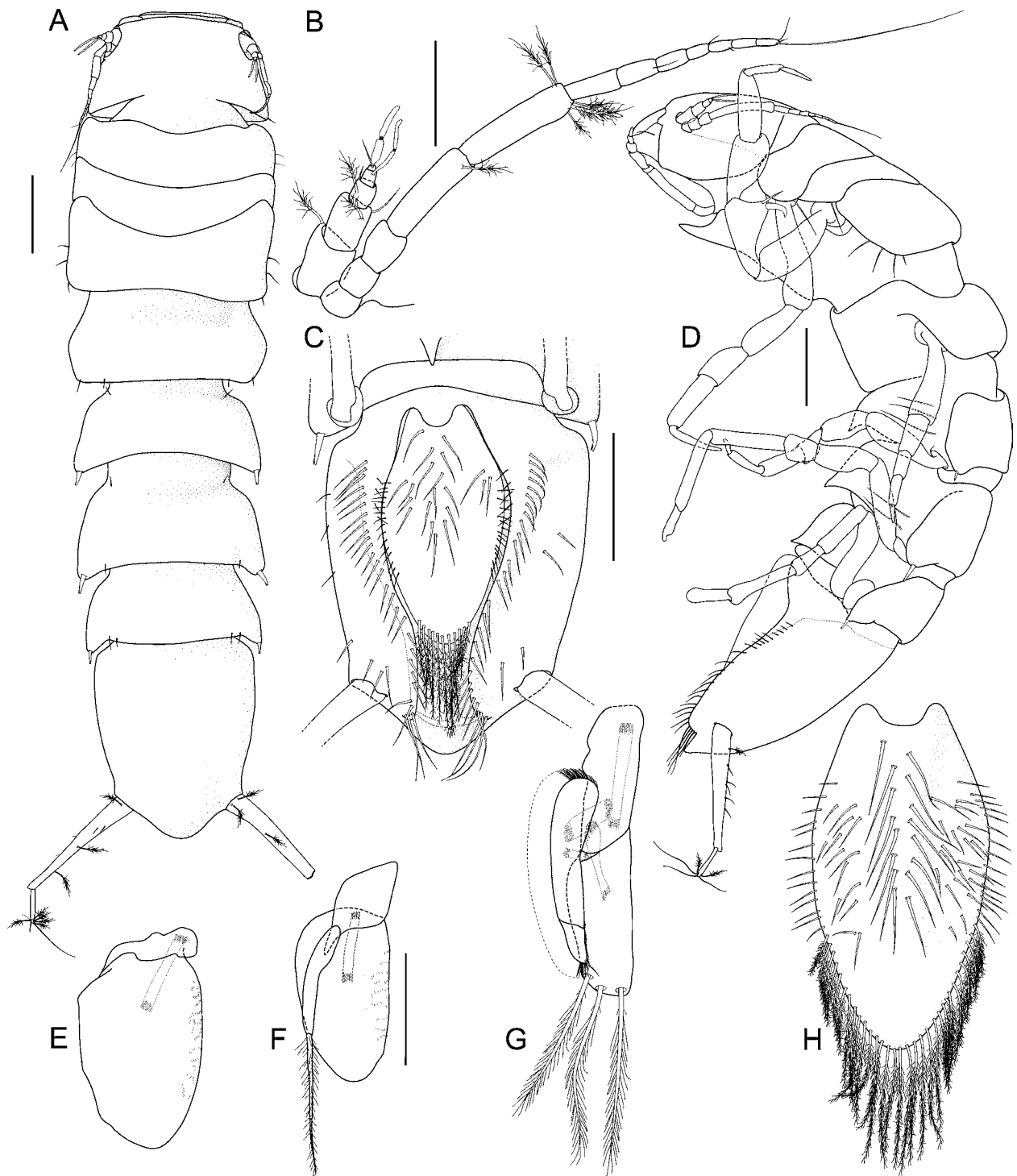


Figure 4. *Macrostylis scotti* n. sp. A–H, paratype non-ovigerous female (ZMH K-42992). **A**, dorsal habitus, imbricate ornamentation (IO) omitted. **B**, antennula and antenna, *in situ*. **C**, ventral pleotelson, IO omitted. **D**, lateral habitus, IO omitted, setae simplified. **E**, ventral pleopod V. **F**, ventral pleopod IV. **G**, ventral pleopod III. **H**, ventral pleopod II (operculum). Scales: A, C, D = 0.5 mm, B = 0.2 mm, E–H = 0.3 mm.

setae on tergite as in female, present, without pedostals. Posterolateral setae on coxae absent.

Pleonite 1. Tergal articulation with pleotelson absent. **Pleotelson.** Sexually dimorphic. Tergite dorsal surface in posterior view uniformly convex. Posterior apex shape and setation as in

female. **Antennula.** Of 5 articles, elongate articles cylindrical, articles decreasing in size from proximal to distal; terminal and penultimate article with several aesthetascs, antepenultimate article with no aesthetascs. **All pereopods.** Length/body-length ratios similar female. **Pereopods I–II.** Ischium

with dorsal setal row of setae marginally. **Pereopod III.** Ischium setation and shape, merus setation and carpus setation as in female. **Pereopod V.** Ischium setation as in female. **Pereopod VII.** Dorsal and ventral margins rows of elongate setae as in female. Penes joined medially. **Pleopod I.** Distally with lateral horns.

***Macrostyliis scotti* n. sp.**

(Figs 2–10)

urn:lsid:zoobank.org:act:8EBFDE96-E5CB-4D62-A56D-8E23B910EDC7

Etymology

The name “*scotti*” is dedicated to the British explorer Robert Falcon Scott CVO, in order to mark the 100th anniversary of his heroic trial to be the first person to reach the geographic South Pole. He reached the pole second, after Roald Amundsen, and died on this ill-fated Terra Nova Expedition around the 29th March 1912.

Type fixation

Holotype (Figs 2, 3): adult male, 5.4 mm, ZMH K-42990, designated here.

Type material examined

Holotype: adult male, 5.4 mm, ZMH K-42990, used for the illustration of the habitus and DNA studies. Paratypes: adult male, 5.1 mm, ZMH K-42991, dissected for illustrations of appendages and habitus as well as DNA studies; non-ovigerous female, 5.3 mm, ZMH K-42992, dissected for illustration of appendages and DNA studies.

Type material – Remarks

The holotype is complete except for posterior pereopods that have been removed from one side for

DNA studies; complete holotype and carcasses of paratype are conserved in 96% EtOH, dissected parts are mounted on slides using Euparal.

Type locality

Collected 04th January 2008 from the slope of the seamount Maud Rise. This is located off Queen Maud Land on the Antarctic continental slope. Samples were taken during the ANDEEP-SYSTCO project with R/V *Polarstern*, station ANTXXIV-2 039-17: start trawl at 64° 28.77' S, 2° 52.69' E; 2,152 m depth; end trawl at 64° 28.66' S, 2° 53.14' E; 2,153 m depth.

Diagnosis

Body heavily calcified, cuticular setules absent. Tergal plates laterally projecting below coxae, coxal articulations ventrally or medioventrally. Ventral spines keeled. Pereonites 1–5 in male with rows of long simple setae along posterolateral margins. Pereonite 3 posterolateral margin not produced posteriorly. Pereonites 3 and 4 ventral spines absent. Pereonite 4 width exceeding pereonite 5 width. Pereonite 6 posterolateral margin rounded. Pereonite 7 ventral spine present, small. Female pleotelson ovoid; waist present, posterior apex length about 0.20 pleotelson length. Antenna article 2 squat. Mandibular incisors not cuspidate, bluntly rounded. Pereopod III ischium dorsal lobe tapering, with 2 prominent apical setae. Pereopod V ischium distodorsally with setae present. Operculum elongate, ovoid, lateral fringe of setae with fluent transition to apical row of pappose setae. Uropod protopod distal margin tapering laterally, endopod articulation subterminally.

Description of non-ovigerous female

Body (Fig. 4A, D). Length 5.3 mm, 4.0 width, subcylindrical, tergite surfaces with very long, simple ventrolateral setae anteriorly of pereopod

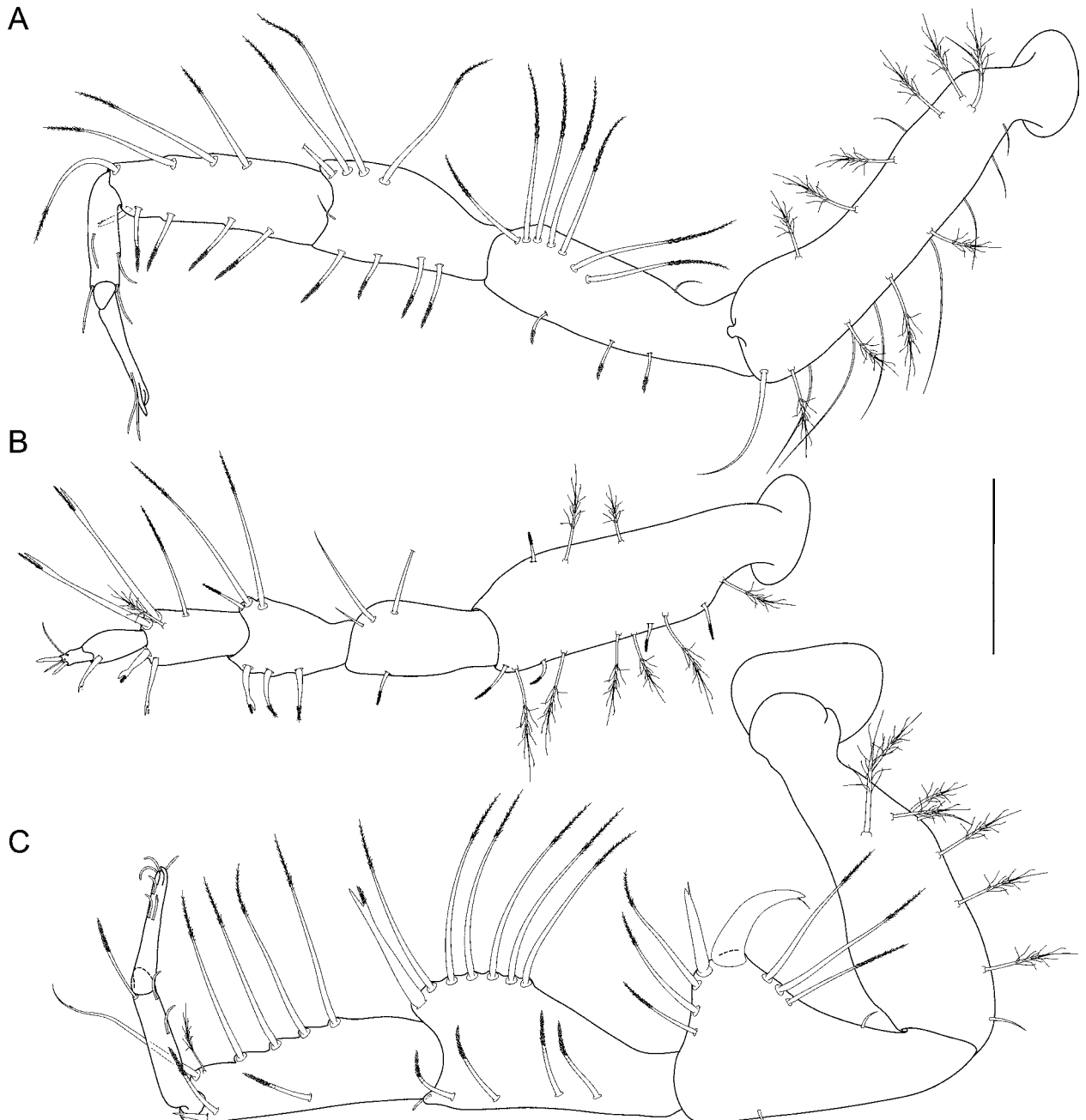


Figure 5. *Macrostyliis scotti* n. sp. A–C, paratype non-ovigerous female (ZMH K-42992). A, pereopod II. B, pereopod IV. C, pereopod III. Scale: A–C = 0.3 mm.

insertions. Tergal plates laterally projecting below coxae. **Ventral spines.** Pereonite 1 spine acute, prominent. Pereonites 3–4 spines absent. Pereonite 5 spine acute, small, placed medially. Pereonite 6 spine acute, prominent, closer to anterior segment border. Pereonite 7 spine small. **Imbricate ornamentation (IO).** Pereonite 4 IO on tergite in a thin irregular anterior transversal band along the collum margin and on bottom of collum; pereonite 5 IO on tergite in a broad transversal band covering anterior half of segment; and on bottom of collum. Oval

areas free from IO probably represent muscular attachments; pereonites 6–7 IO on tergite in a broad transversal band covering more than anterior half of segment; and on bottom of collum. With oval areas free from IO; pleotelson IO covering whole tergite except posterior margin.

Cephalothorax. Length 0.68 width, 0.15 body length; frons straight, frontal furrow and posterolateral setae present. Posterolateral margins blunt. **Fossosome.** Length 0.76 width, 0.19 body length. Lateral tergite margins confluent, ventral

surface keeled; sternite articulations present. **Pereonite 1.** Anterior margin concave; posterolateral setae simple. **Pereonites 2–3.** Posterolateral setae simple, flexibly articulated.

Pereonite 4. Width 1.1 pereonite 5 width, length 0.46 width; pereonal collum present. Lateral margins convex. Posterior tergite margin with 2 simple, asetulate, flexibly articulated setae; setae not extending beyond posterolateral margin. Posterolateral margins rounded; posterolateral setae simple, asetulate, flexibly articulated. **Pereonites 5–7.** Posterolateral margins produced posteriorly, rounded, with bifid, robust, flexibly articulated posterolateral setae. **Pereonite 5.** Length 0.39 width, 0.81 pereonite 4 length. **Pereonite 6.** Length 0.58 width, 1.5 pereonite 5 length. Posterior tergite margin with 2 simple, asetulate, flexibly articulated setae; setae not extending beyond posterolateral margin. **Pereonite 7.** Length 0.46 width. Posterior tergite margin with 4 simple, asetulate, flexibly articulated setae; setae not extending beyond posterolateral margin.

Pleotelson (Fig. 4A,C). Ovoid, waist present, setal ridges not visible in dorsal view, length 0.24 body length, 1.2 width, narrower than pereonite 7; statocysts and dorsal slot-like apertures not visible or absent. Posterior apex convex, smoothly curving medially, slightly concave at uropodal insertions; setae absent. Pleopodal cavity width 0.50 pleotelson width, pre-anal trough width 0.19 pleotelson width. Anal opening subterminally, parallel to frontal plane.

Antennula (Fig. 4B). Length 0.24 head width, 0.27 antenna length, width 1.3 antenna width. Articles decreasing in size from proximal to distal, L/W ratios of articles 1.2, 1.3, 1.3, 1.0, 0.5. Article 1 longest and widest, with 1 broom seta. Articles 2–4 cylindrical. Article 2 with 3 setae: 1 simple, 2 broom. Article 4 with 1 aesthetasc. Article 5 minute, squat, with 2 setae: 1 simple, 1

aesthetasc. Aesthetascs with intermediate belt of constrictions. **Antenna (Fig. 4B).** Length 0.19 body length. Article 1 squat. Article 2 squat, longer than article 1. Article 3 longer than article 1. Article 4 about as long as articles 1–3 together, distally with 1 broom seta. Article 5 longer than article 4, distally with 5 broom setae. Flagellum with 7 articles. **Mouthparts.** See description of adult male.

Pereopod I. Broken, missing. **Pereopod II (Fig. 5A).** Length 0.42 body length; article L/W ratios 3.7, 3.1, 1.6, 2.8, 3.4, 7.3; relative article length ratios 1.0, 0.65, 0.39, 0.52, 0.24, 0.31. Ischium dorsally with 7 simple setae submarginally. Merus dorsally with 4 simple setae; ventrally with 4 medially biserrate, distally fringe-like sensillae. Carpus dorsally with 4 simple setae; ventrally with 5 setae: 4 medially biserrate, distally fringe-like sensillae, 1 bifurcate distally. Dactylus distally with 2 sensillae. **Pereopod III (Fig. 5C).** Length 0.44 body length; article L/W ratios 3.0, 1.6, 1.7, 2.9, 4.2, 5.5; relative article length ratios 1.0, 0.72, 0.60, 0.66, 0.32, 0.34. Ischium dorsal lobe tapering; proximally with 3 simple setae; apex with 2 prominent, robust, bifid setae; apical seta bent towards proximal, spine-like; subapical seta flexibly articulated; distally with 3 simple setae. Merus dorsally with 7 setae: 6 simple, 1 bifurcate; ventrally with 5 setae: 4 medially biserrate, distally fringe-like sensillae in row, 1 small simple distally. Carpus dorsally with 6 setae: 5 simple, in row, 1 broom; ventrally with 3 setae: 2 medially biserrate, distally fringe-like sensillae, 1 bifurcate distally. Dactylus with 3 sensillae.

Pereopod IV (Fig. 5B). Length 0.25 body length; article L/W ratios 3.2, 1.9, 1.3, 1.9, 2.0, 1.7; relative article length ratios 1.0, 0.44, 0.30, 0.30, 0.18, 0.09; carpus laterally flattened. **Pereopod V (Fig. 6A).** Length 0.32 body length; article L/W ratios 2.9, 2.3, 1.4, 3.2, 4.4, 2.7; relative article length ratios 1.0, 0.60, 0.42, 0.60, 0.42, 0.15.

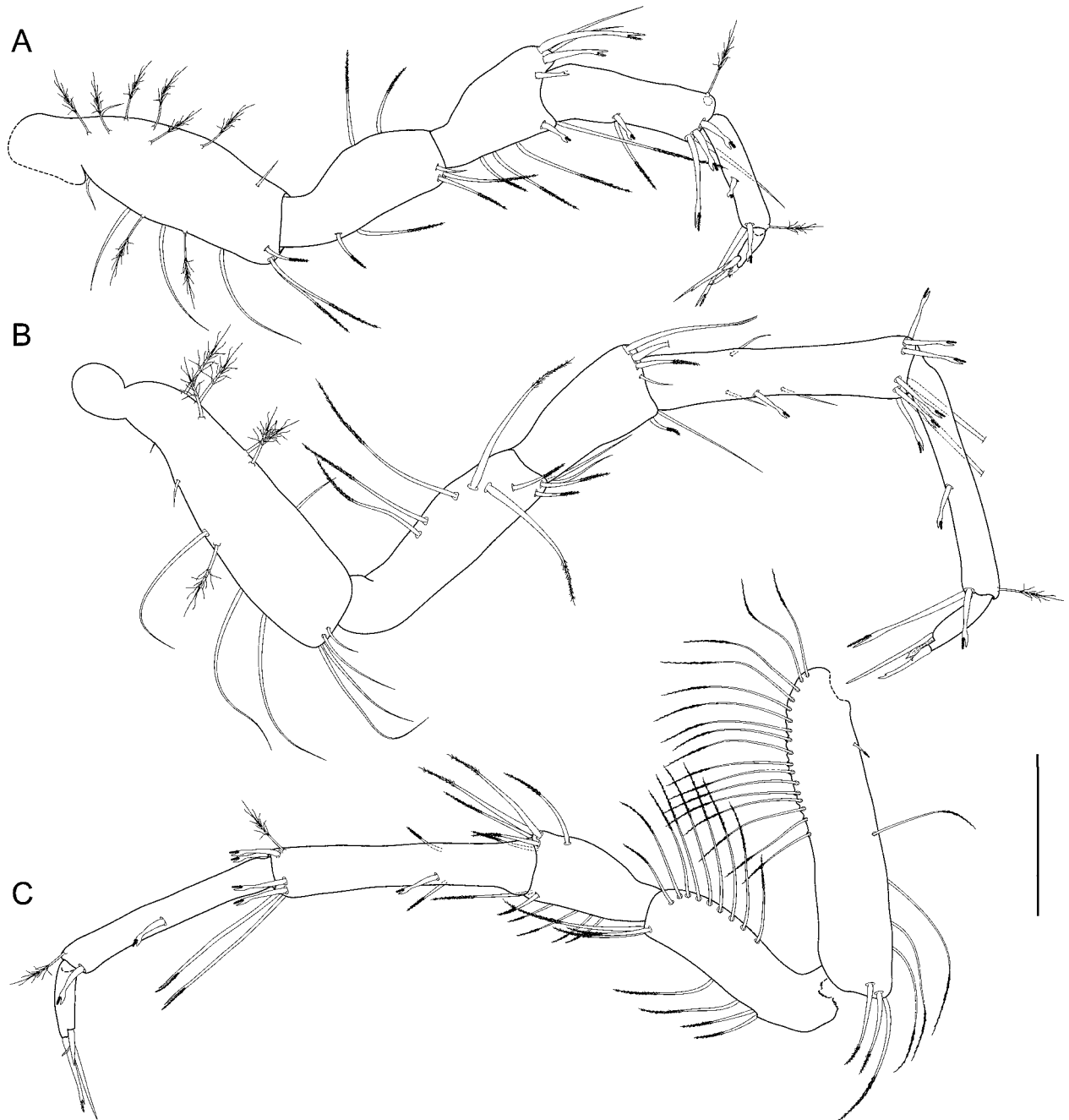


Figure 6. *Macrostylis scotti* n. sp. A–C, paratype non-ovigerous female (ZMH K-42992). A, pereopod V. B, pereopod VI. C, pereopod VII. Scale: A–C = 0.3 mm.

Ischium middorsally with 2 long, pappose setae; distodorsally without seta; midventrally with 2 long, pappose setae; distoventrally with 3 setae: 1 simple, small, 2 long, pappose. Merus distodorsally with 5 setae: 3 bifurcate, pappose, 2 simple; midventrally with 3 long, pappose setae; distoventrally with 2 setae: 1 short, bifurcate, pappose, 1 long, pappose. Carpus distodorsally with 2 setae: 1 broom, 1 broken, missing; distoventrally with 4 setae: 3 bifurcate, pappose, 1 long, simple. **Pereopod VI (Fig. 6B).** Length 0.46 body length;

article L/W ratios 3.9, 3.2, 1.8, 4.1, 6.3, 3.5; relative article length ratios 1.0, 0.64, 0.41, 0.74, 0.67, 0.21. Ischium dorsally with 5 long setae; midventrally without seta; distoventrally with 5 setae. Merus middorsally without seta; distodorsally with 4 setae: 1 minute, simple, 1 pappose, 1 bifurcate, 1 broken; midventrally without seta; distoventrally with 2 setae. Carpus middorsally with 1 seta; distodorsally with 3 bifurcate, pappose setae; midventrally with 3 setae: 1 bifurcate, pappose, laterally, 2 simple, medially; distoventrally with 5

setae: 3 bifurcate, pappose, 2 long, broken medially. **Pereopod VII (Fig. 6C)**. Length 0.42 body length, relative article length ratios 1.0, 0.61, 0.36, 0.80, 0.67, 0.21. Basis length 4.4 width; dorsal margin row of 17 elongate setae present, exceeding beyond proximal half of article, setae longer basis width; ventral margin with row of 4 elongate setae, setae longer basis width. Ischium length 3.1 width, middorsally with 9 long, pappose setae; midventrally with 4 long, pappose setae in row; distoventrally with 3 long, pappose setae. Merus length 1.7 width; distodorsally with 6, midventrally with 4, distoventrally with 2 long, pappose setae respectively. Carpus length 4.5 width; middorsally with 1 pappose seta; distodorsally with 3 setae: 1 broom, 2 bifurcate, pappose; midventrally with 2 setae: 1 bifurcate, pappose, 1 pappose; distoventrally with 4 setae: 2 bifurcate, short, pappose, 2 bifurcate, long, pappose. Propodus length 6.8 width. Dactylus length 3.3 width.

Operculum (Fig. 4C, H). Elongate, length 1.9 width, 0.70 pleotelson dorsal length; apical width 0.87 operculum width; distally not reaching anus, ovoid, ventrally keeled; with lateral fringe consisting of 14–16 pappose setae, with fluent transition to apical row of setae; with 30–33 pappose setae on apex, completely covering anal opening.

Pleopod III (Fig. 4G). Length 3.5 width, protopod length 2.5 width, 0.47 pleopod III length. Exopod length 0.64 pleopod III length; with fringe of fine setae, setae shorter exopod width; subterminal seta present. **Pleopod IV (Fig. 4F)**. Length 2.4 width, endopod length 1.5 width; exopod length 6.0 width, 0.65 endopod length, exopod lateral fringe of setae absent. **Pleopod V (Fig. 4E)**. Present.

Uropod (Fig. 4A). Inserting on pleotelson posterior margin; length 0.83 pleotelson length; protopod length 5.9 width, 0.66 pleotelson length, protopod distal margin tapering laterally, endopod articulation subterminally; endopod length 7.3 width, 0.27

protopod length, endopod width at articulation noticeably narrower than protopod.

Description of adult male

Body (Figs 2, 3A, B, 7A, B). Length 5.1–5.4 mm, 4.5 width. **Cephalothorax**. Frontal furrow present, straight; L/W ratio larger than in female, length 0.92–0.93 width, 0.16 body length; posterolateral corners rounded, posterolateral setae present, posterior margins papillose and setose. **Fossosome**. L/W ratio greater than in female, length 0.88–0.94 width, length/body-length ratio subequal to female; ventrally keeled (Fig. 2B). **Pereonites 1–3**. With 4–5, 2 and 5 long, simple, asetulate setae respectively in rows along posterolateral margins.

Pereonite 4 (Fig. 2A, E). Pereonal collum present, medially convex. Posterolateral margins not produced posteriorly. Posterior tergite margin with 6 simple, asetulate setae. **Pereonite 5**. Length 0.50–0.53 width, 1.1 pereonite 4 length. **Pereonite 6**. Length 0.60 width. **Pereonite 7**. Posterior tergite margin with 4 simple, asetulate, flexibly articulated setae; setae posteriorly not extending beyond posterolateral margin. **Pleonite 1 (Fig. 2C)**. Sternal articulation with pleotelson present.

Pleotelson (Figs 2A, C, 3B, E, 7A, D). L/W ratio in male greater than in female, length 1.4–1.5 width, 0.23–0.26 body length, width subequal pereonite 7 width; rectangular, waist present, setal ridges in dorsal view not visible. Posterior apex convex, almost straight with a narrow, rounded tip; without setae on margin; pleopodal cavity width 0.51–0.54 pleotelson width, pre-anal trough width 0.14–0.17 pleotelson width.

Antennula (Fig. 7C). Length 0.29 head width, 0.26 antenna length, width 1.5 antenna width; article L/W ratios 0.83, 0.78, 0.57, 0.60, 1.0; relative article length ratios 1.0, 0.70, 0.40, 0.30, 0.30. Articles 1–5 squat. Article 1 longest and widest, with 1 broom seta and 2 distally fringe-like

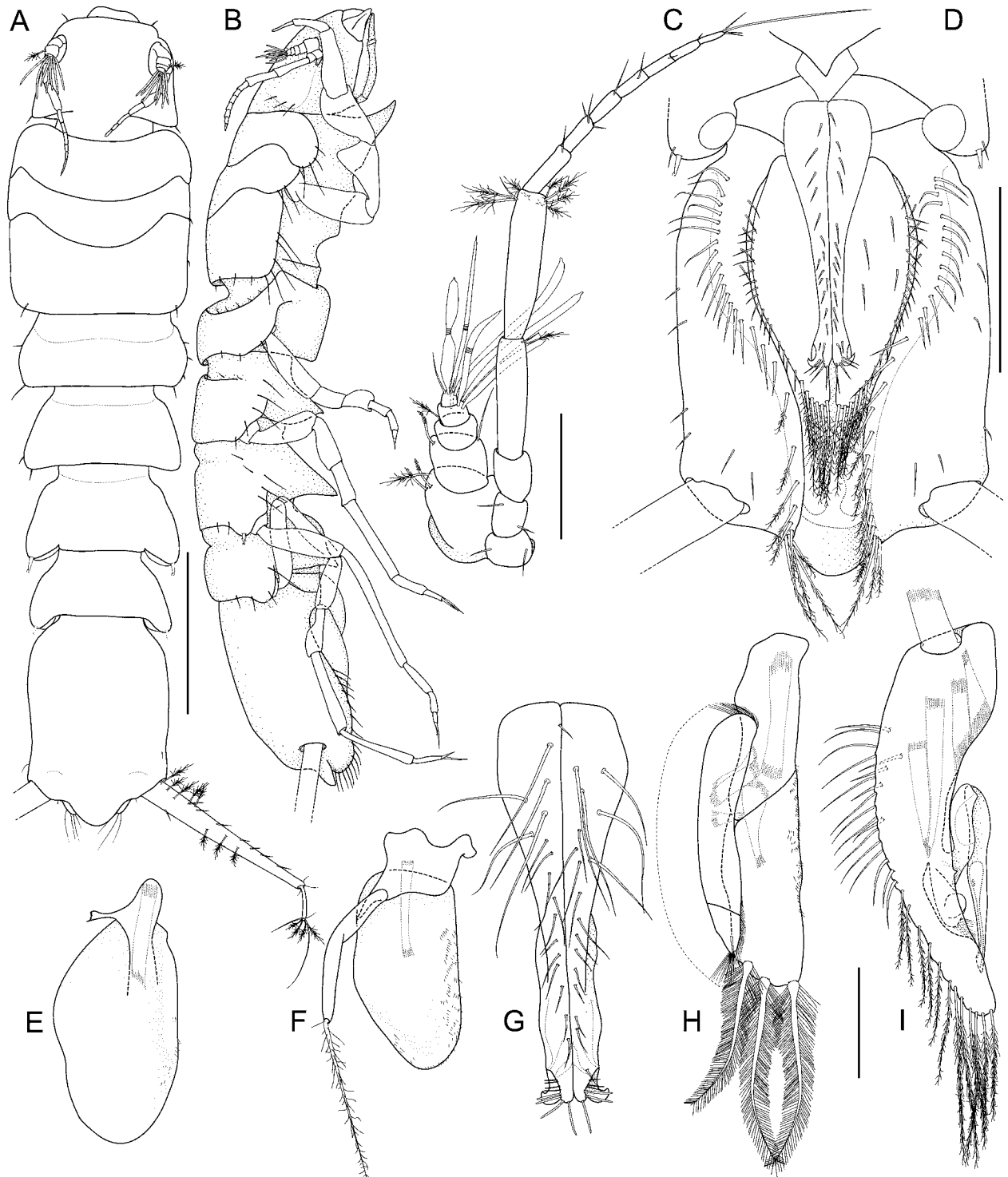


Figure 7. *Macrostylis scotti* n. sp. A–I, paratype adult male (ZMH K-42991). A, habitus dorsal. B, habitus lateral. C, antennule and antenna, *in situ*. D, pleotelson, ventral. E, pleopod V, ventral. F, pleopod IV, ventral. G, pleopods I ventral. H, pleopod III, ventral. I, pleopod II, dorsal. Scales: A, B: 1.0 mm; C, E–I = 0.2 mm; D = 0.5 mm.

sensillae. Article 2 with 2 setae: 1 simple, 1 distally fringe-like sensilla. Article 3 with 1 broom seta. Article 4 with 4 aesthetascs. Article 5 with 6 setae: 2 simple, 4 aesthetascs; aesthetascs with intermediate belt of constrictions. **Antenna (Fig. 7C).** Article 1 squat. Article 2 elongate, longer than article 1. Article 3 squat, longer than article 1.

Article 4 longer than articles 1–3 together, distally with 2 setae: 1 simple, 1 broom. Article 5 longer than article 4, distally with 8 setae: 1 simple, 7 broom.

Mandibles (Fig. 8A, B, D, E). In medial view strongly narrowing from proximal to distal, subtriangular, with lateral setae; left mandible

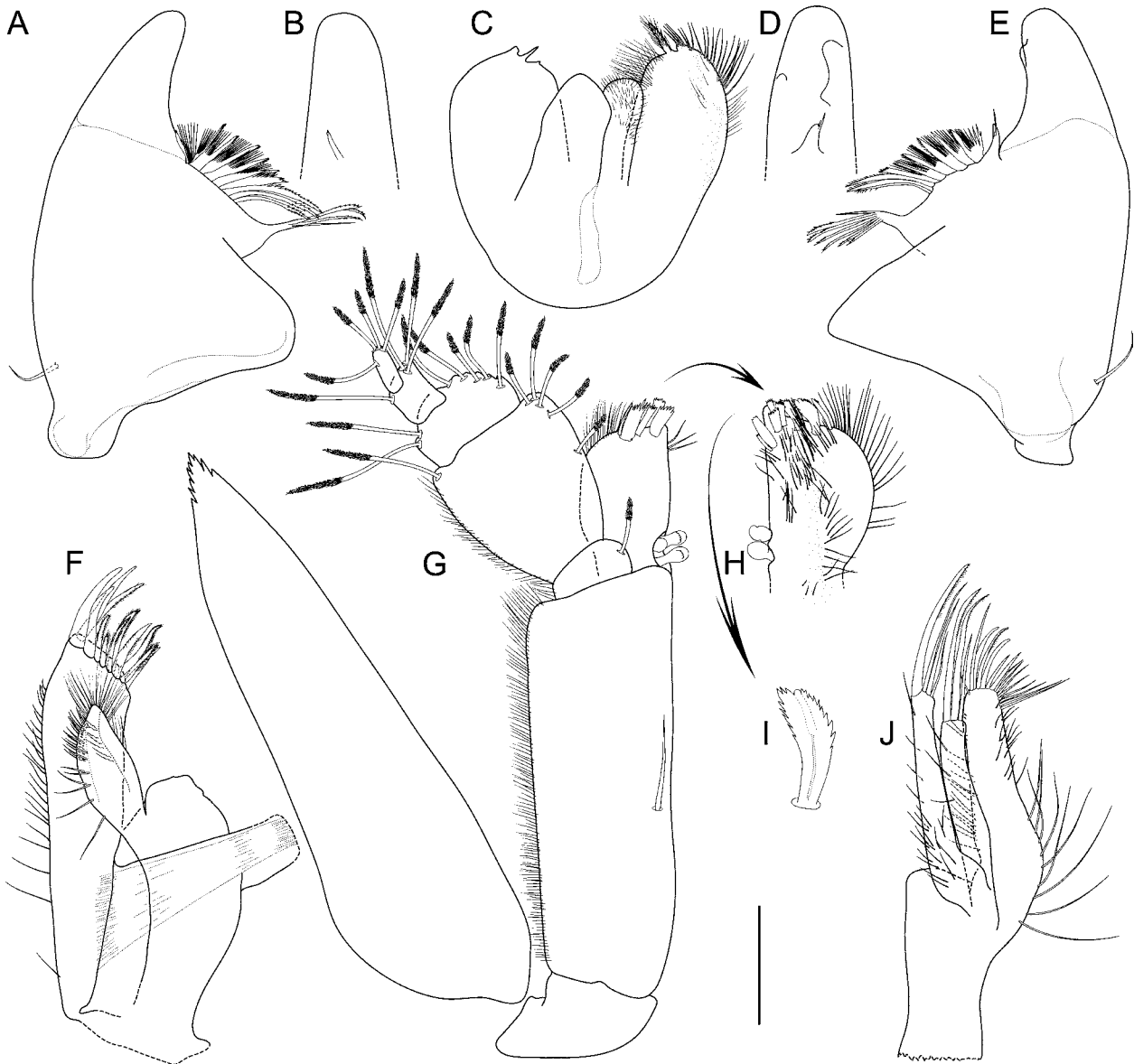


Figure 8. *Macrostylyis scotti* n. sp. A–J, paratype adult male (ZMH K-42991) mouthparts. A, left mandible, dorsal. B, left mandible incisor process, medial. C, paragnaths, ventral, setae omitted on right side. D, right mandible incisor process, medial. E, right mandible, dorsal. F, maxillula, ventral, with medial lobe flipped over. G, maxilliped, ventral. H, maxilliped endite, dorsal. I, fan seta. J, maxilla, ventral. Scales: A–J = 0.1 mm.

incisor process simplified, bluntly rounded, with 1 cusp, *lacinia mobilis* spine-like, adjacent to spine row without separating gap; right mandible incisor process simplified, bluntly rounded, with 3 minute cusps, *lacinia mobilis* spine-like, subsimilar in size to left *lacinia*, adjacent to spine row without gap.

Maxillula (Fig. 8F). Lateral lobe with 12 robust setae. **Maxilla (Fig. 8J).** Lateral lobe with 4 partly serrate setae terminally; middle endite with 3 partly serrate setae terminally; inner endite with 6 partly serrate setae terminally. **Maxilliped (Fig. 8G–I).** Basis length 4.0 width, medioventrally with seta

present. Epipod length 3.6 width, 1.1 basis length; palp wider than endite, article 2 wider than articles 1 and 3, article 1 shorter than article 3.

Pereopod I (Fig. 9A). Length 0.33 body length; article L/W ratios 4.0, 3.2, 1.5, 2.1, 2.8, 4.3; relative article length ratios 1.0, 0.55, 0.30, 0.36, 0.22, 0.20. Ischium dorsally with 6 setae: 1 small, simple proximally, 4 long, distally pappose in submarginal row, 1 small, simple. Merus dorsally with 3 long, distally pappose setae; ventrally with 5 setae: 4 medially serrate, distally fringe-like sensillae, 1 simple, small. Carpus dorsally with 4

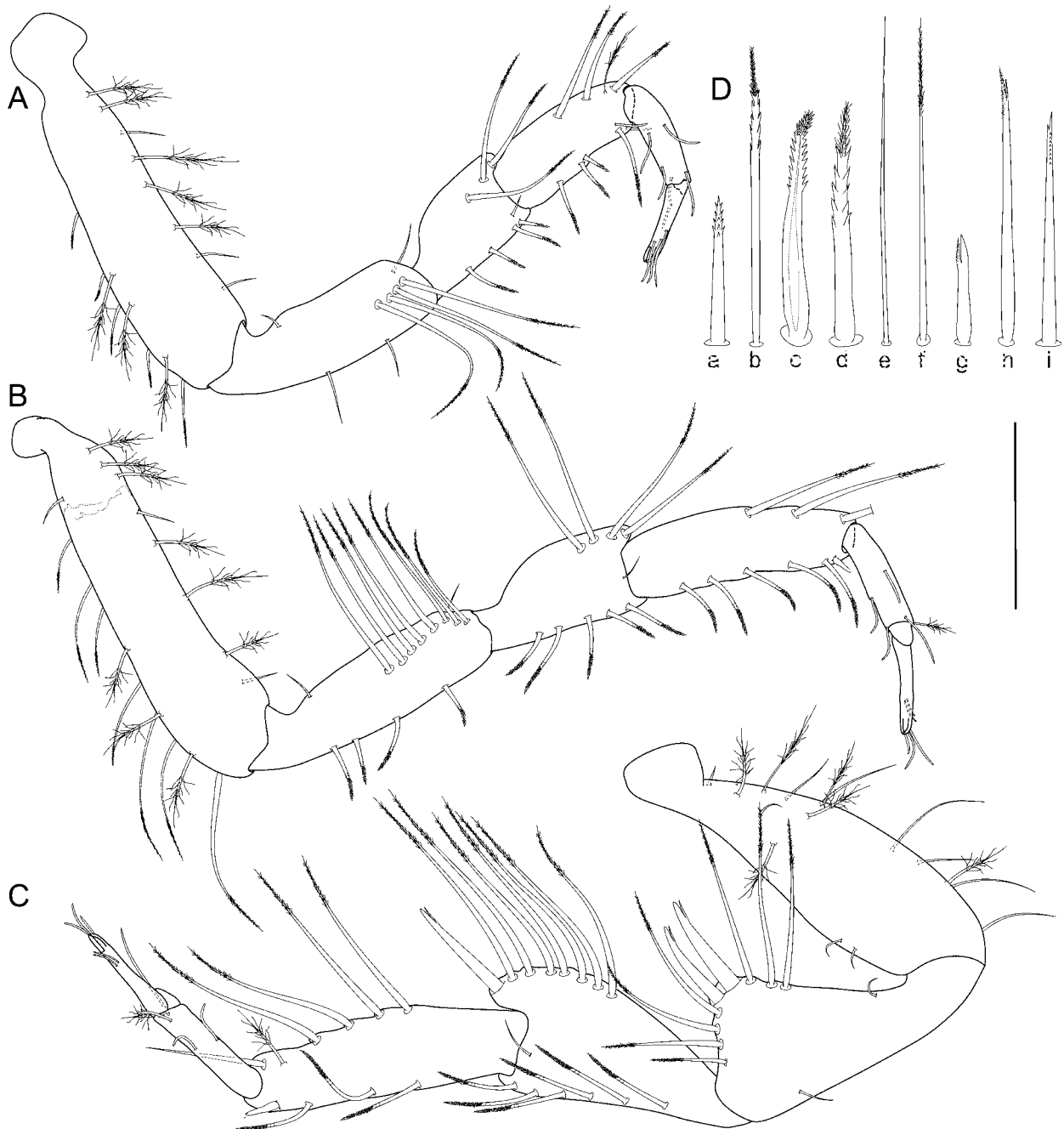


Figure 9. *Macrostylis scotti* n. sp. A–D, paratype adult male (ZMH K-42991). A, pereopod I. B, pereopod II. C, pereopod III. D, setae (at different rates of magnification): a, tripleserrate. b, thin, medially biserrate, distally fringe-like. c, medially biserrate, distally fringe-like, cross-section. d, medially biserrate, distally fringe-like. e, thin, long, asetulate; thin, long distally pappose. f, robust, bifurcate, fringe-like. g, bifurcate, fringe-like. h, i, bifurcate, biserrate. Scale: A–C = 0.3 mm.

setae: 3 long, distally pappose in row and 1 broom seta; ventrally with 4 setae: 3 medially serrate, distally fringe-like sensillae and 1 simple, small mediolaterally. **Pereopod II (Fig. 9B).** Length/body-length ratio sexually dimorphic; length 0.40 body length; article L/W ratios 4.0, 3.3, 1.7, 3.0, 3.4, 6.0; relative article length ratios 1.0, 0.63, 0.38, 0.56, 0.27, 0.28. Ischium dorsally with 9 setae: 1

small, simple proximally, 7 long, distally pappose in submarginal row, 1 short, simple mediolaterally. Merus dorsally with 4 long, distally pappose setae; ventrally with 5 medially serrate, distally fringe-like sensillae. Carpus dorsally with 3 long, distally pappose setae; ventrally with 6 setae: 5 medially serrate, distally fringe-like sensillae and 1 bifurcate, distally fringe-like sensilla.

Pereopod III (Fig. 9C). Length 0.43 body length; article L/W ratios 3.2, 1.8, 1.6, 3.0, 4.2, 5.7; relative article length ratios 1.0, 0.72, 0.57, 0.70, 0.35, 0.28. Ischium sexually dimorphic, triangular, dorsal lobe proximally with 3 distally pappose setae, apex with 2 prominent, robust, spine-like, straight, bifid setae; distally with 4 distally pappose setae. Merus dorsally with 8 setae: 7 distally pappose, 1 robust, bifurcate fringe-like sensilla; ventrally with 6 medially serrate, distally fringe-like sensillae. Carpus dorsally with 6 setae: 5 distally pappose, 1 broom; ventrally with 4 setae: 3 medially serrate, distally fringe-like sensillae and 1 robust, bifurcate, fringe-like sensilla.

Pereopod IV (Fig. 10A). Length 0.22 body length; article L/W ratios 2.9, 2.0, 1.3, 2.1, 2.0, 2.5; relative article length ratios 1.0, 0.51, 0.37, 0.44, 0.19, 0.12. **Pereopod V (Fig. 10B).** 0.34 body length; article L/W ratios 3.4, 2.4, 1.6, 4.5, 6.5, 4.0; relative article length ratios 1.0, 0.61, 0.43, 0.71, 0.51, 0.16. Ischium middorsally with 2 setae; distodorsally with 1 short seta; midventrally with 2 distally pappose setae; distoventrally with 5 distally pappose setae. Merus distodorsally with 6 setae: 2 robust, short, bifurcate, fringe-like sensillae and 4 distally pappose; midventrally with 3 setae: 1 short, robust, bifurcate, fringe-like sensilla and 2 long, thin distally pappose; distoventrally with 3 setae: 2 damaged, 1 long distally pappose. Carpus distodorsally with 1 broom seta; distoventrally with 5 setae: 3 robust, bifurcate, fringe-like sensillae and 2 long, thin, distally pappose.

Pereopod VI (Fig. 10C). Article L/W ratios 3.6, 2.6, 2.2, 5.7, 10.8, 5.0; relative article length ratios 1.0, 0.60, 0.54, 0.89, 0.75, 0.26. Ischium dorsally with 9 simple setae; midventrally with 4 distally pappose setae; distoventrally with 6 distally pappose setae. Merus distodorsally with 8 setae: 2 bifurcate, fringe-like sensillae, 2 bifurcate, biserrate, 4 distally pappose; midventrally with 3

distally pappose setae; distoventrally with 2 setae: 1 bifurcate, biserrate, 1 distally pappose. Carpus middorsally with 3 distally pappose setae; distodorsally with 5 setae: 1 broom, 4 robust, bifurcate, fringe-like sensillae; midventrally with 2 setae: 1 robust, bifurcate, fringe-like sensilla, 1 thin, long, distally pappose; distoventrally with 5 bifurcate, fringe-like sensillae: 3 short, robust, 2 long, bifurcate.

Pereopod VII (Fig. 10D). Length/body-length ratio as in female, length 0.41 body length; relative article length ratios 1.0, 0.61, 0.39, 0.88, 0.71, 0.25; segment L/W ratios sexually dimorphic. Basis length 5.1 width, posterior margin with row of 17 setae, not exceeding beyond proximal half of article, setae longer basis width; ventral margin sexually dimorphic, with row of 8 elongate setae; setae longer basis width. Ischium length 2.8 width; middorsally with 8, midventrally with 5, distoventrally with 4 distally pappose setae respectively. Merus length 2.2 width; distodorsally with 7, midventrally with 2 distoventrally with 2 distally pappose setae respectively. Carpus length 7.0 width; distodorsally with 1 broom seta; midventrally with 1 robust, bifurcate, fringe-like sensilla; distoventrally with 2 setae: 1 robust, bifurcate, fringe-like, 1 long, bifurcate, biserrate. Propodus length 10.0 width. Dactylus length 4.7 width.

Pleopod I (Figs 2C, 7G). Length 0.56 pleotelson length, lateral horns not extending distally beyond medial lobes, distally with 6–8 sensillae, ventrally with setae present. **Pleopod II (Fig. 7I).** Protopod apex tapering, with row of 13–15 setae along entire lateral margin; with 12 pappose setae distally. Endopod distance of insertion from protopod distal margin 0.32 protopod length. Stylet weakly curved, not extending to distal margin of protopod, length 0.48 protopod length. **Uropod (Fig. 7A).** Length 0.99–1.0 pleotelson length; protopod L/W ratio greater than in female, length 6.3–

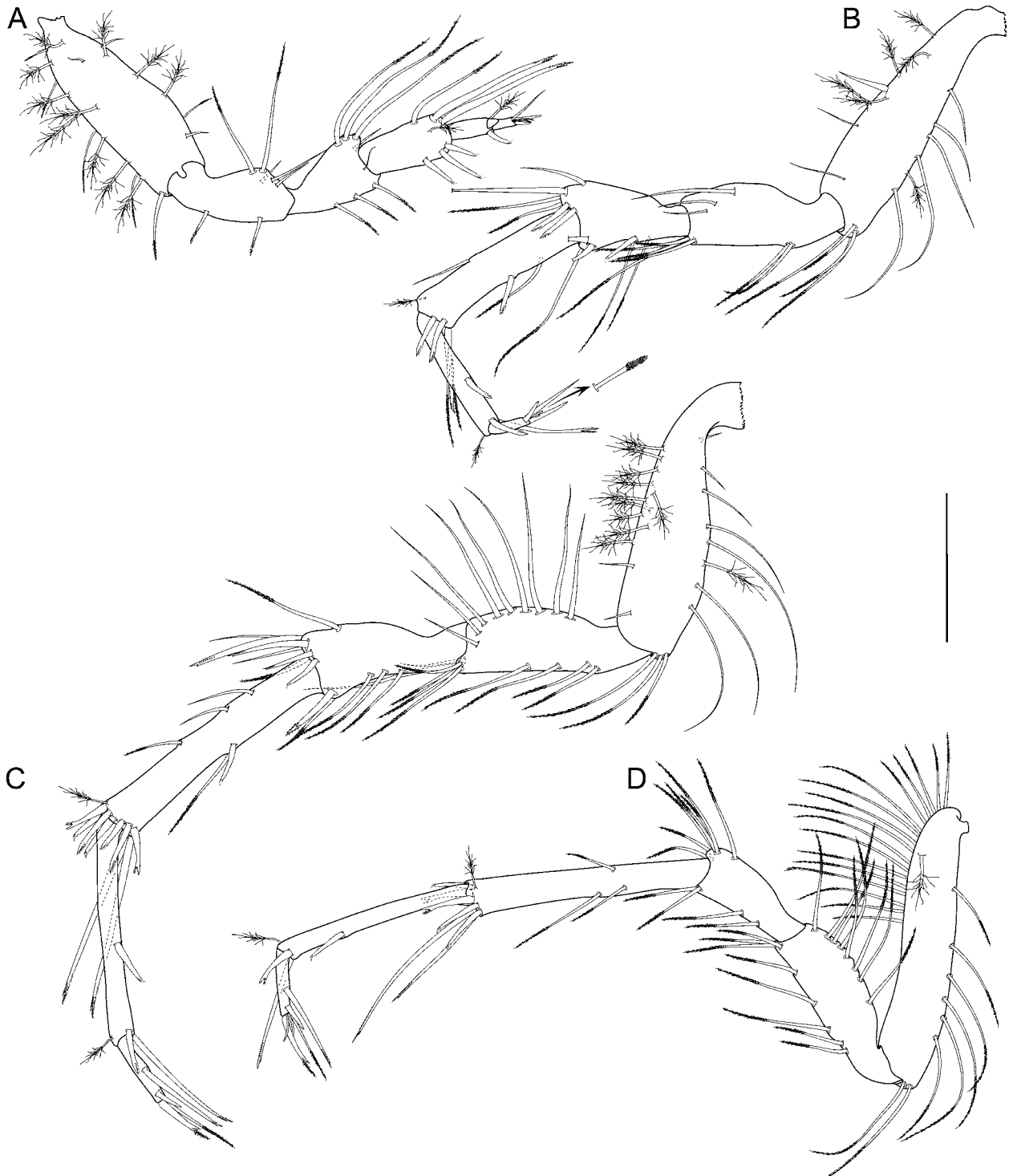


Figure 10. *Macrostyliis scotti* n. sp. A–D, paratype adult male (ZMH K-42991). A, pereopod IV. B, pereopod V. C, pereopod VI. D, pereopod VII. Scale: A–D = 0.3 mm.

7.5 width; distally narrowing, tapering laterally, endopod inserting subterminally; endopod/protopod length ratio 0.19–0.24, smaller than in female; endopod length 8.0–10.5 width, width narrower than protopod.

Remarks

Macrostyliis scotti n. sp. is among the largest

species of Macrostyliidae currently described with only *M. galathea* Wolff, 1956 and *M. magnifica* Wolff, 1962 of similar size or larger than *M. scotti*. This species appears closely related to *M. uniformis* Riehl & Brandt, 2010. The character states shared by both species are e.g. a heavily calcified cuticle of the body and appendages, strong and simple, unidentate mandibular incisors, an oval,

elongate operculum with continuous transition between lateral setal fringe and terminal row of setae. Furthermore, both terminal and subterminal articles of the female antennulae bear one aesthetasc respectively and the pereopod III ischium dorsal lobe features two prominent setae.

A group of species potentially closely related consists of *M. abyssicola* Hansen, 1969, *M. minuta* Menzies, 1962, *M. robusta* Brandt, 2004. Similar to *M. scotti*, these have tergal plates laterally projecting below coxal articulations. In combination with keeled sternites, this allows the pereopods to be positioned close to the sternites. This might have important implications for a burrowing life-style. Further, they share the body free from dense cover with setules, and a subterminally articulating uropod endopod with *M. scotti* and *M. uniformis*. On the other hand, in this group, one can identify a tendency to reduce the antennula as well as the seventh pereopods, which is not the case in *M. scotti*. Among the characters unique for *M. scotti* are the very long setae that can be found laterally on the tergites.

***Macrostylis matildae* n. sp.**

(Figs 11–20)

urn:lsid:zoobank.org:act:CBDDFFA0-5539-4540-B04E-AA9CA1D695A5

Etymology

The name “*matildae*” is the latinized genitive case of “Matilda”, an Old German given name meaning “powerful battler”. It is derived from “Maud”, another variant of the same name, as in Maud Queen consort of Norway (1869–1938), spouse of King Haakon VII. This name is ment to reflect on the type locality seamount Maud Rise and the adjacent Norwegian claim of Antarctica, Queen Maud

Land (Norwegian: Dronning Maud Land).

Type fixation

Holotype (Fig. 11): non-ovigerous female, 1.7 mm, ZMH K-43000, designated here.

Type material examined

Holotype: non-ovigerous female used for habitus illustrations, 1.7 mm, ZMH K- 43000. Paratypes (all from same sample as holotype): 1 ovigerous female with eggs used for habitus illustrations, 2.0 mm, ZMH K-43002; 1 non-ovigerous female dissected for illustrations, 1.9 mm, ZMH K-43003; 1 non-ovigerous female used for SEM, ZMH K-43005; 1 adult male, dissected for illustrations, ZMH K-43004; 1 manca male, dissected for illustration ZMH K-43001; 29 specimens from the type locality: 6 ovigerous females with no eggs; 14 non-ovigerous females; 1 female manca ZMH; 1 manca male ZMH K-43006.

Type locality

Collected 04th January 2008 from the slope of the seamount Maud Rise. This is located off Queen Maud Land on the Antarctic continental slope. Samples were taken during the ANDEEP-SYSTCO project with R/V *Polarstern*, station ANTXXIV-2 039–17: start trawl at 64° 28.77' S, 2° 52.69' E; 2,152 m depth; end trawl at 64° 28.66' S, 2° 53.14' E; 2,153 m depth.

Diagnosis

Body and all external appendages covered with furry coat of cuticular setules. Pereonites 3–4 ventral spines present. Pereonite 4 posterolateral margins produced posteriorly, rounded. Female pereonite 6 length clearly larger pereonite 5 length.

Pereonite 7 ventral spine small; posterolateral margins similar in female and male. Pleotelson shape similar in both sexes, narrowing evenly

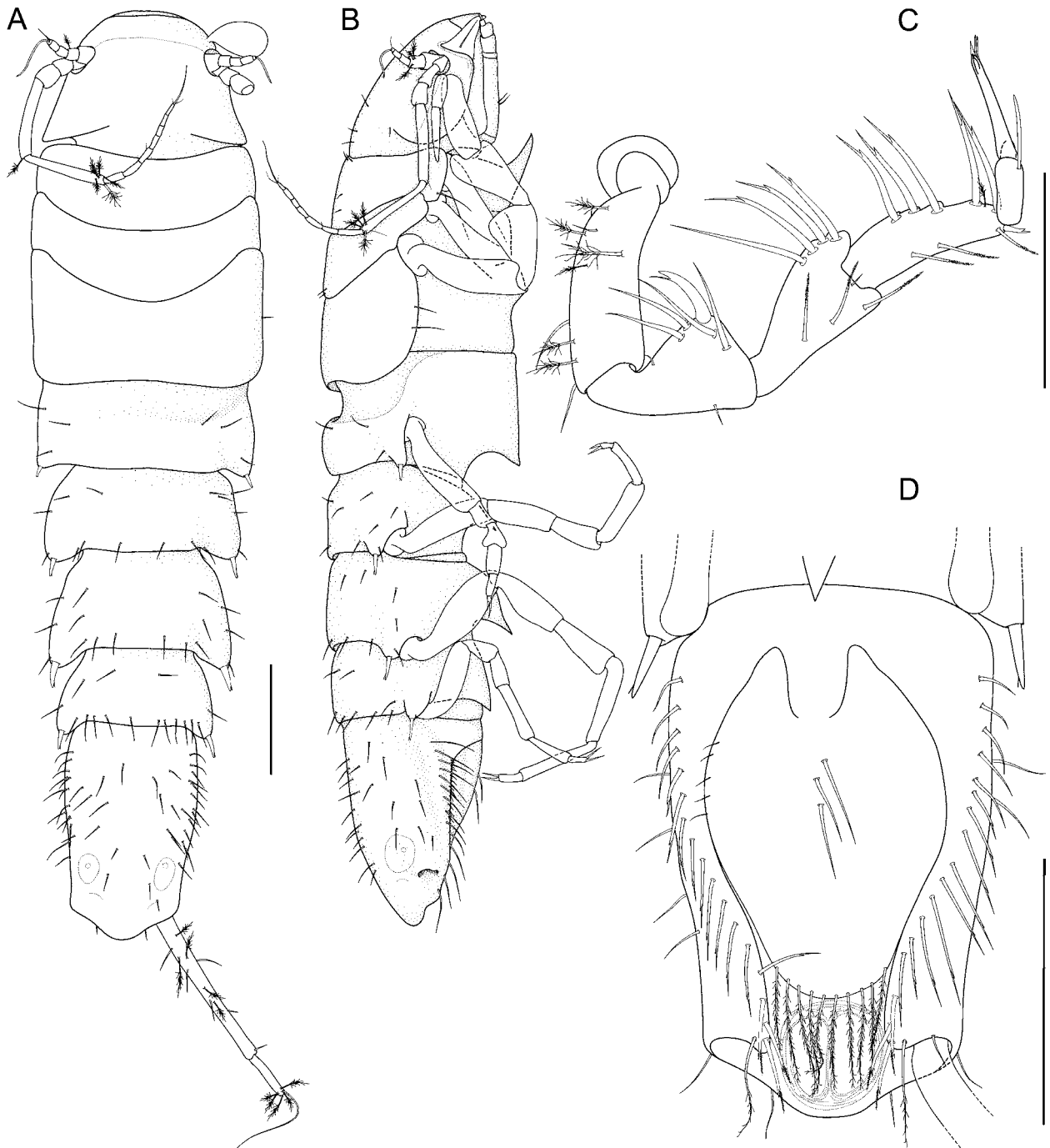


Figure 11. *Macrostylis matildae* n. sp. **A–D**, holotype non-ovigerous female (ZMH K-43000). **A**, habitus dorsal, cuticular setules and imbricate ornamentation (IO) omitted. **B**, habitus lateral, cuticular setules, IO and uropod omitted. **C**, pereopod III. **D**, pleotelson, ventral. Scale: A–D = 0.2 mm.

towards uropod insertions, lateral margins straight, waist present; posterior apex convex, apex length about 0.13 pleotelson length. Pereopod III ischium dorsal lobe triangular, apex with 1 prominent recurved seta. Operculum stout. Uropods and pleotelson respectively of similar length in adult male and female.

Description of non-ovigerous female

Body (Figs 11A, B, 12A, 13A, B). Length 1.7–1.9 mm, 3.8–4.0 width, subcylindrical, tergite surfaces hirsute, densely covered with cuticular setules on all body parts, incl. pereopods and operculum.

Ventral spines. All spines acute. Pereonite 1 spine prominent. Pereonite 3 spine prominent, closer to anterior segment border. Pereonite 4 spine directed posteriorly, small, closer to posterior segment

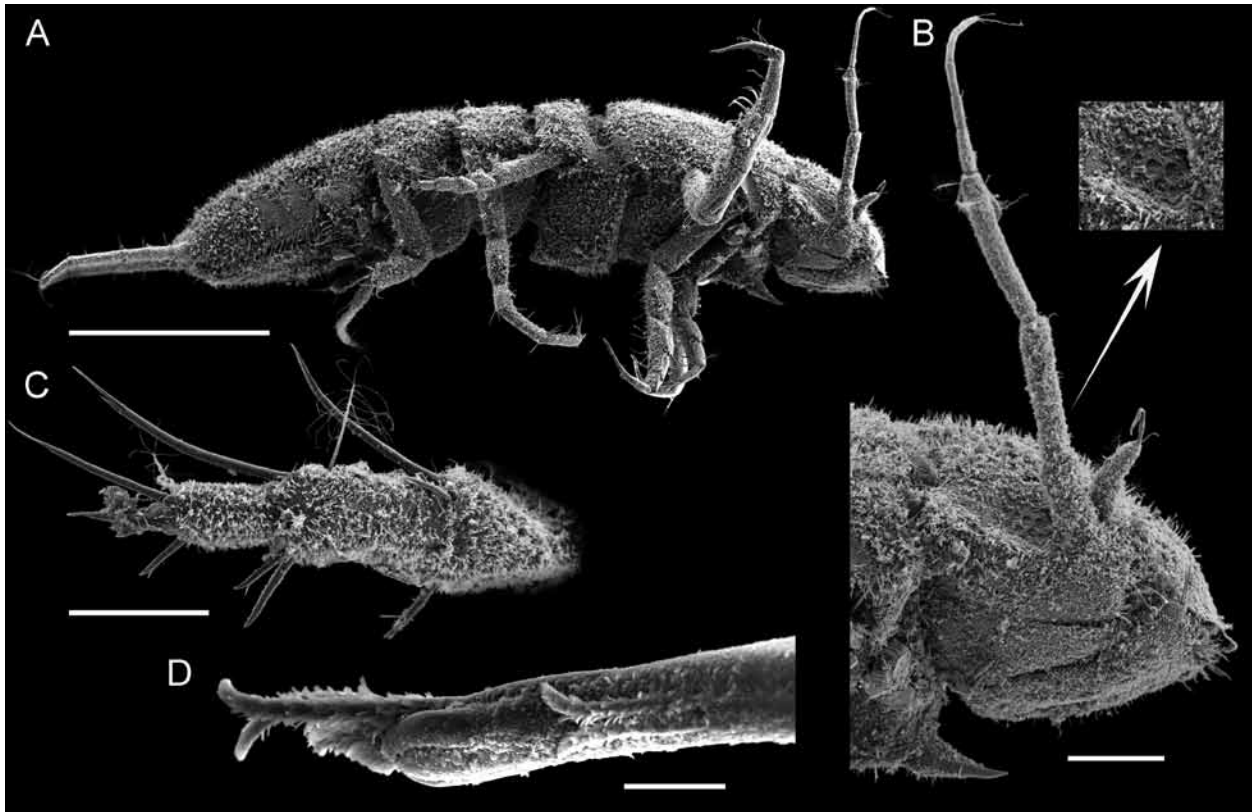


Figure 12. *Macrostylyis matildae* n. sp. A–D, paratype non-ovigerous female (ZMH K-43005), SEM photograph. A, habitus lateral. B, cephalothorax lateral with imbricate ornamentation enlarged. C, pereopod IV, merus–dactylus D, pereopod III dactylus, postero-lateral view. Scale: A = 0.5 mm, B = 0.1 mm, C = 0.05 mm, D = 0.01 mm.

border. Pereonite 5–6 spines prominent, closer to posterior segment border. Pereonite 7 spine small. **Imbricate ornamentation (IO).** Cephalothorax IO dorsally and laterally; pereonite 1–pleotelson IO on all tergites and sternites.

Cephalothorax. Length 0.73–0.84 width, 0.16–0.18 body length; frons convex, with wrinkles, frontal furrow present, slightly convex; dorsal surface with array of setae, in symmetrical arrangement: each side with 3 setae in a transversal row along frontal furrow, 1 seta posteromedially to antennal insertions, 2 setae along posterolateral ridge. Posterolateral setae present, robust, flexibly articulated. Posterolateral margins acute. **Fossosome.** Length 0.84–0.95 width, 0.22–0.24 body length. Lateral tergite margins confluent, ventral surface without keel; sternite articulations present, fully expressed, clearly reaching tergal margin. **Pereonite 1.** Anterior margin concave; poste-

rolateral setae simple. **Pereonite 2–3.** Posterolateral setae simple, flexibly articulated. **Pereonite 4.** Width 1.1 pereonite 5 width, length 0.34–0.41 width; pereonal collum present. Lateral margins curved, narrow in pereonal collum, widest in the middle and slightly concave anterior of posterolateral angles. Posterior tergite margin with 4 simple, thin, flexibly articulated setae; setae extending beyond posterior margin. Posterolateral margins produced posteriorly, rounded. Posterolateral setae bifid, robust, spine-like.

Pereonites 5–7. Posterolateral margins produced posteriorly, rounded. Posterolateral setae bifid, robust, spine-like. **Pereonite 5.** Length 0.42–0.43 width, 0.86–0.94 pereonite 4 length. Posterior tergite margin with 6 simple, flexibly-articulated setae; setae not extending beyond posterolateral margin. **Pereonite 6.** Length 0.50–0.52 width, 1.1–1.2 pereonite 5 length. Posterior tergite margin

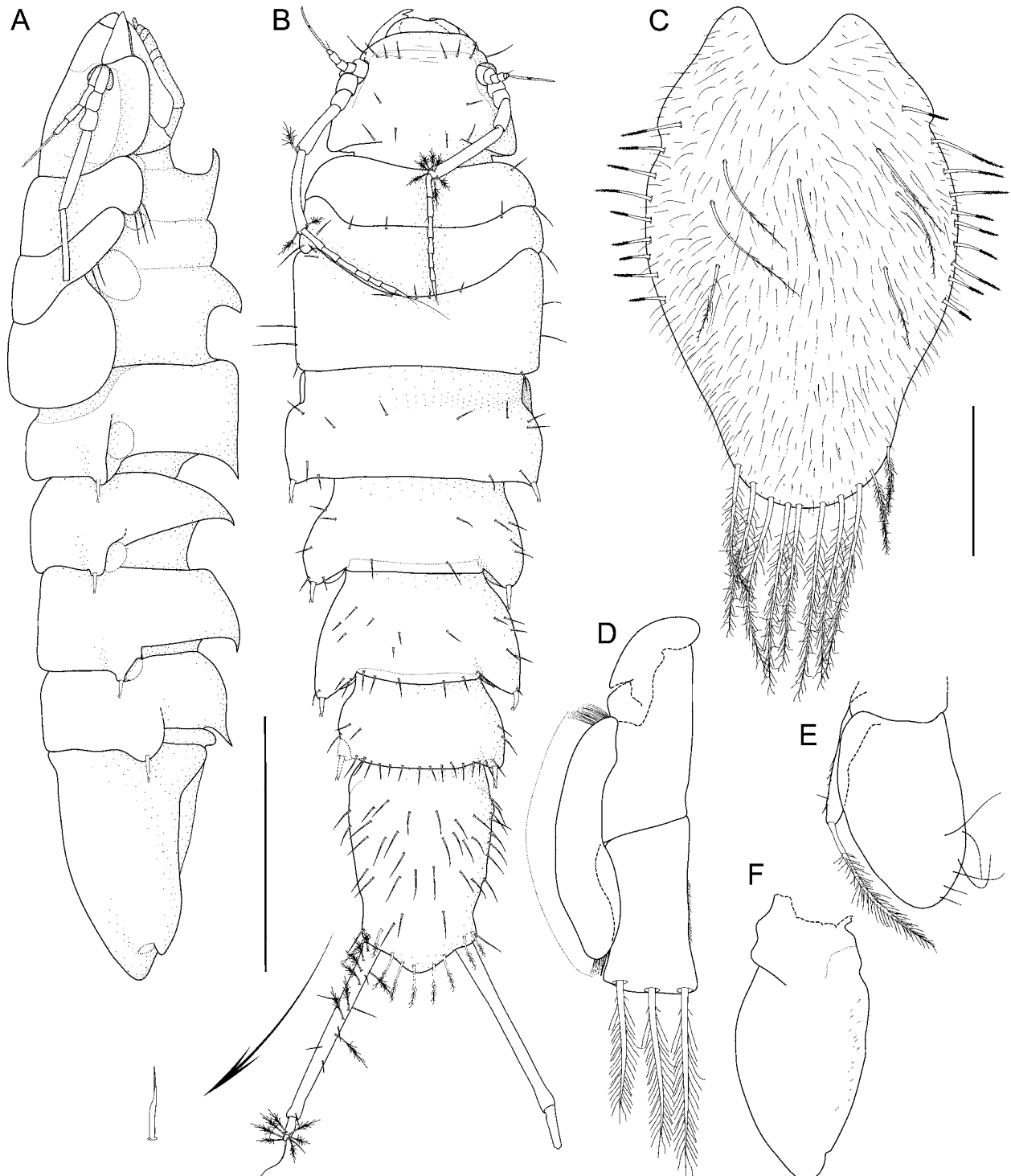


Figure 13. *Macrostylis matildae* n. sp. A–F, paratype non-ovigerous female (ZMH K-43003). **A**, habitus lateral, pereopods dissected, most setae, imbricate ornamentation (IO) and cuticular setules omitted. **B**, habitus, dorsal, cuticular setules, IO and right uropod setation omitted, with pleotelson tergal seta enlarged. **C**, operculum, ventral. **D**, pleopod III, dorsal, exopod setal fringe indicated by dashed line. **E**, pleopod IV, dorsal. **F**, pleopod V, dorsal. Scale: A, B = 0.5 mm, C–F = 0.1 mm.

with 10 simple, flexibly articulated setae; setae extending beyond posterolateral angles. **Pereonite 7.** Length 0.44–0.51 width. Posterior tergite margin with 11–15 simple, flexibly articulated setae; setae extending beyond posterolateral margin.

Pleonite 1. Sternal articulation with pleotelson absent. **Pleotelson (Figs 11A, D, 13B).** Narrowing evenly towards uropod insertions, lateral margins straight, waist present, setal ridges visible in dorsal view, dorsal length 0.22–0.23 body length, 1.4–1.6

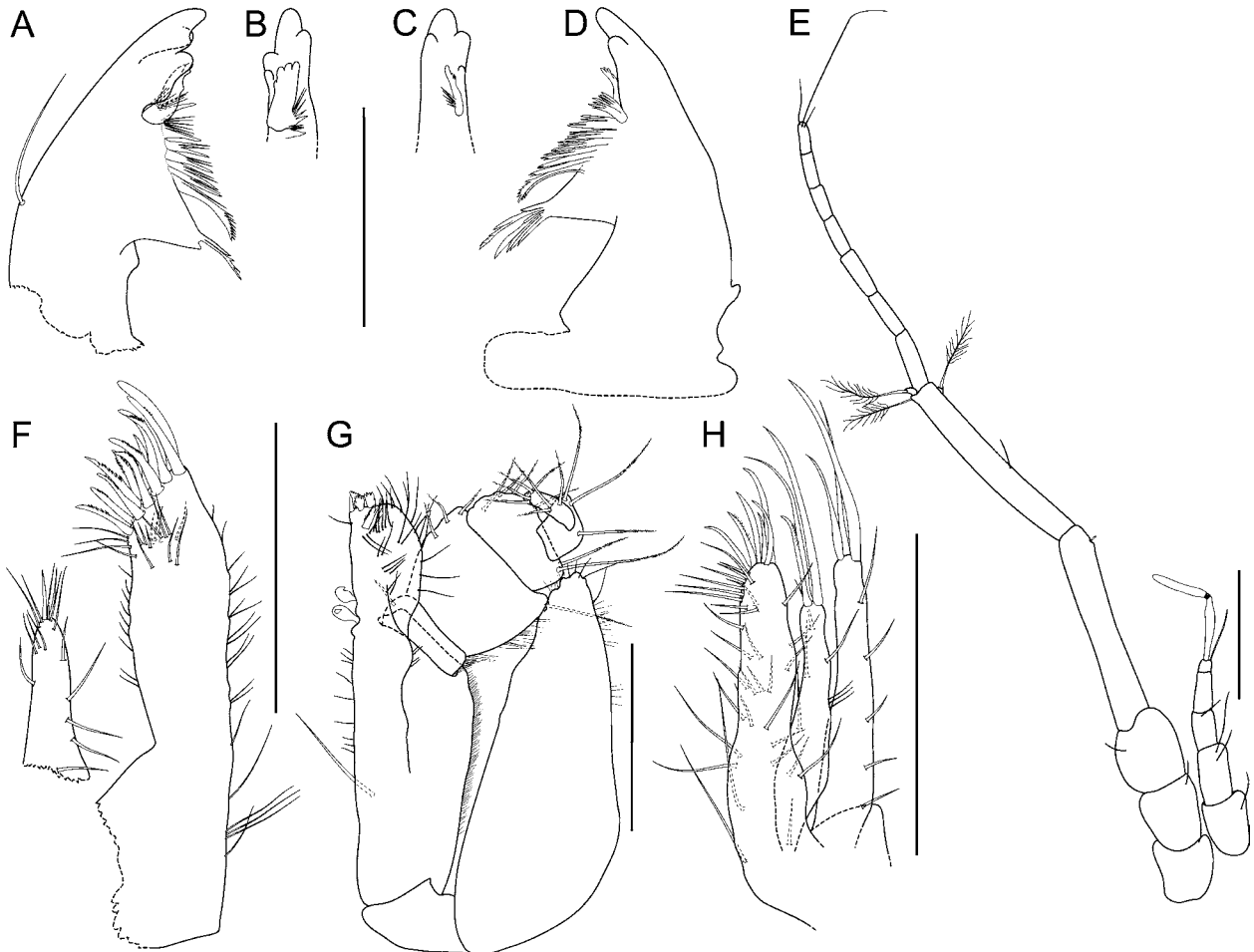


Figure 14. *Macrostylyl matildae* n. sp. **A–H**, paratype non-ovigerous female (ZMH K-43003). **A**, left mandible, dorsal, molar process damaged. **B**, left mandible incisor process and *lacinia mobilis*, medial. **C**, right mandible incisor process and *lacinia mobilis*, medial. **D**, right mandible, dorsal, molar process damaged, lateral seta missing. **E**, antenna and antennula, *in situ*. **F**, maxillula, damaged. **G**, maxilliped, ventral. **H**, maxilla. Scales: A–H = 0.1 mm.

width, narrower than pereonite 7; statocysts present, dorsal slot-like apertures present, diagonal across longitudinal axis, concave. Posterior apex slightly concave at uropod insertions, posteriorly convex, length 0.13 pleotelson length. Posterior apex with 10 pappose setae, positioned on and around apex. Pleopodal cavity width 0.75–0.78 pleotelson width, pre-anal trough width 0.38–0.42 pleotelson width. Anal opening terminally, parallel to frontal plane. *Labrum*. Anterior margin convex.

Antennula (Fig. 14E). Length 0.38 head width, 0.22 antenna length, width 0.69 antenna width. Articles decreasing in width from proximal to distal. Articles 1–4 distinctly longer than wide, cylindrical. Article 1 with 1 broom seta. Article 2 longer than article 1, with 2 broom setae. Article

3 with 1 broom seta. Article 5 squat, with 2 setae: 1 simple, 1 aesthetasc with intermediate belt of constrictions. **Antenna (Fig. 14E).** Length 0.36 body length. Article 1 squat. Articles 2–3 elongate, longer than article 1. Article 4 longer than articles 1–3 together, distally with 1 simple seta. Article 5 length subequal article 4 length, distally with 3 broom setae. Flagellum with 7 articles. **Mandibles (Fig. 14A–D).** In medial view strongly narrowing from proximal to distal; left and right mandible incisor processes multidentate with dorsal and ventral subdistal teeth that partly enclose *lacinia*, left incisor with 4 cusps, *lacinia mobilis* grinding, with 4 cusps; right mandible incisor with 3 cusps, *lacinia mobilis* grinding, clearly smaller than left *lacinia*, with 4 cusps. **Maxillula (Fig. 14F).**

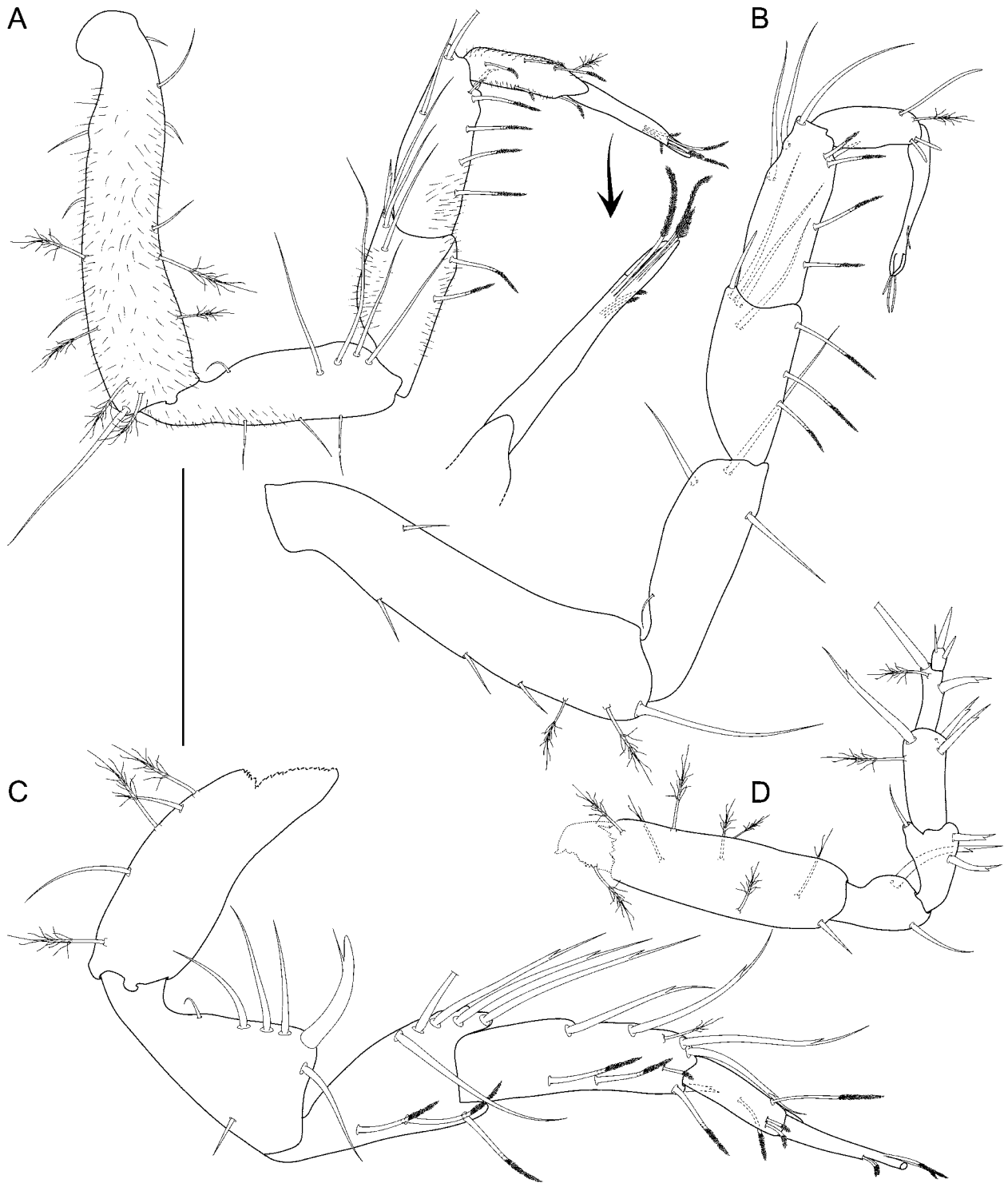


FIGURE 15. *Macrostylis matildae* n. sp. A–D, paratype non-ovigerous female (ZMH K-43003). A, pereopod I. B, pereopod II, cuticular setules omitted. C, pereopod III, cuticular setules omitted, propodus and dactylus twisted 45°. D, pereopod IV, cuticular setules omitted. Scale: A–D = 0.2 mm.

Lateral lobe with 12 robust setae. **Maxilla (Fig. 14H).** Lateral lobe with 3 setae terminally; middle endite with 4 setae terminally; inner endite with 8 setae terminally. **Maxilliped (Fig. 14G).** Basis length 3.3 width, medioventrally with seta present; epipod length 2.7 width, 0.99 basis-endite length; palp wider than endite, article 2 wider than articles

1 and 3, article 1 shorter than article 3.

Pereopod I (Fig. 15A). Length 0.45 body length. Ischium dorsal margin with 5 setae: 1 small proximally, 4 long, thin submarginally. Merus dorsal margin with 4 submarginal setae: 3 long thin, 1 short, bifurcate; ventral margin with 2 medially serrate, distally fringe-like sensillae. Carpus

dorsally with 2 long, thin setae. Dactylus distally with 3 sensillae. **Pereopod II (Fig. 15B)**. Length 0.47 body length. Ischium dorsally with 3 submarginal setae: 1 small proximally, 2 long, thin distally. Merus dorsally with 4 submarginal setae: 3 long and thin, and 1 short, bifurcate; ventrally with 3 medially serrate, distally fringe-like sensillae. Carpus dorsally with 3 long, thin setae; ventrally with 5 setae: 4 medially serrate, distally fringe-like sensillae, 1 short bifurcate. Dactylus distally with 3 sensillae.

Pereopod III (Figs 11C, 12D, 15C). Length 0.47 body length. Ischium dorsal lobe triangular; proximally with 2–3 setae; apex with 1 prominent seta; apical seta robust, bifid, bent towards proximal, spine-like; distally with 1–2 setae. Merus dorsally with 4–6 setae: 1–2 long, thin and 2–4 long, bifurcate; ventrally with 3 medially serrate, distally fringe-like sensillae. Carpus dorsally with 5–6 setae: 4–5 long, bifurcate, 1 broom; ventrally with 4–5 setae: 3–4 medially serrate, distally fringe-like sensillae, 1 short bifurcate. Dactylus distally with 3 sensillae.

Pereopod IV (Figs 12C, 15D). Length 0.25 body length, carpus cylindrical. **Pereopod V (Fig. 16A)**. Length 0.40 body length. Ischium middorsally with 2 setae; distodorsally without seta; midventrally with 1 seta; distoventrally with 3 setae. Merus distodorsally with 4 setae: 2 bifurcate, 2 simple; midventrally with 1 seta; distoventrally with 2 setae: 1 simple, 1 bifurcate. Carpus distodorsally with 1 seta; distoventrally with 3 bifurcate setae. **Pereopod VI (Fig. 16B)**. Length 0.51 body length. Ischium dorsally with 2 setae; midventrally with 4 setae, arranged in bundle; distoventrally with 2 setae. Merus middorsally without seta; distodorsally with 6 setae; midventrally with 2 bifurcate setae, arranged in bundle; distoventrally with 2 setae: 1 long, 1 bifurcate. Distodorsally with 3 setae: 1 broom, and 2 bifurcate; midventrally with

2 bifurcate setae; distoventrally with 4 bifurcate setae. **Pereopod VII (Fig. 16C)**. Length 0.35 body length; basis length 3.8 width, dorsal margin with row of 14 elongate setae, exceeding beyond proximal half of article; setae longer basis width; ventral margin with 2 setae; setae shorter basis width. Ischium length 2.3 width, middorsally with 2 setae, midventrally and distoventrally with 1 seta respectively. Merus length 2.3 width; distodorsally with 3 setae; midventrally and distoventrally with 1 seta respectively. Carpus length 4.7 width, distodorsally with 4, midventrally with 1, distoventrally with 3 bifurcate setae respectively. Propodus length 5.5 width. Dactylus length 4 width.

Operculum (Figs 11D, 13C). Elongate, length 1.6 width, 0.83 pleotelson dorsal length; apical width 0.52 operculum width; distally tapering, not reaching anus; without keel. With lateral fringes of 7–10 setae, distinctly separate from apical row of setae. With 10 pappose setae on apex, completely covering anal opening. **Pleopod III (Fig. 13D)**. Length 2.8 width; protopod length 2.3 width, 0.56 pleopod III length; exopod with fringe of fine setae; setae longer than pleopod III exopod width, length 0.64 pleopod III length, seta subterminally present. **Pleopod V (Fig. 13F)**. Present. **Uropod (Figs 11A, 12A, 13B)**. Inserting on pleotelson posterior margin; length 1.0–1.1 pleotelson length; protopod length 8.8–10.0 width, 0.77–0.88 pleotelson length, protopod distal margin blunt, endopod insertion terminal; endopod length 4.5 width, 0.26–0.30 protopod length, width at articulation narrower than protopod.

Description of adult male

Body (Fig. 17A, B). Length 2.6 mm, 4.2 width. **Cephalothorax**. Length 0.77 width, 0.14 body length. **Fossosome**. Not keeled. **Pereonites 1-3**. With 2, 3, 6–7 long, thin posterolateral setae respectively. **Pereonite 4**. Length 0.52 width. Pereonal collum

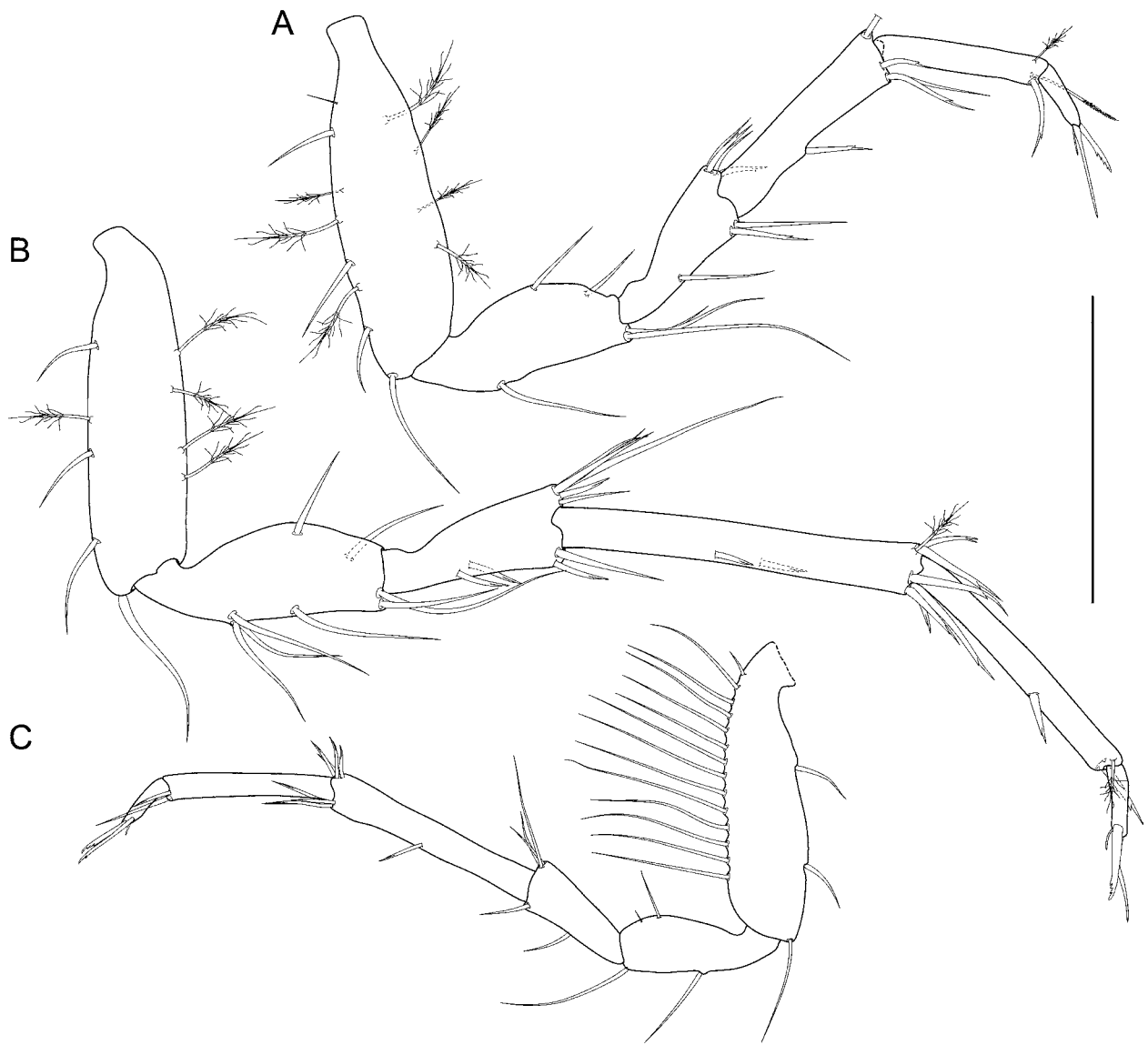


Figure 16. *Macrostyliis matildae* n. sp. A–C, paratype non-ovigerous female (ZMH K-43003). A, pereopod V, cuticular setules omitted. B, pereopod VI, cuticular setules omitted. C, pereopod VII, cuticular setules omitted. Scale: A–C = 0.2 mm.

present, medially convex. Posterolateral margins produced posteriorly. **Pereonite 5.** Length 0.59 width. **Pereonite 6.** Length 0.55 width, 0.90 pereonite 5 length. **Pereonite 7.** Posterior tergite margin with 15 simple, asetulate, flexibly articulated setae; setae not extending beyond posterolateral margin.

Pleonite 1. Sternal articulation with pleotelson present. **Pleotelson (Fig. 17B, C).** Similar to female. Posterior apex length 0.10 pleotelson length, pleopodal cavity width 0.67 pleotelson width, pre-anal trough width 0.33 pleotelson width.

Antennula (Fig. 17D). Length 0.39 head width, width 1.3 antenna width. Article 1 elongate,

longest and widest, with 1 broom seta. Article 2 elongate, with 3 distally fringe-like sensillae. Article 3 squat, with 2 simple setae. Article 4 squat, with 6 aesthetascs. Article 5 squat, with 6 setae: 1 simple, 5 aesthetascs. Aesthetascs with intermediate belt of constrictions. **Antenna (Fig. 17D).** Damaged. Article 1 squat. Article 2 squat, longer than article 1. Article 3 elongate, longer than article 1.

Pereopod I (Fig. 18A, B). Length 0.36 body length. Ischium dorsally with 4 setae. Carpus dorsally with 2 setae: 1 broom, 1 simple; ventrally with 3 setae: 2 medially serrate, distally fringe-like

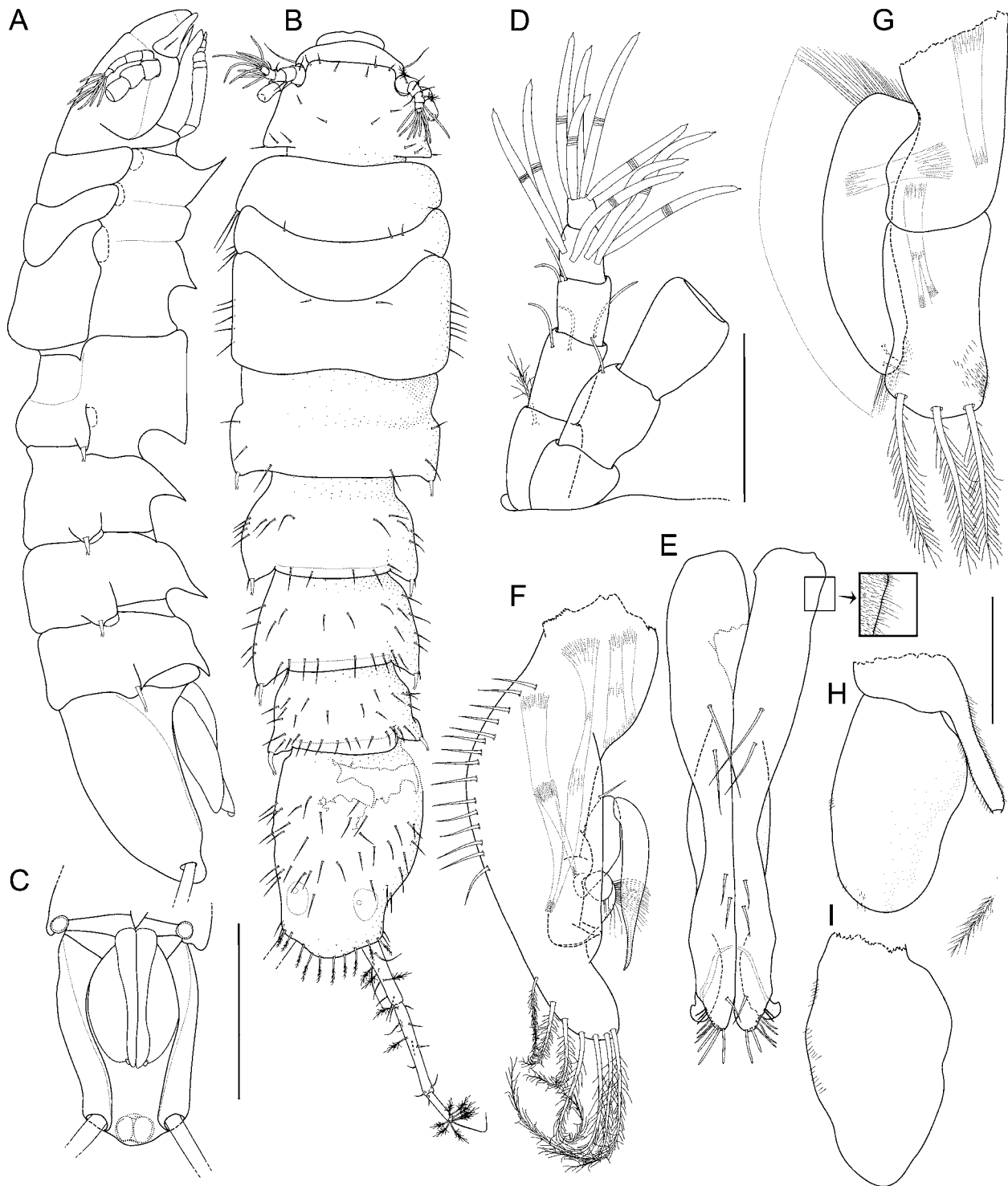


Figure 17. *Macrostyliis matildae* n. sp. A–I, paratype adult male (ZMH K-43004). **A**, habitus, lateral, antenna broken, pereopods dissected, cuticular setules and imbricate ornamentation (IO) omitted. **B**, habitus, dorsal, cuticular setules and IO omitted, pleotelson damaged, left uropod omitted, antennae broken. **C**, pleotelson, ventral, setae and cuticular setules omitted. **D**, antennule and antenna, in situ, antenna broken. **E**, pleopods I, cuticular setules enlarged. **F**, pleopod II, ventral, cuticular setules omitted. **G**, pleopod III. **H**, pleopod IV. **I**, pleopod V. Scales: A–C = 0.5 mm, D–I = 0.1 mm.

sensillae, 1 small simple. **Pereopod II** (Fig. 18C). Length/body-length ratio smaller than in female: length 0.41 body length. Ischium dorsally with 5 long, thin setae. Merus dorsally with 3 setae; ven-

trally with 3 medially serrate, distally fringe-like sensillae. Carpus dorsally with 3 setae: 2 long, thin, 1 broom; ventrally with 5 setae: 4 medially serrate, distally fringe-like sensillae, 1 small, simple. **Pere-**

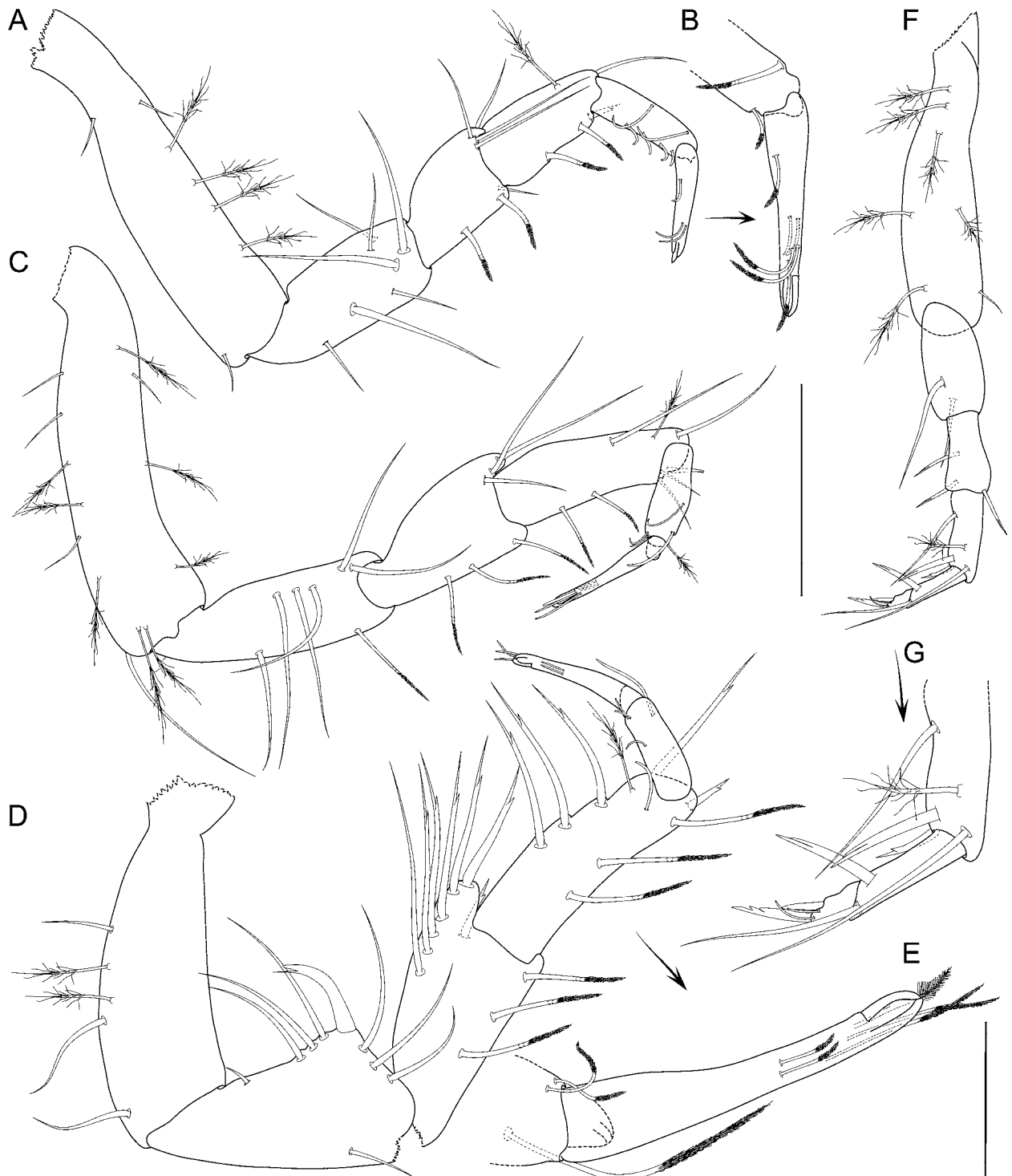


Figure 18. *Macrostyliis matildae* n. sp. A–E, paratype adult male (ZMH K-43004). A, pereopod I, cuticular setules omitted. B, pereopod I dactylus, double size. C, pereopod II. D, pereopod III, cuticular setules omitted. E, pereopod III dactylus, double size. F, pereopod IV, cuticular setules omitted. G, pereopod IV dactylus enlarged. Scales: A,C,D,F = 0.2 mm, E = 0.05 mm.

opod III (Fig. 18D, E). Length 0.44 body length. Ischium dorsal lobe triangular, proximally with 3 simple setae; apex with 1 prominent, robust, spine-like, bifid seta; distally with 3 simple setae. Merus dorsally with 7 setae: 1 long, thin, simple, 6 bifurcate; ventrally with 3 medially serrate, distally

fringe-like sensillae. Carpus dorsally with 5 setae: 4 bifurcate, 1 broom; ventrally with 4 setae: 3 medially serrate, distally fringe-like sensillae, 1 short bifurcate. **Pereopod IV (Fig. 18F, G).** Length 0.23 body length. **Pereopod V (Fig. 19A, B).** Ischium middorsally with 1 seta, distodorsally with 2 bi-



Figure 19. *Macrostylyis matildae* n. sp. **A–C**, paratype adult male (ZMH K-43004). **A**, pereopod V, cuticular setules omitted. **B**, pereopod V dactylus, enlarged. **C**, pereopod VI, cuticular setules illustrated. **D**, pereopod VII, cuticular setules omitted, twisted at carpo-propodal articulation. Scale: A, C, D = 0.2 mm.

furcate setae; midventrally with 3 setae in bundle; distoventrally with 2 setae. Merus distodorsally with 3 setae: 1 long, slim, 2 short, bifurcate; midventrally with 1 bifurcate seta; distoventrally with 3 setae: 1 bifurcate, 1 simple. Carpus distodorsally with 2 setae: 1 broom, 1 simple; distoventrally with 4 short, bifurcate setae. **Pereopod VI (Fig. 19C)**. Length 0.36 body length. Ischium setation as in female: dorsally with 2 setae; midventrally with 4 setae in bundle; distoventrally with 3 setae. Merus distodorsally with 4 setae: 1 short, bifurcate, 3 simple; midventrally with 1 bifurcate seta; distoventrally with 2 setae: 1 bifurcate, 1 long,

simple. Carpus middorsally with 1 bifurcate seta; distodorsally with 4 setae: 1 broom, 3 bifurcate; midventrally with 2 bifurcate setae; distoventrally with 3 bifurcate setae. **Pereopod VII (Fig. 19D)**. Shorter pereopod VI; basis length 3.0 width; dorsal margin with row of 19 elongate setae exceeding proximal half of article; setae longer basis width; ventral margin with 3 setae; setae shorter basis width; ischium length 3.0 width; middorsally with 2 setae; midventrally with 3 setae; distoventrally with 3 setae. Merus length 2.8 width, setation as in female; carpus length 9.0 width; distodorsally with 4 setae: 1 broom, 3 bifurcate; midventrally with

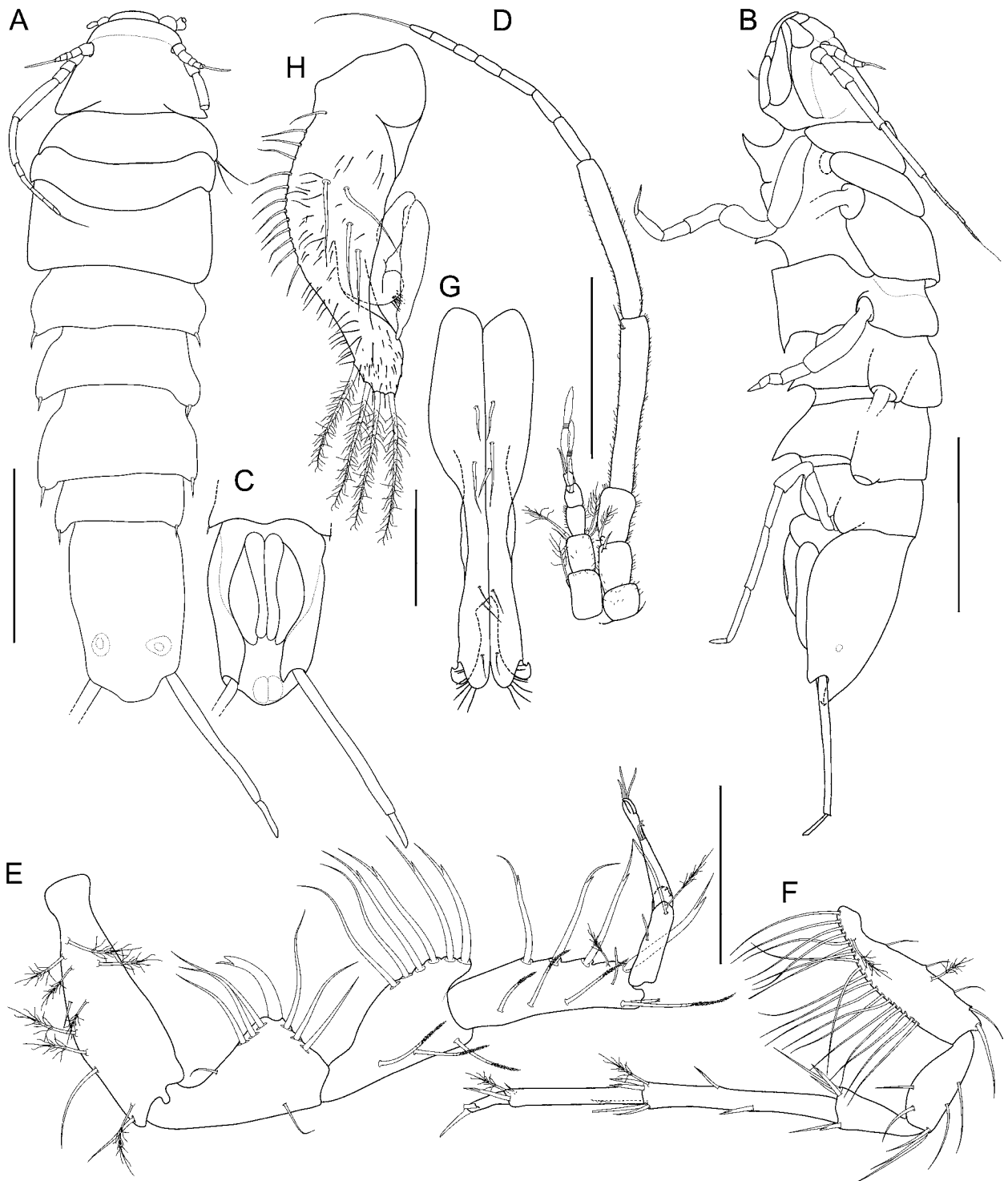


Figure 20. *Macrostyliis matildae* n. sp. **A–C**, paratype juvenile male (ZMH K-43001). **A**, habitus dorsal, cuticular setules and most setae omitted. **B**, habitus lateral, cuticular setules and most setae omitted. **C**, pleotelson, ventral, cuticular setules and setae omitted. **D**, antennule and antenna. **E**, pereopod III. **F**, pereopod VII. **G**, pleopod I. **H**, pleopod II, ventral, cuticular setules omitted. Scale: A–C = 0.5 mm; D–F = 0.2 mm; G, H = 0.1 mm.

3 bifurcate setae; distoventrally with 2 bifurcate setae. Propodus length 8.5 width. Dactylus length 5.0 width.

Pleopod I (Fig. 17E). Length 0.66 pleotelson length, lateral horns not extending distally beyond medial lobes; distally with 8–9 sensillae,

ventral setae present. **Pleopod II (Fig. 17F).** Protopod apex rounded, with 15 setae on proximolateral margin; with 7 pappose setae distally. Endopod distance of insertion from protopod distal margin 0.37 protopod length. Stylet weakly curved, not extending to distal margin of protopod, length

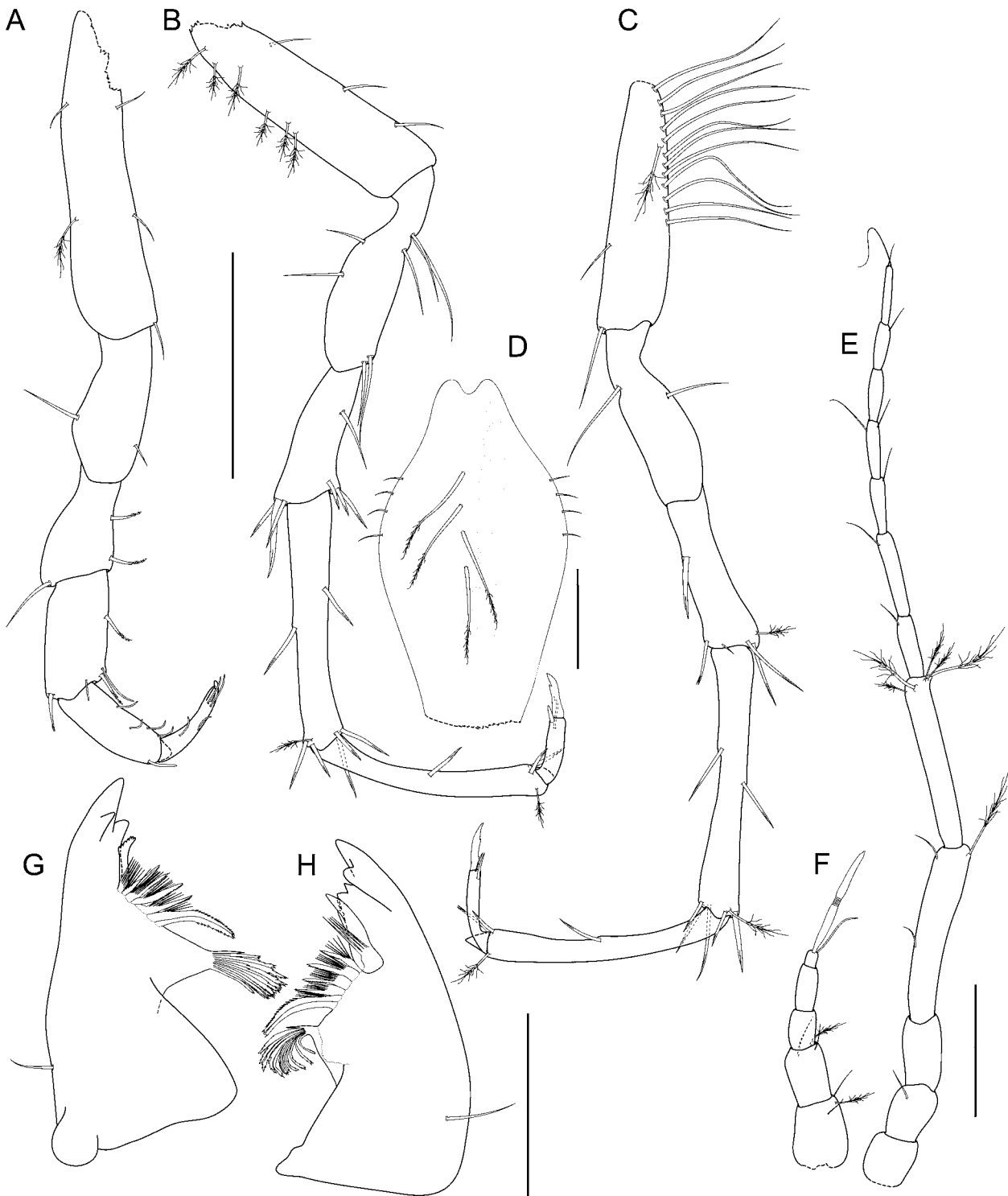


Figure 21. *Macrostylyx sarsi* Brandt, 1992 A–H, holotype non-ovigerous female (BM(NH)1990-40-1). A, pereopod I. B, pereopod VI. C, pereopod VII. D, operculum, apex damaged. E, antenna. F, antennula. G, right mandible, ventral. H, left mandible, ventral. Scale: A–C = 0.2 mm; D–H = 0.1 mm.

0.40 protopod length. **Uropod (Fig. 17B).** Length 0.97 pleotelson length; protopod length 9.2 width; endopod length 0.22 protopod length, less than in female, length 5.0 width.

Remarks

The pleotelson of the best intact adult male specimen available is strongly damaged. This might have affected the measurements related to the pleotelson width. The most distinct character state of this species is the dense coat of cuticular setules

covering all body parts and external appendages. Different from other species of which both adult sexes have been described, no dimorphism can be found in the shape and size ratios of the pleotelson and uropods. Setal microstructures might have been overlooked in several instances due to the small size of the specimens. There are some indications for several pereopodal setae for which no further attributes were described to be mono- or bisetulate. *Macrostylis matildae* n. sp. can be regarded closely related to several species from the Southern and Indian Oceans: *M. expolita* Mezhov, 2003b, *M. latiuscula* Mezhov, 2003b, *M. medioxima* Mezhov, 2003a, *M. sarsi* Brandt, 1992, *M. setulosa* Mezhov, 1992, and *M. vinogradovae* Mezhov, 1992. This is due to the similar body shape and ventral spination; body covered with cuticular setules; pereonite 3 posterolateral spine-like setae absent (not in *M. setulosa*); pereonite 4 posterolateral spine-like setae present; operculum distally narrowing with lateral fringe of setae distinctly separate from apical row of setae.

***Macrostylis antennamagna* Riehl & Brandt, 2010**

urn:lsid:zoobank.org:act:5B09C3B7-6291-458D-BC5E-975BCBD39D80

Macrostylis antennamagna Riehl & Brandt, 2010; pp. 29–43; Figs 9–18.

Modified diagnosis

Body hirsute. Female pleotelson narrowing evenly towards uropod insertions, lateral margins straight, posterior apex slightly concave, posterior apex length 0.15 pleotelson length. Male pleotelson of hour-glass-like shape, posterior apex clearly concave. Female pereonite 4 posterolateral margins produced posteriorly, rounded. Male pere-

onite 4 posterolateral margins not produced posteriorly. Female pereonite 6 shorter pereonite 5, vice versa in male. Female pereonite 3–4 ventral spines present, small, both absent in male. Female and male pereonite 7 ventral spine small. Pereopod III ischium dorsal lobe triangular.

***Macrostylis cerrita* Vey & Brix, 2009**

urn:lsid:zoobank.org:act:3644D8D7-30A9-462E-9DC1-8D19C948EC9C

Macrostylis cerrita Vey & Brix, 2009; pp. 356–370, Figs 1–6.

Modified diagnosis

Body cuticular setules absent. Pereonite 3 posterolateral margins not produced posteriorly. Pereonite 3–4 ventral spines absent. Pereonite 4 lateral margins convex in collum region, concave posteriorly; posterolateral margins not produced posteriorly. Pereonite 7 ventral spine prominent. Pleotelson narrowing evenly towards uropod insertions, lateral margins straight, waist present; posterior apex posteriorly convex, length 0.14 pleotelson length. Pereopod III ischium dorsal lobe tapering, recurved with no apical seta. Pereopod V ischium distodorsally without seta. Operculum elongate, distally tapering, apical width subequal or smaller 0.5 operculum width, lateral fringe of setae distinctly separate from apical row of setae.

Remarks

The original illustration of the habitus (Vey & Brix 2009; Fig. 1B) shows a conspicuous spine laterally on the pleotelson. This spine was not mentioned in the original description text though. The inspection of the holotype revealed that it does not exist. The pereopod III ischium dorsal lobe (Fig.

Key to the Southern-Ocean species of *Macrostylis*

Except where mentioned otherwise, the key is based on females.

1. Pleotelson lateral margins narrowing evenly towards uropod insertions, lateral margins straight (Fig. 22A)... **2**
- Pleotelson rectangular, lateral margins straight, parallel (Fig. 22C)... *Macrostylis gerdesi* (Brandt, 2002)
- Pleotelson ovoid (Fig. 22D)..... **4**
- 2(1). Pereonite 3 ventral spine present (Fig. 22F, G); pleotelson waist present (Fig. 22B, D, E); pereonite 4 ventral spine present (Fig. 22F, G); pereonite 7 ventral spine small (Fig. 22F, H); pereopod III ischium dorsal apex triangular (Fig. 22P)..... **3**
- Pereonite 3 ventral spine absent (Fig. 22H); pereonite 4 spine absent (Fig. 22H); pleotelson waist absent (Fig. 22A); pereonite 7 spine prominent (Fig. 22G); pereopod III ischium dorsal apex tapering, recurved (Fig. 22O)..... *Macrostylis cerrita* Vey & Brix, 2009
- 3(2). Operculum elongate (Fig. 22L, M); pereonite 4 posterolateral margins tapering; pleotelson posterior apex concave (Fig. 22E); pereonite 7 posterolateral margins sexually dimorphic; pereopod III dorsal apex with 2 prominent setae (Fig. 22Q)..... *Macrostylis antennamagna* Riehl & Brandt, 2010
- Operculum stout (Fig. 22N); pereonite 4 posterolateral margins rounded; pleotelson posterior apex convex (Fig. 22A–D); pereonite 7 posterolateral margins similar in female and male; pereopod III ischium dorsal apex with 1 prominent seta (Fig. 22P)..... *Macrostylis matildae* Riehl & Brandt n. sp.
- 4(1). Pleotelson waist absent (Fig. 22A, C); pereonite 4 width subequal pereonite 5 width..... **5**
- Pleotelson waist present (Fig. 22B, D, E); pereonite 4 width exceeding pereonite 5 width..... **6**

Figure 22. Illustrations for identification key to the Macrostylidae of the Southern Ocean (opposite page) **A**, pleotelson of *Macrostylis cerrita* Vey & Brix, 2009, dorsal view, evenly narrowing towards uropodal insertions, lateral margins straight, waist absent. **B**, pleotelson of *M. matildae* n. sp., dorsal view, evenly narrowing towards uropodal insertions, lateral margins straight, waist present. **C**, pleotelson of *M. gerdesi* (Brandt, 2002), dorsal view, lateral margins straight, subparallel. **D**, pleotelson of *M. setulosa* Mezhov, 1992, lateral margins convex, waist present. **E**, pleotelson of *M. antennamagna* Riehl & Brandt, 2010, dorsal view, lateral margins convex, waist present, posterior apex concave. **F**, ventral spines of *M. matildae* with pereonites 3 and 4 spines present, pereonite 7 spine small. **G**, ventral spines of *M. roaldi* Riehl & Kaiser (2012) with pereonites 3 and 4 spines present, pereonite 7 spine prominent. **H**, ventral spines of *M. scotti* n. sp. with pereonites 3 and 4 spines absent, pereonite 7 spine small. **I**, *M. matildae* pereonite 3 posterolateral margin spine-like setae absent, pereonite 4 lateral margin curved, posterolateral margin produced posteriorly, rounded, spine-like setae present.

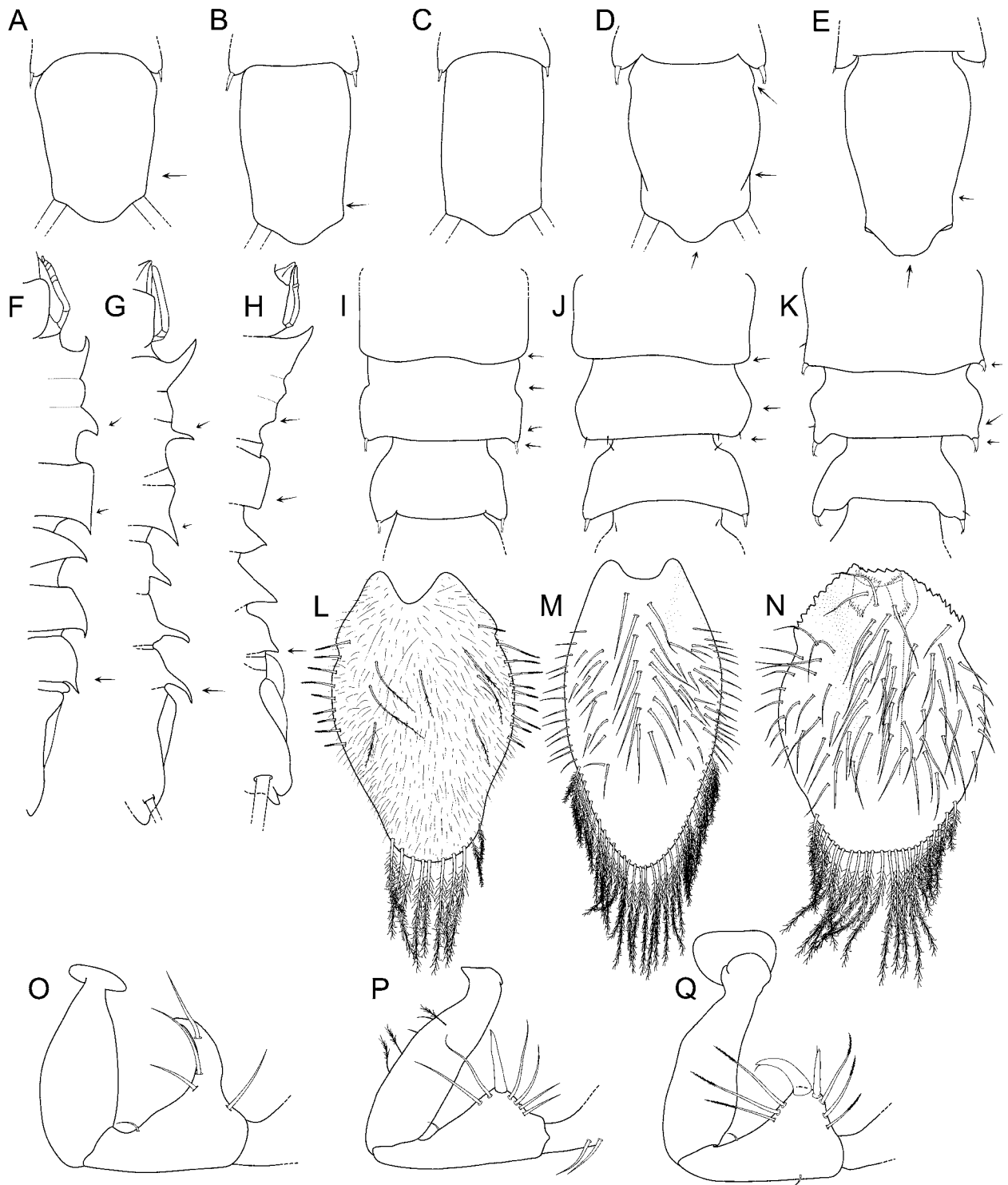


Figure 22 continued. **J**, *M. scotti* pereonite 3 posterolateral margin spine-like setae absent, pereonite 4 lateral margin convex, posterolateral margin not produced posteriorly, rounded, spine-like setae absent. **K**, *M. roaldi* pereonite 3 posterolateral margin spine-like setae present, pereonite 4 lateral margin curved, posterolateral margin produced posteriorly, pointed, spine-like setae present. **L**, *M. matildae* operculum, elongate, distally tapering, with lateral fringe of setae distinctly separate from apical row of pappose setae. **M**, *M. scotti* operculum, elongate, ovoid, with fluent transition between lateral fringe of setae and apical row of pappose setae. **N**, *M. roaldi* operculum, stout, ovoid, with lateral fringe of setae distinctly separate from apical row of pappose setae. **O**, *M. cerrita* pereopod III ischium with tapering dorsal apex and 1 spine-like prominent seta. **P**, *M. roaldi* pereopod III ischium with triangular dorsal apex and 1 prominent spine-like seta. **Q**, *M. scotti* pereopod III ischium with dorsal apex tapering and 2 prominent, spine-like setae.

5(4). Pereonite 4 lateral margins curved, posterolateral margins rounded, posterolateral setae prominent, robust (Fig. 22I); pereopod III ischium dorsal lobe triangular (Fig. 22P); pereonite 6 length clearly larger than pereonite 5 length; operculum distally tapering, lateral fringe of setae distinctly separate from apical row of pappose setae (Fig. 22L).....	<i>Macrostylis sarsi</i> Brandt, 1992 nom. dub.
– Pereonite 4 lateral margins convex, posterolateral margins rounded, posterolateral setae simple, small (Fig. 22J); pereopod III ischium dorsal lobe tapering (Fig. 22Q); pereonite 6 length smaller or subequal to pereonite 5 length; operculum ovoid, lateral fringe of setae with fluent transition to apical row of pappose setae (Fig. 22M).....	<i>Macrostylis uniformis</i> Riehl & Brandt, 2010
6(4). Body cuticular setules absent; Pereonite 3 posterolateral margin not produced posteriorly (Fig. 22I, J); pereonite 6 posterolateral margin rounded.....	7
– Body cuticle with dense cuticular setules, pereonite 3 posterolateral margin produced posteriorly (Fig. 22K); pereonite 6 posterolateral margin tapering.....	8
7(6). Pereonites 3, 4 and 7 ventral spines present (Fig. 22F,G); pereonite 7 spine prominent (Fig. 22G); pereopod III ischium with 1 prominent apical seta (Fig. 22P); operculum as long as pleotelson, distally tapering, lateral fringe of setae distinctly separate from apical row of pappose setae (Fig. 22L), apical setae short.....	<i>Macrostylis vinogradovae</i> Mezhov, 1992
– Pereonites 3 and 4 ventral spine absent (Fig. 22H); pereonite 7 ventral spine present, small (Fig. 22F,H); pereopod III ischium with 2 prominent apical setae (Fig. 22Q); operculum ovoid (Fig. 22M), lateral fringe of setae with fluent transition to apical row of pappose setae, apical setae long	<i>Macrostylis scotti</i> Riehl & Brandt n. sp.
8(6). Pereonite 4 spine present, lateral margins concave in neck region and anteriorly to posterolateral projections (Fig. 22K); pereonite 3 ventral spine present, prominent (Fig. 22F,G); operculum stout (Fig. 22N), ovoid, apical width greater 0.5 operculum width (Fig. 22N).....	<i>Macrostylis roaldi</i> Riehl & Kaiser, 2012
– Pereonite 3 ventral spine present, small; pereonite 4 spine absent (Fig. 22H), lateral margins convex (Fig. 22J); operculum elongate (Fig. 22L,M), distally tapering, apical width up to 0.5 operculum maximum width.....	<i>Macrostylis setulosa</i> Mezhov, 1992

4E) is of remarkable shape and setation. It is tapering, recurved and an apical seta is lacking. A similar ischium is present in *M. balayevi* Mezhov, 1989 *M. quadratura* Birstein, 1970 and *M. tumu-*

losa Mezhov, 1989 where the dorsal lobe is tapering and without apical seta. The recurved apical lobe found in *M. cerrita*, however, might represent a more derived condition. In other species of

the genus, the ischium has a convergently similar, hook-shaped appearance. Instead of a recurved dorsal lobe, however, a hook-shaped apical spine-like seta (Fig. 22O) is present on the dorsal lobe apex. This is the case e.g. in *Macrostylis carinifera* Mezhov, 1988, *M. dorsaetosa* Riehl *et al.*, 2012, *M. papillata* Riehl *et al.* 2012, *M. spinifera* Sars, 1864. Vey and Brix (2009) noticed the lateral mandibular setae and interpreted this character as autapomorphy for *M. cerrita*. However, the mandibular lateral setae have been recognized already before, e.g. in *M. sarsi* (Brandt 1992; Fig. 14) and *M. magnifica* Wolff, 1962 (Mezhov 2000), and are present in all species described since and all type material checked (Riehl, unpublished data). Possibly, those setae are apomorphic for the whole family Macrostylidae. In accordance with the gender agreement stated in Article 31.2 of the ICZN, the species-group name is changed to be feminine.

***Macrostylis gerdesi* (Brandt, 2002)**

urn:lsid:zoobank.org:act:DE164C85-4733-40E3-9721-975940A24F95

Desmostylis gerdesi Brandt, 2002; pp. 618–626, Figs 1–4; *Macrostylis gerdesi* (Brandt, 2002).— Riehl & Brandt, 2010; pp. 43–44; Fig. 19.

Type fixation

Holotype: non-ovigerous female, 1.8 mm length, ZMH K-39915, by original designation.

Type locality

Antarctica, Southern Ocean, Weddell Sea, off Kapp Norvegia: multiple box corer, station 037, 28.2.1996, 71° 31.90'S, 13° 31.20'W; 238 m depth.

Type material

Holotype: non-ovigerous female, 1.8 mm length, ZMH K-39915, dissected; paratype: non-ovigerous female, 1.6 mm length, ZMH K-39916, from type locality.

Type material – Remarks

The holotype carcass got all limbs removed and is strongly damaged. The slides with appendages are in good condition.

Modified diagnosis

Pereonite 3 ventral spine small. Pereonite 4 width subequal pereonite 5 width, posterolateral margins not produced posteriorly, ventral spine absent. Pereonite 6 length shorter pereonite 5 length. Pereonite 7 ventral spine prominent. Pleotelson subrectangular, waist absent, posterior apex convex. Pereopod III ischium dorsal lobe triangular. Pereopod V ischium dorsally with no seta.

***Macrostylis obscura* (Brandt, 1992) nom. dub.**

Desmostylis obscura Brandt, 1992; p. 70, Figs 11–13; *Macrostylis obscura* (Brandt, 1992); Riehl & Brandt (2010); pp. 43–44; Fig. 19.

Remarks

This species and the genus *Desmostylis* Brandt, 1992 were based on a single damaged manca. Both were subsequently transferred to *Macrostylis* Sars, 1864 (Riehl & Brandt 2010). The species was collected from the same box corer sample as *M. sarsi* Brandt, 1992, which is represented by a single subadult female specimen. Both species share several similarities, such as dorsal and lateral setation of the body. Quantitative samples such as box-corer samples often show an aggregated distribution of

single species, so the possibility remains that these specimens are conspecific. Unfortunately, much of each type specimen is missing owing to dissection and subsequent damage and loss at the NHM London. So the types cannot be fully compared to decide whether they are conspecific or not. Another consequence of the manca stage of the only known representative of *M. obscura* is that information suitable and available for comparison with other species of the family is very limited. *M. obscura* is therefore not included in the key presented below and is henceforward regarded *nomen dubium*. In accordance with the gender agreement stated in Article 31.2 of the ICZN, the species-group name is changed to be feminine.

***Macrostylis sarsi* Brandt, 1992 nom. dub.**

(Fig. 21)

Macrostylis sarsi Brandt 1992; pp. 74–78, Figs 14–16.

Type fixation

Ovigerous female, 2.0 mm length, BM(NH) 1990:40:1, by original designation.

Type locality

West Maud Rise, ANT VIII/6 station 1833–1. 65° 10.5'S, 0° 27.4'W; depth 4,335 m, box corer.

Type material

Only holotype available, deposited at the Natural History Museum, London.

Modified diagnosis

Body with furry coat of cuticular setules and scattered spine-like, bifid setae. Pereonite 3 posterolateral margins produced posteriorly. Pereonite 4

width subequal pereonite 5 width, lateral margins curved; posterolateral margins rounded, not produced posteriorly, posterolateral setae present. Pereonite 6 length clearly larger pereonite 5 length. Female pleotelson ovoid, waist absent. Pereopod III ischium dorsal lobe triangular. Pereopod VII length smaller pereopod VI length. Operculum elongate, length exceeding 1.5 width.

Remarks

Based on the illustrations, the holotype is not adult. It is the only specimen available. A potential synonymy with *Macrostylis obscura* (Brandt, 1992) is discussed above. The ventral spines have not been illustrated in the original description, as it was the case in *M. obscura* (Brandt, 1992), described in the same publication, where later ventral spines were found (Riehl & Brandt 2010). The scale provided in the habitus plate is probably incorrect: according to the description, the body should be 2.0 mm long; new measurements based on the scale provided result in a body length of 1.3 mm. All other plates have no scale and hence, re-evaluation of ratios between parts is impossible and hence, original measures were mostly applied here. The holotype carcass is gone missing, slides are available but damaged and dissected parts are mostly in bad condition or lost. Appendages available on slides are: Antennula, antenna, mandibles, pereopod I, pereopods 5–7, operculum (apex broken). The taxonomic identity of this species cannot be determined from its existing type and it is hence considered *nomen dubium*.

***Macrostylis setulosa* Mezhov, 1992**

urn:lsid:zoobank.org:act:8C216677-AD60-4F8B-B55B-34627ABB7479

Macrostylis setulosa Mezhov, 1992; pp. 83–87, Fig. 1.

Type fixation

Holotype: non-ovigerous female, 3.2 mm, Mc-1274, by original designation.

Type material

Holotype: non-ovigerous female, Mc-1274, with 3 stage III mancae; paratype: non-ovigerous female, 2.8 mm, Mc-1275. All material deposited at the Zoological Museum of the Moscow State University.

Type locality

Southern Ocean, Scotia Arc, South Sandwich Islands with R/V *Akademik Kurchatov*, cruise 11, station 880, 57° 07.4' S, 26° 40' W; 757 m depth; by means of the bottom sampler "Okean".

Type material – Remarks

The paratype material collected at stations R/VAkademik *Kurchatov* 927 originate from a very different locality and depth. Type material was not available for comparison but there is a possibility that they are different species. Because of that, the information given by Mezhov about male characters were excluded here and corresponding stations are listed below as further records instead of type locality. The type locality is hence restricted to the locality of the holotype.

Further records

R/V *Akademik Kurchatov*, cruise 11, station 927,

56° 08.4' S, 52° 40' W; 1,660 m depth.

R/V *Dm. Mendeleev*, cruise 43, station 4084-I, 70° 40.6' S, 15° 47.8' W; 4,335 m depth.

R/V *Dm. Mendeleev*, cruise 43, station 4084-II, 70° 53.17' S, 15° 04.51' W; 2,925 m depth.

R/V *Dm. Mendeleev*, cruise 43, station 4085, 60° 33.35'S, 35° 37.1' W; 2,705 m depth.

Modified diagnosis

Pereonite 3 posterolateral margins produced posteriorly, ventral spine present, small. Pereonite 4 lateral margins convex, ventral spine absent. Pleotelson ovoid. Pereopod III ischium dorsal lobe triangular. Operculum elongate, distally tapering, apical width smaller 0.50 operculum width.

Description of non-ovigerous female

Body. Length 2.8–3.2 mm, 4.1 width, subcylindrical; with furry cuticular setules, mainly laterally on tergites V–VII and covering whole pleotelson.

Ventral spines. Pereonite 1 spine acute, prominent. Pereonite 3 spine acute, small, placed medially on midline. Pereonite 4 spine absent. Pereonite 5 spine acute, small, closer to posterior segment border. Pereonite 6 spine acute, prominent, closer to posterior segment border. Pereonite 7 spine prominent.

Cephalothorax. Frons straight, frontal furrow present, convex, almost straight, anterior to antennal articulations; posterolateral margins acute. **Fossosome.** Length 0.82 width, 0.21 body length. Lateral tergite margins confluent, ventral surface without keel; sternite articulations present in rudimental condition. **Pereonite 1.** Anterior margin concave. **Pereonite 3.** Posterolateral margin produced posteriorly, tapering, with lateral constriction anteriorly to seta articulations; posterolateral setae bifid, robust, spine-like. Pereonites 4–7. Posterolateral margins produced posteriorly, tapering. Posterolateral setae bifid, robust, spine-

like. **Pereonite 4.** Width 1.1 pereonite 5 width, length 0.33 width; pereonal collum present. Lateral margins simple concave.

Pereonite 5. Length 0.48 width, 1.3 pereonite 4 length. **Pereonite 6.** Length 0.56 width, 1.2 pereonite 5 length. **Pereonite 7.** Length 0.50 width. **Pleotelson.** Length 0.23 body length, 1.4 width, narrower than pereonite 7; ovoid, setal ridges visible, waist present. Width maximum anterior to waist. Statocysts present, dorsal slot-like apertures transverse across longitudinal axis, convex. Posterior apex length 0.15 pleotelson length, concave at uropod insertions, posteriorly convex, evenly rounded.

Labrum. Anterior margin concave. **Antennula.** Length 0.23 antenna length, width 0.60 antenna width. Articles decreasing in size from proximal to distal. Articles 1–4 distinctly longer than wide, cylindrical. Article 1 longest and widest, with 3 setae: 2 simple, 1 broom. Article 2 with 5 setae: 2 simple, 3 broom. Article 3 with 1 simple seta. Article 5 minute, squat, with 2 setae: 1 simple, 1 aesthetasc. **Antenna.** Article 1 squat. Article 2 elongate, longer than article 1. Article 3 elongate, longer than article 1. Article 4 about as long as articles 1–3 together, distally with 2 simple setae. Article 5 shorter than article 4, distally with 2 broom setae. Flagellum with 6 articles. **Mandibles.** Left and right mandible incisor processes multidentate with dorsal and ventral subdistal teeth that partly enclose lacinia. **Maxilliped.** Basis length 2.9 width; epipod length 3.0 width, 1.0 basis length; palp wider than endite, article 2 wider than articles 1 and 3, article 1 longer than article 3.

Pereopod I. Ischium dorsal margin with 3 submarginal setae. Merus dorsally with 5 setae: 4 in submarginal row, 1 bifurcate distally; ventral margin with 2 setae. Carpus dorsally with 1 seta. Dactylus distally with 3 sensillae. **Pereopod III.** Ischium dorsal lobe triangular; proximally with

4 setae; apex with 1 prominent seta; apical seta robust, bifurcate, recurved, flexibly articulated; distally with 4 setae. Merus dorsally with 11 setae: 4 thin, long, 6 more robust, bifurcate, long, 1 short, spine-like; ventrally with 4 setae. Carpus dorsally with 5 setae, 4 long, bifurcate, 1 broom, ventrally with 5 setae: 4 potentially distally sensillate, 1 short, bifurcate. Dactylus with 3 sensillae. **Pereopod IV.** Carpus subcylindrical.

Operculum. Elongate, length 1.7 width; apical width 0.47 operculum width; distally tapering; with lateral fringe consisting of 9 setae, distinctly separate from apical row of setae; with 16 pappose setae on apex. **Uropod.** Length 0.94 pleotelson length; protopod length 8.3 width, 0.69 pleotelson length, protopod distal margin blunt, endopod insertion terminally; endopod length 6.0 width, 0.36 protopod length, width at articulation clearly narrower than protopod.

***Macrostylis uniformis* Riehl & Brandt, 2010**

urn:lsid:zoobank.org:act:5105DA6E-E793-42B6-A5D7-A4D9F8C5933A *Macrostylis uniformis* Riehl & Brandt, 2010; pp. 19–29, Figs 3–8.

Modified diagnosis

Body heavily calcified, cuticular setules absent. Pereonite 4 width subequal pereonite 5 width, lateral margins convex, posterolateral margins not produced posteriorly, posterolateral setae absent. Pleotelson ovoid, waist absent, posterior apex length about 0.20 pleotelson length. Antenna article 2 elongate, longer than article 1. Mandible incisors simplified, monodentate, bluntly rounded. Pereopod III ischium dorsal lobe tapering, with 2 prominent apical setae. Pereopod V ischium distodorsally with setae present. Operculum ovoid, lateral

fringe of setae with fluent transition to apical row of setae. Uropod protopod distal margin slightly extending laterally, endopod articulation subterminally.

***Macrostylis vinogradovae* Mezhov, 1992**

urn:lsid:zoobank.org:act:7C4763BD-9260-4169-8B1F-F666097CB142

Macrostylis vinogradovae Mezhov, 1992; p. 87, Fig. 2.

Type fixation

Holotype: non-ovigerous female, 2.6 mm, Mc-1279, by original designation.

Type material

Holotype: non-ovigerous female, Mc-1279, DM station 4084-II; paratype: female fragment, 1.2 mm, Mc-1280, DM station 4084-I. All material deposited at the Zoological Museum of the Moscow State University.

Type locality

Southern Ocean, southeastern Weddell Sea, off Kapp Norvegia, Dronning Maud Land, with R/V Dm. Mendeleev, cruise 43, station 4084-II, 70° 53.17' S, 15° 04.51' W; 2,925 m depth; by means of the bottom sampler "Okean".

Type material – Remarks

Only the holotype is complete and the only other specimen is a strongly-damaged fragment of which substantial parts are missing. Further, the paratype was collected from a very different depth (bathyal vs. abyssal). An allocation of both specimens to the same species is therefore put in doubt. The type locality is consequently restricted here to the coll-

ection locality of the holotype.

Further records

Southern Ocean, southeastern Weddell Sea, off Kapp Norvegia, Dronning Maud Land, with R/V Dm. Mendeleev, cruise 43, station 4084-I, 70° 40.6' S, 15° 47.8' W; 4,335 m depth; by means of the bottom sampler "Okean".

Modified diagnosis

Pereonite 3 posterolateral margins not produced posteriorly. Pereonite 4 wider than pereonite 5, lateral margins convex, posterolateral margins produced posteriorly, tapering, posterolateral setae spine-like, robust. Pleotelson ovoid, waist present, setal ridges visible. Ischium dorsal lobe triangular; apex with 1 prominent seta; distally with no seta. Operculum elongate, subsimilar pleotelson length, distally tapering, ventrally keeled, apical width smaller 0.50 operculum width, apical setae short.

Description female

Body. Length 2.6 mm, subcylindrical. **Ventral spines.** All spines acute. Pereonite 1 spine prominent. Pereonite 3 spine small, closer to anterior segment border. Pereonite 4 spine directed posteriorly, small, closer to posterior segment border. Pereonite 5 spine prominent, medially. Pereonite 6 spine prominent, closer to posterior segment border. Pereonite 7 spine prominent. **Imbricate ornamentation (IO).** Pereonites 4–7 IO most distinct at collum.

Cephalothorax. Length 0.84 width, 0.16 body length; frons straight, frontal furrow present, straight, slightly anteriorly to antennulae insertions. **Fossosome.** Length 0.94 width, 0.23 body length. Lateral tergite margins confluent, ventral surface without keel; sternite margins present, not fully expressed. **Pereonite 1.** Anterior margin concave. **Pereonite 4.** Width 1.2 pereonite 5 width,

length 0.41 width; pereonal collum present. Lateral margins convex. Posterolateral margins produced posteriorly, tapering. Posterolateral setae bifid, robust, spine-like. Pereonites 5–7. Posterolateral margin produced posteriorly, rounded; posterolateral setae bifid, robust.

Pereonite 5. Length 0.45 width, subequal pereonite 4 length. **Pereonite 6.** Length 0.70 width, 1.4 pereonite 5 length. **Pleotelson.** Ovoid, waist present, setal ridges visible, length 0.20 body length, 1.56 width, narrower than pereonite 7; statocysts present, dorsal slot-like apertures present. Posterior apex concave at uropod insertions, posteriorly broadly rounded, convex, length 0.21 pleotelson length.

Maxilliped. Basis length 3.8 width; epipod length 3.1 width, 1.0 basis length; palp width subequal basis width, article 2 wider than articles 1 and 3, article 1 and 3 subequal in length.

Pereopod III. Length 0.47 body length. Ischium dorsal lobe triangular; proximally with 2 setae; apex with 1 prominent, robust, bifurcate, straight seta; distally with no seta. Merus dorsally with 5 setae, ventrally with 3 setae. Carpus dorsally and ventrally with 4 setae respectively. **Pereopod IV.** Length 0.25 body length.

Operculum. Elongate, length 1.8 width, 1.0 pleotelson dorsal length; apical width 0.43 operculum width; distally tapering, ventrally keeled; with lateral fringe consisting of 11–12 setae, distinctly separate from apical row of setae; with 11 short, pappose setae on apex, completely covering anal opening. **Uropod.** Inserting on posterior pleotelson margin; length 1.1 pleotelson length; protopod length 8.2 width, 0.85 pleotelson length, distal margin blunt, endopod insertion terminally; endopod 0.33 protopod length, width at articulation subsimilar protopod width.

Molecular results

The 16S alignment is characterized by a proportion of invariable sites (p_{invar}) of 0.32246. The Xia-test for variation saturation resulted in $I_{\text{ss}} = 0.5452$, significantly smaller than $I_{\text{ss}.c}$ (= 0.6866 assuming a symmetrical topology). The sequences have consequently experienced little saturation. 135 characters are constant, 47 variable characters are parsimony-uninformative, 230 characters are parsimony informative. Both, the Bayesian and the ML phylogenetic analyses resulted in the same topology and very similar branch length (Fig. 23). Macrostylidae and all morphologically assigned macrostylid species are monophyletic and well supported. The MP analysis resulted in a similar topology but several nodes were not supported. Intraspecific uncorrected p -distances between 0.0–0.3 were observed within macrostylids. Interspecific variability ranges from 23.3 % uncorrected p -distance between *Macrostylis matildae* n. sp. and *M.* sp. SYSTCO#4 to 31.1 % between *M. roaldi* and *M.* sp. SYSTCO#4. Attempts to amplify COI sequences for both new species were unsuccessful. From a small number of specimens of *M. matildae* n. sp., the 12S fragment could be sequenced successfully. As GenBank contained 12S sequences of only two other Janiroidean isopod species by time of submission of this manuscript, no analysis could be conducted.

Discussion

The family Macrostylidae is currently considered monotypic (Riehl & Brandt 2010). To date, probably due to strong overall morphological similarity between the species, no approach has been taken to revise the genus *Macrostylis* and to erect further genera. Taxonomic studies are often difficult to

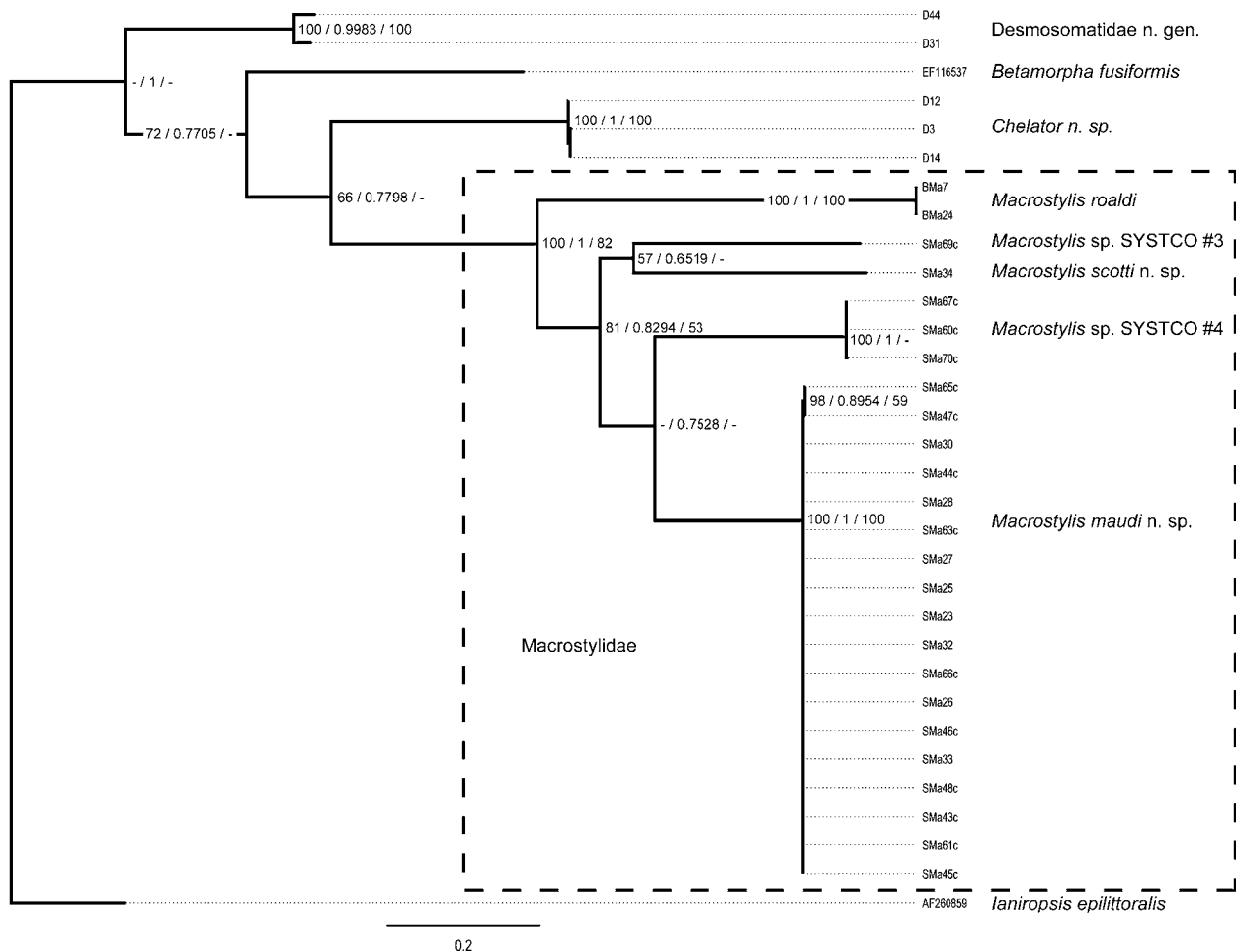


Figure 23. Cladogram of Maximum Likelihood (ML), Bayesian and Maximum Parsimony (MP) phylogenetic analyses. Node labels are statistical support values (ML fast bootstrap / posterior probability / MP bootstrap). ML: best tree; Bayesian: consensus tree; MP: 50 % Majority Rule consensus tree; outgroup set to *Ianiropsis epilittoralis*.

compare as different terminologies and character sets have been used or specimens of different stage or gender. The microscopic methods and views of different authors vary. We hence compiled data for all previously described species of this genus from the Southern Ocean applying a consistent terminology and methodology. Our study of type material and literature data from ten out of eleven known Southern Ocean macrostylids revealed these to be distinct and morphologically diverse. It is yet too early to infer intrafamilial relationships from the morphology but this study is another step towards a phylogeny and revision of the family. Even though character analyses and phylogenetic inference are still lacking, certain groupings begin to take shape and are discussed in the remarks of

the new-described species.

Characters used to distinguish species in the key

The family Macrostylidae is characterized by a large number of apomorphies (see e.g. Riehl & Brandt 2010) which makes it easy to delineate from other families. The species, on the other hand, are often hard to tell apart and we hence provide a new identification key to the Southern Ocean species in this article. A recent key by Vey & Brix (2009) is outdated due to new descriptions (Riehl & Kaiser 2012; Riehl & Brandt 2010). Additionally, this key as well as previous ones provided by Kussakin (1999), Wolff (1956) and Menzies (1962)

compared adult male specimens with females. For reasons explained above, this is often not possible or may easily lead to incorrect identification.

The key presented here is based on and suitable for identification of females and juvenile males. It has limited potential for the specific identification of adult males. Such a key has not been developed because male specimens are rare and in many cases unknown. Females were encountered more often in deep-sea samples (Riehl *et al.* 2012) and are known for all Southern Ocean species of Macrostylidae. Adult males have been described only for few species including the here described ones (e.g. *Macrostylis antennamagna* Riehl & Brandt, 2010; *M. roaldi* Riehl & Kaiser, 2012). So at present, knowledge about the morphology of adult males is scarce for Macrostylidae from the Southern Ocean and in general.

Development and sexual dimorphism

Sexual dimorphisms have been identified in a wide range of janiroidean isopods, also Macrostylidae (Riehl *et al.* 2012). Among the most obvious characters in which adult males of Macrostylidae differ from females are a more slender body, the increased number of antennular aesthetascs, size of antennule and antenna in relation to body size and the shape of the pleotelson (Sars 1864; Hansen 1916; Mezhov 1989; Riehl & Brandt 2010; Riehl *et al.* 2012). Above that, there is evidence that the expression of the cuticular imbricate ornamentation (e.g. in *Macrostylis papillata* Riehl *et al.*, 2012) and the length of the pereopods, especially pereopod VII might be strongly affected by sexual dimorphism (e.g. in *M. longipes* Hansen, 1916 and *M. longipedis* Brandt, 2004). Future taxonomic work on this group should pay attention to sexually dimorphic traits as these might hold valuable information for phylogenetic studies on the family.

Dimorphic characters in *Macrostylis scotti* n. sp. are the shape and measures of the pleotelson (also ventrally) and the length-width ratio of the longer pereopod VII articles.

While pereopod VII length / body length ratio is similar between male and female specimens, the seventh walking leg of the female is built more robust compared to the male i.e. they have a smaller L/W ratio. A similar pattern can be observed in pereopod VII of *M. matildae* n. sp. *M. matildae* shows very little dimorphism. The antennule of the adult male bears a dense assemblage of aesthetascs on the terminal and subterminal articles, as typical in Macrostylidae (compare e.g. *M. scotti* n. sp., *M. spinifera* Sars, 1864 (Sars 1899), *M. antennamagna* Riehl & Brandt, 2010 and *M. papillata* Riehl *et al.*, 2012). As discussed by Riehl *et al.* (2012), a change in the size and setation of the antennule can be observed that occurs with the adult moult. Fig. 20D shows the antennule of a juvenile male which is pre-adult. This is indicated by the pleopod I, which has the distolateral horns already developed. Characters remaining juvenile, however, are the relative short length of pleopod I when compared to pleopod II (Fig. 20C), the short and blunt pleopod II stylet (Fig. 20H) which does not have a developed pore and canal, and an antennula which is similar to the female but bears one additional aesthetasc on the fourth article.

Molecular phylogeny

Intraspecific distances are very low. Variability might be underrepresented due to sampling bias as specimens for each species were collected from one locality only. Contrastingly, interspecific distances are extremely high and no species pair in the phylogenetic trees has a particularly close relationship. Based on the position in the cladogram (Fig. 23), branch length and uncorrected *p*-distan-

ces, *Macrostylis matildae* n. sp. is closest to *M. sp.* SYSTCO#4, with 23.3 % uncorrected *p*-distance separating them. *Macrostylis roaldi* however, is the most basally derived macrostylid in the 16S ML tree. Its separation from the other macrostylids is 28.5–31.1 % uncorrected *p*-distance and thus extremely high when compared to the few existing genetic data sets for deep-sea isopods (e.g. Brix *et al.* 2011; Raupach *et al.* 2007; Brökeland & Raupach 2008). Such high variability in the 16S gene is indicative for rather old and higher-level (i.e. generic) divergence (Wetzer 2002; Brix *et al.* submitted). There is no reference data available for Macrostylidae to compare our results with. This nevertheless contradicts the current monotypy of Macrostylidae. It furthermore shows that Macrostylidae, similar to other isopod families like Munnopsidae, are old and divergent.

The lack of recognized diversity above species level in the current system may thus be artificial. It is probably a reflection of the overall morphological similarity in Macrostylidae (Riehl & Brandt 2010) which is grounded mainly in the numerous complex synapomorphies related to the digging lifestyle (Hessler & Strömberg 1989; Wägele 1989), i.e. the short, laterally inserting antennulae and antennae, spade-like head, the fossosoma, specialized pereopods 1–4, statocysts present in the pleotelson, presence of ventral spines, etc. These could be regarded as key innovations (Assis & de Carvalho 2010) which evolved early in macrostylid evolution and lead to the success of the group. Furthermore, a digging lifestyle may result in environmentally caused convergence somewhat similar to what can be observed in stygofauna (Baratti *et al.* 1999) or subterranean crustaceans (Kornobis *et al.* 2011). Consequently and different from free-living potential sister taxa such as Munnopsidae, possible evolutionary trajectories in habitus morphology are likely to be more

constrained.

Much more detailed morphological and molecular data are hence necessary to evaluate the evolutionary history and superspecific diversity of this taxon. A broad survey of the morphology of the currently described species of this family is needed to test the molecular data (reciprocal illumination; Hennig 1950). Desmosomatidae and Munnopsidae were previously considered potential sister taxa for Macrostylidae (Wägele 1989; Raupach *et al.* 2004) and where thus chosen to test the monophyly in the phylogenetic analyses presented in this paper. Uncorrected *p*-distances of those taxa to any macrostylids range from 31.6–38.8 % and are thus very high but not clearly distinct from maximum nucleotide variability within Macrostylidae. This mirrors either old age of the clades or high mutational rates in the 16S fragment and is indicative for some degree of nucleotide-variability saturation in the dataset. The polyphyly of Desmosomatidae in the 16S tree is worth mentioning and potentially caused by long-branch attraction due to missing intermediates (see e.g. Wägele & Mayer 2007) but a detailed analysis of this phenomenon is beyond the scope of this article.

Acknowledgements

Jörundur Svavarsson and one anonymous reviewer are thanked for their effort and helpful suggestions which led to an improved manuscript. The authors are grateful to the crew of R/V *Polarstern* and to the Alfred Wegener Institute (AWI) for logistic support which made sampling possible. The effort of all pickers and sorters of the material at the Zoological Museum Hamburg and the German Center for Marine Biodiversity Research is kindly acknowledged. Dr. Marina Maljutina corrected TR's translation of a Russian key to the species of

Macrostylidae by Kussakin (1999) and her review of an earlier version of this manuscript largely improved this article. Dr. Stefanie Kaiser is thanked for creating the map. Dr. Saskia Brix kindly provided a microscope to prepare the illustrations and Dr. Karin Meissner gave access to her photo equipment. Gratitude is owed to Buz Wilson and the department of Marine Invertebrates at the Australian Museum for providing working space and support for TR during the preparation of this manuscript. Renate Walter kindly assisted at the SEM. Miranda Lowe kindly made type material available at the Natural History Museum, London. Kathrin Philipps-Bussau and Petra Wagner assisted with the loan of type material at the Zoological Museum Hamburg. DNA laboratory work was possible due to great help from Amy Driskell and Andrea Ormos at the Smithsonian Laboratories of Analytical Biology. The new species could be collected with financial support from the German Federal Ministry for Education and Research (BMBF) to AB. TR was financially supported by the British Antarctic Survey (BAS) during sampling, by the CeDAMar taxonomic-exchange program during sequencing and by the German National Academic Foundation (Studienstiftung des deutschen Volkes) during the preparation of the manuscript. This is ANDEEP publication #167.

References

- Assis, L. & De Carvalho, M. (2010) Key innovations: further remarks on the importance of morphology in elucidating systematic relationships and adaptive radiations. *Evolutionary Biology*, 37(4), 247–254. <http://dx.doi.org/10.1007/s11692-010-9098-z>
- Baratti, M., Bazzicalupo, M., De Filippo, C. & Massana, G. (1999) Detection of genetic variability in stygobitic isopods using rapid markers. *Crustaceana*, 72(7), 625–634. <http://dx.doi.org/10.1163/156854099503672>
- Barnard, K.H. (1920) Contribution to the crustacean fauna of South Africa No. 6. Further additions to the list of marine Isopoda. *Annals of the South African Museum*, 17, 319–428.
- Bathmann, U. (2010) *The expedition of the research vessel "Polarstern" to the Antarctic in 2007/2008 (ANT-XXIV/2)*. Ulrich Bathmann (Ed.) Berichte zur Polar- und Meeresforschung = Reports on polar and marine research; 604. Bremerhaven: Alfred-Wegener-Institut für Polar- und Meeresforschung, 205 pp.
- Benson, D.A., Karsch-Mizrachi, I., Lipman, D.J., Ostell, J. & Wheeler, D.L. (2008) GenBank. *Nucleic Acids Research*, 36(Database issue), D25–30. <http://dx.doi.org/10.1093/nar/gkm929>
- Birstein, Y.A. (1970) New Crustacea Isopoda from the Kurile-Kamchatka Trench area. In: Bogorov, V.G. (Ed.) *Fauna of the Kurile-Kamchatka Trench and its environment*. Academy of Sciences of the USSR. Proceedings of the Institute of Oceanology 86, pp. 308–356. (In Russian)
- Birstein, Y.A. (1973) *Deep water isopods (Crustacea. Isopoda) of the north-western part of the Pacific Ocean*. Akademiya Nauk, SSSR, Moscow, 213 pp. (In Russian)
- Brandt, A. (1992a) New Asellota from the Antarctic deep sea (Crustacea, Isopoda, Asellota), with descriptions of two new genera. *Zoologica Scripta*, 21(1), 57–78. <http://dx.doi.org/10.1111/j.1463-6409.1992.tb00310.x>
- Brandt, A. (1992b) Origin of Antarctic Isopoda (Crustacea, Malacostraca). *Marine Biology*, 113, 415–423. <http://dx.doi.org/10.1007/BF00349167>
- Brandt, A. (2002) *Desmostylis gerdesi*, a new species (Isopoda: Malacostraca) from Kapp Norvegia, Weddell Sea, Antarctica. *Proceedings of the Biological Society of Washington*, 115(3), 616–627.
- Brandt, A. (2004) New deep-sea species of Macrostylidae (Asellota: Isopoda: Malacostraca) from the Angola Basin off Namibia, South West Africa. *Zootaxa*, 448, 1–35.
- Brandt, A., Brix, S., Brökeland, W., Choudhury, M., Kaiser, S. & Malyutina, M.V. (2007a) Deep-sea isopod biodiversity, abundance, and endemism in the Atlantic sector of the Southern Ocean—Results from the ANDEEP I–III expeditions. *Deep-Sea Research Part II*, 54(16–17), 1760–1775. <http://dx.doi.org/10.1016/j.dsr2.2007.07.015>
- Brandt, A., Gooday, A.J., Brandao, S.N., Brix, S., Brökeland, W., Cedhagen, T., Choudhury, M., Cornelius, N., Danis, B., de Mesel, I., Diaz, R.J., Gillan, D.C., Ebbe, B., Howe, J.A., Janussen, D., Kaiser, S., Linse, K., Malyutina, M.V., Pawlowski, J., Raupach, M.J. & Vanreusel, A. (2007b) First insights into the biodiversity and biogeography of the Southern Ocean deep sea. *Nature*, 447(7142), 307–311. <http://dx.doi.org/10.1038/nature05827>
- Brandt, A., De Broyer, C., Gooday, A.J., Hilbig, B. & Thomson, M.R.A. (2004) Introduction to ANDEEP (ANtartic benthic DEEP-sea biodiversity: colonization history and recent community patterns)—a

- tribute to Howard L. Sanders. *Deep-Sea Research Part II: Topical Studies in Oceanography*, 51(14-16), 1457–1465. <http://dx.doi.org/10.1016/j.dsr2.2004.08.006>
- Brandt, A., Bathmann, U., Brix, S., Cisewski, B., Flores, H., Göcke, C., Janussen, D., Kräufigsky, S., Kruse, S., Leach, H., Linse, K., Pakhomov, E., Peeken, I., Riehl, T., Sauter, E., Sachs, O., Schüller, M., Schrödl, M., Schwabe, E., Strass, V., van Franeker, J.A. & Wilmsen, E. (2011a) Maud Rise – a snapshot through the water column. *Deep Sea Research Part II: Topical Studies in Oceanography*, 58(19–20), 1962–1982. <http://dx.doi.org/10.1016/j.dsr2.2011.01.008>
- Brandt, A., Ebbe, B. & Bathmann, U. (2011b) Southern Ocean biodiversity—From pelagic processes to deep-sea response. *Deep Sea Research Part II: Topical Studies in Oceanography*, 58(19–20), 1945–1947. <http://dx.doi.org/10.1016/j.dsr2.2011.05.003>
- Brandt, A., Linse, K. & Schüller, M. (2009) Bathymetric distribution patterns of Southern Ocean macrofaunal taxa: Bivalvia, Gastropoda, Isopoda and Polychaeta. *Deep Sea Research Part I: Oceanographic Research Papers*, 56(11), 2013–2025. <http://dx.doi.org/10.1016/j.dsr.2009.06.007>
- Brandt, A., Elsner, N., Brenke, N., Golovan, O., Malyutina, M.V., Riehl, T., Schwabe, E. & Würzberg, L. (2013) Epifauna of the Sea of Japan collected via a new epibenthic sledge equipped with camera and environmental sensor systems. *Deep Sea Research Part II: Topical Studies in Oceanography*, 86–87, 43–55. <http://dx.doi.org/10.1016/j.dsr2.2012.07.039>
- Brenke, N. (2005) An epibenthic sledge for operations on marine soft bottom and bedrock. *Marine Technology Society Journal*, 39(2), 10–21. <http://dx.doi.org/10.4031/002533205787444015>
- Brenke, N., Guilini, K. & Ebbe, B. (2011) Characterization of the seafloor at the SYSTCO stations based on video observations and ground truthing sedimentology. *Deep Sea Research Part II: Topical Studies in Oceanography*, 58(19–20), 2043–2050. <http://dx.doi.org/10.1016/j.dsr2.2011.05.007>
- Brix, S., Riehl, T. & Leese, F. (2011) First genetic data for *Haploniscus rostratus* and *Haploniscus unicornis* from neighbouring deep-sea basins in the South Atlantic. *Zootaxa*, 2838, 79–84.
- Brix, S., Leese, F., Riehl, T. & Kihara, T.-C. (submitted) A new genus and new species of Desmosomatidae Sars, 1897 (Isopoda) from the east South-Atlantic abyss described by means of integrative taxonomy. *Marine Biodiversity*.
- Brökeland, W. & Raupach, M.J. (2008) A species complex within the isopod genus *Haploniscus* (Crustacea: Malacostraca: Peracarida) from the Southern Ocean deep sea: a morphological and molecular approach. *Zoological Journal of the Linnean Society*, 152(4), 655–706. <http://dx.doi.org/10.1111/j.1096-3642.2008.00362.x>
- Dallwitz, M.J. (1974) A flexible computer program for generating identification keys. *Systematic Biology*, 23(1), 50–57. <http://dx.doi.org/10.1093/sysbio/23.1.50>
- Dallwitz, M.J. (1980) A general system for coding taxonomic descriptions. *Taxon*, 29(1), 41–46. <http://dx.doi.org/10.2307/1219595>
- Dallwitz, M.J. (1993) *DELTA and INTKEY. Advances in computer methods for systematic biology: artificial intelligence, databases, computer vision*. Johns Hopkins University Press, Baltimore, pp. 287–296.
- Dallwitz, M.J., Paine, T.A. & Zurcher, E.J. (2010) *User's guide to the DELTA editor*. Available from: <http://delta-intkey.com/> (Accessed 25 Sep. 2012)
- Drummond, A.J., Ashton, B., Buxton, S., Cheung, M., Cooper, A., Duran, C., Field, M., Heled, J., Kearse, M., Markowitz, S., Moir, R., Stones-Havas, S., Sturrock, S., Thierer, T. & Wilson, A. (2011) *Geneious v5.4*. Available from: <http://www.geneious.com/> (Accessed 24 Jul. 2013)
- Folmer, O., Black, M., Hoeh, W., Lutz, R. & Vrijenhoek, R. (1994) DNA primers for amplification of mitochondrial cytochrome c oxidase subunit I from diverse metazoan invertebrates. *Molecular Marine Biology and Biotechnology*, 3(5), 294–299.
- Gurjanova, E. (1933) Die marinen Isopoden der Arktis. *Fauna Arctica*, 6(5), 391–470. (In German)
- Hansen, H.J. (1916) Crustacea Malacostraca: The order Isopoda. *Danish Ingolf Expedition*, 3(5), 1–262.
- Hennig, W. (1950) *Grundzüge einer Theorie der phylogenetischen Systematik*. Deutscher Zentralverlag, Berlin, 370 pp.
- Hessler, R.R. (1970) *The Desmosomatidae (Isopoda, Asellota) of the Gay Head-Bermuda Transect*.
- Arrhebus, G.O.S., Cox, C.S., Fager, E.W., Hand, C.H., Newberry, T., & Schaefer, M.B. (Eds), Bulletin of the Scripps Institution of Oceanography 15, University of California Press, Berkeley, Los Angeles, London, 185 pp.
- Hessler, R.R. & Thistle, D. (1975) On the place of origin of deep-sea isopods. *Marine Biology*, 32(2), 155–165. <http://dx.doi.org/10.1007/BF00388508>
- Hessler, R.R. & Strömberg, J.O. (1989) Behavior of janiroidean isopods (Asellota), with special reference to deep sea genera. *Sarsia*, 74(3), 145–159.
- Huelsensbeck, J.P. & Ronquist, F. (2001) MRBAYES: Bayesian inference of phylogenetic trees. *Bioinformatics*, 17(8), 754–755. <http://dx.doi.org/10.1093/bioinformatics/17.8.754>
- Kaiser, S., Barnes, D.K.A. & Brandt, A. (2007) Slope and deep-sea abundance across scales: Southern Ocean isopods show how complex the deep sea can be. *Deep-Sea Research Part II: Topological Studies in Oceanography*, 54(16–17), 1776–1789. <http://dx.doi.org/10.1016/j.dsr2.2007.07.006>

- Kaiser, S., Barnes, D.K.A., Linse, K. & Brandt, A. (2008) Epibenthic macrofauna associated with the shelf and slope of a young and isolated Southern Ocean island. *Antarctic Science*, 20(03), 281–290.
- Kaiser, S., Barnes, D.K.A., Sands, C.J. & Brandt, A. (2009) Biodiversity of an unknown Antarctic Sea: assessing isopod richness and abundance in the first benthic survey of the Amundsen continental shelf. *Marine Biodiversity*, 39(1), 27–43. <http://dx.doi.org/10.1007/s12526-009-0004-9>
- Kaiser, S., Griffiths, H.J., Barnes, D.K.A., Brandão, S.N., Brandt, A. & O'Brien, P.E. (2011) Is there a distinct continental slope fauna in the Antarctic? *Deep Sea Research Part II: Topical Studies in Oceanography*, 58(1–2), 91–104. <http://dx.doi.org/10.1016/j.dsr2.2010.05.017>
- Kaiser, S., Brandão, S.N., Brix, S., Barnes, D.K.A., Bowden, D.A., Ingels, J., Leese, F., Schiaparelli, S., Arango, C.P., Badhe, R., Bax, N., BLazewicz-Paszkowycz, M., Brandt, A., Brenke, N., Catarino, A.I., David, B., De Ridder, C., Dubois, P., Ellingsen, K.E., Glover, A.G., Griffiths, H.J., Gutt, J., Halanych, K.M., Havermans, C., Held, C., Janussen, D., Lörz, A.-N., Pearce, D.A., Pierrat, B., Riehl, T., Rose, A., Sands, C.J., Soler-Membrives, A., Schüller, M., Strugnell, J.M., Vanreusel, A., Veit-Köhler, G., Wilson, N.G. & Yasuhara, M. (2013) Patterns, processes and vulnerability of Southern Ocean benthos. *Marine Biology*, 1–23 http://dx.doi.org/10.1007/978-1-59745-251-9_3
- Katoh, K., Asimenos, G. & Toh, H. (2009) Multiple Alignment of DNA Sequences with MAFFT. Posada, D. (Ed.) *Bioinformatics for DNA Sequence Analysis*, Methods in Molecular Biology 537, pp. 39–64.
- Katoh, K., Misawa, K., Kuma, K. & Miyata, T. (2002) MAFFT: a novel method for rapid multiple sequence alignment based on fast Fourier transform. *Nucleic Acids Research*, 30(14), 3059–3066. <http://dx.doi.org/10.1093/nar/gkf436>
- Kavanagh, F.A. & Wilson, G.D.F. (2007) Revision of the genus *Haplomesus* (Isopoda: Asellota: Ischnomesidae) with erection of four new genera. *Invertebrate Systematics*, 21(5), 487–535. <http://dx.doi.org/10.1071/IS06031>
- Kornobis, E., Pálsson, S., Sidorov, D.A., Holsinger, J.R. & Kristjánsson, B.K. (2011) Molecular taxonomy and phylogenetic affinities of two groundwater amphipods, *Crangonyx islandicus* and *Crymostygius thingvallensis*, endemic to Iceland. *Molecular Phylogenetics and Evolution*, 58(3), 527–539. <http://dx.doi.org/10.1016/j.ympev.2010.12.010>
- Kussakin, O.G. (1999) Marine and brackishwater likefooted Crustacea (Isopoda) from the cold and temperate waters of the Northern Hemisphere Suborder Asellota. Part 2. Families Joeropsididae, Nannoniscidae, Desmosomatidae, Macrostylidae. Alimov, A.F. (Ed.), Keys to the Fauna of the USSR, Zoological Institute of the Russian Academy of Sciences, St. Petersburg, pp. 1-383. (In Russian)
- Latreille, P.A. (1802) Histoire naturelle générale et particulière des Crustacés et des Insectes. In: de Buffon, G.L.L. (Ed.) Histoire Naturelle, nouvelle édition, accompagnée des notes. 1802–1805, Paris, pp. 1–467. (In French)
- Lins, L.S.F., Ho, S.Y.W., Wilson, G.D. F. & Lo, N. (2012) Evidence for Permo-Triassic colonization of the deep sea by isopods. *Biology Letters*, 8(6), 979–982. <http://dx.doi.org/10.1098/rsbl.2012.0774>
- Machida, R.J., Miya, M.U., Nishida, M. & Nishida, S. (2004) Large-scale gene rearrangements in the mitochondrial genomes of two calanoid copepods *Eucalanus bungii* and *Neocalanus cristatus* (Crustacea), with notes on new versatile primers for the srRNA and COI genes. *Gene*, 332, 71–78. <http://dx.doi.org/10.1016/j.gene.2004.01.019>
- Machida, R.J. & Tsuda, A. (2010) Dissimilarity of species and forms of planktonic *Neocalanus* copepods using mitochondrial COI, 12S, nuclear ITS, and 28S gene sequences. *PLoS ONE*, 5(4), e10278. <http://dx.doi.org/10.1371/journal.pone.0010278>
- Meinert, F.V.A. (1890) *Crustacea Malacostraca*. Videnskabelige udbytte af kanonbaden "Hauchs Dogter", 147–230 pp. (In Danish)
- Menzies, R.J. (1952) Some marine asellote isopods from northern California, with descriptions of nine new species. *Proceedings of the United States National Museum*, 102(3293), 117–159.
- Menzies, R.J. (1962) The isopods of abyssal depths in the Atlantic Ocean. In: Barnard, J. L., Menzies, R.J. & Bacescu, M.C. (Eds.) *Abyssal Crustacea*. Vema Research Series, Columbia University Press, New York, 79–206 pp.
- Menzies, R.J. & George, R.Y. (1972) Isopod Crustacea of the Peru-Chile Trench. *Anton Bruun Report*, 9, 1–124.
- Meyer, C.P., Geller, J.B. & Paulay, G. (2005) Fine scale endemism on coral reefs: archipelagic differentiation in turbid gastropods. *Evolution*, 59(1), 113–125. <http://dx.doi.org/10.1111/j.0014-3820.2005.tb00899.x>
- Mezhov, B.V. (1988) The first findings of Macrostylidae (Isopoda, Asellota) in the Indian Ocean. *Zoologicheskii Zhurnal*, 67(7), 983–994. (In Russian)
- Mezhov, B.V. (1989) Two new species of *Macrostylis* (Isopoda, Macrostylidae) from the trenches of the Pacific Ocean and comments on the morphology of *M. galathea*. *Zoologicheskii Zhurnal*, 68(8), 33–40. (In Russian)
- Mezhov, B. V. (1992) Two new species of the genus *Macrostylis* G.O.Sars, 1864 (Crustacea Isopoda Asellota Macrostylidae) from the Antarctic. *Arthropoda Selecta*, 1(2), 83–87.
- Mezhov, B.V. (2000) Addition to the fauna of isopod crustacean genus *Macrostylis* G.O. Sars, 1864 (Crustacea: Isopoda: Macrostylidae) of the Atlantic and Arctic oceans,

- with descriptions of three new Atlantic species. *Arthropoda Selecta*, 9(2), 69–83.
- Mezhov, B.V. (2003a) New abyssal species of the genus *Macrostylis* G.O. Sars, 1864 (Crustacea: Isopoda: Macrostylidae) from the northwestern part of the Indian Ocean. *Arthropoda Selecta*, 12(1), 1–8.
- Mezhov, B.V. (2003b) Three new species of the genus *Macrostylis* G.O. Sars, 1864 (Crustacea: Isopoda: Macrostylidae) from the Indian Ocean. *Arthropoda Selecta*, 12(2), 95–100.
- Nylander, J.A.A. (2004) *MrModeltest. Version: 2*. Evolutionary Biology Center, Uppsala University, Available from: <http://www.abc.se/~nylander/mrmodeltest2/mrmodeltest2.html> (Accessed 25 Sep. 2012)
- Palumbi, S.R., Martin, A., Romano, S., McMillan, W.O., Stice, L. & Grabowski, G. (1991) *The simple fool's guide to PCR*, Version 2. Available from: <http://palumbi.stanford.edu/SimpleFoolsMaster.pdf> (2012-09-25)
- Ratnasingham, S. & Hebert, P.D.N. (2007) bold: The Barcode of Life Data System (<http://www.barcodinglife.org>). *Molecular Ecology Notes*, 7(3), 355–364. <http://dx.doi.org/10.1111/j.1471-8286.2007.01678.x>
- Raupach, M. J., Held, C. & Wägele, J.-W. (2004) Multiple colonization of the deep sea by the Asellota (Crustacea: Peracarida: Isopoda). *Deep Sea Research Part II: Topical Studies in Oceanography*, 51, 1787–1795. <http://dx.doi.org/10.1016/j.dsr2.2004.06.035>
- Raupach, M.J., Malyutina, M.V., Brandt, A. & Wägele, J.-W. (2007) Molecular data reveal a highly diverse species flock within the munnopsoid deep-sea isopod *Betamorpha fusiformis* (Barnard, 1920) (Crustacea: Isopoda: Asellota) in the Southern Ocean. *Deep Sea Research Part II: Topical Studies in Oceanography*, 54(16–17), 1820–1830. <http://dx.doi.org/10.1016/j.dsr2.2007.07.009>
- Riehl, T. & Brandt, A. (2010) Descriptions of two new species in the genus *Macrostylis* Sars, 1864 (Isopoda, Asellota, Macrostylidae) from the Weddell Sea (Southern Ocean), with a synonymisation of the genus *Desmostylis* Brandt, 1992 with *Macrostylis*. *Zookeys*, 57, 9–49. <http://dx.doi.org/10.3897/zookeys.57.310>
- Riehl, T. & Kaiser, S. (2012) Conquered from the deep sea? A new deep-sea isopod species from the Antarctic shelf shows pattern of recent colonization. *PLoS ONE*, 7, 11, e49354. <http://dx.doi.org/10.1371/journal.pone.0049354>
- Riehl, T., Wilson, G.D.F. & Hessler, R.R. (2012) New Macrostylidae Hansen, 1916 (Crustacea: Isopoda) from the Gay Head- Bermuda transect with special consideration of sexual dimorphism. *Zootaxa*, 3277, 1–26.
- Ronquist, F. & Huelsenbeck, J.P. (2003) MrBayes 3: Bayesian phylogenetic inference under mixed models. *Bioinformatics*, 19(12), 1572–1574. <http://dx.doi.org/10.1093/bioinformatics/btg180>
- Sars, G.O. (1864) *Om en anomal Gruppe af Isopoder*. Forhandlinger Videnskapselskapet I Kristiania, Anar 1863. 205–221 pp. (*In Norwegian*)
- Sars, G.O. (1899) *An account of the Crustacea of Norway: with short descriptions and figures of all the species: Isopoda*. Cammermeyer, A. (Ed.), Bergen Museum, Bergen.
- Stamatakis, A. (2006) RAxML-VI-HPC: maximum likelihood-based phylogenetic analyses with thousands of taxa and mixed models. *Bioinformatics*, 22(21), 2688–2690. <http://dx.doi.org/10.1093/bioinformatics/btl446>
- Swofford, D.L. (2002) PAUP*: phylogenetic analysis using parsimony (* and other methods). Sunderland, MA: Sinauer Associates.
- Tsang, L.M., Chan, B.K.K., Shih, F.-L., Chu, K.H. & Allen Chen, C. (2009) Host-associated speciation in the coral barnacle *Wanella milleporae* (Cirripedia: Pyrgomatidae) inhabiting the *Millepora* coral. *Molecular Ecology*, 18(7), 1463–1475. <http://dx.doi.org/10.1111/j.1365-294X.2009.04090.x>
- Vey, A. & Brix, S. (2009) *Macrostylis cerrita* sp. nov., a new species of Macrostylidae (Isopoda: Asellota) from the Southern Ocean. *Zootaxa*, 2096, 356–370.
- Wägele, J.-W. (1989) *Evolution and phylogeny of isopods. New data and the state of affairs*. E. Schweizerbart'sche Verlagsbuchhandlung. (Zoologica), Stuttgart, 262 pp. (*In German*)
- Wägele, J.-W. & Mayer, C. (2007) Visualizing differences in phylogenetic information content of alignments and distinction of three classes of long-branch effects. *BMC Evolutionary Biology*, 7(1), 147. <http://dx.doi.org/10.1186/1471-2148-7-147>
- Wetzer, R. (2002) Mitochondrial genes and isopod phylogeny (Peracarida: Isopoda). *Journal of Crustacean Biology*, 22(1), 1–14.
- Wilson, G.D.F. (1989) *A systematic revision of the deep-sea subfamily Lipomerinae of the isopod crustacean family Munnopsidae*. Cox, C.S., Fleminger, A., Kooyman, G.L., & Rosenblatt, R.H., (Eds.) Bulletin of the Scripps Institution of Oceanography 27, University of California Press, Berkeley, Los Angeles, London, 138 pp.
- Wilson, G.D.F. (1999) Some of the deep-sea fauna is ancient. *Crustaceana*, 72(8), 1019–1030. <http://dx.doi.org/10.1163/156854099503915>
- Wilson, G.D.F. (2008) A review of taxonomic concepts in the Nannoniscidae (Isopoda, Asellota), with a key to the genera and a description of *Nannoniscus oblongus* Sars. *Zootaxa*, 1680, 1–24.

Wolff, T. (1956) Isopoda from depths exceeding 6000 meters. *Galathea Report*, 2, 85–157.

Wolff, T. (1962) The systematics and biology of bathyal and abyssal Isopoda Asellota. *Galathea Report*, 6(3), 1–320. [http://dx.doi.org/10.1016/0011-7471\(65\)91573-1](http://dx.doi.org/10.1016/0011-7471(65)91573-1)

Xia, X. & Xie, Z. (2001) DAMBE: software package for data analysis in molecular biology and evolution. *Journal of Heredity*, 92(4), 371–373. <http://dx.doi.org/10.1093/jhered/92.4.371>

Xia, X., Xie, Z., Salemi, M., Chen, L. & Wang, Y. (2003) An index of substitution saturation and its application. *Molecular Phylogenetics and Evolution*, 26(1), 1–7.

Author contributions

The study was conceived by myself. Specimens were identified, dissected and illustrated by myself. The fundamental database was developed by myself with contributions from G.D.F. Wilson. The manuscript was written by myself with contributions from A. Brandt. Fieldwork was conducted by A. Brandt and myself. The molecular part of this study was conducted by myself at the Smithsonian National Museum of Natural History with contributions from A. Driskell, A. Ormos and K. Jeskulke. SEM images were created with the help of R. Walter. This study was conducted in the framework of the SYSTCO project led by A. Brandt.

Chapter 5

Urstylidae – a new family of abyssal isopods (Crustacea: Asellota) and its phylogenetic implications

Published as: Riehl, T., Wilson, G. D. F. and Maljutina, M. V. (2014) Urstylidae – A new family of deep-sea isopods and its phylogenetic implications. *Zoological Journal of the Linnean Society*, 170, 245–296. DOI: 10.1111/zoj.12104.

Abstract

We report three new species of isopod crustaceans that belong to a rare higher taxon of asellote Isopoda. This taxon does not fit into current classifications. The isopods occurred in abyssal soft sediments, near manganese nodules, and in the vicinity of hydrothermal vents. Given their wide spatial occurrence across the Atlantic and Pacific Oceans, a cosmopolitan distribution is assumed. A cladistic analysis revealed a close relationship with the Macrostylidae, a common representative of the deep-sea macrofauna. Analyses of character evolution across the Janiroidea showed sufficient synapomorphies to justify the erection of *Urstylis* gen. nov. and the new family Urstylidae based on the three new species. All taxa are described in this paper. Urstylidae is characterized, amongst other apomorphies, by an elongate habitus with spade-like head; uropods are long, styliform; one pleonite is free; antennal merus and carpus are relatively short; the first pereopod is carpo-propodosubchelate, and more robust and shorter than pereopod II. Several characters, such as the pereopods' posterior scale-like claw that basally encloses the distal sensilla may be interpreted as ancestral when compared to the situation in the highly derived Macrostylidae.

Keywords: benthos – cladistics – deep sea – Janiroidea – Macrostylidae – parsimony – taxonomy – *Urstylis solicopia* sp. nov. – *Urstylis thiotyntlus* sp. nov. – *Urstylis zapiola* sp. nov.

Introduction

The asellote isopod superfamily Janiroidea Sars, 1897, is the most speciose superfamily amongst isopods. It currently comprises 22 accepted families (Schotte *et al.*, 2013) plus seven genera with uncertain affinities (Wilson, 2013). Janiroidea gave rise to the oldest of isopod lineages in the deep sea (Raupach, Held and Wägele, 2004; Raupach *et al.*, 2009), probably before the advent of the Triassic (Lins *et al.*, 2012). Today, most deep-sea janiroid families have a wide or cosmopolitan distribution, and are commonly encountered in abyssal soft sediments (Hessler and Thistle, 1975; Hessler, Wilson and Thistle, 1979). Despite decades of sampling the deep sea, however, only a small fraction of the deep-sea floor has been studied (Ramirez-Llodra *et al.*, 2010) and rare taxa continue to be revealed that do not fit in any of the currently established groups (see e.g. Just, 2005; Osborn, Madin and Rouse, 2011).

Isopods that did not fit into current classifications were encountered during the Woods Hole Oceanographic Institution programs (Rex *et al.*, 1993; Wilson, 1998). They were not treated taxonomically owing to uncertainty about their affinities. Subsequently, this same type of isopod has appeared in samples from the Pacific Ocean, both the Clarion-Clipperton Fracture Zone (CCFZ; Thistle and Wilson, 1987, 1996; Wilson, 1987a); and the Galapagos Rift Zone (Grassle *et al.*, 1985); and were more recently collected again in the CCFZ by the Russian scientific centre ‘Yuzhmorgeologia’, the Federal State Unitary Geological Enterprise, Southern Scientific and Production Association for Marine Geological Operations, Gelendzhik.

These new species had a habitus that resembled Macrostylidae Hansen, 1916. One was marked as ‘Macrostylidae new genus’ in publications that listed this species (Thistle and Wilson, 1987). A

careful account of their morphology showed that they had none of the apomorphic characters of macrostylids, so a more detailed analysis of the three species was undertaken. The culmination of evidence has convinced us that sufficient information was available to add another family to the Janiroidea, Urstylidae fam. nov., comprising one new genus and three species. The potential relationships of this new family amongst Janiroidea are discussed, with a consideration of apomorphic features of both the Macrostylidae and the new family.

Material and Methods

Sampling

Sampling was conducted during various US and Russian cruises by different institutions. Samplers employed were box corers (Hessler and Jumars, 1974) or epibenthic sled (Sanders, Hessler and Hampson, 1965). Please refer to the type localities and further records of the respective new species for detailed information.

Terminology

Terminology is largely based on previous work on Janiroidea (Wilson, 1989; Riehl and Brandt, 2010, 2013). Ratios described as ‘near’ or ‘subequal’ are defined as being $\pm 5\%$ of the second measurement (Kavanagh and Wilson, 2007). For reasons of comparability, the podomeres of the antenna are named in this paper instead of numbering them. The close relationship between the new taxa and Macrostylidae makes assumptions of homologies necessary and given the difference in article numbers between them, consecutive numbering of the articles would lead to confusion. The presence or absence of the antenna first article is obscured by simply counting the basal podomeres owing to its transformations

across the entire order (Wilson, 2009). We hence adopted the nomenclature used by Hansen (1893) for Malacostraca: the first three articles are named 'precoxa', 'coxa', and 'basis'. The antennal scale (i.e. rudimentary exopod or squama) is located at the basis and allows the antennal articles to be homologized across all isopod taxa.

Character Matrices and Cladistic Analysis

The data were assembled and analysed following Wirkner and Richter's (2010) approach. For the taxon sampling, an exemplar approach (Yeates, 1995; Prendini, 2001) was chosen. A character matrix was assembled in MESQUITE (Maddison and Maddison, 2011) starting with the data from Wilson (2009). All major asellotan groups and all families of the Janiroidea were covered; the non-asellotan taxa were removed. The character set was subsequently expanded to address many derived features found in the Janiroidea, with synapomorphies of all families of this group. From the available taxonomic-systematic literature, species were selected according to the following rationale: (1) wherever possible, we used the type species of the type genus for each family so that the resulting classification is unambiguous.

Types were chosen wherever the available descriptions fulfilled certain quality standards (completeness and detail of description and illustrations, availability of type material). In some cases, we used nontype species owing to incomplete descriptions. (2) Species for which DNA was available to the authors from online repositories or otherwise were chosen because this will allow a combined analysis of morphological and molecular data sets. (3) Species with exceptionally detailed descriptions were chosen in some cases where neither (1) nor (2) applied. The exemplar character coding was not followed when a character state was not known for the exemplar species but the state had a consistent

condition across all other species of the genus or family. The evolution of the entire clade Janiroidea is beyond the scope of this publication and will be addressed separately (T. Riehl and G. D. F. Wilson, unpubl. data). To evaluate the phylogenetic position of the three new species, we reduced the set of exemplar taxa to those that are potentially (or at least superficially) related. The exemplars chosen belong to the families Desmosomatidae Sars, 1897, Janirellidae Menzies, 1956, Katianiridae Svavars-son, 1987, Macrostylidae Hansen, 1916, Mesosignidae Schultz, 1969, Nannoniscidae Hansen, 1916, and Thambematidae Stebbing, 1913.

We excluded many families owing to their fundamentally different morphologies (e.g. Munnopsidae Lilljeborg, 1864, Munnidae Sars, 1897, Santiidae Wilson, 1987b, Dendrotionidae Vanhöffen, 1914, Haplomunnidae Wilson, 1976) or because of significant differences in copulatory structures: Ischnomesidae Hansen, 1916 and Haploniscidae Hansen, 1916 have a dorsal opening to the spermathecal duct ('cuticular organ'), whereas the families considered here have lateral openings. Our selection was also based on previous analyses which showed that this suite of families at least has proximity to Macrostylidae (Wägele, 1989; Raupach *et al.*, 2009).

After the sister-group relationship with macrostylids was established in a preliminary analysis with limited taxon number, the macrostylid taxon sampling was broadened so that the terminals cover the morphological diversity currently known for this family. All currently known species of *Macrostylis* were studied for this purpose as well as recently collected and undescribed material. The selection of macrostylid terminals was made to represent the fundamental range of morphological variability across this family. The terminals represent clades within this family that have been identified by morphological and molecular means (Riehl

and Brandt, 2013; T. Riehl, unpubl. data). This approach was taken to test whether both groups are reciprocally monophyletic. Our interpretation is restricted to establishing the position of the new taxa.

The morphology of the three new species was analysed using light microscopy and scanning electron microscopy (SEM; see taxonomy section below). Comparative analysis with the other Janiroidea led to character conceptualization where characters were defined and explained and assumptions of homology were made. States of 407 characters were newly defined or in some cases adopted from previous studies (e.g. Wilson, 1985, 2009; Brusca and Wilson, 1991). All were used in the analysis but states for only those 75 characters relevant for the new taxa and their systematic relationships are outlined, defined, and discussed in detail.

Characters are constructed to be independent from each other. Our aim was to decompose morphologies into the smallest homologous characters with consistent states that are real alternatives (i.e. distal margin rounded vs. acute, rather than round vs. not round). We separated independent features into different characters to avoid mixing nonhomologous states (i.e. presence/absence features are separate from structural features of the present state). A cladistic analysis was used to infer the most parsimonious relationship scenarios amongst the terminals and to test the homology hypotheses defined in the character concepts. The character matrix was evaluated using TNT (Goloboff, Farris and Nixon, 2008), in a thorough analysis with the following settings: the root was forced to *Janira maculosa* Leach, 1814 based on previous studies suggesting a basal position of Janiridae in the Janiroidea (Wägele, 1989); a 'new technology' analysis was conducted with sectorial search, ratchet, drift, and tree fusing (all at standard settings); seed was set to 12345 and the minimum tree length was

found 100 times.

A strict consensus tree was generated from the four equally shortest trees retained. The consensus tree was resampled following the jackknife algorithm with a removal probability of 25% and 10 000 replicates. Relative and absolute Bremer support values were derived from tree-bisection-reconnection (TBR; Goloboff and Farris, 2001). The complete data set has been deposited in TREEBASE under the following URL: <http://purl.org/phylo/treebase/phylo/phylo/study/TB2:S14396>. Finally, the evolutionary interpretation of the character changes was carried out.

Taxonomy

Whole specimens were transferred from 70–96% ethanol to an ethanol-glycerine solution (1:1) and subsequently to glycerine. For illustration of appendages in standard views, dissected parts were temporarily mounted on slides following Wilson (2008) and stained with methyl green or chlorazol black. Dissected appendages were mounted on permanent slides using Euparal following Riehl and Kaiser (2012) in the cases of the specimens archived in Hamburg (ZMH K) and Vladivostok (MIMB). The specimens deposited in Sydney (AM P.) and Washington D.C. (USNM) were mounted as follows: the parts were transferred from glycerine to a 50:50 pure ethanol and turpeneol solution in a relatively deep and straight-sided dish. The turpeneol-ethanol mixture is turbulent because the ethanol evaporates quickly, and the solution thus will tend to run over flat or curved surfaces. After approximately 5 min, the parts were transferred to Euparal. A Carl Zeiss Leo 1525 microscope was used for SEM and the specimen was mounted on a specimen holder after Pohl (2010).

Character states were coded using the computer software DELTA (Dallwitz, 1980, 1993; Dallwitz, Paine and Zurcher, 2010) to generate

descriptions. A database previously used for Macrostylidae (Riehl and Kaiser, 2012; Riehl, Wilson and Hessler, 2012; Riehl and Brandt, 2013) was adopted. An identification key and species' diagnoses were prepared using KEY (Dallwitz, 1974) as implemented in DELTA. The key was manually complemented with further characters to allow more exact identification. Measurements were taken from line drawings using either the distance-measurement tool embedded in Adobe Acrobat Professional or ImageJ and in accordance with the methods described by Hessler (1970). A stage micrometer was used for calibration.

All appendages' article-length ratios are given in proximal to distal order, excluding setae. Many ratios are used for descriptions in this paper. To avoid multiple repetition of the word 'times,' these are reported as a multiplier of an object of a telegraphic phrase to indicate the size of the subject of the phrase (see Wilson, 1989). For example, 'endopod length 2.2 width' means 'the length of the endopod is 2.2 times its width.' This example is mathematically equivalent to the equation ' $L = 2.2W$ '. Dependent object clauses, separated off by a comma, do not repeat the subject. Descriptions of pereopod setae are provided in proximal to distal and lateral to medial order of description in accordance with Riehl *et al.* (2012).

Line drawings were created with the programs Inkscape and Adobe Illustrator following Coleman (2003, 2009).

Results

Character Conceptualization

In the following section, we discuss the concepts for the characters that appear synapomorphies for

the Macrostylidae and Urstylidae, relative to a selected set of outgroup taxa. This reduced character set does not discuss all characters in the matrix used in the analysis, although we provide the complete matrix as Supporting Information Appendix S1. This data set is too limited to infer relationships within or between the other taxa used.

Antennula and antenna articulation position on the cephalothorax

Anteriorly inserting first antennula or antenna articles are widely distributed in Janiroidea. The articulations sit in a transverse plane. In Macrostylidae, the articulation sockets are positioned on the dorsolateral surface of the cephalothorax. In this case, the plane of the articulation is tilted lateroventrally resulting in a dorsolateral orientation (see e.g. Riehl *et al.*, 2012: fig. 7). Another distinct direction of the articulation of the antennula can be found in Echinothambematidae, where it is tilted slightly anteroventrally and laterally resulting in a dorsal and anterolateral orientation. The antennal articulation is in the transverse plane. In Haplomunnidae (not treated here), the lateral aspect found in Echinothambematidae is absent. Here, the antennular and antennal articulations are orientated anterodorsally.

Character 1. Antennula articulation position: 0 = anteriorly; 1 = dorsolaterally; 2 = anterodorsally.

Character 2. Antenna articulation position: 0 = anteriorly; 1 = dorsolaterally.

Antennula basal article orientation

In most species, the first article projects anteriorly. In Macrostylidae a posterodorsal projection can be found. Echinothambematidae have a highly flexible first article that can occupy every orientation from anterolaterally to dorsally; and in Haplomunnidae and some Dendrotionidae (not treated here), the first article projects anterodorsally.

Character 3. Antennula basal article orientation: 0 = anteriorly; 1 = posterodorsally; 2 = anterodorsally; 3 = anterolaterally to dorsally.

Antennula flagellum aesthetasc number per article in adult male

Most Janiroidea have one aesthetasc per flagellar segment in the male. Several taxa, mostly with a small flagellum, have more aesthetascs per antennular segment (two to five); in some cases, substantially more than five aesthetascs per segment are present.

Character 4. Antennula flagellum aesthetasc number in adult male per article: 0 = one; 1 = two to five; 2 = six or more.

Antennula hypertrophy in adult males

Whereas the lengths and widths of antennulae are similar in both sexes in many Janiridae and ‘munoid’ taxa (Wägele, 1989), some groups, such as Macrostylidae have a thicker antennula in adult males (article width increased relative to length) than in the females, also referred to as hypertrophy.

Character 5. Antennula hypertrophy in adult males: 0 = absent; 1 = present.

Antenna axis

In most Isopoda, the antenna in relaxed position has a curved axis. Basal podomeres that are cuneiform (wedge-shaped) provide the basis for this as the articular planes are not parallel. Although the first article is usually positioned and projecting anteriorly, the antenna on the whole can thus be directed posteriorly. In some groups, all podomeres are approximately cylindrical with proximal and distal articulations aligned. In these cases, bending of the axis is the result of articulation only.

Character 6. Antenna axis: 0 = curved; 1 = straight.

Antenna article 3 (basis) scale

The exopod of the crustacean antenna is called the squama, scale, or scaphocerite (McLaughlin, 1980). It is located on the basis of the limb (Wägele, 1989). In Asellota, this exopod is rudimentary, or completely absent.

Character 7. Antenna article 3 (basis) scale (presence): 0 = present; 1 = absent.

Antennal basal article 1 (precoxa)

We consider two distinct states in which the first podomere of the antenna is either present and fully articulated, or absent (Wägele, 1983; Brusca and Wilson, 1991).

Character 8. Antennal basal article 1 (precoxa): 0 = present; 1 = absent.

Antenna article 3 (basis) length relative to articles 2 and 4

The antenna basis is either longer than coxa and ischium or at most subsimilar in length.

Character 9. Antenna article 3 (basis) length (vs. articles 2 and 4): 0 = longer; 1 = subsimilar or shorter.

Antenna article 6 (carpus) length relative to the combined lengths of podomeres 1–4

The carpus of the antenna occurs in two states in the Janiroidea: distinctly longer than the preceding articles (precoxa–ischium) combined or relatively short in comparison to articles 1–4.

Character 10. Antenna article 6 length (vs. podomeres 1–4): 0 = longer; 1 = subsimilar or shorter.

Mandibular lateral seta

A seta is present laterally on the mandible body in Macrostylidae, approximately at the location of the palp articulation in other groups. Seta-like objects occurring in *Mexicope* are located more ventrally and occur next to the mandible palp. These are con-

sidered analogous because of differences in structure and location.

Character 11. Mandibular lateral seta: 0 = absent; 1 = present.

Differentiation of the lacinia mobilis on the right mandible

The right *lacinia mobilis* may be either indistinguishable from the remainder of the spine row or differentiated to form a heavily calcified and movable tooth-like structure (Richter, Edgecombe and Wilson, 2002).

Character 12. Mandibular right *lacinia mobilis*: 0 = indistinguishable; 1 = differentiated.

Mandibular palp

In Janiroidea, the palp is plesiomorphically present and apomorphically absent across various groups.

Character 13. Mandibular palp: 0 = present; 1 = absent.

Maxilliped palp article 2 width and length ratios

Three distinct conditions are recognized with respect to the width relationships of the first (ischium) and second (merus) palp articles of the maxilliped. Maximal widths are measured perpendicularly to the palp axis (character 14). The maxilliped article 2 (merus) shows considerable variability in the relationship between lateral length (LL) and medial length (ML) as well as between LL and width. Here, we define three states for the LL-width relationship: the LL is either subsimilar to the width, distinctly smaller, or distinctly greater (character 15). Further, we distinguish the state in which the lateral length is subequal to or exceeds the medial length from the state in which the lateral length is distinctly shorter than the medial length (character 16).

Character 14. Maxilliped palp article 2 width (vs. article 1 width): 0 = wider; 1 = subsimilar; 2 = nar-

rower.

Character 15. Maxilliped palp article 2 lateral length vs. width: 0 = $LL \approx \text{width}$; 1 = $LL < \text{width}$; 1 = $LL > \text{width}$.

Character 16. Maxilliped palp article 2 lateral vs. medial length: 0 = $LL \geq ML$; 1 = $LL < ML$.

Maxilliped palp article 4 length–width ratio

Articles with a length that clearly exceeds the width are considered elongate. Where length and width are subsimilar, the article is short. Maximum width and length of the maxilliped article 4 (propodus) are used.

Character 17. Maxilliped palp article 4 L/W ratio: 0 = $L \approx W$; 1 = $L > W$.

Posterolateral setae on pereonites

Posterolateral setae are defined as those robust setae that are located on or near the apex of posterolateral tergite projections, and are clearly directed posteriorly. Such setae are usually prominent in that they are the only setae on an otherwise asetose cuticle or because they exceed other setae in close proximity in length, width, and/or robustness.

Character 18. Posterolateral setae on pereonites: 0 = absent; 1 = present.

Pereonite tagmosis and functional groupings

Throughout the Isopoda, the body has functional groupings or tagmata wherein limbs within a group have similar morphological construction and orientation.

Character 19. Pereonal tagmosis, functional groupings: 0 = 4:3; 1 = 3:1:3.

Anterior pereonites' size relative to posterior pereonites

Width and depth of the anterior pereonites (tagma) may be increased significantly in comparison to posterior body segments, resulting in an overall

posteriorly narrowing body shape.

Character 20. Anterior vs. posterior pereonites size: 0 = subsimilar; 1 = wider, deeper.

Anterior pereonites' integration relative to posterior pereonites

Different levels of integration are defined by the expression of the intersegment articulation. Integration is low when segments are freely articulated, spaced, and movable against each other. Highly integrated segments form a compact subsection of the body with confluent outlines and tight articulations.

Character 21. Anterior pereonites integration: 0 = low; 1 = high.

Anterior pereonites lateral margins (transition between segments)

Whereas in most Asellota the lateral outline is notched between the segments, in Macrostylidae the segments of the anterior pereonites have a seamless transition creating an entire outline.

Character 22. Anterior pereonites' transition between segments: 0 = notched; 1 = entire.

Anterior pereonites' sternite margins (fusion)

The cuticular membrane at segment borders allows the segments to move against each other. Where segments are highly integrated; movability may be lost, the segment margins may fuse.

Character 23. Anterior pereonites' sternite margins: 0 = expressed; 1 = (partly) fused.

Tergal projections laterally on anterior pereonites 2–4 and posterior pereonites 6–7 (presence)

This character differentiates between the condition in which the tergites project laterally beyond the lateral margin of the coxae and the condition in which the coxae are aligned with the tergites or project beyond. Anterior and posterior segments

are treated separately.

Character 24. Tergal projections laterally on anterior pereonites 2–4: 0 = absent; 1 = present.

Character 25. Tergal projections laterally on anterior pereonites 5–7: 0 = absent; 1 = present.

Oostegites on pereopods 1 and 2

The number of oostegites and the legs involved in creating the pouch can vary across the Janiroidea.

Character 26. Pereopod 1 oostegite: 0 = present; 1 = absent.

Character 27. Pereopod 2 oostegite: 0 = present; 1 = absent.

Pereonite 4 anterior collum

The presence of a collum in pereonite 4 is apomorphic for the Macrostylidae (Riehl *et al.*, 2012).

Character 28. Pereonite 4 anterior collum: 0 = absent; 1 = present.

Position of the coxa insertion on pereonite 4

The coxal insertion on pereonite 4 is located either anteriorly or medially on the lateral margin.

Character 29. Pereonite 4 coxa insertions: 0 = anterolateral; 1 = mediolateral.

Ventral spines on pereonites 1 and 2

In pereonite 1, a clear distinction can be made when the spine either assumes a ventral-posterior orientation or is directed anteriorly and projects ventrally to the cephalothorax. As species groups show considerable variation, we have treated each pereonite individually.

Character 30. Pereonite 1 ventral spine orientation (if present): 0 = anteriorly; 1 = ventrally and posteriorly.

Character 31. Pereonite 2 ventral spine: 0 = absent; 1 = present.

Anterior pereopods' coxae shape

The coxae of the anterior pereopods are either ring-like projections with clear coxa–body articulations or they are embedded into the ventral pereonal cuticle, which is referred to as ‘disc-like’.

Character 32. Anterior pereopods coxae: 0 = ring-like; 1 = disc-like.

Coxa setation of anterior and posterior pereopods

The degree of setation on the coxae varies considerably across the janiroideans, although those taxa that have the coxa in a more ventral position or reduced typically have unadorned coxae.

Character 33. Anterior pereopods' coxae setation: 0 = present; 1 = absent.

Character 34. Posterior pereopods' coxae setation: 0 = present; 1 = absent.

Pereopod I–IV orientation

The anterior locomotory appendages of Janiroidea are either orientated anteriorly and held in a ventrolateral position, or their orientation is somewhat dorsal and held in a lateral position.

Characters 35–38. Pereopods I–IV orientation: 0 = ventrolateral; 1 = dorsolateral.

Shape of dactylus posterior (ventral) claw of the anterior and posterior pereopods

The diversely modified setae that form the ventral dactylar claws (Wilson, 1985) appear in diverse shapes. They are often claw-shaped similar to the dorsal claw. Further forms of modification are flattened, scale-like claws; elongate structures that are dorsally concave and ventrally keeled; straight, unarticulated spines; hand-shaped, serrate claws (see Wilson, 1985). In the posterior pereopods, claws may have retained (or regained) a simple seta-like appearance. Anterior and posterior claws show considerable differences in some taxa, these have

been coded separately.

Character 39. Shape of the anterior pereopod dactylus posterior claw (if present): 0 = claw-like; 1 = scale-like; 2 = thin elongate, with ventral carina, distally tapering, clinging to distal sensilla, 3 = thin, unarticulated spine; 4 = broad, serrate.

Character 40. Posterior pereonites' dactylus posterior claw (if present) shape: 0 = claw-like; 1 = scalelike; 2 = seta-like.

Position of the dactylus distal sensillae in the anterior and posterior pereopods relative to the claws

Distally on janiroidean dactyli and adjacent to the dorsal claw, small modified setae can be found that have a probable sensory function and are commonly referred to as sensillae (Wilson, 1989; Riehl and Brandt, 2010). Their number is variable, usually up to three. Their shape resembles a thin, flexible tube, often with fringe-like microstructure (Riehl and Brandt, 2010). The positional relationship of the dorsal and ventral claws to the distal sensillae (Wilson, 1985) can be sorted into three different categories: the sensilla(e) may be located between the claws in close proximity, basally enclosed by a large dorsal and a short scalelike ventral claw, or the two claws form a canal within which the sensilla is enclosed.

Character 41. Anterior pereopods' dactylus distal sensillae: 0 = not enclosed; 1 = enclosed; 2 = basally enclosed.

Character 42. Posterior pereopods' dactylus distal sensillae: 0 = not enclosed; 1 = basally enclosed.

Pereopod I dactylus distal sensillae

In most families, these sensillae are short and do not project beyond the dorsal claw. In Urstylidae, these sensillae are elongate and project beyond the claws. In Macrostylidae, one distal sensilla is thick and immovable and is enclosed by dorsal and

medial claws.

Character 43. Pereopod I dactylus distal sensillae: 0 = short, slender; 1 = long; 2 = thick, robust.

Length of the anterior pereopods' dactylus medial sensillae

Medially on the dactylus of Janiroidea, a single or small clutch of sensillae is present. These can either be rather short in a way that they do not distally project beyond the claws, or they are enlarged and project distally.

Character 44. Anterior pereopods' dactylus medial sensillae: 0 = short, thin; 1 = elongate, swollen.

Pereopod I ischium dorsal margin

A dorsally projecting ischium of the first pereopod can be distinguished from an ischium with subparallel dorsal and lateral margins (character 45). The projections differ largely in their extent (character 46). Where the projection is small, it has a rounded or triangular appearance; the width of the article is smaller than its length. A large projection is defined by a tapering shape and an article width that exceeds its length.

Character 45. Pereopod I ischium dorsal margin: 0 = subparallel; 1 = projecting.

Character 46. Pereopod I ischium dorsal margin projection: 0 = small; 1 = large.

Pereopod I merus shape

Measurement of the dorsal length (taking into account also distodorsal processes) in relation to the article's maximal width allows short and elongate merus to be distinguished. A short merus is characterized by having a dorsal length subequal to or shorter than its width. Usually, a distinct distodorsal projection is present. Long merus have a dorsal length exceeding their width. Distodorsal projections are absent or minute in this case.

Character 47. Pereopod I merus shape: 0 = short; 1

= long.

Pereopod I carpus shape

Five shapes of the first pereopod carpus are defined (Just and Wilson, 2004, 2007; Wilson, 1987b): a triangular carpus has a short dorsal margin and a much longer ventral margin; trapezoid means that the segment is proximally slender and distally widening, dorsal and ventral margins have sub-similar lengths; an elongate carpus has parallel dorsal and ventral margins, is slender and multiple times longer than wide; quadrate refers to a short carpus with length subsimilar to width and parallel margins; a sickle shape is present when dorsal and ventral margins are parallel, with the ventral margin concave and the dorsal margin convex.

Character 48. Pereopod I carpus shape: 0 = triangular; 1 = trapezoid; 2 = elongate; 3 = quadrate; 4 = sickle-shaped.

Pereopod I opposition between carpus and propodus

This character addresses whether the carpus and propodus are involved to form a subchela. Subchelae can vary a lot in their degree of opposition, whereas the opposition alone does not define a chela. To identify a subchela as such, structures associated in grasping need to be present as well: ventral projections, spine-like setae, or rows of spinules.

Character 49. Pereopod I opposition between carpus and propodus: 0 = absent; 1 = present.

Pereopod I length in relation to pereopod II

Three categories of length can be distinguished in pereopod I compared to pereopod II. These patterns were recognized by Hessler (1970) for Desmosomatidae and we extend their generality. Regarding the length, the categories shorter and subsimilar or longer are discriminated.

Character 50. Pereopod I length vs. pereopod II: 0 = distinctly shorter; 1 = subsimilar or longer.

Pereopods II and III merus, carpus, and propodus form and setation

Fundamental transformations to pereopods II and III occur amongst the janiroideans, although defining these changes should avoid sole reference to assumed habits, such as ‘ambulatory’ or ‘fossorial’. Limited information on approximate functions of the limbs is available from behavioural observations (Hessler and Strömberg, 1989) and so we have added parenthetic comments, but the characters are defined on morphology. The ‘ambulatory’ state is defined by a short paucisetose merus, and carpus and propodus without or with only ventral robust setae and subparallel margins. Two distinct ‘fossorial’ states are defined and considered analogous rather than homologous because of fundamental structural differences: the first can be recognized by its short, paucisetose merus, and multiple rows of robust setae on the carpus and propodus, both with broadened margins. The second ‘fossorial’ state is characterized by an elongate ischium, merus, and carpus, all with broadened margins and dorsal and ventral rows of robust setae, propodus slender and paucisetose.

Character 51. Pereopod II form: 0 = ‘ambulatory’; 1 = ‘fossorial I’; 2 = ‘fossorial II’.

Character 52. Pereopod III form: 0 = ‘ambulatory’; 1 = ‘fossorial I’; 2 = ‘fossorial II’.

Pereopod III carpo-propodal joint rotation

A rotation of the third pereopod at the carpo-propodal joint is one of the synapomorphies for Macrostylidae (see Riehl and Kaiser, 2012: fig. 4c). As a consequence, the propodus and dactylus angle dorsolaterally instead of ventrally in relation to the limb, or posteriorly along the body axis. The articular plate at the propodo-dactylar joint, usually

positioned laterally on the limb, has a dorsomedial position and the medial sensillae of the dactylus assume a dorsal position.

Character 53. Pereopod III carpo-propodal joint rotation: 0 = absent; 1 = present.

Pereopod III ischium form

The presence of a strong projection of the pereopod III ischium dorsal margin is apomorphic for Macrostylidae. Most other janiroideans have only a distal increase in width if anything, but never have a distinctive bulge midlength on the ischium.

Character 54. Pereopod III ischium form: 0 = straight or slightly vaulted; 1 = with dorsal lobe.

Pereopod III ischium dorsal setation

The ischial projection of the Macrostylidae is furnished with robust and fine setae that are especially useful for species group delimitation (but see Riehl and Kaiser, 2012). Most species have one or two robust setae at the apex of the projection. Other janiroideans have few, if any, ischial setae in a dorsal midlength position.

Character 55. Pereopod III ischium dorsal setation: 0 = setation minor or absent; 1 = setation prominent.

Pereopod IV

Several conditions of the fourth pereopod can be distinguished regarding its overall length and its carpus length. The leg-length categories (character 56) are highly elongate when the length exceeds the body length, in extreme cases up to several times; subsimilar to preceding and subsequent pereopods; or distinctly shorter than pereopods III and V. For the carpus, the following length categories (character 57) are recognized: clearly longer than merus and near propodus length; subsimilar merus length, longer propodus; subsimilar to merus and propodus.

Character 56. Pereopod IV length: 0 = elongate; 1 = subsimilar; 2 = shorter.

Character 57. Pereopod IV carpus (elongation): 0 = longer merus, subsimilar propodus; 1 = subsimilar merus, longer propodus; 2 = subsimilar merus and propodus.

Paired sensory organ dorsally on pleotelson

The paired sensory organs present on the pleotelson of Macrostylidae (Hansen, 1916; Wägele, 1989) and two of the *Urstylis* species are homologized based on similarity in position and underlying anatomy. They are located dorsally in the posterior half of the pleotelson, either as broom setae (= penicillate setae) or in cavities that contain crystalline structures and are interpreted as statocysts.

Character 58. Pleotelson dorsal paired sensory organ (type; if present): 0 = statocyst; 1 = broom seta.

Pleopodal cavity posterior form

The margin of the pleopodal cavity is usually defined by the opercular pleopods. It is considered closed when the opercular pleopods seal off the cavity with the ventrally emerging posterior wall of the pleopodal cavity. It is open when a preanal trough extends the pleopodal cavity to the posterior apex of the pleotelson. In the latter case, the opercular pleopods may or may not extend caudally to the pleotelson apex.

Character 59. Pleopodal cavity posteriorly: 0 = closed; 1 = open.

Pleotelson lateroventral setal rows and ridges

Ventrally on the pleotelson of Macrostylidae, ridges follow the margin of the pleopodal cavity (character 60). They extend from the posterior end of the preanal trough to the anterior region of the pleotelson where in some species they divide from the pleopodal cavity and continue along the lateral

cuticle of the pleotelson. Alongside these rows, macrostylids have rows of long and relatively robust setae (character 61). These also occur in janiroideans that do not feature the ridges, such as Urstylidae, or other taxa not treated here such as Pleurocopidae, Santiidae, some Paramunnidae, and some Munnopsidae (Syneurycopinae, *Microcope* Malyutina, 2008). Setae and ridges are thus considered independent and have been separately coded.

Character 60. Pleotelson lateroventral ridges: 0 = absent; 1 = present.

Character 61. Pleotelson lateroventral setal rows: 0 = absent; 1 = present.

Anus position with regard to pleopodal cavity

Typically, the anus is either covered by the opercular pleopods and thus inside the pleopodal cavity, or it is exposed and outside the cavity. Where the opercular pleopods are shorter than the pleopodal cavity the anus is situated within the cavity but still exposed.

Character 62. Anus position with regard to pleopodal cavity: 0 = inside; 1 = outside.

Male pleopod I medial & lateral lobe arrangement

The first pleopod in Janiroidea has grooves distally on the dorsal surface that guide the second pleopod stylet motion during copulation (Wilson, 1987b). The position of these grooves determines the border between medial and lateral lobes of the pleopod distal apex. The position of the lobes with regard to each other is often group-specific. The lateral and medial lobes can, for instance, be either arranged lateral to each other and in the same plane or the medial lobes override the lateral lobes ventrally.

Character 63. Male pleopod I medial and lateral lobes arrangement: 0 = lateral; 1 = medial lobes ventrally 'overriding' lateral lobes.

Type of setae distally on the female pleopod II

Using a light microscope, the setae on the distal margin of the female opercular pleopod appear to be asetulate in most Janiroidea. *Macrostylis* species are special in having pappose setae, whereas *Urstylis thiotyntlus* has apically sensillate setae.

Character 64. Female pleopod II distal setae (type): 0 = simple; 1 = pappose; 2 = sensillate.

Length of setae distally on the female pleopod II

Whereas most taxa with an apical row of setae on the operculum feature only relatively short setae, in Urstylidae, Macrostylidae, and Mesosignidae, these setae are distinctly longer, partly covering the anus. We define short as being subequal or less than one quarter of the operculum length and long as significantly larger than this.

Character 65. Female pleopod II distal setae (length): 0 = short; 1 = long.

Female pleopod II lateral fringe of fine setae

The opercular pleopod II of the female janiroideans has marginal setae, either distally that may or may not cover the anus, or laterally. Amongst the taxa studied here, most species had a fringe of setae laterally, although *Urstylis zapiola*, *Janirella*, *Echinothambema*, *Desmosoma*, and *Pseudomesus* lacked the setae.

Character 66. Female pleopod II lateral fringe of fine setae (presence): 0 = absent; 1 = present.

Length of the male pleopod II stylet

The Janiroidea show substantial variability in the length of the male pleopod II endopodal stylet, so this feature is likely to be more useful for defining subgroups rather than being distinctive at the family level. The stylet is basally a relatively short straight (e.g. *Janirella*) or curved (e.g. *Janira*) structure and both forms can be seen amongst the Macrostylidae and Urstylidae. Amongst other taxa not included

in this analysis, the stylet may be also sinusoidal (e.g. *Munella*) or coiled (e.g. *Dendromunna*, some Munnopsidae). We consider the stylet to be short when it does not project beyond the distal tip of the protopod; it is intermediate when its projects distinctly beyond the protopod tip but is shorter than 1.5 times the protopod length; otherwise it is long.

Character 67. Male pleopod II stylet length: 0 = short; 1 = intermediate; 2 = long.

Male pleopod II exopod form

The pleopod II exopod in Janiroidea is a short, unarticulate ramus, often with a distal hook (Wilson, 1987b). We find it either to be short and stout with its length not exceeding its width, or elongate when clearly longer than wide.

Character 68. Male pleopod II exopod form: 0 = stout; 1 = elongate.

Pleopod III exopod

The third pleopod shows consistent patterns across the families of the Janiroidea (Wilson, 1985, 1989: figs 36, 37) so that length, width, and expression of segmentation are useful apomorphic features. The plesiomorphic form is a broadly operculate, biarticulate exopod with a fringe of short plumose setae. The exopod becomes less important and undergoes a variety of independent reductions amongst the families of Janiroidea. As these shape and setation characters appear to be independent, they are divided into relative length and width features. The exopod occurs as either mono- or biarticulate (character 69). Three different width categories are distinguished: significantly broader than the endopod, subsimilar to the endopod width, distinctly narrower (character 70). Distally on the exopod, single or multiple conspicuous setae are situated either apically, subapically on the dorsal surface, or distributed along the apical margin (character 71).

Character 69. Pleopod III exopod: 0 = biarticula-

te; 1 = monoarticulate.

Character 70. Pleopod III exopod width (vs. endopod): 0 = subsimilar; 1 = narrower.

Character 71. Pleopod III exopod distal setae (position): 0 = apically; 1 = subapically; 2 = apical and lateral margins.

Uropod position in relation to anus position, in taxa in which the uropods insert posterolaterally

In the Asellota, Microcerberidae, and Phreatoicoidea, the uropods insert near the posterior pleotelson margin, either on the ventral margin or below it, although some Janiroidea have the uropods inserting well above the pleotelson margin on the dorsal surface (e.g. Paramunnidae and Munnidae; not treated here). For those taxa that have the uropods placed posteriorly at the posterolateral margin (above the pleopodal cavity margin but typically below the pleotelson dorsal surface), the uropods are located in direct proximity to the anus in many taxa (Desmosomatidae, Nannoniscidae, some Munnopsidae) and in the cases of the Joeropsiidae, some Munnopsidae (Ilyarachninae and Lipomerinae), and some undescribed Desmosomatidae (not treated here) even cover the anus. Plesiomorphically (Asellidae, Janiridae), the uropods insert adjacent to the anus but typically with a small separation. In Macrostylidae, Urstylidae, and several other taxa with long, styliform uropods, the latter insert some distance laterally to the anus.

Character 72. Uropod insertion (where posterolateral) relative to anus: 0 = adjacent; 1 = separate.

Presence of uropod exopod

The uropod exopod is absent across several groups of Janiroidea independently of the position or overall size of the uropod.

Character 73. Uropod exopod (presence): 0 = present; 1 = absent.

Uropod exopod length relative to endopod length and shape

Where the uropod exopod is present, three length categories are distinguished in comparison with the endopod length: Both rami are either subsimilar, the exopod is distinctly shorter but a recognizable elongate ramus, or the exopod may be vestigial, squat, shorter than long, and immovable because of its small size, although full articulation may be present.

Character 74. Uropod rami relative length: 0 = subsimilar; 1 = exopod smaller; 2 = exopod vestigial.

Uropod endopod length in relation to the protopod length

Depending on the length of the uropod protopod, the length of the endopod can be relatively long or short. Macrostylidae and Urstylidae have extremely elongate uropods; in the majority of species most of the length consists of the protopod. Other families were included in our analysis because they also have elongate uropods, and small or vestigial endopods.

Character 75. Uropod endopod length vs. protopod length: 0 = longer; 1 = subsimilar or shorter.

Systematics

Asellota Latreille, 1802

Janiroidea Sars, 1897

Urstylidae Fam. Nov.

Zoobank registration

urn:lsid:zoobank.org:act:5FAFBD95-32CB-4C73-B904-3DA4C73447B5

Type genus

Urstylis gen. nov., designated here.

Composition

Urstylis gen. nov.

Family diagnosis

Cephalothorax spatulate, widening posteriorly, prognathous. Pleotelson anterior margin 'stalked', not directly adjacent to preceding pereonites. Antenna merus and carpus both subsimilar or shorter than podomeres 1–4 together; merus shorter than carpus. Antennal scale present as rudimentary, unarticulated spine. Maxilliped palp article 2 width subequal to article 1 width. Pereopodal coxae setose. Pereopod I carposubchelate, more robust and shorter than pereopod II; ischium with dorsal setose lobe, carpus trapezoidal, widening distally, with dorsal and ventral margin lengths subsimilar. Pereopods II–VII similar in size and shape. Posterior pereopods dactylus posterior (ventral) claw scale-like, flattened in cross-section; distal sensillae basally enclosed between dorsal and ventral claws. Male pleopod I medial lobes ventrally 'overriding' lateral lobes. Male pleopod II exopod thick and slightly longer than wide. Pleopod III exopod bisegmented with clear articulation; distal article much narrower than proximal article, inserting distomedially; projecting near distal tip of endopod. Uropod insertions at posterolateral pleotelson margin; uropods long, styliform, exopod rudimentary (assumed for *Urstylis thiotyntlus* gen. et sp. nov.).

Family description

Body elongate, more slender in male than in female (assumed for *U. thiotyntlus*). **Cephalothorax** spatulate, with anterolateral insertions of antennulae and antennae; lateral margins setose. Pereonal tagmiosis 4:3. **Pereonites 1–4** lateral margins subpar-

allel, anteriorly rounded, and posteriorly abruptly narrowing (fossosome absent); articulations fully expressed, movable; lateral margins setose, pereonal collum absent. Coxae inserting lateroventrally, visible in lateral view. Posterolateral margins of pereonites 5–7 rounded, lateral margins setose. **Pleonite 1** tergal and sternal articulations with pleotelson present, dorsally with two setae at posterior tergite margin.

Pleotelson subrectangular, elongate, lateral outline with weak waist separating longer anterior and shorter posterior convex margin, posterior margin concave at uropod insertions; apex convex, broadly rounded, ventrally with setal ridges absent; longitudinal trough absent. Anal opening parallel to frontal plane. Marsupium with four pairs of oostegites (pereopods I–IV), oopore lateroventrally (Fig. 1). Antennula and antenna orientated anteriorly.

Antennula of six articles, axis inflected at articulation of elongate articles 1 and 2, article 1 longest and widest; aesthetascs simple, tubular. **Antenna** with six podomeres, precoxa–ischium squat, ischium elbow joint, article insertions at right angles, basis with unarticulated small spine (probably homologous with scale), flagellar articles each with several thin, tubular aesthetascs, more in male than in female. **Mandible** without palp, incisor process multidentate, gracile, much thinner than basal region; *lacinia mobilis* grinding or crushing, multidentate, right lacinia clearly smaller than left lacinia, left mandible incisor with dorsal cusps forming right angle to distal and ventral cusps. **Maxilliped** basis medioventrally with seta absent; palp narrower than basis, wider than endite, first article distolateral lobe present, fourth article distomedial lobe present.

Pereopodal coxae ring-shaped, setose; dactyli with two claws inserted terminally; ventral claw much smaller than dorsal claw, scale-like,

basally enclosing distal sensillae. **Pereopod I** modified, shortest and broadest, ischium with dorsal setose lobe, carpus broader distally, laterally flattened; pereopods II–VII similar in size, shape, and setation, getting slightly more slender from II to VII, carpus-propodus elongate, cylindrical, lengthening from pereopods II to VI. **Opercular pleopods** distally setose; setae asetulate.

Male pleopod I proximally with subparallel lateral margins, distally widening, with no distolateral horns, lateral lobes not extending distally beyond medial lobes. **Male pleopod II** protopod slender, tapering distally, narrower than pleopod I. Female operculum stout, ovoid, without keel, broadly rounded distally, ventrally overlapping the lateral margins of the pleopodal cavity, distally not reaching anus. **Pleopod III** protopod and endopod subequal in length and width, endopod with three plumose distal setae, setae longer than endopod; exopod biarticulate, with distinct articulation, lateral outline not continuous, with lateral fringe of fine setae mostly restricted to proximal article, distal article length approximately 0.33 times proximal article length, approximately 0.5 times proximal article width, with conspicuous subterminal seta shorter than distal article.

Pleopod IV exopod subequal in length to endopod, elongate, flat, with lateral fringe of fine setae, setae longer than exopod width, distally with plumose seta, seta slightly smaller than exopod. Pleopod V uniramous. Uropod long, styliform, biramous, exopod squat, minute, wider than long, with one or few setae; protopod exceeding the length of the pleotelson (known only in *Urstylis zapiola* and *Urstylis solycopia manca*).

Distribution

Species of Urstylidae have been found exclusively on abyssal soft sediments. They are known to occur in the western South Atlantic, near manganese

nodules in the tropical North Pacific, and in the vicinity of hydrothermal vents near the Galapagos.

Urstylis gen nov.

Zoobank registration

urn:lsid:zoobank.org:act:E046CF0B-5DBA-4077-8C54-0F206467EE8C

Gender

The ending ‘-is’ is nominative singular feminine, as in *Macrostylis*.

Type species

Urstylis zapiola sp. nov., designated here.

Etymology

Based on the likely basal position of this genus to Macrostylidae and supposedly primitive character states, the Old High German prefix ‘Ur-’, meaning ‘thoroughly’ was chosen. It adds the meaning proto-, primitive, or original to nouns with which it is combined. This prefix was especially chosen in honour of Robert R. Hessler, who employed this prefix for naming ancestral character states or modelled ancestral species. The root ‘-stylis’ refers to the shape of the uropods that characterize species of *Urstylis* and the related Macrostylidae. It is based on the Greek $\sigma\tau\upsilon\lambda\acute{\iota}\varsigma$ which is the complementary feminine form of $\sigma\tau\upsilon\lambda\omicron\varsigma$ (stylos; masculine), meaning column or pillar.

Composition

Urstylis zapiola sp. nov., *U. solycopia* sp. nov., *U. thiotyntlus* sp. nov.

Generic diagnosis

Pereon without sternal spines, not keeled. Pereonites 1–4 not tightly packed with anterior submargi-

nal row of setae and lateral margin setose, posterolateral margin without prominent spine-like seta. Long setae on pedestal (uncalcified) articulations along lateral and anterior tergite margins. Pleotelson waist well pronounced, paired dorsal sensory organ present. Pereopod I positioned ventrally, orientated anteriorly, ischium dorsal lobe not longer than merus dorsal lobe.

***Urstylis zapiola* gen. et sp. nov.**

Figures 1–9

Zoobank registration

urn:lsid:zoobank.org:act:3948B113-52B4-4CF5-93B7-710C67C9EA25

Etymology

This name refers to the type locality on the Zapiola Drift, a topographical feature in the Argentine Basin underlying a deep-sea current strongly influencing the deep Argentine Basin sediments (Flood, Shor and Manley, 1993) called the Zapiola Anticyclone (de Miranda, Barnier and Dewar, 1999). It is a feminine noun in apposition.

Type fixation

Adult male holotype USNM 1208013, designated here.

Type material examined

USNM 1208013: adult male holotype, 1.9 mm. USNM 1208014: adult female paratype, 1.8 mm. AM P.90631: adult male paratype [dissected, parts on two slides (AM P.90631.001)]. USNM 1208015: adult male, 1.9 mm, head damaged, uropod ~0.8 mm; adult male 1.9 mm. AM P.67340: four brooding females, 1.7 mm; two brooding females, 1.6 and 1.8 mm; four females, 1.6, 1.8, 1.9 mm (twice); three adult males, 1.5 mm (twice), 1.7 mm; three

individuals fragmented, two females, male. George D. F. Wilson (GDFW) collection: male paratype (sectioned on four slides), 1.6 mm.

Type locality

Argentine Basin, 43°33.0'S, 48°58.1'W, 5208–5223 m, Woods Hole Oceanographic Institution Research Vessel (R/V) Atlantis II cruise 60, benthic station 247A, 17.03.1971, epibenthic sled. *Urstylis zapiola* was collected in a particularly large epibenthic sample. The isopod composition of this sample is provided in Supporting Information Appendix S2.

Further records

Known only from the type locality.

Type material – remarks

Only two specimens, both male, retained uropods and so the least damaged specimen was used for the holotype. Of the brooding females, two had embryos in the brood pouch, only three each. The males were typically heavily calcified whereas the females were not.

Diagnosis

Body subcylindrical; pleotelson length/width ratio 1.5, waist well pronounced, paired dorsal sensory organ located in tergal cuticular tubercles; pereonites 4 and 5 subequal; pereonite 6 slightly longer than pereonite 5; pereonite 7 posterolateral margins not projecting posteriorly; pereopod I ischium dorsal lobe with one seta. Pereopods V–VII ischium and carpus without strong seta mid-dorsally.

Description of female

Body (Fig. 2C) length 1.8 mm, 4.0 width. Ventral spines on pereonites 1–7 absent. Cephalothorax – pleotelson with imbricate ornamentation covering all tergites, sternites, and opercular pleopods.

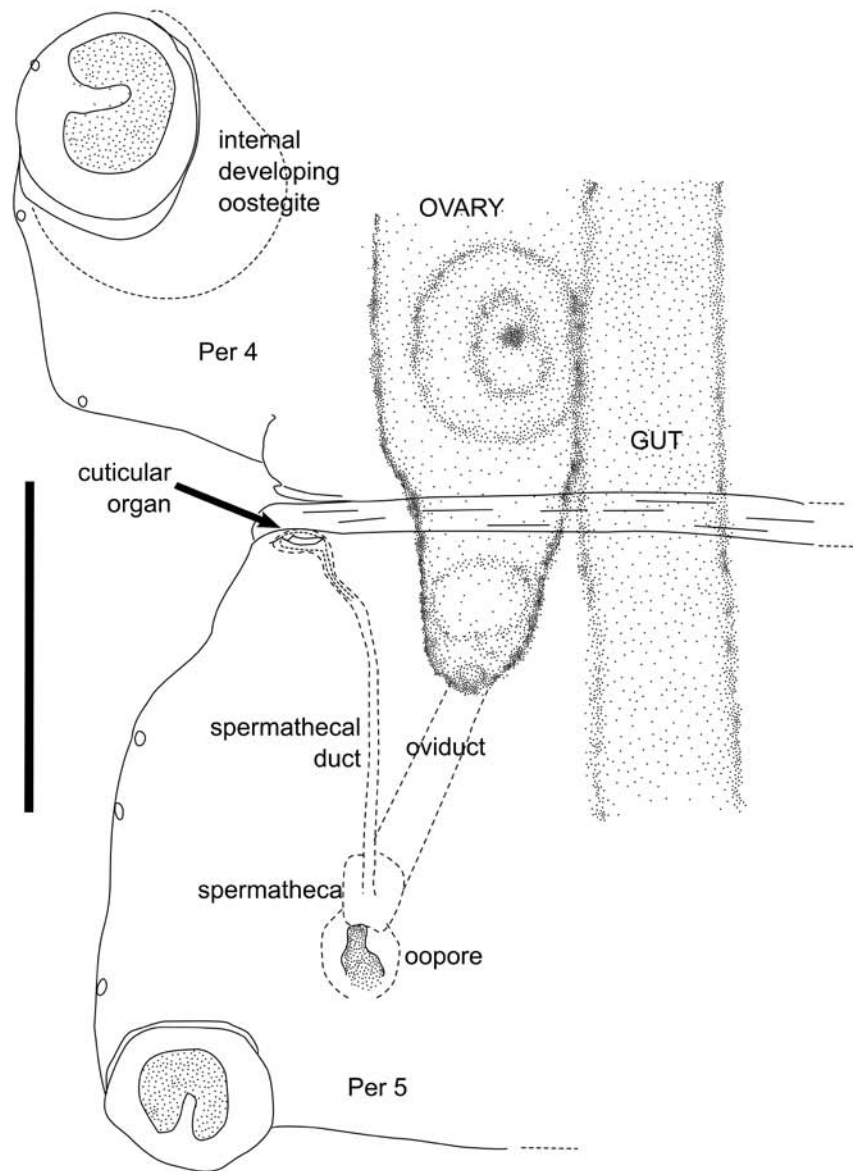


Figure 1. *Urstylis zapiola* gen. et sp. nov., adult female paratype USNM 1208014, ventral view of pereonites (Per) 4, 5, showing arrangement of reproductive organs, internal oostegite and gut; legs omitted for clarity. Scale bar = 0.1 mm.

Cephalothorax (Figs 2C, 6C) length 0.80 width, 0.18 body length; frons in dorsal view convex, smooth, frontal furrow present, convex anterior margin adjacent to clypeus, not projecting; antennal articulations anteriorly. Posterolateral margins angular, blunt (angle $> 90^\circ$). Posterolateral setae on cephalothorax and pereonites 1–7 asensillate, simple. **Pereonites 1–3** with row of setae on anterior tergite margin. Pereonite 1 length 0.2 width, 0.05 body length, anterior margin concave. Pereonite 2 length 0.36 width, 0.09 body length. Pereonite 3 length 0.35 width, 0.09 body length.

Pereonite 4 width 1.2, pereonite 5 width, length 0.42 width, 0.10 body length; lateral margins anteriorly and posteriorly convex with medial concavity. Posterolateral margins rounded. **Pereonites 5–7** length subequal, each 0.08–0.09 body length, narrowing from 5 to 7. Posterior margins setose; setae asensillate, simple, flexibly articulating, short. Posterolateral margins produced posteriorly, rounded. **Pereonite 5** length 0.42 width, 0.85 pereonite 4 length. Posterior margin with four setae. **Pereonite 6** length 0.49 width, 1.1 pereonite 5 length. Posterior margin with six setae. **Pereonite 7** length 0.51

width. Posterior margin with six setae.

Pleonite 1 length 0.25 pereonite 7 length, width 0.52 pereonite 7 width. **Pleotelson** length 0.22 body length, 1.5 width, width 0.95 pereonite 7 width; paired dorsal organ on the tergal surface in cuticular tubercles; apex length 0.13 pleotelson length, laterally with four simple setae. Pleopodal cavity width 0.79 pleotelson width.

Antennula (Fig. 3F) relative length ratios of articles 1.0, 0.70, 0.33, 0.33, 0.33, 0.33, L/W ratios of articles 1.5, 2.0, 1.0, 1.0, 2.0, 2.0. Article 1 with one simple seta. Article 2 with one simple seta. Article 4 with two simple setae. Article 6 with two aesthetascs, aesthetascs simple, tubular. **Antenna (Fig. 3F)** length 0.18 body length. Ischium angular with medial projection, about as long as coxa. Merus about as long as coxa, basis, and ischium together, articulating distolaterally on ischium, antennal proximodistal axis with distinctly sharp bend. Carpus longer than merus, articulating distolaterally on merus, antennal proximodistal axis with distinctly sharp bend between merus and carpus. Flagellum with eight articles and two to six short setae distally on each article.

Pereopod I (Fig. 4) length 0.26 body length; article L/W ratios 3.3, 1.3, 0.67, 1.2, 1.5, 1.0; relative article length ratios 1.0, 0.40, 0.20, 0.35, 0.30, 0.10. Ischium longer than wide, dorsal margin with two setae: one long, simple on dorsal lobe apex and one short, simple proximally. Merus dorsal margin with two long, simple setae, ventral margin with two setae: one simple, one robust, bifid. Carpus distodorsally with two long, simple setae, ventrally with three setae: one short, robust, bifid, one long, slender, one monoserrate, robust, bifid. Propodus dorsally with two simple setae: one long distally and one small, more proximally; ventrally with two setae: one simple, slender, one bifid, robust; with row of setules proximally to bifid seta. Dactylus distally with three sensillae, dorsal claw length 1.0

dactylus length, robust.

Pereopod II slightly longer than pereopod I. Ischium dorsally with one simple seta on dorsal lobe apex. Merus dorsally with two simple setae distally on apex, ventrally with one simple seta distally. Carpus with one distodorsal and two ventral simple setae. **Pereopod III (Fig. 4F)** length 0.34 body length; article L/W ratios 3.6, 2.2, 1.0, 3.0, 3.3, 2.5; relative article length ratios 1.0, 0.61, 0.28, 0.67, 0.56, 0.28. Ischium dorsal lobe flat and rounded; proximally and on apex without seta; distally with one simple seta. Merus dorsally on apex with one simple seta, ventrally with two simple setae. Carpus dorsally with four setae: one simple medially, one broom seta and two simple distally, ventrally with three simple setae. Dactylus distally with two sensillae.

Operculum (Fig. 5C) length 1.5 width, 0.82 pleotelson dorsal length. Apical width 0.82 operculum maximal width. Lateral fringe of setae absent. With 14 pappose setae on apex, completely covering anal opening. **Uropod** broken in female.

Female genital system

Female copulatory duct (cuticular organ) (Fig. 1). The opening for the spermathecal duct is located ventrally adjacent to the articular membrane at the anterior corner of pereonite 5. The spermathecal duct extends medially toward the posterior margin of the ovary and then has a sharp turn posteriorly. Rather than intersecting the oviduct midway, the duct ends in an indistinctly demarcated region just inside the oopore; the position of this structure is consistent with it being the spermatheca, although no sperm were observed in that region.

The duct was highly reflective in the preparatory female specimen studied (USNM 1208014), so it may have contained sperm from a prior mating encounter as insemination in janiroideans occurs well before the parturial moult (Veuille, 1980; Wilson,

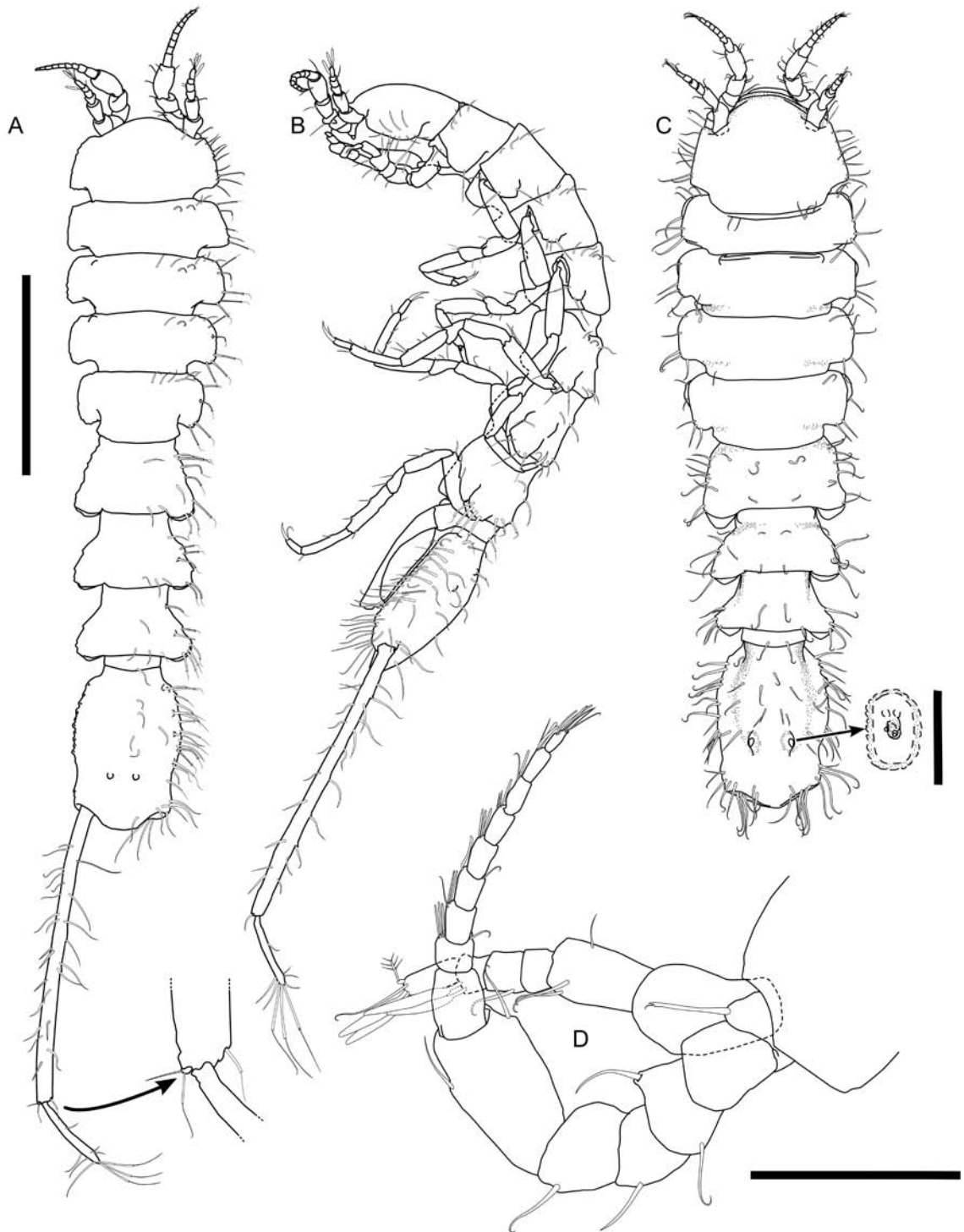


Figure 2. *Urstyliis zapiola* gen. et sp. nov. **A, B**, adult male holotype USNM 1208013. **C**, adult female paratype USNM 1208014. **D**, adult male paratype, AM P. 90631. **A**, dorsal habitus with enlargement of uropodal exopod. **B**, lateral habitus. **C**, dorsal habitus with enlargement of structure on pleotelson. **D**, antennula and antenna, *in situ*, lateral view. Scale bars = 0.5 mm, (A–C); 0.1 mm (D); 0.05 mm (C enlargement).

1987b, 1991). **The oopore** was medial and anterior to the coxa of pereopod V, and the oviduct continued in a dorsomedial direction to the ovary, which terminated just beyond the anterior margin of pereonite 5. **The ovae** were indistinct and did not fill the lumen of the ovary, indicating that the female

was not fully in reproductive condition. The female was at least in preparatory condition because developing oostegites were observed on pereonites 1–4 beneath the cuticle adjacent to the coxae (Fig. 1).

Description of adult male

Body (Figs 2, 6) length 2.0 mm, 4.5 width. **Cephalothorax (Fig. 6)** frontal ridge absent; length/width ratio subequal to female, length 0.83 width, 0.16 body length; without setae dorsally, posterolateral corners rounded, posterolateral setae present.

Pereonite 1 length 0.31 width, 0.06 body length.

Pereonite 2 length 0.37 width, 0.07 body length.

Pereonite 3 length 0.41 width, 0.08 body length.

Pereonite 4 width 1.1 pereonite 5 width, length 0.56 width. **Pereonites 5–7** similar in shape, size and setation, subequal in length to pereonite 4. Length 0.6 width.

Pleonite 1 length 0.23 pereonite 7 length, with two simple setae. **Pleotelson** in dorsal view similar to female. Length 1.4 width, 0.22 body length, width 0.95 pereonite 7 width. Posterior apex length 0.13 pleotelson length, pleopodal cavity width 0.81 pleotelson width.

Antennula (Figs 2D, 6C) length 0.48 head width, 0.50 antenna length, width 1.0 antenna width; article L/W ratios 1.8, 1.3, 0.5, 1.0, 0.5, 3.0; relative article length ratios 1.0, 0.57, 0.14, 0.29, 0.14, 0.43; of six articles; terminal and penultimate articles with two tubular aesthetascs, respectively.

Antenna (Fig. 2D) length 0.18 body length, basal articles slightly more stout than in female, flagellum of nine articles, precoxa–ischium squat, globular, coxa–ischium longer than precoxa; ischium distally with one simple seta. Merus longer than ischium, distally with one simple seta. Carpus slightly stouter than in female, with two subdistal setae.

Mandibles (Fig. 3) molar with two spines and two to three setulate spines; left mandible incisor process with five cusps, *lacinia mobilis* with four denticles; right mandible incisor process with four cusps, *lacinia mobilis* spine-like, with eight denticles. **Maxillula (Fig. 7B, C)** lateral lobe terminally with 11 robust and three slender setae.

Maxilla (Fig. 7D) lateral lobe length subsimilar to middle lobe length, with six setae terminally, four long, two shorter distomedially; middle lobe with five setae terminally, four long, one short distomedially; medial lobe terminally with seven setae, medially with a setal row.

Maxilliped (Figs 6C, 7E, F) basis length 3.9 width, with two coupling hooks; endite distally truncate, with three fan setae, eight slender setae, and one spine-like seta distomedially, lateral margin with row of setae; epipod length 2.8 width, 0.81 basis length. Palp article 1 shorter than article 3, distomedially with one seta, distolateral extension short, length 0.21 article 1 length, rounded; article 2 wider than articles 1 and 3, with two distomedial setae; article 3 with five medial setae; article 4 distomedial extension minute, with four setae; article 5 terminally with four setae.

Pereopods I–VII (Figs 4, 5) dactylus dorsal claw subequal to dactylus in length with one sensilla inserting terminally. **Pereopod I (Fig. 4A)** length 0.22 body length; article L/W ratios 3.0, 1.8, 0.80, 1.4, 1.7, 2.0; relative article length ratios 1.0, 0.5, 0.22, 0.39, 0.28, 0.11. Ischium dorsally with one simple seta. Merus setation as in female, dorsally with two long, bifid setae, ventrally with three setae: one thin, one robust, bifid distally and one small more laterally at mero-carpal articulation. Carpus with two distodorsal long setulate, bifid setae, ventrally with three setae: one thin, two robust, bifid. Propodus with one long distodorsal seta and two short, ventral setae.

Pereopod II (Fig. 4B) length 0.27 body length; article L/W ratios 3.4, 2.0, 1.0, 2.8, 4.0, 4.0; relative article length ratios 1.0, 0.59, 0.29, 0.65, 0.47, 0.24. Ischium dorsally with one simple seta on apex. Merus dorsally with two simple setae on apex, ventrodistally with one simple seta. Carpus dorsodistally with one small, simple seta, ventrally with two setae. **Pereopod III (Fig. 4D)** length 0.30

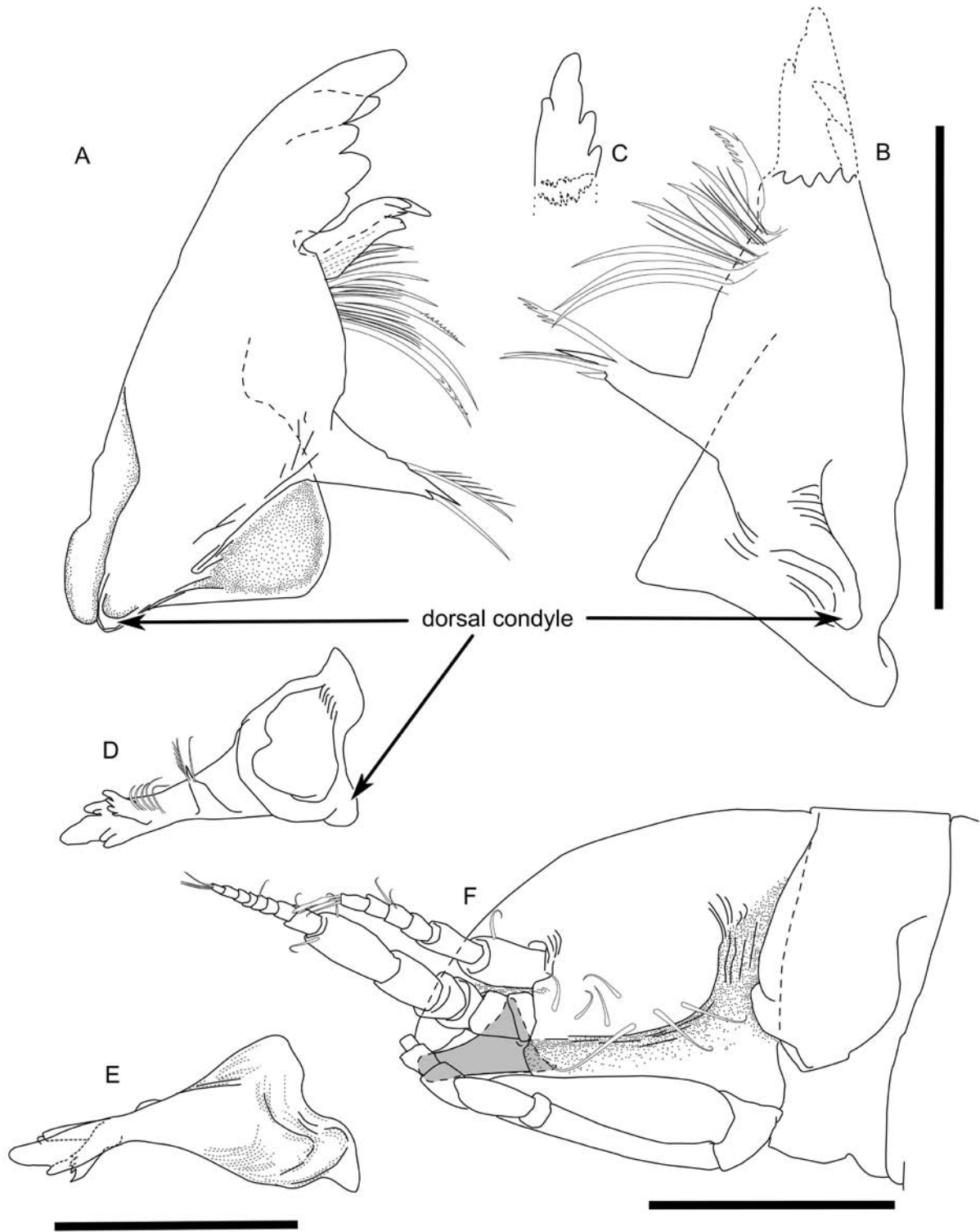


Figure 3. *Urstylis zapiola* gen. et sp. nov., mandibles. **A–E**, adult male paratype AM P. 90631, **F**, adult female paratype USNM 120801. **A**, left mandible, dorsal view. **B**, right mandible, dorsal view. **C**, right incisor process. **D**, **E**, left mandible, medial view and lateral view, respectively. **F**, head, left lateral view, showing antennula and antenna as well as position of mandible (darkened). Scale bars = 0.1 mm (A–C); 0.1 mm (D, E); 0.2 mm (F).

body length; article L/W ratios 3.6, 2.5, 0.80, 3.0, 3.3, 2.5; relative article length ratios 1.0, 0.56, 0.22, 0.67, 0.56, 0.28. Setation as in female. **Pereopod IV (Fig. 4E)** length 0.3 body length; article L/W ratios 3.4, 2.8, 1.0, 3.3, 3.3, 2.5; relative article

length ratios 1.0, 0.65, 0.29, 0.76, 0.59, 0.29.

Pereopods V–VII (Fig. 8) similar to pereopods II–IV in size, carpi and propodi slightly more elongate; setation similar: ischium dorsally without seta; midventrally with two simple setae. Merus

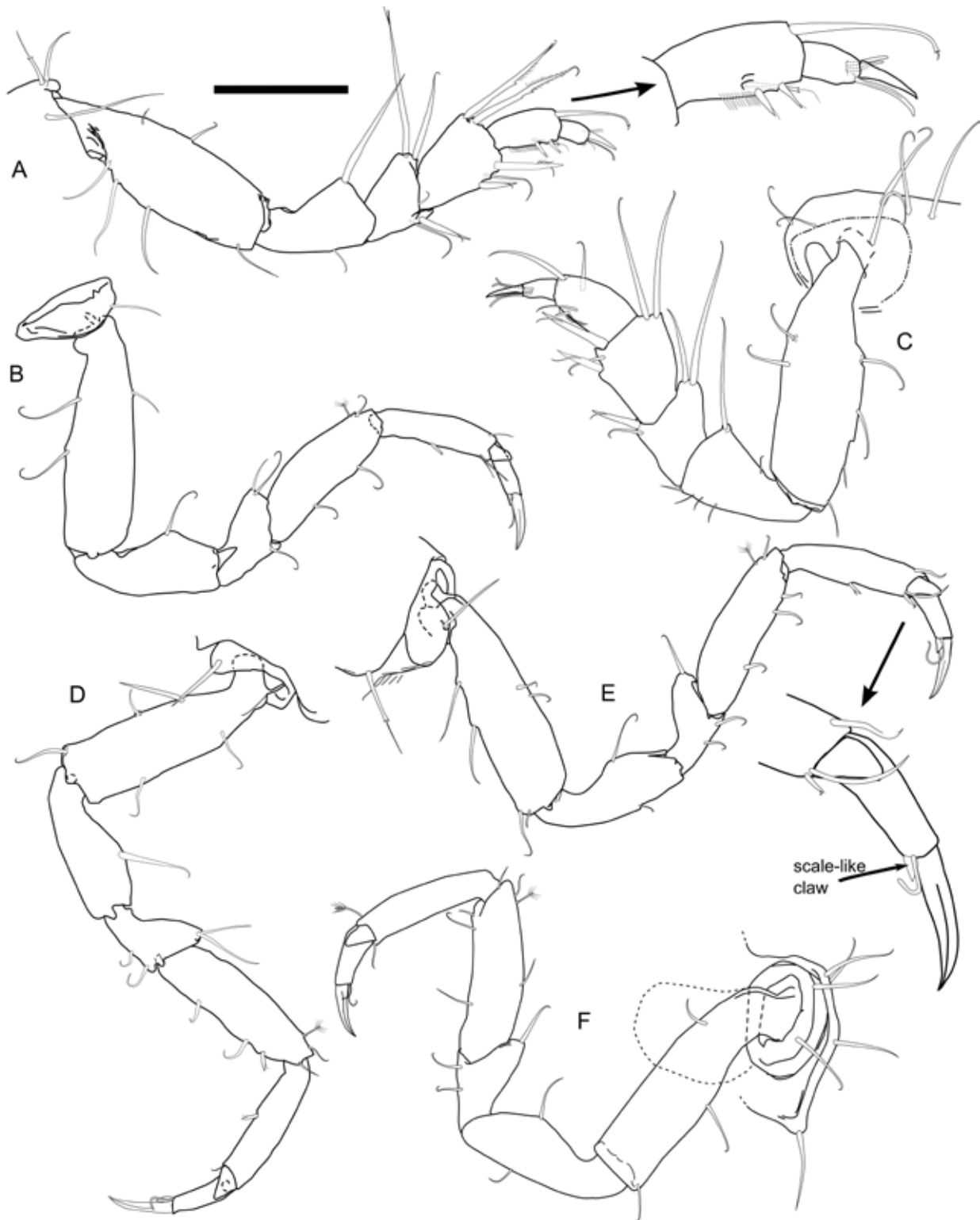


Figure 4. *Urstylis zapiola* gen. et sp. nov., anterior pereopods. **A, B, D, E**, adult male paratype AM P. 90631. **C, F**, adult female paratype USNM 120801. **A, C**, pereopod I. **B, D, E**, pereopods II–IV; **E**, pereopod IV with enlargement of dactylus and claws (arrow). **F**, pereopod III. Scale bar = 0.1 mm.

distodorsally with two setae: one minute, one long, prominent; midventrally and distoventrally with one simple seta; distodorsally with one bifid seta; midventrally with two robust, bifid setae; distoventrally with one robust, bifid seta.

Pereopod V (Fig. 8A) 0.31 body length; article L/W ratios 3.0, 2.75, 1.25, 3.25, 6.5, 2.5; relative article length ratios 1.0, 0.73, 0.33, 0.87, 0.87, 0.33. **Pereopod VI (Fig. 8B)** length 0.34 body length; article L/W ratios 3.4, 3.0, 1.5, 3.5, 4.3, 2.0;

relative article length ratios 1.0, 0.71, 0.35, 0.82, 0.76, 0.24. **Pereopod VII (Fig. 8C)** length 0.31 body length, slightly smaller pereopod VI length; article L/W ratios 3.5, 2.5, 2.0, 4.7, 6.5, 2.0 relative article length ratios 1.0, 0.71, 0.43, 1.0, 0.93, 0.29.

Pleopod I (Figs 5B, 9A, B) length 0.73 pleotelson length, 2.5 width, distal width 1.3 proximal width. Distomedial lobes with ten long, simple setae altogether; distoventrally with minute, simple setae present, in semicircular arrangement on both sides. **Pleopod II (Fig. 9C)** protopod apex tapering, with rounded tip, distolateral margin with ten thin setae. Endopod distance of insertion from protopod distal margin 0.36 protopod length. Stylet sinuous, narrowing distally to sperm-duct opening, extending beyond distal margin of protopod, length 0.95 protopod length; sperm-duct opening located 0.17 stylet length from stylet proximal margin. Exopod length 0.32 protopod length, with rows of fine and minute setae laterodistally. **Pleopod III (Fig. 9D)** length 2.1 width, protopod length 1.7 width, 0.53 pleopod III length; endopod plumose terminal setae longer than endopod, medial seta longest, 0.80 pleopod III length. Exopod length 0.84 pleopod III length, proximal article broadened distally, width 0.85 endopod width; distal article length 0.30 proximal article length, width 0.30 proximal article width, subterminally with one seta; lateral fine setae about as long as exopod width. **Pleopod IV (Fig. 9E)** length 1.9 width, endopod length 1.8 width, about twice as long as protopod. Exopod length 3.3 width, 1.1 endopod length; terminal plumose seta length 0.88 exopod length. **Pleopod V (Fig. 9F)** length 2.4 width. **Uropod (Fig. 2A, B)** length 2.4 pleotelson length; protopod length 17.6 width; with numerous scattered simple setae. Endopod inserting terminally, length 0.28 protopod length, 8.6 width, width narrower than protopod. Exopod minute, length about 0.05 endopod length, globular, with two setae.

Remarks

Urstylis zapiola was collected in a particularly large epibenthic sample (WHOI 247) from the abyssal plain of the Argentine Basin: 1316 individuals and 72 species of isopods. This locality is below 5200 m, showing that isopod species richness can be high, even at the greatest abyssal depths, contra the source-sink theory of Rex *et al.* (2005) that abyssal diversity should be a subset of and therefore smaller than bathyal diversity. For a detailed taxa list see also Supporting Information Appendix S2.

Urstylis solicopia sp. et gen. nov.

Figures 11–21

Zoobank registration

urn:lsid:zoobank.org:act:8BCACEA0-2180-4CB8-ACF5-0F36DE73A3B8

Etymology

The species name refers to the type locality in the Pacific Ocean (Clarion-Clipperton Fracture Zone; CCFZ) being rich in manganese nodules (Fig. 10). The epithet *solicopia* is derived from the Latin words *solis*, singular genitive of *solum* earth, bottom, and *copia* meaning plentiful translating into *of plentiful bottom*. It is a feminine adjective.

Type fixation

Ovigerous female holotype, 2.0 mm, ZMH K-43070, designated here.

Type material examined

ZMH K-43070: ovigerous female holotype, 2.0 mm, station (st.) 8717. ZMH K-43052: non-ovigerous female paratype, 2.0 mm, st. 8581, greatly damaged; ZMH K-43053: one non-ovigerous female anterior fragment, sputter-coated for SEM,

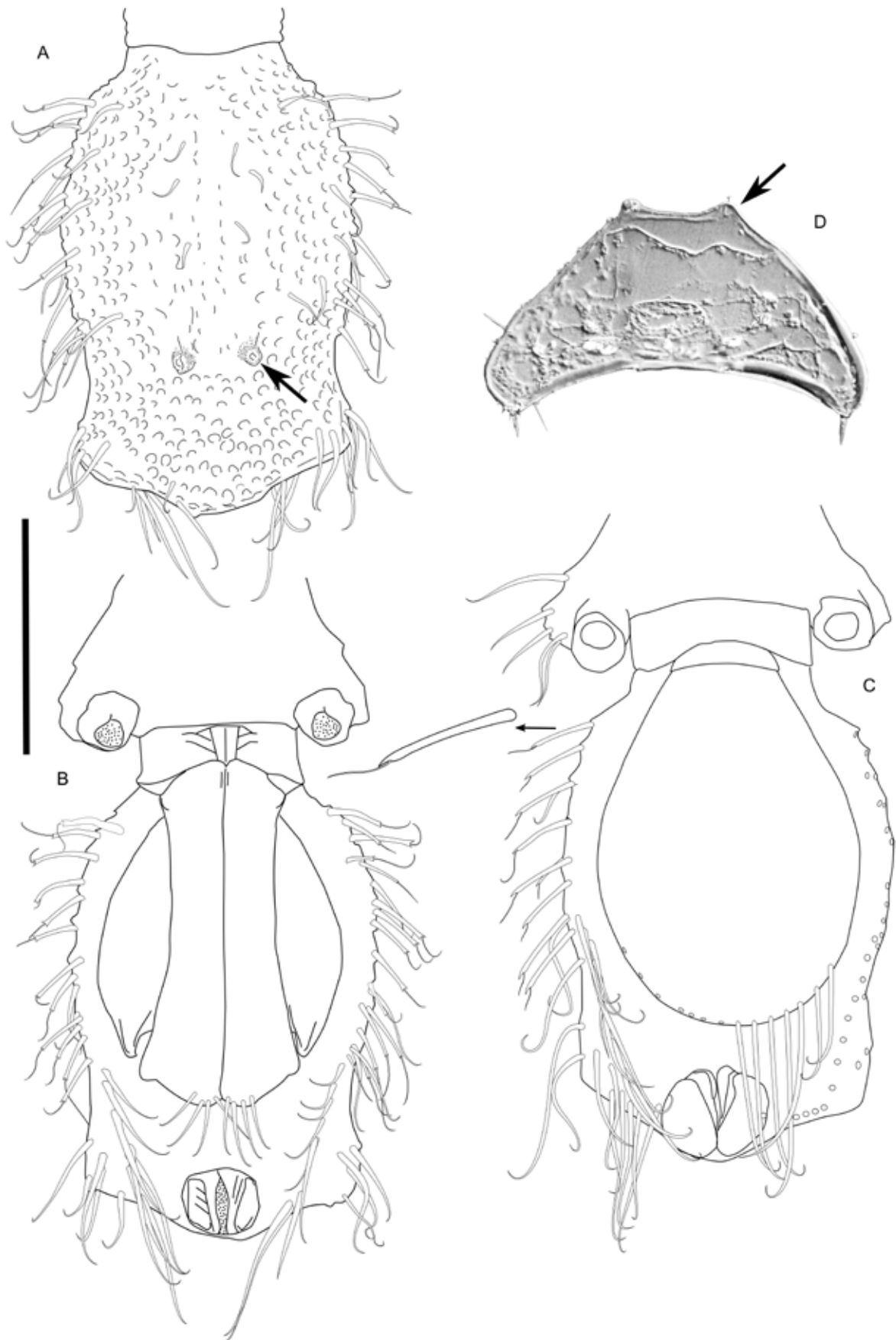


Figure 5. *Urstylis zapiola* gen. et sp. nov., pleotelson. **A, B**, adult male paratype AM P. 90631, dorsal and ventral views, respectively. **C**, adult female paratype USNM 120801, pleotelson ventral view. **D**, section through transversal plane of the pleotelson at the location of the paired dorsal cuticular tubercles (arrow). Scale bar = 0.2 mm.

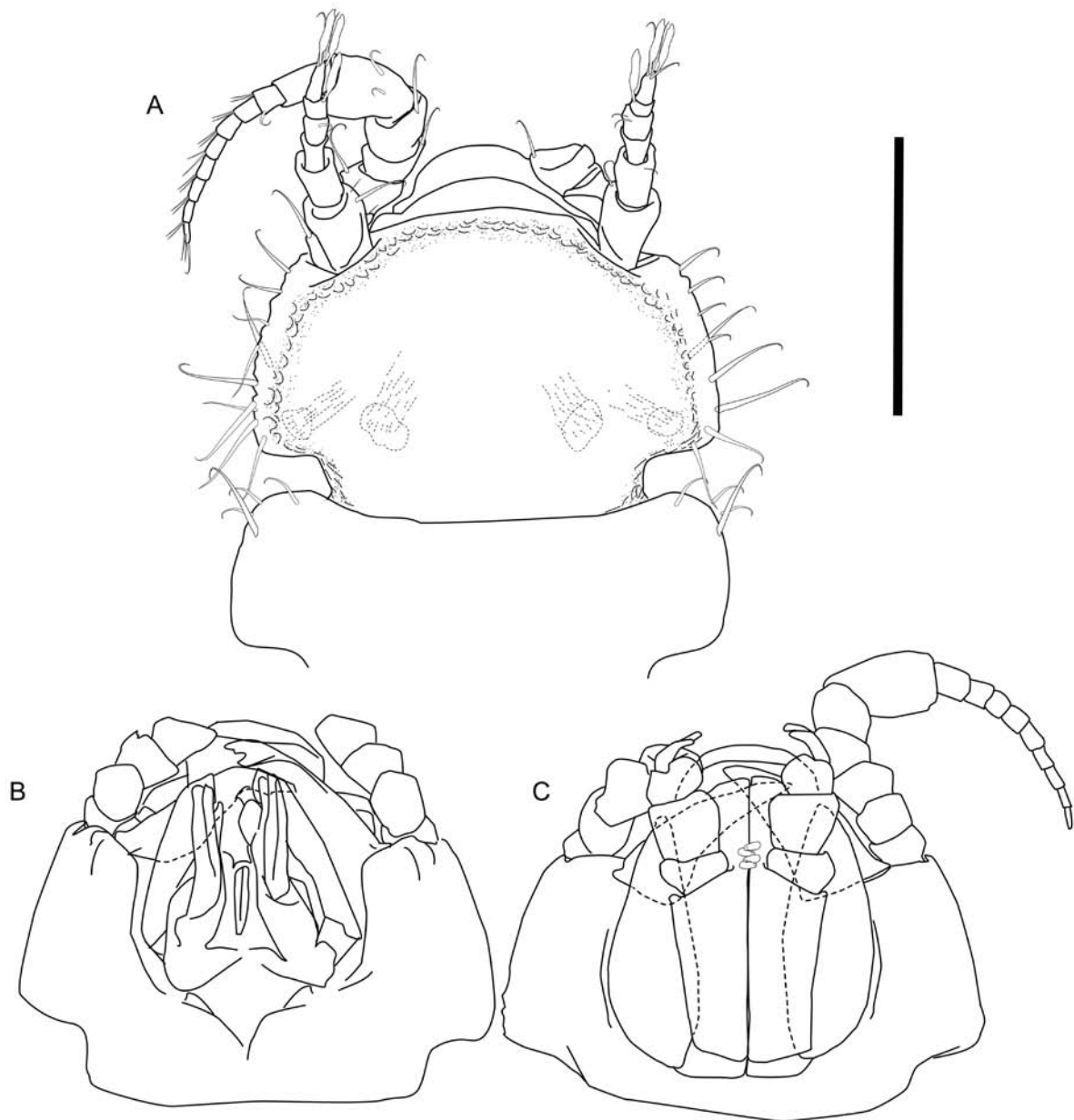


Figure 6. *Urstylis zapiola* gen. et sp. nov., views of head. A–C, adult male paratype, AM P. 90631. A, dorsal view, dotted structures showing internal attachment of mandibular muscles. B, C, ventral view, without and with maxilliped, respectively. Scale bar = 0.2 mm.

st. 8687; ZMH K-43054: juvenile female paratype, 1.7 mm, st. 8698; ZMH K-43055: adult male paratype, 2.1 mm, st. 8581, dissected for illustrations; MIMB 28178: adult male paratype, 1.7 mm, st. 8719; ZMH K-43057: juvenile female paratype, 1.2 mm, st. 8670; ZMH K-43058, juvenile female paratype, 1.6 mm, st. 8571; ZMH K-43059: non-ovigerous female paratype, 2.0 mm, st. 8615, greatly damaged; ZMH K-43060: juvenile male paratype, 1.1 mm and juvenile female paratype, 1.2 mm; st. 8660; MIMB 28178: one juvenile female, 1.6 mm,

and two mancae paratypes, 1.1 mm, st. 8717; ZMH K-43062: juvenile female paratype, 1.5 mm, st. 8721; ZMH K-43069: ovigerous female paratype, 2.0 mm, st. 213.

Type locality

Collected with box corer from the Russian claim in the Clarion-Clipperton Fracture Zone manganese nodule area during several expeditions by the Russian Scientific Centre ‘Yuzhmorgeologia’ (Federal State Unitary Geological Enterprise,

Southern Scientific and Production Association for Marine Geological Operations), Gelendzhik (Table 1). The locality is characterized by soft sediment with manganese nodules of varying size and density (Fig. 10).

Type material – remarks

The holotype ovigerous female and several paratypes show some shrinking artefacts possibly caused by treatment with ethanol and low degree of calcification. These caused the depressions shown in the habitus illustrations of the female. The natural condition is shown in the SEM figures. Uropods are broken and missing in the complete type series except in one manca, which is extremely damaged and therefore not illustrated.

Further records

GDFW collection: USA National Oceanic and Atmospheric Administration (NOAA) Deep Ocean Mining Study (DOMES), 0.25 m² box corer samples: DJ08, manca, DJ08 24.xi.1977 9°25.23'N, 151°4.46'W, 5205 m; DJ32, manca, 30.xi.1977, 9°16.00'N, 151°56.10'W, 5043 m; DJ39, manca, 03.xii.1977, 9°35.80'N, 151°6.80'W, 5117 m; GDFW collection, DJ46, brooding female, five mancae, 19.v.1978, 9°28.00'N, 151°27.60'W, 5216 m; DJ49, manca, 20.v.1978, 9°23.40'N, 151°25.30'W, 5171 m; DJ73, manca, 27.v.1978, 9°28.10'N, 151°15.60'W, 5107 m.

Diagnosis

Body dorsoventrally flattened, tergite surfaces rather hirsute; pereonite 4 width subequal to pereonite 5 width, pereonite 6 shorter pereonite 5; pereonite 7 posterolateral margins projecting posteriorly. Pleotelson length/width ratio 1.3, paired dorsal organ expressed as pedestal broom setae articulating on flat conical elevations. Pereopod I ischium dorsal lobe with two setae; pereopods'

V–VII ischium and carpus mid-dorsally with seta present.

Description of female

Body (Figs 11A, B, 12A, C, E) length 2.0 mm, 3.4 width, dorsoventrally slightly flattened, tergite surfaces hirsute, with long setae on pedestal (calcified) articulations along lateral and anterior tergite margins. **Ventral spines** on pereonites 1–7 absent. **Imbricate ornamentation** on cephalothorax–pleotelson covering whole tergite. **Cephalothorax–pereonite VII** posterolateral setae simple, asensillate.

Cephalothorax (Figs 11A, B, 12A–E) length 0.61 width, 0.13 body length; frons in dorsal view convex, smooth, frontal ridge present, slightly convex; dorsal surface with array of setae. Posterolateral margins angular, blunt; posterolateral setae asensillate, simple, flexibly articulated on calcified pedestal articulations. **Pereonite 1** length 0.24–0.29 width, 0.07 body length, anterior margin straight. **Pereonite 2** length 0.28–0.32 width, 0.08–0.09 body length. **Pereonite 3** length 0.32–0.37 width, 0.09–0.10 body length. **Pereonite 4** width 1.1 pereonite 5 width, length 0.37–0.38 width; lateral margins in dorsal view convex, almost parallel; posterolateral margins rounded.

Pereonites 5–7 (Fig. 11A, B) of similar shape, diminishing in length and width from 5 to 7. Posterior tergite margins with four simple, asensillate, flexibly articulating setae; setae long, extending beyond posterolateral margin. Posterolateral margins rounded. Coxae setose, setae simple, asensillate, on pedestals. **Pereonite 5** length 0.45 width, 1.1 pereonite 4 length. **Pereonite 6** length 0.44 width, 0.91 pereonite 5 length. **Pereonite 7** length 0.43–0.75 width. Pleonite 1 length 0.32 pereonite 7 length, dorsally with two setae.

Pleotelson length 0.22–0.24 body length, 1.25–1.32 width, slightly wider than or as wide

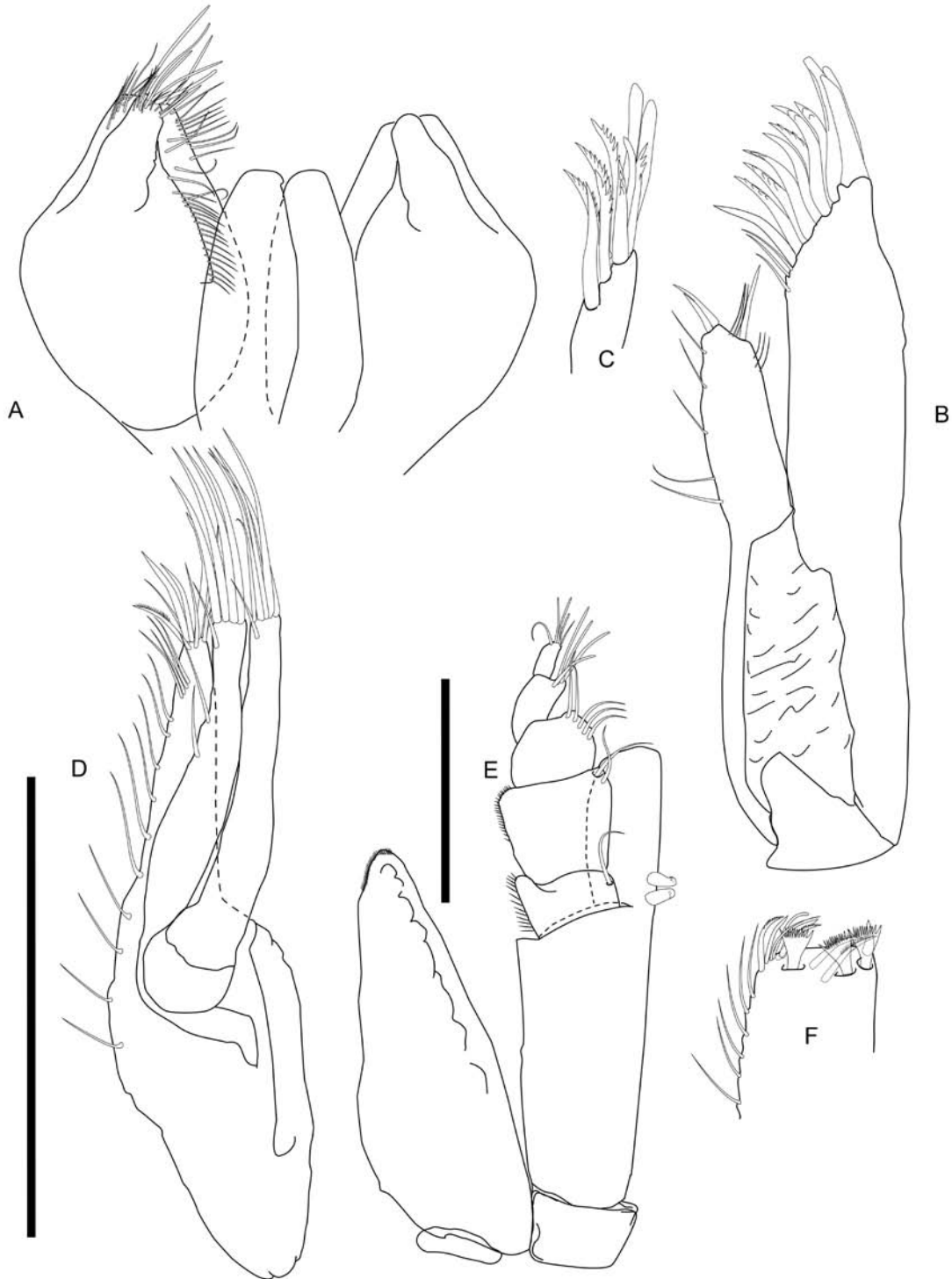


Figure 7. *Urstylis zapiola* gen. et sp. nov., mouthparts in ventral view. A–F, adult male paratype AM P. 90631. A, paragnaths. B, maxillula. C, maxillula lateral lobe, medial view. D, maxilla. E, maxilliped. F, maxilliped endite, distal margin, enlargement of E. Scale bars = 0.1 mm (A–D); 0.1 mm (E).

as pereonite 7; paired dorsal organ expressed as pedestal broom setae. Posterior margin straight or slightly concave laterally at uropod insertions, apex convex, length 0.13–0.18 pleotelson length, posterolaterally with four simple setae. Pleopodal cavity width 0.80 pleotelson width.

Antennula (Fig. 11C) length 0.45 head width, 0.54 antenna length; width 0.90 antenna width. Article 1 without setae. Article 2 with six simple setae. Article 3 length subequal width, with one simple seta. Article 4 length subequal width, with two simple setae. Article 5 distinctly

longer than wide, cylindrical. Article 6 with two aesthetascs. **Antenna (Fig. 11C)** length 0.18 body length; relative length ratios of articles 1.0, 1.3, 1.3, 1.3, 2.0, 2.3, L/W ratios of articles 0.75, 1.0, 0.80, 1.0, 2.5, 2.3. Basis angular with dorsolateral projection; longer than coxa. Ischium angular with medial projection, longer than coxa. Merus shorter than articles 1–3 together, distally with one simple seta. Merus articulating distolaterally on ischium, antennal proximodistal axis with distinctly sharp bend. Carpus longer than merus, distally with seven simple setae. Flagellum with nine articles. **Mouthparts** as in male.

Pereopod I–VII (Figs 13–15) dactyli with two claws and two sensillae inserting terminally and two sensillae subdistally, pereopod I dorsal claw subequal to dactylus in length, ventral claw length 0.5 dorsal claw length, pereopods' II–VII dorsal claw length about 0.6 dactylus length, ventral claw scale-like, tiny, length 0.23–0.25 dorsal claw length. **Pereopod I (Figs 13A, 14A–E)** length 0.24 body length; article L/W ratios 2.9, 1.5, 0.67, 1.3, 2.0, 2.0; relative article length ratios 1.0, 0.45, 0.20, 0.40, 0.30, 0.10. Ischium dorsal margin with two simple setae, dorsal lobe projecting near basal width of article. Merus dorsal margin with two simple setae, one long, one short, ventral margin with two setae, one small, simple, one long, bifid, monoserrate. Carpus dorsally with two simple setae. Articular plate on propodus absent; dactylus distally with two sensillae, dactylus dorsal claw length 1.0 dactylus length. **Pereopod II (Figs 13B, 14G)** length 0.30 body length; article L/W ratios 3.5, 1.0, 2.0, 2.5, 3.3, 2.5; relative article length ratios 1.0, 0.48, 0.24, 0.48, 0.48, 0.24. Ischium dorsally with two simple setae, one long medially, one short distally, with dorsal setae on dorsal margin. Merus dorsally with two simple setae, one long, one short and slender, with dorsal setae on dorsal margin, ventrally with two simple

setae: one short medially, one long distally. Carpus distodorsally with one simple seta, ventrally with three bifid setae.

Pereopod III (Fig. 13C) length 0.31 body length; article L/W ratios 3.5, 2.2, 1.0, 2.8, 3.7, 2.0: relative article length ratios 1.0, 0.52, 0.24, 0.52, 0.52, 0.19. Ischium with one simple, not prominent seta on apex. Merus dorsally with two long, simple setae, ventrally with two short, simple setae. Carpus distodorsally with one broom seta and one short simple seta; ventrally with three setae: one bifid medially, one simple and one bifid subdistally. **Pereopod IV** length 0.31 body length, about as long as neighbouring pereopods; article L/W ratios 3.0, 2.2, 1.0, 3.3, 3.7, 2.0; relative article length ratios 1.0, 0.61, 0.28, 0.72, 0.61, 0.22.

Pereopods V–VII (Fig. 15) similar in setation. Ischium mid-dorsally with one simple seta, distodorsally with setae absent, midventrally with two simple setae. Merus distodorsally with two setae, one simple, slender, one bifid, midventrally with one simple, small seta, distoventrally with two setae, one simple, long, one simple, small. Carpus mid-dorsally and distodorsally with one bifid seta respectively, distoventrally with three bifid setae. **Pereopod V** length 0.33 body length; article L/W ratios 3.4, 2.2, 1.8, 3.3, 6.5, 2.5; relative article length ratios 1.0, 0.65, 0.41, 0.76, 0.76, 0.29. **Pereopod VI** length 0.35 body length; article L/W ratios 4.3, 2.8, 2.0, 5.0, 7.5, 2.5; relative article length ratios 1.0, 0.65, 0.47, 0.88, 0.88, 0.29. **Pereopod VII** length 0.37 body length; relative article length ratios 1.0, 0.61, 0.50, 0.83, 0.89, 0.28; article L/W ratios 3.6, 2.8, 2.3, 5.0, 8.0, 2.5.

Operculum (Fig. 11D, E) ovoid, length 1.1 width, 0.69 pleotelson dorsal length; apical width 0.82 operculum maximal width. Lateral fringe consisting of ten to eleven setae, with fluent transition to row of 17 asetulate apical setae. Apical setae completely covering anal opening. **Uropod** (meas-

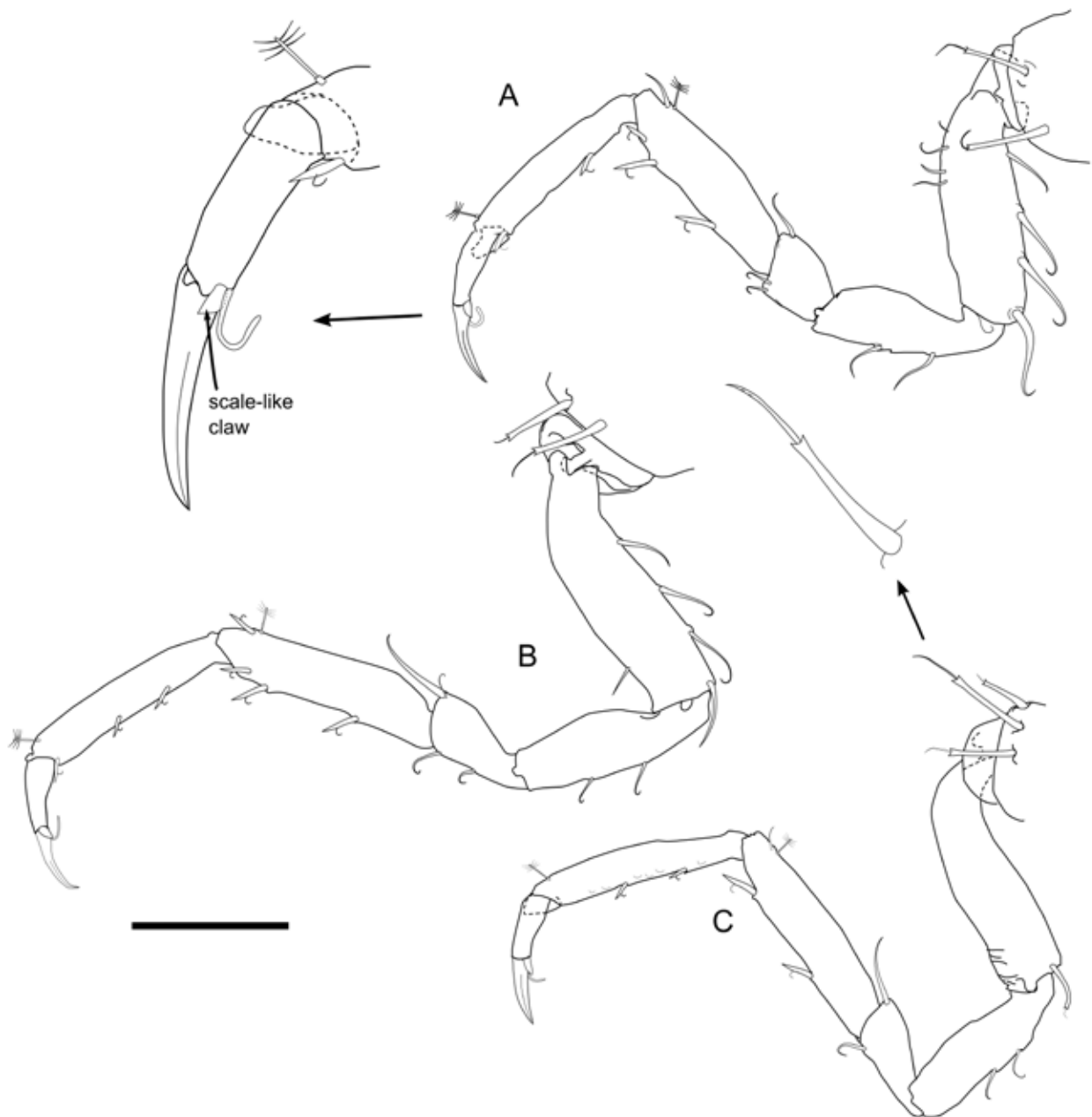


Figure 8. *Urstylis zapiola* gen. et sp. nov., posterior pereopods. A–C, adult male paratype AM P. 90631, pereopods V–VII. Scale bar = 0.1 mm.

ured from other material) length 2.8 pleotelson length; protopod length 23.3 width, 2.1 pleotelson length, protopod distal margin blunt, endopod insertion terminal; endopod length 12.1 width, 0.37 protopod length, endopod width; exopod length 0.05 endopod length.

Description of adult male

Body (Fig. 16A, C) length 2.1 mm, 4.0 width.

Cephalothorax frontal ridge present, slightly convex; length/width ratio larger than in female,

length 0.74 width, 0.15 body length; with conspicuous dorsal array of setae: four simple setae in a quadrate arrangement, posterolateral setae absent, posterior margins setulose. **Pereonite 1** length 0.20 width, 0.05 body length. **Pereonite 2** length 0.36 width, 0.09 body length. **Pereonite 3** length 0.34 width, 0.09 body length. **Pereonite 4** posterolateral margins not produced posteriorly.

Pleotelson (Fig. 16A, C, D) in dorsal view similar to female, constricted anteriorly to uropod articulation, width maximum anterior to waist,

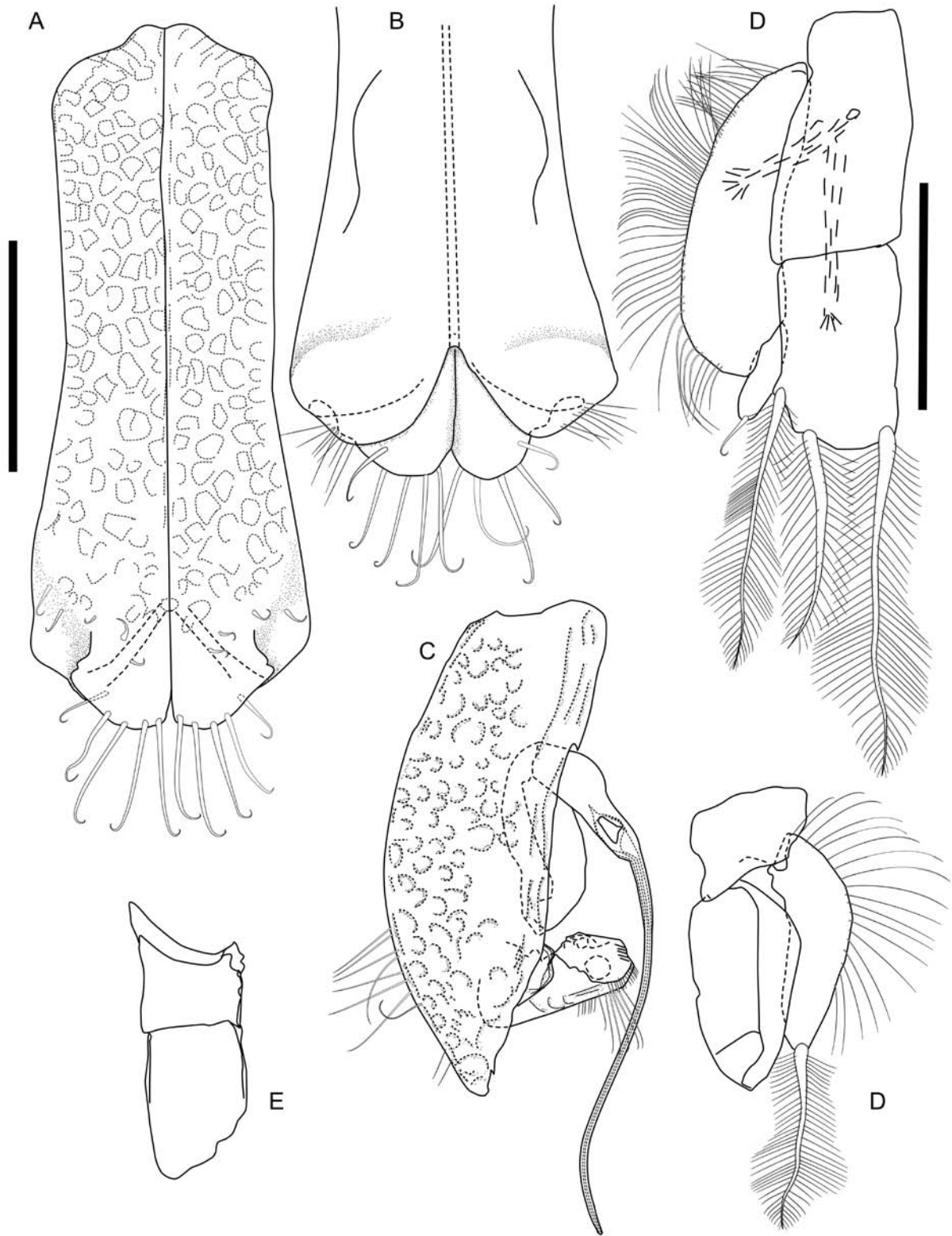


Figure 9. *Urstylis zapiola* gen. et sp. nov., pleopods, adult male paratype AM P. 90631. A, B, pleopod I, ventral and dorsal view, respectively. C–E, pleopods II–V, ventral view. Scale bar = 0.1 mm (A, C–F).

setal ridges not visible in dorsal view; length/width ratio in male subequal to female, 0.23 body length, width subequal peronite 7 width, tergite with several projecting and calcified pedestals with

setal articulations. Posterior apex length 0.14 pleotelson length, pleopodal cavity width 0.87 pleotelson width.

Antennula (Fig. 16B) length 0.81 head

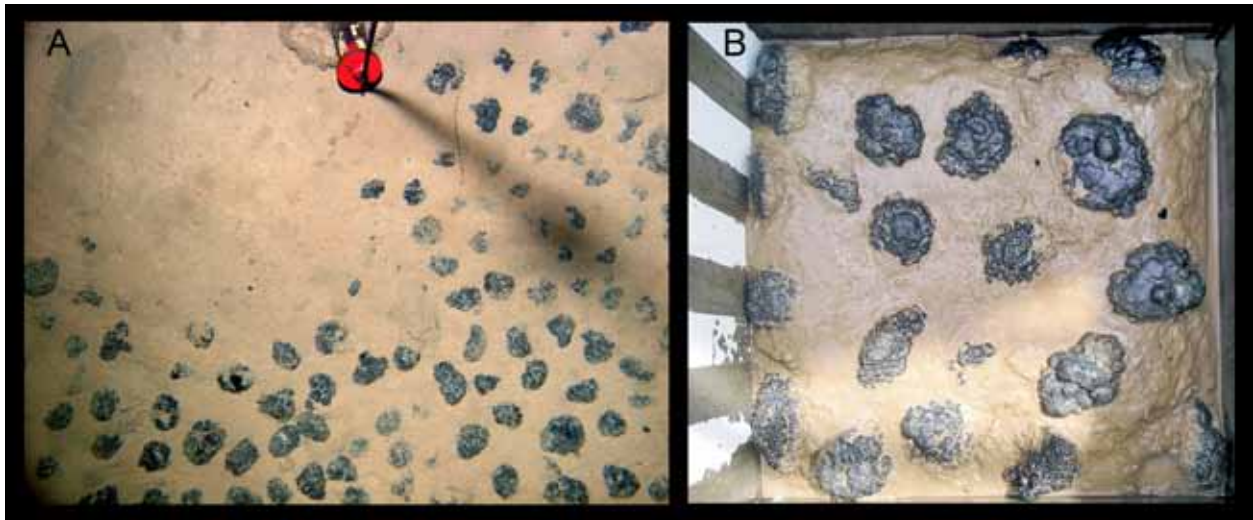


Figure 10. Bottom characteristics in the Russian claim in the Clarion-Clipperton Fracture Zone manganese-nodule area at the type locality of *Urstylis solicipia* gen. et sp. nov. Station 90, R/V Yuzhmorgeologia cruise 4–06; 13°13.11780'N, 134°29.49900'W; 4804 m. A, photograph taken by autonomous camera mounted on giant box corer before impact. B, box core sample, size of sample 0.25 m², scale: one interval on left inner wall of the box = 5 cm. Courtesy of Slava Melnik, State Scientific Center Yuhzmorgeologia.

width, 0.57 antenna length, width 0.88 antenna width; article L/W ratios 1.7, 2.0, 1.0, 1.0, 1.0, 2.0; relative article length ratios 1.0, 0.83, 0.25, 0.25, 0.25, 0.30; terminal and penultimate articles with two aesthetascs respectively. Article 1 with two simple setae and one broom seta. Article 2 with five setae: two simple, three broom. Article 3 with one simple seta and one broom seta. Article 4–5 both with one simple seta. Article 6 elongate, distinctly longer than article 5. **Antenna (Fig. 16B)** length 0.29 body length, flagellum of six to nine articles, article length–width ratios subsimilar in males and females. Merus distally with four simple setae and one broom seta. Carpus distally with ten setae: five simple, five broom.

Mandible (Fig. 17) molar process apex with two spines and three setulate setae; left mandible incisor process with five cusps, *lacinia mobilis* with four denticles; right mandible incisor process with four cusps, *lacinia mobilis* with six denticles. **Maxillula (Fig. 18A)** lateral lobe terminally with 11 robust and three slender setae. **Maxilla (Fig. 18B)** lateral lobe with five setae terminally: one robust, serrate, two simple, two slender, simple;

middle lobe with five setae terminally: three robust, serrate, two slender, simple; medial lobe terminally with six setae: two short, robust, laterally, two long, robust, two slender, simple.

Maxilliped (Fig. 18C, D) basis length 3.9 width; endite distally with two fan setae; with two coupling hooks; palp articles 1 and 2 subsimilar in width, article 1 distomedially with one seta, distolateral lobe length 0.35 article 1 length, article 2 wider than article 3, article 1 shorter than article 3, article 4 distomedial extension with three setae, article 5 with five distal setae; epipod length 2.6 width, 0.85 basis length, distolaterally fringed with setulae.

Pereopods I–VI (Figs 19, 20) similar to those in female in size, proportions and setation. **Pereopod VII** length 0.42 body length, shorter than pereopod VI; relative article length ratios 1.0, 0.74, 0.58, 1.1, 1.1, 0.26. Article L/W ratios: 3.8, 2.8, 2.8, 6.7, 6.7, 2.5. **Pleopod I (Figs 16D, 21A)** length 0.84 pleotelson length, distal width 1.6 proximal width, distomedial lobes rounded, distally with six to eight long setae, distolateral lobes with five to seven small setae, ventral surface subdis-

Table 1. *Urstylis solycopia* gen. et sp. nov. type locality. Details of sampling locations and dates.

R/V name	Project #	Station #	Lat.	Long.	Depth [m]	Date
Yuzhmorgeologia	4-06	90	13° 13.11780' N	134° 29.49900' W	4804	15.08.2006
Yuzhmorgeologia	18-01	213	13° 53.24598' N	129° 06.48198' W	4750	27.07.2003
Gelendzhik	4-08	8571	12° 59.67060' N	133° 46.29540' W	4790	22.07.2009
Gelendzhik	4-08	8581	13° 04.77720' N	133° 57.27540' W	4840	24.07.2009
Gelendzhik	4-08	8615	13° 22.21440' N	133° 55.15320' W	4905	28.07.2009
Gelendzhik	4-09	8660	12° 50.52120' N	133° 23.60700' W	4824	19.12.2010
Gelendzhik	4-09	8670	12° 55.36980' N	133° 37.71120' W	5031	24.12.2010
Gelendzhik	4-09	8687	13° 09.42720' N	133° 21.59220' W	4882	06.01.2011
Gelendzhik	4-09	8698	13° 16.17480' N	133° 25.06380' W	4947	05.01.2011
Gelendzhik	4-09	8717	13° 28.17420' N	133° 30.07080' W	4889	02.01.2011
Gelendzhik	4-09	8719	13° 29.02080' N	133° 32.77380' W	4860	30.12.2010
Gelendzhik	4-09	8721	13° 30.13380' N	133° 30.50220' W	4859	30.12.2010

R/V, Research Vessel.

tally with five short setae on each side. **Pleopod II** (**Fig. 21B**) protopod with fringe of > 32 thin setae on distolateral margin; apex projected, narrowly rounded. Endopod distance of insertion from protopod distal margin 0.35 protopod length. Stylet sublinear, extending beyond distal margin of protopod, length 0.88 protopod length.

Pleopod III (**Fig. 21C**) length 1.8 width, protopod length 2.0 width, 0.56 pleopod III length, endopod terminal plumose setae longer than endopod. Exopod length 0.84 pleopod III length, proximal article as wide as endopod, with fringe of fine setae; seta length subsimilar to pleopod III exopod width; distal article length 0.36 proximal article length, width 0.47 proximal article width, conspicuous subterminal seta present. **Pleopod IV** (**Fig. 21D**) length 2.0 width, endopod length 1.7 width, exopod length 4.7 width, exopod length 0.78 endopod length, lateral fringe of setae present. **Pleopod V** (**Fig. 21E**) length 2.4 width.

Remarks

Urstylis solycopia gen. et sp. nov. is the most setose species currently known for this genus. The anterior tergites bear rows of setae along their anterior margin as well as medially across the segments. The

posterior tergites have medial and posterior rows of simple setae. Another distinguishing feature is that all pereonal and pleonal tergites of *U. solycopia* are covered with imbricate ornamentation and to a lesser degree the sternites, too. Dorsally on the pleotelson, a pair of broom setae on flat, cone-shaped elevations is located in approximately the same position as the tubercles in *U. zapiola* or the statocysts in *Macrostylis*.

The operculum of this species has a lower length–width ratio than in *U. zapiola*. The 0.25 m² box corer samples from the USA National Oceanic and Atmospheric Administration (NOAA) Deep Ocean Mining Study (DOMES) collected by GDFW and colleagues in 1977–1978 provide data on the population of this species at DOMES site A. The species appeared in six out of 55 samples with a total of 11 individuals. As the samples were open box corers with no partitions, the total area sampled is 13.75 m², which gives a population density of this species of 0.8 individuals per square meter, based on random expectations. As most species do not occur randomly but show patchy (underdispersed) distributions (Kaiser and Barnes, 2008), the effective density can be expected to be much higher. Despite the large number of samples coll-

ected at DOMES site A, no males were found, suggesting that, as observed in haploniscids (Brökeland, 2010), macrostylids (Riehl and Kaiser, 2012), and tanaids, the males occur at a lower density than females or juveniles. The expectation that juveniles should be the most frequent size class is borne out by these samples.

Urstylis thiotyntlus gen. et sp. nov.

Figures 22–25

Zoobank registration

urn:lsid:zoobank.org:act:E3150B05-CAC6-4C03-B0AB-71FB6DB862FD

Diagnosis

Body subcylindrical; anterior pereonites medioventrally keeled; all sternites with projecting spines; spines directed posteriorly; without dorsal setae, posterolateral margins of all pereonites with prominent, robust spine-like seta; pereonites 1–4 tightly packed, pereonite 4 wider than pereonite 5, posterolateral margin with prominent, spine-like seta and simple setae; pereonite 6 shorter than pereonite 5; pereonite 7 posterolateral margins not projecting posteriorly. Pleotelson rectangular, length 2.0 width, waist weakly pronounced; paired dorsal sensory organ absent. Pereopod I projecting laterally and dorsally, ischium dorsal setose lobe longer than merus dorsal lobe, with three enlarged setae; pereopods V–VI ischium with seta mid-dorsally, carpus mid-dorsally with no seta. Female pleopod II distal setae apically sensillate.

Etymology

This name, derived from the Greek words *theiodes* meaning sulphur-like and *tyntlos* mud, refers to the

sulphide-rich sediments around the hydrothermal mounds of the Galapagos mid-ocean ridge system. It is a masculine noun in apposition.

Type fixation

Adult female holotype, 1.6 mm, USNM 1208016, designated here.

Type material examined

USNM 1208016: adult female holotype. USNM 1208017: manca stage 1 paratype.

Type locality

Galapagos Hydrothermal Mounds region, R/V Gillis st. 301 ('away from mounds' – see Grassle *et al.*, 1985), 0°35.0'N, 86°05.7'W, 2730 m, box core (one of 25 subcores).

Type material – remarks

Holotype female missing antennal flagellum and uropods; several pereopods broken at basis; pleopod II (operculum) removed and mounted on slide. Manca stage 1 specimen missing antennae and uropods.

Description of female

Body (Fig. 22) subcylindrical, length 1.6 mm, 4.0 width, tergite surfaces hirsute, setation of lateral tergal margins present, with long setae along lateral margins of pereonites; posterior pereonites and pleotelson with dorsal robust setae. **Ventral spines** acute, keel-like, directed posteriorly. Pereonite 1 spine small. Pereonite 2 spine small, placed midway on midline. Pereonites 3 and 4 spines small, closer to posterior segment border. Pereonite 5 spine absent. Pereonite 6 spine prominent, triangular in lateral view, closer to posterior segment border. Pereonite 7 spine prominent. Imbricate ornamentation absent on all pereonites.

Cephalothorax length 0.61 width, 0.14

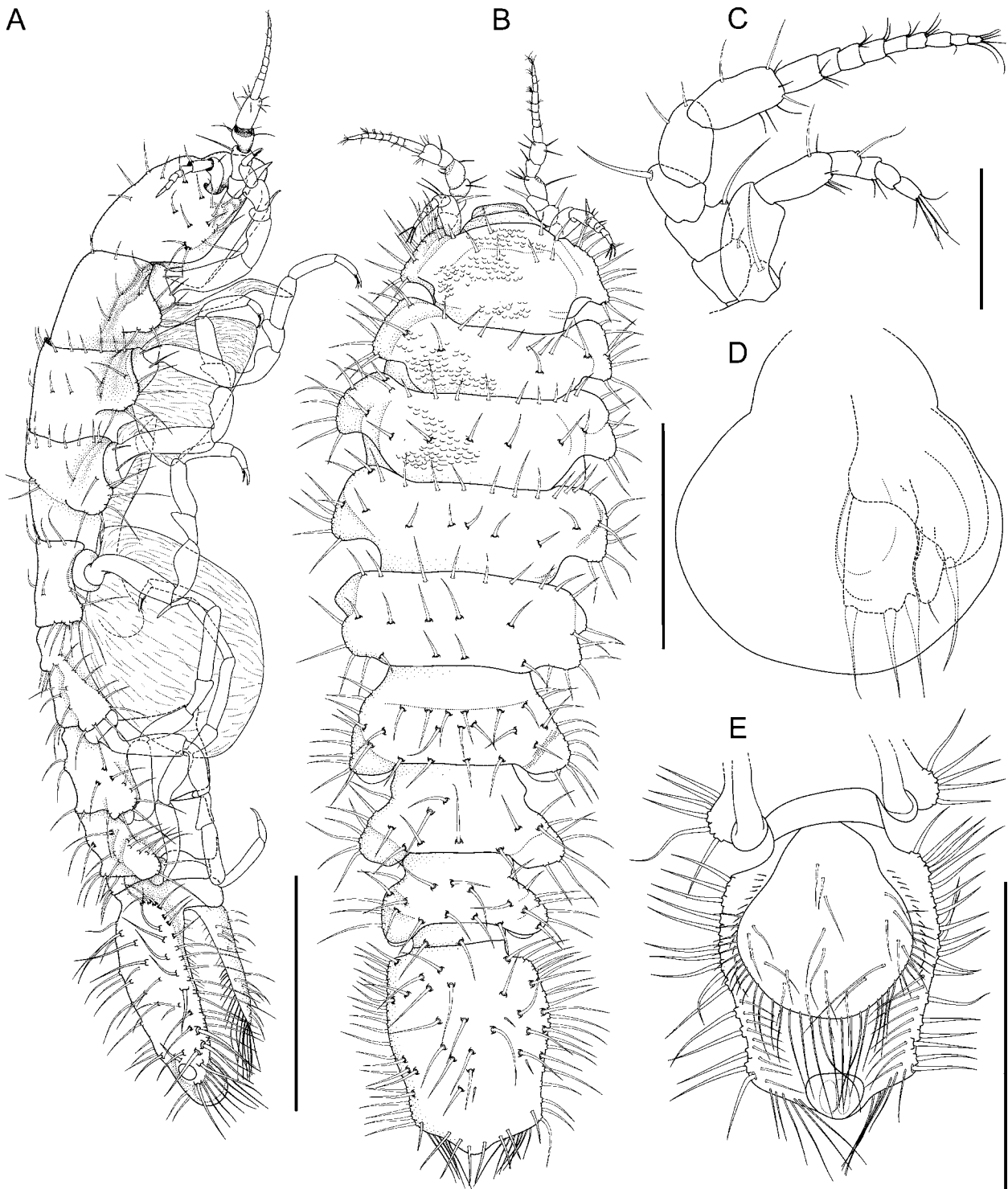


Figure 11. *Urstylis solicipia* gen. et sp. nov., ovigerous female holotype ZMH K-43070. **A**, habitus, lateral. **B**, habitus, dorsal. **C**, antennula and antenna, dorsomedial, *in situ*. **D**, pleopods, ventral, *in situ*. **E**, pleotelson, ventral. Scale bars = 0.5 mm (A, B, E); 0.1 mm (C); 0.2 mm (D).

body length; frons in dorsal view convex, smooth, frontal furrow present, convex anterior margin adjacent to clypeus, not projecting. Posterolateral setae present. Posterolateral margins angular, blunt. **Pereonite 1** length 0.35 width, 0.08 body length, anterior margin straight. Posterolateral setae asen-

sillate, simple. **Pereonite 2** length 0.33 width, 0.08 body length. Posterolateral setae robust. **Pereonite 3** length 0.42 width, 0.10 body length; posterolateral setae asensillate, robust, flexibly articulated. **Pereonite 4** width 1.04 pereonite 5 width, length 0.63 width; lateral margins curved, in dorsal view

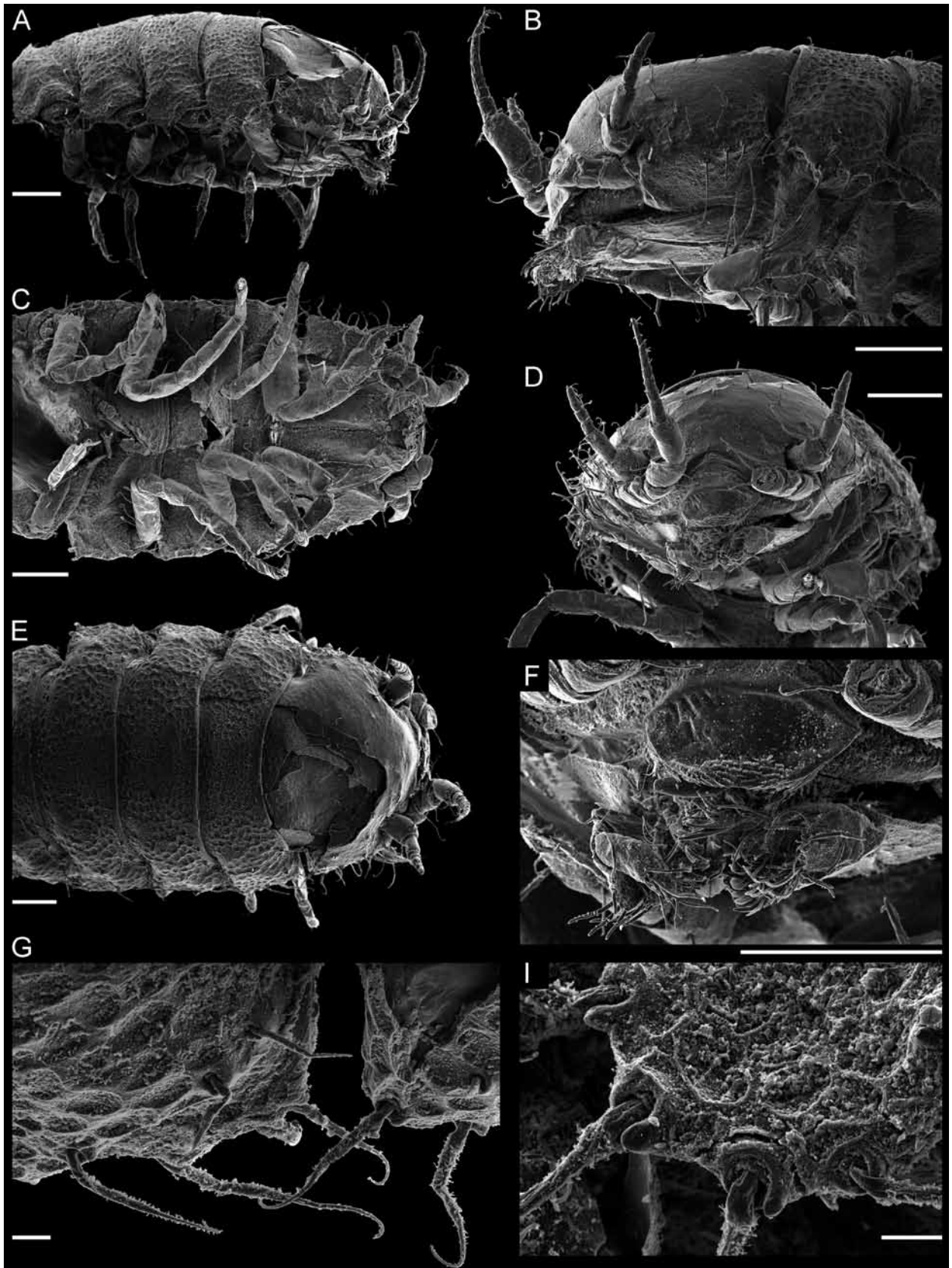


Figure 12. *Urstylis solicopia* gen. et sp. nov., paratype female fragment ZMH K-43053. **A**, lateral habitus. **B**, lateral cephalothorax. **C**, ventral habitus. **D**, frontal head. **E**, dorsal habitus. **F**, mouthfield. **G**, cephalothorax right posterolateral margin and pereonite anterolateral margin. **H**, pereonite 2 posterolateral margin, lateral view. Scale bars = 0.1 mm (A–F); 10 µm (G, H).

lateral margins narrowing posteriorly to coxae, with distinct indentation posterior to coxa. Posterolateral margins tapering. Posterolateral setae sensillate, robust, flexibly articulated.

Pereonites 5–7 posterior tergite margin with two sensillate, robust, flexibly articulated setae; setae extending beyond posterolateral margin. Posterolateral margins not produced posteriorly. Tergite posterolateral setae sensillate, robust. **Pereonite 5** length 0.75 width, 0.80 pereonite 4 length. **Pereonite 6** length 0.59 width, 0.94 pereonite 5 length. **Pereonite 7** length 0.56 width.

Pleotelson (Fig. 22A, B) length 0.26 body length, 2.0 width, narrower than pereonite 7; paired dorsal sensory organ absent. Posterior margin apex length 0.11 pleotelson length. Posterior apex setae absent. Pleopodal cavity width 0.85 pleotelson width. Labrum anterior margin in dorsal view concave. Concavity on left side, margin sinusoid, no distal cuticular spinules.

Antennula (Fig. 22E) length 0.51 head width, length 0.46 antenna length, width 0.69 antenna width; relative length ratios of articles 1.0, 0.75, 0.34, 0.28, 0.18, 0.34; L/W ratios of articles 1.8, 2.3, 1.4, 1.2, 1.1, 2.2. Article 1 distinctly longer than wide, dorsally flattened, ventrally semicircular, longest and widest. Articles 2–4 distinctly longer than wide. Article 3 with one asensillate seta. Article 4 with one asensillate large, distally curled seta. Article 5 length subequal to width. Terminal article with two simple tubular aesthetascs. **Antenna (Fig. 22F)** length 0.25 body length. Basis angular with dorsolateral projection, shorter than coxa, rudimentary scale present. Ischium longer than coxa. Merus longer than coxa, basis, and ischium combined, distally with two asensillate setae, articulating distolaterally on ischium, antennal proximodistal axis with distinctly sharp bend. Carpus longer than merus, distally with one asensillate seta. Flagellum with nine articles.

Mandibles (Figs 22C, D, 23A): left mandible incisor process simplified, mono- or bidentate rounded, blunt; right mandible incisor process multidentate with dorsal and ventral subdistal teeth that partly enclose lacinia. **Maxilliped (Fig. 23A)** with three coupling hooks, article 2 wider than articles 1 and 3, article 1 shorter than article 3, article 4 distomedial extension present; epipod length 2.8 width, 0.87 basis length. Anterior pereopodal coxae ring-shaped, coxal setation present.

Pereopod I (Fig. 24A) positioned laterally and dorsally; length 0.28 body length; article L/W ratios 1.96, 0.83, 0.90, 1.64, 2.43, 4.27; relative article length ratios 1.00, 0.62, 0.41, 0.55, 0.35, 0.30; ischium dorsal margin with lobe projecting much greater than basal width of segment, with three enlarged setae: one simple seta, two distally biserrate. Merus dorsal margin with two setae: one simple, one distally bidentate; ventral margin with three setae: two distally curled, one robust subdistally sensillate. Carpus dorsally with two distally biserrate setae. Propodus with one long distodorsal seta and one short ventral seta, articular plate on propodus absent; dactylus distally with two sensillae, dorsal claw length slightly shorter than dactylus.

Pereopod II (Fig. 24B) longer than pereopod I, length 0.37 body length; article L/W ratios 4.0, 2.3, 1.3, 2.6, 3.3, 4.0; relative article length ratios 1.0, 0.50, 0.31, 0.46, 0.30, 0.26. Ischium dorsally with 1 distally curled simple seta. Merus dorsally with two setae, ventrally with one seta; setae distally curled simple. Carpus dorsally with one broom seta, ventrally with three setae: one distally curled, simple and two robust, subdistally sensillate. Dactylus distally with one sensilla, dorsal claw length similar to dactylus length.

Pereopod III (Fig. 25A) length 0.39 body length; article L/W ratios 3.4, 2.0, 1.8, 2.5, 3.0, 4.0; relative article length ratios 1.00, 0.48, 0.44, 0.50,

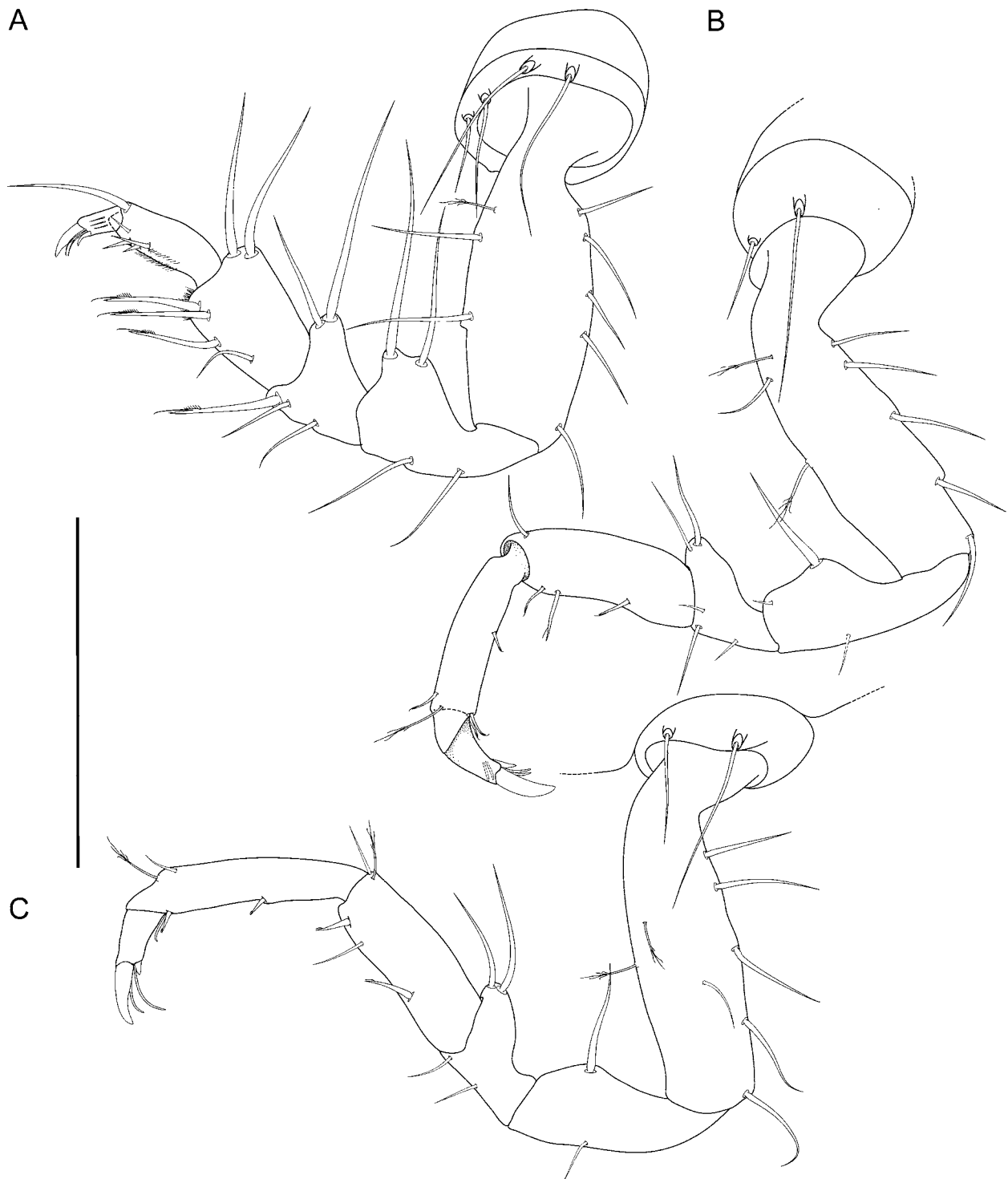


Figure 13. *Urstylis solicopia* gen. et sp. nov., ovigerous female holotype ZMH K-43070. **A**, pereopod I. **B**, pereopod II. **C**, pereopod III. Scale bar = 0.2 mm.

0.36, 0.34. Ischium with no seta proximodorsally, dorsal lobe flat, rounded; proximally with one seta. Merus dorsally with two simple, distally curled setae, at dorsodistal margin, ventrally with two simple, distally curled setae, along ventral margin. Carpus dorsally with two simple setae, ventrally with three setae: two simple marginally, one sen-

sillate robust distally. Dactylus with one sensilla.

Pereopod IV (Fig. 25B) length 0.48 body length, more robust and longer than pereopod III (~43% longer); article L/W ratios 4.7, 2.9, 1.6, 3.0, 3.7, 5.9; relative article length ratios 1.0, 0.63, 0.36, 0.48, 0.32, 0.30. **Pereopod V (Fig. 25C)** length 0.39 body length; article L/W ratios 5.8, 2.9,

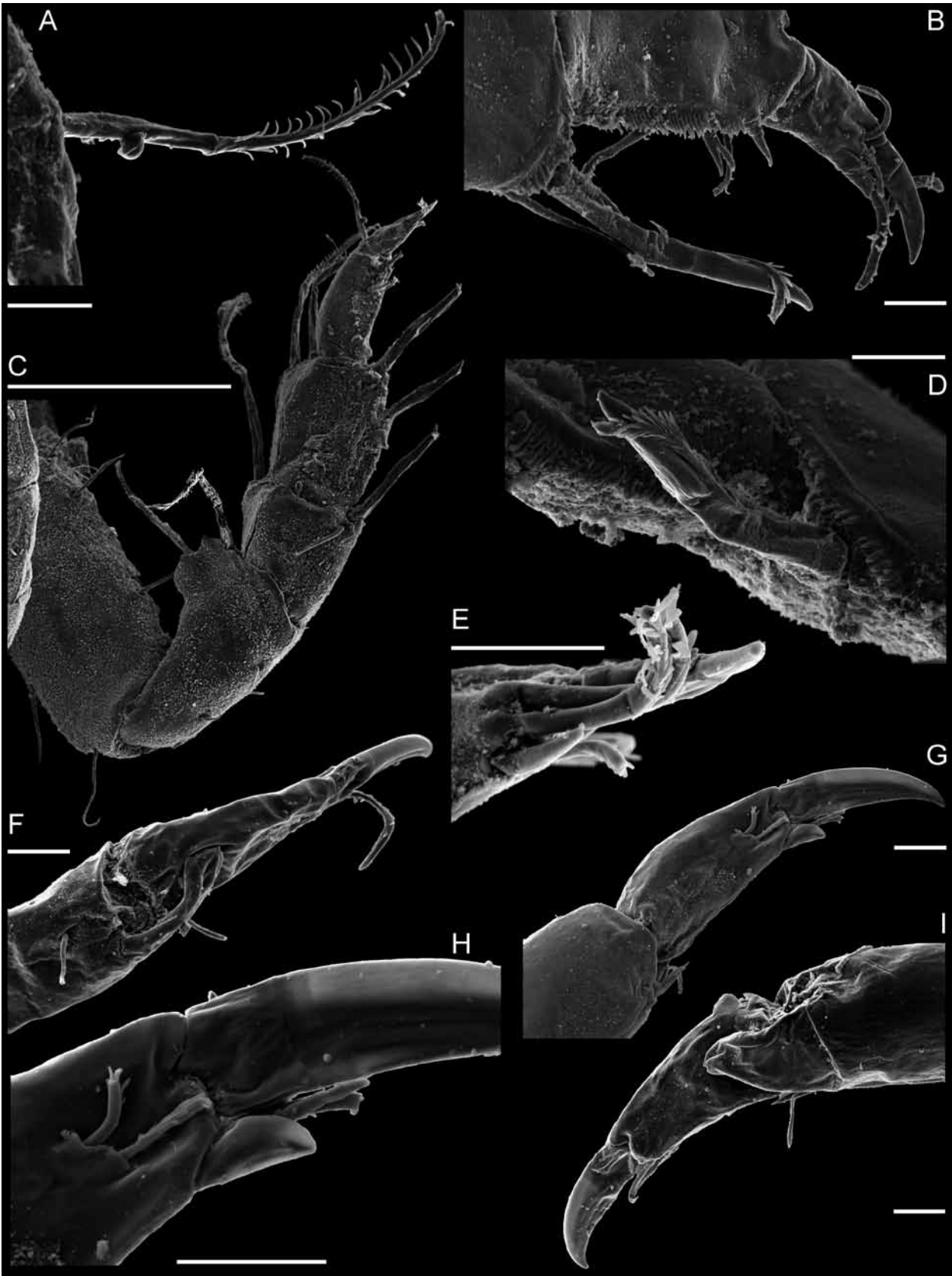


Figure 14. *Urstylis solicopia* gen. et sp. nov., paratype female fragment ZMH K-43053. **A**, pereopod I propodus distodorsal margin bisetulate seta. **B**, medial pereopod I propodus, dactylus. **C**, lateral pereopod I. **D**, pereopod I carpus distoventral margin robust seta with subdistal fringe-like sensilla. **E**, pereopod I ventral dactylus. **F**, pereopod II dorsal dactylus. **G**, pereopod II medial dactylus. **H**, close-up of G. **I**, pereonite 2 lateral dactylus. Scale bars = 10 μ m (A, B, D–I); 0.1 mm (C).

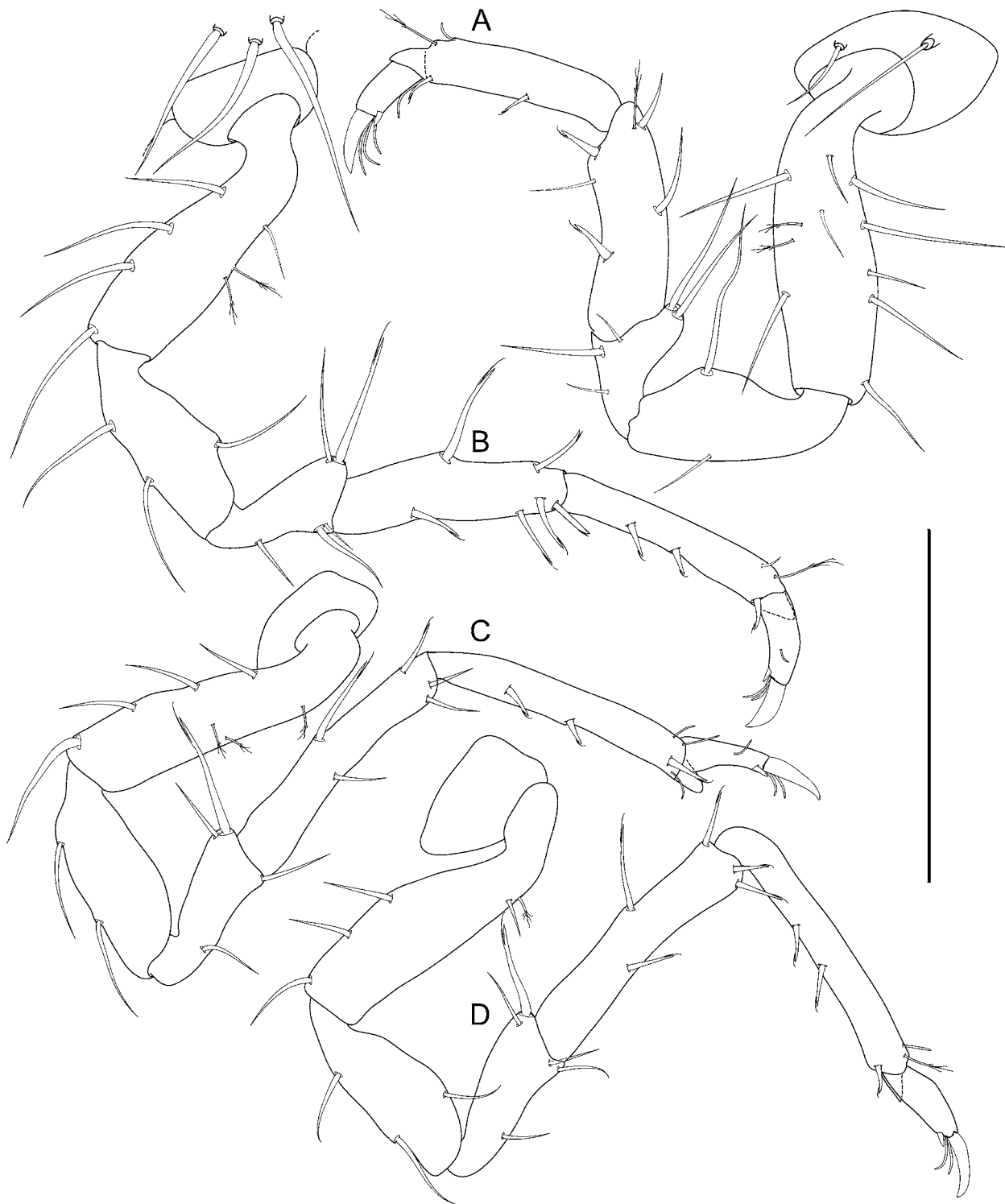


Figure 15. *Urstylis solycopia* gen. et sp. nov., ovigerous female holotype ZMH K-43070. **A**, pereopod IV. **B**, pereopod V. **C**, pereopod VI. **D**, pereopod VII. Scale bar = 0.2 mm.

3.4, 5.5, 7.3, 6.3; relative article length ratios 1.0, 0.61, 0.51, 0.65, 0.65, 0.41. Ischium mid-dorsally with one small simple seta, midventrally with two simple distally curled setae. Merus distoventrally with one simple distally curled seta. Carpus disto-

dorsally with two setae: one simple, one penicillate; midventrally with one seta; distoventrally with two elongate, robust, sensillate setae.

Pereopod VI (Fig. 25D) length 0.48 body length; article L/W ratios 4.7, 3.8, 4.5, 9.1, 8.5, 2.9; relative article length ratios 1.0, 0.73, 0.75, 1.12, 0.93, 0.52. Ischium dorsally with one seta, midven-

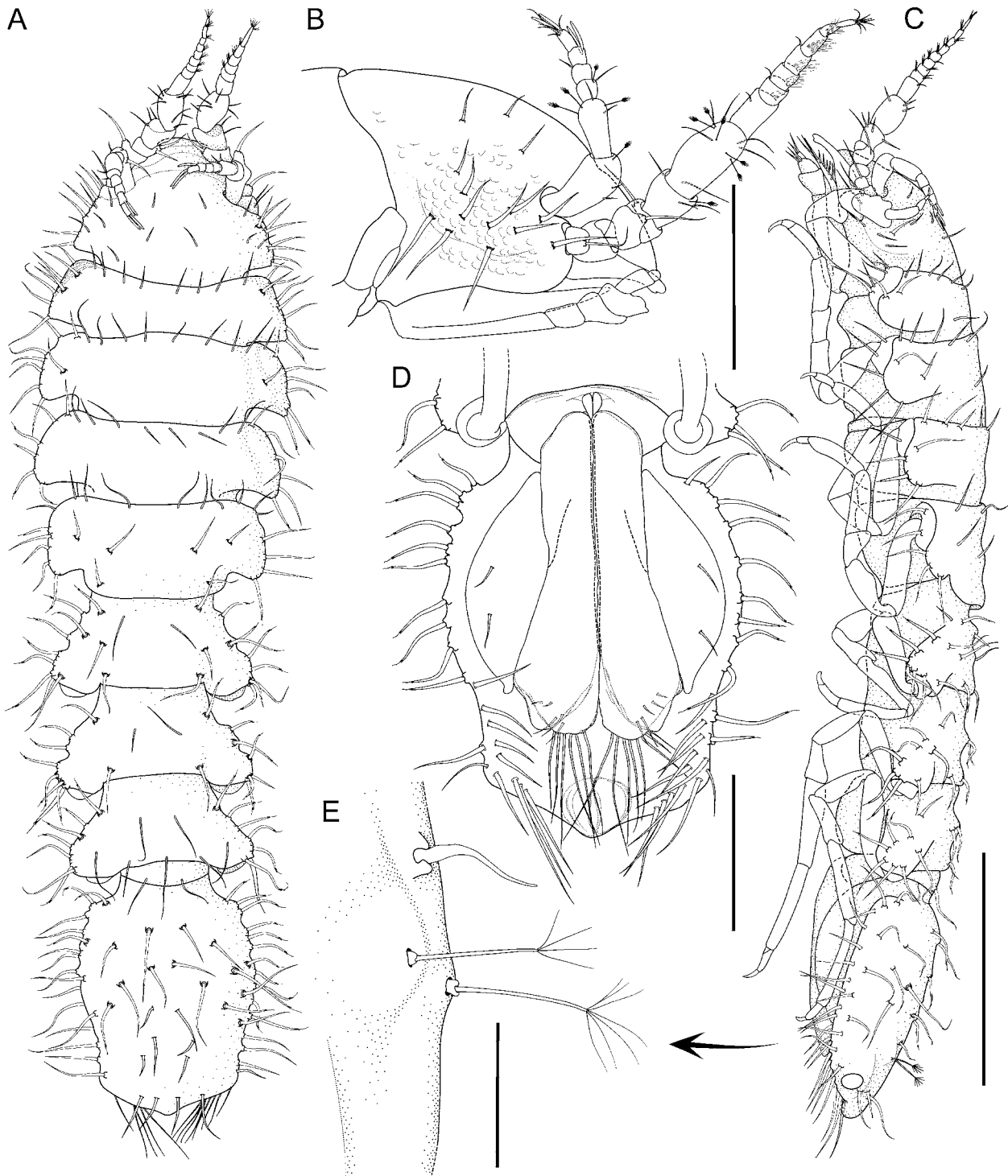


Figure 16. *Urstylis solicipia* gen. et sp. nov., adult male paratype ZMH K-43055. A, habitus, dorsal. B, cephalothorax, lateral. C, habitus, lateral. D, pleotelson, ventral. Scale bars = 0.5 mm (A, C); 0.3 mm (B); 0.2 mm (D); 0.05 mm (E).

trally with two distally curled simple setae. Merus distodorsally with one distally curled simple seta; midventrally with one distally curled simple seta; distoventrally with one simple seta. Distodorsally with two simple setae; midventrally with two thin robust sensillate setae; distoventrally with two thin robust sensillate setae. **Pereopod VII** basis ventral

margin with row of three elongate setae; setae shorter than basis width.

Operculum (Fig. 23C) length 1.4 width, 0.82 pleotelson dorsal length; apical width 0.50 operculum width; distally tapering. With lateral fringe consisting of eight bifurcate distally sensillate setae, with continuous transition to apical row

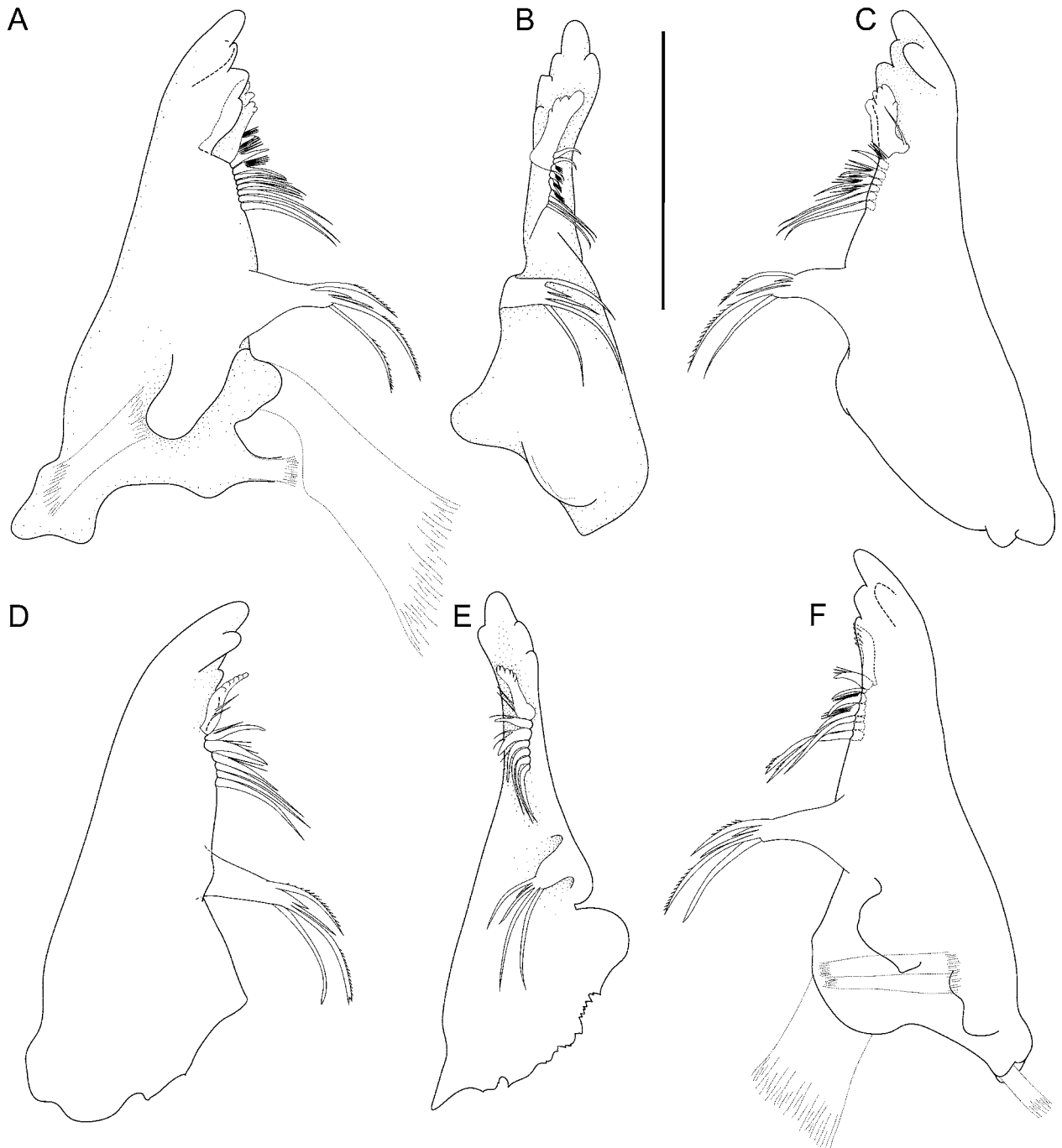


Figure 17. *Urstylis solicopia* gen. et sp. nov., adult male paratype ZMH K-43055. A–C, left mandible. D–F, right mandible. Scale bar = 0.1 mm.

of 17 setae; apical setae asetulate, distally sensillate, extending to anal opening. **Pleopod III** (Fig. 23B) length 2.3 width; protopod length 2.4 width, 0.61 pleopod III length. **Uropod** broken.

Remarks

Urstylis thiotyntlus gen. et sp. nov. differs from the other two species in the genus by its laterally positioned pereopod I. This limb is further modified by being more robust and having distinctive dorsal

projections on the ischium, merus, and carpus, all of which bear large distally denticulate setae.

The attitude of the first pereopod is reminiscent of that seen in macrostylids and the Desmosomatidae although, in these taxa, the relevant limbs are pereopods II–III. Given that this limb position is common amongst desmosomatid and macrostylid species known to be fossorial (Hessler and Strömberg, 1989), we infer that this species may also be fossorial.

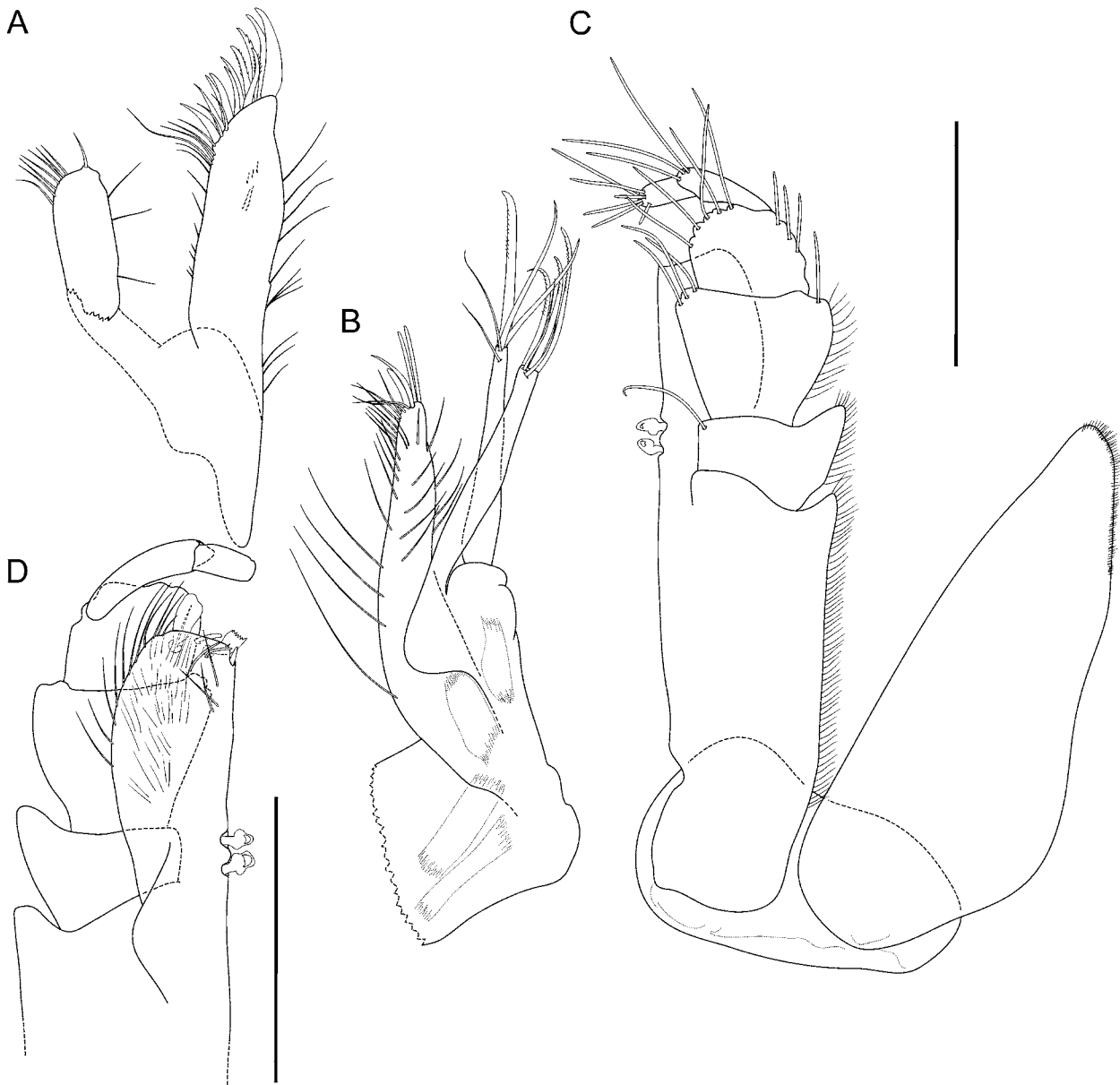


Figure 18. *Urstyliis solicipia* gen. et sp. nov., adult male paratype ZMH K-43055. **A**, maxillula. **B**, maxilla. **C**, maxilliped, ventral, endite setation omitted. **D**, maxilliped endite close-up, dorsal. Scale bars = 0.1 mm.

Differences between pereopods II–IV and V–VI are more pronounced and pereopod I is more derived than in *U. zapiola* and *U. solicipia*. *Urstyliis thiotyntlus* presages the robust midventral spines seen in *Macrostyliis* species with the possession of keel-like spines on most sternites, which only occur amongst other species of *Urstyliis* as v-shaped midline keels of *U. zapiola* sp. nov. males. *Urstyliis thiotyntlus* also lacks the distinctive dorsal organs occurring on the pleotelson of *U. zapiola*, but has a distinctively narrow pleotelson.

Of the three species, *U. thiotyntlus* has the least number of setae on the dorsal surfaces, and

these setae are shorter and more robust. Pereonites 1–4 are more integrated and relatively wide relative to the posterior body part in comparison to the other *Urstyliis* species. This species was collected as part of a study of the Galapagos hydrothermal sedimentary community by Grassle *et al.* (1985).

Although the Gillis sample 301 (containing this species) was taken away from hydrothermal mounds, it is still within a nautical mile of the mounds. As such, this background sedimentary community probably is still influenced by nearby hydrothermal activity. Gillis 301, however, is somewhat more diverse than samples taken amongst

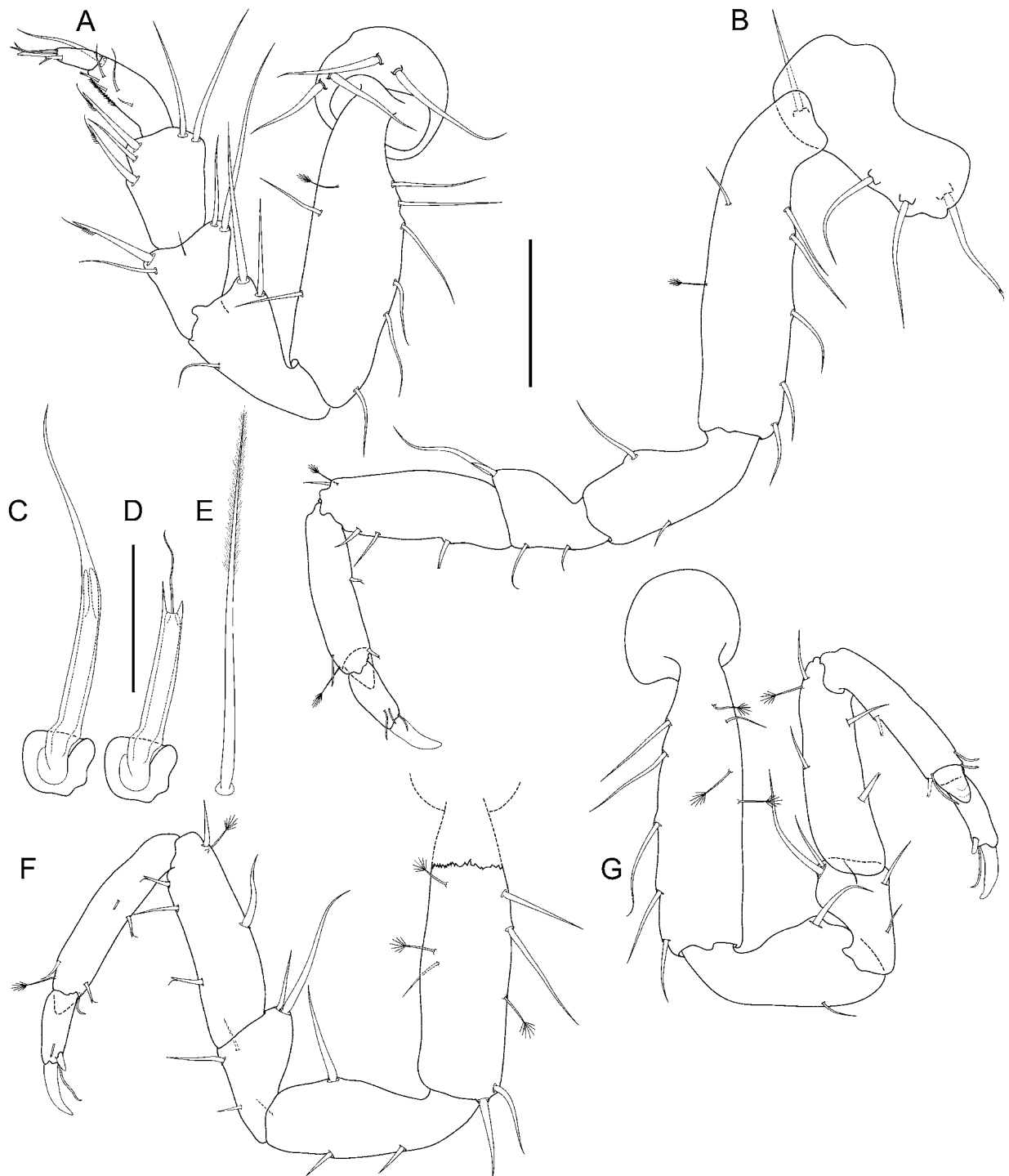


Figure 19. *Urstylis solicipia* gen. et sp. nov., adult male paratype ZMH K-43055. **A**, pereopod I. **B**, pereopod II. **C**, simple seta as found on the trunk cuticle and pereopods with indicated internal structures. **D**, simple seta with cuticle broken and internal tissue exposed distally. **E**, bisetulate seta. **F**, pereopod III. **G**, pereopod IV. Scale bars = 0.1 mm (A, B, F, G); 0.025 mm (C–E).

the hydrothermal mounds (Grassle *et al.*, 1985). above).

Overall, the isopod diversity of the Galapagos hydrothermal mounds region is high. The appearance of this species in one single sample thus concurs with the rare appearance of *Urstylis* in the high isopod diversities observed for the CCFZ (Thistle and Wilson, 1987, 1996) and Argentine Basin (see

Phylogenetic Results

Both TNT analyses, thorough and fast, retained four shortest trees with a best score of 677 (Fig. 26). The three new species form a monophyletic

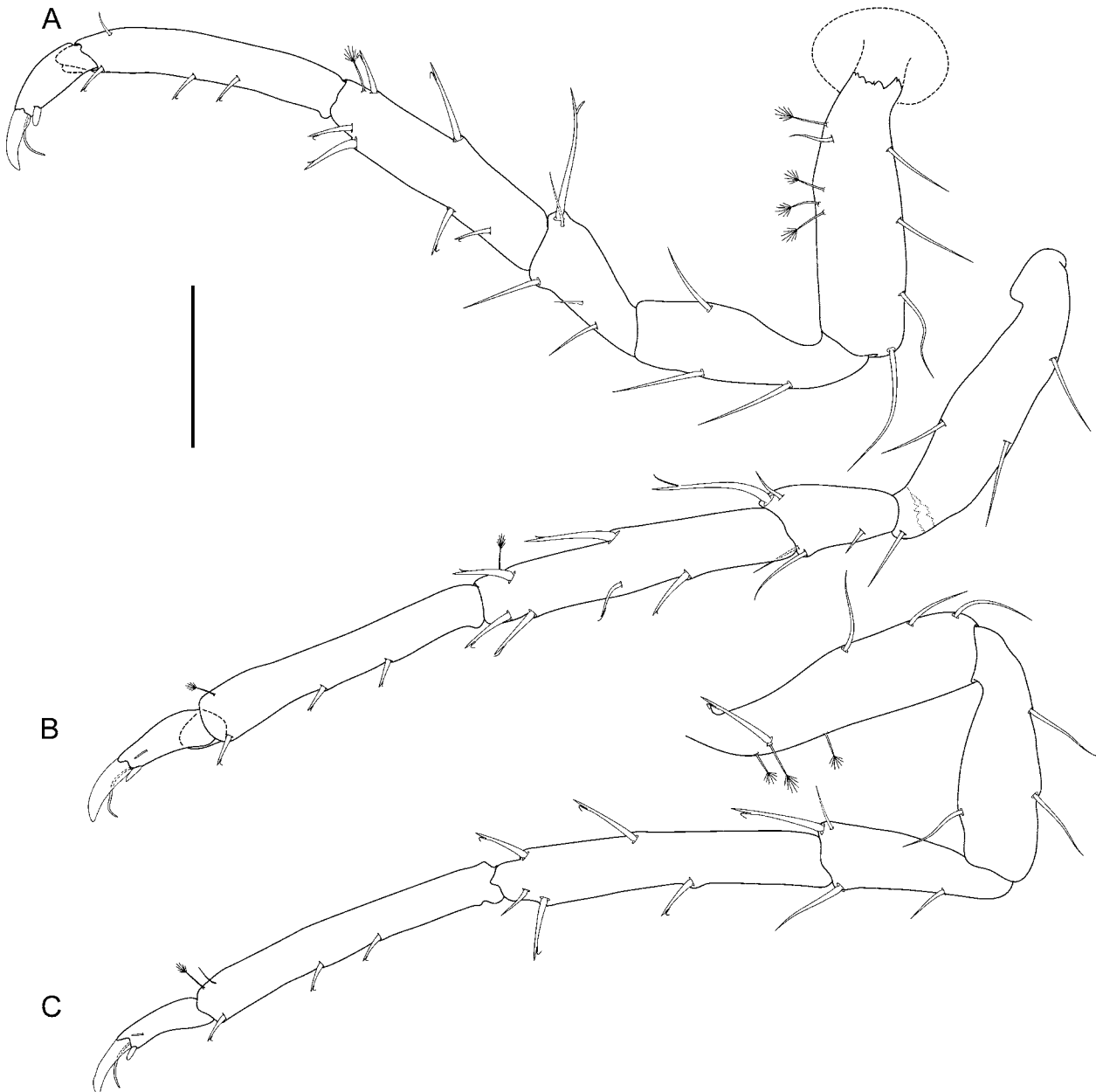


Figure 20. *Urstylis solicipia* gen. et sp. nov., adult male paratype ZMH K-43055. **A**, pereopod V. **B**, pereopod VI, basis broken and lost, ischium damaged. **C**, pereopod VII. Scale bar = 0.1 mm.

group, henceforward referred to as Urstylidae. It is supported by 14 synapomorphies, a jackknife value of 97, Bremer support of 9, and relative (rel.) Bremer value of 64 (Fig. 27; see also Discussion). Macrostylidae were found to be the closest related to Urstylidae with ten synapomorphies supporting this clade (jackknife 98, Bremer 8, rel. Bremer 62).

Macrostylidae are nevertheless distinctly separated by 43 synapomorphies (jackknife 100, Bremer > 10, rel. Bremer 100). The most basally derived clade comprises Echinothambematidae, Janirellidae, Katianiridae, and Mesosignidae. The

sister clade to Macrostylidae and Urstylidae is Thambematidae. Desmosomatidae and Nannoniscidae have separate positions respectively basally to Thambematidae.

Discussion

The three new species are placed within the 'higher Janiroidea' because of the typical, highly derived janiroid opercular pleopods of the males (Wilson, 1987b). Their bodies are elongate and slender,

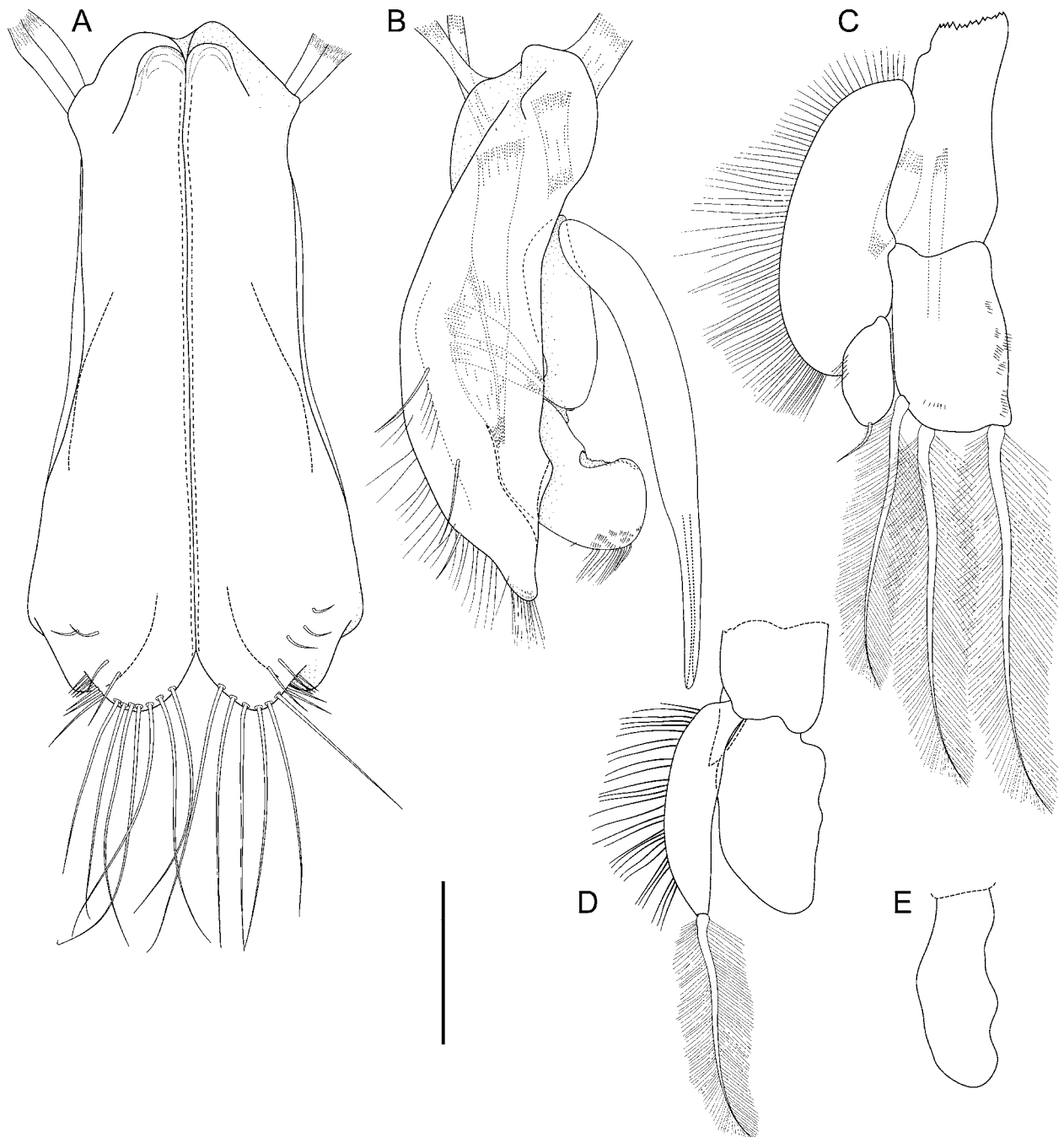


Figure 21. *Urstylis solycopia* gen. et sp. nov., adult male paratype ZMH K-43055. **A**, pleopod I. **B**, pleopod II, ventral. **C**, pleopod III. **D**, pleopod IV. **E**, pleopod V. Scale bar = 0.1 mm.

lateral tergal projections are absent, and the anterior pereopods feature rows of relatively robust setae on both ventral and dorsal margins that are typical features of a fossorial lifestyle as seen, e.g. in *Eugerdella* and Macrostylidae (Hessler and Strömberg, 1989). A close relationship to the ‘munnoïd’ taxa *sensu* Wägele (1989) can thus be excluded. Consequently, those taxa were not considered in the analyses presented here.

A reduction in the length of the antennula,

flattened triangular molar processes, and a long mandibular spine row are characteristic for the desmosomatid–nannoniscid–macrostylid clade as inferred by Wägele (1989) and the new species share these character states. They furthermore share a distomedial process on the maxilliped carpus (palp article 3). Analogous conditions, however, occur in Janirellidae Munnidae, Paramunnidae, Munnopsidae, *Xostylus*, and Katianiridae. Further inter- or intrafamilial relationships are beyond the scope

of this work and will be addressed separately (T. Riehl and G. D. F. Wilson, unpubl. data). The data set used for this study is reduced with regard to the taxa used and therefore, relationships within clades other than the macrostylid–urstylid clade have to be treated with care.

The Phylogenetic Relationship between Urstylidae and Macrostylidae

Affinity between the new species and Macrostylidae was validated by the parsimony analyses (Fig. 26), depicted by a long list of synapomorphies (Fig. 27). Superficially close groups such as Echinothambematidae, *Dactylostylis*, and Katianiridae have a fundamentally different underlying morphology. The broad pleotelson with elongate styliform uropods articulating distinctly separate from the anus has thus evolved at least twice independently.

The prognathous, spade-like head that is posteriorly widened and fits into the anterior margin of pereonite 1 is an important homology. In taxa that have a presumed burrowing lifestyle, such as Macrostylidae and Urstylidae, some Desmosomatidae and Nannoniscidae (Hessler and Strömberg, 1989), the anterior pereonites (1–3) are often broader and deeper than the posterior pereonites, giving the body a posteriorly tapering shape. The enlarged dimensions of the anterior pereonites may reflect increased musculature. Although this is a synapomorphy for Urstylidae and Macrostylidae, it has independently evolved in some desmosomatids and nannoniscids (character 20).

The results are inconclusive about the sternal spines that are present in *U. thiotyntlus*, most (but not all) macrostylids, some Nannoniscidae, and rarely in Desmosomatidae (characters 30, 31). These may have a common origin in the *Urstylis*–*Macrostylis* clade but an independent origin is equally as parsimonious. Although basally derived

taxa, especially those with long antennular flagellae, have one aesthetasc per flagellar segment in the male (character 4), Macrostylidae and the new species have several of these chemosensory setae on the distal segments. This can be interpreted as a chemosensory enhancement for sexual purposes (females typically have only one to two aesthetascs) and possibly as compensation for the reduction of aesthetasc-bearing segments. Within Asellota, the antennal basis length (character 9) often exceeds the length of coxa and ischium respectively, especially in taxa of the ‘munnopsoid radiation’. Urstylids and macrostylids, however, have subsimilar length relationships of the basal antenna podomeres. Our analyses also suggest independent reduction of this segment in *Pseudomesus* and in some of the basally derived taxa.

Several mandibular characters support a macrostylid–urstylid relationship. The right *lacinia mobilis* (character 12) evolved from a spine-row member to a heavily calcified structure independently in *Echinothambema*, *Dactylostylis*, and in the last common ancestor of the macrostylid–urstylid clade. A mandibular palp is plesiomorphically present in most groups of Janiroidea, although reduced multiple times across this monophyletic group (character 13), such as in Munnidae, *Pleurocope*, some Paramunnidae, Nannoniscidae, Haplomunnidae, Desmosomatidae, and some Munnopsidae. Its absence is an apomorphic character for the macrostylid–urstylid clade.

More similarities between the two families are found on the body segments. Specialized setae are present on posterolateral tergite margins of the pereonites in Macrostylidae and *U. thiotyntlus* (character 18). In other taxa, although setae might be generally present, such specialized configuration is absent. The setal distribution and robustness varies across the species of *Macrostylis*: most commonly they are spine-like in pereonites 5–7. Our data

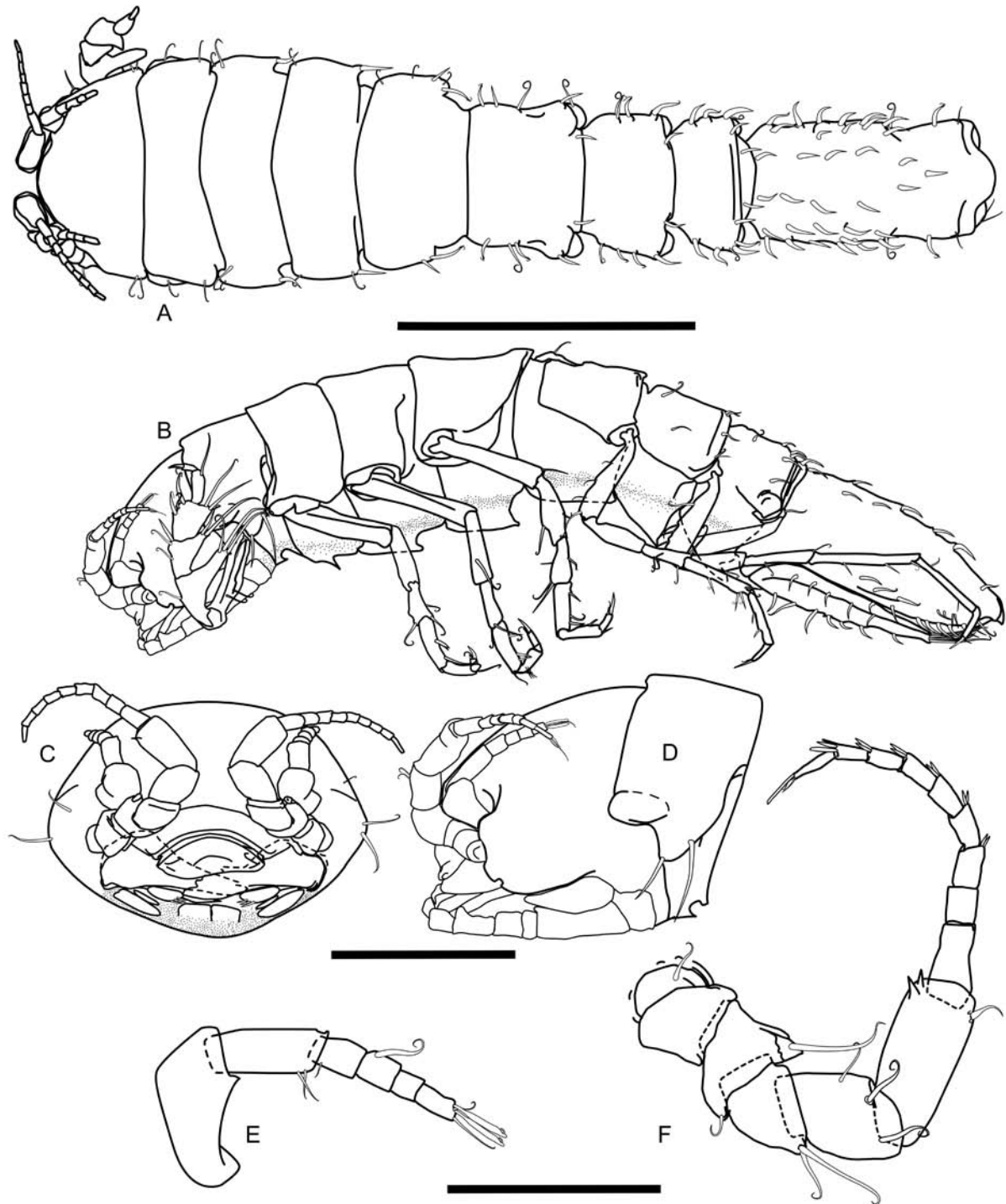


Figure 22. *Urstylis thiotyntlus* gen. et sp. nov., holotype female USNM 1208016. **A**, dorsal habitus. **B**, ventral habitus. **C**, **D**, head anterior and left lateral view, respectively. **E**, antennula, lateral view. **F**, antenna, medial view. Scale bars = 0.5 mm (A, B); 0.2 mm (C, D); 0.1 mm (E, F).

suggest either independent origins or a secondary reduction in *U. solicipia* and *U. zapiola*.

Further evidence for their close relationship is present on the pleotelson. Elongate setae constituting the apical setal row on the operculum (character 65) are rather uncommon amongst Janiroidea. This state is synapomorphic for the ma-

crostylid–urstylid clade and a homoplasy in mesosignids and katianirids. *Urstylis thiotyntlus* is clearly distinguished from the other new species but similar to some macrostylids, for example with regard to robust, spine-like posterolateral setae (character 18). These are present in the majority of macrostylids but missing in other species of *Ursty-*

lis and all of the outgroup taxa.

A common origin can thus be neither verified nor excluded. Other features of *U. thiotyntlus* must be considered derived. The ischium dorsal margin of pereopod I is dorsally expanded as in most Janiroidea (character 45). This lobe is usually located on the distodorsal region of the article and is simply rounded or almost triangular. The condition present in *U. solicipia* and *U. zapiola* is thus plesiomorphic. The subparallel margins found in Macrostylidae, several Paramunnidae, Nannoniscidae, and Munnopsidae (not treated here), as well as the extremely expanded dorsal lobe found in *U. thiotyntlus* (character 46), must be considered as (multiple independent) derivations.

New Insights on the Evolution of the Highly Derived Macrostylidae

Urstylidae show many plesiomorphic character states indicating a more basal derivation than the Macrostylidae. This is depicted by translating unique synapomorphies into branch length (Fig. 27). The free pleonite expressed in all three species is one example of a plesiomorphic character. A pleon with five freely articulated pleonites is present in most malacostracan crustaceans. Throughout the isopods, many groups show tendencies for the integration of the posterior pleonites into a pleotelson. Thus, the pleotelson has differing compositions amongst the major groupings of Isopoda (Wägele, 1989; Brusca and Wilson, 1991; Brandt and Poore, 2003; Wilson, 2009).

The pattern of articulation loss between pleonite 1 and the pleotelson defines clusters of taxa within the Janiroidea. Macrostylidae are variable in this regard but mostly show a loss of articulation (Kussakin, 1999; Riehl *et al.*, 2012).

More evidence that Urstylidae is not as highly derived as Macrostylidae or, for example,

many Nannoniscidae or Desmosomatidae, can be seen in the lower degree of tagmosis (character 19). Although Macrostylidae can be considered to have the most-derived tagmosis amongst the before-mentioned taxa, Desmosomatidae and Nannoniscidae often have a clear distinction in form and setation of the anterior and posterior pereopods. In Urstylidae, pereopods II–VII are fairly similar. Additionally, the integration of the segments (characters 21–23) is less derived than in Macrostylidae: the segments appear to be movable against each other and are laterally equally spaced.

Several morphological features of Urstylidae seem to represent intermediate conditions assuming an evolutionary trajectory from a primitive janirid-like ancestor (Wägele, 1989) to the highly derived Macrostylidae. The relatively strong anterior habitus, also present in *Eugerdella* for example, may have a common origin in all three groups (character 20). The specific organization and shape of the pereopodal claws and dactylar sensillae (characters 39–44) is incompletely studied but nevertheless, evolutionary patterns can be observed across all the Janiroidea, based on the few species that have been studied in detail (Wilson, 1985). The ventral claw on the dactylus of most janiroideans is typically either seta-like or more robustly claw-like, although several groups, such as Haploniscidae (not treated here), and Urstylidae have distinctly flattened or scale-like ventral claws (character 39). In Macrostylidae, this claw is thin and elongate, dorsally concave, often with a ventral carina, distally tapering and bending upwards, clinging to the distal sensilla. Whereas in most taxa, the anterior and posterior pereopods have similar claws, in Urstylidae for example, the Macrostylidae show substantial differences. Here, the posterior claws are shaped like simple or serrate setae, generally subcircular in cross-section (character 40). The shape of the ventral claw by

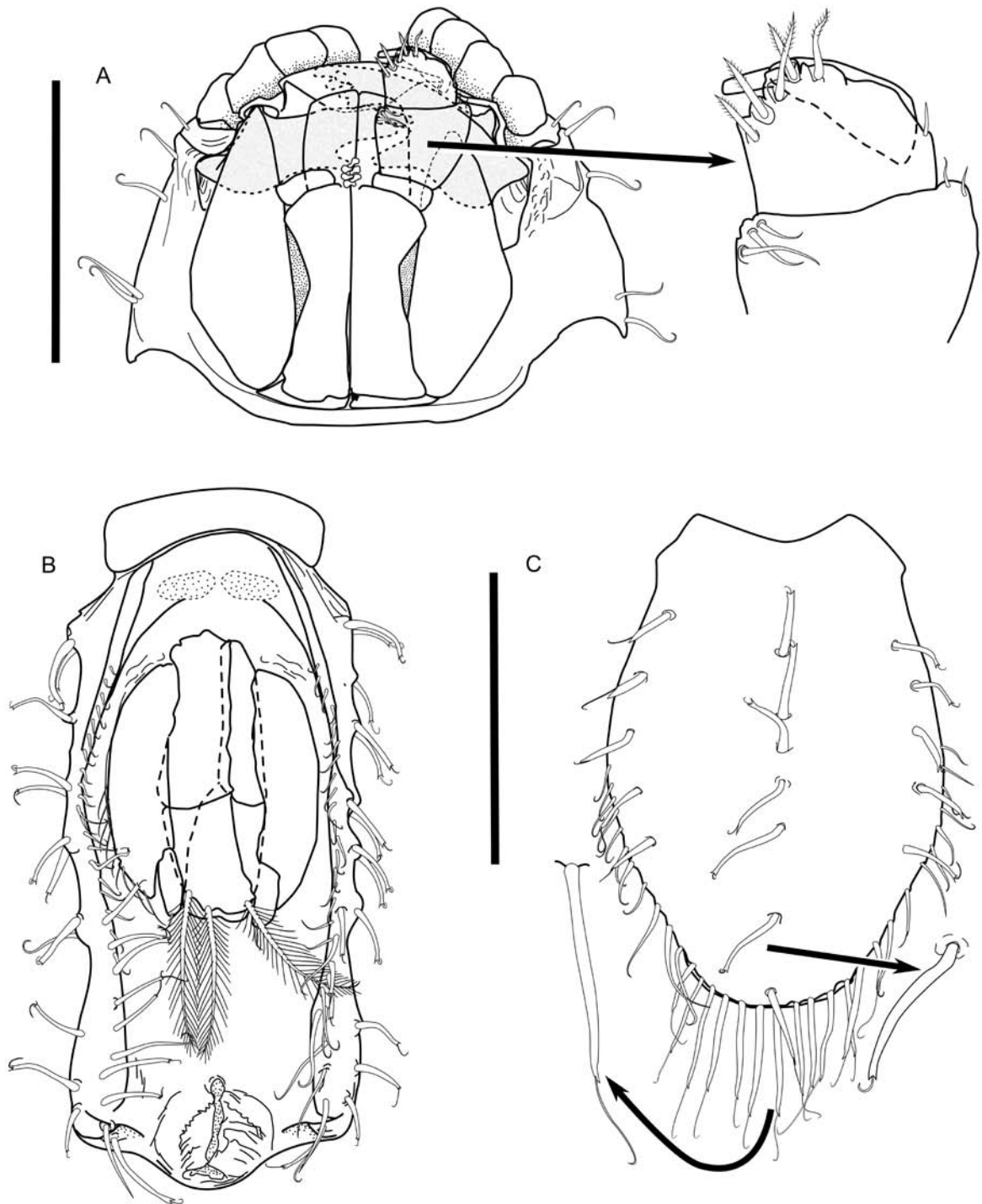


Figure 23. *Urstylis thiotyntus* gen. et sp. nov., holotype female USNM 1208016. **A**, maxilliped, ventral view, with enlargement of palp articles 2–3. **B**, pleotelson, ventral view, operculum removed to show pleopod III. **C**, operculum ventral view. Scale bars = 0.2 mm (A); 0.2 mm (B, C).

itself does not provide sufficient information regarding a potential evolutionary trajectory. The basal inclusion of the distal sensilla by the claws (characters 41, 42), however, may be interpreted as an intermediate state in Urstylidae. The macrostylid anterior dactylus is furnished with claws that cover the distal sensilla along its entire dorsal and

ventral margins. Distal sensillae plesiomorphically sit between the dorsal and ventral claws and are fully exposed. This claw apomorphy is probably not homologous to the enclosed claws of the Munnopsidae (Wilson, 1989). That is because, unlike the Munnopsidae, the distal sensilla in *Macrostylis* is uniquely thick and has lost the fringe-like mi-

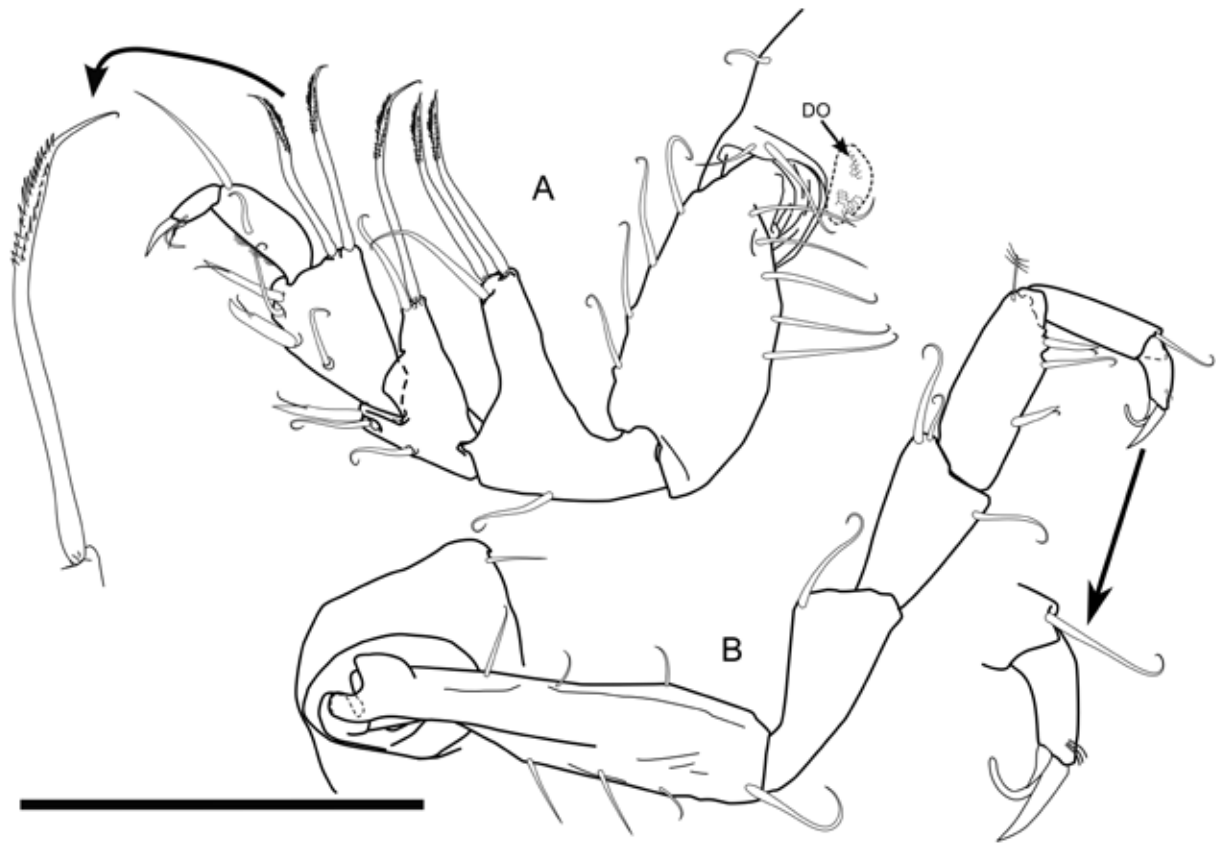


Figure 24. *Urstylis thiotyntlus* gen. et sp. nov., holotype female USNM 1208016. **A**, pereopod I, lateral view. **B**, pereopod II, lateral view, with enlargement of dactylus and claws (arrow). Scale bar = 0.2 mm.

crostructure (character 43).

The elongate, rod-like uropods inserting at the posterolateral margin in distinct separation from the anus (character 87) was one of the characters that initially led to allocation of the new taxa to Macrostylidae (Thistle and Wilson, 1987) and seems indeed to be of common origin. Interestingly, detailed study of the uropods revealed the presence of a vestigial exopod (character 73). Again, this situation may represent the ancestral condition from the macrostylid perspective. In the latter taxon, the uropod exopod is completely reduced.

The interpretation of the paired sensory organ (character 58) on the pleotelson is problematic. The subcuticular organ of Macrostylidae discovered by Hansen (1916) has never been analysed anatomically or physiologically. In *U. zapiola*, we identified a pair of cuticular tubercles that seem to house a cavity, which resembles the macrostylid

organ as it is filled with some sort of crystalline structure (Fig. 2C). Given this agreement in position and form, we assume a homology between the structures in Macrostylidae and *U. zapiola*. In *U. solicopia*, a pair of broom setae (= penicillate setae) was found in a similar position and arising from cuticular elevations. Although anatomical studies are needed, such as on the innervation of both structures, we hypothesize a common origin of both types of sensory organs. Indeed, these tubercles and broom setae can be found in a wide range of Janiroidea including many Haploniscidae (e.g. Brökeland and Wägele, 2004: Fig. 26), some Munnopsidae (e.g. Malyutina, 2003: electronic supplement Fig. 1), and in the nannoniscid genus *Austroniscus* (S. Kaiser, pers. comm.), which may indicate a fundamental synapomorphy rooted deep within the whole superfamily. Unfortunately, not much attention has been paid to these structures in

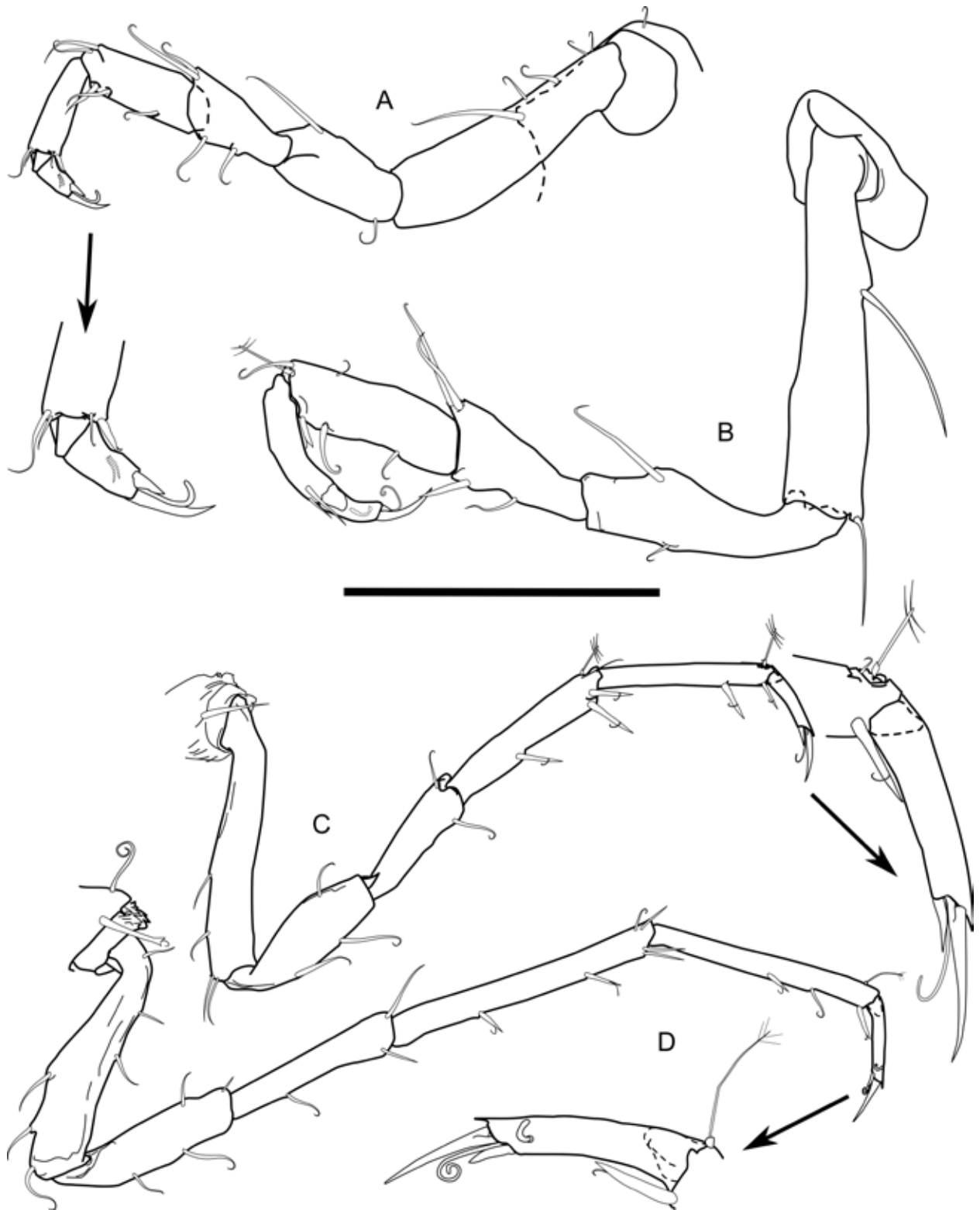


Figure 25. *Urstylis thiotyntlus* gen. et sp. nov., holotype female USNM 1208016. A–D, pereopods III–VI, left side, lateral view. A, C, showing enlargement of dactylus. D, pereopod VI dactylus, right side, lateral view. Scale bar = 0.2 mm (A–D).

the taxonomic literature. Owing to their small size, they may have been overlooked in many cases. Consequently this character was left unscored in our database for most taxa; confirmation of the homology of these structures in urstylids and macro-

stylids remains to be found.

Classificatory Consequences

According to our results, Macrostylidae is the

Figure 26 (opposite page). Strict consensus of four most parsimonious trees, based on morphological characters, analysed under equal weights, showing the position of Urstylidae amongst potentially related Janiroidea. The terminal taxa are exemplars representing families (bold font; not to scale): *J. maculosa* Leach, 1814; *J. priseri* Chardy, 1972; *D. acutispinis* Richardson, 1911; *E. aculeata* Mezhev, 1981; *K. bilobata* Gurjanova, 1930; *M. usheri* Menzies, 1962a; *N. oblongus* Sars, 1870; *T. platycarpus* Hessler, 1970; *P. brevicornis* Hansen, 1916; *D. lineare* Sars, 1864; *E. serrata* Brix, 2006; *T. amicum* Stebbing, 1912; *M. papillata* Riehl, Wilson and Hessler, 2012; *M. elongata* Hansen, 1916; *M. minuta* Menzies, 1962b; *M. scotti* Riehl and Brandt, 2013; *M. curticornis* Birstein, 1973; *M. matildae* Riehl and Brandt, 2013; *M. spinifera* Sars, 1864; *M. antennamagna* Riehl and Brandt, 2010; *M. subinermis* Hansen, 1916; *M. roaldi* Riehl and Kaiser, 2012; *M. magnifica* Wolff, 1962; *M. ovata* Birstein, 1970; *U. thiotyntlus* sp. nov.; *U. solicipia* sp. nov.; *U. zapiola* sp. nov. Support values above branches are derived from jackknife resampling (10 000 repetitions; removal probability = 25; group frequencies). Below the branches, Bremer support (from 3758 trees, cut 0) and relative Bremer support (from 2344 trees, cut 0) are given. In cases for which absolute Bremer supports are followed with a question mark (?), the respective groups are supported by a value of 10 or higher. Jackknife values below 50 are not shown.

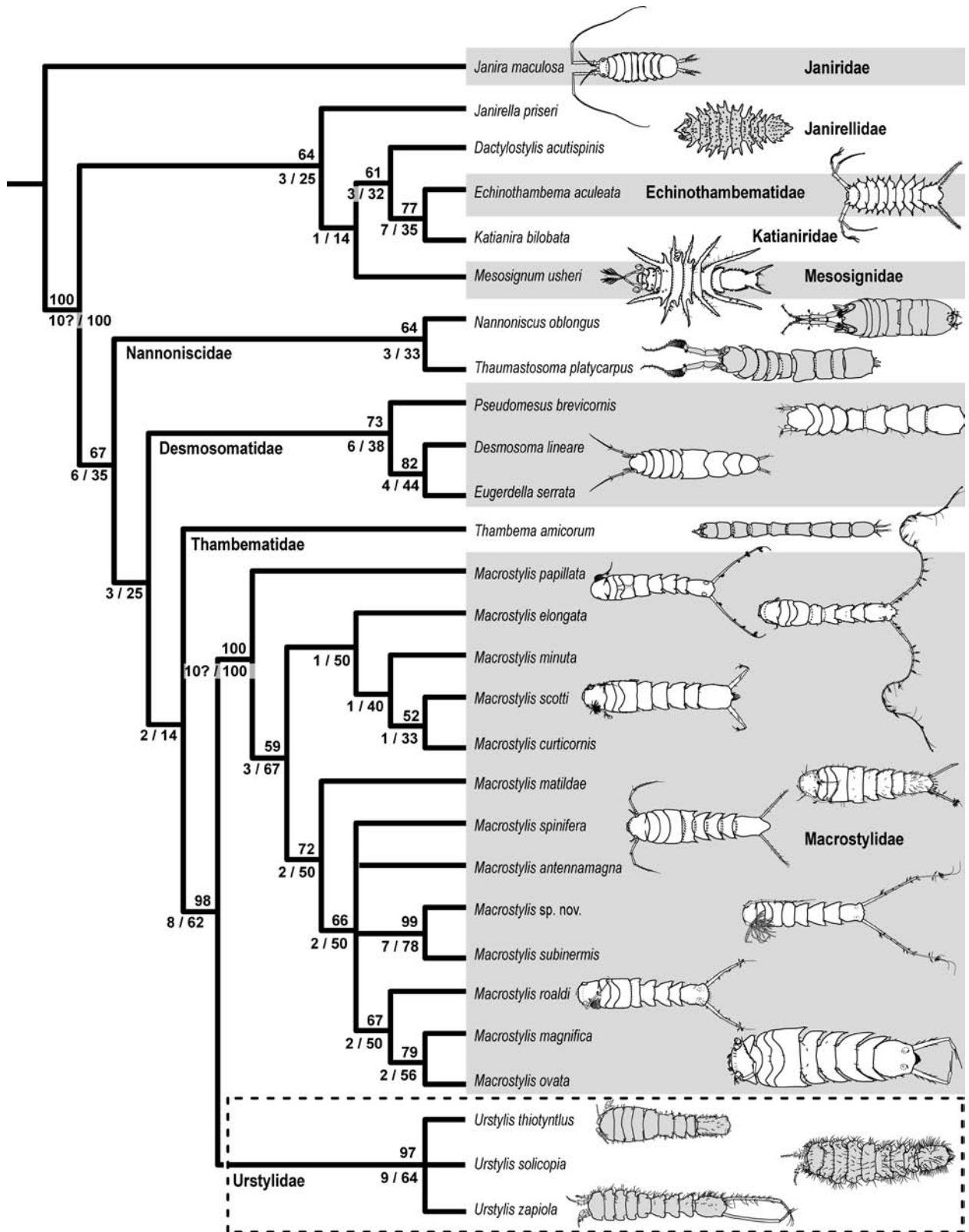
sister group to the new species but the *Urstylis* species share numerous derived character states. One example is the relatively short carpus (character 10) of the antenna. This podomere is elongate throughout the Asellota and, because this is also found in phreatoicids, it probably represents the plesiomorphic condition. In Janiroidea, however, this article is often distinctly longer than the combined length of the preceding articles, such as many Janiridae, Macrostylidae, Janirellidae, and Munnopsidae. Other group-specific characters lie in the proportions of the maxilliped (characters 14–17): the length–width ratio of the maxilliped palp article 2 (merus) is highly variable across Janiroidea. Some groups, such as Mesosignidae and *Dactylostylis*, show a consistently narrow article 2. Across the other families, both merus that are as long as wide and merus that are wider than long commonly occur.

The carposubchelate first pereopod (character 49) and the ventral comb of spinules are plesiomorphic, as seen in the Asellidae and Phreatoicidae. The inclusion of the dactylus, however, to form a carpopropodosubchela furnished with ventral robust setae participating in grasping are evolutionary novelties that independently arose in Urstylidae, Desmosomatidae, and Nannoniscidae. The first pereopod undergoes multiple other trans-

formations throughout the Asellota. Plesiomorphically (e.g. amongst Phreatoicidae, Asellidae, Stenetriidae, and other basal asellotans) the first pereopods are shorter than more posterior pereopods (character 50). In the Janiridae, males have a larger first pereopod than females, but this is complicated by the second pereopod also being sexually dimorphic in the species *Janira maculosa*.

In Macrostylidae, pereopod I is subsimilar in length to the second pereopod, whereas in the Urstylidae, it is always shorter – plesiomorphically according to our analyses. Amongst basally derived asellotes, the limb is plesiomorphically propodosubchelate (Wilson, 1987b, 2009), and it appears as a more leg-like structure in the basally derived janiroideans such as Janiridae, possibly via intermediate states (Wilson, 1986) in which both the carpus and propodus become enlarged (e.g. Munnidae and Paramunnidae).

Amongst the more derived janiroideans, a subchelate state occurs but with the palm being the carpus and the movable finger being the propodus and dactylus together. This pattern is complicated by several taxa having the propodosubchelate state amongst apparently more derived taxa (e.g. *Pleurocope* or *Torwolia*). To capture the transformations, many of which seem to be independent, the shapes of the carpus (character 48) and propodus as well as



the degree to which they oppose one another (character 49) are treated here as separate characters. In the plesiomorphic propodosubchelate state, the carpus is triangular, but it is trapezoidal (unique in Urstylidae and analogous to *Thaumastosoma* in the context of our analysis) or rectangular, and elonga-

te in the walking-leg-like pereopods. Other unique features can be found in the pleopods.

The short and stout male pleopod II exopod found in Janiroidea (character 68) is remarkably elongate in Urstylidae. A rather large number of complex synapomorphies for the three new

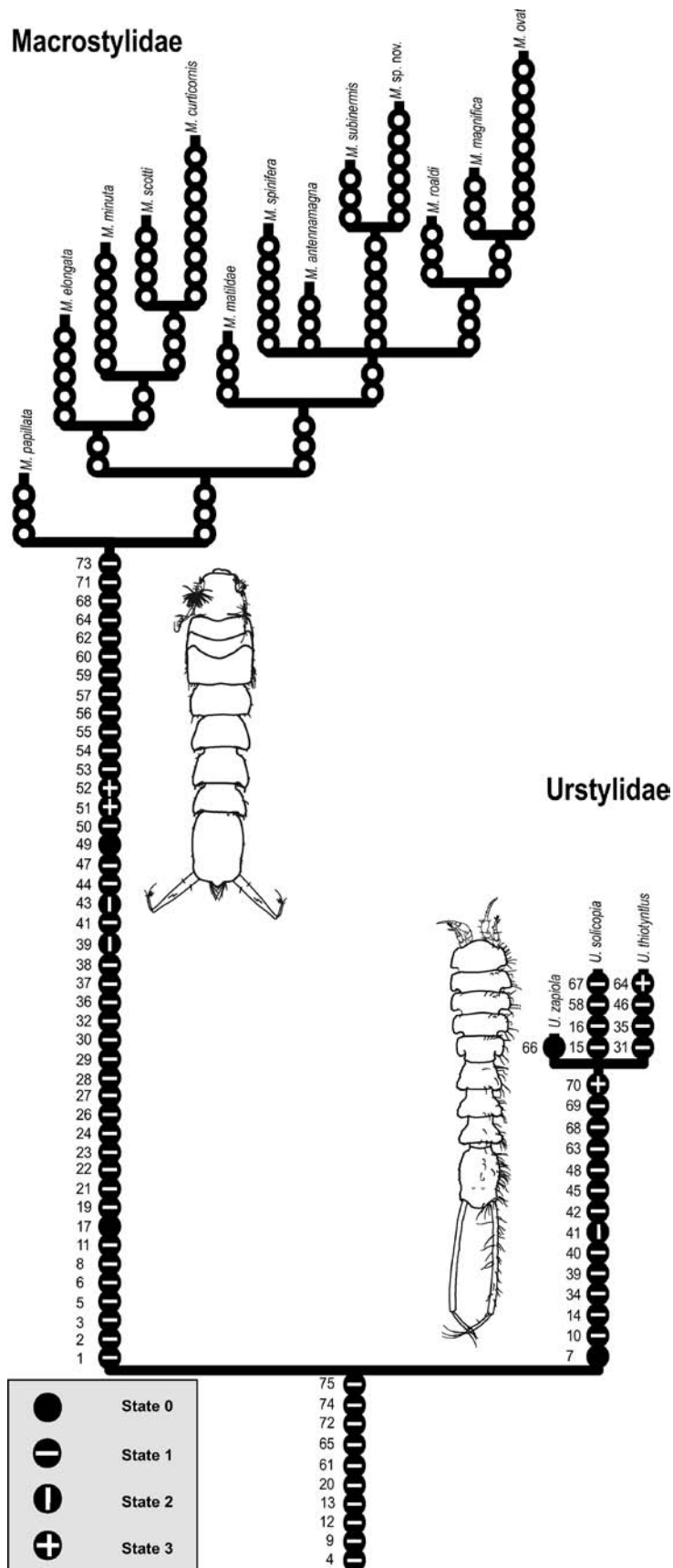


Figure 27. Synapomorphies for Urstylidae and subtaxa, as well as for Macrostylidae and their joint clade common to all four shortest trees mapped on the phylogenetic tree (Fig. 26). The number of synapomorphies is translated into branch length. Apomorphies for Macrostylidae are indicated but detailed information is omitted as these exceed the scope of this paper. Urstylidae fam. nov. is defined by 14 unique synapomorphies. Macrostylidae are highly derived and their large number (43) of synapomorphies is the main argument against the inclusion of *Urstylis* gen. nov. in this family. A sister-group relationship of both families is supported by ten shared apomorphies. M., *Macrostylis*; U., *Urstylis*.

Key to the species of Urstylidae

1. Body without sternal spines, (females) not keeled; pereonite 4 posterolateral margins rounded, with simple setae; pereonite 6 posterolateral margins produced posteriorly, rounded; pleotelson rather stout ($L/W < 1.5$), with anterior and posterior convex outline separated by concave waist; pereopod I positioned ventrally and orientated anteriorly, ischium dorsal margin projecting near basal width of segment.....2
- Body with sternal spines, partly keeled; pereonite 4 posterolateral margins acutely tapering, with robust, spine-like setae; pereonite 6 posterolateral margins not produced; pleotelson elongate ($L/W > 1.5$), subrectangular, waist only weakly pronounced, lateral margins subparallel; pereopod I positioned lateroventrally and orientated dorsolaterally, ischium dorsal margin projection much greater than basal width of segment.....*Urstylis thiotyntlus* sp. nov.
2. Body subcylindrical; pereonite 7 without posterolateral protrusions; pereopod VII shorter than pereopod VI; operculum with lateral setal fringe absent.....*Urstylis zapiola* sp. nov.
- Body dorsoventrally flattened; pereonite 7 with posterolateral protrusions similar to pereonite 6; pereopod VII length subsimilar pereopod VI length; operculum with lateral setal fringe present*Urstylis solycopia* sp. nov.

species as well as for Macrostylidae was accumulated. These outnumber the joint synapomorphies multiple times, so including the new taxa in Macrostylidae would result in a less definable group. Additionally, within the genus *Macrostylis* more (morphological) diversity is present than suggested by the monotypy of the family (Fig. 27). Macrostylids have never been revised systematically and the absence of generic diversity is owing to a lack of taxonomic effort rather than a lack of morphological variability (Riehl and Brandt, 2013). Riehl and Brandt (2013) found relatively large genetic divergence within macrostylids and hypothesized that thorough analyses are likely to reveal substantial

morphological diversity within *Macrostylis*.

Although all currently known macrostylids were studied, only a small subset was chosen here for practical reasons to represent the family. Nevertheless, because these represent distinct major clades within the monotypic family (T. Riehl, unpubl. data), the basal synapomorphies are likely to be fundamental for this taxon as a whole and the reciprocal monophyly can be generalized. As Macrostylidae internal relationships are beyond the scope of this paper, such characters have mostly been omitted in the analyses and character conceptualization.

Considering the clear distinction of the new

species from macrostylids overall, inclusion within this family would have negative practical effects on the concept of Macrostylidae. We thus are justified in the erection of a new family-level taxon: Urstylidae. We argue that this decision provides a more conservative and durable nomenclature.

Biogeographic Considerations

The phylogenetic analysis has another outcome that combines with other research on the age of deep-sea isopod groups. The low average density (approximately one individual in every 1.25 m) at which these isopods occur shows that they are rare in the fauna, but apparently the species are extremely widespread geographically. As we can conceive of no mechanism that would rapidly transport populations between the South Atlantic and the North Pacific, we conclude that their ancestors came to the two regions by crawling or perhaps movement by occasional erosive currents. The results of Lins *et al.* (2012) centre the branch leading to the Macrostylidae in the mid-Permian around 275 Mya (credibility interval ranges from the Upper Carboniferous to the upper Triassic). Our analyses place the Urstylidae on this branch. The geographical distance (~14 350 km) separating the *Urstylis* localities implies that the ancestral population began spreading several hundred million years ago. Thus, we believe the application of the prefix 'Ur' to the family name to be apt.

Acknowledgements

The invaluable support of A. Brandt to T. R. and M. V. M. is gratefully appreciated. S. Melnik is thanked for providing specimens and data from the Russian State Scientific Centre Yuhzmorgeologia expeditions and photographs from the type locality. F. Friedrich and R. Walter assisted with the

SEM. Financial support was granted by a PhD fellowship of the German National Academic Foundation (Studienstiftung des deutschen Volkes) and a Geddes fellowship of the Australian Museum to T. R. M. V. M. received funding from the Russian Foundation of Basis Research (Projects 11-04-98586). USA National Science Foundation grants to H. L. Sanders, J. F. Grassle (Woods Hole Oceanographic Institution) and R. R. Hessler (Scripps Institution of Oceanography) supported the collection and processing of the Atlantic Argentine Basin and Pacific hydrothermal mound samples. USA National Oceanographic and Atmospheric Administration contracts to P. A. Jumars (University of Washington), R. R. Hessler and G. D. F. W. (Scripps Institution of Oceanography) supported the collection and processing of the DOMES samples. S. Kaiser and two anonymous reviewers kindly provided constructive criticism on this work, which led to an improved paper.

References

- Birstein YA. 1970. New Crustacea Isopoda from the Kurile-Kamchatka Trench area. In: Bogorov VG, ed. Fauna of the Kurile-Kamchatka Trench and its environment. Proceedings of the Shirshov Institute of Oceanology (Vols 1–2, Vol. 86: 1). Moscow: Academy of Sciences of the USSR, 308–356.
- Birstein YA. 1973. Deep water isopods (Crustacea. Isopoda) of the north-western part of the Pacific Ocean. *Akademiya Nauk, SSSR: Moscow*, 1–213.
- Brandt A, Poore GCB. 2003. Higher classification of the flabelliferan and related Isopoda based on a reappraisal of relationships. *Invertebrate Systematics* 17: 893–923.
- Brix S. 2006. A new species of Desmosomatidae (Isopoda: Crustacea) from the deep Southern Ocean: *Eugerdella serrata* sp. nov. including remarks to the morphological variability within *Eugerdella* Hessler, 1970. *Mitteilungen aus dem Hamburger zoologischen Museum und Institut*, 69–84.
- Brökeland W. 2010. Description of four new species from the *Haploniscus unicornis* Menzies, 1956 complex (Isopoda: Asellota: Haploniscidae). *Zootaxa* 2536: 1–35.
- Brökeland W, Wägele J-W. 2004. Redescription of three

- species of *Haploniscus* Richardson, 1908 (Isopoda, Asellota, Haploniscidae) from the Angola Basin. *Organisms Diversity & Evolution* 4: 237–239.
- Brusca RC, Wilson GDF. 1991. A phylogenetic analysis of the Isopoda with some classificatory recommendations. *Memoirs of the Queensland Museum* 31: 143–204.
- Chardy P. 1972. *Janirella priseri* sp. n., Isopode abyssal de l'Atlantique nord. *Crustaceana. Supplement* 3: 11–18.
- Coleman CO. 2003. "Digital inking": how to make perfect line drawings on computers. *Organisms Diversity & Evolution* 3: 303–304.
- Coleman CO. 2009. Drawing setae the digital way. *Zoosystematics and Evolution* 85: 305–310.
- Dallwitz MJ. 1974. A flexible computer program for generating identification keys. *Systematic Biology* 23: 50–57.
- Dallwitz MJ. 1980. A general system for coding taxonomic descriptions. *Taxon* 29: 41–46.
- Dallwitz MJ. 1993. DELTA and INTKEY. In: Fortuner R, ed. *Advances in computer methods for systematic biology: artificial intelligence, databases, computer vision*. Baltimore, MD: Johns Hopkins University Press, 287–296. Available at: <http://delta-intkey.com>
- Dallwitz MJ, Paine TA, Zurcher EJ. 2010. User's guide to the DELTA editor. Available at: <http://delta-intkey.com>
- De Miranda AP, Barnier B, Dewar WK. 1999. On the dynamics of the Zapiola Anticyclone. *Journal of Geophysical Research* 104 (C9): 21137–21149.
- Flood RD, Shor AN, Manley PL. 1993. Morphology of abyssal mudwaves at project MUDWAVES sites in the Argentine Basin. *Deep Sea Research Part II: Topical Studies in Oceanography* 40: 859–888.
- Goloboff PA, Farris JS. 2001. Methods for quick consensus estimation. *Cladistics* 17: S26–S34.
- Goloboff PA, Farris JS, Nixon KC. 2008. TNT, a free program for phylogenetic analysis. *Cladistics* 24: 774–786.
- Grassle JF, Brown-Leger LS, Morse-Porteous L, Petrecca RF, Williams I. 1985. Deep-sea fauna in the vicinity of hydrothermal vents. *Bulletin of the Biological Society of Washington* 6: 443–452.
- Gurjanova E. 1930. Beiträge zur Fauna der Crustacea-Malacostraca des arktischen Gebietes. *Zoologischer Anzeiger* 86: 231–248.
- Hansen HJ. 1893. Zur Morphologie der Gliedmassen und Mundtheile bei Crustaceen und Insekten. *Zoologischer Anzeiger* 16: 193–212.
- Hansen HJ. 1916. Crustacea Malacostraca: the order Isopoda. *Danish Ingolf Expedition* 3: 1–262.
- Hessler RR. 1970. The Desmosomatidae (Isopoda, Asellota) of the Gay Head-Bermuda Transect. *Bulletin of the Scripps Institution of Oceanography* (Vol. 15). Berkeley, Los Angeles, CA, London: University of California Press.
- Hessler RR, Jumars PA. 1974. Abyssal community analysis from replicate box cores in the central North Pacific. *Deep Sea Research and Oceanographic Abstracts* 21: 185–209.
- Hessler RR, Strömberg JO. 1989. Behavior of janiroidean isopods (Asellota), with special reference to deep sea genera. *Sarsia* 74: 145–159.
- Hessler RR, Thistle D. 1975. On the place of origin of deep-sea isopods. *Marine Biology* 32: 155–165.
- Hessler RR, Wilson GDF, Thistle D. 1979. The deep-sea isopods: a biogeographic and phylogenetic overview. *Sarsia* 64: 67–75.
- Just J. 2005. Xenosellidae, a new family of Janiroidea (Asellota: Isopoda: Crustacea), for *Xenosella coxospinosa* gen. nov., sp. nov., from the marine bathyal of eastern Australia. *Zootaxa* 1085: 21–32.
- Just J, Wilson GDF. 2004. Revision of the *Paramunna* complex (Isopoda: Asellota: Paramunnidae). *Invertebrate Systematics* 18: 377–466.
- Just J, Wilson GDF. 2007. Revision of *Austrosignum* Hodgson and *Munnogonium* George & Strömberg (Paramunnidae) with descriptions of eight new genera and two new species. (Crustacea: Isopoda: Asellota). *Zootaxa* 1515: 1–29.
- Kaiser S, Barnes DKA. 2008. Southern Ocean deep-sea biodiversity: sampling strategies and predicting responses to climate change. *Climate Research* 37: 165–179.
- Kavanagh FA, Wilson GDF. 2007. Revision of the genus *Haplomesus* (Isopoda: Asellota: Ischnomesidae) with erection of four new genera. *Invertebrate Systematics* 21: 487–535.
- Kussakin OG. 1999. Marine and brackish-water isopods from cold and temperate waters of the Northern Hemisphere suborder Asellota. Part 2. Families Joeropsididae, Nannoniscidae, Desmosomatidae, Macrostylidae. *Keys to the fauna of the SSSR, Vol. 3*. St. Petersburg: A. F. Alimov, Publication of the Zoological Institute of the Russian Academy of Sciences.
- Latreille PA. 1802. Histoire naturelle générale et particulière des Crustacés et des Insectes. Histoire Naturelle generale et particuliere, nouvelle edition, accompagnee des notes, Vol. 3. Paris: G. L. L. Buffon, Dufart.
- Leach WE. 1814. Crustaceology. In: Brewster D, ed. *The Edinburgh Encyclopædia*. Edinburgh: A. Balfour, 383–437.
- Lilljeborg W. 1864. Bidrag til kändedommen om de inom

- Sverige och Norrige förekommande Crustaceer af Isopodernas underordning och Tanaidernas familj. Inbjudningsskrift till Åhörande af de Offentliga Föreläsningar. Upsala: CA. Leffler, Konglige Academie Boktryckare, 31 pp.
- Lins LSF, Ho SYW, Wilson GDF, Lo N. 2012. Evidence for Permo-Triassic colonization of the deep sea by isopods. *Biology Letters* 8: 979–982.
- Maddison WP, Maddison DR. 2011. Mesquite: a modular system for evolutionary analysis. Available at: <http://mesquiteproject.org>
- Malyutina MV. 2003. Revision of *Storothyngura* Vanhöffen, 1914 (Crustacea: Isopoda: Munnopsididae) with descriptions of three new genera and four new species from the deep South Atlantic. *Organisms Diversity & Evolution* 3: 245–252.
- Malyutina MV. 2008. *Microcope* gen. nov.—a new deep-sea genus of Munnopsidae (Crustacea, Isopoda, Asellota), with description of two new species from the Southern Hemisphere. *Zootaxa* 1866: 555–574.
- McLaughlin PA. 1980. Comparative morphology of recent crustacea. San Francisco, CA: W. H. Freeman.
- Menzies RJ. 1956. New abyssal tropical Atlantic isopods with observations on their biology. *American Museum Novitates* 1798: 1–16.
- Menzies RJ. 1962a. The zoogeography, ecology, and systematics of the Chilean marine isopods. Reports of the Lund University Chile Expedition 1948–1949, Vol. 42. Lund: CWK Gleerup.
- Menzies RJ. 1962b. The isopods of abyssal depths in the Atlantic Ocean. In: Barnard JL, Menzies RJ, Bacescu MC, eds. *Abyssal Crustacea*, Vema Research Series, Vol. 1. New York: Columbia University Press, 79–206.
- Mezhov BV. 1981. Isopoda. In: Kuznetsov AP, Mironov AN, eds. *Benthos of the Submarine mountains Marcus-Necker and adjacent Pacific regions*. Moscow: Academy of Sciences of the U.S.S.R. P. P. Shirshov Institute of Oceanology, 62–82.
- Osborn KJ, Madin LP, Rouse GW. 2011. The remarkable squidworm is an example of discoveries that await in deepelagic habitats. *Biology Letters* 7: 449–453.
- Pohl H. 2010. A scanning electron microscopy specimen holder for viewing different angles of a single specimen. *Microscopy Research and Technique* 73: 1073–1076.
- Prendini L. 2001. Species or supraspecific taxa as terminals in cladistic analysis? Groundplans versus exemplars revisited. *Systematic Biology* 50: 290–300.
- Ramirez-Llodra E, Brand A, Danovaro R, De Mol B, Escobar E, German CR, Levin LA, Martinez Arbizu P, Menot L, Buhl-Mortensen P, Narayanaswamy BE, Smith CR, Tittensor DP, Tyler PA, Vanreusel A, Vecchione M. 2010. Deep, diverse and definitely different: unique attributes of the world's largest ecosystem. *Biogeosciences* 7: 2851–2899.
- Raupach MJ, Held C, Wägele J-W. 2004. Multiple colonization of the deep sea by the Asellota (Crustacea: Peracarida: Isopoda). *Deep Sea Research Part II: Topical Studies in Oceanography* 51: 1787–1795.
- Raupach MJ, Mayer C, Malyutina MV, Wägele J-W. 2009. Multiple origins of deep-sea Asellota (Crustacea: Isopoda) from shallow waters revealed by molecular data. *Proceedings of the Royal Society B: Biological Sciences* 276: 799–808.
- Rex MA, McClain CR, Johnson NA, Etter RJ, Allen JA, Bouchet P, Warén A. 2005. A source-sink hypothesis for abyssal biodiversity. *The American Naturalist* 165: 163–178.
- Rex MA, Stuart CT, Hessler RR, Allen JA, Sanders HL, Wilson GDF. 1993. Global-scale latitudinal patterns of species diversity in the deep-sea benthos. *Nature* 365: 636–639.
- Richardson H. 1911. Les crustacés isopodes du Travailleur et du Talisman: formes nouvelles. *Bulletin du Museum National d'Histoire Naturelle* 17: 518–534.
- Richter S, Edgecombe GD, Wilson GDF. 2002. The *lacinia mobilis* and similar structures—a valuable character in arthropod phylogenetics? *Zoologischer Anzeiger – A Journal of Comparative Zoology* 241: 339–361.
- Riehl T, Brandt A. 2010. Descriptions of two new species in the genus *Macrostylis* Sars, 1864 (Isopoda, Asellota, Macrostylidae) from the Weddell Sea (Southern Ocean), with a synonymisation of the genus *Desmostylis* Brandt, 1992 with *Macrostylis*. *Zookeys* 57: 9–49.
- Riehl T, Brandt A. 2013. Southern Ocean Macrostylidae reviewed with a key to the species and new descriptions from Maud Rise. *Zootaxa* 3692: 160–203.
- Riehl T, Kaiser S. 2012. Conquered from the deep sea? A new deep-sea isopod species from the Antarctic shelf shows pattern of recent colonization. *PLoS ONE* 7: e49354.
- Riehl T, Wilson GDF, Hessler RR. 2012. New Macrostylidae Hansen, 1916 (Crustacea: Isopoda) from the Gay Head-Bermuda transect with special consideration of sexual dimorphism. *Zootaxa* 3277: 1–26.
- Sanders HL, Hessler RR, Hampson GR. 1965. An introduction to the study of deep-sea benthic faunal assemblages along the Gay Head-Bermuda transect. *Deep Sea Research and Oceanographic Abstracts* 12: 845–867.
- Sars GO. 1864. Om en anomal Gruppe af Isopoder. *Forhandlinger Videnskaps-Selskapet, Anar* 1863. Christiania, 205–221.
- Sars GO. 1870. Nye Dybvandscrustaceer fra Lofoten. Særskilt aftrykt af Videnskaps-Selskapet, *Forhandlinger for* 1869. Christiania, 147–174.

- Sars GO. 1897. On some additional Crustacea from the Caspian Sea. *Annales du Musée Zoologique Academie Imperiale des Sciences St. Petersburg* 2: 273–305.
- Schotte M, Boyko CB, Bruce NL, Poore GCB, Taiti S, Wilson GDF. 2013. Isopoda, Janiroidea. World marine, freshwater and terrestrial isopod crustaceans database. Available at: <http://www.marinespecies.org/Isopoda/aphia.php?p=taxdetails&id=155716>
- Schultz GA. 1969. The marine isopod crustaceans. Hampton, NJ: William C. Brown Company.
- Stebbing TRR. 1912. On the Crustacea Isopoda of the ‘Porcupine’ expedition – abstract. *Proceedings of the Zoological Society of London* 4: 42.
- Stebbing TRR. 1913. On the Crustacea Isopoda from the ‘Porcupine’ expedition. *Transactions of the Zoological Society of London* 20: 231–246.
- Svavarsson J. 1987. Reevaluation of *Katianira* in Arctic waters and erection of a new family, Katianiridae (Isopoda: Asellota). *Journal of Crustacean Biology* 7: 704–720.
- Thistle D, Wilson GDF. 1987. A hydrodynamically modified, abyssal isopod fauna. *Deep-Sea Research. Part A. Oceanographic Research Papers* 34: 73–87.
- Thistle D, Wilson GDF. 1996. Is the HEBBLE isopod fauna hydrodynamically modified? A second test. *Deep-Sea Research Part I* 43: 545–554.
- Vanhöffen E. 1914. Die Isopoden der Deutschen Südpolar-Expedition 1901–1903. In: Drygalsky E, ed. *Deutsche Südpolarexpedition 1901–1903. Zoologie (Vol. 7)*. Berlin: Georg Reimer, 449–598.
- Veuille M. 1980. Sexual behaviour and evolution of sexual dimorphism in body size in *Jaera* (Isopoda Asellota). *Biological Journal of the Linnean Society* 13: 89–100.
- Wägele J-W. 1983. On the homology of antennal articles in Isopoda. *Crustaceana* 45: 31–37.
- Wägele J-W. 1989. Evolution und phylogenetisches System der Isopoda: Stand der Forschung und neue Erkenntnisse. *Zoologica (Vol. 140)*. Stuttgart: E. Schweizerbart’sche Verlagsbuchhandlung.
- Wilson GDF. 1976. The systematics and evolution of *Haplomunna* and its relatives (Isopoda, Haplomunnidae, new family). *Journal of Natural History* 10: 569–580.
- Wilson GDF. 1985. The systematic position of the Ilyarachnoid Eurycopidae (Crustacea, Isopoda, Asellota). Unpublished PhD dissertation, University of California, San Diego.
- Wilson GDF. 1986. Evolution of the female cuticular organ in the Asellota (Crustacea, Isopoda). *Journal of Morphology* 190: 297–305.
- Wilson GDF. 1987a. Crustacean communities of the manganese nodule province (DOMES site A compared with DOMES site C). Report for the National Oceanic and Atmospheric Administration Office of Ocean and Coastal Resource Management (Ocean Minerals and Energy) no. NA-84-ABH-0030 (p. 44). La Jolla, California 92093: Scripps Institution of Oceanography.
- Wilson GDF. 1987b. The road to the Janiroidea: comparative morphology and evolution of the asellote isopod crustaceans. *Journal of Zoological Systematics & Evolutionary Research* 25: 257–280.
- Wilson GDF. 1989. A systematic revision of the deep-sea subfamily Lipomerinae of the isopod crustacean family Munnopsidae. *Bulletin of the Scripps Institution of Oceanography (Vol. 27)*. Berkeley, Los Angeles, CA, London: University of California Press.
- Wilson GDF. 1991. Functional morphology and evolution of isopod genitalia. In: Bauer RT, Martin JW, eds. *Crustacean sexual biology*. New York: Columbia University Press, 228–245.
- Wilson GDF. 1998. Historical influences on deep-sea isopod diversity in the Atlantic Ocean. *Deep Sea Research Part II: Topical Studies in Oceanography* 45: 279–301.
- Wilson GDF. 2008. A review of taxonomic concepts in the Nannoniscidae (Isopoda, Asellota), with a key to the genera and a description of *Nannoniscus oblongus* Sars. *Zootaxa* 1680: 1–24.
- Wilson GDF. 2009. The phylogenetic position of the Isopoda in the Peracarida (Crustacea: Malacostraca). *Arthropod Systematics & Phylogeny* 67: 159–198.
- Wilson GDF. 2013. Janiroidea incertae sedis. In: Schotte M, Boyko CB, Bruce NL, Poore GCB, Taiti S, Wilson GDF, eds. *World marine, freshwater and terrestrial isopod crustaceans database*. Available at: <http://www.marinespecies.org/Isopoda/aphia.php?p=taxdetails&id=268172> on 18 September 2013.
- Wirkner CS, Richter S. 2010. Evolutionary morphology of the circulatory system in Peracarida (Malacostraca; Crustacea). *Cladistics* 26: 143–167.
- Wolff T. 1962. The systematics and biology of bathyal and abyssal Isopoda Asellota. *Galathea Report* 6: 1–320.
- Yeates DK. 1995. Groundplans and exemplars: paths to the tree of life. *Cladistics* 11: 343–357.

Supporting Information

Additional Supporting Information may be found

in the online version of this article at the publisher's web-site:

Appendix S1. Urstylidae matrix trees: http://onlinelibrary.wiley.com/store/10.1111/zoj.12104/asset/supinfo/zoj12104-sup-0001-appendix_s1.nex?v=1&s=2d1511887fec307b4583a636731a8987eaf085d7

Appendix S2. Information on isopod diversity at type locality of *Urstylis zapiola*:

Remarks on the faunal composition at the type locality of *Urstylis zapiola* sp. nov., gen. nov.

Urstylis zapiola was collected in a particularly large epibenthic sample (WHOI 247) from the abyssal plain of the Argentine Basin: subsample A; the sample was so large that it was split into two parts. This subsample had 1,316 individuals and 72 species of isopods with representatives of the families Munnopsidae (21 species), Desmosomatidae (12), Nannoniscidae (9), Ischnomesidae (5), Macrostylidae (5 - including *Urstylis*), Haploniscidae (5), Acanthaspidiidae (3), Dendrotionidae (1), Haplommunnidae (1), Paramunnidae (1), Mesosignidae (1), Thambematidae (1), incertae sedis (*Xostylus* and *Sugoniscus*), Arcturidae (3), Serolidae (1), Paranthuridae (1). This locality is below 5,200m showing that isopod species richness can be high, even at the greatest abyssal depths.

Author contributions

This study was designed by myself. Preliminary species identification was conducted by G.D.F. Wilson and M.V. Malyutina amongst others. Specimens were dissected and illustrated by myself and G.D.F. Wilson with contributions from M.V. Malyutina. All digital artwork was conducted by G.D.F. Wilson and myself. The phylogenetic database was developed and the analyses performed

by myself with contributions from G.D.F. Wilson. The taxonomic database was built by myself with contributions from G.D.F. Wilson. I developed the descriptions. The manuscript was written by myself with contributions from G.D.F. Wilson and M.V. Malyutina.

Chapter 6

A comparative review of the morphology of Macrostylidae (Isopoda) from the phylogenetic perspective

Uⁿpublished manuscript

Abstract

The isopod family Macrostylidae (Crustacea) shows interesting distribution patterns across all oceans and can be found from sublittoral to the hadal zone. Macrostylids may thus provide fascinating clues on the colonization history of continental shelves, slopes, abyssal basins and deep-ocean trenches. A lack of insight on this group's evolutionary history, however, currently does not allow using this taxon as a model group. In this paper, the current knowledge of macrostylid morphology is reviewed to improve our understanding of their phylogeny. A cladistic analysis of macrostylids in the context of related taxa of their parent superfamily Janiroidea was conducted. It allows, for the first time, to discuss their apomorphies in the light of potential key innovations that lead to the success of this group. Moreover, character concepts are established through a comparative study of macrostylid morphology. We are thus setting the baseline for understanding the relationships and colonization history of Macrostylidae across oceans and depths.

Key words: deep sea – Janiroidea – character states – sexual dimorphism – key innovations – evolution – phylogenetic systematics

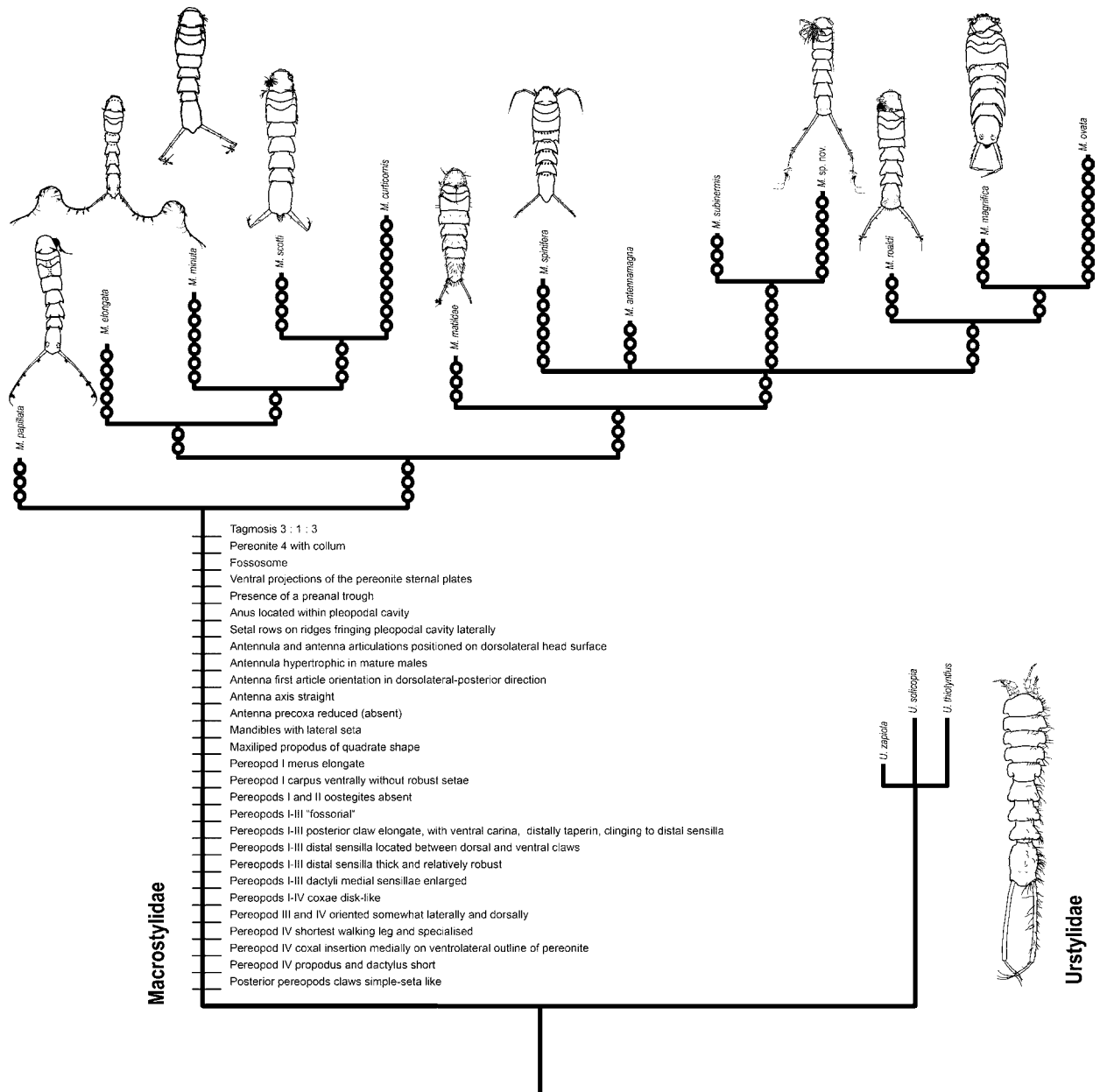


Figure 1. Excerpt of strict consensus of four most parsimonious trees, based on the morphological character dataset by Riehl et al. (2014), analyzed under equal weights, showing the synapomorphies of Macrostyliidae. The terminal taxa are exemplar species. Ingroup taxa: *M. papillata* Riehl, Wilson & Hessler, 2012; *M. elongata* Hansen, 1916; *M. minuta* Menzies, 1962; *M. scotti* Riehl & Brandt, 2013; *M. curticornis* Birstein, 1973; *M. matildae* Riehl & Brandt, 2013; *M. spinifera* Sars, 1864; *M. antennamagna* Riehl & Brandt, 2010; *M. subinermis* Hansen, 1916; *M. roaldi* Riehl & Kaiser, 2012; *M. magnifica* Wolff, 1962; *M. ovata* Birstein, 1970. Outgroup: *U. thiotyntus* Riehl et al 2014; *U. solicipia* Riehl et al 2014; *U. zapiola* Riehl et al 2014. The number of synapomorphies is translated into branch length. M, *Macrostyliis*; U, *Urstyliis*.

Introduction

The isopod family Macrostyliidae Hansen, 1916 (Asellota, Janiroidea) is cosmopolitan in the deep sea (Kussakin 1999; Riehl and Brandt 2010). Macrostyliids are common members of bathyal and abyssal communities (Brandt et al. 2005, 2007b; Wilson 2008b) where they are thought to prima-

rily live as endofauna in soft sediments (Thistle and Wilson 1987, 1996; Hessler and Strömberg 1989). The family has a remarkable depth distribution (Hessler et al. 1979; Brandt et al. 2009) extending from sublittoral (e.g. *Macrostyliis spinifera* Sars, 1864 at ~ 30 m depth (Sars 1899)) down to the deepest hadal trenches (e.g. *M. mariana* Wolff, 1956 at 10,730 m). Due to their wide bathymetric

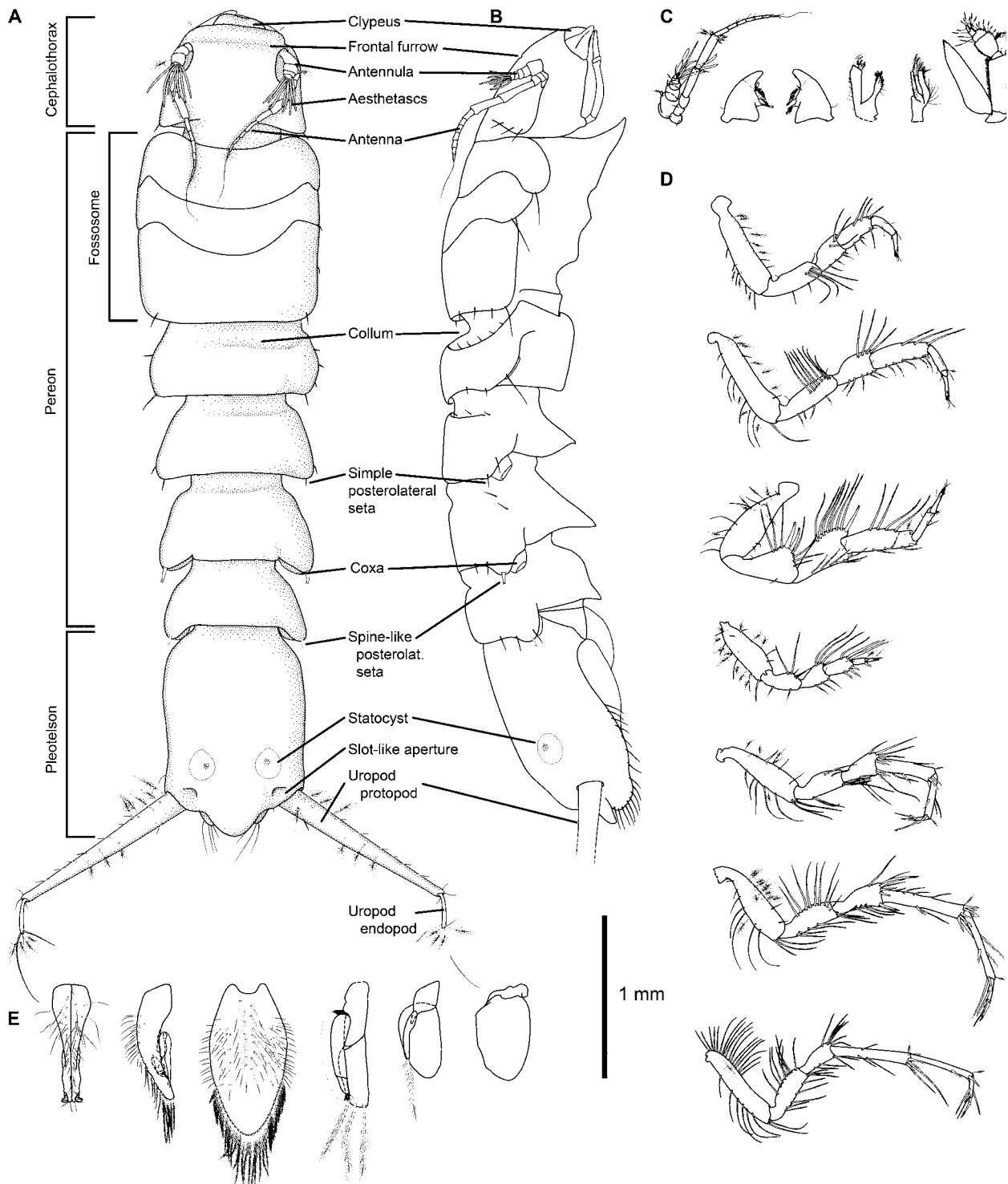


Figure 2. Schematic illustration of general morphological features of Macrostylidae (Crustacea: Isopoda) based upon and modified after drawing of *Macrostylis scotti* Riehl & Brandt, 2013. **A:** habitus dorsal. **B:** habitus lateral. **C:** head appendages from left to right: antennula and antenna, left and right mandibles, Maxillula, maxilla, maxilliped. **D:** pereopods 1–7. **E:** pleotelson appendages from left to right: male pleopods I, male pleopod II, female operculum, pleopods III–V. B

and geographic range, phylogenetic estimates in Macrostylidae might provide fascinating clues on shelf-to-deep-sea colonizations (Riehl and Kaiser 2012).

However, despite their relatively frequent occurrence in deep-sea benthic samples (Sars 1864;

Beddard 1886; Hult 1941; Wolff 1962; Birstein 1970), until now macrostylid relationships remain unclear (Riehl and Brandt 2013). Despite molecular data pointing to high interspecific divergence (Riehl and Brandt 2013), the family is currently considered monotypic with only a single genus

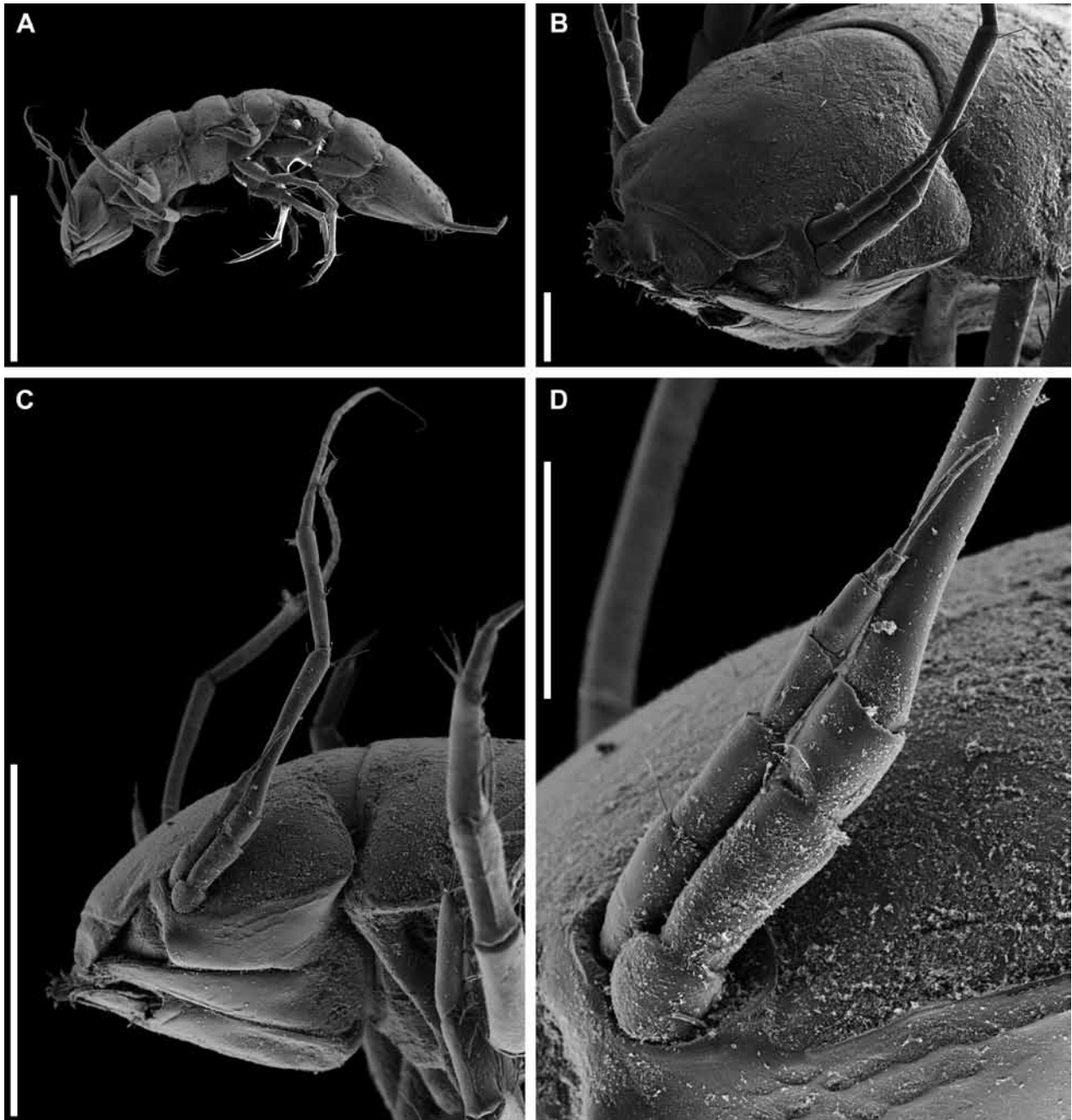


Figure 3. *Macrostylis* sp. (DIVA 3 #7) non-ovigerous female. **A:** habitus lateral. **B:** cephalothorax, dorsolateral. **C:** cephalothorax, antennula and antenna, lateral. **D:** antennula, close-up. Scales: A = 1.0 mm; B,D = 100 μ m; C = 0.5 mm.

Macrostylis Sars, 1864 (Riehl and Brandt 2010). Genetic insights, however, are relatively scarce for macrostylids as for deep-sea organisms in general (Zardus *et al.* 2006; Brix *et al.* 2011; Havermans *et al.* 2013; Kaiser *et al.* 2013). Morphologically, intrafamilial relationships seem to be concealed by high interspecific conformity (Riehl and Brandt 2010) as well as strong sexual dimorphism (Riehl *et al.* 2012).

A recently published phylogenetic analysis suggested Urstylidae Riehl, Wilson and Malyu-

tina, 2014 to represent the closest extant relative of Macrostylidae (Riehl *et al.* 2014). It included, amongst other Janiroidea, a limited but representative macrostylid taxon sampling. Here, we build upon this dataset to review the synapomorphies of Macrostylidae in the light of evolutionary key innovations (Mayr 1960). Furthermore, a comparative study of macrostylid morphology is conducted. Morphological characters are outlined and hypotheses about homological states are made. We hence set the baseline for future thorough analyses

on inner-macrostyliid relationships and a revision of this so far monotypic family.

Material and methods

Taxon- and Character Sampling

The taxonomic literature available for Macrostyliidae was reviewed and type as well as other collection material was extensively studied (Table 1). Samples were collected during the BIOICE project with different Icelandic, Norwegian and Faroe vessels, during the ANDEEP and ANDEEP-SYSTCO projects with Research Vessel (RV) Polarstern (ANT XIX/2-3, XXII-3; (Brandt *et al.* 2007a; Brandt *et al.* 2011)), the KuramBio project with RV Sonne (SO223, Brandt and Malyutina, 2012), the DIVA-3 and IceAGE projects with RV Meteor (M79/1, M85/3; Brix, 2011). The vast majority of samples was collected by means of epibenthic sledges (Brenke 2005; Brandt *et al.* 2013).

Terminology

Terminology is largely based on previous work on Janiroidea (Hessler 1970; Wilson 1989; Riehl and Brandt 2010; Riehl and Brandt 2013; Wilson 2013; Riehl *et al.* 2014). A glossary is provided in the electronic supplement to define taxon-specific terms. The podomeres of the antenna are named following Hansen's (1893) approach.

Morphology

The morphology of Macrostyliidae was analyzed using light microscopy and scanning-electron microscopy (SEM) (see taxonomy section below). For light microscopy, whole specimens were transferred from 70–96% ethanol to an ethanol-glycerine solution (1:1) and subsequently to glycerine. For illustration of appendages in standard views,

dissected parts were temporarily mounted on slides following Wilson (2008a) and stained with Methyl Green or Chlorazol Black.

For SEM, specimens were gradually transferred to 99% ethanol and subsequently critical-point dried. A Carl Zeiss Leo 1525 microscope was used for SEM and specimens were mounted according to the methods described by Riehl *et al.* (2012) or on a specimen holder after Pohl (2010). SEM photographs were edited using Adobe Photoshop CS5. For figure assembly, structures of interest were cropped and backgrounds removed without altering the structures themselves. Line illustrations (taxonomic drawings and trees) were prepared using Adobe® Illustrator® following the methods of Coleman (Coleman 2003, 2009; see also Appendix 2).

Phylogeny

Starting with a review of the synapomorphies of the isopod family Macrostyliidae, character concepts are proposed in the second part of the paper.

For the review of macrostyliid synapomorphies, a recently published morphological dataset (Riehl *et al.* 2014) was re-analyzed following the same methods. The morphological traits of the ingroup (= Macrostyliidae) were compared with related deep-sea taxa of the Janiroidea Sars, 1897 (Desmosomatidae Sars, 1897; Echinothambematidae Menzies, 1956, Janirellidae Menzies, 1956; Katianiridae Svavarsson, 1987; Nannoniscidae Hansen, 1916; Thambematidae Stebbing, 1913; Urstyliidae Riehl, Wilson and Malyutina, 2014). The dataset was evaluated in Mesquite (Maddison and Maddison 2011) and analyzed phylogenetically using a parsimony approach in TNT (Goloboff *et al.* 2008). The dataset was originally composed to evaluate the relationships of the Urstyliidae but contained a representative taxon sampling of Mac-

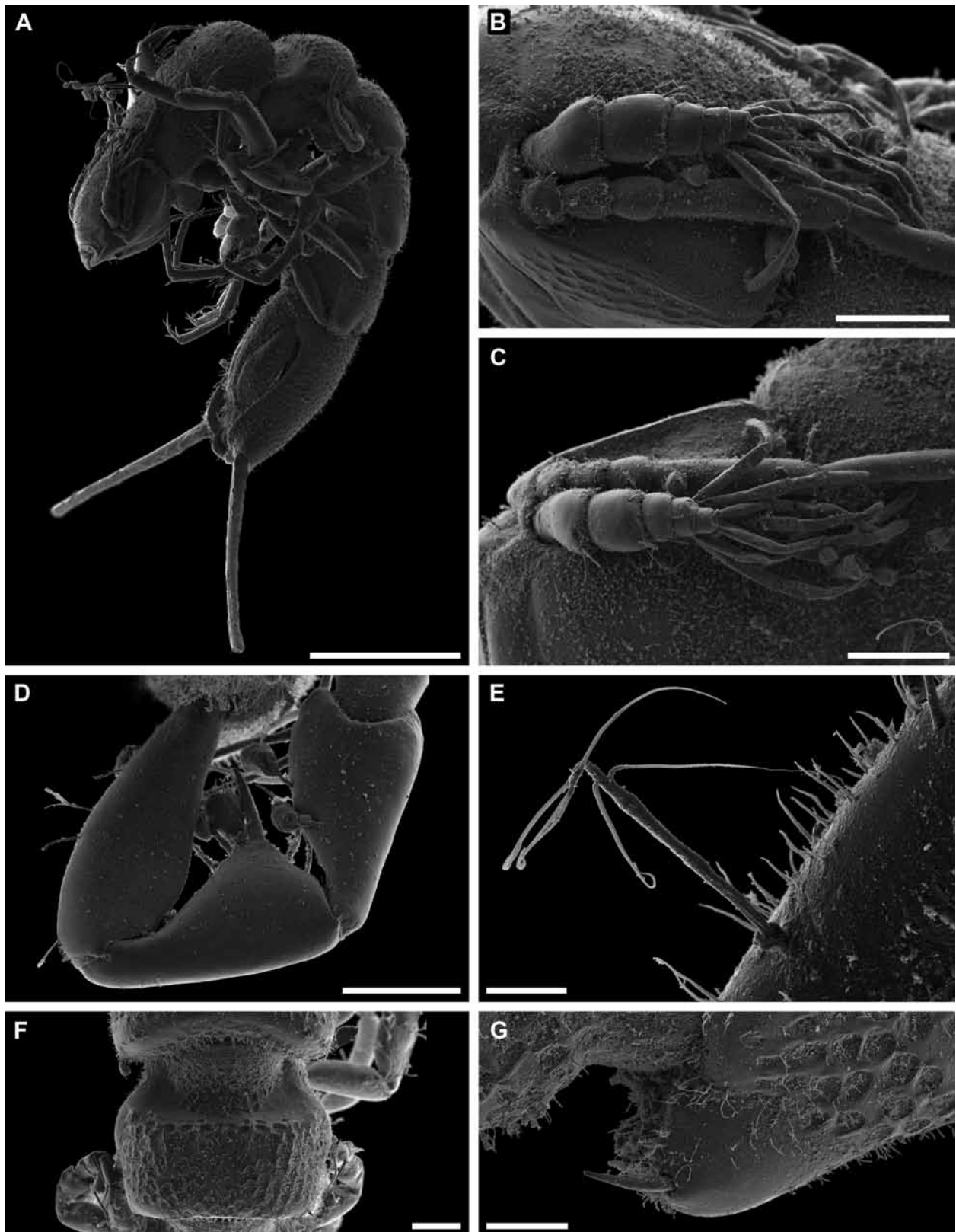


Figure 4. *Macrostylis* sp. (KuramBio #6) adult male. **A:** habitus. **B:** antennula, close-up, lateral. **C:** antennula, close-up, dorsal. **D:** pereopod III ischium, anterior. **E:** broom seta on pereopod VII basis. **F:** pereonite 4 with large collum, dorsal. **G:** pereonite 5 posterolateral margin and seta, dorsal. Scales: A = 0.5 mm; B–D, F = 100 μ m; E = 10 μ m; G = 50 μ m.

rostylidae as well. Hence, in this paper we interpret the results from a new perspective, focussing on the synapomorphies of Macrostylidae.

To set the baseline for a macrostylid phylo-

geny, interspecific differences were analyzed and homology hypotheses were made. This character conceptualization follows the approach presented by Wirkner and Richter (2010). States of 117 cha-

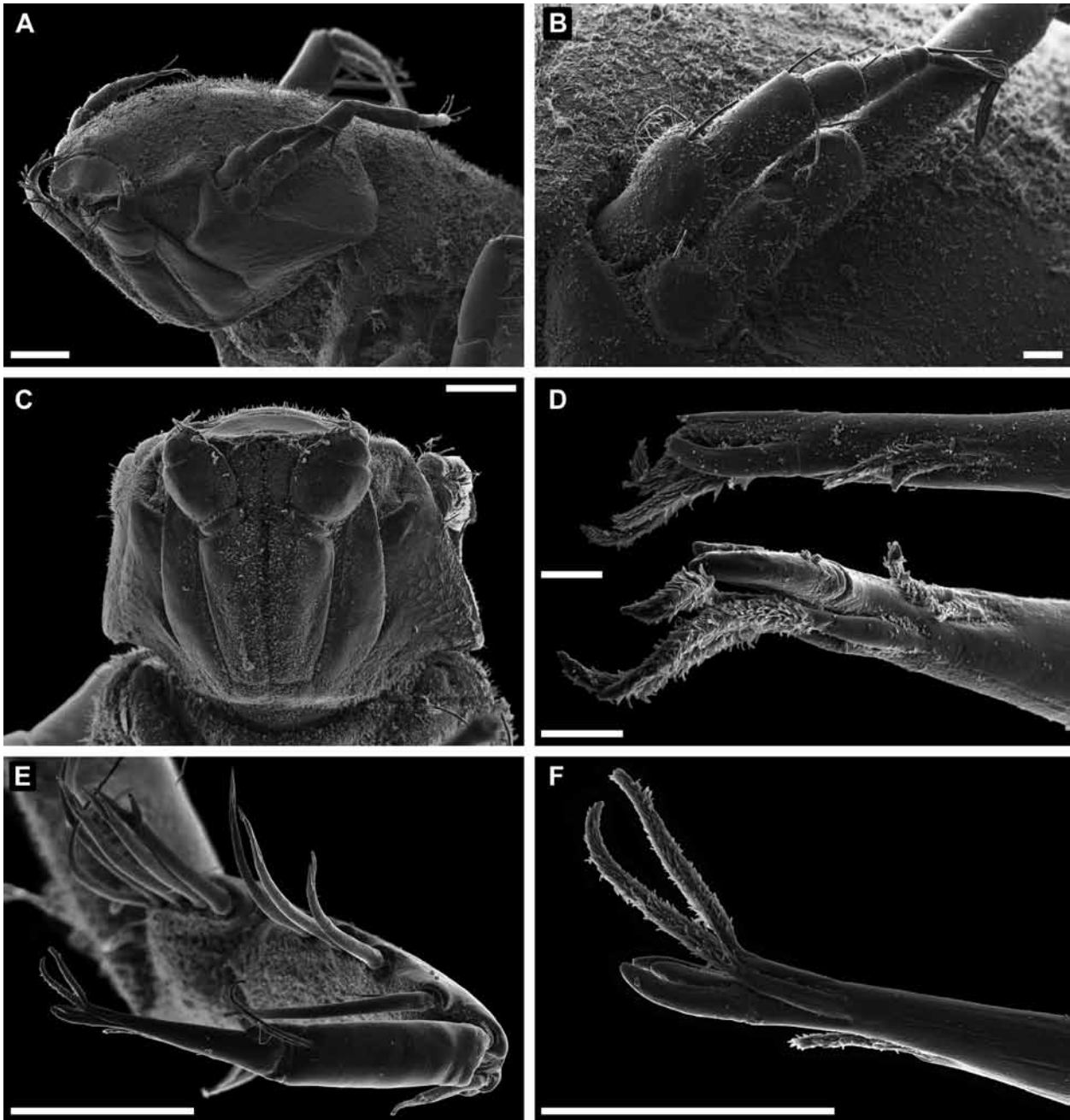


Figure 5. *Macrostylys* sp. (KuramBio #6) non-ovigerous female. **A:** cephalothorax. **B:** antennula, close-up, lateral. **C:** cephalothorax, maxillipeds ventral. **D:** pereopod dactylus claws and sensillae, ventral (top) and lateral (bottom). **E–F:** pereopod III propodus, dactylus, dorsal (anterior). Scales: A, C, E = 100 μm ; B = 20 μm ; D, F = 10 μm .

racters were newly defined.

Key innovations in macrostyloid evolution

Macrostyliidae comprises a robustly supported monophyletic branch of the Janiroidea tree. The macrostyloid clade is characterized by a long list of apomorphic characters compared to other groups (Figure 1). It seems to be highly derived and ho-

mogeneous in comparison with potentially related taxa, such as Thambematidae, Urstyliidae, Desmosomatidae and Nannoniscidae (Wägele 1989; Riehl *et al.* 2014).

Cephalothorax and head appendages

The macrostyloid head comprises several characters that seem to be evolutionary novelties unique to this taxon. The articulation socket shared by the antennula and antenna (see e.g. Fig. 2A, B, Fig. 3B, C, Fig. 4A–C, Fig. 5A, B), unlike in any other janiroid

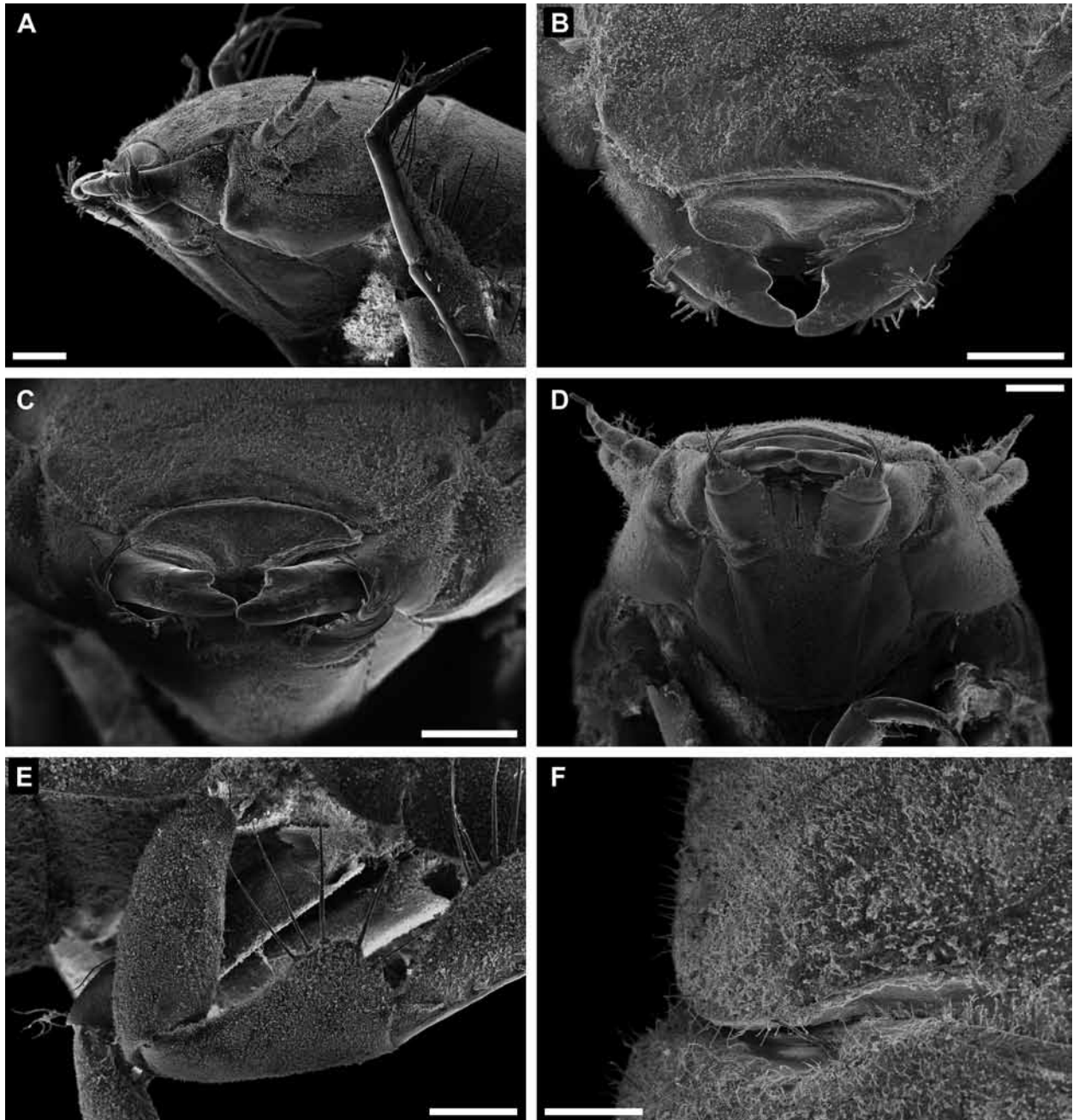


Figure 6. *Macrostylis subinermis* Hansen, 1916 non-ovigerous female. **A:** cephalothorax lateral. **B:** clypeus, labrum and mandibles, dorsal. **C:** mouthparts, frontal. **D:** cephalothorax, maxillipeds, ventral. **E:** pereopod III ischium, lateral (posterior). **F:** cephalothorax posterolateral margin. Scales: A–E = 100 μm ; F = 50 μm .

isopod, is positioned on the dorsolateral surface of the cephalothorax (Fig. 2). Similarly apomorphic is the orientation of the first antennal article in a dorsolateral and posterior direction (Fig. 6D) and the relatively straight axis of the antenna where all segments are cylindrical with aligned articulations (Fig. 3C). These novelties may be adaptations related to burrowing behavior, where the head is used to push into the sediment such as it appears to be in *Macrostylis* species (Hessler and Strömberg 1989). The closest known relatives, such as

Urstylidae, and most of the more distantly related Janiroidea have the plesiomorphic anterior articulation and orientation of the basal articles of antennula and antenna, and diverse variations of cuneiform antenna segments that allow for a curved or bent axis of the relaxed antenna (Riehl *et al.* 2014). Intermediate conditions for these head characters are presently not known.

Size increase of the antennulae in adult males (compare Fig. 4A, B with Fig. 5A, B) might be the result of sexual selection and an outbreeding

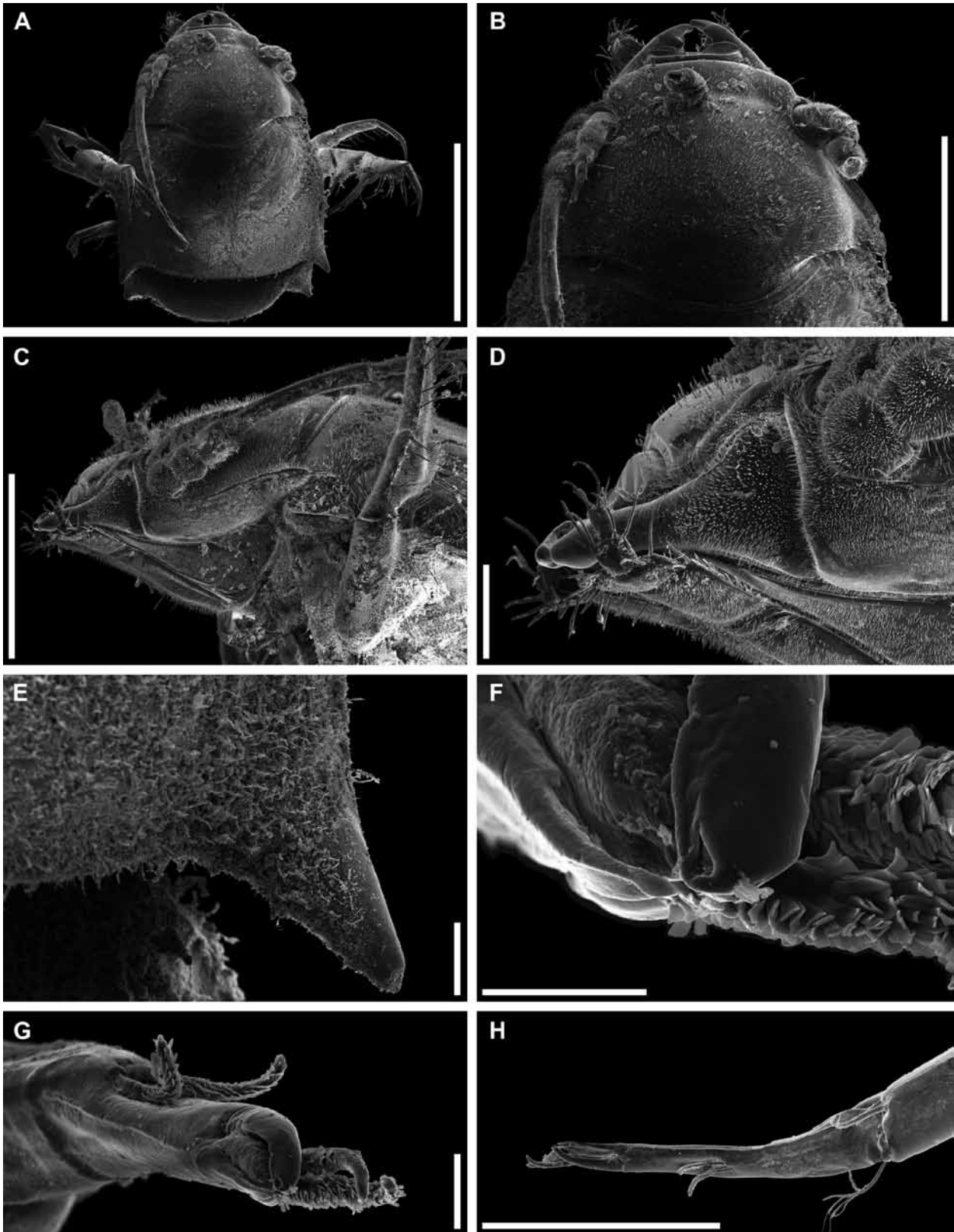


Figure 7. *Macrostylis magnifica* Wolff, 1962 juvenile female. **A:** cephalothorax and fossosome, dorsal. **B:** cephalothorax, dorsal. **C:** cephalothorax, lateral. **D:** mandibles, lateral. **E:** pereonite 3 posterolateral projection, dorsal. **F, G:** pereopod III dactylus claws. **H:** pereopod III dactylus. Scales: A=1.0 mm; B, C: 0.5 mm; D, H = 100 μ m; E = 50 μ m; E = 5.0 μ m.

mate-search strategy (Riehl *et al.* 2012). Although males are often not known or poorly (if at all) illustrated in the literature, similar enlargements can be observed in katianirids and most munnopsids

as well. Its evolution might be triggered by the reduction of the general antennular size and must be considered homoplastic in the latter taxa according to the analysis by Riehl *et al.* (2014).

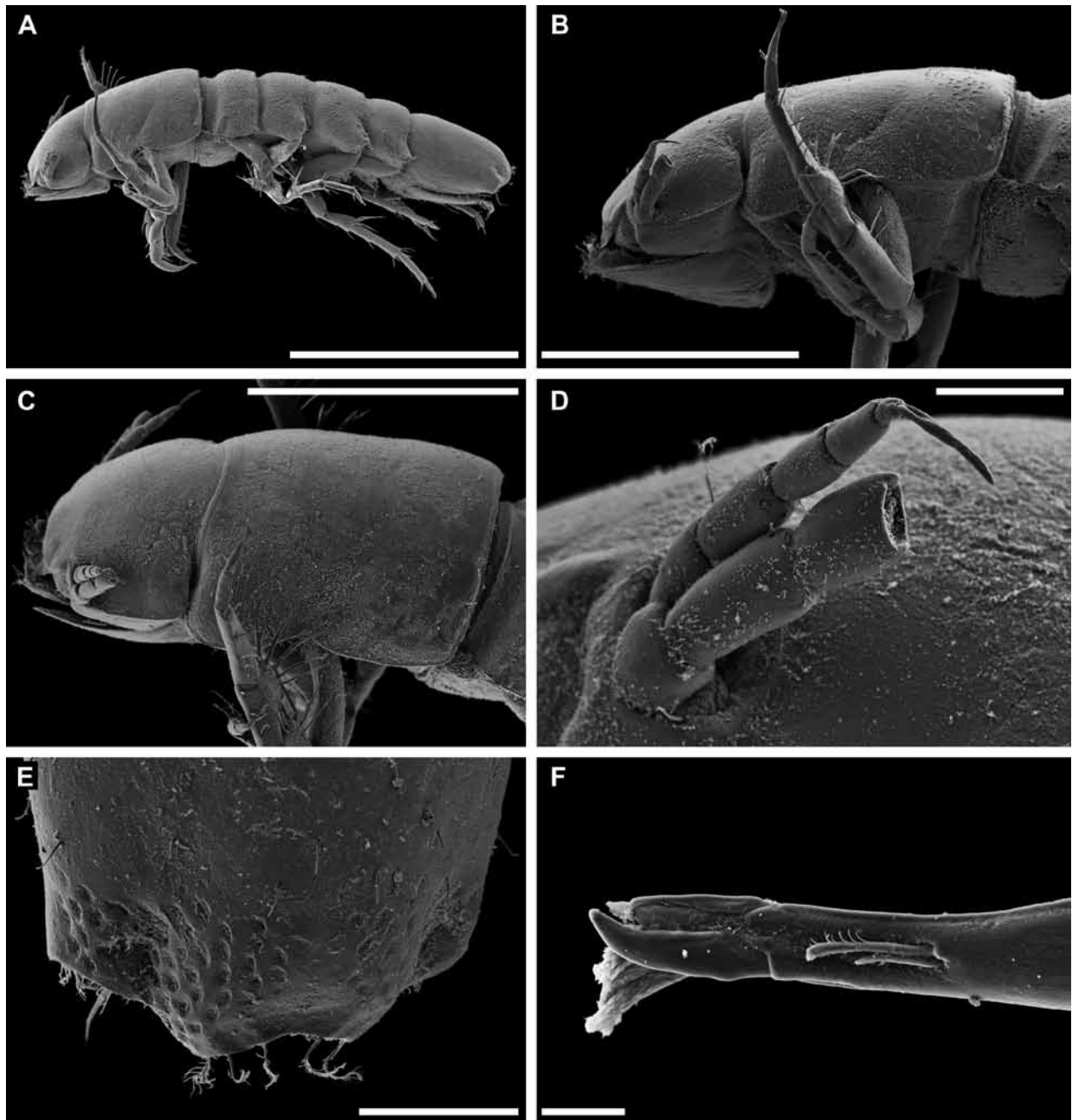


Figure 8. *Macrostylis* sp. (Diva 3 #7) non-ovigerous female. **A:** habitus, dorsolateral. **B:** cephalothorax and fossosome, lateral. **C:** cephalothorax and fossosome, dorsal. **D:** antennula, close-up, lateral. **E:** pleotelson posterior margin. **F:** pereopod III dactylar claws, lateral (ventral). Scales: A = 1.0 mm; B, C = 0.5 mm; D = 50 μ m; E = 100 μ m; F = 10 μ m.

Besides the antennula, the macrostylid antenna also shows indications of reductions. Whereas the occurrence of a precoxa in the antennal protopod is limited to some genera of the Cirolanidae Dana, 1853, Ligiidae Leach, 1814 and Microcerberidae Karaman, 1933 as well as most of the Asellota, the antennal protopod consists of coxa and basis only in all other groups (Hansen 1893; Wägele 1983; Brusca and Wilson 1991) making up altogether five podomeres (coxa–carpus). Amongst the Asellota, a precoxa, and thus six podomeres, are commonly

present in all superfamilies (Aselloidea, Janiroidea, Gnathostenetroidea, and Stenetroidea) and can therefore be considered synapomorphic for the Asellota (Brusca and Wilson 1991). The discovery of the probably “primitive” genus *Vermectias* Just and Poore, 1992, also possessing a precoxa, supports this hypothesis. Amongst the Janiroidea, the precoxa got reduced at least twice independently: in the Macrostylidae as well as the Echinothamematidae Menzies, 1956 and Katianiridae Svavars-son, 1987. A seta projecting from below the base of

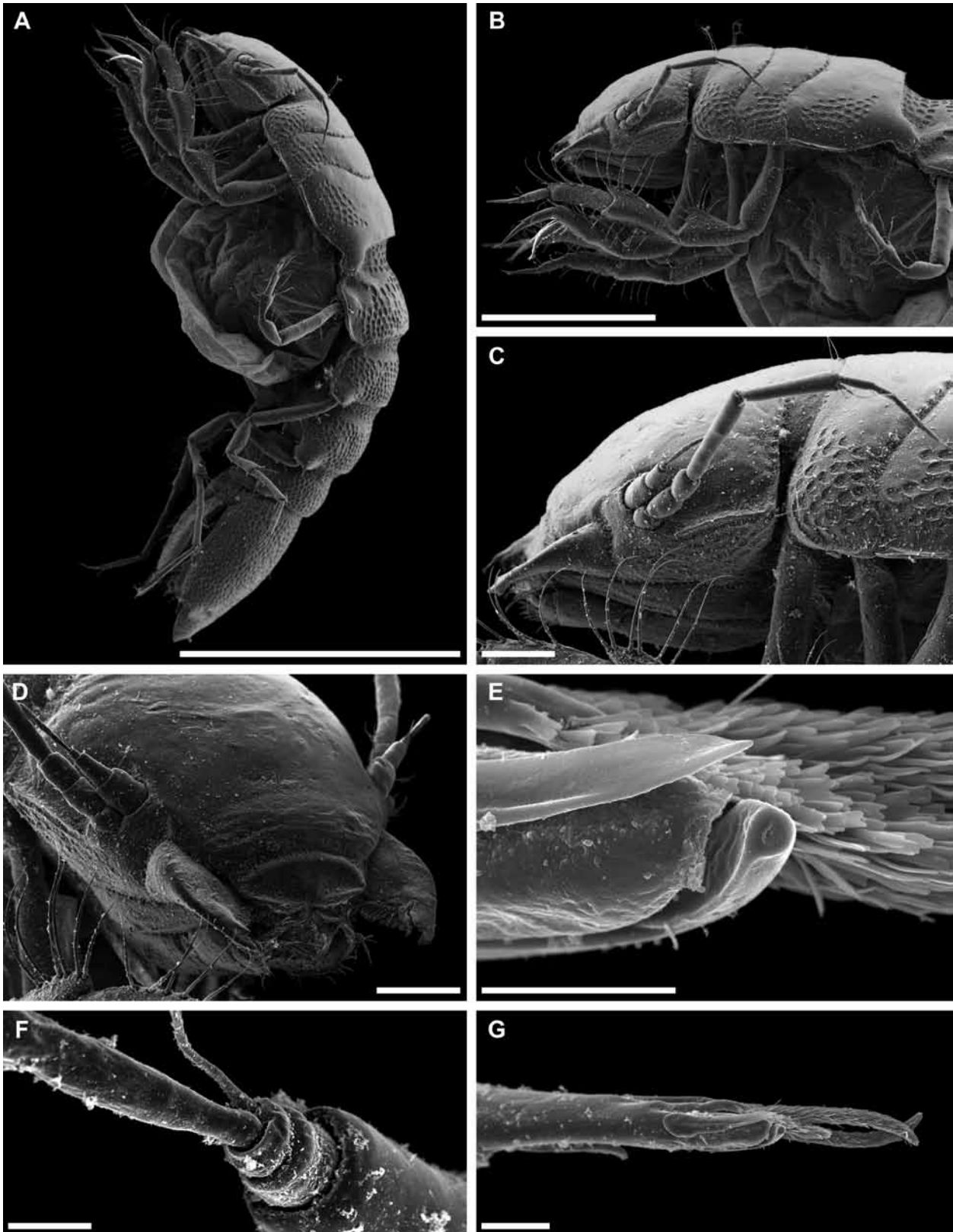


Figure 9. *Macrostyliis* aff. *minuta* Menzies, 1962 (Diva 3 #2) ovigerous female. **A:** habitus lateral. **B:** anterior body, lateral. **C:** cephalothorax, antennae, lateral. **D:** cephalothorax, frontal. **E, G:** pereopod III dactylar claws. **F:** antenna distal articles. Scales: A = 1.0 mm; B = 0.5 mm; C, D = 100 μ m; E = 5.0 μ m; F, G = 10 μ m.

the coxa may be interpreted as a remainder of the precoxa (see e.g. Fig. 3D).

The exopod of the antenna is reduced to various degrees across the Asellota (Wägele 1983). There is no evidence, though, for a rudimentary

exopod in Macrostyliidae. In Urstylidae, an unarticulated projection might represent the exopod (Riehl *et al.* 2014), its complete absence may thus be apomorphic for Macrostyliidae.

While the anterior direction of the mandi-

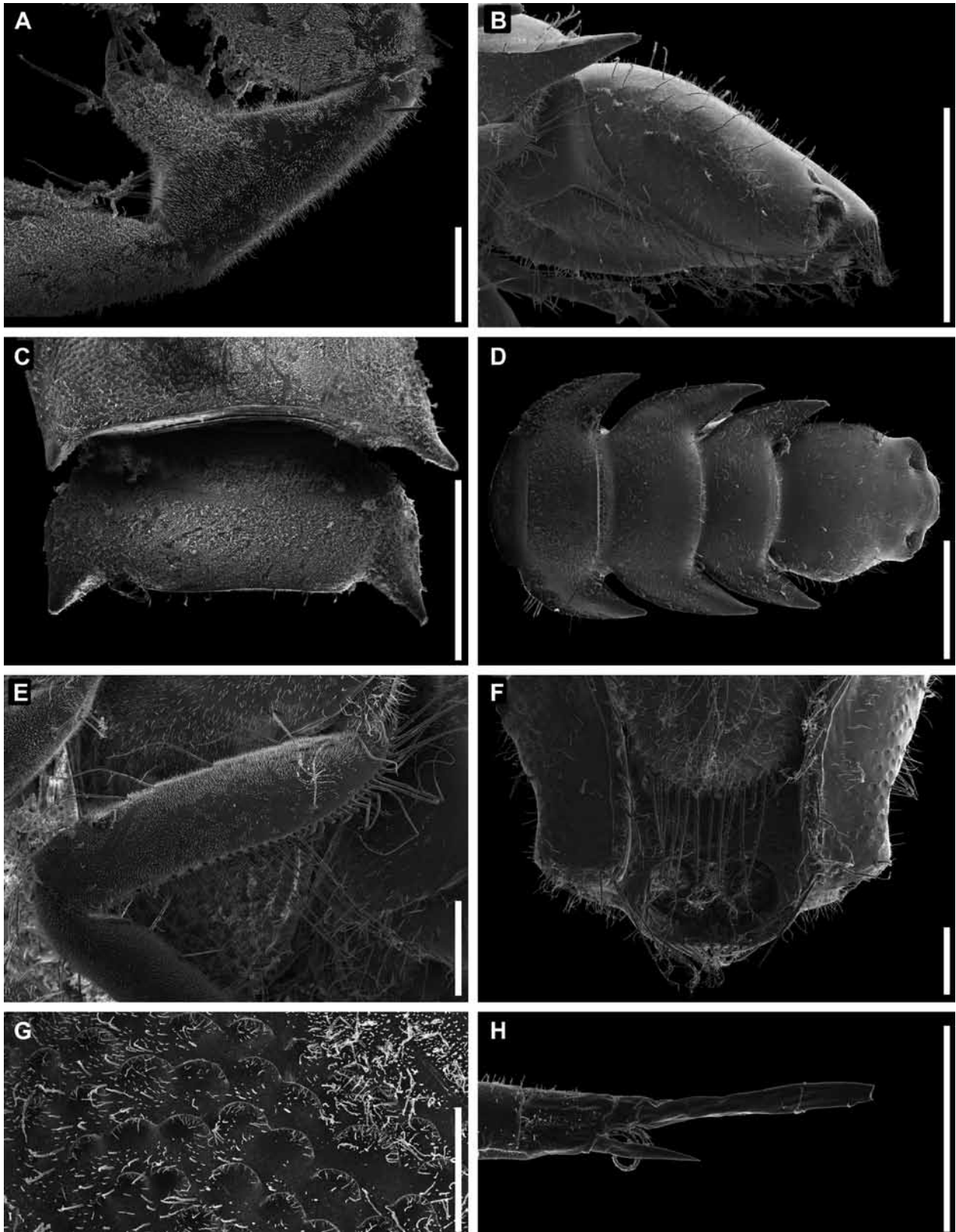


Figure 10. *Macrostylis magnifica* Wolff, 1962 juvenile female. **A:** pereopod III ischium. **B:** pleotelson, lateral. **C:** pereonite 4, dorsal. **D:** posterior pereonites and pleotelson, dorsal. **E:** pereopod VII basis, lateral (anterior). **F:** pleotelson posterior margin, operculum, pleopodal cavity, anus. **G:** imbricate ornamentation. **H:** pereopod VII dactylus. Scales: A = 100 μ m; B–D: 0.5 mm; E, F = 100 μ m; G, H = 50 μ m.

ble (Fig. 6A–D) and the lack of the mandibular palp are character states shared with Urstylidae, a simple seta laterally on the mandibular coxa occurs independently in macrostylids (Fig. 7D) and echi-

nothambematids (Riehl *et al.*, 2014). Vey and Brix (2009) hypothesized that this seta may be a remainder of the reduced palp. Since the approximate similarity in their location is the only evidence that

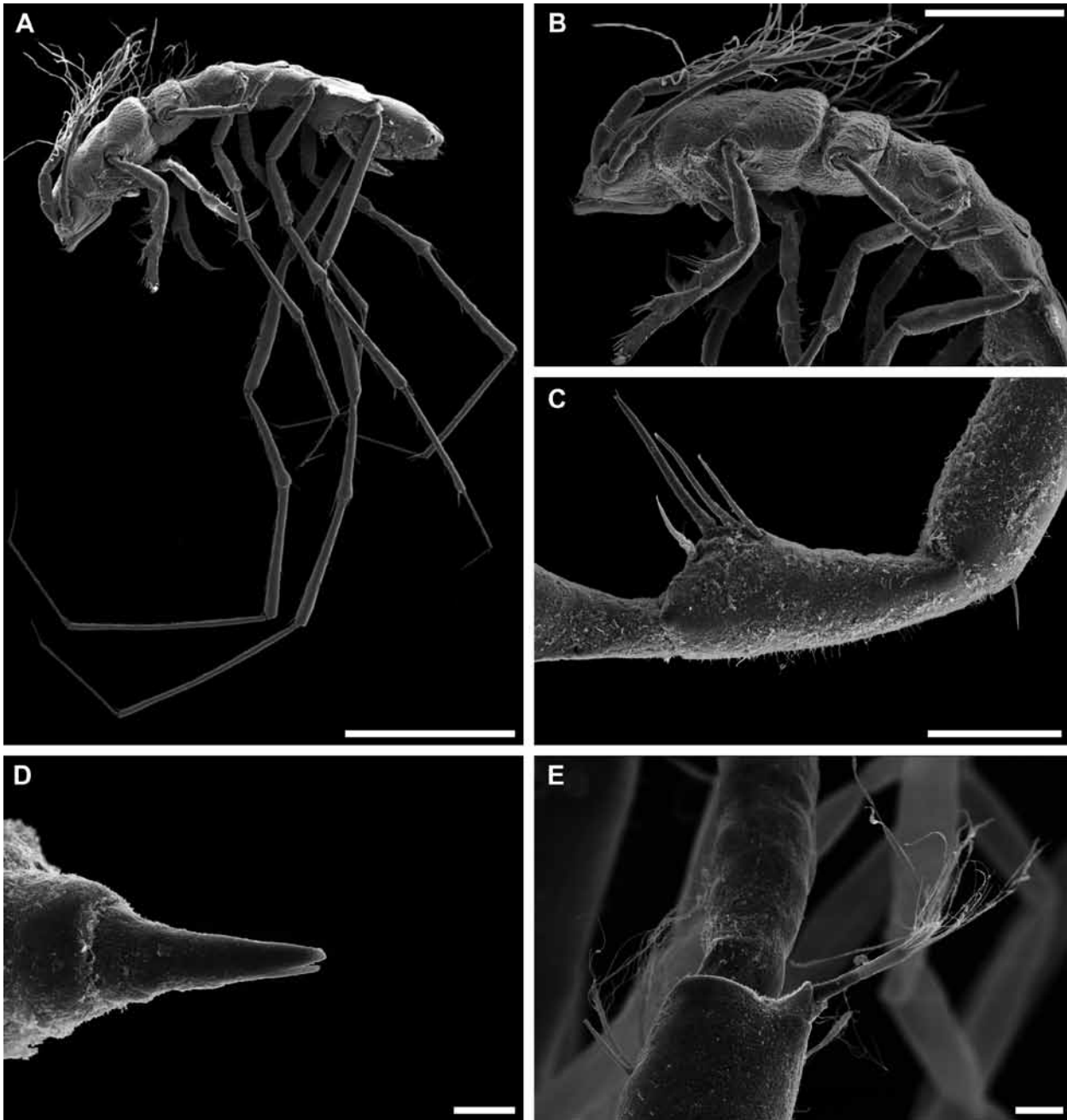


Figure 11. *Macrostylys* sp. (ANDEEP #9) copulatory male. **A:** habitus, lateral. **B:** anterior body and antennae, lateral. **C:** pereopod III ischium, lateral (posterior). **D:** pereiopod 4 posterolateral spine-like seta (robust, bifid seta). **E:** antenna carpus distal margin seta (pedestal broom seta). Scales: A = 1.0 mm; B = 0.5 mm; C = 100 μ m; D, E = 10 μ m.

might support a common origin, uncertainty about the derivation of this seta remains. Furthermore, the likely common loss of the palp in Macrostyliidae and Urstylidae, with the latter not possessing the lateral seta, may be held against Vey and Brix's (2009) hypothesis. An assumption of analogy is, in this case, favoured instead.

Maxillipeds have an opercular function for the mouth field (e.g. Fig. 5C, Fig. 6D). The shapes of their components reflect the contour of the mouth field outlines and group-specific homolo-

gies can thus be expected. The propodus of the maxilliped (palp article 4) is elongate in all of the janiroideans studied by Riehl *et al.* (2014), except in *Macrostylys* that apomorphically has a quadrate propodus (Fig. 5A, Fig. 7D).

Pereon

Probably the most profound evolutionary novelty present in macrostyliid morphology is the unique arrangement of pereonal functional groupings, also referred to as tagmosis. Most isopods have

Table 1. Species of the isopod genus *Macrostyliis* examined in scanning-electron microscopy. Material indicated whether paratypes (PT) or other material was examined. F = female, M = male, ovi = ovigerous, copul = copulatory, RP = Rothlisberg & Percy-sledge, EBS = epibenthic sledge, C-EBS = camera-epibenthic sledge. Coordinates are provided in decimal degrees.

Species	Author, date	Status	Material	Collection #	Area	Res. vessel	Cruise	Station	Gear	Lat.	Long.
<i>magnifica</i>	Wolff, 1962	other	non-ovi F	BIICE 2863	N Atlantic	Biarni Seemundsson		B-13-95 734	RP sledge	61.170	-18.043
<i>subinermis</i>	Hansen, 1927	other	1 non-ovi F	BIICE 2647	N Atlantic, Iceland	Haakon Mosby	HM-1-94	14	Detr. Sledge	68.082	-15.322
<i>subinermis</i>	Hansen, 1928	other	1 copul M	BIICE 2647	N Atlantic, Iceland	Haakon Mosby	HM-1-94	14	Detr. Sledge	68.082	-15.322
<i>uniformis</i>	Riehl & Brandt, 2010	PT	1 non ovi F, 3.5 mm (1Ma81)	ZMH K-42174	S Ocean, N Weddell Sea	Polarstern	ANDEEP II	137	EBS	-63.750	-33.797
sp. Kurambio #06	n. sp.	other	1 copul M		NW Pacific, Kurile-Kamitchatka Trench	Sonne	Kurambio	SO223-2-9	C-EBS	46.246	155.544
sp. Kurambio #06	n. sp.	other	1 non-ovi F		NW Pacific, Kurile-Kamitchatka Trench	Sonne	Kurambio	SO223-2-9	C-EBS	46.246	155.544
sp. ANDEEP #9	n. sp.	other	1 copulatory M (Ma25)	Ma25	S Ocean, Weddell Sea	Polarstern	ANDEEP III	PS61/080-9	EBS	-70.646	-14.724
sp. DIVA 3 sp. # 7	n. sp.	other	1 non ovi F, 1 male	D2M90 D3M98	SW Atlantic	Meteor	DIVA 3	M79/1 583	EBS	-14.990	-29.943
<i>antennamagna</i>	Riehl & Brandt, 2010	PT	1 copul M 2.8 mm (1Ma60)	ZMH K-42172	S Ocean, N Weddell Sea	Polarstern	ANDEEP II	138-6	EBS	-64.028	-39.128
DIVA 3 sp. #02	n. gen. et sp.	other		D3M88 D3M89	SW Atlantic	Meteor	DIVA 3	M79/1 583	EBS	-14.990	-29.943

either of two forms, a 3:4 state or a 4:3 state. In the first, three anterior (typically all prehensile limbs) angle anteriorly, and four more elongate limbs angle posteriorly. In the second state, four limbs angle anteriorly and three posteriorly, with typically only the first limb being prehensile if any. This was presumed, until recently, to be the plesiomorphic condition for the order (Wilson 2009) and found e.g. in some Janiridae as well as most other Janiroidea. Within the Janiroidea, with their multiplicity of body forms, two derived tagmatizations can be found nested within the tagmosis 4:3. The natasome, where three posterior limbs are paddle-shaped, is not discussed further here as it is characteristic of the Munnopsidae and an adaptation for swimming (Hessler *et al.* 1979; Wilson 1989). In Macrostylidae, the anterior tagma consists of pereonites 1–3 (Wolff 1962). It is forming a compact body section of immovable, highly integrated segments (Fig. 2, Fig. 7A). This integration of the anterior pereonites in Macrostylidae is called fossosome (Wilson 2005; Riehl and Brandt 2010).

In some macrostylids, the integration is even more advanced by partly fusion of the anterior body segments in the sternites (Riehl *et al.*, 2014) but also in the tergites (Fig. 8A–C). Nannoniscidae, Desmosomatidae and Urstylidae, also with fossorial anterior pereonites, have their pereonite borders fully expressed and the articles seem independently movable. In the Macrostylidae, however, the anterior pereonites form a compact subrectangular structure (Fig. 2A, Fig. 7A, Fig. 8A, C). The lateral outlines are confluent (Fig. 8C).

Macrostylids additionally have a unique configuration of the brood pouch (Fig. 9A). In Janiroidea, oostegites are plesiomorphically present on the first four pairs of pereopods (Hessler 1982; Wilson 2009), but not more posteriorly as in many other isopods (e.g., Cymothoida). Oostegites are always absent from the maxillipeds in the

Janiroidea but present, for example, in Aselloidea (e.g. Stoch *et al.*, 1996). On the first pereonite, oostegites are always absent in Macrostylidae and sometimes in Thambematidae Stebbing, 1913 where they were reduced independently (Riehl *et al.* 2014). Oostegites on the second pereonites are absent in Macrostylidae but always present in other janiroideans, where reported. Because the condition of oostegites has not been reported or illustrated for many taxa, the matrix remained unscored for several taxa and the results are partly inconclusive. Coding these data is further complicated because many taxa have internally developing oostegites, so that a brooding female must be recorded to observe the state of these characters. This is the case, for example, in macrostylids (Riehl unpublished data) and urstylids (Riehl *et al.* 2014) and could be synapomorphic for their common monophylum.

Amongst the most characteristic features of Macrostylidae are ventral processes of their sternites (Fig. 2B, Fig. 7C). Ventral spine projections of the pereonite sternites frequently (but not always (Fig. 4A)) occur in Macrostylidae as well as in *Urstylis thiotyntlus*, Nannoniscidae Hansen, 1916 and rarely in Desmosomatidae Sars, 1897. Although uncertainty remains, these spines seem to be of independent origins in the various families. Exclusive for Macrostylidae is the sickle-like shape and anterior direction of the sternite 1 spine that projects below the head. Only a minority of the presently known species, *Macrostylis curticornis* Birstein, 1973, *M. longula* Birstein, 1970, *M. profundissima* Birstein, 1970, *M. quadratura* Birstein, 1970, *M. reticulata* Birstein, 1973, *M. sensitiva* Birstein, 1970, *Macrostylis* sp. KuramBio #6 (Fig. 4, Fig. 5), lacks this sickle-shaped spine. Whether the rounded, sharp keels that these species exhibit (Fig. 4A) as ventral projections are reductions or represent the plesiomorphic state remains to be identified. These species all occur in close prox-

imity in the North-west Pacific and a phylogeny might thus reveal a common origin for the absence of the spine on the first sternite.

The fourth pereonite in Macrostylidae is distinct from both anterior and posterior segments in shape and regarding its limbs. It can be considered a separate tagma. Anteriorly, a collum allows high freedom of mobility against the fossosome (e.g. Fig. 2A, B, Fig. 4F, Fig. 8A). Although the collum is present to a degree in Macrostylidae on all pereonites posterior to the fossosome and its expression is highly variable, it is often most strongly developed in some species on pereonite 4 (e.g. Kussakin, 1999; Riehl *et al.*, 2012).

Pereopods

The body tagmatization of macrostylids is expressed not only in the pereonite arrangement but in specialized anterior pereopods as well. Most janiroideans have limbs that are directed ventrally from their lateral insertion, but several groups are distinct in placing the limbs more dorsally emerging from a lateral position (Fig. 3A, Fig. 4A, Fig. 7A, Fig. 8A, B). This is apparent for pereopods II–III in the macrostylids and some desmosomatids. The lateral and dorsal orientation of the pereopods appears to be related to the anteriorly burrowing habit of the Macrostylidae (Hessler and Strömberg 1989), suggesting that the condition for pereopod I in *U. thiotyntlus* (Riehl *et al.* 2014) may also be an independent burrowing adaptation. The anterior pereopods of macrostylids are not prehensile, which is the case in the related Urstylidae and some Desmosomatidae, but from anterior to posterior progressively robust and setose with dorsal and ventral rows of setae on merus, carpus and propodus (Fig. 2D).

The coxae of the anterior pereopods in Macrostylidae have gone through a peculiar transformation: they are imbedded into the ventral

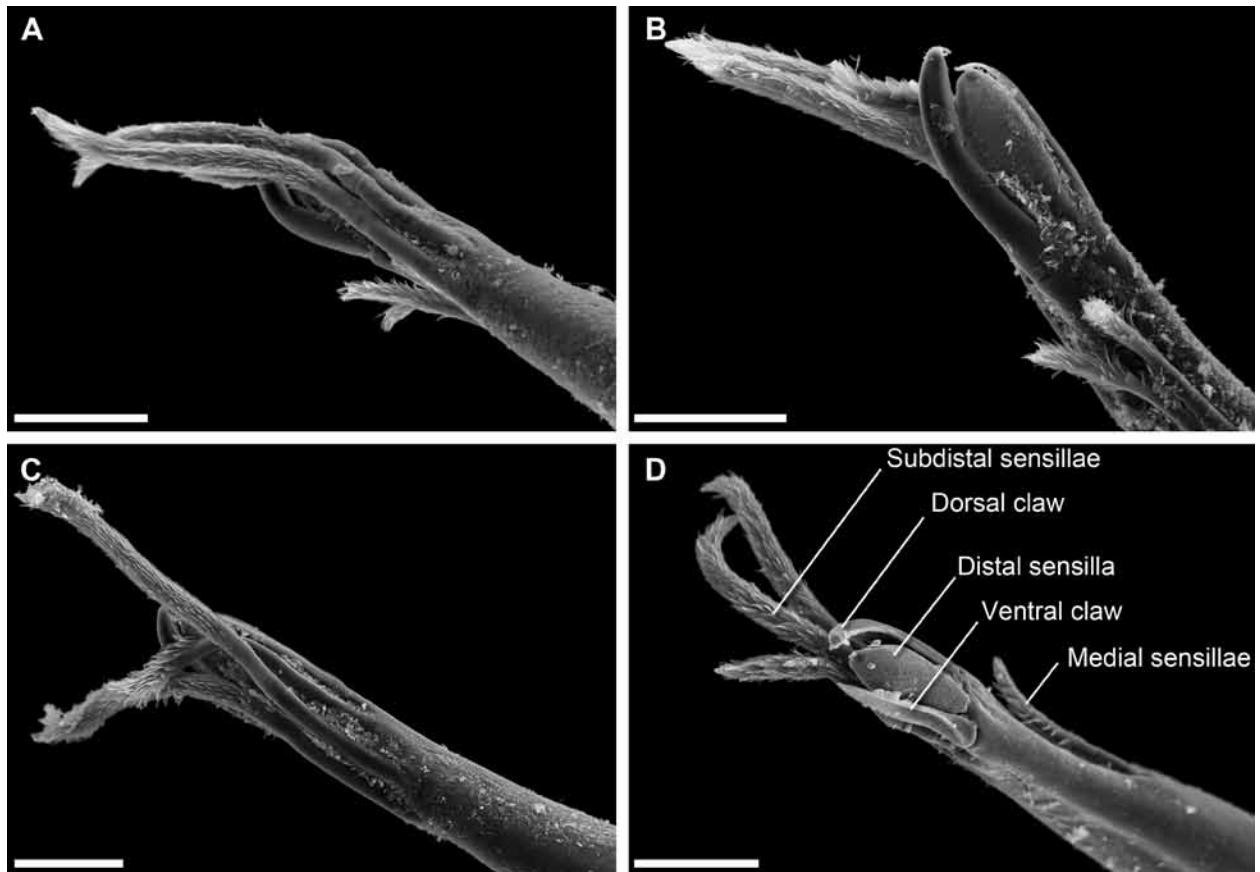


Figure 12. *Macrostyliis* aff. *minuta* Menzies, 1962 (Diva 3 #2) ovigerous female dactylar claws of anterior pereopodal tagma. **A, B:** pereopod I. **C:** pereopod II. **D:** pereopod III. Scales: A–D = 10 μ m.

cuticle, and seem completely inflexible – this is referred to as a “disk-like” coxa that does not project. The plesiomorphic state is a ring-like coxa that projects from the pereonite and generally has a visible coxa-body articulation (Wägele 1989). A condition similar to macrostyliids was observed in *Xostylis longiflagellatus* Birstein, 1970 and *Echinothambema* Menzies, 1956 where it might have evolved independently (Riehl *et al.* 2014).

The first three pereopods of macrostyliids are highly modified. These “fossorial” legs are characterized by the elongation of the merus in combination with broadened margins of ischium, merus and carpus as well as increased setation of all three articles (Fig. 2D). In basally derived groups like the Janiridae Sars, 1897, these limbs are elongate and with only a few robust setae on the ventral margin of the carpus and propodus. Munnopsidae Lilljeborg, 1864, Munnidae Sars, 1897 and Dendrotonidae Vanhöffen, 1914 have

pereopods that might be ambulatory, but are also exceptionally long, often longer than the body. In Desmosomatidae and *Thaumastosoma* Hessler, 1970, the carpus and propodus of pereopods II–III are also robust and densely setose, with the addition of second, more dorsal row of robust setae. Due to the differential shape of the articles, especially the merus, and the location of the setal rows, an independent, parallel evolution rather than a homology is assumed.

The elongate merus in pereopod I (but also all the other pereopods) is another evolutionary novelty that arose in macrostyliids (Fig. 2D). In most Janiroidea, especially those with a robust carpusubchelate pereopod I, the merus is short (dorsal length subequal to width or smaller) and features a distodorsal expansion. This merus structure mirrors the form of the carpus in those taxa that are propodosubchelate, suggesting that the expansion adds mechanical strength to the subchelate limb. In

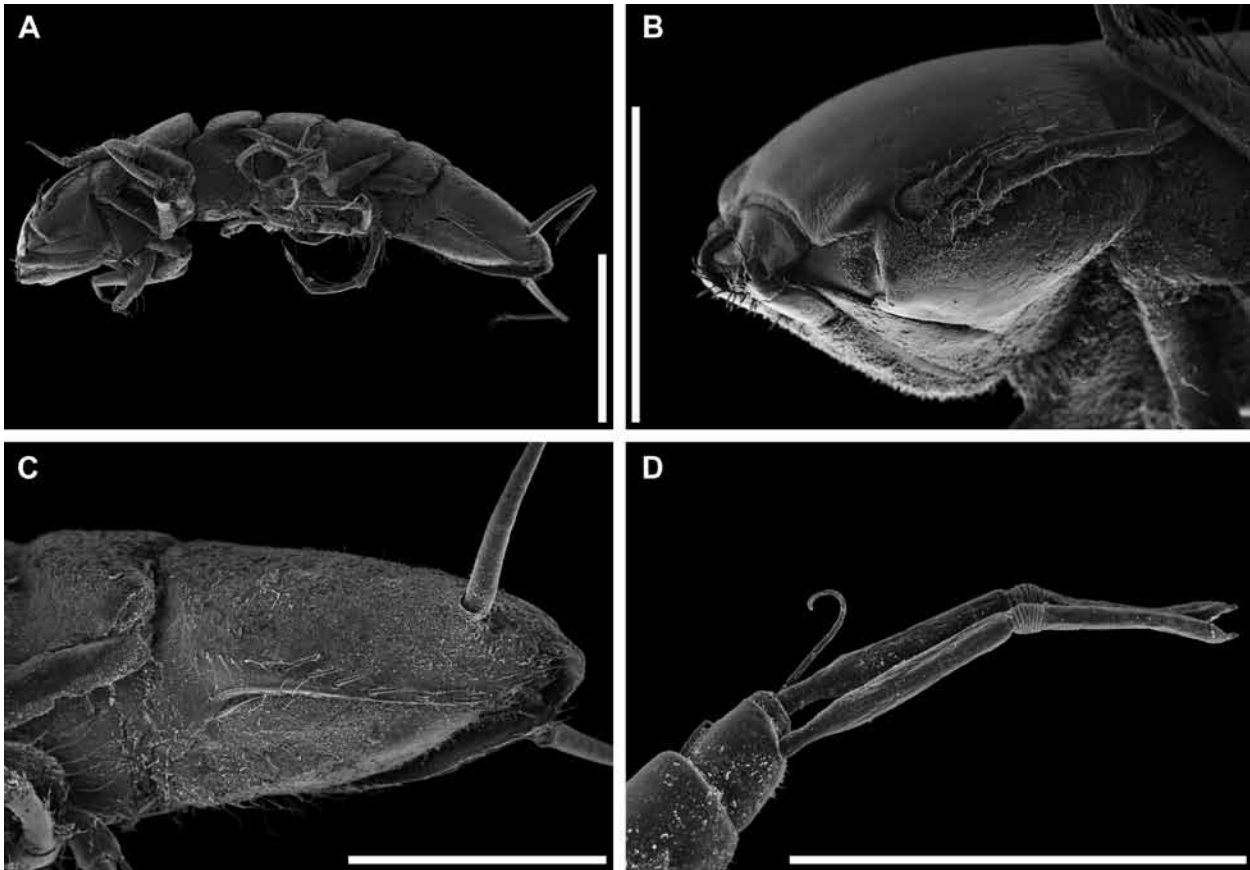


Figure 13. *Macrostylys uniformis* Riehl and Brandt, 2010 non-ovigerous female. Images were modified after Riehl (2009). **A:** habitus ventrolateral. **B:** cephalothorax, lateral. **C:** pleotelson, ventrolateral. **D:** antennula distal articles and aesthetascs.

taxa with a less prehensile first pereopod, such as Macrostylidae or Mesosignidae Schultz, 1969, this article is elongate (length exceeding width) and the distodorsal process is either weakly expressed or completely absent.

The third pereopod of Macrostylidae shows several characters unique to this family, but with high variability so that species-specific patterns can be recognized (Riehl *et al.* 2012; Riehl and Kaiser 2012). The ischium bears a peculiar mid-dorsal projection (Fig. 4D, Fig. 6E, Fig. 10A, Fig. 11C) that can assume a rounded, tapering or triangular shape. It is further commonly fitted with a row of long setae of which one or two on the projection apex are prominent, robust and spine-like. There are species known that lack the dorsal projections and pronounced setation on the ischium (T. Riehl, unpubl. data). It remains to be clarified whether this is the plesiomorphic condition or a secondary reduction.

The carpo-propodal joint rotation of pereopod III (Fig. 5E, Riehl and Kaiser (2012): Fig. 4B) and the dorsolateral orientation of pereopod IV (Fig. 3A, Fig. 4A, Fig. 9A) of the macrostylids are unique and may be used in burrowing as well. Typically, across the Janiroidea the fourth pereopod follows the shape and length of preceding walking legs. In Macrostylidae, however, this leg is the shortest of all pereopods (Fig. 2D; except for pereopod VII that may be underdeveloped in some species), probably linked with the dorsolateral orientation.

Moreover, the anterior tagma is characterized by a unique claw arrangement (Fig. 5D, F, Fig. 7G, H, Fig. 8F, Fig. 9E, G, Fig. 12). The diversely modified setae that form the ventral dactylar claws (Wilson 1985) appear in diverse shapes across Janiroidea. In Macrostylidae, this seta is thin and elongate, features a ventral carina, and is distally tapering (Fig. 12D). It is clinging to the distal sensilla, which is uniquely shaped as well (see below).

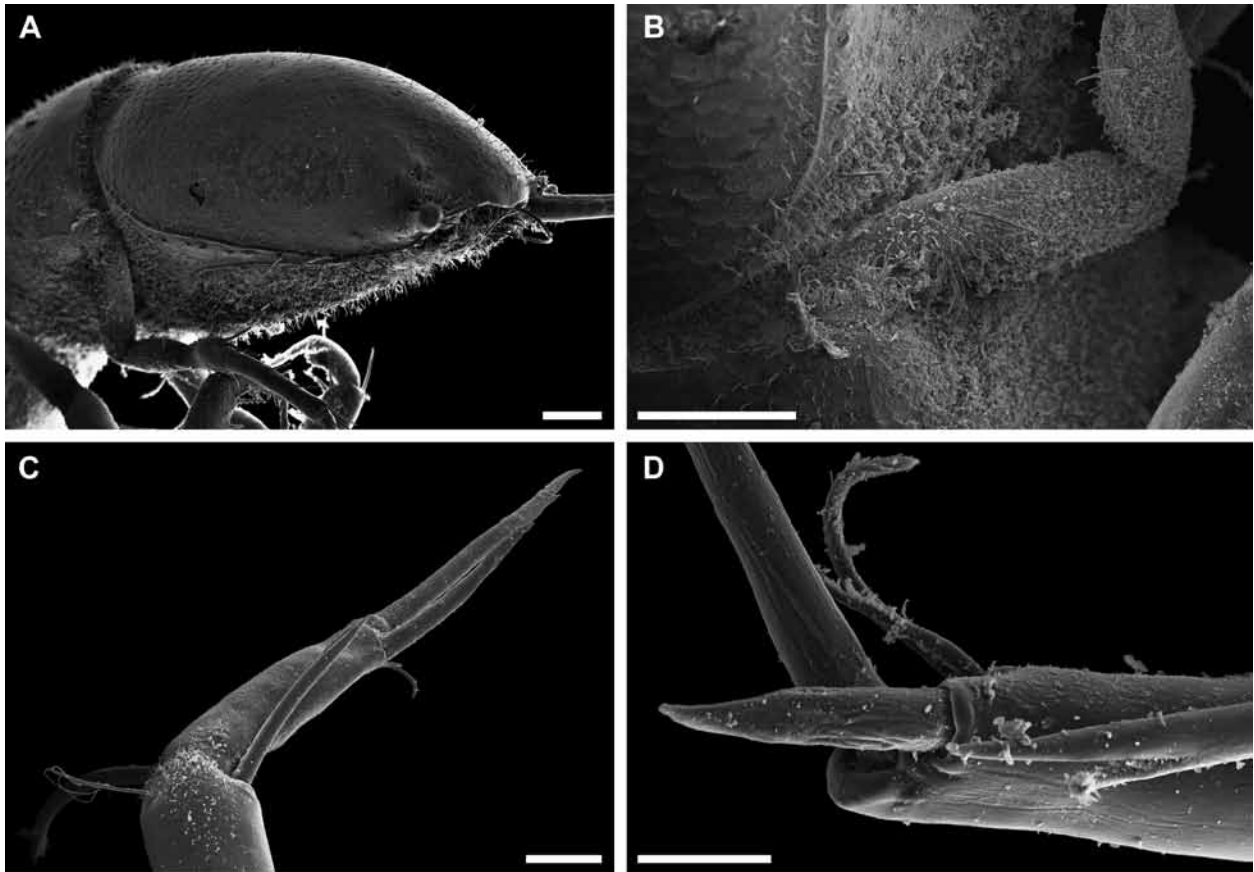


Figure 14. *Macrostylis* sp. (KuramBio #6) non-ovigerous female. **A:** pleotelson. **B:** pereopod VII, lateral. **C:** pereopod VII dactylus. **D:** pereopod IV dactylus claws and sensillae. Scales: A, B = 100 μ m; C = 10 μ m; D = 20 μ m.

In other Janiroidea, on the contrary, this seta is often claw-shaped and thus similar to the dorsal claw. Alternatively it may assume a flattened, scale-like shape; or represent elongate structures that are dorsally concave and ventrally keeled; straight, unarticulated spines; hand-shaped, serrate claws (see, e.g. Wilson, 1985). In the posterior pereopods of Macrostylidae, claws have retained (or regained) a simple seta-like appearance (e.g. Fig. 10H).

The distal sensillae (Wilson, 1989; Riehl and Brandt, 2010) that are located distally on janiroidean dactyli and adjacent to the dorsal claw are variable in number within Janiroidea but occur as single seta in macrostylids (Riehl *et al.* 2014). Their location between dorsal and ventral claws is taxon specific (Fig. 12). Its thick shape is unique to the Macrostylidae as well. The dactylus of the anterior legs is exclusive in *Macrostylis* in several ways. Next to the peculiar shape and arrangement of the claws and the distal sensilla, the subterminal

sensillae located medially of the dactylus, otherwise short, slim and tube-like structures, are enlarged here and distally project beyond the claws (Fig. 5D, F, Fig. 12).

The macrostylid pereopod IV is reduced in size (Riehl *et al.*, 2014; char. 56) and does not lay with either the anterior or posterior limbs, articulating medially on the lateroventral margin (Fig. 3A, Fig. 9A, Fig. 11A, B) with a dorsolateral orientation. Its setation and the directions of the article joints are equally different from both the anterior legs as well as the posterior legs. Most deep-sea janiroideans, with their fundamental asellotan 4:3 tagmosis, have the pereopod IV coxae inserting on the anterolateral margin of pereonite 4, so that the fourth pereopod angles forward.

In Janiridae, the coxa is located medially on the lateral segment outline, independently of the orientation of the pereopod. Probably independently from the plesiomorphic condition that is found

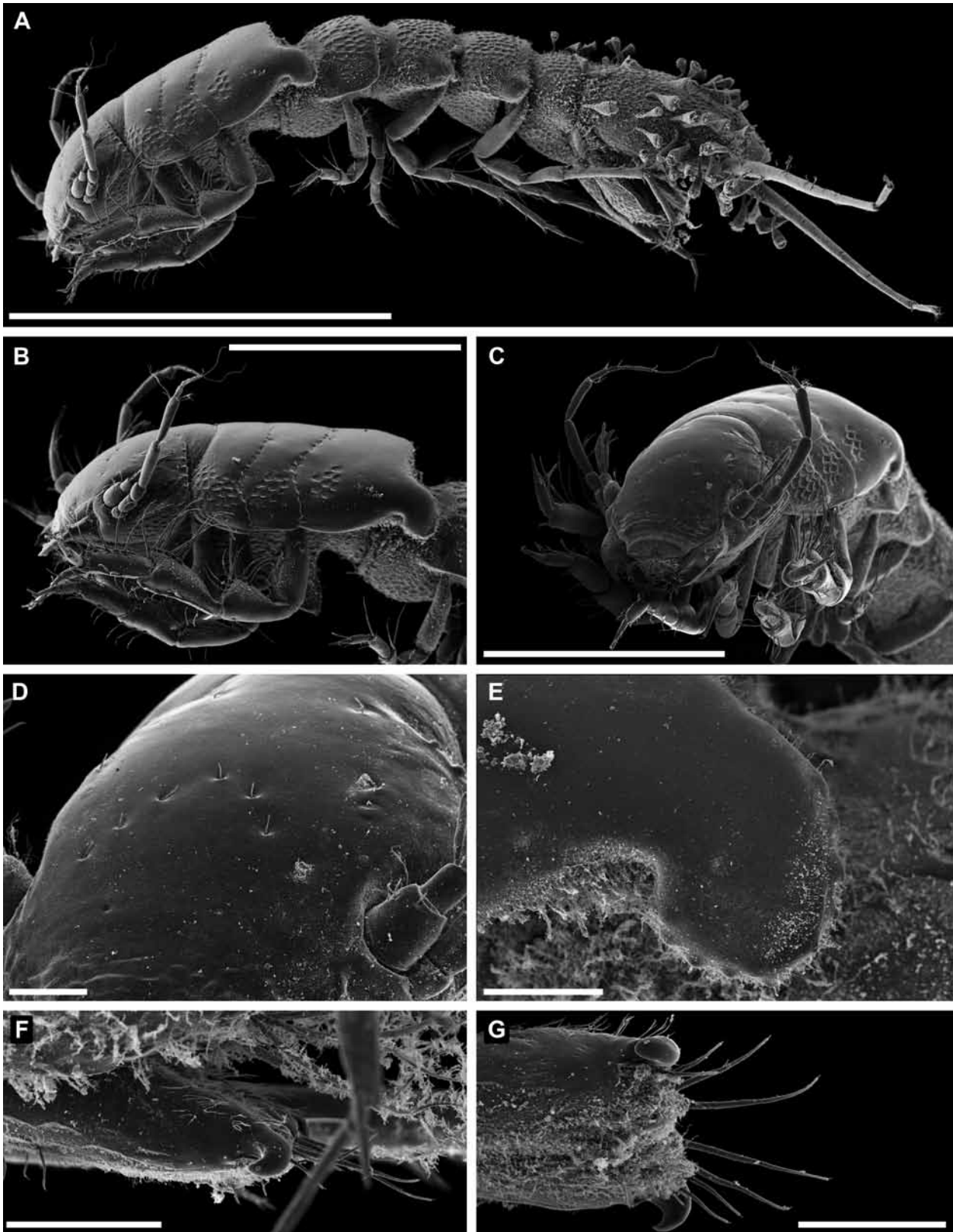


Figure 15. *Macrostylis* aff. *minuta* Menzies, 1962 (Diva 3 #2) copulatory male. **A:** habitus lateral. **B:** anterior body, lateral. **C:** cephalothorax, antennae, frontolateral. **D:** frons. **E:** pereonite 3 posterolateral projection, lateral. **F:** pleopod I *in situ*, lateral. **G:** pleopod I ventral. Scales: A = 1.0 mm; B, C = 0.5 mm; D–G = 50 μ m.

in Janiridae, the articulation position has also changed in Macrostylidae to a more medial position on the lateral margin. The pereopod IV carpus typically follows the shape of preceding limbs,

but may differ in some cases. In the macrostylids, with their odd tagmosis, the pereopod IV carpus is subsimilar or shorter than the usually short merus. Propodus as well as dactylus are short as well,

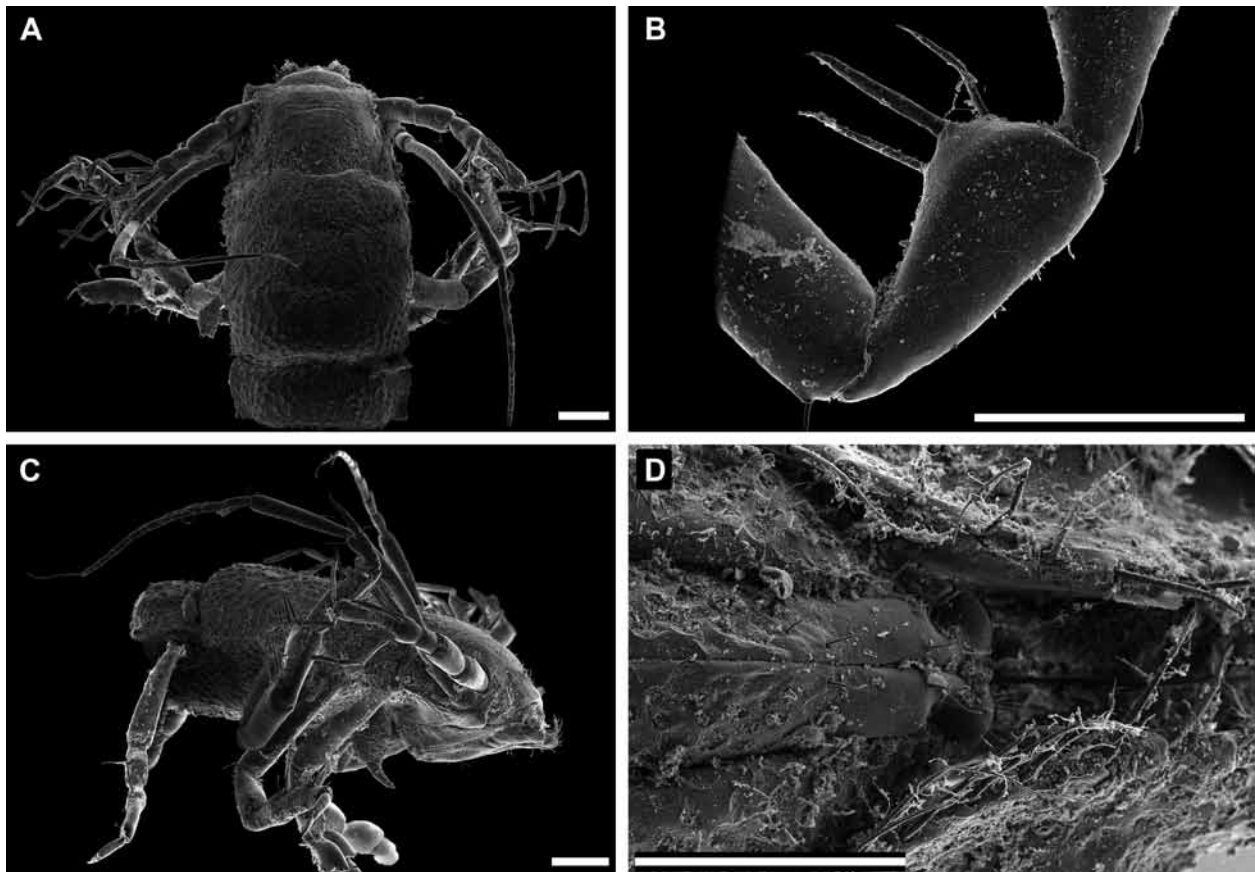


Figure 16. *Macrostylylis subinermis* Hansen, 1916 copulatory male. **A:** anterior body, dorsal. **B:** pereopod III ischium. **C:** anterior body, lateral. **D:** pleopod II, ventral. Scales: A–D = 100 μ m.

about carpus length when combined. The Urstyliidae follow the typical pattern where the carpus is longer than wide and near the length of the propodus. A few taxa, such as *Halacarsantia* Wolff, 1989, have robust prehensile pereopods with sub-similar carpus and propodus, both shorter than the merus. This over-all pattern creates the typical and apomorphic macrostyloid tagmosis of 3:1:3.

Pleotelson

There is a certain similarity between macrostyliids and *Dactylostylis* Richardson, 1911 as well as Echinothambematidae Menzies, 1956 regarding their uropods. The pleotelson of Macrostyliidae, however, features several characters unique to this family that outweigh any superficial similarity with both groups regarding the V-shaped arrangement of long, styliform uropods (Fig. 2).

The preanal trough, for example, (Fig. 10F) posteriorly extends the pleopodal cavity to the

pleotelson apex, resulting in the cavity to be open posteriorly. A similar pattern can be observed in Janirellidae, which is a homoplasy in the light of the latest analysis (Riehl *et al.* 2014). Probably as consequence of the caudal projection of the pleopodal cavity, the anus of macrostyliids is situated within the cavity (Fig. 10F). The prominent setal rows (Fig. 10B, F, Fig. 13C) that can be found fringing the pleopodal cavities of both Macrostyliidae and Urstyliidae (also in Syneurycopinae Wolff, 1962 and *Microcope* Malyutina, 2008) are found to be situated on ridges (Fig. 10B, Fig. 14A) only in Macrostyliidae.

Finally, a paired sensory organ dorsally in the macrostyloid pleotelson (Hansen 1916; Wägele 1989) is exclusive to the group (Fig. 2A, B). Such subcuticular cavities that contain crystalline structures can be found in all macrostyloid species. Their connection to the slot-like apertures (Mezhov 2003) that are located more posteriorly on the pleo-

telson tergite remains to be shown. However, they are interpreted as statocysts (Wägele 1992). The apertures might represent the openings of a cuticular invagination, analogous to the general structure of statocysts in other crustaceans (Sekiguchi and Terazawa 1997).

Statocysts are equilibrium organs, meaning they detect the spatial position and its changes. While this function has important implications to the eye movement and swimming behavior of, for example, many decapods and mysids (Sandeman and Okajima 1972; Neil 1975; Neil and Ansell 1995; Sekiguchi and Terazawa 1997), macrostylids lack eyes and neither is there any evidence for natatory behavior in macrostylid isopods. At the current stage of knowledge, drawing connections between the statocysts and the assumed digging lifestyle are mere speculation. Detailed anatomical and behavioral studies remain to be conducted.

Character conceptualization

Since the discovery and phylogenetic allocation of Urstylidae, the view upon the position of Macrostylidae Hansen, 1916 in the janiroid tree of life seems better understood (Riehl *et al.* 2014). As discussed above, the branch leading to the macrostylids is characterized by a relatively long list of synapomorphies and is thus indicating a high specialization of this taxon. The largest gap that remains in our understanding of the evolution of this isopod family refers to its interspecific relationships. Until now, Macrostylidae is considered monotypic (Riehl and Brandt 2010). Yet similar and thus potentially related species can be found in different oceans and across large depth ranges (T. Riehl, unpubl. data). Intra-familial phylogenies might help to explain these patterns. In the following section, we discuss the concepts for potential

apomorphies for subgroups of the family. Plesiomorphic conditions are represented by exemplars of the Urstylidae and Desmosomatidae Sars, 1897 (Wägele 1989; Riehl *et al.* 2014).

Body characters

Cephalothorax posterior margins.

The spade-shaped head of macrostylids is widest posteriorly (Fig. 2A, Fig. 5C, Fig. 7A). The articulation of the head with pereonite 1 is clearly narrower than the overall width of the head at its posterior margin. Laterally to the articulation, the head of macrostylids features distinct margins. These margins are either smooth (Fig. 3B, Fig. 6F) or papillose (Fig. 9C) and can be free of setae or carry one or multiple setae.

Char. 1. Cephalothorax posterior margins papillae: 0 = absent; 1 = present.

Char. 2. Cephalothorax posterior margins setae: 0 = absent; present.

Ventral spines

Ventral projections of the pereonal sternites can appear in distinct shapes and orientation in a variety of taxa. Spine-shaped projections are characteristic for (though not always present in) Macrostylidae (Hansen 1916; Wolff 1956; Mezhev 1989; Kusakin 1999). Macrostylid species that completely lack ventral spines have been reported exclusively from the northern Pacific Ocean (Birstein 1970; Birstein 1973), for example *Macrostylis curticornis* Birstein, 1973 and *M. profundissima* Birstein, 1970.

Ventral spines are also found in some Nannoniscidae, Echinothambematidae and Urstylidae but a common origin is only likely in macrostylids and urstylids (Riehl *et al.* 2014). Consequently, the homology concepts defined here are restricted in

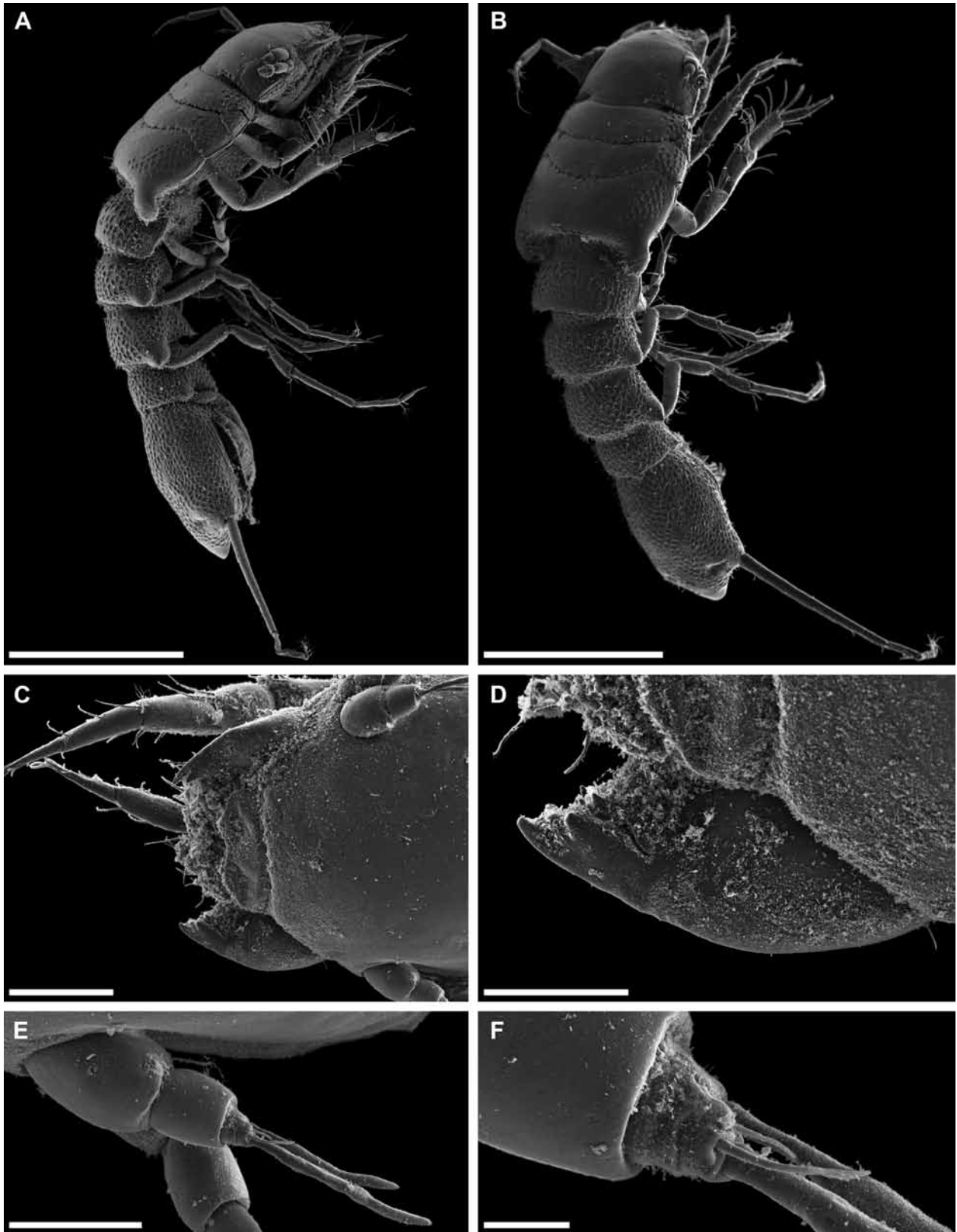


Figure 17. *Macrostylis* aff. *minuta* Menzies, 1962 (Diva 3 #2) copulatory male. **A:** habitus lateral. **B:** habitus, dorsolateral. **C:** frons, labrum, mandibles. **D:** mandible, dorsal. **E:** antennula, dorsal. **F:** antennula distal segments. Scales: A, B = 0.5 mm; C = 100 μ m; D, E = 50 μ m; F = 10 μ m.

their validity to macrostylids and urstylids only. The presence of ventral spines is variable for every segment and these are thus coded separately. In pereonite 1, a clear distinction can be made when the projection is either spine-shaped or blunt and

when the spine either assumes a ventral-posterior orientation such as in *Urstylis thiotyntlus* Riehl, Wilson and Malyutina, 2014 or is directed anteriorly and projects ventrally to the cephalothorax as found in many macrostylids (Fig. 2B).

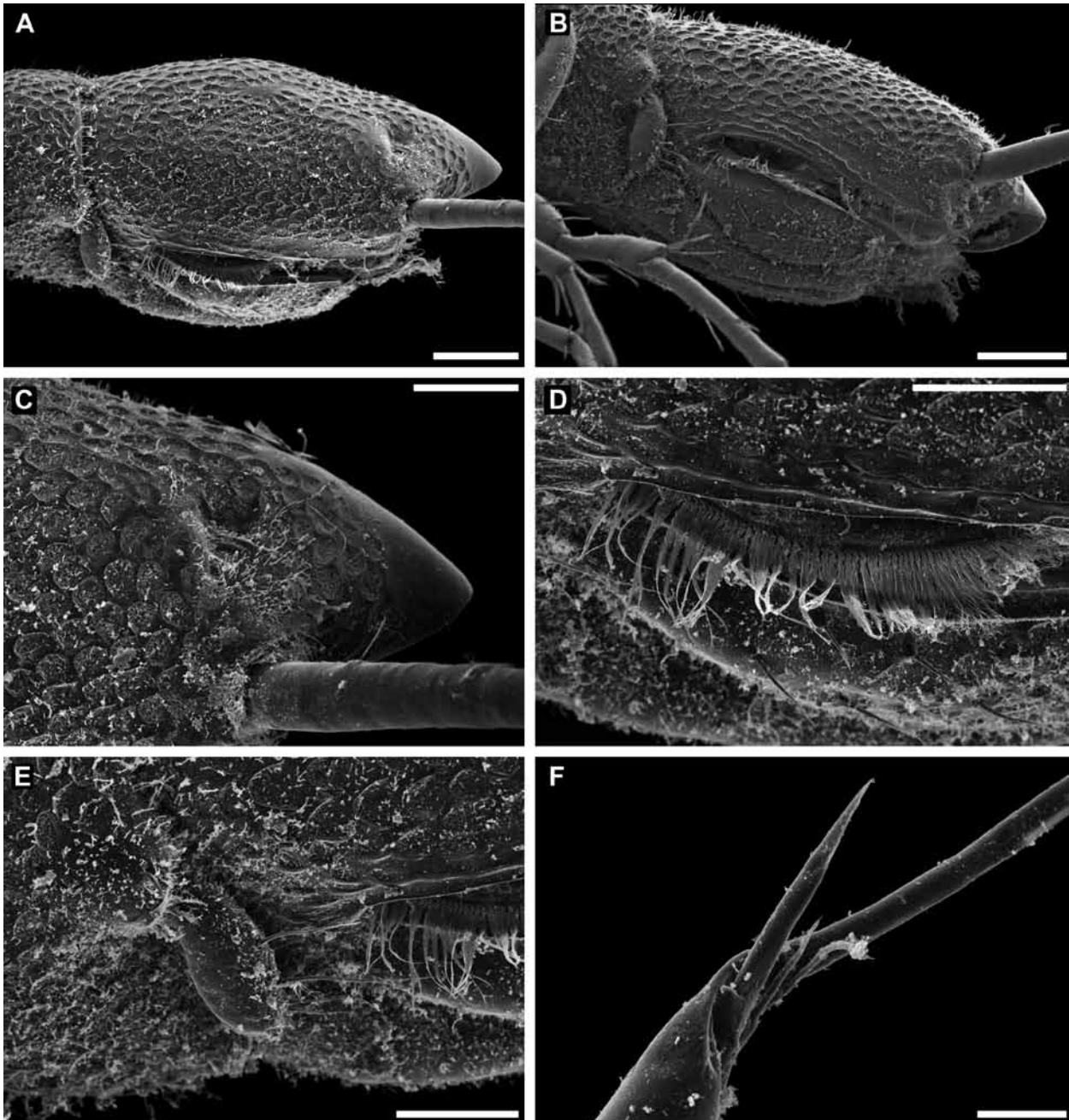


Figure 18. *Macrostylis* aff. *minuta* Menzies, 1962 (Diva 3 #2) copulatory male. **A:** pleotelson, lateral. **B:** pleotelson, ventrolateral. **C:** slot-like apertures. **D:** pleopod III, lateral fringe of setae. **E:** pereopod VII. **F:** antennula distal segments. Scales: A, B = 100 μ m; C–E = 50 μ m; F = 10 μ m.

Chars 3–9. Pereonites 1-7 ventral projection: 0 = absent; 1 = present.

Char. 10. Pereonite 1 ventral projection (shape; if present): 0 = blunt; 1 = spine.

Char. 11. Pereonite 1 ventral projection orientation (if present): 0 = anteriorly; 1 = ventrally & posteriorly; 2 = ventrally.

Posterolateral setae on cephalothorax and pereonites

Following Riehl *et al.* (2014), posterolateral setae

are defined as setae that are located on or near the apex of posterolateral tergite projections, and are clearly directed posteriorly. These setae are usually prominent in that they are the only setae on an otherwise asetose cuticle or because they exceed other setae in close proximity in length, width and/or robustness. Posterolateral setae have been identified on the cephalothorax (Fig. 7B) and all pereonites (e.g. Fig. 4G, Fig. 11B, D) but their presence and characteristics are variable and often species specific. They may have or have not a spine-like

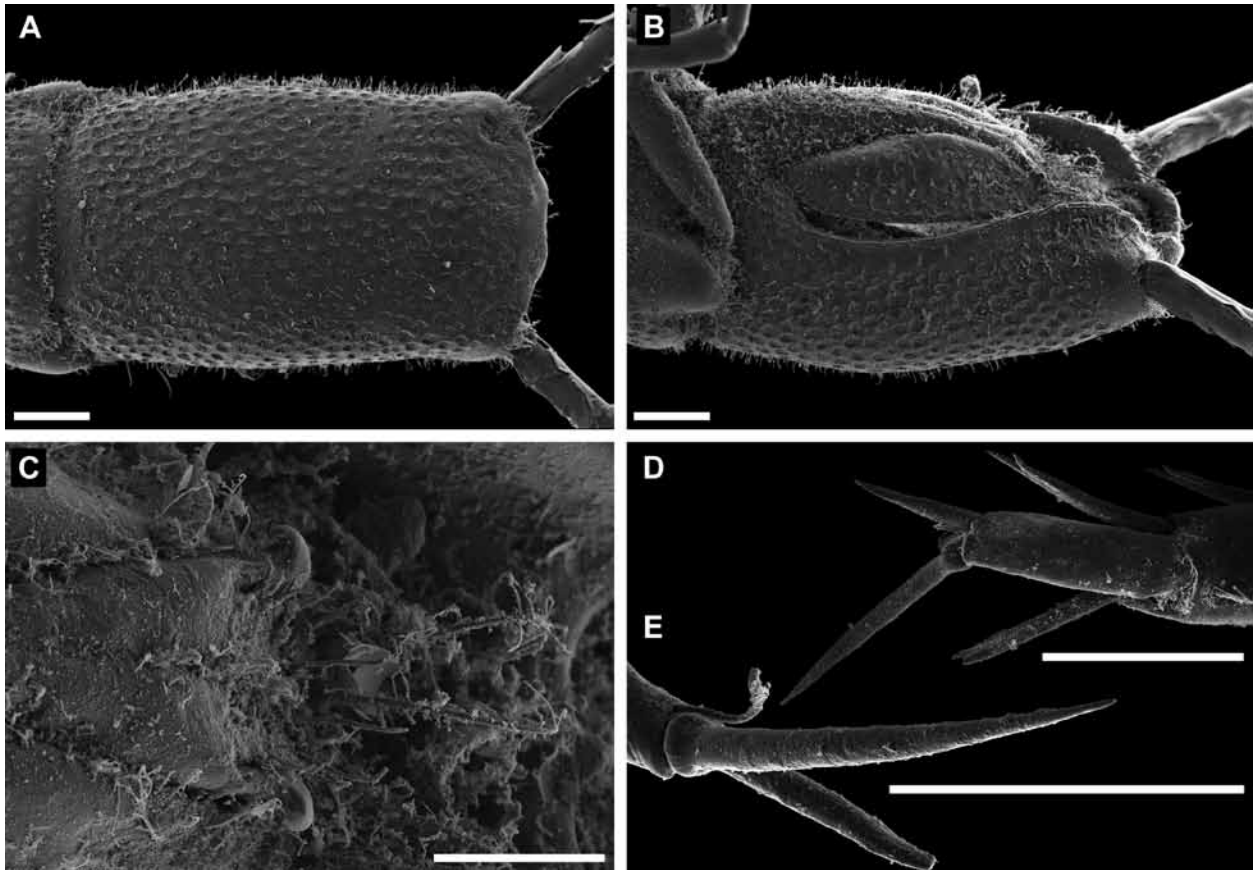


Figure 19. *Macrostylis* sp. (KuramBio #6) adult male. **A:** pleotelson, dorsal. **B:** pleotelson ventrolateral. **C:** pleopod I distal tip, ventral. **D, E:** pereonite 5 posterolateral margin and seta, dorsal. Scales: A, B = 100 μ m; C–E = 50 μ m.

appearance (Fig. 11B, D) and a subdistal sensilla (bifid; Fig. 11D) (Riehl 2009; Riehl and Brandt 2010).

Because there is considerable variation with regard to both presence and shape of posterolateral setae throughout Macrostylidae, each segment is treated here independently.

Chars 12–19. Posterolateral setae on cephalothorax through pereonite 7 (presence): 0 = absent; 1 = present.

Chars 20–27. Posterolateral setae on cephalothorax through pereonite 7 substructures (presence): 0 = absent; 1 = present.

Chars 28–35. Posterolateral setae on cephalothorax through pereonite 7 robustness: 0 = simple; 1 = robust.

Chars 36–44. Posterolateral setae on cephalothorax through pereonite 7 articulation: 0 = flexibly articulated; 1 = spine-like.

Pereonites 1–3 (if fossosome) posterolateral projections (presence)

Most macrostylids, urstylids or desmosomatids have no posterolateral projections of their first three pereonites (Fig. 8C). In most macrostylids, the first two body segments have confluent lateral margins with the subsequent segment. The posterolateral margin of pereonite 3 is usually broadly rounded and not projecting either. However, some macrostylid species have projections in selected or all three anterior segments. The projections of the third segment can either taper off and culminate in spine-like setae (e.g. *M. magnifica* Wolff, 1962; see Fig. 7A, E), or constitute blunt and papillose outgrowths (*M. minuta* Menzies, 1962; see Fig. 15A, C, F). The presence of such processes can in cases be sexually dimorphic: processes may only be present in adult males (T. Riehl, unpubl. data).

Char. 45. Pereonites 1 and 2 posterolateral margins: 0 = conjunct with subsequent pereonite;

1 = projecting posteriorly.

Char. 46. Pereonite 3 posterolateral margins: 0 = broadly rounded, not projecting; 1 = with acute projection that culminates in a posterolateral seta; 2 = with papillose and blunt posterolateral projections.

Char. 47. Anterior pereonites posterolateral projections (sexual dimorphism): 0 = similar in male and female; 1 = females without, males with projections.

Pereonites 1–4 ventral projection of tergites and orientation of coxae

Most commonly amongst Janiroidea, the lateral tergite margins of the anterior four pereonites are located somewhat dorsally to the coxae. This is independent of the presence or absence of lateral tergal projections such as lappets or spines. The coxae of the respective segments are in these cases oriented laterally and ventrally as well as potentially towards anterior. Riehl and Brandt (2013) described a second condition where the tergal margins are projecting ventrally for the species *Macrostylis scotti* Riehl and Brandt, 2013. In combination with a shift of the tergite margin towards lateroventrally relative to the coxae, the plain of articulation is turned towards medially. The bases of the respective limbs assume a medioventral orientation. A similar and potentially homologous condition has been found in other species of the family, namely *M. minuta* Menzies, 1962 and *M. robusta* Brandt, 2004 as well as several undescribed species (Fig. 9A–C, Fig. 13A, Fig. 15A, B).

Char. 48. Pereonites 1–4 ventral projection of tergites and orientation of coxae: 0 = not projecting; 1 = projecting.

Sternal keels on the anterior pereonites

Sternal keels are angular projections along the ventral midline. In cross-section through the trans-

verse plane, the sternal outlines in these taxa are laterally concave and ventrally tapering. In some species of macrostylids, the ventral carina stretches entirely from the anterior border of pereonite 1 to the posterior margin of pereonite 3 (e.g. in *M. scotti* Riehl *et al.* 2012).

Char. 49. Anterior pereonites sternal keel (presence): 0 = absent; 1 = present.

Char. 50. Anterior pereonites sternal keel (shape): 0 = interrupted; 1 = entire.

Pereonite 4 integration into anterior or posterior tagmata

While the fourth pereonite is plesiomorphically a member of the anterior tagma and thus resembling the general shape and function of pereonites 1–3 (to a variable degree), in macrostylids, this segment shows some variability. In most species, its shape (lateral and posterior outlines) is distinct from both the anterior and the posterior segments (Fig. 1, Fig. 2A, Fig. 4F). There are species, however, that show strong similarity between the fourth segment and either the anterior (Fig. 16A) or the posterior (Fig. 10C) tagma. As there are opposing patterns present in mature males and females of some species, this sexual dimorphism is coded separately, where present.

Char. 51. Pereonite 4 integration to other tagmata (in female): 0 = resembling anterior segments; 1 = distinct from anterior and posterior tagmata; 2 = resembling posterior segments.

Char. 52. Pereonite 4 integration to other tagmata sexual dimorphism: 0 = absent; 1 = present.

Char. 53. Pereonite 4 integration to other tagmata (in male): 0 = resembling anterior segments; 1 = distinct from anterior and posterior tagmata; 2 = resembling posterior segments.

Pereonite 4 anterior collum

While the presence of a collum on the fourth pere-

onite is a synapomorphy for the species of Macrostylidae according to Riehl *et al.* (2014), there is considerable variation across macrostylids regarding the extend of the collum. We distinguish short collum (Fig. 16A), where the depression constitutes up to half the length of pereonite 4, from longer ones (Fig. 4F).

Char. 54. Pereonite 4 anterior collum: 0 = up to 50% pereonite 4 length; 1 = longer 50% pereonite 4 length.

Pereonite 7 state of development in adult specimens (heterochrony: hypomorphosis)

Across various groups of Janiroidea, species have developed functionally reduced posterior pereonites. This tendency is reflected in the integration and fusion of segments, for example in many Ischnomesidae Hansen, 1916, Nannoniscidae and Haploniscidae Hansen, 1916.

In Macrostylidae, fusion of posterior pereonites cannot be found. Nevertheless, some species have their seventh pereonite retarded (Fig. 14A, Fig. 18A, B, E): the size is inferior relative to preceding segments; the shape, e.g. posterolateral projections that might be present in preceding segments, are not or only minimally developed; the limbs are short and their setation is underdeveloped, they assume an attitude similar to that found in mancae where ischium through dactylus of both legs lie under the pleotelson close together and probably without function. Besides the seventh pereonite, other features of the body display the regular developmental trajectory. This paedomorphosis can thus be explained by an earlier offset of the development in the affected body parts. This evolutionary phenomenon occurring multiply and independently across Janiroidea, agrees with the definition of hypomorphosis (Reilly *et al.* 1997).

Previous papers discussing this phenomenon contradicted each other by explaining their

observations with the terms neoteny (Brökeland and Brandt 2004), or progenesis (Kavanagh *et al.* 2006). Since both terms are ambiguously defined and partly synonyms, we neither agree nor disagree but name the heterochronic changes of the ontogeny more precisely.

Char. 55. Pereonite 7 state of development: 0 = underdeveloped; 1 = fully developed.

Pleonite 1 dorsal margin expression

In Asellota, pleonites 1–3 are plesiomorphically present (Brusca and Wilson 1991; Just and Poore 1992). A complete absence of free pleonites, however, can be observed in several unrelated groups of Janiroidea. The presence of a transverse ridge anteriorly on the pleon indicates the expression of an articulation between the first pleonite and the pleotelson (see Riehl *et al.* (2012): Fig. 8D).

Char. 56. Pleonite 1 dorsal margin expression: 0 = absent; 1 = present.

Pleotelson lateroventral setal rows and ridges

Ventrally on the pleotelson of some Macrostylidae, ridges follow the margin of the pleopodal cavity (Fig. 10B, Fig. 14A, but see Fig. 13C, Fig. 18A, B, Fig. 19B). They extend from the posterior end of the preanal trough to the anterior region of the pleotelson where in some species they divide from the pleopodal cavity and continue along the lateral cuticle of the pleotelson. Alongside these ridges, macrostylids have rows of long and relatively robust setae. These also occur in macrostylids and other janiroideans that do not feature the ridges, such as Urstylidae, Pleurocopidae Fresi and Schiecke, 1972, Santiidae Wilson, 1987, some Paramunnidae Vanhöffen, 1914 (e.g. *Austronanus* Hodgson, 1910) and Munnopsidae (e.g. *Microcope* Malyutina, 2008). Setae and ridges are thus considered independent and were separately coded.

Char. 56. Pleotelson lateroventral ridges: 0 =

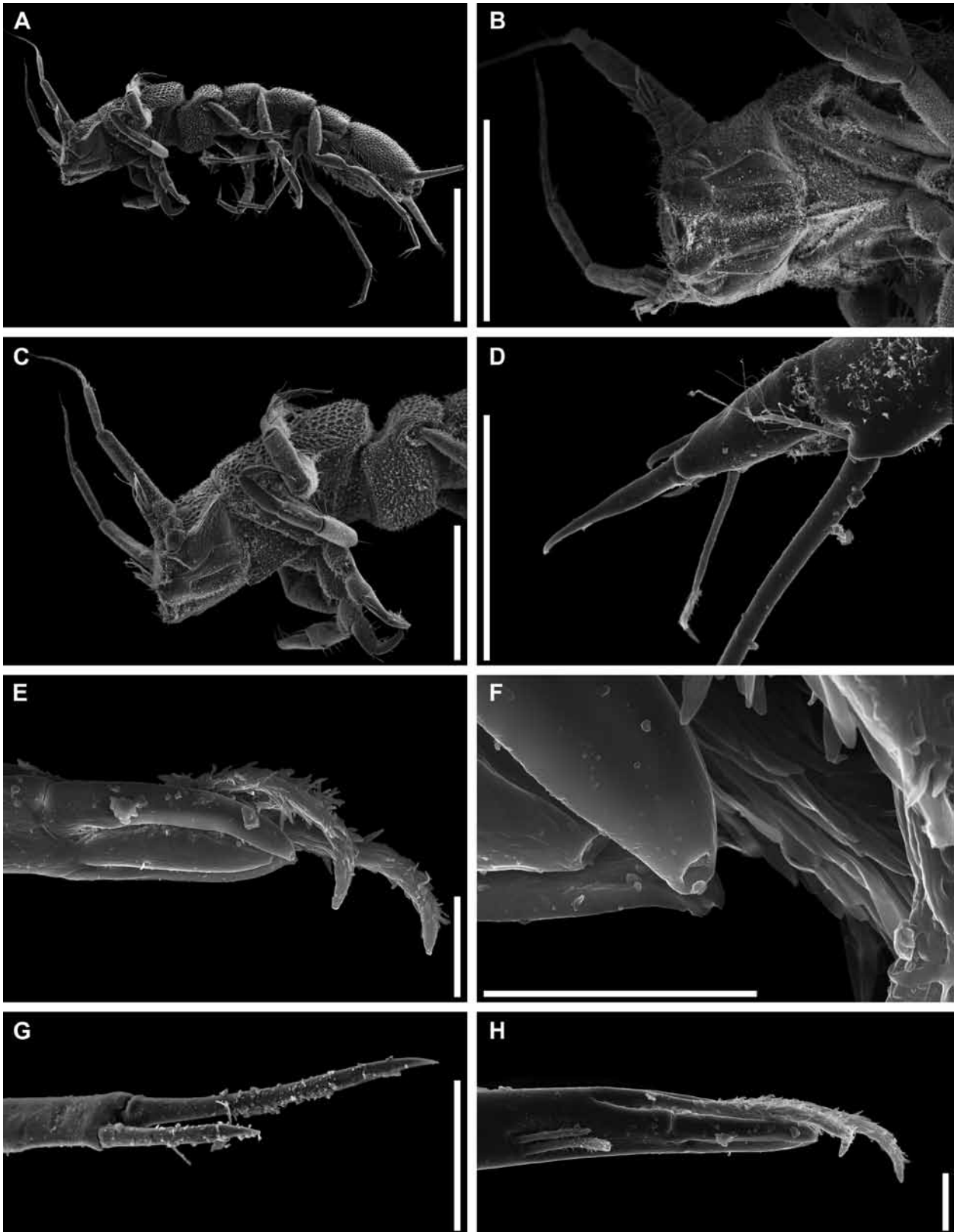


Figure 20. *Macrostylis antennamagna* Riehl and Brandt, 2010 copulatory male. **A:** habitus lateral. **B:** cephalothorax ventral. **C:** anterior body, lateral. **D:** pereopod IV dactylus, dorsal. **E, F, H:** pereopod III dactylar claws. **G:** pereopod dactylar claws. Scales: A = 1.0 mm; B, C = 0.5 mm; D, G = 50 μ m; E, H = 10 μ m; F = 5.0 μ m. Images modified after Riehl (2009).

absent; 1 = present.

Char. 57. Pleotelson lateroventral ridges: 0 = restricted to follow the pleopodal-cavity margin; 1 = anteriorly extending laterally and dorsally.

Char. 58. Pleotelson lateroventral setal rows: 0 =

absent; 1 = present.

Anus position with regard to pleopodal cavity

Typically, the anus is either covered by the opercular pleopods and thus inside the pleopodal cavity,

or it is exposed and outside the cavity. Where the opercular pleopods are shorter than the pleopodal cavity the anus is situated within the cavity but still exposed (Fig. 10F).

Char. 59. Anus position with regard to pleopodal cavity: 0 = inside; 1 = outside.

Head appendage characters

Antennula article number

The antennula of most macrostyloid species consists of five articles (Fig. 3D, Fig. 4B, C, Fig. 5B, Fig. 8D, Fig. 16C). We assume this to be the plesiomorphic state for this family. According to Riehl *et al.* (2014), however, this might be a reduced condition from the Janiroidea perspective. Both further reductions (Fig. 9C, F, Fig. 17C, E, F) as well as higher numbers of articles can be observed frequently in the Macrostylidae (see e.g. Kussakin, 1999).

Char. 60. Antennula article number: 0 = five; 1 = four; 2 = three; 3 = two; 4 = one; 5 = 6 or more.

Female antennula terminal article shape and size

Considering the relative length of the terminal antennula article, which is article 5 in the majority of species, two states are differentiated: the small state is characterized by a joint that is more than one tenth of the antennula first article length while the minute state defines articles that are one tenth in length or smaller. Regarding the shape, two states are found in macrostylids. The terminal article is considered elongate, when its length is subsimilar to its width or greater (Fig. 3D, Fig. 16A, C); it is squat when its width exceeds its length but it is clearly projecting (Fig. 5B, Fig. 8D).

Char. 61. Antennula terminal article size (in female): 0 = short; 1 = minute.

Char. 62. Antennula terminal article shape (in female): 0 = squat; 1 = elongate.

Antennula article shape sexual dimorphism (in macrostylids with 5 antennula articles)

In all currently known macrostyloid females and immature males, the size of the antennula articles decreases in length and width from proximal to distal. In the adult males, however, two distinct conditions can be identified that are independent of the male enlargement that seems to be always present in subadult and fully mature macrostyloid males: the pattern can be either similar to that observed in females and immature males (compare Fig. 4B with Fig. 5B), or articles one, two and five are elongate, while articles three and four are comparably short – usually wider than long (e.g. in *Macrostylis spinifera* Sars, 1864; compare Fig. 6A with Fig. 16A, C; see also Fig. 11A, B).

Char. 63. Antennula article shape sexual dimorphism: 0 = absent; 1 = present, in male: articles 1, 2, 5 elongate, 3 and 4 short.

Antennula flagellum aesthetasc number

In macrostyloid females, either one aesthetasc is present and only on the terminal article (Fig. 3B, C) or both terminal and subterminal articles bear one aesthetasc respectively (Fig. 13D). Species with aesthetascs on the antepenultimate flagellar article are currently not known for *Macrostylis*. The majority of Janiroidea have one aesthetasc per flagellar segment in the male. Predominantly those taxa that have a small flagellum are characterized by more than one aesthetascs per antennular segment (Fig. 4B, C). Rarely, substantially more than 5 aesthetascs per segment are present (Riehl *et al.* 2014), such as in *Macrostylis longipedis* Brandt, 2004 (see also Fig. 11A, B, Fig. 16A, C).

Char. 64. Antennula flagellum aesthetasc presence on subterminal article (in female): 0 = absent; 1 =

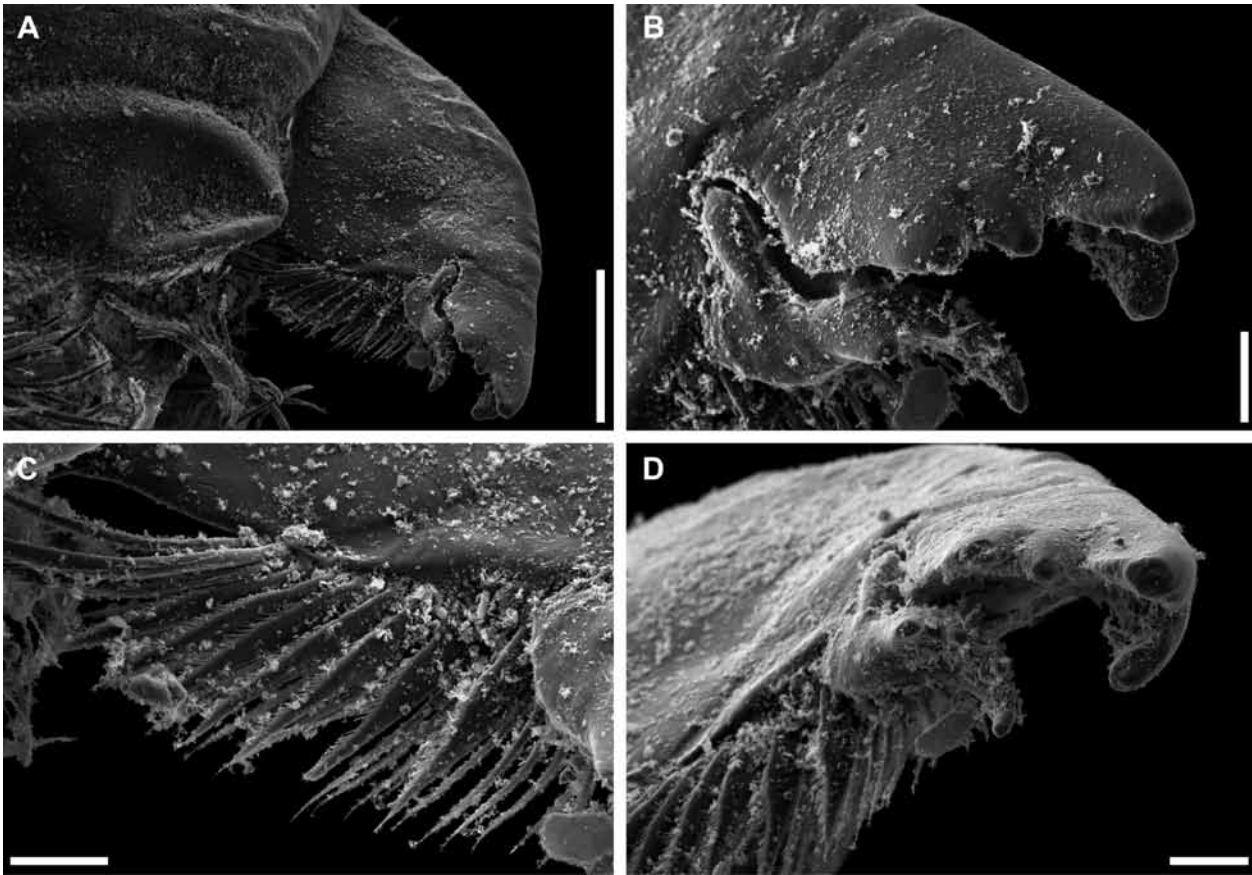


Figure 21. *Macrostylis* aff. *minuta* Menzies, 1962 (Diva 3 #2) ovigerous female left mandible. **A:** overview. **B:** incisor and *lacinia mobilis*. **C:** spine row. **D:** Incisor and *lacinia mobilis*, medial view. Scales: A = 50 μ m; B–D = 10 μ m.

present.

Char. 65. Antennula flagellum aesthetasc number per article (in adult male): 0 = one; 1 = two to five; 2 = six or more.

Antennula enlargement in adult males

In Macrostylidae as well as some Munnopsidae, mature males have significantly enlarged antennulae (compare Fig. 4B with Fig. 5B). This sexual dimorphism affects especially the width in some species also the length of the limb. In many Janiridae and “munnoid” taxa (Wägele 1989), male and female antennulae are subsimilar in their relative sizes.

Char. 66. Antennula enlargement in adult males: 0 = absent; 1 = present.

Antenna article 5 & 6 (merus & carpus) length

Merus and carpus of the antenna occur in two states in the Janiroidea: distinctly longer than the

preceding articles (precoxa–ischium) combined or relatively short in comparison to articles 1–4. In Macrostylidae, those species with a shorter or subsimilar article 6 can be discerned from those with the sixth article exceeding article five length.

Char. 67. Antenna article 5 length (vs. podomeres 1–4): 0 = subsimilar or shorter; 1 = longer.

Char. 68. Antenna article 6 length (vs. podomeres 1–4): 0 = subsimilar or shorter; 1 = longer.

Char. 69. Antenna article 6 length (vs. article 5 length): 0 = subsimilar or shorter; 1 = longer.

Antenna enlargement in adult males

In macrostylids, such as *M. antennamagna* Riehl and Brandt, 2010 (Fig. 20A–C), the metamorphosis of the adult male also includes changes in the antenna. The podomeres of the latter are distinctly increased in size when compared to the female or subadult males, analogous to the changes that occur in the antennula.

Char. 70. Antenna enlargement in adult males: 0 = absent; 1 = present.

Shape of mandibular coxa

Two distinct shapes of the mandible coxa are distinguished in Macrostylidae. In medial view, the robust mandible type it is gradually narrowing towards distally, culminating in the incisor. This type of mandible has a straight coxal axis. The more slender mandible type has a “neck” proximally to the incisor, which is the narrowest area of the coxa. From there, the coxa is slightly widening towards distally. In the latter mandible type, the incisor is frequently bent towards ventrally – the coxal axis is curved.

Char. 71. Mandibular coxa (shape): 0 = robust; 1 = slender.

Char. 72. Mandibular coxa (shape): 0 = straight; 1 = bent.

Mandible incisor teeth arrangement

Most Janiroidea have multidentate incisor processes. These are featuring multiple teeth arranged in an approximate linear way. This is considered the plesiomorphic condition from the macrostylid perspective (Riehl *et al.* 2014). Within Macrostylidae, two distinct forms can be identified that both differ significantly from the plesiomorphic state. Most macrostylids have multidentate incisors with one or few teeth both on the dorsal and ventral sides subdistally to a single, strong, mediate tooth (Fig. 21). The incisor teeth thus form a concavity that partly houses the *lacinia mobilis*. In few selected species, the incisor appears relatively simple consisting of one blunt tooth and without further cusps (Riehl and Brandt 2010; Riehl and Brandt 2013).

Char. 73. Mandible incisor process (shape): 0 = multidentate, linear arrangement; 1 = monodentate, rounded; 2 = multidentate with subdistal teeth.

Differentiation of the movable laciniae on the mandibles

The right *lacinia mobilis* may be either indistinguishable from the remainder of the spine row or differentiated to form a movable tooth-like structure (Richter *et al.* 2002; Riehl *et al.* 2014). In macrostylids where the *laciniae* are differentiated, its cuticle is either weakly calcified and fragile with multiple scale- or spine-like distal tips or it is heavily calcified with broad humps much alike the left *lacinia*. The size of the right *lacinia mobilis* is either subsimilar or distinctly smaller than the left one.

Char. 74. Mandibular left *lacinia mobilis*: 0 = indistinguishable; 1 = differentiated.

Char. 75. Mandibular left *lacinia mobilis* shape and robustness (where differentiated): 0 = weakly calcified; 1 = heavily calcified.

Char. 76. Mandibular right *lacinia mobilis*: 0 = indistinguishable; 1 = differentiated.

Char. 77. Mandibular right *lacinia mobilis* shape and robustness (where differentiated): 0 = weakly calcified; 1 = heavily calcified.

Char. 78. Mandibular right *lacinia mobilis* relative size (where differentiated): 0 = distinctly smaller left *lacinia*; 1 = subsimilar left *lacinia*.

Maxilliped palp propodus distomedial projection.

The maxilliped is a transformed thoracopod with an opercular function (besides others) in Asellota. Distomedially in the maxilliped propodus, a projection may be present.

Char. 79. Maxilliped palp propodus distomedial projection: 0 = absent; 1 = present.

Maxilliped palp dactylus presence

The maxilliped palp is usually consisting of five articles (ischium–dactylus) but several variations can be observed across Janiroidea. In Katianiridae

Svavarsson, 1987 and one species of Macrostylidae (T. Riehl, unpubl. data), for example, only four palp articles are present. There is indication that despite the superficial similarity, these phenomena are not homologous. While an elongated second article and the positions and orientations of the articulations and segments in Katianiridae indicate a fusion of merus and carpus, in some macrostylids the fifth article appears to be not expressed (T. Riehl, unpubl. data). In the context of this paper, only the expression of the maxilliped dactylus is of interest.

Char. 80. Maxilliped palp dactylus: 0 = present; 1 = absent.

Pereopod characters

Coxa setation of anterior and posterior pereopods

The coxal setation varies substantially in the Janiroidea. Commonly, the coxae lack setation when they are located in a more ventral position or reduced. This is the case, for example, in the anterior pereonites of Macrostylidae. Most species of this family have a setose posterior coxae as well, even though exposed. Nevertheless, setose coxae rarely occur in macrostylids (T. Riehl, unpubl. data) as in urstylids, which might represent the plesiomorphic condition from the macrostylid point of view.

Char. 81. Anterior pereonites coxae setation (presence): 0 = present; 1 = absent.

Char. 82. Posterior pereonites coxae setation (presence): 0 = present; 1 = absent.

Anterior pereopods coxae orientation

The majority of janiroideans has the coxae of the anterior pereonites oriented somewhat lateroventrally. Along with ventrally projecting lateral

tergite margins in some macrostylids, such as *M. scotti* Riehl and Brandt, 2013, the orientation of the coxae is changed to a more medial direction. In lateral view, they are obscured in these species by the tergal margin.

Char. 83. Anterior pereopods coxae orientation: 0 = lateroventrally; 1 = medioventrally

Pereopod III ischium form

The presence of a projection of the pereopod III ischium dorsal margin is apomorphic for Macrostylidae (Riehl *et al.* 2014). Most other janiroideans have only a distal increase in width of this article if anything, but never have a distinctive bulge midlength on the ischium. Within Macrostylidae, distinct shapes are delineated. A flat and rounded projection implies that both proximal and distal 'slopes' are somewhat convex and the apex broadly rounded.

A long and tapering projection is characterized by two concave slopes. Lobes of a triangular shape have somewhat straight slopes. We further differentiate distally protruding projections, where the proximal slope is convex and the distal slope clearly concave, from semicircular projections as well as hook-shaped acute projections.

Char. 84. Pereopod III ischium form: 0 = straight or slightly vaulted; 1 = with dorsal lobe. We further differentiate distally protruding projections, where the proximal slope is convex and the distal slope clearly concave, and semicircular projections.

Char. 85. Pereopod III ischium dorsal lobe form (if present): 0 = flat, rounded; 1 = triangular; 2 = tapering; 3 = distally protruding; 4 = broadly rounded, semicircular; 5 = hook-shaped, recurved.

Pereopod III ischium dorsal setation

The ischial projection of the Macrostylidae is frequently prominently setose (Kussakin 1999; Riehl and Kaiser 2012; Riehl *et al.* 2014). Most species

of this family bear a dorsal row of setae consisting of simple setae on the proximal and distal slopes of the projection and sometimes one prominent seta on its apex, rarely a second prominent seta subapically. There is, however, considerable variation in these characters. The apical and subapical setae vary in their shape and robustness as well as in their articulation. Prominent is defined here as outstanding with regard to their size in comparison to the direct neighbours in the setal row. We distinguish between straight and recurved, robust and simple, as well as spine-like and flexibly articulating prominent setae. Other Janiroidea have distinctly different setal configurations, commonly consisting of few, if any, ischial setae (Riehl *et al.* 2014).

Char. 86. Pereopod III ischium dorsal row of seta distally to lobe apex (presence): 0 = present; 1 = absent.

Char. 87. Pereopod III ischium dorsal setation: 0 = setation minor or absent; 1 = setation prominent.

Char. 88. Pereopod III ischium apical seta (size): 0 = common; 1 = prominent.

Char. 89. Pereopod III ischium apical seta (shape): 0 = straight; 1 = curved.

Char. 90. Pereopod III ischium apical seta (articulation): 0 = flexibly articulated; 1 = spine-like.

Char. 91. Pereopod III ischium subapical prominent setae (size): 0 = common; 1 = prominent.

Char. 92. Pereopod III ischium subapical seta (shape): 0 = straight; 1 = recurved.

Char. 93. Pereopod III ischium subapical seta (articulation): 0 = flexibly articulated; 1 = spine-like.

Char. 94. Pereopod III ischium dorsal row of seta distally to lobe apex (presence): 0 = present; 1 = absent.

Pereopod IV carpus shape

Plesiomorphically, the carpus width is subsimilar along the whole length of the article with margins

parallel and width near depth. In some macrostylids, this article is extended at the dorsal and ventral margins and thus appears flattened. The carpus width thus shows two distinct conditions: it is considered slender when its width is subsimilar its depth and does not widen significantly relative to the width at the mero-carpal articulation. A flat carpus is recognized by its dorsal and ventral margins extending clearly beyond the width at the mero-carpal articulation and a greater width compared to its depth.

Char. 95. Pereopod IV carpus shape: 0 = slender; 1 = flattened.

Pereopod VII development and reduction (heterochrony, hypomorphosis)

In species that display pedomorphism in their seventh pereonite, three distinct developmental conditions are distinguished regarding the developmental condition of the seventh pereopod. In most species, the pereopod VII is fully developed and thus subsimilar to pereopod VI regarding length and setation. Some species have the seventh walking legs retarded. These characters appear to have stopped ontogeny at a manca stage as they are paucisetose, relatively short and held midventrally under the opercular pleopods. This negative offset can be explained by hypomorphosis (Reilly *et al.* 1997). Reduced seventh pereopods consist only of coxa and basis. These variations in the development of the seventh walking leg can occur independently of the pedomorphism of the seventh pereonite and are hence coded separately.

Char. 96. Pereopod VII in adult specimens: 0 = fully developed; 1 = underdeveloped; 2 reduced.

Pereopod V–VII sexual length dimorphism

While in most macrostylids, as in other Janiroidea, the adult male's posterior walking legs have subsimilar relative length proportions compared to

the conspecific females, some species show sexual length dimorphism. In these species, for example *Macrostylis subinermis* Hansen, 1916 (Kussakin 1999), the adult males have elongated seventh pereopods.

Char. 96. Pereopod VII length in adult male vs. female: 0 = subsimilar; 1 = distinctly longer in male.

Pereopod VII basis posterior margin setation

Amongst Macrostylidae, some species bear a dense row of setae along the posterior margin of their pereopod VII basis. This is unique amongst Isopoda. The setae may be either short and no longer than the width of the basis or distinctly longer. The distribution of the setal row is either limited to the proximal half of the basis or stretching beyond.

Char. 97. Pereopod VII basis posterior margin row of setae (presence): 0 = absent; 1 = present.

Char. 98. Pereopod VII basis posterior margin setae (length): 0 = short; 1 = long.

Char. 99. Pereopod VII basis posterior margin row of setae (distribution): 0 = limited to proximal half; 1 = beyond proximal half.

Pleotelson appendage characters

Male pleopod I medial & lateral lobe arrangement

In Urstylidae, the pleopod I lobes the medial lobes lie flat and parallel to each other. The medial lobes partly override the lateral lobes ventrally (Riehl *et al.* 2014). In Macrostylidae, the lateral and medial lobes can be commonly arranged lateral to each other and in the same plane. Two distinct shapes are distinguished in Macrostylidae: in most species, the lateral lobes are lateroventrally projecting and hook-shaped, such as in *Macrostylis spinifera* Sars,

1864; alternatively, for example in *M. subinermis* Hansen, 1916, the lateral lobes are merely bluntly rounded and not projecting while the medial lobes project clearly beyond the lateral lobes distally and in some cases also project ventrally.

Char. 100. Male pleopod I medial & lateral lobe arrangement: 0 = lateral; 1 = medial lobes ventrally “overriding” lateral lobes; 2 = medial lobes projecting distally (and sometimes ventrally), lateral lobes not projecting.

Male pleopod I relative to pleopod II

In Janiroidea, the male first and second pleopods form the operculum that encloses the branchial cavity. These two pairs of appendages may either lay flat in one plane or form a vaulted operculum that clearly projects ventrally beyond the margin of the branchial cavity. The condition where the first pleopods are clearly not projecting to the second pleopods’ distal margins is distinguished from the state where they are projecting to the second pleopods’ distal tips or beyond. In the first case, they may be distally as well as laterally embedded into the second pereopods. In the latter condition, the second pleopods distally touch each other. The distal part of the first pleopods may be curved ventrally in a way that it projects ventrally beyond the second pleopod margins.

Char. 101. Male operculum (shape): 0 = flat, even; 1 = vaulted.

Char. 102. Male pleopod I length vs. pleopod II length: 0 = clearly shorter; 1 = subsimilar or longer.

Char. 103. Pleopods II distally: 0 = rounded, distinctly separate from each other; 1 = distally enclosing first pleopods, touching each other.

Char. 104. Pleopods I distally: 0 = straight, level with second pleopods; 1 = curved ventrally, projecting ventrally beyond second pleopod margins.

Length of setae distally on the female pleopod II (operculum)

While in most taxa with an apical row of setae on the operculum feature only relatively short setae, in Urstylidae, Macrostylidae, and Mesosignidae, these setae are distinctly longer, partly covering the anus. We define short as being subequal or less than $\frac{1}{4}$ operculum length and long as significantly larger than $\frac{1}{4}$ operculum length.

Char. 105. Female operculum distal setae (length): 0 = short; 1 = long.

Female operculum lateral fringe of fine setae

The opercular pleopod II of the female janiroideans has marginal setae, either distally that may or may not cover the anus, or laterally. Among the Macrostylidae, either a gradual transition between the lateral fringes and the distal row of pappose setae occurs or they are distinctly separated.

Char. 106. Female operculum lateral fringe of fine setae (presence): 0 = absent; 1 = present.

Char. 107. Female operculum lateral and distal setae (transition): 0 = gradual; 1 = separated.

Female operculum shape and relative length

In Asellota, the female second pleopods are fused to form an unpaired monoarticulate appendage (Wilson 1987) that in Janiroidea seals off the branchial chamber as an operculum (Wägele 1989). Its shape largely follows the outline of the pleopodal cavity. We discern between ovoid opercula and those that appear distally tapering because their outline is concave distolaterally. Along the ventral midline, a broadly rounded keel may be present. This keel may or may not constitute a longitudinal furrow (Birstein 1973). Only few macrostylid species have operculi that completely seal off the pleopodal cavity. Predominantly, the operculum does not project to the anus.

Char. 108. Female operculum shape: 0 = distally tapering; 1 = ovoid.

Char. 109. Female operculum keel: 0 = present; 1 = absent.

Char. 110. Female operculum keel longitudinal furrow: 0 = present; 1 = absent.

Char. 111. Female operculum length: 0 = overlapping or completely covering anus; 1 = not projecting to anus.

Pleopod III exopod

Although the third pleopod shows consistent patterns across several families of the Janiroidea ((Wilson 1985; Wilson 1989): Figs 36, 37) so that length, width and expression of segmentation are useful apomorphic features (Riehl *et al.* 2014), there is variability present within the Macrostylidae as well. The exopod, for example, is either uniarticulate or plesiomorphically biarticulate. Also plesiomorphically, the exopod is fringed by short plumose setae. Within Macrostylidae, these setae are always simple but appear singly or in small numbers and only close to the ramus' distal tip.

Char. 112. Pleopod III exopod: 0 = biarticulate; 1 = monoarticulate.

Char. 113. Pleopod III exopod distal setae (number and position): 0 = one apically; 1 = more than 1 on apical and lateral margins; 2 = absent.

Pleopod IV exopod fringe of setae

Laterally on the macrostylid exopod of pleopod IV, a row of setae may be present or not.

Char. 114. Pleopod IV exopod lateral row of setae: 0 = absent; 1 = present.

Pleopod IV presence of large pappose seta distally on exopod

The presence of a single large, pappose seta distally on the pleopod IV exopod is deeply rooted within the Janiroidea although multiple variations

occur. Urstylids, thambematids, desmosomatids and nannoniscids follow this pattern, which is also commonplace amongst macrostylids. For the latter family, this consequently represents the plesiomorphic condition. Rarely, however, the seta is absent in species of *Macrostylis* (T. Riehl, unpubl. data.).

Char. 115. Pleopod IV exopod distal pappose seta (presence): 0 = present; 1 = absent.

Uropod endopod length in relation to the protopod length

Macrostylidae, similar to Urstylidae, have extremely elongate uropods, where commonly most of the length consists of the protopod. However, there is considerable variation across the family.

Char. 116. Endopod length vs. protopod length: 0 = longer; 1 = subsimilar or shorter.

Shape of uropod protopod distal margin and location of endopod articulation

The protopod may either have a subparallel or homogeneously narrowing protopod that has the endopod articulation at its distal margin; or the protopod may taper off towards laterally and projecting beyond the endopod articulation.

Char. 117. Uropod protopod-endopod articulation: 0 = subterminally; 1 = terminally.

Potentially informative characters

Only the dorsal habitus as well as certain appendages have gained attention throughout the complete taxonomic history of the Macrostylidae. Consequently, for many morphological features, especially anatomical characters, the current knowledge is insufficient.

The imbricate ornamentation is one of the previously neglected characters and seems widely distributed across macrostylids (Aydogan *et al.* 2000; Riehl *et al.* 2012; Riehl and Brandt 2013).

Similar microstructures (e.g. honey-comb patterns, reticulate patterns) have been observed across other isopod and peracarid groups as well (Brix *et al.* submitted; Moreira 1974; Bruce 1992; Brökeland and Wägele 2004; Brökeland and Brandt 2006; Kaiser 2008; Rehm 2009; Kaiser and Marner 2012) that may in some cases be homologous. Their form and distribution as well as sexual dimorphisms are likely to hold valuable information for taxonomy and systematics of these isopods. However, because assessment of such unapparent structures usually requires scanning electron microscopy or other imaging techniques that were infrequently used in the past, our knowledge is scarce.

The degree of integration of the first three pereonites into the fossosome potentially deserves more attention as well. The expression of the segment borders between the tergal as well as sternal plates, for example, shows considerable variation (compare Fig. 8C with 9B).

The location of the spermathecal duct has been discussed multiple times (Wolff 1962; Veuille 1978; Wilson 1986; Wilson 1987; Brusca and Wilson 1991; Wilson 1991; Just 2005) and continues to be a useful character for phylogeny and classification of the janiroideans. This character has allowed Riehl *et al.* (2014) to exclude those taxa from the analysis that have a dorsal opening to the spermathecal duct (e.g. Haploniscidae, Ischnomesidae, Dendrotionidae) or the largely shallow-water taxa such as Munnidae and Santiidae where this structure is located ventrally (Wilson 1986; Wilson 1991).

Most higher janiroideans used in previous analyses (Riehl *et al.* 2014) and in the present paper are assumed to have the pore in the articular membrane anteriorly on pereonite 5, including *Urstylis* (Riehl *et al.* 2014), while *Macrostylis* has the pore positioned somewhat more posteriorly, and not in the articular membrane (see Riehl *et al.*

(2012): Fig. 1), a state that is possibly derived from the urstylid condition. A generality of this condition in Macrostylidae (as in other taxa) can only be assumed since observations are currently lacking for all but one species of this family.

The significant differences of the male pleopod I distal lobes between some species of macrostylids (compare Fig. 15G with Fig. 16D) might be reflected in their mating behavior as well as the arrangement of the female genitalia. Until now, the latter have been identified only for one species.

Conclusions

Macrostylidae are characterized by a unique, distinct and highly derived morphology (Fig. 2), which can be interpreted in the light of key innovations in the sense of Mayr (1960): as behaviorally important synapomorphies that are connected with a major adaptive radiation and that are presumed to have had major influence on the latter.

Regarding intra-familial relationships, these many shared apomorphies seem to outweigh distinguishing characters and to have hindered delineation of subtaxa, such as genera, within the family. Since macrostylids are a relatively successful group both in ecological and evolutionary terms (Hessler *et al.* 1979; Kaiser *et al.* 2007; Brandt *et al.* 2007b; Wilson 2008a; Brandt *et al.* 2009), we assume that their unique and distinct morphology might be connected with a major adaptive radiation in the early phylogenetic history of this group. The typical macrostylid morphology (Fig. 2) is thus hypothesized to represent behaviorally important synapomorphies, or “key innovations” (Mayr 1960).

Macrostylid morphology is characterized by a set of reductions, for example in the anten-

nae, pereonal segment borders and pereonites. As assumed before on the basis of collection data (Thistle and Wilson 1987; Harrison 1989; Wilson 2008a), morphology (Wägele 1989) and behavioral observations (Hessler and Strömberg 1989), we interpret most of the unique but consistent morphological features of macrostylids as adaptations to burrowing habits (Wolff 1962) that may have facilitated the success of Macrostylidae. Yet thorough behavioral observations remain to be conducted.

Nevertheless, the high degree of similarity on the one hand and the high diversity and large distribution on the other hand seem to contradict each other. They indicate a lack of selective pressure and niche-related differentiation or rather conserving selection in the gross morphology of the group over their some 250 my evolution (Lins *et al.* 2012). It is still mysterious, what the factors may be that drive speciation in the abyss.

While the common appearance of macrostylids features various adaptations, many of them reductions that may be connected to an endobenthic live style, adult (or terminal (Riehl *et al.* 2012)) males of various species change their appearance with their adult moult. Increased relative sizes of antennula, antenna, aesthetascs, posterior pereopods, and uropods likely have not evolved under natural selection as they seem disadvantageous for living within the sediment. Instead, sexual selection may be the driving force behind the evolution of such seemingly obscure body shapes as found in the adult male of *Macrostylis subinermis*. Similarly, more intensive behavioral observations than presently available (Hessler and Strömberg 1989) would help to solidify such speculations.

These sexual dimorphisms, besides further characters presented in this paper, illustrate that despite the general morphological homogeneity of this group (Riehl and Brandt 2010), significant variation in morphological characters exists. Alt-

though relationships remain to be inferred by means of phylogenetic analyses prior to a fundamental revision of Macrostyliidae, several subgroups already become apparent.

The first of these subgroups includes those species that have a pronounced sexual dimorphism: In *Macrostyliis subinermis* Hansen, 1916 and *M. longipedis* Brandt, 2004, for example, males go through a metamorphosis when they moult into mature state. The antennula articles then have peculiar length ratios (e.g. with the terminal article elongate) and several appendages, such as antennula, seventh pereopods and uropods, can be extremely elongated. It is, however, problematic to allocate a species to this group. Firstly, only mature males expose the typical characters and these are often rare in the samples. Secondly, the sexual dimorphisms may make allocation of mature males with their conspecific females as well as juvenile males problematic as long as only morphological data is considered.

Another subgroup that becomes apparent is characterized by various degrees of reduction and hypomorphosis of their antennulae and seventh pereopods. An additional characteristic is the shift of the coxal articulations into a more medial direction that is connected to ventrally projecting tergite margins of pereonites 1–4. This group may include species such as *M. minuta* Menzies, 1962, *M. robusta* Brandt, 2004 and *M. uniformis* Riehl and Brandt, 2010.

However, for most species of *Macrostyliis*, group allocation currently remains unclear. Their systematic position and the solidity of the above hypothesized groups are to be evaluated in a phylogenetic context. A biogeographical study on the Macrostyliidae may reveal interesting patterns, especially related to their evolutionary history. The subgroups discussed above, for instance, seem to have a cosmopolitan distribution, which might indicate multiple circumglobal colonizations by ma-

crostyliids. Species lacking the anteriorly directed spine on the first pereonite, conversely, seem to have a narrow geographic distribution in the North Pacific. They are particularly interesting since their occurrence around and within the Kurile-Kamchatka Trench indicate that a phylogenetic analysis might reveal novel ideas about the origin of hadal fauna.

Finally, multiple species of the predominantly bathyal and abyssal macrostyliids occur on the shelf of North America (G.D.F. Wilson, personal communication), Northern Europe (Sars 1899; Hansen 1916), Western Australia (T. Riehl, unpubl. data) and at various locations around Antarctica (Brandt 2002; Brandt *et al.* 2011; Riehl and Kaiser 2012). More are likely to be revealed with increasing sampling effort in previously unsampled areas (e.g., Kaiser *et al.* 2013) and using the appropriate gear. This disjunct distribution across continental shelves points towards multiple independent colonizations of the shallows by deep-sea taxa.

Acknowledgements

The invaluable support of George D.F. Wilson to TR is gratefully appreciated. Frank Friedrich and Renate Walter assisted with the SEM. Financial support was granted by a Ph.D. fellowship of the German National Academic Foundation (Studienstiftung des deutschen Volkes) and a Geddes fellowship of the Australian Museum to TR.

References

Aydogan, A., Wägele, J.-W. and Park, J. Y. (2000) New deep-sea isopods (Crustacea. Isopoda. Asellota) from the Atacama-Trench. *Mitteilungen-Museum für Naturkunde in Berlin*, 76(2), 175–194 (Zoologische Reihe).

Beddard, F. E. (1886) Report on the Isopoda collected by HMS

- Challenger during the years 1873–76. Part 2. Report of the Voyage of HMS Challenger, 17, 1–178.
- Birstein, Y. A. (1970) New Crustacea Isopoda from the Kurile-Kamchatka Trench area. In: Bogorov, V. G. (Ed.) Fauna of the Kurile-Kamchatka Trench and its environment. pp 308–356. Moscow: Academy of Sciences of the USSR. (Proceedings of the Shirshov Institute of Oceanology; 86).
- Birstein, Y. A. (1973) Deep water isopods (Crustacea: Isopoda) of the north-western part of the Pacific Ocean. *Akademiya Nauk, SSSR*: Moscow, 1–213.
- Bober, S. and Riehl, T. (accepted) Adding depth to line-artwork by digital stippling – A step-by-step guide to the method. *Organisms Diversity & Evolution*.
- Brandt, A. (2002) *Desmostylis gerdesi*, a new species (Isopoda: Malacostraca) from Kapp Norvegia, Weddell Sea, Antarctica. *Proceedings of the Biological Society of Washington*, 115(3), 616–627.
- Brandt, A. (2004) New deep-sea species of Macrostylidae (Asellota: Isopoda: Malacostraca) from the Angola Basin off Namibia, South West Africa. *Zootaxa*, 448, 1–35.
- Brandt, A., Bathmann, U., Brix, S., Cisewski, B., Flores, H., Göcke, C., Janussen, D., Krägefsky, S., Kruse, S., Leach, H., Linse, K., Pakhomov, E., Peeken, I., Riehl, T., Sauter, E., Sachs, O., Schüller, M., Schrödl, M., Schwabe, E., Strass, V., van Franeker, J. A. and Wilmsen, E. (2011) Maud Rise – a snapshot through the water column. *Deep Sea Research Part II: Topical Studies in Oceanography*, 58(19-20), 1962–1982.
- Brandt, A., Brenke, N., Andres, H.-G., Brix, S., Guerrero-Kommritz, J., Mühlenhardt-Siegel, U. and Wägele, J.-W. (2005) Diversity of peracarid crustaceans (Malacostraca) from the abyssal plain of the Angola Basin. *Organisms Diversity & Evolution*, 5(Supplement 1), 105–112.
- Brandt, A., Brix, S., Brökeland, W., Choudhury, M., Kaiser, S. and Malyutina, M. V. (2007a) Deep-sea isopod biodiversity, abundance, and endemism in the Atlantic sector of the Southern Ocean—Results from the ANDEEP I–III expeditions. *Deep-Sea Research Part II*, 54(16-17), 1760–1775.
- Brandt, A., De Broyer, C., De Mesel, I., Ellingsen, K. E., Gooday, A. J., Hilbig, B., Linse, K., Thomson, M. R. A. and Tyler, P. A. (2007b) The biodiversity of the deep Southern Ocean benthos. *Philosophical Transactions of the Royal Society B: Biological Sciences*, 362(1477), 39–66.
- Brandt, A., Elsner, N., Brenke, N., Golovan, O., Malyutina, M. V., Riehl, T., Schwabe, E. and Würzberg, L. (2013) Epifauna of the Sea of Japan collected via a new epibenthic sledge equipped with camera and environmental sensor systems. *Deep Sea Research Part II: Topical Studies in Oceanography*, 86-87, 43–55.
- Brandt, A., Linse, K. and Schüller, M. (2009) Bathymetric distribution patterns of Southern Ocean macrofaunal taxa: Bivalvia, Gastropoda, Isopoda and Polychaeta. *Deep Sea Research Part I: Oceanographic Research Papers*, 56(11), 2013–2025.
- Brandt, A. and Malyutina, M. V. (2012) The German-Russian deep-sea expedition KuramBio (Kurile Kamchatka Biodiversity Study): to the Kurile Kamchatka Trench and abyssal plain on board of the R/V Sonne, 223rd Expedition, July 21th - September 7th 2012 [online]. Hamburg: University of Hamburg; Biozentrum Grindel & Zoologisches Museum Hamburg. (R/V Sonne Cruise Reports).
- Brenke, N. (2005) An epibenthic sledge for operations on marine soft bottom and bedrock. *Marine Technology Society Journal*, 39(2), 10–21.
- Brix, S. (2011) Short Cruise Report RV Meteor M85/3 [online]. Hamburg: Institute of Oceanography, University of Hamburg.
- Brix, S., Riehl, T. and Leese, F. (2011) First genetic data for *Haploniscus rostratus* and *Haploniscus unicornis* from neighbouring deep-sea basins in the South Atlantic. *Zootaxa*, 2838, 79–84.
- Brix, S., Leese, F., Riehl, T. and Kihara, T.-C. (in press) A new genus and new species of Desmosomatidae Sars, 1897 (Isopoda) from the east South-Atlantic abyss described by means of integrative taxonomy. *Marine Biodiversity*.
- Bruce, N. L. (1992) A new genus of hemibranchiate sphaeromatid isopod crustacean from tropical Western Australia. *Journal of natural history*, 26(6), 1263–1272.
- Brusca, R. C. and Wilson, G. D. F. (1991) A phylogenetic analysis of the Isopoda with some classificatory recommendations. *Memoirs of the Queensland Museum*, 31, 143–204.
- Brökeland, W. and Brandt, A. (2004) Two new species of Ischnomesidae (Crustacea: Isopoda) from the Southern Ocean displaying neoteny. *Deep-Sea Research Part II*, 51(14-16), 1769–1785.
- Brökeland, W. and Brandt, A. (2006) New records of *Mastigoniscus* Lincoln, 1985 (Isopoda: Asellota: Haploniscidae) in the Southern Ocean, with descriptions of three new species. *Mitteilungen aus dem Hamburgischen Zoologischen Museum und Institut*, 103, 85–128.
- Brökeland, W. and Wägele, J.-W. (2004) Redescription of three species of *Haploniscus* Richardson, 1908 (Isopoda, Asellota, Haploniscidae) from the Angola Basin. *Organisms Diversity & Evolution*, 4(4), 237–239.
- Coleman, C. O. (2003) "Digital inking": how to make perfect line drawings on computers. *Organisms Diversity & Evolution*, 3(4), 303–304.
- Coleman, C. O. (2009) Drawing setae the digital way. *Zoosystematics and Evolution*, 85(2), 305–310.

- Dana, J. D. (1853) On the classification of the Crustacea Choristopoda or Tetradecapoda. *American Journal of Science and Arts Series 2*, 14(41), 297–316.
- Fresi, E. and Schiecke, U. (1972) *Pleurocope dasyura* Walker, 1901 and the Pleurocopidae New Family (Isopoda, Asellota). *Crustaceana*, S3, 207–213 (Studies on Peracarida (Isopoda, Tanaidacea, Amphipoda, Mysidacea, Cumacea)).
- Goloboff, P. A., Farris, J. S. and Nixon, K. C. (2008) TNT, a free program for phylogenetic analysis. *Cladistics*, 24(5), 774–786.
- Hansen, H. J. (1893) Zur Morphologie der Gliedmassen und Mundtheile bei Crustaceen und Insekten. *Zoologischer Anzeiger*, 16, 193–212.
- Hansen, H. J. (1916) Crustacea Malacostraca: The order Isopoda. *Danish Ingeolf Expedition*, 3(5), 1–262.
- Harrison, K. (1989) Are deep-sea asellote isopods infaunal or epifaunal? *Crustaceana*, 56(3), 317–319.
- Havermans, C., Sonet, G., d'Udekem d'Acoz, C., Nagy, Z. T., Martin, P., Brix, S., Riehl, T., Agrawal, S. and Held, C. (2013) Genetic and morphological divergences in the cosmopolitan deep-sea amphipod *Eurythenes gryllus* reveal a diverse abyss and a bipolar species. *PLoS ONE*, 8(9), e74218.
- Hessler, R. R. (1970) The Desmosomatidae (Isopoda, Asellota) of the Gay Head-Bermuda Transect. (Arrhebus, G. O. S., Cox, C. S., Fager, E. W., Hand, C. H., Newberry, T., and Schaefer, M. B., Eds.) Berkeley, Los Angeles, London: University of California Press, 15, 1–185. Available from: <http://escholarship.org/uc/item/1mn198vx>.
- Hessler, R. R. (1982) The structural morphology of walking mechanisms in eumalacostracan crustaceans. *Philosophical Transactions of the Royal Society of London. B, Biological Sciences*, 296(1081), 245–298.
- Hessler, R. R. and Strömberg, J. O. (1989) Behavior of janiroidean isopods (Asellota), with special reference to deep sea genera. *Sarsia*, 74(3), 145–159.
- Hessler, R. R., Wilson, G. D. F. and Thistle, D. (1979) The deep-sea isopods: a biogeographic and phylogenetic overview. *Sarsia*, 64(1-2), 67–75.
- Hodgson, T. V. (1910) Crustacea IX. Isopoda. In: Harmer, S. F. (Ed.) *National Antarctic Expedition 1901-1904. Natural History*. p 77. (Zoology and Botany).
- Hult, J. (1941) On the soft-bottom isopods of the Skagerak. *Zoologiska Bidrag från Uppsala*, 21, 1–234.
- Just, J. (2005) Xenosellidae, a new family of Janiroidea (Asellota: Isopoda: Crustacea), for *Xenosella coxospinosa* gen. nov., sp. nov., from the marine bathyal of eastern Australia. *Zootaxa*, 1085, 21–32.
- Just, J. and Poore, G. C. (1992) Vermectiadiidae, a new primitive asellote isopod family with important phylogenetic implications. *Journal of Crustacean Biology*, 12(1), 125–144.
- Kaiser, S. (2008) First record and new species of the genus *Hebefustis* Siebenaller and Hessler, 1977 (Isopoda: Asellota: Nannoniscidae) from the deep Weddell Sea Basin. *Zootaxa*, 1866, 467–481.
- Kaiser, S., Barnes, D. K. A. and Brandt, A. (2007) Slope and deep-sea abundance across scales: Southern Ocean isopods show how complex the deep sea can be. *Deep-Sea Research Part II: Topological Studies in Oceanography*, 54(16-17), 1776–1789.
- Kaiser, S., Brandão, S. N., Brix, S., Barnes, D. K. A., Bowden, D. A., Ingels, J., Leese, F., Schiaparelli, S., Arango, C. P., Badhe, R., Bax, N., Blazewicz-Paszkwowycz, M., Brandt, A., Brenke, N., Catarino, A. I., David, B., Ridder, C. D., Dubois, P., Ellingsen, K. E., Glover, A. G., Griffiths, H. J., Gutt, J., Halanych, K. M., Havermans, C., Held, C., Janussen, D., Lörz, A.-N., Pearce, D. A., Pierrat, B., Riehl, T., Rose, A., Sands, C. J., Soler-Membrives, A., Schüller, M., Strugnell, J. M., Vanreusel, A., Veit-Köhler, G., Wilson, N. G. and Yasuhara, M. (2013) Patterns, processes and vulnerability of Southern Ocean benthos: a decadal leap in knowledge and understanding. *Marine Biology*, 160(9), 2295–2317.
- Kaiser, S. and Marner, M. (2012) A new species of *Pentaceration* Just, 2009 (Isopoda, Asellota, Paramunnidae) from the Challenger Plateau, New Zealand (Tasman Sea). *Zoosystematics and Evolution*, 88(2), 171–184.
- Karaman, S. (1933) *Microcerberus stygius*, der dritte Isopod aus dem Grundwasser von Skoplje, Jugoslavien. *Zool. Anz.*, 102, 165–169.
- Kavanagh, F. A., Wilson, G. D. F. and Power, A. M. (2006) Heterochrony in *Haplomesus* (Crustacea: Isopoda: Ischnomesidae): revision of two species and description of two new species. *Zootaxa*, 1120, 1–33.
- Kussakin, O. G. (1999) Marine and brackish-water isopods from cold and temperate waters of the Northern Hemisphere Suborder Asellota. Part 2. Families Joeropsididae, Nannoniscidae, Desmosomatidae, Macrostylidae. (Alimov, A. F., Ed.) St. Petersburg: Publication of the Zoological Institute of the Russian Academy of Sciences, pp. 1-383. (Keys to the Fauna of the SSSR).
- Leach, W. E. (1814) Crustaceology. In: Brewster, D. (Ed.) *The Edinburgh Encyclopædia*. pp 383–437. Edinburgh: A. Balfour.
- Lilljeborg, W. (1864) Bidrag til kannedommen om de inom Sverige och Norrige förekommande Crustaceer af Isopodernas underordning och Tanaidernas familj. Inbjudningsskrift till Åhörande af de Offentliga Föreläsningar. C. A. Leffler, Kongl. Acad. Boktryckare, Upsala., 31 pp.
- Lins, L. S. F., Ho, S. Y. W., Wilson, G. D. F. and Lo, N. (2012) Evidence for Permo-Triassic colonization of the deep sea by

- isopods. *Biology Letters*, 8(6), 979–982.
- Maddison, W. P. and Maddison, D. R. (2011) Mesquite: a modular system for evolutionary analysis. [online]. Version: 2.75. Available from: <http://mesquiteproject.org>.
- Malyutina, M. V. (2008) *Microcope* gen. nov.–a new deep-sea genus of Munnopsidae (Crustacea, Isopoda, Asellota), with description of two new species from the Southern Hemisphere. *Zootaxa*, 1866, 555–574.
- Mayr, E. (1960) The emergence of evolutionary novelties. *Evolution after Darwin*, 1, 349–380.
- Menzies, R. J. (1956) New abyssal tropical Atlantic isopods with observations on their biology. *American Museum Novitates*, 1798, 1–16.
- Menzies, R. J. (1962) The isopods of abyssal depths in the Atlantic Ocean. In: Barnard, J. L., Menzies, R. J., and Bacescu, M. C. (Eds.) *Abyssal Crustacea*. pp 79–206. New York: Columbia University Press. (Vema Research Series).
- Mezhov, B. V. (1989) Two new species of *Macrostylis* (Isopoda, Macrostylidae) from the trenches of the Pacific Ocean and comments on the morphology of *M. galathea*. *Zoologicheskii Zhurnal*, 68(8), 33–40.
- Mezhov, B. V. (2003) Three new species of the genus *Macrostylis* G.O. Sars, 1864 (Crustacea: Isopoda: Macrostylidae) from the Indian Ocean. *Arthropoda Selecta*, 12(2), 95–100.
- Moreira, P. S. (1974) New records and a new species of *Serolis* (Crustacea, Isopoda, Flabellifera) from southern Brazil. *Boletim do Instituto Oceanográfico*, 23, 121–153.
- Neil, D. M. (1975) The mechanism of statocyst operation in the mysid shrimp *Praunus flexuosus*. *The Journal of Experimental Biology*, 62(3), 685–700.
- Neil, D. M. and Ansell, A. D. (1995) The orientation of tail-flip escape swimming in decapod and mysid crustaceans. *Journal of the Marine Biological Association of the United Kingdom*, 75(01), 55–70.
- Pohl, H. (2010) A scanning electron microscopy specimen holder for viewing different angles of a single specimen. *Microscopy Research and Technique*, 73(12), 1073–1076.
- Rehm, P. (2009) Description of a new subspecies *Diastylis enigmatica rossensis* (Crustacea: Peracarida: Cumacea) from the Ross Sea, Antarctica. *Helgoland Marine Research*, 63(2), 149–158.
- Reilly, S. M., Wiley, E. O. and Meinhardt, D. J. (1997) An integrative approach to heterochrony: the distinction between interspecific and intraspecific phenomena. *Biological Journal of the Linnean Society*, 60(1), 119–143.
- Richardson, H. (1911) Les crustacés isopodes du Travailleur et du Talisman: formes nouvelles. *Bulletin du Museum National d'Histoire Naturelle*, 17, 518–534.
- Richter, S., Edgecombe, G. D. and Wilson, G. D. F. (2002) The *lacinia mobilis* and similar structures—a valuable character in arthropod phylogenetics? *Zoologischer Anzeiger-A Journal of Comparative Zoology*, 241(4), 339–361.
- Riehl, T. (unpublished data) First record of Macrostylidae (Isopoda: Janiroidea) from the Australian continental shelf – basal position or highly derived?
- Riehl, T. (2009) *Macrostylidae Hansen, 1916 (Crustacea, Malacostraca): state of the art, new results and perspectives*. Diplomarbeit. Universität Hamburg.
- Riehl, T. and Brandt, A. (2010) Descriptions of two new species in the genus *Macrostylis* Sars, 1864 (Isopoda, Asellota, Macrostylidae) from the Weddell Sea (Southern Ocean), with a synonymisation of the genus *Desmostylis* Brandt, 1992 with *Macrostylis*. *Zookeys*, 57, 9–49.
- Riehl, T. and Brandt, A. (2013) Southern Ocean Macrostylidae reviewed with a key to the species and new descriptions from Maud Rise. *Zootaxa*, 3692(1), 160–203.
- Riehl, T. and Kaiser, S. (2012) Conquered from the deep sea? A new deep-sea isopod species from the Antarctic shelf shows pattern of recent colonization. *PLoS ONE*, 7(11), e49354.
- Riehl, T., Wilson, G. D. F. and Hessler, R. R. (2012) New Macrostylidae Hansen, 1916 (Crustacea: Isopoda) from the Gay Head-Bermuda transect with special consideration of sexual dimorphism. *Zootaxa*, 3277, 1–26.
- Riehl, T., Wilson, G. D. F. and Malyutina, M. V. (2014) Urstylidae – A new family of deep-sea isopods and its phylogenetic implications. *Zoological Journal of the Linnean Society*, 170, 245–296.
- Sandeman, D. C. and Okajima, A. (1972) Statocyst-induced eye movements in the crab *Scylla serrata* I. The sensory input from the statocyst. *Journal of Experimental Biology*, 57(1), 187–204.
- Sars, G. O. (1864) Om en anomal Gruppe af Isopoder. *Forhandlinger Videnskaps-Selskapet, Anar 1863*. pp 205–221. Christiania.
- Sars, G. O. (1897) On some additional Crustacea from the Caspian Sea. *Annales du Musée Zoologique Academie Imperiale des Sciences St. Petersburg*, 2, 273–305.
- Sars, G. O. (1899) An account of the Crustacea of Norway: with short descriptions and figures of all the species: Isopoda. (Cammermeyer, A., Ed.) Bergen: Bergen Museum.
- Schultz, G. A. (1969) *How To Know The marine isopod crustaceans*. Hampton, New Jersey: William C. Brown Company, pp.1-359.

- Sekiguchi, H. and Terazawa, T. (1997) Statocyst of *Jasus edwardsii pueruli* (Crustacea, Palinuridae), with a review of crustacean statocysts. *Mar. Freshwater Res.*, 48(8), 715–720.
- Stebbing, T. R. R. (1913) On the Crustacea Isopoda from the “Porcupine” expedition. *Transactions of the Zoological Society of London*, 20, 231–246.
- Stoch, F., Valentino, F. and Volpi, E. (1996) Taxonomic and biogeographic analysis of the *Proasellus coxalis*-group (Crustacea, Isopoda, Asellidae) in Sicily, with description of *Proasellus montalentii* n. sp. *Hydrobiologia*, 317(3), 247–258.
- Svavarsson, J. (1987) Reevaluation of *Katianira* in Arctic waters and erection of a new family, *Katianiridae* (Isopoda: Asellota). *Journal of Crustacean Biology*, 7(4), 704–720.
- Thistle, D. and Wilson, G. D. F. (1987) A hydrodynamically modified, abyssal isopod fauna. *Deep-Sea Research. Part A. Oceanographic Research Papers*, 34(1), 73–87.
- Thistle, D. and Wilson, G. D. F. (1996) Is the HEBBLE isopod fauna hydrodynamically modified? A second test. *Deep-Sea Research Part I*, 43(4), 545–554.
- Vanhöffen, E. (1914) Die Isopoden der Deutschen Südpolar-Expedition 1901-1903. In: Drygalsky, E. von (Ed.) *Deutsche Südpolarexpedition 1901-1903*. pp 449–598. Berlin: Georg Reimer. (Zoologie; 25).
- Veuille, M. (1978) Biologie de la reproduction chez *Jaera* (Isopode Asellote) II. Evolution des organes reproducteurs femelles. *Cahiers de Biologie Marine*, 19(4), 385–395.
- Vey, A. and Brix, S. (2009) *Macrostylis cerritus* sp. nov., a new species of Macrostylidae (Isopoda: Asellota) from the Southern Ocean. *Zootaxa*, 2096, 356–370.
- Wilson, G. D. F. (1985) The systematic position of the Ilyarachnoid Eurycopidae (Crustacea, Isopoda, Asellota). Dissertation. San Diego: University of California San Diego.
- Wilson, G. D. F. (1986) Evolution of the female cuticular organ in the Asellota (Crustacea, Isopoda). *Journal of Morphology*, 190(3), 297–305.
- Wilson, G. D. F. (1987) The road to the Janiroidea: Comparative morphology and evolution of the asellote isopod crustaceans. *Journal of Zoological Systematics & Evolutionary Research*, 25(4), 257–280.
- Wilson, G. D. F. (1989) A systematic revision of the deep-sea subfamily Lipomerinae of the isopod crustacean family Munnopsidae. (Cox, C. S., Fleminger, A., Kooyman, G. L., and Rosenblatt, R. H., Eds.) Berkeley, Los Angeles, London: University of California Press. (Bulletin of the Scripps Institution of Oceanography). ISBN 0-520-09745-9.
- Wilson, G. D. F. (1991) Functional morphology and evolution of isopod genitalia. In: Bauer, R. T. and Martin, J. W. (Eds.) *Crustacean Sexual Biology*. pp 228–245. New York: Columbia University Press.
- Wilson, G. D. F. Glossary for Isopoda Asellota terms. [online] (2005) (Asellota (Crustacea: Isopoda) Glossary). Available from: <http://www-personal.usyd.edu.au/~buz/Asellota/asell-glossary.html>. [Accessed 2013-06-11].
- Wilson, G. D. F. (2008a) A review of taxonomic concepts in the Nannoniscidae (Isopoda, Asellota), with a key to the genera and a description of *Nannoniscus oblongus* Sars. *Zootaxa*, 1680, 1–24.
- Wilson, G. D. F. (2008b) Local and regional species diversity of benthic Isopoda (Crustacea) in the deep Gulf of Mexico. *Deep-Sea Research Part II: Topological Studies in Oceanography*, 55(24-26), 2634–2649.
- Wilson, G. D. F. (2009) The phylogenetic position of the Isopoda in the Peracarida (Crustacea: Malacostraca). *Arthropod Systematics & Phylogeny*, 67(2), 159–198.
- Wilson, G. D. F. Glossary for anatomical terms of Asellota. [online] (2013) (<http://www.scamit.org>). Available from: [http://](http://www.scamit.org)

www.scimit.org/taxontools/toolbox-new/ARTHROPODA/Subphylum%20Crustacea/Class%20Malacostraca/Subclass%20Eumalacostraca/Superorder%20Peracarida/Order%20Isopoda/Suborder%20Asellota/-OTHER%20USEFUL%20TOOLS/Wilson_Asellota_Glossary_20130930.pdf. [Accessed 2013-10-23].

Wirkner, C. S. and Richter, S. (2010) Evolutionary morphology of the circulatory system in Peracarida (Malacostraca; Crustacea). *Cladistics*, 26(2), 143–167.

Wolff, T. (1956) Isopoda from depths exceeding 6000 meters. *Galathea Report*, 2, 85–157.

Wolff, T. (1962) The systematics and biology of bathyal and abyssal Isopoda Asellota. *Galathea Report*, 6(3), 1–320.

Wolff, T. (1989) The genera of Santiidae Kussakin, 1988, with the description of a new genus and species (Crustacea, Isopoda, Asellota). *Steenstrupia*, 15(7), 177–191.

Wägele, J.-W. (1983) On the homology of antennal articles in Isopoda. *Crustaceana*, 45(1), 31–37.

Wägele, J.-W. (1989) Evolution und phylogenetisches System der Isopoda: Stand der Forschung und neue Erkenntnisse [Evolution and phylogeny of isopods. New data and the state of affairs]. Stuttgart: E. Schweizerbart'sche Verlagsbuchhandlung. (Zoologica). ISBN 978-3-510-55026-5.

Wägele, J.-W. (1992) Isopoda. In: Harrison, F. W. and Humes, A. G. (Eds.) *Crustacea*. pp 529–617. New York, Chichester, Brisbane, Toronto, Singapore: Wiley-Liss. (Microscopic Anatomy of Invertebrates). ISBN 0-471-56842-2.

Zardus, J. D., Etter, R. J., Chase, M. R., Rex, M. A. and Boyle, E. E. (2006) Bathymetric and geographic population structure in the pan-Atlantic deep-sea bivalve *Deminucula atacellana* (Schenck, 1939). *Molecular Ecology*, 15(3), 639–651.

Author contributions

This study was designed and conducted by myself.

The manuscript was written by myself with contributions from A. Brandt. R. Walter assisted with taking SEM images. This research benefitted from uncountable discussions with G.D.F. Wilson. New material was collected during the ANDEEP, BIOICE, DIVA-3, and KuramBio expeditions organized by A. Brandt (ANDEEP, KuramBio), J. Svarsson (BIOICE), and P. Marínez Arbizu (DIVA-3). I assisted during field work in the DIVA-3 and KuramBio cruises.

Chapter 7

Multiple colonization of the continental shelves by deep-sea fauna - Insights to the phylogeny of Macrostylidae (Isopoda) from mitochondrial and nuclear DNA as well as morphology

Unpublished manuscript

Abstract

Macrostylid isopods are predominantly distributed in the abyssal and their lack of eyes as well the phylogenetic position supports a deep-sea origin of this group. Shallow water species clearly belonging to this family have nevertheless been reported from continental shelves of the Antarctic, Arctic and Boreal regions, as well as Australia. In the present paper, we investigated the evolutionary history of the shelf macrostylids. We are testing whether the presence of all or some of the shelf species across continents can be traced back to a common emergence from deeper waters, thus before the disintegration of Gondwana or even Pangaea, or whether each individual shelf species has a unique origin from a bathyal or abyssal predecessor. Through ancestral state reconstruction, we further investigate the depth origin for macrostylids. We analyzed mitochondrial and nuclear rRNAs in a Bayesian framework as well as morphological data with a parsimony approach. Although the resulting phylogenetic scenarios are prone to incongruence, we found evidence supporting several subclades within Macrostylidae across datasets. The unrelatedness of the continental-shelf species from Antarctica, Australia, and Europe in all three datasets analyzed suggests multiple independent emergent events and supports an abyssal origin for macrostylids.

Introduction

The understanding of the evolutionary and colonization histories of the largest ecosystem on our planet, the oceans below the continental-shelf breaks (depending on geography, usually situated between 200 and 1000 m depth (Smith *et al.* 2008)), is remarkably scarce (Ramirez-Llodra *et al.* 2010; Rex and Etter 2010). Much effort has been spent on identifying the age and origin of this deep-sea fauna with contradicting conclusions, mostly due to a lack of preserved fossil remains of actual deep-sea organisms (Smith and Stockley 2005). A relatively recent colonization of the deep-sea by shelf fauna was widely assumed since evidence from, for example, deep-drilling projects suggests recurring large-scale anoxia in the deep sea throughout the Phanerozoic (Weissert 1981) as a consequence of climate warming (Hay 2008), especially during the Turonian stage of the Cretaceous (Weissert 1981; Hay 2002; Alegret *et al.* 2003). The fauna has, according to this theory, repeatedly reinvaded the deep sea after mass extinctions (Menzies and Imbrie 1958; Menzies *et al.* 1961; Jacobs and Lindberg 1998).

However, based on both biogeographic and molecular-clock data, a fairly old age of at least parts of the deep-sea benthos has been suggested dating back to the late Paleozoic or early Mesozoic (Wilson 1999; Strugnell *et al.* 2008; Lins *et al.* 2012; Thuy *et al.* 2012). And despite the evident deposition of organic carbon-rich sediments during the Cretaceous, some scientists have the opinion that ocean circulation, and thus oxygen supply to the deep seabed in the Cretaceous were not quite different from today (Arthur and Sageman 1994; Hay 2008). Oxygen-depleted zones, or Oxygen-Minimum Zones (OMZ) have existed rather on lower shelves and along the slopes than stretching across whole ocean basins (Diaz and Rosen-

berg 1995). Therefore, while there is evidence that large-scale anoxia in the deep marine ecosystems during the Cretaceous have had severe effects on parts of the fauna, very likely these were limited only to severely impacted regions rather than distributed globally. Some groups, such as the isopod crustaceans, may have consequently survived deep-water anoxic events *in situ*. Likewise, the bathyal OMZs may have acted as barriers preventing renewed deep-sea colonization (and vice versa) over thousands of years and have thus promoted evolution in isolation (White 1988; Wilson 1999).

Amongst the deep-sea organisms, macrofaunal isopods are relatively well studied (Rex and Etter 2010) and numerically important (Sanders *et al.* 1965; Hessler and Sanders 1967; Brandt *et al.* 2007). They are thought to have colonized the abyssal zone (i.e. areas below 3000 m (Smith *et al.* 2008)) multiple times (Wilson 1980; Raupach *et al.* 2004, 2009) where they diverged *in situ* and generated a highly specialized fauna (Hessler and Thistle 1975). The latter is characterized chiefly by the absence of eyes (Hessler and Thistle 1975) and adaptations to coping with the only food sources widely available, which are phytodetritus, protozoans and (patchily and rarely) carcasses, wood, and alife (Dayton and Hessler 1972; Wolff 1976; Suchanek *et al.* 1985; Gudmundsson *et al.* 2000; Brökeland *et al.* 2010; Würzberg *et al.* 2011; Jamieson *et al.* 2012).

While some groups, such as Munnidae and Paramunnidae may have colonized bathyal and abyssal depths rather recently (Wilson 1980; Lins *et al.* 2012), other colonization events may date back to before the mass extinctions which occurred at the end of the Palaeozoic and during the Mesozoic (Wilson 1999; Lins *et al.* 2012). It has been recently proposed that, for example, the ancestors of the family Macrostylidae Hansen, 1916 are the lineage that colonized the deep-sea first of the

isopods and that has modern-day representatives. This would have occurred more than 250 million years ago (Ma) (Lins *et al.* 2012).

While immigrations from shelf into the deep sea are relatively well-established scenarios, invasions from the deep sea into shallow-water environments are less well understood. Besides corals (Lindner *et al.* 2008; Pante *et al.* 2012), and peccinid molluscs (Berkman *et al.* 2004), isopods are amongst the few organism groups for which an emergence scenario, thus a colonization from offshore to onshore, has been discussed.

Some of the highly adapted deep-sea isopods show great depth distribution (Brandt *et al.* 2009), and may occur in the shallows, especially at high latitudes (Hessler *et al.* 1979; Svavarsson *et al.* 1993). There is taxonomic, ecological and phylogenetic evidence for such polar emergence, as a colonization process occurring over evolutionary time scales, mostly from the Antarctic (Menzies *et al.* 1973; Brandt 1992, 1999; Thatje *et al.* 2005; Kaiser *et al.* 2011; Strugnell *et al.* 2011). Here, a “thermohaline express way” (Kussakin 1973; Strugnell *et al.* 2008) has been suggested to facilitate across-depth migration of organisms due to deep-water formation (submergence), upwelling (emergence) as well as a general lack of a thermocline in the water column. Similar observations of deep-sea taxa in the shallows have been made in cold boreal and Arctic waters (Svavarsson *et al.* 1993). The paramunnid genus *Pleurogonium* Sars, 1864 is one example of “re-colonization” of the shallows from the deep which is prevalent in the North Atlantic (Wilson 1980).

The isopod family Macrostylidae seems to be another example of an emergent taxon. Macrostylids are known to inhabit all ocean depths from the shallow sublittoral, e.g. *Macrostylis spinifera* Sars, 1864 at ~30 m depth, to the deepest hadal trenches, such as *M. mariana* Mezhev, 1993 from

the bottom of the Mariana Trench at almost 11,000 m depth (Kussakin 1999; Brandt *et al.* 2009; Riehl and Brandt 2010). The lack of eyes and their mostly abyssal distribution as well as phylogenetic evidence suggest a deep-sea origin of this group (Hessler *et al.* 1979; Wägele 1989; Raupach *et al.* 2004; Riehl *et al.* 2014). Disjunct findings of shelf representatives in Antarctica (Brandt 2002; Riehl and Kaiser 2012; Riehl and Brandt 2013), Australia (T. Riehl, unpubl. data), Europe (Sars 1864; Meinert 1890; Malyutina and Kussakin 1996) and North America (T. Riehl, G.D.F. Wilson, unpubl. data), however, raise the question whether these disjunct shelf occurrences of macrostylids represent relicts from single or few colonization events before the early Jurassic when the disintegrations of Pangea and Gondwana occurred (~175 Ma), or whether the shallows have been colonized independently and more recently.

In contrast to the potentially great age of this isopod family (Lins *et al.* 2012), the 85 currently recognized species of Macrostylidae (Table 1) have all been assigned to the genus *Macrostylis* Sars, 1864. Considering their observed high molecular divergence (Riehl and Brandt 2013), this monotypy might indicate an overlooked morphological diversity on the superspecific levels and/or selective pressures that conserved their general morphology over time. Recent morphological studies show that Macrostylidae is highly derived and the number of characterizing synapomorphies, thus conserved features, is high (Riehl *et al.* 2014). This is in line with the ancient-origin theory (Lins *et al.* 2012). However, the lack of within-family variability may indicate as well that present-day similarity across macrostylids is the consequence of eradication of much of the macrostylid diversity in rather recent times.

Asking whether the disparate occurrences of macrostylids in shallow seas have one common

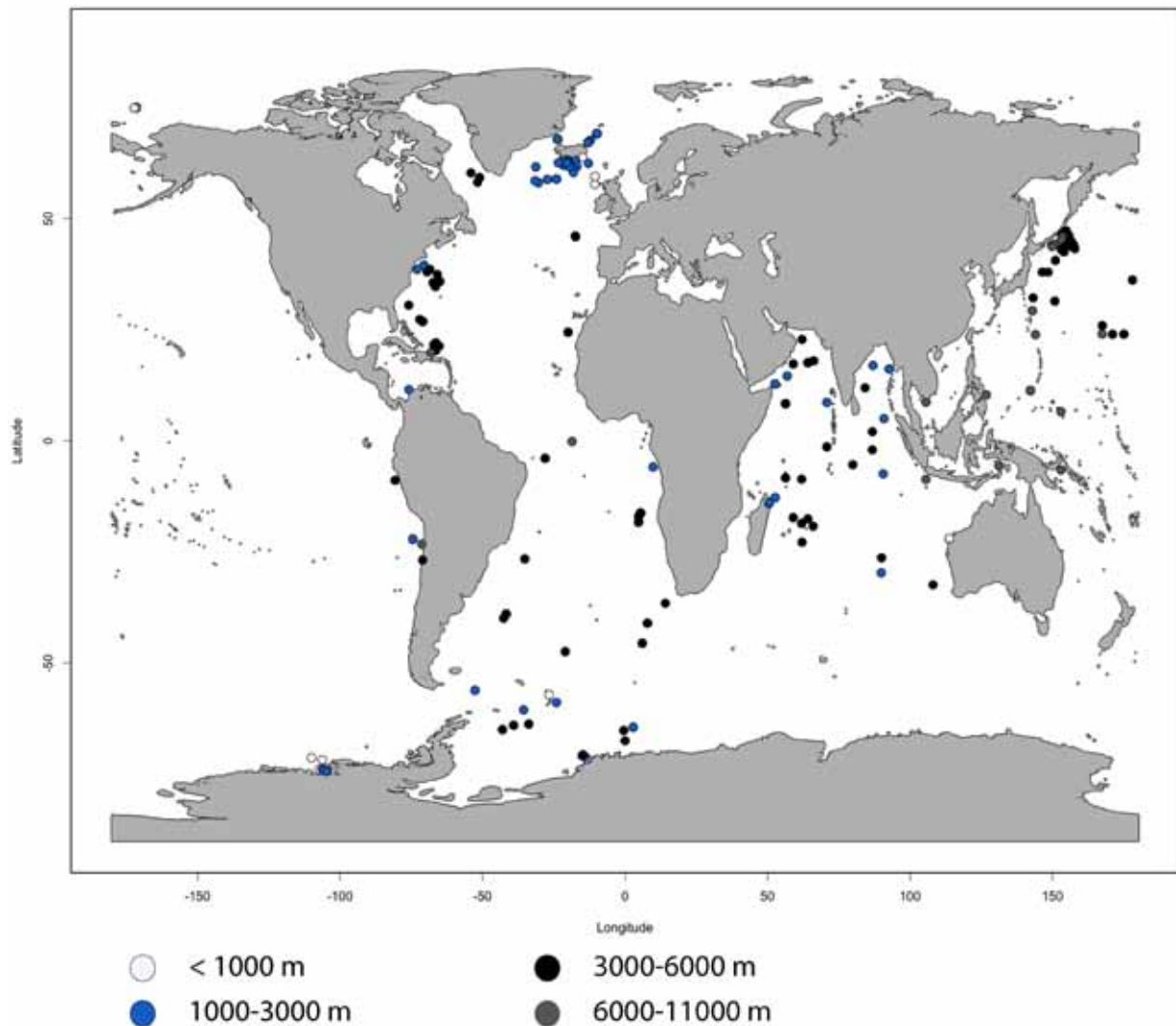


Figure 1. Distribution map of Macrostylidae (Isopoda: Asellota) in the world ocean. Each record is represented by a circle. Shelf species (above 1000 m) are indicated in white, bathyal species in blue, abyssal and hadal species are represented by black and grey circles respectively. This distribution map contains all taxonomic records (original descriptions and published additional records of described species as well as new records for material examined morphologically or genetically in this paper (see table 1).

or multiple independent origins, we performed the first comprehensive phylogenetic analyses for this family based on DNA data and morphology. Upon this phylogenetic-systematic reasoning, macrostylid classification is discussed and colonization processes are reconstructed.

Methods

Morphology

A new dataset of morphological characters was assembled in DELTA (Dallwitz 1980, 1993) and Mesquite (Maddison and Maddison 2011). The characters used are based on previous homology hypotheses (Riehl and Brandt in prep.). A dataset recently published by Riehl *et al.* (2014; Chapter

5) was added upon and Urstylidae, Thambematidae, Desmosomatidae and Nannoniscidae were used as outgroup. Altogether, the matrix comprised 480 characters and 81 taxa. Characters were developed from previously available datasets (Riehl and Kaiser 2012; Riehl *et al.* 2012, 2014; Riehl and Brandt 2013; Chapters 2-5) using their terminology.

For character scorings, type material was analyzed where available (Table 1). Otherwise, original descriptions and new collections were the source for the data. Several species (described and new) have been (re-)collected during recent expeditions to the Antarctic, North and South Atlantic as well as the Western North Pacific (Table 2) and were thus available for analyses as well. These were predominantly sampled by means of epibenthic sledges (Rothlisberg and Percy 1976; Brenke 2005; Brandt *et al.* 2013). Since subadult and adult males can vary drastically from females (Riehl *et al.* 2012), characters were scored separately for both sexes with special consideration of sexual dimorphisms. Males tend to occur less frequently in samples compared to females. Accordingly, scorings were based mostly on female characters.

Several species were described on the basis of one single specimen only. In cases where species descriptions were based on males, these had to be excluded from analyses for above-mentioned reasons. Where descriptions were of poor quality and type material was unavailable or damaged, species were excluded as well.

Cladistic analyses

The homology concepts were tested in a parsimony framework (Wirkner and Richter 2010) using TNT (Goloboff *et al.* 2008). The search routine was set to find the optimal score 50 times independently, using defaults of “xmult” plus 50 cycles of tree-drifting (Goloboff 1999). No target score was

defined. For consensus calculation, trees were temporarily collapsed with tree-bisection and reconnection (TBR).

Absolute and relative bremer supports (Goloboff and Farris 2001) were calculated by TBR-swapping the trees found, keeping note of the number of steps needed to lose each group. Trees were illustrated using Mesquite and the graphics were enhanced in Adobe® Illustrator®.

Molecular methods

To gain high-quality DNA from deep-sea Macrostylidae, methods according to Riehl *et al.* (under review; Appendix 3) were followed including amplification and sequencing protocols (see also Brix *et al.* in press, 2011; Dreyer and Wägele 2001, 2002; Raupach *et al.* 2004; Riehl and Kaiser 2012; Riehl and Brandt 2013). They were collected during the ANDEEP-SYSTCO (Brandt *et al.* 2010), DIVA 3 (Martínez Arbizu *et al.* 2014), IceAGE (Brix *et al.* 2012), and KuramBio (Brandt and Malyutina 2012) expeditions with the German research vessels METEOR, POLARSTERN, and SONNE. Sampling data are listed in Table 1.

Raw sequence files and chromatograms were managed, and checked for quality in Geneious (Drummond *et al.* 2011). To exclude sequences derived from contaminations, NCBI Blast searches were conducted. GenBank numbers for the 16S and 18S sequences generated during this project will be provided upon acceptance of this manuscript.

Comparison of alignment methods

Different alignment methods were applied for the rRNA sequences using the EMBL web server (Goujon *et al.* 2010; McWilliam *et al.* 2013) and compared regarding the proportion of unresolved nodes in the resulting Maximum Likelihood (ML) trees of fast RAxML (Stamatakis 2006) analyses

(trees not shown here). ClustalW2 (Larkin *et al.* 2007) was chosen since it represents one of the most widely used multiple-alignment programs. MAFFT (Kato *et al.* 2002) with the Q-INS-I algorithm was chosen for the alignments of ribosomal RNA sequences because it takes into account the RNA's secondary structure in its version 7.110 (Kato and Toh 2008; Kato *et al.* 2009). Further widely applied alignment methods that we tested were MUSCLE (Edgar 2004) and T-Coffee (Notredame *et al.* 2000).

Moreover, to evaluate the effect of ambiguous sites on the phylogenetic signal/noise relationship, each alignment was treated on the GBLOCKS (Castresana 2000) server applying default as well as least stringent settings for DNA sequences in order to keep as much information as possible. The alignments that resulted in the best-supported topology were subsequently used for a thorough Bayesian analysis.

Tree-independent exploration of phylogenetic signal

NeighbourNet analysis was performed with SplitTree (Huson 1998) in order to evaluate clade support and phylogenetic information content of preliminary and reduced (in terms of taxon composition) datasets. Edge length is a proxy for split support of a grouping. This method offers reciprocal illumination *sensu* Hennig (1965) for the phylogenetic inference as it helps to distinguish noise from signal and to visualize long branches (Wägele and Mayer 2007).

Outgroup choice

We tested three isopod families of varying relatedness to the ingroup for their usefulness as outgroup. Molecular sequences of the families Janirellidae Menzies, 1956, Desmosomatidae Sars, 1897 and Munnopsidae Lilljeborg, 1864 were chosen from

Brix *et al.* (in press), Osborn (2009) and Raupach *et al.* (2009). Previous molecular and morphological data suggest a potential sister-group relationship of Desmosomatidae or Munnopsidae with Macrostyliidae (Wägele 1989; Raupach *et al.* 2004, 2009; Riehl *et al.* 2014). These families were also chosen because these were the only closely related groups of which sufficient DNA markers were available on GenBank across the chosen markers.

Based on preliminary alignments, NeighborNet networks were constructed with SplitsTree and fast preliminary ML analyses run with RAxML. Long branches were identified. In cases, where outgroup relationships with the ingroup had conflicting signal (no long edges), the respective outgroup taxa were removed.

Phylogenetic analysis

The individual alignments were analyzed phylogenetically using MrBayes (Ronquist and Huelsenbeck 2003) to conduct a Bayesian analysis. The Akaike Information Criterion (Akaike 1974) was used to detect the best-fitting model as evaluated by MrModeltest2 (Nylander 2004). The analysis was run for 30,000,000 generations, with six independent chains. Every thousandth generation was sampled. For generating the consensus, a burnin of 25% was used. The outgroup was forced to *Janirella* in the 18S analysis and *Chelator* in the 16S analysis. Trees were illustrated using FigTree ver. 1.31 and the graphics were enhanced in Adobe Illustrator.

Shelf colonization

In our phylogenetic reconstructions, we found shallow-water species nested within clades of deep-water macrostyliids. We therefore hypothesize that the shallow-water species have evolved from deep-sea lineages.

Depth regimes were scored as discrete character states using approximate maximum continental-shelf depth (1000 m) as lower limit of the sublittoral although we are aware that the shelf break occurs at much shallower depth aside from Antarctica (Smith *et al.* 2008). However, the maximum depth for the shelf break was chosen to account for variation in this geological attribute around the globe. Furthermore, the maximum sill depth of the Greenland-Iceland-Faroe Ridge at around 850 m is important for the discussion of our results and lies roughly in the same depth category.

The bathyal was coded to reach from 1000–3000 m depth and the third depth regime defined as below 3000 m depth. Using consensus trees inferred from morphological and molecular data (the latter not shown but discussed), ancestral depth distribution was reconstructed using Wagner parsimony in Mesquite (Maddison and Maddison 2011).

The discontinuous nature of hadal trenches dictates that their faunas can only be linked via abyssal intermediates. Since there can be no direct exchange of faunal elements from hadal to the sublittoral, hadal and abyssal have been merged here. Nevertheless, it is worth mentioning that eleven of the species in the dataset have so far only been collected from hadal depths, and one (*M. grandis*) occurs in and outside the Kurile-Kamchatka Trench at abyssal as well as hadal depths.

Results

Morphological results

Of 85 described macrostyloid species, 51 were included in the analyses and eight additional undescribed species were added. We tried to reach a good match between morphological and genetic

datasets; however, for most of the previously described species, no DNA data are available. Vice versa, many of the recently collected species that we were able to extract DNA from have not yet been described. We included these into the morphological matrix, as far as the condition of the specimens at hand allowed. Based on morphological re-examination (and DNA similarity), *Macrostyliis ovata* has been found synonymous with *M. grandis*; *M. longipes* is a synonym of *M. subinermis*. Thus, overall a dataset comprising 58 species could be assembled.

In the cladistic analysis, 16,985,250,982 rearrangements were examined in total. Best score (shortest tree) was 1164 and 32 equally short trees were retained (Figure 2). As could be expected from previous analyses (Riehl and Brandt in prep.; Riehl *et al.* 2014), Macrostyliidae formed a well-supported monophyletic clade with Bremer/relative Bremer support of 10/100 and a resampling frequency of 100.

Macrostyliis papillata and *M. belayaevi* paraphyletically formed the most basally derived macrostyliids followed by a small clade including *M. tumulosa*, *M. galathaea*, *M. uniformis* and *M. scotti*. The latter is characterized by the presence of an aesthetasc on the subterminal antennula article of the female whereas other macrostyliids have only a single aesthetasc and on the terminal article only. Except from *M. tumulosa*, this group shares medioventrally oriented anterior coxae, and ventrolateral setal ridges on the pleotelson.

Subsequently, the remaining species are distributed across two major distinct branches. The smaller of the two clades (henceforward called “Abyssicola clade”) is characterized by a recessed position of the anus and a small, often blunt, sternal projection of the first pereonite. This clade includes species that do not show strong sexual dimorphism. Their seventh pereonites are usually

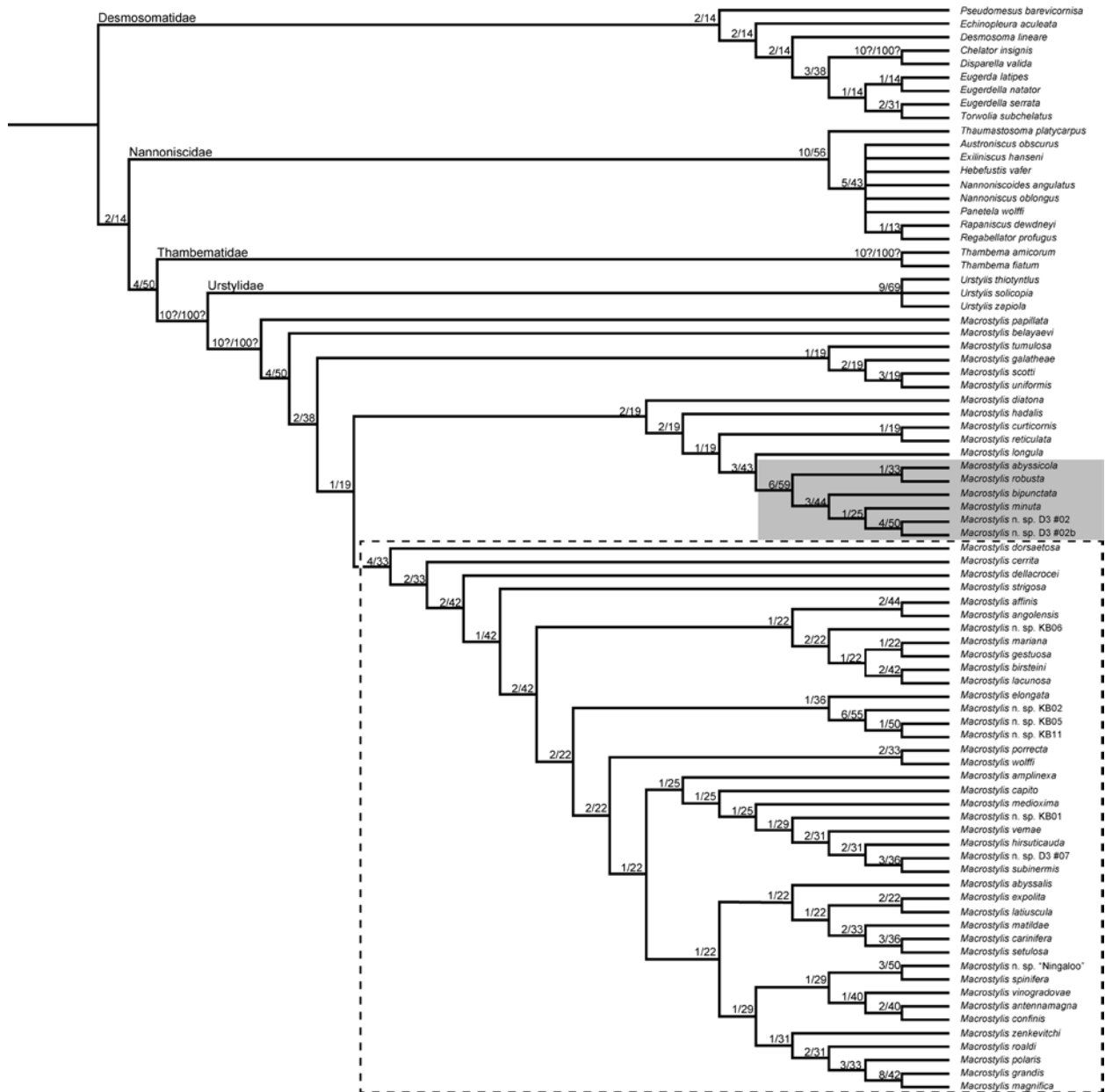


Figure 2. A morphology-based scenario of the evolutionary history of Macrostylidae (Isopoda: Asellota). Strict consensus of 32 equally short trees derived from a parsimony analysis using TNT (Goloboff *et al.* 2008). Total rearrangements examined were 16,985,250,982. Best score was 1164 and 32 trees were retained. The labels on branches show absolute and relative Bremer supports (Goloboff and Farris 2001). Groups indicated with a question mark (?) are those for which the absolute Bremer supports appear to be 10 or more. Highlighted are two monophyletic groups within Macrostylidae that reappear consistently across morphological and DNA analyses: the “*Macrostylis abyssicola* group” (grey background) is robustly supported as monophyletic in all three analyses. The sexually dimorphic “*Macrostylis sensu stricto*” reappears in all analyses but “rogue taxa” cluster within this clade to varying degrees across datasets and it is thus not consistently composed and its monophyly could not be supported.

rather reduced in the expression of their postero-lateral projections and the seventh walking legs are commonly not longer than the preceding appendages. Nested within this clade is a strongly supported group comprising *M. abyssicola*, and *M. robusta* on the one branch and *M. minuta* as well as two undescribed species on the other hand (Figure

2). These species share a sharp ventral keel on the fossosome sternum, ventrally projecting lateral tergal plates on pereonites 1–4, and a reduction of the seventh pereonite and its appendages as well as the antennula. The species of the “*M. minuta*” subclade have their seventh pereopods reduces in a most peculiar way: only the basis is present. Addi-

tionally, these species share strange posterolateral projections on the third pereonite.

All remaining species were recovered in a large clade that has the following synapomorphies: the carpus of the antenna (article 5 in macrostylids, see Hansen (1893), and Riehl *et al.* (2014) for discussion) exceeds the combined lengths of the proximal short podomeres of the antenna; ventrolateral ridges are present on the pleotelson; the uropod protopod of the female is shorter than the pleotelson length; the posterolateral margins of the sixth and seventh pereonites feature only one prominent seta that is robust; the antennal coxa is more than twice as long as the basis (secondarily reduced in several species, though); the lateral fringe of setae on the operculum is distinctly separate from the apical row of pappose setae; and the shape of the operculum is distally tapering (tongue-shaped) with concave distolateral margins.

This large clade comprises the type species of the family, *M. spinifera*, and all macrostylids that show a pronounced sexual dimorphism featuring elongations of antennulae, sixth and seventh pereopods and an increase in the number and length of the aesthetascs in the copulatory males. It also includes a relatively well-supported clade supported by a unique shape of the first male pleopods where the lateral lobes are reduced and instead, the medial lobes seem to have taken over their function as stylet guide, which is achieved by the hook-shaped lateral lobes in all other species of the family. We refer to this clade in the following discussion as *Macrostylis sensu stricto*.

Molecular results

Estimation of phylogenetic signal

Alignments treated with GBlocks resulted in trees that showed identical or very similar relationships

compared to their untreated counterparts. Since branch support values, however, were generally distinctively smaller than in the untreated alignments, these results were discarded. Comparisons of bootstrap supports across alignment methods resulted in a preference for ClustaW2 alignments for both 16S and 18S.

The amount of conflicting evidence as shown by the NeighborNet network (see supplement) is reflecting the conflict in the dataset by showing a star-shaped network with inly few central supporting edges and multiple long branches arising directly from the center.

Phylogeny based on mitochondrial 16S and nuclear 18S rRNA

While the analysis based on the morphological dataset resulted in a well-resolved topology (although not always convincingly supported; Figure 2), both molecular phylogenies show extended polytomies due to unsupported deeper relationships (Figures 3, 4).

The 16S fragment comprised the most complete dataset of 31 morphologically discriminated “morpho species”. In congruence with the morphological data, the “Abyssicola” group has been recovered monophyletically and well supported. Likewise, *Macrostylis s. str.* forms a large and diverse monophyletic clade, however with a slightly different taxon composition. All other morpho-species form single entities or cluster in groups of 2–5. All branch off a large basal polytomy. Within *Macrostylis curticornis*, we found evidence for considerable divergence which should provoke further morphological analyses. *M. grandis* and *M. ovata* are synonyms. The same was found for *M. subinermis* and *M. longipes*.

The 18S phylogeny contains 26 morphospecies of which all but one (*Macrostylis* n. sp. D3

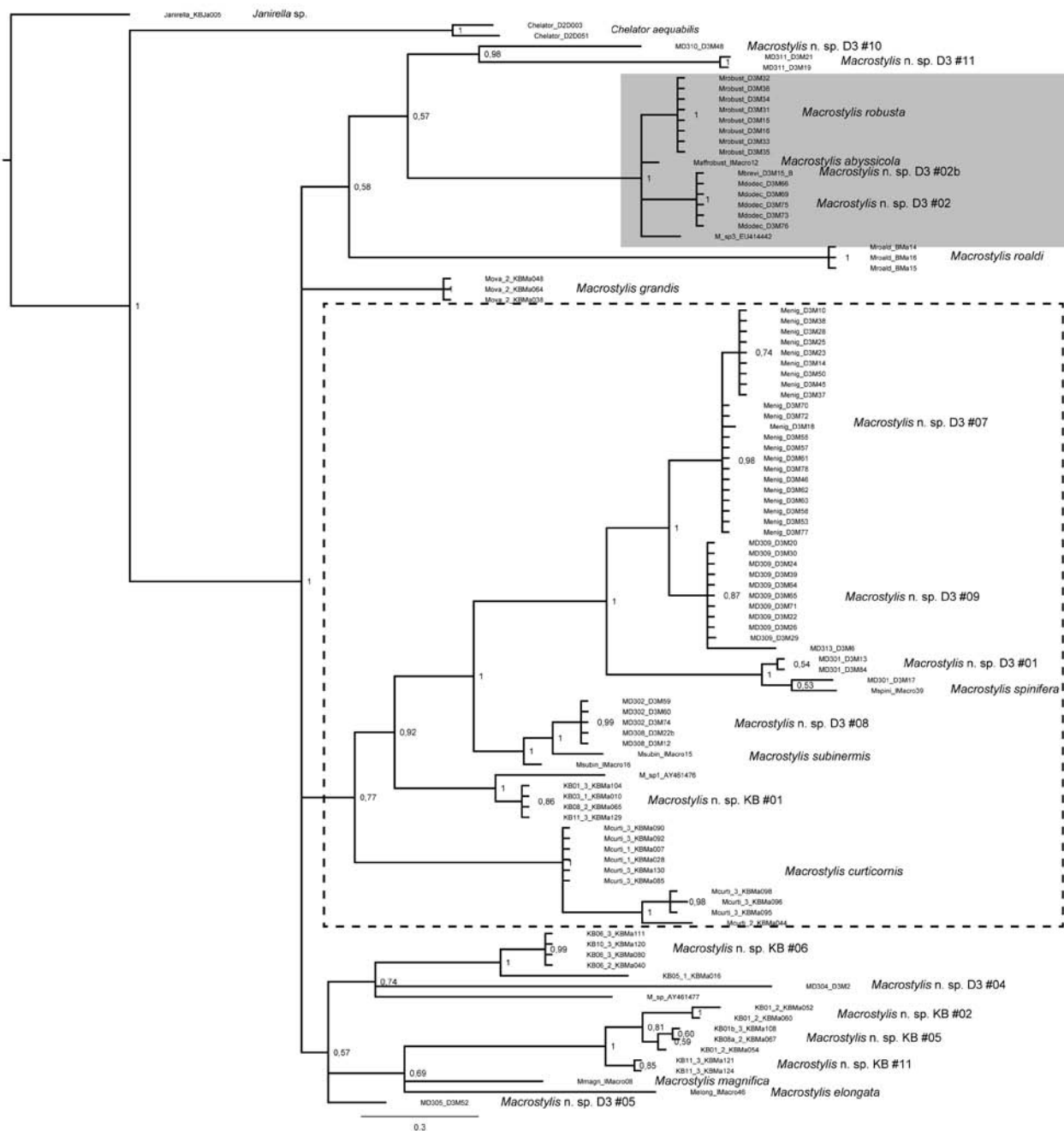


Figure 3. Bayesian phylogenetic reconstruction of the evolutionary history of Macrostylidae (Isopoda: Asellota) – 18S. The tree is a consensus and the Bayesian analysis was based on 104 nuclear 18S rRNA sequences including two desmosomatids and a janirellid as outgroup. Sequences for *Chelator aequabilis* Brix and Leese, in press and previously published macrostylid sequences (Raupach *et al.* 2004; Riehl and Kaiser 2012; Riehl and Brandt 2013) were retrieved from GenBank. Support values are posterior probabilities and nodes with support below 0.5 have been collapsed. Two monophyletic groups within Macrostylidae that reappear consistently across morphological and DNA analyses are highlighted: the “*Macrostylis abyssicola* group” (grey background) is robustly supported as monophyletic in all three analyses. The sexually dimorphic “*Macrostylis sensu stricto*” reappears in all analyses but “rogue taxa” cluster within this clade to varying degrees across datasets and it is thus not consistently composed and its monophyly could not be supported.

02b) were recovered. Again, there is divergence within *M. curticornis* pointing to multiple species hidden in this morphospecies. *Macrostylis subinermis* is paraphyletic in this tree. Overall, again, the

“Abyssicola” clade is well supported and *Macrostylis s. str.* has been resolved but once more, with a slightly different taxon composition.

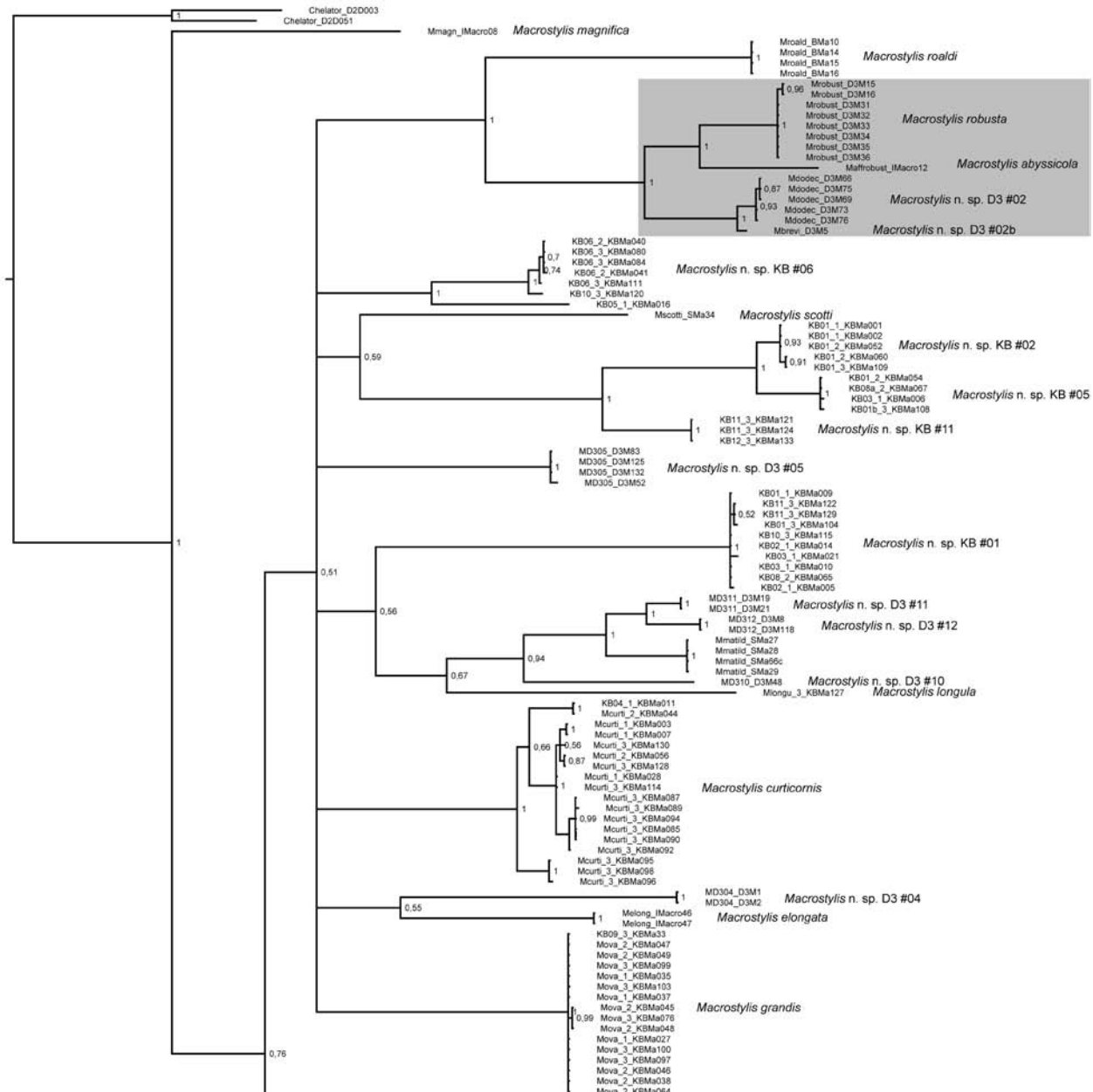


Figure 3. (first part; continuation next page). Bayesian phylogenetic reconstruction of the evolutionary history of Macrostylidae (Isopoda: Asellota) – 16S. The tree is a consensus and the Bayesian analysis was based on 210 mitochondrial 16S rRNA sequences including two desmosomatids as outgroup. Support values are posterior probabilities and nodes with support below 0.5 have been collapsed. The desmosomatid *Chelator aequabilis* Brix and Leese, in press was used as outgroup (Brix et al. in press). Next to mostly new sequences, previously published sequences (Riehl & Kaiser 2012; Riehl & Brandt 2013) were retrieved from GenBank. Two monophyletic groups within Macrostylidae that reappear consistently across morphological and DNA analyses are highlighted: the “*Macrostylis abyssicola* group” (grey background) is robustly supported as monophyletic in all three analyses. The sexually dimorphic “*Macrostylis sensu stricto*” reappears in all analyses but “rogue taxa” cluster within this clade to varying degrees across datasets and it is thus not consistently composed and its monophyly could not be supported.

Colonization reconstruction

The ancestral state reconstruction of depth occurrence based on morphological data (Figure 5) suggests six invasions of the bathyal from abyssal

depths. Borne out of these, four independent emergence events to depths shallower than 1000 m depths are supported. Even when considering the actual depths of the continental shelf at the respective regions (~ 1000 m in Antarctica; ~ 200

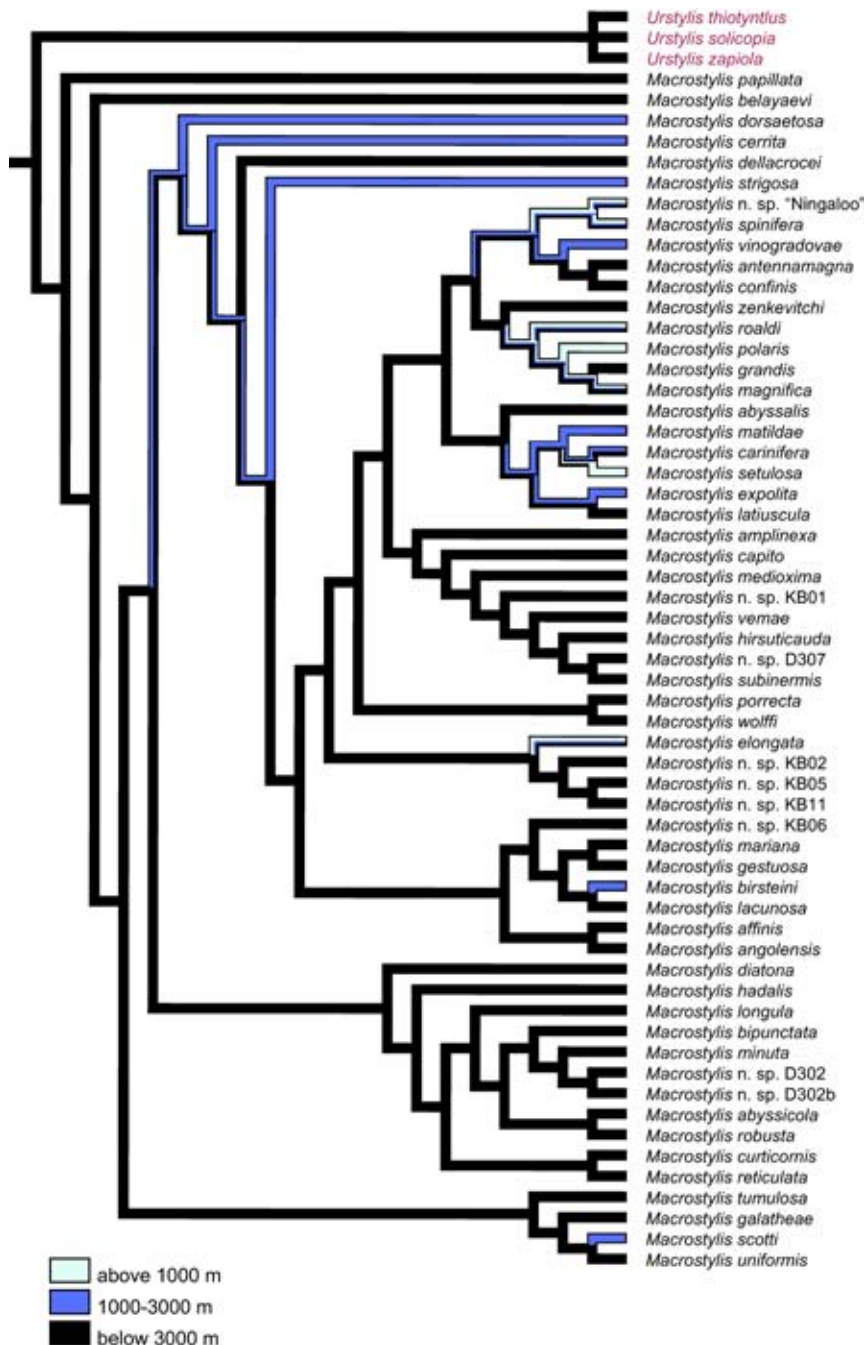


Figure 5. The abyss-shelf colonization history of Macrostylidae (Isopoda: Asellota). Based on the strict consensus (Figure 2), an ancestral state reconstruction was conducted using depth zones sublittoral (0–1000 m), bathyal (1000–3000 m) and abyssal + hadal (>3000 m depth) as discrete characters and a parsimony reconstruction scheme as implemented in Mesquite (Maddison and Maddison 2011). White bars indicate a depth occurrence above 1000 m, blue indicate a bathyal distribution and black bars represent abyssal and hadal species. Species (and predecessors) occurring across more than one depth zone have mixed coloration. An abyssal origin of Macrostylidae is most parsimonious. Within Macrostylidae, six emergence events into the bathyal became apparent, of which four evolved into a shelf emergence.

Discussion

Phylogeny

Despite previously being regarded as monotypic (Riehl and Brandt 2010; Riehl and Kaiser 2012; Riehl *et al.* 2012), at least two major clades have diverged within Macrostylidae far back in evolutionary times. From all datasets included in this study, similar main groups have been recovered.

First of all and best supported, the “Abyssicola” clade has been congruently retrieved from all three datasets. The monophyly of this group seems highly plausible, due to the high complexity of the reductions apparent in these species (hypomorphosis; see Chapter 6).

While the *Macrostylis s. str.* group comprises similar main taxa in all trees, to overall composition of this clade is different in all treatments. We would like to point out that the homology of the complex sexual dimorphisms expressed by several species of this clade on the one hand (see Chapters

2 and 6) and the derived shape of the first male pleopod in a subset of these seem unlikely to have evolved multiple times independently. The proportion of homoplastic character thus seems relatively high and may require further and more elaborate data examination.

Morphological uniformity

These results are remarkable in the light of comparison with closely-related families, most of all with the Munnopsidae. The latter has evolved secondary natatory capabilities with related specializations in morphology. On the generic and subfamily levels, Munnopsidae is among the most diverse janiroid families, comprising nine subfamilies and 44 genera which are morphologically highly diverse (Thistle and Hessler 1976; Wilson 1989; Malyutina and Brandt 2004, 2006, 2007; Osborn 2009). Macrostylidae, on the other hand, expose a remarkable morphological uniformity. The deep-sea environment is generally rather uniform and stable in physical parameters and it has been hypothesized that this may favor an “orthogenetic” pattern of structural adaptation, which means evolution towards an endpoint (Giere 2009). Furthermore, similar environmental conditions imply similar selective pressures resulting in analogous adaptations (Giere 2009). Even in the highly diverse Munnopsidae, highly similar species occur (Wilson 1982; Raupach *et al.* 2007) and the high diversity on the superspecific levels may be related to the evolution of the munnopsid-specific swimming mode and thus an increased accessibility for various new ecological niches.

Alternatively (or additionally), the uniform macrostylid appearance could be related to constraints imposed by an endobenthic lifestyle. The fossosome is among the most obvious characters that always allow allocation to this family. Behavioral observations (Hessler and Strömberg 1989),

sampling evidence (Harrison 1989; Wilson 2008) and morphology (Thistle and Wilson 1987; Wägele 1989) suggest that most if not all species of the family live below the surface within the top layer of soft sediments. As with other endobenthic groups of isopods, such as Thambematidae and also subterranean amphipods or non-arthropod taxa, living in the interstitial or digging through sediment puts certain constraints on the evolution of morphological traits. In many cases, “under-ground” taxa have a tendency to evolve a worm-like habitus, are difficult to distinguish (“cryptic species”) or their morphology does not provide sufficient phylogenetic information to systematize them due to convergent evolution of tryglomorphous or comparable features (Seilacher 1984; Lee 1998; Kornobis *et al.* 2011; Pipan and Culver 2012).

Ancient divergence

The wide and disjunctive geographic distribution of small clades or even species pairs in the trees (e.g. *M. spinifera* from the North Atlantic and *M. sp. n.* “Ningaloo” from Australia) suggests a highly chaotic colonization history. To realize the observed geographic and phylogenetic distributions considerable time is required. That is even more the case when considering the strictly benthic lifestyle of macrostylids (discussed in Chapter 3).

Colonization patterns and potential refuge scenarios

We could show that with a likely origin of macrostylids in depth greater than 3000 m, the occurrence of species on the slopes and shelves are a consequence of multiple emergence events, i.e. migration up the slope (Brandt 1992). While in the molecular datasets, shelf and slope species are not well represented, the morphological data suggests

seven independent emergence events in total. Four independent shelf invasions are the most parsimonious scenario when considering both the morphological as well as the molecular scenarios of evolution. The reconstructed scenarios are especially convincing since bathyal intermediates are recovered in all cases of emergence up to shelf depths. However, bathyal species are underrepresented in the molecular data and accordingly, such pattern could not be shown in the 16S and 18S trees (and these have hence been omitted in this paper). When putting these invasions of the bathyal and sublittoral by isopods into a historic context, climate change and continental drift need to be considered.

Abyssal anoxia/dysoxia as well as rising temperatures, for example during the Cretaceous, are thought to have had severe effects on the inhabitants of the deep sea (Jacobs and Lindberg 1998; Horne 1999). These anoxic events were the consequence of high surface productivity and/or stagnation of the thermohaline circulation (Sarmiento *et al.* 1988). It has been suggested that the Antarctic slope might represent a refuge for re-colonization of the abyss (but also for shelf fauna) following adverse climate-induced changes in the abyssal and shelf environments (Kaiser *et al.* 2011)).

Recurring expansions and retreats of Antarctic glaciers have been connected to an increased eurybathy in certain taxa on the one hand, and allopatric speciation through local extinction and isolation on the other hand (Clarke *et al.* 1992; Brey *et al.* 1996; Brandt 2005). Oscillating OMZs may have had similar effects (White 1988) on the lower shelf and the bathyal fauna. Despite the importance that depth-related factors seem to have on the benthic organisms (Etter and Rex 1990; Brix and Svavarsson 2010; Jennings *et al.* 2013; Schnurr *et al.* 2014), the Southern Ocean shelf and slope may thus favor eurybathic taxa; and enhanced eurybathy may be the preadaptation required to ‘conquer’

another depth zone (but see Brandão *et al.* 2010). *Macrostyliis roaldi* is an example for a relatively eurybathic species recorded from roughly 500–1500 m on the shelf and upper slope of the Amundsen Sea. Yet, the phylogenetic position of this species and its relations remain contradictory. The morphological results suggest an intermediate position between the abyssal *M. zenkevitchi* and *M. polaris* from the Arctic shelf. This monophyletic clade is deeply nested within *Macrostyliis s. str.* On the contrary, both 18S and 16S analyses favor (but weakly supported) a basal position to the “Abyssicola” group. The latter is known only from the abyss of the North and South Atlantic. Especially the long branch leading to *M. roaldi* in the 18S consensus tree points out that this species is strongly differentiated from other macrostyliids (also shown in the NeighborNet networks in the supplement).

Certainly, improved sampling effort on neighboring shelf areas but also on the poorly sampled slope and in the even less known abyss off Pine Island Bay (Kaiser *et al.* 2009; Linse *et al.* 2013) may yield macrostyliids that are closer related and would thus allow for a more detailed inspection of the shelf colonization by deep-sea isopods in the Pacific sector of the Southern Ocean. It is interesting to note, though, that an affinity to *M. polaris* does not appear implausible from the morphological perspective. Unfortunately, only juvenile males are known for this species to date, thus leaving gaps in the data matrix, and molecular data is not available for *M. polaris*. The second Southern Ocean macrostyliid occurring at shelf depth is *M. setulosa* recorded in only one sample from the Scotia Arc off the South Sandwich Islands. This species seems to be related to bathyal and abyssal species, including *M. matildae* from the adjacent Lazarev Seamount Maud Rise (Brandt *et al.* 2011).

Besides the Southern Ocean with its unique series of glacial expansions and retreats on the con-

tinental shelf, the Arctic (including the Northern Seas) and the North Atlantic are another yet contrasting example of an environment favoring eurybathy. That is first of all due to the semi-isolated geography of the area north of the Greenland-Iceland-Faroe (GIF) Ridge, but also due to a relatively recent onset of the deep-basin ventilation with oxygenated water (Svavarsson *et al.* 1993) and its relatively young geological age (Dahl 1972; Dahl *et al.* 1976).

Past hypoxic or dysoxic conditions in the deep Nordic Seas and the Arctic deep basins are thought to have had an impoverishing effect on their faunas or have even prevented establishment of a diverse fauna as found south of the GIF Ridge (Berggren and Schnitker 1983; Thiede *et al.* 1998). These areas still have a low diversity today, in contrast to the North Atlantic deep sea (Sanders *et al.* 1965; Sanders 1968; Svavarsson *et al.* 1990). The shallow GIF Ridge with a maximum saddle depth of 850 m has been hypothesized to act as a physical barrier for the northward dispersal of abyssal fauna, thus allowing only eurybathic deep-sea species to invade northwards (Svavarsson *et al.* 1993). It is therefore not surprising that three of the four macrostylids found in shallow depths of Icelandic and adjacent European waters are eurybathic: *Macrostylis elongata*, *M. spinifera*, and *M. subinermis* are covering bathyal and sublittoral depths while *M. magnifica* is the only macrostylid species recorded to date with a depth range ranging from abyssal to sublittoral depths. This observation may reflect adaptations to changes in deep-water temperature and oxygenation and the necessity to evade anoxia in the abyss or bathyal OMZs.

However, the distribution of black shales, that are commonly formed during periods of anoxia (Ingall *et al.* 1993), suggests that not unlike today, also in the Cretaceous, oxygen-minimum zones were rather located on the slope than in the

abyss (Diaz and Rosenberg 1995) thus rendering this regions unsuitable as refuge. Evidence for this scenario has been presented also for the Antarctic (Doyle and Whitham 1991).

It has been suggested that the most common oxygen-related phenomenon was oxygen stratification where deep and shallow oxygenated water masses are separated by intermediate “death zones” of anoxia/dysoxia (Wilson 1999). These divisions of the water column by mid-water oxygen-minimum zones (OMZ) have strong effects on the benthonic fauna where they are grounded (Levin and Gage 1998; Gutiérrez *et al.* 2000; Levin *et al.* 2000, 2009). Under the assumption that OMZs existed on a global scale during the anoxia/dysoxia periods occurring throughout the Mesozoic, they may have acted as barriers to dispersal across depth and restricted the transmigration across the bathyal zone from abyssal to shelf and *vice versa* (Wilson 1999). Evolution in isolation was the consequence for both shallow-water and abyssal faunas (White 1988). We can draw limited conclusions from the present data but the ancestral state reconstruction favors a common emergence for *Macrostylis spinifera* and the new species from Australia. The scenario requires the assumption of an emergence before the disintegration of Pangaea and an *in situ* survival on the shelves. Unfortunately, the Australian species was not available for molecular analyses, so the morphological result cannot be corroborated. Nevertheless, we interpret this finding as showing the potential of the continental shelves to act as refuge for ancient deep-sea groups.

An alternative survival scenario for the antique (i.e. pre-Triassic) abyssal fauna does not require the assumption of slope or shelf colonization. On the contrary, despite dramatically different oceanographic regimes with increased water temperatures and a likely interruption of the thermohaline circulation, deep-water formation was

likely still possible wherever high-density and saline surface water were produced, transporting oxygenated water to the deep seabed, for example Halothermal Circulation (HTC; (Horne 1999)). The processes occurring in deep-water formation areas, though, would have critically influenced the deep-water oxygen concentration (Sarmiento *et al.* 1988). Nevertheless, despite the fact that warm water has a lower capacity in dissolving oxygen than cold water masses (Weiss 1970), present-day evidence suggests that this may still have been sufficient for maintaining an abyssal fauna (Jumars 1976; Diaz and Rosenberg 1995; Levin and Gage 1998). And beyond the possibility of deep-ocean ventilation by HTC, there is evidence suggesting that a cold-water component has been present, possibly throughout the Phanerozoic, challenging the hypothesis that the abyss was mainly anoxic (Horne 1999; see also Hay 2008).

While some regions, such as the North and South Atlantic, were probably uninhabitable due to de-oxygenation (Weissert 1981; Kennett and Stott 1991, 1995), other regions were probably not. Especially in the Pacific Ocean, adverse climatic periods of the Cretaceous might have been survived *in situ* because evidence for anoxic conditions on the abyssal seafloor has not been found everywhere (Weissert 1981).

Macrostylids mainly occur at abyssal depths. The ancestral state reconstruction does not support a single reversal and on this background it is most parsimonious to assume that major anoxic conditions in the sea were survived by abyssal macrostylid isopods *in situ*.

Conclusions

Our study suggests that Macrostylidae are much more diverse and phylogenetically structured than

suggested by their previous classification and monotypy. Several subgroups were consistently revealed by phylogenetic analyses of morphological and molecular data and this may be a first step towards a revision of the family. Yet, discordances between the datasets currently prevail, which means that phylogenetic relationships cannot be unambiguously inferred.

On the complex background of climatic and paleoceanographic variations, the phylogeny of macrostylids can be interpreted as mirroring equally complex biogeographic consequences to those changes. Macrostylidae has an abyssal origin, nevertheless, shelf macrostylids have been collected from Antarctic, Australian, European and North American waters. Phylogenetic evidence suggests that these species are not in all cases close allies but have their closest relatives at bathyal or abyssal depths. This result points to multiple independent colonization events within this deep-sea family. Disjunct geographic distribution of subclades suggests a possible shelf emergence dating back to before the disintegration of Gondwana in the Jurassic thus rendering the shelf as a potential refuge for ancient and highly specialized deep-sea fauna. However, there is no evidence for re-colonization of the abyss from shelf or slope and it can thus be assumed that macrostylids predominantly survived the Phanerozoic mass extinction in the abyss.

Acknowledgements

The crews and captains of R/Vs METEOR, POLARSTERN and SONNE are greatly acknowledged for their support at sea. We would like to thank all people at the German Center for Marine Biodiversity Research in Hamburg and Wilhelmshaven as well as at the Zoological Museum Hamburg, AG NTII, who helped sorting

samples. Saskia Brix-Elsig and Pedro Martinez Arbizu provided support with travel funds to visit the Laboratories for Analytical Biology (LAB), Smithsonian Institution (SI), National Museum of Natural History. Amy Driskell and Andrea Ormos gave invaluable support at LAB. T. Chad Walter is kindly acknowledged due to his generous help to get along at SI. Discussions with George D. F. (Buz) Wilson helped much to improve the manuscript. Sarah Schnurr kindly created the distribution map. Molecular laboratory work was possible due to travel funds by the *University of Hamburg Foundation* (Universitätsstiftung Hamburg) and the *Census of the Diversity of Abyssal Marine Life* (CeDAMar) taxonomic exchange program. During the preparation of the manuscript and data analyses, TR was funded by the *German National Academic Foundation* (Studienstiftung des deutschen Volkes).

References

Akaike, H. (1974) A new look at the statistical model identification. *Automatic Control, IEEE Transactions on*, 19(6), 716–723.

Alegret, L., Molina, E. and Thomas, E. (2003) Benthic foraminiferal turnover across the Cretaceous/Paleogene boundary at Agost (southeastern Spain): paleoenvironmental inferences. *Marine Micropaleontology*, 48(3), 251–279.

Arthur, M. A. and Sageman, B. B. (1994) Marine shales: depositional mechanisms and environments of ancient deposits. *Annual Review of Earth and Planetary Sciences*, 22, 499–551.

Berggren, W. A. and Schnitker, D. (1983) Cenozoic marine environments in the north Atlantic and Norwegian-Greenland Sea. *Structure and Development of the Greenland-Scotland Ridge*. pp 495–548. Springer.

Berkman, P. A., Cattaneo-Vietti, R., Chiantore, M. and Howard-Williams, C. (2004) Polar emergence and the influence of increased sea-ice extent on the Cenozoic biogeography of pectinid molluscs in Antarctic coastal areas. *Deep Sea Research Part II: Topical Studies in Oceanography*, 51(14–16), 1839–1855 (ANDEEP (Antarctic benthic DEEP-sea) biodiversity: colonization history and recent community

patterns: a tribute to Howard L. Sanders).

Brandão, S. N., Sauer, J. and Schön, I. (2010) Circumantarctic distribution in Southern Ocean benthos? A genetic test using the genus *tt*(Crustacea, Ostracoda) as a model. *Molecular Phylogenetics and Evolution*, 55(3), 1055–1069.

Brandt, A. (1992) Origin of Antarctic Isopoda (Crustacea, Malacostraca). *Marine Biology*, 113, 415–423.

Brandt, A. (1999) On the origin and evolution of Antarctic Peracarida (Crustacea, Malacostraca). *Scientia Marina*, 63(S1), 261–274.

Brandt, A. (2002) *Desmostylis gerdesi*, a new species (Isopoda: Malacostraca) from Kapp Norvegia, Weddell Sea, Antarctica. *Proceedings of the Biological Society of Washington*, 115(3), 616–627.

Brandt, A. (2005) Evolution of Antarctic Biodiversity in the Context of the Past: The Importance of the Southern Ocean Deep Sea. *Antarctic Science*, 17(04), 509–521.

Brandt, A., Bathmann, U., Brix, S., Cisewski, B., Flores, H., Göcke, C., Janussen, D., Krägefsky, S., Kruse, S., Leach, H., Linse, K., Pakhomov, E., Peeken, I., Riehl, T., Sauter, E., Sachs, O., Schüller, M., Schrödl, M., Schwabe, E., Strass, V., van Franeker, J. A. and Wilmsen, E. (2011) Maud Rise – a snapshot through the water column. *Deep Sea Research Part II: Topical Studies in Oceanography*, 58(19-20), 1962–1982.

Brandt, A., Ebbe, B. and Sauter, E. J. (2010) ANDEEP - SYSTCO: SYSTem COupling in the deep Southern Ocean - from census to ecosystem functioning. *The expedition of the research vessel "Polarstern" to the Antarctic in 2007/2008 (ANT-XXIV/2)*. Ulrich Bathmann., pp 78–83. Bremerhaven: Alfred-Wegener-Institut Für Polar- und Meeresforschung. (604). ISBN 1866-3192.

Brandt, A., Elsner, N., Brenke, N., Golovan, O., Malyutina, M. V., Riehl, T., Schwabe, E. and Würzberg, L. (2013) Epifauna of the Sea of Japan collected via a new epibenthic sledge equipped with camera and environmental sensor systems. *Deep Sea Research Part II: Topical Studies in Oceanography*, 86-87, 43–55.

Brandt, A., Gooday, A. J., Brandao, S. N., Brix, S., Brökeland, W., Cedhagen, T., Choudhury, M., Cornelius, N., Danis, B., de Mesel, I., Diaz, R. J., Gillan, D. C., Ebbe, B., Howe, J. A., Janussen, D., Kaiser, S., Linse, K., Malyutina, M. V., Pawlowski, J., Raupach, M. J. and Vanreusel, A. (2007) First insights into the biodiversity and biogeography of the Southern Ocean deep sea. *Nature*, 447(7142), 307–311.

Brandt, A., Linse, K. and Schüller, M. (2009) Bathymetric distribution patterns of Southern Ocean macrofaunal taxa: Bivalvia, Gastropoda, Isopoda and Polychaeta. *Deep Sea Research Part I: Oceanographic Research Papers*, 56(11), 2013–2025.

Brandt, A. and Malyutina, M. V. (2012) *The German-*

- Russian deep-sea expedition KuramBio (Kurile Kamchatka Biodiversity Study): to the Kurile Kamchatka Trench and abyssal plain on board of the R/V Sonne, 223rd Expedition, July 21th - September 7th 2012 [online]. Hamburg: University of Hamburg; Biozentrum Grindel and Zoologisches Museum Hamburg. (R/V Sonne Cruise Reports).
- Brenke, N. (2005) An epibenthic sledge for operations on marine soft bottom and bedrock. *Marine Technology Society Journal*, 39(2), 10–21.
- Brey, T., Dahm, C., Gorny, M., Klages, M., Balke, M. and Arntz, W. E. (1996) Do antarctic benthic invertebrates show an extended level of eurybathy? *Antarctic Science*, 8(01), 3–6.
- Brix, S., Bauernfeind, W., Brenke, N., Blazewicz-Paszkowycz, M., Borges, V., Buldt, K., Cannon, J., Diaz Agras, G., Fiege, D., Fiorentino, D., Haraldsdóttir, S., Hoffmann, S., Holst, S., Hüttmann, F., Jeskulke, K., Jennings, R. M., Kocot, K., Khodami, S., Lucas Rodriguez, Y., Martinez Arbizu, P., Meißner, K., Mikkelsen, N., Miller, M., Murray, A., Neumann, H., Ostman, A., Riehl, T., Schnurr, S., Svavarsson, J. and Yasuhara, M. (2012) *IceAGE - Icelandic marine Animals: Genetics and Ecology* [online]. Hamburg: Senatskommission für Ozeanographie der Deutschen Forschungsgemeinschaft MARUM – Zentrum für Marine Umweltwissenschaften der Universität Bremen Leitstelle Deutsche Forschungsschiffe Institut für Meereskunde der Universität Hamburg. (METEOR Reports; 85-3).
- Brix, S., Leese, F., Riehl, T. and Kihara, T.-C. (in press) A new genus and new species of Desmosomatidae Sars, 1897 (Isopoda) from the east South-Atlantic abyss described by means of integrative taxonomy. *Marine Biodiversity*, .
- Brix, S., Riehl, T. and Leese, F. (2011) First genetic data for *Haploniscus rostratus* and *Haploniscus unicornis* from neighbouring deep-sea basins in the South Atlantic. *Zootaxa*, 2838, 79–84.
- Brix, S. and Svavarsson, J. (2010) Distribution and diversity of desmosomatid and nannoniscid isopods (Crustacea) on the Greenland–Iceland–Faeroe Ridge. *Polar biology*, 33(4), 515–530.
- Brökeland, W., Guðmundsson, G. and Svavarsson, J. (2010) Diet of four species of deep-sea isopods (Crustacea: Malacostraca: Peracarida) in the South Atlantic and the Southern Ocean. *Marine Biology*, 157(1), 177–178.
- Castresana, J. (2000) Selection of conserved blocks from multiple alignments for their use in phylogenetic analysis. *Molecular Biology and Evolution*, 17(4), 540–552.
- Clarke, A., Crame, J. A., Stromberg, J.-O. and Barker, P. F. (1992) The Southern Ocean benthic fauna and climate change: A historical perspective [and Discussion]. *Philosophical Transactions of the Royal Society of London. Series B: Biological Sciences*, 338(1285), 299–309.
- Dahl, E. (1972) The Norwegian Sea deep water fauna and its derivation. *Ambio Special Report*, 19–24.
- Dahl, E., Laubier, L., Sibuet, M. and Stromberg, J.-O. (1976) Some quantitative results on benthic communities of the deep Norwegian Sea. *Astarte*, (9), 61–79.
- Dallwitz, M. J. (1980) A general system for coding taxonomic descriptions. *Taxon*, 29(1), 41–46.
- Dallwitz, M. J. (1993) DELTA and INTKEY. In: Fortuner, R. (Ed.) *Advances in computer methods for systematic biology: artificial intelligence, databases, computer vision*. pp 287–296. Baltimore: Johns Hopkins University Press.
- Dayton, P. K. and Hessler, R. R. (1972) Role of biological disturbance in maintaining diversity in the deep sea. *Deep Sea Research and Oceanographic Abstracts*, 19(3), 199–208.
- Diaz, R. J. and Rosenberg, R. (1995) Marine benthic hypoxia: a review of its ecological effects and the behavioural responses of benthic macrofauna. *Oceanography and marine biology. An annual review*, 33, 245–03.
- Doyle, P. and Whitham, A. G. (1991) Palaeoenvironments of the Nordenskjöld Formation: an Antarctic Late Jurassic—Early Cretaceous black shale-tuff sequence. *Geological Society, London, Special Publications*, 58(1), 397–414.
- Dreyer, H. and Wägele, J.-W. (2001) Parasites of crustaceans (Isopoda: Bopyridae) evolved from fish parasites: Molecular and morphological evidence. *Zoology*, 103, 157–178.
- Dreyer, H. and Wägele, J.-W. (2002) The Scutocoxifera tax. nov. and the information content of nuclear ssu rDNA sequences for reconstruction of isopod phylogeny (Peracarida: Isopoda). *Journal of Crustacean Biology*, 22(2), 217–234.
- Drummond, A. J., Ashton, B., Buxton, S., Cheung, M., Cooper, A., Duran, C., Field, M., Heled, J., Kearse, M., Markowitz, S., Moir, R., Stones-Havas, S., Sturrock, S., Thierer, T. and Wilson, A. (2011) *Geneious v5.4* [online]. Version: 5.4. Available from: <http://www.geneious.com/>.
- Edgar, R. C. (2004) MUSCLE: multiple sequence alignment with high accuracy and high throughput. *Nucl. Acids Res.*, 32(5), 1792–1797.
- Etter, R. J. and Rex, M. A. (1990) Population differentiation decreases with depth in deep-sea gastropods. *Deep Sea Research Part I: Oceanographic Research*, 37(8), 1251–1261.
- Goloboff, P. A. (1999) Analyzing large data sets in reasonable times: solutions for composite optima. *Cladistics*, 15(4), 415–428.
- Goloboff, P. A. and Farris, J. S. (2001) Methods for quick consensus estimation. *Cladistics*, 17(1), S26–S34.
- Goloboff, P. A., Farris, J. S. and Nixon, K. C. (2008) TNT, a free program for phylogenetic analysis. *Cladistics*, 24(5), 774–786.

- Goujon, M., McWilliam, H., Li, W., Valentin, F., Squizzato, S., Paern, J. and Lopez, R. (2010) A new bioinformatics analysis tools framework at EMBL-EBI. *Nucleic Acids Research*, 38(Web Server), W695–W699.
- Gudmundsson, G., von Schmalensee, M. and Svavarsson, J. (2000) Are foraminifers (Protozoa) important food for small isopods (Crustacea) in the deep sea? *Deep Sea Research Part I: Oceanographic Research Papers*, 47(11), 2093–2109.
- Gutiérrez, D., Gallardo, V. A., Mayor, S., Neira, C., Vásquez, C., Sellanes, J., Rivas, M., Soto, A., Carrasco, F. and Baltazar, M. (2000) Effects of dissolved oxygen and fresh organic matter on the bioturbation potential of macrofauna in sublittoral sediments off Central Chile during the 1997/1998 El Niño. *Marine Ecology Progress Series*, 202, 81–99.
- Hansen, H. J. (1893) Zur Morphologie der Gliedmassen und Mundtheile bei Crustaceen und Insekten. *Zoologischer Anzeiger*, 16, 193–212.
- Hansen, H. J. (1916) Crustacea Malacostraca: The order Isopoda. *Danish Ingolf Expedition*, 3(5), 1–262.
- Harrison, K. (1989) Are deep-sea asellote isopods infaunal or epifaunal? *Crustaceana*, 56(3), 317–319.
- Hay, W. W. (2002) A new view of Cretaceous paleoceanography. In: Michalik, J. (Ed.) *Tethyan/Boreal Cretaceous Correlation*. pp 11–37. Bratislava, Slovak Rep.: VEDA Publishing House of the Slovak Academy of Sciences.
- Hay, W. W. (2008) Evolving ideas about the Cretaceous climate and ocean circulation. *Cretaceous Research*, 29(5–6), 725–753 (Life and the environment during the Cretaceous 7th International Symposium on the Cretaceous).
- Hennig, W. (1965) Phylogenetic systematics. *Annual Review of Entomology*, 10(1), 97–116.
- Hessler, R. R. and Sanders, H. L. (1967) Faunal diversity in the deep sea. *Deep Sea Research and Oceanographic Abstracts*, 14(1), 65–70.
- Hessler, R. R. and Strömberg, J. O. (1989) Behavior of janiroidean isopods (Asellota), with special reference to deep sea genera. *Sarsia*, 74(3), 145–159.
- Hessler, R. R. and Thistle, D. (1975) On the place of origin of deep-sea isopods. *Marine Biology*, 32(2), 155–165.
- Hessler, R. R., Wilson, G. D. F. and Thistle, D. (1979) The deep-sea isopods: a biogeographic and phylogenetic overview. *Sarsia*, 64(1-2), 67–75.
- Horne, D. J. (1999) Ocean circulation modes of the Phanerozoic: implications for the antiquity of deep-sea benthonic invertebrates. *Crustaceana*, 999–1018.
- Huson, D. H. (1998) SplitsTree: A Program for Analyzing and Visualizing Evolutionary Data. *Bioinformatics*, 14, 68–73.
- Ingall, E. D., Bustin, R. M. and Van Cappellen, P. (1993) Influence of water column anoxia on the burial and preservation of carbon and phosphorus in marine shales. *Geochimica et Cosmochimica Acta*, 57(2), 303–316.
- Jacobs, D. K. and Lindberg, D. R. (1998) Oxygen and evolutionary patterns in the sea: Onshore/offshore trends and recent recruitment of deep-sea faunas. *Proceedings of the National Academy of Sciences*, 95(16), 9396–9401.
- Jamieson, A. J., Fujii, T. and Priede, I. G. (2012) Locomotory activity and feeding strategy of the hadal munnopsid isopod *Rectisura cf. herculea* (Crustacea: Asellota) in the Japan Trench. *The Journal of Experimental Biology*, 215(17), 3010–3017.
- Jennings, R. M., Etter, R. J. and Ficarra, L. (2013) Population differentiation and species formation in the deep sea: The potential role of environmental gradients and depth. *PLoS ONE*, 8(10), e77594.
- Jumars, P. A. (1976) Deep-sea species diversity: does it have a characteristic scale. *Journal of Marine Research*, 34(2), 217–246.
- Kaiser, S., Barnes, D. K. A., Sands, C. J. and Brandt, A. (2009) Biodiversity of an unknown Antarctic sea: assessing isopod richness and abundance in the first benthic survey of the Amundsen continental shelf. *Marine Biodiversity*, 39(1), 27–43.
- Kaiser, S., Griffiths, H. J., Barnes, D. K. A., Brandão, S. N., Brandt, A. and O'Brien, P. E. (2011) Is there a distinct continental slope fauna in the Antarctic? *Deep Sea Research Part II: Topical Studies in Oceanography*, 58(1-2), 91–104.
- Katoh, K., Asimenos, G. and Toh, H. (2009) Multiple Alignment of DNA Sequences with MAFFT. (Posada, D., Ed.) *Bioinformatics for DNA Sequence Analysis*, 537, 39–64 (Methods in Molecular Biology).
- Katoh, K., Misawa, K., Kuma, K. and Miyata, T. (2002) MAFFT: a novel method for rapid multiple sequence alignment based on fast Fourier transform. *Nucleic Acids Research*, 30(14), 3059–3066.
- Katoh, K. and Toh, H. (2008) Recent developments in the MAFFT multiple sequence alignment program. *Briefings in Bioinformatics*, 9(4), 286–298.
- Kennett, J. P. and Stott, L. D. (1991) Abrupt deep sea warming, paleoceanographic changes and benthic extinctions at the end of the Paleocene. *Nature*, 353, 225–229.
- Kennett, J. P. and Stott, L. D. (1995) Terminal Paleocene mass extinction in the deep sea: association with global warming. *Effects of past global change on life*, 94–107.
- Kornobis, E., Pálsson, S., Sidorov, D. A., Holsinger, J. R. and Kristjánsson, B. K. (2011) Molecular taxonomy and phylogenetic affinities of two groundwater amphipods,

- Crangonyx islandicus* and *Crymostygius thingvallensis*, endemic to Iceland. *Molecular Phylogenetics and Evolution*, 58(3), 527–539.
- Kussakin, O. G. (1973) Peculiarities of the geographical and vertical distribution of marine isopods and the problem of deep-sea fauna origin. *Marine Biology*, 23(1), 19–34.
- Kussakin, O. G. (1999) *Marine and brackish-water isopods from cold and temperate waters of the Northern Hemisphere Suborder Asellota. Part 2. Families Joeropsididae, Nannoniscidae, Desmosomatidae, Macrostylidae.* (Alimov, A. F., Ed.) St. Petersburg: Publication of the Zoological Institute of the Russian Academy of Sciences. (Keys to the Fauna of the SSSR).
- Larkin, M. A., Blackshields, G., Brown, N. P., Chenna, R., McGettigan, P. A., McWilliam, H., Valentin, F., Wallace, I. M., Wilm, A. and Lopez, R. (2007) Clustal W and Clustal X version 2.0. *Bioinformatics*, 23(21), 2947–2948.
- Levin, L. A. and Gage, J. D. (1998) Relationships between oxygen, organic matter and the diversity of bathyal macrofauna. *Deep-Sea Research Part II*, 45(1-3), 129–163.
- Levin, L. A., Gage, J. D., Martin, C. and Lamont, P. A. (2000) Macrobenthic community structure within and beneath the oxygen minimum zone, NW Arabian Sea. *Deep Sea Research Part II: Topical Studies in Oceanography*, 47(1–2), 189–226.
- Levin, L. A., Whitcraft, C. R., Mendoza, G. F., Gonzalez, J. P. and Cowie, G. (2009) Oxygen and organic matter thresholds for benthic faunal activity on the Pakistan margin oxygen minimum zone (700–1100 m). *Deep Sea Research Part II: Topical Studies in Oceanography*, 56(6–7), 449–471 (Benthic Biological and Biogeochemical Patterns and Processes Across an Oxygen Minimum Zone (Pakistan Margin, NE Arabian Sea)).
- Lilljeborg, W. (1864) Bidrag til k annedommen om de inom Sverige och Norrige f orekommande Crustaceer af Isopodernas underordning och Tanaidernas familj. *Inbjudningsskrift till  h rande af de Offentliga F rel sningar: C. A. Leffler, Kongl. Acad. Boktryckare, Upsala.*, 31 pp.
- Lindner, A., Cairns, S. D. and Cunningham, C. W. (2008) From offshore to onshore: multiple origins of shallow-water corals from deep-sea ancestors. *PLoS One*, 3(6), e2429.
- Lins, L. S. F., Ho, S. Y. W., Wilson, G. D. F. and Lo, N. (2012) Evidence for Permo-Triassic colonization of the deep sea by isopods. *Biology Letters*, 8(6), 979–982.
- Linse, K., Griffiths, H. J., Barnes, D. K., Brandt, A., Davey, N., David, B., De Grave, S., d’Udekem d’Acoz, C., El aume, M., Glover, A. G., Hemery, L. G., Mah, C., Mart n-Ledo, R., Munilla, T., O’Loughlin, M., Pierrat, B., Sauc de, T., Sands, C. J., Strugnell, J. M. and Enderlein, P. (2013) The macro- and megabenthic fauna on the continental shelf of the eastern Amundsen Sea, Antarctica. *Continental Shelf Research*, 68, 80–90.
- Maddison, W. P. and Maddison, D. R. (2011) *Mesquite: a modular system for evolutionary analysis.* [online]. Version: 2.75. Available from: <http://mesquiteproject.org>.
- Malyutina, M. V. and Kussakin, O. G. (1996) Addition to the Polar Sea bathyal and abyssal Isopoda (Crustacea). Part 1. Anthuridea, Valvifera, Asellota (Ischnomesidae, Macrostylidae, Nannoniscidae). *Zoosystematica Rossica*, 4(1), 49–62.
- Mart nez Arbizu, P., Brix, S., Kaiser, S., Brandt, A., George, K. H., Arndt, H., Hausmann, K., T rkay, M., Renz, J., Hendrycks, E., Reiss, H., D az Agras, G. and Pawlowski, J. (2014) *Cruise No. M79/1. Deep-Sea Biodiversity, Current Activity, and Seamounts in the Atlantic.* Bremen, Germany: DFG-Senatskommission f r Ozeanographie. (METEOR Reports; Cruise No. M79/1).
- McWilliam, H., Li, W., Uludag, M., Squizzato, S., Park, Y. M., Buso, N., Cowley, A. P. and Lopez, R. (2013) Analysis Tool Web Services from the EMBL-EBI. *Nucleic Acids Research*, 41(W1), W597–W600.
- Meinert, F. V. A. (1890) Crustacea malacostraca. *Videnskabelige udbytte af kanonbaden "Hauchs Dogter".* pp 147–230.
- Menzies, R. J. (1956) New abyssal tropical Atlantic isopods with observations on their biology. *American Museum Novitates*, 1798, 1–16.
- Menzies, R. J., George, R. Y. and Rowe, G. T. (1973) *Abyssal environment and ecology of the world oceans.* New York: John Wiley and Sons. ISBN 0-471-59440-7.
- Menzies, R. J. and Imbrie, J. (1958) On the antiquity of the deep sea bottom fauna. *Oikos*, 9(2), 192.
- Menzies, R. J., Imbrie, J. and Heezen, B. C. (1961) Further considerations regarding the antiquity of the abyssal fauna with evidence for a changing abyssal environment. *Deep Sea Research (1953)*, 8(2), 79–90, IN1, 91–94.
- Mezhov, B. V. (1993) Three new species of *Macrostylis* G.O. Sars, 1864 (Crustacea Isopoda Asellota Macrostylidae) from the Pacific Ocean. *Arthropoda Selecta*, 2(3), 3–9.
- Notredame, C., Higgins, D. G. and Heringa, J. (2000) T-Coffee: A novel method for fast and accurate multiple sequence alignment. *Journal of molecular biology*, 302(1), 205–217.
- Nylander, J. A. A. (2004) *MrModeltest.* Version: 2. Evolutionary Biology Center, Uppsala University.
- Osborn, K. J. (2009) Relationships within the Munnopsidae (Crustacea, Isopoda, Asellota) based on three genes. *Zoologica Scripta*, 38(6), 617–635.
- Pante, E., France, S. C., Couloux, A., Cruaud, C., McFadden, C. S., Samadi, S. and Watling, L. (2012) Deep-sea origin and in-situ diversification of chrysogorgiid octocorals. *PLoS ONE*,

Ramirez-Llodra, E., Brandt, A., Danovaro, R., De Mol, B., Escobar, E., German, C. R., Levin, L. A., Martinez Arbizu, P., Menot, L., Buhl-Mortensen, P., Narayanaswamy, B. E., Smith, C. R., Tittensor, D. P., Tyler, P. A., Vanreusel, A. and Vecchione, M. (2010) Deep, diverse and definitely different: unique attributes of the world's largest ecosystem. *Biogeosciences*, 7(9), 2851–2899.

Raupach, M. J., Held, C. and Wägele, J.-W. (2004) Multiple colonization of the deep sea by the Asellota (Crustacea: Peracarida: Isopoda). *Deep Sea Research Part II: Topical Studies in Oceanography*, 51, 1787–1795.

Raupach, M. J., Mayer, C., Malyutina, M. V. and Wägele, J.-W. (2009) Multiple origins of deep-sea Asellota (Crustacea: Isopoda) from shallow waters revealed by molecular data. *Proceedings of the Royal Society B: Biological Sciences*, 276, 799–808.

Rex, M. A. and Etter, R. J. (2010) *Deep-sea biodiversity - Pattern and scale*. 1. ed. Harvard University Press. ISBN 0674036077.

Riehl, T. and Brandt, A. (in prep.) A comparative review of the morphology of Macrostylidae (Isopoda) from the phylogenetic perspective.

Riehl, T. and Brandt, A. (2010) Descriptions of two new species in the genus *Macrostylis* Sars, 1864 (Isopoda, Asellota, Macrostylidae) from the Weddell Sea (Southern Ocean), with a synonymisation of the genus *Desmostylis* Brandt, 1992 with *Macrostylis*. *Zookeys*, 57, 9–49.

Riehl, T. and Brandt, A. (2013) Southern Ocean Macrostylidae reviewed with a key to the species and new descriptions from Maud Rise. *Zootaxa*, 3692(1), 160–203.

Riehl, T., Brenke, N., Brix, S., Driskell, A., Kaiser, S. and Brandt, A. (under review) Field and laboratory methods for DNA barcoding and molecular-systematic studies on deep-sea isopod crustaceans. *Polish Polar Research*, .

Riehl, T. and Kaiser, S. (2012) Conquered from the deep sea? A new deep-sea isopod species from the Antarctic shelf shows pattern of recent colonization. *PLoS ONE*, 7(11), e49354.

Riehl, T., Wilson, G. D. F. and Hessler, R. R. (2012) New Macrostylidae Hansen, 1916 (Crustacea: Isopoda) from the Gay Head-Bermuda transect with special consideration of sexual dimorphism. *Zootaxa*, 3277, 1–26.

Riehl, T., Wilson, G. D. F. and Malyutina, M. V. (2014) Urstylidae – A new family of deep-sea isopods and its phylogenetic implications. *Zoological Journal of the Linnean Society*, 170, 245–296.

Ronquist, F. and Huelsenbeck, J. P. (2003) MrBayes 3: Bayesian phylogenetic inference under mixed models. *Bioinformatics (Oxford, England)*, 19(12), 1572–1574.

Rothlisberg, P. C. and Percy, W. G. (1976) An epibenthic sampler used to study the ontogeny of vertical migration of *Pandalus jordani* (Decapoda, Caridea). *Fisheries Bulletin*, 74, 994–997.

Sanders, H. L. (1968) Marine benthic diversity: a comparative study. *American naturalist*, 243–282.

Sanders, H. L., Hessler, R. R. and Hampson, G. R. (1965) An introduction to the study of deep-sea benthic faunal assemblages along the Gay Head-Bermuda transect. *Deep Sea Research and Oceanographic Abstracts*, 12(6), 845–867.

Sarmiento, J. L., Herbert, T. D. and Toggweiler, J. R. (1988) Causes of anoxia in the world ocean. *Global Biogeochemical Cycles*, 2(2), 115–128.

Sars, G. O. (1864) Om en anomal Gruppe af Isopoder. *Forhandlinger Videnskaps-Selskapet, Anar 1863 in Christiania*, 205–221.

Sars, G. O. (1897) On some additional Crustacea from the Caspian Sea. *Annales du Musée Zoologique Academie Imperiale des Sciences St. Petersburg*, 2, 273–305.

Schnurr, S., Brandt, A., Brix, S., Fiorentino, D., Malyutina, M. and Svavarsson, J. (2014) Composition and distribution of selected munnopsid genera (Crustacea, Isopoda, Asellota) in Icelandic waters. *Deep Sea Research Part I: Oceanographic Research Papers*, 84, 142–155.

Smith, A. B. and Stockley, B. (2005) The geological history of deep-sea colonization by echinoids: roles of surface productivity and deep-water ventilation. *Proceedings of the Royal Society B: Biological Sciences*, 272(1565), 865–869.

Smith, C. R., De Leo, F. C., Bernardino, A. F., Sweetman, A. K. and Martínez Arbizu, P. (2008) Abyssal food limitation, ecosystem structure and climate change. *Trends in Ecology and Evolution*, 23(9), 518–528.

Stamatakis, A. (2006) RAxML-VI-HPC: maximum likelihood-based phylogenetic analyses with thousands of taxa and mixed models. *Bioinformatics*, 22(21), 2688–2690.

Strugnell, J. M., Cherel, Y., Cooke, I. R., Gleadall, I. G., Hochberg, F. G., Ibáñez, C. M., Jorgensen, E., Laptikhovskiy, V. V., Linse, K., Norman, M., Vecchione, M., Voight, J. R. and Allcock, A. L. (2011) The Southern Ocean: Source and sink? *Deep Sea Research Part II: Topical Studies in Oceanography*, 58(1-2), 196–204.

Strugnell, J. M., Rogers, A. D., Prodöhl, P. A., Collins, M. A. and Allcock, A. L. (2008) The thermohaline expressway: the Southern Ocean as a centre of origin for deep-sea octopuses. *Cladistics*, 24(6), 853–860.

Suchanek, T. H., Williams, S. L., Ogden, J. C., Hubbard, D. K. and Gill, I. P. (1985) Utilization of shallow-water seagrass detritus by Caribbean deep-sea macrofauna: [delta] 13C evidence. *Deep Sea Research Part A. Oceanographic*

Research Papers, 32(2), 201–214.

Svavarsson, J., Brattegard, T. and Strömberg, J. O. (1990) Distribution and diversity patterns of asellote isopods (Crustacea) in the deep Norwegian and Greenland Seas. *Progress in Oceanography*, 24, 297–310.

Svavarsson, J., Stromberg, J. O. and Brattegard, T. (1993) The deep-sea asellote (Isopoda, Crustacea) fauna of the Northern Seas: species composition, distributional patterns and origin. *Journal of Biogeography*, 537–555.

Thatje, S., Hillenbrand, C.-D. and Larter, R. (2005) On the origin of Antarctic marine benthic community structure. *Trends in Ecology & Evolution*, 20(10), 534–540.

Thiede, J., Winkler, A., Wolf-Welling, T., Eldholm, O., Myhre, A. M., Baumann, K.-H., Henrich, R. and Stein, R. (1998) Late Cenozoic history of the polar North Atlantic: results from ocean drilling. *Quaternary Science Reviews*, 17(1), 185–208.

Thistle, D. and Wilson, G. D. F. (1987) A hydrodynamically modified, abyssal isopod fauna. *Deep-Sea Research. Part A. Oceanographic Research Papers*, 34(1), 73–87.

Thuy, B., Gale, A. S., Kroh, A., Kucera, M., Nummerger-Thuy, L. D., Reich, M. and Stöhr, S. (2012) Ancient origin of the modern deep-sea fauna. *PLoS one*, 7(10), e46913.

Weiss, R. F. (1970) The solubility of nitrogen, oxygen and argon in water and seawater. *Deep Sea Research and Oceanographic Abstracts*, 17, 721–735.

Weissert, H. (1981) The environment of deposition of black shales in the early Cretaceous - an ongoing controversy. [online], Available from: http://archives.datapages.com/data/sepmsp/SP32/The_Environment_of_Deposition.htm. [Accessed 2014-04-06].

White, B. N. (1988) Oceanic anoxic events and allopatric

speciation in the deep sea. *Biological Oceanography*, 5(4), 243–259.

Wilson, G. D. F. (1980) New insights into the colonization of the deep sea: Systematics and zoogeography of the Munnidae and the Pleurogoniidae comb. nov. (Isopoda; Janiroidea). *Journal of Natural History*, 14(2), 215–236.

Wilson, G. D. F. (1999) Some of the deep-sea fauna is ancient. *Crustaceana*, 72(8), 1019–1030.

Wilson, G. D. F. (2008) Local and regional species diversity of benthic Isopoda (Crustacea) in the deep Gulf of Mexico. *Deep-Sea Research Part II: Topological Studies in Oceanography*, 55(24-26), 2634–2649.

Wirkner, C. S. and Richter, S. (2010) Evolutionary morphology of the circulatory system in Peracarida (Malacostraca; Crustacea). *Cladistics*, 26(2), 143–167.

Wolff, T. (1976) Utilization of seagrass in the deep sea. *Aquatic Botany*, 2(0), 161–174.

Würzberg, L., Peters, J. and Brandt, A. (2011) Fatty acid patterns of Southern Ocean shelf and deep sea peracarid crustaceans and a possible food source, foraminiferans. *Deep Sea Research Part II: Topical Studies in Oceanography*, 58(19–20), 2027–2035.

Wägele, J.-W. (1989) *Evolution und phylogenetisches System der Isopoda: Stand der Forschung und neue Erkenntnisse [Evolution and phylogeny of isopods. New data and the state of affairs]*. Stuttgart: E. Schweizerbart'sche Verlagsbuchhandlung. (Zoologica). ISBN 978-3-510-55026-5.

Wägele, J.-W. and Mayer, C. (2007) Visualizing differences in phylogenetic information content of alignments and distinction of three classes of long-branch effects. *BMC Evolutionary Biology*, 7(1), 147.

Table 1. Records for *Macrostylis* species used in the 16S and 18S phylogenies. Coordinates are given in decimal degrees. Research vessels (R/V) involved in sampling campaigns were R/V Sonne (SO) during the KuramBio project, R/V Meteor (M) during the IceAGE and DIVA 3 campaigns; additional sequences were retrieved from GenBank (Rupapach *et al.* 2004; Riehl and Kaiser, 2012, Riehl and Brandt, 2013). Geographical abbreviations: E = East; N = North; W = West; S = South; GenBank accession numbers for 16S and 18S rRNA sequences are to be announced (TBA) upon acceptance of this manuscript.

Field ID	species	Station	Lat.	Long.	Depth	Ocean	Region	16S	18S
KBMa003	curticornis	SO223-1-10	43.973	157.304	5423	NW Pacific	Kurile-Kamchatka	TBA	TBA
KBMa007	curticornis	SO223-1-10	43.973	157.304	5423	NW Pacific	Kurile-Kamchatka	TBA	TBA
KBMa010	curticornis	SO223-1-10	43.973	157.304	5423	NW Pacific	Kurile-Kamchatka	TBA	TBA
KBMa011	curticornis	SO223-1-10	43.973	157.304	5423	NW Pacific	Kurile-Kamchatka	TBA	TBA

Table 1 continued. Records for *Macrostylis* species used in the 16S and 18S phylogenies.

Field ID	species	Station	Lat.	Long.	Depth	Ocean	Region	16S	18S
KBMa028	curticornis	SO223-2-9	46.227	155.557	4866	NW Pacific	Kurile-Kamchatka	TBA	TBA
KBMa044	curticornis	SO223-2-9	46.227	155.557	4866	NW Pacific	Kurile-Kamchatka	TBA	TBA
KBMa085	curticornis	SO223-3-9	47.231	154.698	4988	NW Pacific	Kurile-Kamchatka	TBA	TBA
KBMa090	curticornis	SO223-3-9	47.231	154.698	4988	NW Pacific	Kurile-Kamchatka	TBA	TBA
KBMa092	curticornis	SO223-3-9	47.231	154.698	4988	NW Pacific	Kurile-Kamchatka	TBA	TBA
KBMa096	curticornis	SO223-4-3	46.909	154.501	5961	NW Pacific	Kurile-Kamchatka	TBA	TBA
KBMa098	curticornis	SO223-4-3	46.909	154.501	5961	NW Pacific	Kurile-Kamchatka	TBA	TBA
KBMa130	curticornis	SO223-7-9	43.048	152.991	5216	NW Pacific	Kurile-Kamchatka	TBA	TBA
KBMa040	KuramBio sp.6	SO223-2-9	46.227	155.557	4866	NW Pacific	Kurile-Kamchatka	TBA	TBA
KBMa041	KuramBio sp.6	SO223-2-9	46.227	155.557	4866	NW Pacific	Kurile-Kamchatka	TBA	TBA
KBMa080	KuramBio sp.6	SO223-2-9	46.227	155.557	4866	NW Pacific	Kurile-Kamchatka	TBA	TBA
KBMa081	KuramBio sp.6	SO223-10-6	41.199	150.096	5250	NW Pacific	Kurile-Kamchatka	TBA	TBA
KBMa111	KuramBio sp.6	SO 223-5-9	43.592	153.965	5378	NW Pacific	Kurile-Kamchatka	TBA	TBA
KBMa120	KuramBio sp.6	SO 223-6-11	42.493	154.001	5290	NW Pacific	Kurile-Kamchatka	TBA	TBA
KBMa016	KuramBio sp.5	SO223-1-10	43.973	157.304	5423	NW Pacific	Kurile-Kamchatka	TBA	TBA
KBMa001	KuramBio sp.2	SO223-1-10	43.973	157.304	5423	NW Pacific	Kurile-Kamchatka	TBA	TBA
KBMa002	KuramBio sp.2	SO223-1-10	43.973	157.304	5423	NW Pacific	Kurile-Kamchatka	TBA	TBA
KBMa052	KuramBio sp.2	SO223-2-9	46.227	155.557	4866	NW Pacific	Kurile-Kamchatka	TBA	TBA
KBMa060	KuramBio sp.2	SO223-2-9	46.227	155.557	4866	NW Pacific	Kurile-Kamchatka	TBA	TBA
KBMa109	KuramBio sp.2	SO223-5-9	43.592	153.965	5378	NW Pacific	Kurile-Kamchatka	TBA	TBA
KBMa076	grandis	SO223-3-9	47.231	154.698	4988	NW Pacific	Kurile-Kamchatka	TBA	TBA
KBMa097	grandis	SO223-4-3	46.909	154.501	5961	NW Pacific	Kurile-Kamchatka	TBA	TBA
KBMa099	grandis	SO223-4-3	46.909	154.501	5961	NW Pacific	Kurile-Kamchatka	TBA	TBA
KBMa103	grandis	SO223-4-3	46.909	154.501	5961	NW Pacific	Kurile-Kamchatka	TBA	TBA
KBMa104	KuramBio sp.1	SO223-5-9	43.592	153.965	5378	NW Pacific	Kurile-Kamchatka	TBA	TBA
KBMa115	KuramBio sp.1	SO223-5-9	43.592	153.965	5378	NW Pacific	Kurile-Kamchatka	TBA	TBA
KBMa121	KuramBio sp.11	SO223-6-11	42.493	154.001	5290	NW Pacific	Kurile-Kamchatka	TBA	TBA
KBMa122	KuramBio sp.1	SO223-6-11	42.493	154.001	5290	NW Pacific	Kurile-Kamchatka	TBA	TBA
KBMa124	KuramBio sp.11	SO223-6-11	42.493	154.001	5290	NW Pacific	Kurile-Kamchatka	TBA	TBA
KBMa129	KuramBio sp.1	SO223-6-11	42.493	154.001	5290	NW Pacific	Kurile-Kamchatka	TBA	TBA
KBMa133	KuramBio sp.11	SO223-9-9	40.592	150.999	5399	NW Pacific	Kurile-Kamchatka	TBA	TBA
KBMa065	KuramBio sp.01	SO223-2-9	46.227	155.557	4866	NW Pacific	Kurile-Kamchatka	TBA	TBA
KBMa038	grandis	SO223-3-9	47.231	154.698	4988	NW Pacific	Kurile-Kamchatka	TBA	TBA
KBMa045	grandis	SO223-3-9	47.231	154.698	4988	NW Pacific	Kurile-Kamchatka	TBA	TBA
KBMa046	grandis	SO223-4-3	46.909	154.501	5961	NW Pacific	Kurile-Kamchatka	TBA	TBA
KBMa047	grandis	SO223-4-3	46.909	154.501	5961	NW Pacific	Kurile-Kamchatka	TBA	TBA
KBMa048	grandis	SO223-3-9	47.231	154.698	4988	NW Pacific	Kurile-Kamchatka	TBA	TBA
KBMu048	grandis	SO223-3-9	47.231	154.698	4988	NW Pacific	Kurile-Kamchatka	TBA	TBA
KBMa064	grandis	SO 23-4-3	46.909	154.501	5961	NW Pacific	Kurile-Kamchatka	TBA	TBA
KBMa127	longula	SO223-6-11	42.493	154.001	5290	NW Pacific	Kurile-Kamchatka	TBA	TBA
IMacro8	magnifica	M85/3 979	60.358	-18.137	2568	N Atlantic	Iceland Basin	TBA	TBA
IMacro46	elongata	M85/3 1019	62.939	-20.744	914	N Atlantic	Iceland Basin	TBA	TBA
IMacro47	elongata	M85/3 1019	62.939	-20.744	914	N Atlantic	Iceland Basin	TBA	TBA
IMacro1	spinifera	M85/3 1019	62.939	-20.744	914	N Atlantic	Iceland Basin	TBA	TBA

Table 1 continued. Records for *Macrotylis* species used in the 16S and 18S phylogenies.

Field ID	species	Station	Lat.	Long.	Depth	Ocean	Region	16S	18S
IMacro18	spinifera	M85/3 1019	62.939	-20.744	914	N Atlantic	Iceland Basin	TBA	TBA
IMacro39	spinifera	M85/3 1010	62.552	-20.395	1385	N Atlantic	Iceland Basin	TBA	TBA
IMacro49	spinifera	M85/3 1019	62.939	-20.744	914	N Atlantic	Iceland Basin	TBA	TBA
IMacro58	spinifera	M85/3 1019	62.939	-20.744	914	N Atlantic	Iceland Basin	TBA	TBA
IMacro12	abyssicola	M85/3 1057	61.642	-31.356	2505	N Atlantic	Irminger Basin	TBA	TBA
D3M1	DIVA-3 sp. 04	M79/1 532	-35.986	-49.013	4605.4	SW Atlantic	Argentine Basin	TBA	TBA
D3M2	DIVA-3 sp. 04	M79/1 532	-35.986	-49.013	4605.4	SW Atlantic	Argentine Basin	TBA	TBA
D3M5	DIVA-3 sp. 02b	M79/1 532	-35.986	-49.013	4605.4	SW Atlantic	Argentine Basin	TBA	TBA
D3M6	DIVA-3 sp. 13	M79/1 534	-36.010	-49.026	4607.8	SW Atlantic	Argentine Basin	TBA	TBA
D3M8	DIVA-3 sp. 12	M79/1 534	-36.010	-49.026	4607.8	SW Atlantic	Argentine Basin	TBA	TBA
D3M10	DIVA-3 sp. 07	M79/1 554	-26.578	-35.213	4484.7	SW Atlantic	Argentine Basin	TBA	TBA
D3M12	DIVA-3 sp. 08	M79/1 554	-26.578	-35.213	4484.7	SW Atlantic	Argentine Basin	TBA	TBA
D3M14	DIVA-3 sp. 07	M79/1 554	-26.578	-35.213	4484.7	SW Atlantic	Argentine Basin	TBA	TBA
D3M14	„group 11“	M79/1 554	-26.578	-35.213	4484.7	SW Atlantic	Argentine Basin	TBA	TBA
D3M15	robusta	M79/1 554	-26.578	-35.213	4484.7	SW Atlantic	Argentine Basin	TBA	TBA
D3M16	robusta	M79/1 554	-26.578	-35.213	4484.7	SW Atlantic	Argentine Basin	TBA	TBA
D3M18	DIVA-3 sp. 07	M79/1 554	-26.578	-35.213	4484.7	SW Atlantic	Argentine Basin	TBA	TBA
D3M19	DIVA-3 sp. 11	M79/1 554	-26.578	-35.213	4484.7	SW Atlantic	Argentine Basin	TBA	TBA
D3M20	DIVA-3 sp. 09	M79/1 554	-26.578	-35.213	4484.7	SW Atlantic	Argentine Basin	TBA	TBA
D3M21	DIVA-3 sp. 11	M79/1 554	-26.578	-35.213	4484.7	SW Atlantic	Argentine Basin	TBA	TBA
D3M22	DIVA-3 sp. 09	M79/1 554	-26.578	-35.213	4484.7	SW Atlantic	Argentine Basin	TBA	TBA
D3M23	DIVA-3 sp. 07	M79/1 554	-26.578	-35.213	4484.7	SW Atlantic	Argentine Basin	TBA	TBA
D3M24	DIVA-3 sp. 09	M79/1 554	-26.578	-35.213	4484.7	SW Atlantic	Argentine Basin	TBA	TBA
D3M25	DIVA-3 sp. 07	M79/1 554	-26.578	-35.213	4484.7	SW Atlantic	Argentine Basin	TBA	TBA
D3M26	DIVA-3 sp. 09	M79/1 554	-26.578	-35.213	4484.7	SW Atlantic	Argentine Basin	TBA	TBA
D3M28	DIVA-3 sp. 07	M79/1 554	-26.578	-35.213	4484.7	SW Atlantic	Argentine Basin	TBA	TBA
D3M29	DIVA-3 sp. 09	M79/1 554	-26.578	-35.213	4484.7	SW Atlantic	Argentine Basin	TBA	TBA
D3M30	DIVA-3 sp. 09	M79/1 554	-26.578	-35.213	4484.7	SW Atlantic	Argentine Basin	TBA	TBA
D3M31	robusta	M79/1 554	-26.578	-35.213	4484.7	SW Atlantic	Argentine Basin	TBA	TBA
D3M32	robusta	M79/1 554	-26.578	-35.213	4484.7	SW Atlantic	Argentine Basin	TBA	TBA
D3M33	robusta	M79/1 554	-26.578	-35.213	4484.7	SW Atlantic	Argentine Basin	TBA	TBA
D3M34	robusta	M79/1 554	-26.578	-35.213	4484.7	SW Atlantic	Argentine Basin	TBA	TBA
D3M35	robusta	M79/1 554	-26.578	-35.213	4484.7	SW Atlantic	Argentine Basin	TBA	TBA
D3M36	robusta	M79/1 554	-26.578	-35.213	4484.7	SW Atlantic	Argentine Basin	TBA	TBA
D3M37	DIVA-3 sp. 07	M79/1 554	-26.578	-35.213	4484.7	SW Atlantic	Argentine Basin	TBA	TBA
D3M38	DIVA-3 sp. 07	M79/1 554	-26.578	-35.213	4484.7	SW Atlantic	Argentine Basin	TBA	TBA
D3M39	DIVA-3 sp. 09	M79/1 554	-26.578	-35.213	4484.7	SW Atlantic	Argentine Basin	TBA	TBA
D3M45	DIVA-3 sp. 07	M79/1 580	-14.982	-29.942	5131	SW Atlantic	Brazil Basin	TBA	TBA
D3M46	DIVA-3 sp. 07	M79/1 580	-14.982	-29.942	5131	SW Atlantic	Brazil Basin	TBA	TBA
D3M48	DIVA-3 sp. 10	M79/1 580	-14.982	-29.942	5131	SW Atlantic	Brazil Basin	TBA	TBA
D3M50	DIVA-3 sp. 07	M79/1 580	-14.982	-29.942	5131	SW Atlantic	Brazil Basin	TBA	TBA
D3M51	DIVA-3 sp. 07	M79/1 580	-14.982	-29.942	5131	SW Atlantic	Brazil Basin	TBA	TBA
D3M53	DIVA-3 sp. 07	M79/1 604	-3.961	-28.089	5179.8	W Atlantic	Brazil Basin	TBA	TBA
D3M55	DIVA-3 sp. 07	M79/1 604	-3.961	-28.089	5179.8	W Atlantic	Brazil Basin	TBA	TBA
D3M57	DIVA-3 sp. 07	M79/1 604	-3.961	-28.089	5179.8	W Atlantic	Brazil Basin	TBA	TBA
D3M58	DIVA-3 sp. 07	M79/1 604	-3.961	-28.089	5179.8	W Atlantic	Brazil Basin	TBA	TBA
D3M59	DIVA-3 sp. 02	M79/1 604	-3.961	-28.089	5179.8	W Atlantic	Brazil Basin	TBA	TBA
D3M60	DIVA-3 sp. 02	M79/1 604	-3.961	-28.089	5179.8	W Atlantic	Brazil Basin	TBA	TBA
D3M61	DIVA-3 sp. 07	M79/1 604	-3.961	-28.089	5179.8	W Atlantic	Brazil Basin	TBA	TBA
D3M62	DIVA-3 sp. 07	M79/1 604	-3.961	-28.089	5179.8	W Atlantic	Brazil Basin	TBA	TBA
D3M63	DIVA-3 sp. 07	M79/1 604	-3.961	-28.089	5179.8	W Atlantic	Brazil Basin	TBA	TBA

Table 1 continued. Records for *Macrostylis* species used in the 16S and 18S phylogenies.

Field ID	species	Station	Lat.	Long.	Depth	Ocean	Region	16S	18S
D3M64	DIVA-3 sp. 09	M79/1 604	-3.961	-28.089	5179.8	W Atlantic	Brazil Basin	TBA	TBA
D3M65	DIVA-3 sp. 09	M79/1 604	-3.961	-28.089	5179.8	W Atlantic	Brazil Basin	TBA	TBA
D3M66	DIVA-3 sp. 02	M79/1 604	-3.961	-28.089	5179.8	W Atlantic	Brazil Basin	TBA	TBA
D3M70	DIVA-3 sp. 07	M79/1 604	-3.961	-28.089	5179.8	W Atlantic	Brazil Basin	TBA	TBA
D3M71	DIVA-3 sp. 09	M79/1 605	-3.958	-28.078	5188.5	W Atlantic	Brazil Basin	TBA	TBA
D3M72	DIVA-3 sp. 07	M79/1 605	-3.958	-28.078	5188.5	W Atlantic	Brazil Basin	TBA	TBA
D3M73	DIVA-3 sp. 02	M79/1 605	-3.958	-28.078	5188.5	W Atlantic	Brazil Basin	TBA	TBA
D3M74	DIVA-3 sp. 02	M79/1 605	-3.958	-28.078	5188.5	W Atlantic	Brazil Basin	TBA	TBA
D3M75	DIVA-3 sp. 02	M79/1 605	-3.958	-28.078	5188.5	W Atlantic	Brazil Basin	TBA	TBA
D3M76	DIVA-3 sp. 02	M79/1 605	-3.958	-28.078	5188.5	W Atlantic	Brazil Basin	TBA	TBA
D3M77	DIVA-3 sp. 07	M79/1 605	-3.958	-28.078	5188.5	W Atlantic	Brazil Basin	TBA	TBA
D3M78	DIVA-3 sp. 07	M79/1 605	-3.958	-28.078	5188.5	W Atlantic	Brazil Basin	TBA	TBA
D3M79	DIVA-3 sp. 07	M79/1 605	-3.958	-28.078	5188.5	W Atlantic	Brazil Basin	TBA	TBA
D3M84	DIVA-3 sp. 01	M79/1 554	-26.578	-35.213	4484.7	SW Atlantic	Argentine Basin	TBA	TBA
D3M105	DIVA-3 sp. 01	M79/1 534	-36.010	-49.026	4607.8	SW Atlantic	Argentine Basin	TBA	TBA
D3M111	DIVA-3 sp. 07	M79/1 580	-14.982	-29.942	5131	SW Atlantic	Argentine Basin	TBA	TBA
D3M115	DIVA-3 sp. 07	M79/1 580	-14.982	-29.942	5131	SW Atlantic	Argentine Basin	TBA	TBA
D3M116	DIVA-3 sp. 07b	M79/1 532	-35.986	-49.013	4605.4	SW Atlantic	Argentine Basin	TBA	TBA
D3M118	DIVA-3 sp. 12	M79/1 534	-36.010	-49.026	4607.8	SW Atlantic	Argentine Basin	TBA	TBA
D3M120	DIVA-3 sp. 07b	M79/1 534	-36.010	-49.026	4607.8	SW Atlantic	Argentine Basin	TBA	TBA
D3M122	DIVA-3 sp. 01	M79/1 534	-36.010	-49.026	4607.8	SW Atlantic	Argentine Basin	TBA	TBA
D3M125	DIVA-3 sp. 05	M79/1 554	-26.578	-35.213	4484.7	SW Atlantic	Argentine Basin	TBA	TBA
D3M129	DIVA-3 sp. 09	M79/1 554	-26.578	-35.213	4484.7	SW Atlantic	Argentine Basin	TBA	TBA
D3M130	DIVA-3 sp. 09	M79/1 554	-26.578	-35.213	4484.7	SW Atlantic	Argentine Basin	TBA	TBA
D3M131	DIVA-3 sp. 08	M79/1 561	-35.232	-26.580	4484	SW Atlantic	Argentine Basin	TBA	TBA
D3M132	DIVA-3 sp. 05	M79/1 561	-35.232	-26.580	4484	SW Atlantic	Argentine Basin	TBA	TBA
SMa34	scotti	ANTXX-IV-2 039-17	-64.480	2.878	2152	S Ocean	Lazarev Sea	KC715769	NA
SMa27	matildae	ANTXX-IV-2 039-17	-64.480	2.878	2152	S Ocean	Lazarev Sea	KC715764	NA
SMa28	matildae	ANTXX-IV-2 039-17	-64.480	2.878	2152	S Ocean	Lazarev Sea	KC715765	NA
SMa29	matildae	ANTXX-IV-2 039-17	-64.480	2.878	2152	S Ocean	Lazarev Sea	TBA	NA
SMa66c	matildae	ANTXX-IV-2 039-17	-64.480	2.878	2152	S Ocean	Lazarev Sea	KC715780	NA
BMa10	roaldi	BIO04-EBS-3A	-74.398	-104.632	504	S Ocean	Amundsen Sea	JX260339	NA
BMa14	roaldi	BIO04-EBS-1A	-74.360	-104.746	1414	S Ocean	Amundsen Sea	JX260338	JX260351
BMa15	roaldi	BIO04-EBS-1A	-74.360	-104.746	1414	S Ocean	Amundsen Sea	JX260337	JX260350
BMa16	roaldi	BIO04-EBS-1A	-74.360	-104.746	1414	S Ocean	Amundsen Sea	JX260336	JX260349
NA	sp. 3 MR-2008	NA	NA	NA	NA	S Ocean	NA	NA	EU414442
NA	sp. 1-JW-2004	NA	NA	NA	NA	S Ocean	NA	NA	AY461476
NA	sp. 2-JW-2004	NA	NA	NA	NA	S Ocean	NA	NA	AY461477
IMacro2	subinermis	M85/3 1144	67.868	-23.696	1281	N Atlantic	Denmark Strait	TBA	TBA
IMacro3	subinermis	M85/3 1148	67.847	-23.696	1248.8	N Atlantic	Denmark Strait	TBA	TBA
IMacro4	subinermis	M85/3 1148	67.847	-23.696	1248.8	N Atlantic	Denmark Strait	TBA	TBA
IMacro5	subinermis	M85/3 1149	67.843	-23.698	1246	N Atlantic	Denmark Strait	TBA	TBA
IMacro6	subinermis	M85/3 1149	67.843	-23.698	1246	N Atlantic	Denmark Strait	TBA	TBA
IMacro7	subinermis	M85/3 1149	67.843	-23.698	1246	N Atlantic	Denmark Strait	TBA	TBA
IMacro9	subinermis	M85/3 1155	69.115	-9.912	2203.8	N Atlantic	Norwegian Basin	TBA	TBA

Field ID	species	Station	Lat.	Long.	Depth	Ocean	Region	16S	18S
IMacro10	subinermis	M85/3 1155	69.115	-9.912	2203.8	N Atlantic	Norwegian Basin	TBA	TBA
IMacro11	subinermis	M85/3 1017	62.931	-20.774	891.7	N Atlantic	Iceland Basin	TBA	TBA
IMacro17	subinermis	M85/3 1006	62.552	-23.389	1386.8	N Atlantic	Iceland Basin	TBA	TBA
IMacro20	subinermis	M85/3 1010	62.552	-20.395	1384.8	N Atlantic	Iceland Basin	TBA	TBA
IMacro21	subinermis	M85/3 1017	62.931	-20.774	891.7	N Atlantic	Iceland Basin	TBA	TBA
IMacro23	subinermis	M85/3 1017	62.931	-20.774	891.7	N Atlantic	Iceland Basin	TBA	TBA
IMacro24	subinermis	M85/3 1017	62.931	-20.774	891.7	N Atlantic	Iceland Basin	TBA	TBA
IMacro25	subinermis	M85/3 1017	62.931	-20.774	891.7	N Atlantic	Iceland Basin	TBA	TBA
IMacro27	subinermis	M85/3 1149	67.843	-23.698	1246	N Atlantic	Denmark Strait	TBA	TBA
IMacro28	subinermis	M85/3 1017	62.931	-20.774	891.7	N Atlantic	Iceland Basin	TBA	TBA
IMacro29	subinermis	M85/3 1017	62.931	-20.774	891.7	N Atlantic	Iceland Basin	TBA	TBA
IMacro30	subinermis	M85/3 1155	69.115	-9.912	2203.8	N Atlantic	Norwegian Basin	TBA	TBA
IMacro31	subinermis	M85/3 1184	67.644	-12.162	1819.3	N Atlantic	Norwegian Basin	TBA	TBA
IMacro32	subinermis	M85/3 1194	67.078	-13.055	1573.5	N Atlantic	Norwegian Sea	TBA	TBA
IMacro33	subinermis	M85/3 989	61.711	-19.549	1912.3	N Atlantic	Iceland Basin	TBA	TBA
IMacro34	subinermis	M85/3 989	61.711	-19.549	1912.3	N Atlantic	Iceland Basin	TBA	TBA
IMacro35	subinermis	M85/3 1191	67.079	-13.064	1574.7	N Atlantic	Norwegian Sea	TBA	TBA
IMacro36	subinermis	M85/3 1191	67.079	-13.064	1574.7	N Atlantic	Norwegian Sea	TBA	TBA
IMacro37	subinermis	M85/3 1191	67.079	-13.064	1574.7	N Atlantic	Norwegian Sea	TBA	TBA
IMacro38	subinermis	M85/3 1191	67.079	-13.064	1574.7	N Atlantic	Norwegian Sea	TBA	TBA
IMacro40	subinermis	M85/3 1155	69.115	-9.912	2203.8	N Atlantic	Norwegian Basin	TBA	TBA
IMacro41	subinermis	M85/3 1196	67.097	-13.007	1612	N Atlantic	Norwegian Sea	TBA	TBA
IMacro42	subinermis	M85/3 1196	67.097	-13.007	1612	N Atlantic	Norwegian Sea	TBA	TBA
IMacro44	subinermis	M85/3 1196	67.097	-13.007	1612	N Atlantic	Norwegian Sea	TBA	TBA
IMacro51	subinermis	M85/3 1155	69.115	-9.912	2203.8	N Atlantic	Norwegian Basin	TBA	TBA
IMacro52	subinermis	M85/3 1155	69.115	-9.912	2203.8	N Atlantic	Norwegian Basin	TBA	TBA
IMacro53	subinermis	M85/3 1155	69.115	-9.912	2203.8	N Atlantic	Norwegian Basin	TBA	TBA
IMacro55	subinermis	M85/3 1155	69.115	-9.912	2203.8	N Atlantic	Norwegian Basin	TBA	TBA
IMacro57	subinermis	M85/3 1155	69.115	-9.912	2203.8	N Atlantic	Norwegian Basin	TBA	TBA
IMacro60	subinermis	M85/3 1010	62.552	-20.395	1384.8	N Atlantic	Iceland Basin	TBA	TBA
IMacro61	subinermis	M85/3 1191	67.079	-13.064	1574.7	N Atlantic	Norwegian Sea	TBA	TBA

Author contributions

This study was designed and conducted by myself. The manuscript was written by myself. This research benefitted from uncountable discussions with G.D.F. Wilson. New material was collected during the ANDEEP, BIOICE, DIVA-3, IceAGE and KuramBio expeditions organized by A. Brandt (ANDEEP, KuramBIO), J. Svavarsson (BIOICE), S. Brix, (IceAGE) and P. Marínez Arbizu (DIVA-3). I contributed during field work in the DIVA-3, IceAGE and KuramBio cruises.

Chapter 8

General Discussion

In this thesis, I investigated potential reasons for the uniform morphology of the deep-sea isopod family Macrostylidae Hansen, 1916, explored the phylogenetic origin of this family as well as its colonization history. Morphological character analyses led to the discovery of an aberrant morphology in the males of some macrostylid species (Chapter 2). I found that the otherwise high morphological similarity between species can be explained by convergent evolution (Chapter 7). Though the lack of morphological diversity might indicate a young age, high genetic divergence (Chapter 4) suggests that Macrostylidae is of a considerable age.

The description of a new isopod family (Urstylidae; Chapter 5) shed new light on the origin of macrostylids. Unravelling the phylogenetic position of Macrostylidae amongst the Janiroidea, I found urstylids to be the sister taxon of macrostylids. Many of the urstylid characters are plesiomorphic, thus they constitute a link between the highly derived Macrostylidae and more basally derived taxa, such as Thambematidae.

Finally, analyzing the relationships of Macrostylidae, the origin and colonization history of shallow-water macrostylids was revealed (Chapters 3, 7). An abyssal origin is likely for Macrostylidae in general and several independent offshore-onshore migrations were the best and most parsimonious explanation for the disjunct findings of macrostylids in various continental shelves.

The “uniform” morphology of Macrostylidae and its contrast in DNA data

I studied interspecific variation in macrostylid characters (Chapters 2–4, 6) to unravel the evolutionary background of their morphological uniformity. Based on the variation of these characters, I

established homology hypotheses (Chapters 5–6), and reconstructed the evolutionary history of this group (Chapter 7).

Since fossils are unavailable for deep-sea isopods, a comparison between geographic distribution of the species and their relationships was conducted to rule out one of the alternative possibilities that macrostylids were either not as old as previously thought and hence had no time for diversification, or that macrostylids have retained a high morphological similarity despite an old age.

A lack of taxonomic effort spent on this group was disregarded as a potential third explanation. It is unlikely since other janiroid taxa of comparable or even younger age, where species diversity and distribution have gained similar attention (roughly counted in terms of taxonomic publications), still comprise several well defined genera, for instance the Nannoniscidae Hansen, 1916, and Janirellidae Menzies, 1956 (see Worms 2013).

Sexual dimorphism in Macrostylidae

Initially, the two new species *Macrostylis papillata* Riehl, Wilson and Hessler, 2012 and *M. dorsaetosa* Riehl, Wilson and Hessler, 2012 were described (Chapter 2). Both species turned out to be key species to the understanding of macrostylid morphology and evolution.

Analyses of stage development in *M. dorsaetosa* led to the discovery of a remarkable sexual dimorphism (SD; Riehl *et al.* 2012). In some species of the family dramatic changes occur during the adult molt of the males. This metamorphosis includes a change in the size, and shape of the antennula, posterior walking legs and uropods, but also the body shape in general becomes significantly more slender (Riehl *et al.* 2012). This phenomenon is only weakly expressed in *M. dorsaetosa* and thus it was possible to allocate conspecific

males and females without the help of DNA evidence. However, it was hypothesized that this phenomenon may be much more “extreme” in other species and could be amongst the reasons why for almost 50% of the species described for this family, only one gender was known. Examples of such cases include *Macrostylis longipedis* Brandt, 2004, *M. urceolata* Mezhov, 1989, and *M. viriosa* Mezhov, 1999. Significant taxonomic problems due to sexual dimorphism have become apparent as well in other groups of animals (Sibley 1957; Kelley 1993; Johnson *et al.* 2009; Brökeland 2010) and in chapter 7, I could support this hypothesis by finding *M. longipes* Hansen, 1916 a synonym of *M. subinermis* Hansen, 1916; and several other species showing extended SD could be collected during recent expeditions and safely allocated using DNA barcoding (Riehl *et al.* under review; Hajibabaei *et al.* 2007).

These findings also have important implications for future taxonomic practice in general. It has become clear how copulatory males can be identified as such: the presence of several aesthetascs on both terminal and subterminal antennula articles is the main characteristic, not only a size increase in the antennula. The latter may to some extent occur in subadult or juvenile males as well (Riehl and Kaiser 2012; Riehl *et al.* 2012). The length of the first pleopods in relation to the length of the second pleopods is on the contrary not necessarily illuminating since their arrangement varies strongly between species. To safely deduce adulthood of a specimen, more information has to be considered, for instance regarding the development and arrangement of the distal setae and lobes on the first pleopod (Riehl and Brandt in prep.).

Due to this metamorphosis, taxonomic allocation based on morphology alone is impossible in some species, especially since subadult individuals are generally very similar between the species. The

combination of morphological and molecular techniques has proven helpful for dealing with sexual and ontogenetic polymorphisms, for example in tanaids (Larsen 2001) and is encouraged to become commonplace in deep-sea isopods taxonomy (see Appendix 3).

Sexual variation in macrostyloid adults may strongly exceed interspecific female variation. It seems obvious that in a group with high similarity, the aberrant male morphology should be explored and used for taxonomy and phylogenetic studies. However, since macrostyloid males tend to be rare in the samples compared to females (T. Riehl, pers. observation), and for most of the previously described species, only one sex has been described, we are far from using this source of phylogenetic information to its whole extend.

It might be hence also required to change taxonomic practice regarding male singletons. When conspecific females are unknown and DNA data are unavailable male morphology holds limited information both for taxonomy and phylogeny. The purely morphological description of single male specimens as new species, for example, is thus explicitly discouraged. That is even more so in case of subadult males which are sometimes different from both juveniles and copulatory males as well as from females (compare Riehl and Kaiser 2012; Riehl *et al.* 2012).

Since there are no DNA data available for many species of the family yet, conspecificity for other separately described species could not be tested so far. SD may in cases hinder taxonomic allocation of conspecifics, but on the other hand this phenomenon is a source of morphological (and generally biological (Butler *et al.* 2007)) diversity and thus I integrated SD into further discussion about understanding macrostyloid evolution.

First, SD constitutes variability that can be coded as morphological characters. I included mul-

tuple SD character in the character database to apply this knowledge in phylogenetic studies (Chapters 5, 7). The differences expressed by some macrostylid males have been hypothesized to be homologous (Chapter 6) and amongst those traits characterizing distinct lineages within Macrostylidae. They may thus be synapomorphies for *Macrostylis sensu stricto*, yet due to incongruence between the two molecular and the morphological datasets (Chapter 7), uncertainty remains and currently no robust classificatory changes can be achieved (Riehl and Brandt in prep., in prep.b). Nevertheless, this variability exists and the phylogenetic signal it carries, though not unambiguously, has been largely supported by molecular data (Chapter 7).

Second, I discussed the potential importance of SD for macrostylid evolution, especially trying to consider the environmental peculiarities of the deep sea. I found sexual selection to be the most convincing explanation for the evolution of the thickened antennulae with a dramatically increased number and size of the olfactory setae (aesthetascs) that can be found in some macrostylids. Such increased size of the olfactory organs are apparent in many arthropods (Schafer and Sanchez 1976; Martens 1987; Jourdan *et al.* 1995; Koh *et al.* 1995; Fernandes *et al.* 2004) and can be attributed to search for and location of conspecific receptive females. Competition in search for mating partners is a driving force in the evolution of SD in terrestrial isopods (Lefebvre *et al.* 2000). Even though behavioral observations on deep-sea isopods are scarce (Hessler and Strömberg 1989), it is not difficult to imagine that in a nutrient-limited environment with low animal densities (Sanders and Hessler 1969), competition in mate finding may be prevalent. Food source partitioning as an alternative explanation for the evolution of sexual dimorphism (Slatkin 1984; Shine 1989) in Macrostylidae can be neglected since male and female mandibles

show no considerable variation (T. Riehl, unpubl. data). However, testing the cause of such sexual dimorphisms in deep-sea isopods may be problematic since more mechanisms than sexual selection may be operating simultaneously (Slatkin 1984; Hedrick and Temeles 1989) and empirical studies may prove difficult to conduct in the remote deep-sea environment.

High genetic divergence

While understanding the morphology of macrostylid sexual dimorphisms and their evolutionary implications were the first attempt for tackling the seeming morphological uniformity of this group, DNA data represented a second approach. The first mitochondrial DNA sequences available for Macrostylidae (Chapters 3–4) contrasted the morphological uniformity and suggested rather high divergences between the species (Riehl and Brandt 2013). Distances between species in 16S rRNA reached from 23.3–31.1% (uncorrected *p*-distances), and these values are comparably high to those found between genera and even families in other Janiroidea (Brix *et al.* in press, 2011; Raupach and Wägele 2006; Brökeland and Raupach 2008; Osborn 2009).

These data show that Macrostylidae, similar to for example Munnopsidae, are old and genetically divergent. The lack of recognized diversity above species level in the current system may thus reflect the high number of complex synapomorphies (Chapters 5–7) but also convergent evolution that is possibly related to an endobenthic lifestyle (Hessler and Strömberg 1989; Wägele 1989).

Potential explanations for a morphological uniformity

Despite the discovery of remarkable sexual dimor-

phisms in some macrostylids (that are complex and thus likely to be homologous), and high genetic divergence, both pointing to a significant evolutionary history in Macrostylidae, the overall morphological variability in macrostylids can still be considered low (Chapter 7). The phylogenetic assessment of macrostylid morphology is prone to a relatively high degree of conflicting signal and hence the tree based on morphology contains only few robustly supported clades. This finding suggests homoplasy in the dataset that could be explained by evolutionary convergence.

The generally limited environmental variability in the deep sea has been suggested to account for high degrees of similarity in endobenthic deep-sea meiofauna due to similar selective pressures (Giere 2009). Furthermore, environmental constraints from living “under-ground” are thought to cause morphological convergence. Digging through deep-sea sediments may impose selective pressure somewhat similar to what can be observed in stygofauna (Baratti *et al.* 1999) or subterranean environments (Nevo 1979; Lee 1998; Kornobis *et al.* 2011; Pipan and Culver 2012). An endobenthic lifestyle was hypothesized for macrostylids (Thistle and Wilson 1987; Hessler and Strömberg 1989; Wägele 1989; Riehl *et al.* 2014) and may account for a suitable explanation of the macrostylid uniformity.

Similar to observations on other cosmopolitan genera (as well as other taxa) of the deep-sea macrofauna (Hessler and Wilson 1983), frequent occurrence of the preferential habitat across the oceans could be the explanation for their wide distribution (Wilson and Hessler 1987). The inability for macrostylids to migrate fast and over long distances (discussed in Chapter 3), and thus isolation by distance (Wright 1938, 1943; Teske *et al.* 2007) alone may explain the genetic divergence of macrostylid species.

The origin of macrostylids in shallow waters, on the slope and in the abyss

Urstylidae – new hints for the evolution of macrostylid morphology

By reconstructing the evolutionary history of Macrostylidae in their parent superfamily Janiroidea, I investigated the phylogenetic origin of this family. In chapter 5, I described three new species that did not fit into the current isopod classification but showed some superficial similarity with macrostylids. By determining their phylogenetic position amongst Janiroidea, they were found in a position basally to the monotypic Macrostylidae (Riehl *et al.* 2014). Nevertheless, they were sufficiently different to justify the erection of a distinct new family Urstylidae Riehl, Hessler, and Malyutina, 2014.

The discovery of Urstylidae allowed a new perspective on macrostylid evolution. A remarkably high number of apomorphies have been found to support Macrostylidae, indicating that this family is highly derived (Riehl and Brandt in prep.; Riehl 2012, 2013; Riehl *et al.* 2014) which may further blur the view on distinct macrostylid subgroups (discussed above).

Urstylidae show numerous plesiomorphic traits, such as the free first pleonite or a low degree of specialization in their tagma and appendages. Remarkably, the sensory organs present on the pleotelson of *Urstylis solicipia* Riehl, Wilson and Hessler, 2014 and *U. zapiola* Riehl, Wilson and Hessler, 2014 may represent distinct evolutionary stages that ultimately led to the paired organ present in the macrostylid pleotelson and commonly interpreted as statocyst. These and other characters link the derived macrostylid morphology to that found

in related groups of the Janiroidea. The apparent plesiomorphic states expressed in several urstylid characters may provoke using the term “living fossil” in connection with the Urstylidae.

Evolution of deep-sea Isopoda and the origin of Macrostylidae

The hypothesized scenario of an onshore-diversification, subsequent deep-sea invasion and finally extinction (Jacobs and Lindberg 1998) is contradicted in the light of macrostylid distribution patterns and phylogeny. The origin of macrostylids was dated to before the Permo-Triassic boundary (Lins *et al.* 2012). The current core distribution of this group is the abyssal (Chapter 7, Fig.1) and *in-situ* diversification is apparent in the light of high molecular divergence (Chapter 4) thus showing a parallel to previous findings in Munnopsidae (Hessler and Thistle 1975; Thistle and Hessler 1976) and Desmosomatidae (Hessler 1970). The discovery and phylogenetic classification of the genus *Urstylis* Riehl, Wilson and Malyutina, 2014 (Chapter 5) as the sister taxon to Macrostylidae solidifies the deep-sea route of the macrostylid clade since Urstylidae seems to be exclusively abyssal (Chapter 7).

As previously hypothesized for other deep-sea Asellota as well, macrostylids seem to represent an ancient clade with a Paleozoic origin (Wilson 1999). It is evident from ostracod and foraminiferan fossil records that great faunal change took place at the Cretaceous-Paleogene boundary (Steineck and Thomas 1996; Alegret *et al.* 2003; Alegret and Thomas 2007). The generality of an uninhabitable deep sea during anoxia/dysoxia events of the Cretaceous and afterwards, however, might thus be put in doubt even further. Similar limitations of the anoxia-related attempt to explain abyssal biodiversity have been found for echinoids

as well (Smith and Stockley 2005).

Shelf colonization

In this thesis, I was able to show that shallow-water representatives of Macrostylidae are the result of multiple independent emergence events (Chapter 7). Similar observations have been made, for example with the munnopsid genera *Echinozone* Sars, 1897 and *Baeonectes* Wilson, 1982 (Thistle and Hessler 1976; Wilson 1999) but also beyond isopods (Brandt 1992; Berkman *et al.* 2004; Pante *et al.* 2012).

These findings show that abyssal, bathyal and sublittoral faunas are not strictly exclusive, but that rather repeatedly and independently, the slopes and shelves have been colonized from the deep (Chapter 7). Very likely, emergence and submergence are continuously and simultaneously ongoing processes (Brandt 2005) that may have played an important role for the survival of the faunas both of the deep sea as well as the continental shelves during periods of unfavorable climatic conditions. However, only emergence and no reversal could be substantiated in the ancestral state reconstruction (Chapter 7).

On the Antarctic shelf and slope, diachronous ice-sheet extensions are thought to have had tremendous effects on the fauna of the Southern Ocean (Riehl and Kaiser 2012; Chapter 3) and helped to generate diversity on the Antarctic shelf (Clarke *et al.* 1992), but also contributed to a specialized slope fauna (Kaiser *et al.* 2011); and similarly, expansions and retreats of anoxic zones in the deep sea might have led to allopatric speciation of faunal elements there (White 1988; Rogers 2000) rather than completely eradicating the fauna.

During the anoxic events of the Cretaceous period, thus both the oxygenated shelf as well as abyssal regions may have acted as refuges for

fauna highly impacted by oxygen minimum zones on the slopes and deeper shelf areas.

Macrostylid classification

Across the phylogenetic datasets, incongruence does currently not allow for a complete revision of the family. Within the macrostylid tree of life, several clades could be identified in mitochondrial (16S) and nuclear DNA (18S) as well as morphological characters (Riehl and Brandt in prep., in prep.b), however, all but one were contradicted or found paraphyletic in at least one of the three datasets (Chapter 7).

The only robustly supported clade is characterized by length (and other) reductions instead of elongations. Sexual dimorphisms are limited in these species to few subtle variations in body size, antennula width and pleotelson shape. *Macrostylis abyssicola* Hansen, 1916 was the first species described from this clade. The sharp sternal keel on the fossosome, and a medioventral orientation of the anterior four pairs of coxae through ventrally produced lateral tergal margins are synapomorphies. The species of this group are further recognized by small and reduced (in terms of article numbers) antennulae and antennae, minimally (if at all) produces posterolateral projections of the posterior tergites and hypomorphosis in the seventh pereonite and its appendages.

Three species nested within the larger “Abyssicola” group have been found to constitute a robust subclade that can be identified by the absence of ischium through dactylus of the seventh pereopods: *Macrostylis minuta* Menzies, 1962 as well as two undescribed species collected during the DIVA 3 cruise in the tropical West Atlantic.

Strong sexual dimorphisms, amongst other characters, characterize a second clade retrieved

from all three datasets. This clade includes *Macrostylis spinifera* Sars, 1864, the type species of the family. Consequently, the possibility to restrict and newly define the genus *Macrostylis* Sars, 1864 could be given, but currently homoplasy leads to incongruence in taxon composition across datasets.

However, within this clade, both distinctly different shapes of the first male pleopod are represented. Without much knowledge about macrostylid mating behavior it can only be guessed that such morphological difference may imply fundamental differences in the function of these copulatory appendages.

For classificatory changes, though, more taxonomic studies are required to determine the character states of several species for which adult males are not yet studied, including *M. spinifera*. Besides increased morphological effort, examination of additional molecular sequence data might help clarifying the picture.

Conclusions and Outlook

Morphological and molecular data were gathered that help understanding the evolutionary history of Macrostylidae, a cosmopolitan family of asellote isopods. The new taxonomic, systematic and phylogenetic results on macrostylids presented in this thesis revealed remarkable sexual dimorphisms and that deep-sea and continental-shelf faunas are interconnected (Riehl and Brandt in prep.). The macrostylid ancestor likely was already a deep-sea species (Riehl *et al.* 2014). Its descendants colonized all oceans and depths, including several independent colonisations of the continental shelves (Riehl and Brandt in prep.). Using the macrostylids as a model, I could thus show that the abyss represents a source of biodiversity for the shallower depth zones.

The profound uniformity met in the macrostyloid morphology may be a result of convergent evolution and a consequence of environmental constraints (digging lifestyle) and stabilizing selection.

Future research in macrostyloid isopods may focus on “filling the gaps” in the knowledge of sexual dimorphisms since this might hold the key for understanding macrostyloid relationships. Detailed descriptions of both female and male specimens (both in adult stage) should be the standard procedure. The combined application of morphological and molecular information allows for reciprocal illumination (Hennig 1950) in this context.

The phylogeny of the Macrostylidae and even more of the whole Janiroidea is still in large parts unresolved. Exploring the phylogenetic position of several taxa *insertae sedis*, such as *Xostylus* Menzies, 1962, may hold important ramifications for understanding deep-sea isopod evolution. Addressing this question with improved morphological and molecular datasets might as well help tackling the question of the age of the deep-sea isopods. To realize this, sampling protocols suitable for DNA extraction (see Appendix 3) should be consistently applied.

References

Alegret, L., Molina, E. and Thomas, E. (2003) Benthic foraminiferal turnover across the Cretaceous/Paleogene boundary at Agost (southeastern Spain): paleoenvironmental inferences. *Marine Micropaleontology*, 48(3), 251–279.

Alegret, L. and Thomas, E. (2007) Deep-Sea environments across the Cretaceous/Paleogene boundary in the eastern South Atlantic Ocean (ODP Leg 208, Walvis Ridge). *Marine Micropaleontology*, 64(1–2), 1–17.

Baratti, M., Bazzicalupo, M., De Filippo, C. and Massana, G. (1999) Detection of genetic variability in stygobitic isopods using rapid markers. *Crustaceana*, 72(7), 625–634.

Berkman, P. A., Cattaneo-Vietti, R., Chiantore, M. and

Howard-Williams, C. (2004) Polar emergence and the influence of increased sea-ice extent on the Cenozoic biogeography of pectinid molluscs in Antarctic coastal areas. *Deep Sea Research Part II: Topical Studies in Oceanography*, 51(14–16), 1839–1855 (ANDEEP (Antarctic benthic DEEP-sea) biodiversity: colonization history and recent community patterns: a tribute to Howard L. Sanders).

Brandt, A. (1992) Origin of Antarctic Isopoda (Crustacea, Malacostraca). *Marine Biology*, 113, 415–423.

Brandt, A. (2004) New deep-sea species of Macrostylidae (Asellota: Isopoda: Malacostraca) from the Angola Basin off Namibia, South West Africa. *Zootaxa*, 448, 1–35.

Brandt, A. (2005) Evolution of Antarctic Biodiversity in the Context of the Past: The Importance of the Southern Ocean Deep Sea. *Antarctic Science*, 17(04), 509–521.

Brix, S., Leese, F., Riehl, T. and Kihara, T.-C. (in press) A new genus and new species of Desmosomatidae Sars, 1897 (Isopoda) from the east South-Atlantic abyss described by means of integrative taxonomy. *Marine Biodiversity*, .

Brix, S., Riehl, T. and Leese, F. (2011) First genetic data for *Haploniscus rostratus* and *Haploniscus unicornis* from neighbouring deep-sea basins in the South Atlantic. *Zootaxa*, 2838, 79–84.

Brökeland, W. (2010) Description of four new species from the *Haploniscus unicornis* Menzies, 1956 complex (Isopoda: Asellota: Haploniscidae). *Zootaxa*, 2536, 1–35.

Brökeland, W. and Raupach, M. J. (2008) A species complex within the isopod genus *Haploniscus* (Crustacea: Malacostraca: Peracarida) from the Southern Ocean deep sea: a morphological and molecular approach. *Zoological Journal of the Linnean Society*, 152(4), 655–706.

Butler, M. A., Sawyer, S. A. and Losos, J. B. (2007) Sexual dimorphism and adaptive radiation in *Anolis* lizards. *Nature*, 447(7141), 202–205.

Clarke, A., Crame, J. A., Stromberg, J.-O. and Barker, P. F. (1992) The Southern Ocean Benthic Fauna and Climate Change: A Historical Perspective [and Discussion]. *Philosophical Transactions of the Royal Society of London. Series B: Biological Sciences*, 338(1285), 299–309.

Fernandes, F. de F., Pimenta, P. F. P. and Linardi, P. M. (2004) Antennal sensilla of the new world screwworm fly, *Cochliomyia hominivorax* (Diptera: Calliphoridae). *Journal of Medical Entomology*, 41(4), 545–551.

Giere, O. (2009) Evolutionary and Phylogenetic Effects in Meiobenthology. *Meiobenthology*. pp 235–241. Berlin, Heidelberg: Springer. ISBN 978-3-540-68657-6, 978-3-540-68661-3.

Hajibabaei, M., Singer, G. A. C., Hebert, P. D. N. and Hickey, D. A. (2007) DNA barcoding: how it complements taxonomy,

- molecular phylogenetics and population genetics. *Trends in Genetics*, 23(4), 167–172.
- Hansen, H. J. (1916) Crustacea Malacostraca: The order Isopoda. *Danish Ingolf Expedition*, 3(5), 1–262.
- Hedrick, A. V. and Temeles, E. J. (1989) The evolution of sexual dimorphism in animals: Hypotheses and tests. *Trends in Ecology & Evolution*, 4(5), 136–138.
- Hennig, W. (1950) *Grundzüge einer Theorie der phylogenetischen Systematik*. Berlin: Deutscher Zentralverlag.
- Hessler, R. R. (1970) *The Desmosomatidae (Isopoda, Asellota) of the Gay Head-Bermuda Transect* [online]. (Arrhebus, G. O. S., Cox, C. S., Fager, E. W., Hand, C. H., Newberry, T., and Schaefer, M. B., Eds.) Berkeley, Los Angeles, London: University of California Press. Available from: <http://escholarship.org/uc/item/1mn198vx>.
- Hessler, R. R. and Strömberg, J. O. (1989) Behavior of janiroidean isopods (Asellota), with special reference to deep sea genera. *Sarsia*, 74(3), 145–159.
- Hessler, R. R. and Thistle, D. (1975) On the place of origin of deep-sea isopods. *Marine Biology*, 32(2), 155–165.
- Hessler, R. R. and Wilson, G. D. F. (1983) The origin and biogeography of malacostracan crustaceans in the deep sea. In: Sims, R. W., Price, J. H., and Whalley, P. E. S. (Eds.) *Evolution, time, and space: the emergence of the biosphere*. pp 227–254. London: Academic Press. (Systematics Association Special Publication; 23).
- Jacobs, D. K. and Lindberg, D. R. (1998) Oxygen and evolutionary patterns in the sea: Onshore/offshore trends and recent recruitment of deep-sea faunas. *Proceedings of the National Academy of Sciences*, 95(16), 9396–9401.
- Johnson, G. D., Paxton, J. R., Sutton, T. T., Satoh, T. P., Sado, T., Nishida, M. and Miya, M. (2009) Deep-sea mystery solved: astonishing larval transformations and extreme sexual dimorphism unite three fish families. *Biology Letters*, 5(2), 235–239.
- Jourdan, H., Barbier, R., Bernard, J. and Ferran, A. (1995) Antennal sensilla and sexual dimorphism of the adult ladybird beetle *Semiadalia undecimnotata* Schn. (Coleoptera: Coccinellidae). *International Journal of Insect Morphology and Embryology*, 24(3), 307–322.
- Kaiser, S., Griffiths, H. J., Barnes, D. K. A., Brandão, S. N., Brandt, A. and O'Brien, P. E. (2011) Is there a distinct continental slope fauna in the Antarctic? *Deep Sea Research Part II: Topical Studies in Oceanography*, 58(1-2), 91–104.
- Kelley, J. (1993) Taxonomic implications of sexual dimorphism in *Lufengpithecus*. *Species, Species Concepts, and Primate Evolution*. WH Kimbel and LB Martin., pp 429–458. New York: Plenum Press.
- Koh, Y. H., Park, K. C. and Boo, K. S. (1995) Antennal sensilla in adult *Helicoverpa assulta* (Lepidoptera: Noctuidae): morphology, distribution, and ultrastructure. *Annals of the Entomological Society of America*, 88(4), 519–530.
- Kornobis, E., Pálsson, S., Sidorov, D. A., Holsinger, J. R. and Kristjánsson, B. K. (2011) Molecular taxonomy and phylogenetic affinities of two groundwater amphipods, *Crangonyx islandicus* and *Crymostygius thingvallensis*, endemic to Iceland. *Molecular Phylogenetics and Evolution*, 58(3), 527–539.
- Larsen, K. (2001) Morphological and molecular investigation of polymorphism and cryptic species in tanaid crustaceans: implications for tanaid systematics and biodiversity estimates. *Zoological Journal of the Linnean Society*, 131(3), 353–379.
- Lee, M. S. Y. (1998) Convergent evolution and character correlation in burrowing reptiles: towards a resolution of squamate relationships. *Biological Journal of the Linnean Society*, 65(4), 369–453.
- Lefebvre, F., Limousin, M. and Caubet, Y. (2000) Sexual dimorphism in the antennae of terrestrial isopods: a result of male contests or scramble competition? *Canadian Journal of Zoology*, 78(11), 1987–1993.
- Lins, L. S. F., Ho, S. Y. W., Wilson, G. D. F. and Lo, N. (2012) Evidence for Permo-Triassic colonization of the deep sea by isopods. *Biology Letters*, 8(6), 979–982.
- Martens, K. (1987) Homology and functional morphology of the sexual dimorphism in the antenna of *Sclerocypris* Sars, 1924 (Crustacea, Ostracoda, Megalocypridinae). *Bijdragen tot de Dierkunde*, 57(2), 183–190.
- Menzies, R. J. (1956) New abyssal tropical Atlantic isopods with observations on their biology. *American Museum Novitates*, 1798, 1–16.
- Menzies, R. J. (1962) The isopods of abyssal depths in the Atlantic Ocean. In: Barnard, J. L., Menzies, R. J., and Bacescu, M. C. (Eds.) *Abyssal Crustacea*. pp 79–206. New York: Columbia University Press. (Vema Research Series).
- Mezhov, B. V. (1989) Two new species of *Macrostylis* (Isopoda, Macrostylidae) from the trenches of the Pacific Ocean and comments on the morphology of *M. galathea*. *Zoologicheskii Zhurnal*, 68(8), 33–40.
- Mezhov, B. V. (1999) Four new species of the genus *Macrostylis* (Crustacea, Isopoda, Macrostylidae) from the Atlantic Ocean abyssal zone. *Zoologicheskii Zhurnal*, 78(12), 1417–1423.
- Nevo, E. (1979) Adaptive convergence and divergence of subterranean mammals. *Annual Review of Ecology and Systematics*, 10(1), 269–308.
- Osborn, K. J. (2009) Relationships within the Munnopsidae (Crustacea, Isopoda, Asellota) based on three genes. *Zoologica*

Pante, E., France, S. C., Couloux, A., Cruaud, C., McFadden, C. S., Samadi, S. and Watling, L. (2012) Deep-sea origin and in-situ diversification of chrysogorgiid octocorals. *PLoS ONE*, 7(6), e38357.

Pipán, T. and Culver, D. C. (2012) Convergence and divergence in the subterranean realm: a reassessment. *Biological Journal of the Linnean Society*, 107(1), 1–14.

Raupach, M. J. and Wägele, J.-W. (2006) Distinguishing cryptic species in Antarctic Asellota (Crustacea: Isopoda)—a preliminary study of mitochondrial DNA in *Acanthaspidia drygalskii*. *Antarctic Science*, 18(02), 191–198.

Riehl, T. (2012) On the phylogenetic position of Macrostylidae in the Janiroidea. Oral paper at the 13th International Deep-Sea Biology Symposium, Wellington, New Zealand.

Riehl, T. (2013) Filling in the phylogenetic gaps of deep-sea isopods. Oral paper at the BioSyst.EU - Global Systematics!, Vienna, Austria.

Riehl, T. and Brandt, A. (in prep.) A comparative review of the morphology of Macrostylidae (Isopoda) from the phylogenetic perspective. Chapter 6.

Riehl, T. and Brandt, A. (in prep.) Multiple colonization of the continental shelves by deep-sea fauna. Insights to the phylogeny of Macrostylidae (Isopoda) from mitochondrial and nuclear DNA as well as morphology. Chapter 7.

Riehl, T. and Brandt, A. (2013) Southern Ocean Macrostylidae reviewed with a key to the species and new descriptions from Maud Rise. *Zootaxa*, 3692(1), 160–203.

Riehl, T., Brenke, N., Brix, S., Driskell, A., Kaiser, S. and Brandt, A. (under review) Field and laboratory methods for DNA barcoding and molecular-systematic studies on deep-sea isopod crustaceans. *Polish Polar Research*.

Riehl, T. and Kaiser, S. (2012) Conquered from the deep sea? A new deep-sea isopod species from the Antarctic shelf shows pattern of recent colonization. *PLoS ONE*, 7(11), e49354.

Riehl, T., Wilson, G. D. F. and Hessler, R. R. (2012) New Macrostylidae Hansen, 1916 (Crustacea: Isopoda) from the Gay Head-Bermuda transect with special consideration of sexual dimorphism. *Zootaxa*, 3277, 1–26.

Riehl, T., Wilson, G. D. F. and Malyutina, M. V. (2014) Urstylidae – A new family of deep-sea isopods and its phylogenetic implications. *Zoological Journal of the Linnean Society*, 170, 245–296.

Rogers, A. D. (2000) The role of the oceanic oxygen minima in generating biodiversity in the deep sea. *Deep Sea Research Part II: Topical Studies in Oceanography*, 47(1–2), 119–148.

Sanders, H. L. and Hessler, R. R. (1969) Ecology of the deep-

sea benthos. *Science*, 163(874), 1419.

Sars, G. O. (1864) Om en anomal Gruppe af Isopoder. *Forhandlinger Videnskaps-Selskapet, Anar 1863 in Christiania*, 205–221.

Sars, G. O. (1897) On some additional Crustacea from the Caspian Sea. *Annales du Musée Zoologique Academie Imperiale des Sciences St. Petersburg*, 2, 273–305.

Schafer, R. and Sanchez, T. V. (1976) The nature and development of sex attractant specificity in cockroaches of the genus *Periplaneta*. I. Sexual dimorphism in the distribution of antennal sense organs in five species. *Journal of Morphology*, 149(2), 139–157.

Shine, R. (1989) Ecological causes for the evolution of sexual dimorphism: a review of the evidence. *Quarterly Review of Biology*, 419–461.

Sibley, C. G. (1957) The evolutionary and taxonomic significance of sexual dimorphism and hybridization in birds. *The Condor*, 59(3), 166–191.

Slatkin, M. (1984) Ecological causes of sexual dimorphism. *Evolution*, 38(3), 622–630.

Smith, A. B. and Stockley, B. (2005) The geological history of deep-sea colonization by echinoids: roles of surface productivity and deep-water ventilation. *Proceedings of the Royal Society B: Biological Sciences*, 272(1565), 865–869.

Steineck, P. L. and Thomas, E. (1996) The latest Paleocene crisis in the deep sea: Ostracode succession at Maud Rise, Southern Ocean. *Geology*, 24(7), 583–586.

Teske, P., Papadopoulos, I., Zardi, G., McQuaid, C., Edkins, M., Griffiths, C. and Barker, N. (2007) Implications of life history for genetic structure and migration rates of southern African coastal invertebrates: planktonic, abbreviated and direct development. *Marine Biology*, 152(3), 697–711.

Thistle, D. and Hessler, R. R. (1976) Origin of a Deep-Sea Family, the Ilyarachnidae (Crustacea: Isopoda). *Systematic Biology*, 25(2), 110–116.

Thistle, D. and Wilson, G. D. F. (1987) A hydrodynamically modified, abyssal isopod fauna. *Deep-Sea Research. Part A. Oceanographic Research Papers*, 34(1), 73–87.

White, B. N. (1988) Oceanic anoxic events and allopatric speciation in the deep sea. *Biological Oceanography*, 5(4), 243–259.

Wilson, G. D. F. (1982) *Systematics of a species complex in the deep-sea genus Eurycope, with a revision of six previously described species (Crustacea, Isopoda, Eurycopidae)*. Berkley, Los Angeles, London: University of California Press. (Bulletin of the Scripps Institution of Oceanography). ISBN 0-520-0968-9.

Wilson, G. D. F. (1999) Some of the deep-sea fauna is ancient. *Crustaceana*, 72(8), 1019–1030.

Wilson, G. D. F. and Hessler, R. R. (1987) Speciation in the deep sea. *Annual Reviews in Ecology and Systematics*, 18(1), 185–207.

Worms. *Janiroidea*. In: Schotte, M., Boyko, C.B., Bruce, N.L., Poore, G.C.B., Taiti, S., Wilson, G.D.F. (Eds). [online] (2013). Available from: <http://www.marinespecies.org/aphia.php?p=taxdetails&id=155716>. [Accessed 2014-04-04].

Wright, S. (1938) Size of population and breeding structure in relation to evolution. *Science*, 87(2263), 430–2264.

Wright, S. (1943) Isolation by Distance. *Genetics*, 28(2), 114–138.

Wägele, J.-W. (1989) *Evolution und phylogenetisches System der Isopoda: Stand der Forschung und neue Erkenntnisse [Evolution and phylogeny of isopods. New data and the state of affairs]*. Stuttgart: E. Schweizerbart'sche Verlagsbuchhandlung. (Zoologica). ISBN 978-3-510-55026-5.

Appendix 1

Glossary of terms relevant for the morphology of Macrostylidae

Unpublished work.

Remarks

This glossary provides definitions of morphological terms. It is based on Wilson (1989, 2013) (with an emphasis on the Asellota and the asellotan superfamily Janiroidea), McLaughlin (1980), Watling (1989), Wägele (1992), Wetzler and Brusca (1997) and Garm (2004) (Isopoda and Crustacea) as well as previous work on Macrostylidae (Wolff 1956, 1962; Riehl and Brandt 2010, 2013; Riehl and Kaiser 2012; Riehl *et al.* 2012). Previous definitions were updated and/or modified according to special macrostylid characters.

Abdomen: see pleotelson.

Accessory seta is a usually slender and long seta articulating proximally to the claws on pereopod dactyli. It may be covered with fringe-like microstructures. [Synonymy: fringe-like sensilla sensu Riehl and Brandt (2010)].

Aesthetascs are specialized sensory setae found in macrostylids on the antennula. A macrostylid aesthetasc is usually longer than the individual antennula articles and tubular and has a thin cuticle. In many species of this family, medially along the aesthetascs, a “concertina-like” constriction has been observed. Supposedly, aesthetascs have chemosensory function (Wägele 1992) and play a role in mate finding. This can be assumed because there are usually more aesthetascs in adult male specimens than in females or immature males (Riehl *et al.* 2012). [Synonymy: sensory filament, see also: seta].

Antenna is the second paired cephalic appendage. In Macrostylidae, it consists of three short and two long podomeres as well as a flagellum of variable length. The short three articles are assumed to be homologous to coxa, basis and ischium of the walking legs. The precoxa (Hansen 1893) is absent in Macrostylidae as a result of a reduction (Riehl *et al.* 2014). [Synonymy: antenna II; plural: antennae; see also: antennula].

Antennal scale is the exopod of the crustacean antenna (McLaughlin 1980). It is located on the basis of the appendage (Wägele 1983) and reduced to various degrees across Asellota (Riehl *et al.* 2014). It is absent in Macrostylidae. [Synonymy: scaphocerite; squama].

Antennula is the first of the paired cephalic appendages. It typically consists of three podomeres (Wägele 1983) and a taxon-specific number of additional distal articles comprising the flagellum. The flagellar articles, in macrostylids only the most distal articles, bear aesthetascs. In Macrostylidae, the overall number of antennula articles reported varies from one to five. Length and diameter of articles commonly decrease gradually towards the distal end but there are diversions from this pattern in the mature males of some species. [Synonymy: antenna I, antennule; plural: antennulae; see also: sexual dimorphism].

Article is a limb segment. [Synonymy: podomere; see also: basis, coxa, dactylus, ischium, flagellum,

merus, propodus].

Articular plate is a small plate of triangular shape, located distally on the posterior side of the pereopodal propodi. Articular plates cover the posterior articular condyle of the propodo-dactylar joint and may allow for an extra degree of freedom of the dactylus and is synapomorphic for isopods (Wilson and Keable 2002; Wilson 2003, 2009).

Articulation is a flexible joint between segments of the body or of appendages. The connection between setae and the general cuticle or sometimes between setules and the setal shaft may also be referred to as articulations. The cuticle is thin and desclerotized in articulations to allow movement. In spine-like setae, the articulation is reduced and the seta fixed.

Basis is the second article of a thoracic appendage and the third article of the antenna. [Plural: bases; see also: maxilliped, pereopod, protopod].

Bifid describes a structure with two distal tips (e.g. in bifid seta (Hessler 1970; Riehl and Brandt 2010)).

Bifid seta is a seta which features a subterminal setule or sensillum, a sensory organ [Synonymy: sensory spine (Brandt 1988); see also: seta].

Bifurcate seta is a seta with two subsimilar robust cusps. Lumen is extending in both parts of the split. Clear distinction to bifid setae not always possible.

Biserrate seta describes a seta with two rows of denticles along its shaft. [Synonymy: two-sided serrate seta; see also: seta].

Bisetulate describes an object such as a seta as bearing two rows of setules apically on opposite sides of the setal shaft. [See also: seta, setule].

Bristle: see seta.

Brood pouch: see marsupium.

Brooding female is an adult female with fully-developed oostegites that form a brood pouch.

Broom seta is a sensory seta for reception of water movements relative to body movements. With pedestal articulation and long setules arranged in a pappose or sometimes plumose manner distally on the shaft (Hessler 1970; Brix 2007; Riehl and Brandt 2010). In macrostylids, broom setae are located on antennula, antenna, pereopods and uropods. In *Urstylis solicopia*, broom setae occur dorsally on the

pleotelson (Riehl *et al.* 2014). [Synonymy: penicillate seta].

Carpus is the fifth article of a thoracopod or the sixth article of antennula and antenna [See also: pereopod].

Cephalon is the anteriormost tagma of crustaceans bearing two pairs of antennae, three pairs of mouthparts (mandible, maxillula, maxilla), the mouth and plesiomorphically the eyes, which are reduced in macrostylids. In isopods, it is fused with the first thoracic segment bearing the maxilliped to form a cephalothorax. [Synonymy: head; see also: cephalothorax].

Cephalothorax is the anterior body unit comprising (in Isopoda) head and the first thoracomere. The mouth opening, clypeus, antennulae and antennae as well as four pairs of mouthparts (mandible, maxillula, maxilla, maxilliped) are located on the cephalothorax. Similar to other typical deep-sea taxa, but unlike their shallow-water relatives, the macrostylid cephalothorax bears no eyes. [Synonymy: cephalon, head; see also: tagma].

Claw (dactylar) is a modified seta located distally on the dactylus. It is more or less heavily sclerotized and may have a sharp tip; sometimes it bears substructures. [Synonymy: dorsal claw; anterior claw; unguis; see also seta].

Claw (secondary dactylar) is a modified seta located distally on dactylus, ventrally to dactylar claw. It may resemble the latter but is often smaller or thinner and articulating slightly more proximally on dactylus. Dactylar claw and secondary dactylar claw often form a functional unit (Just 2005). [Synonymy: ventral claw; unguis; posterior claw (Wilson 1985); see also: seta].

Clypeus is an anterior sternal region of the cephalothorax located between frons, labrum, mandibular fossae and antennal articulations. Related to the prognathous head in macrostylids and urstylids, their heads show remarkable transformations and fusions. The slightly sloping frons is connected to the clypeus via a smooth transition. The frontal furrow, which is not always present, demarks the posterior margin of the clypeus. The clypeus is articulating with the labrum on its ventral margin with a distinct suture line. In Joeropsididae, the clypeus forms a pseudorostrum. [Synonymy: epistome].

Collum is a Latin term meaning ‘neck’ and refers to a constricted region anterior to the widest section of the pereonite where the preceding segment overrides the narrowed anterior region of a segment (Riehl *et al.* 2012). [See also: pereonite].

Coupling hook is a modified seta on the medial margin of the maxilliped’s basal endite with bulbous, recurved and denticulate tips. They couple with their paired counterparts so that both maxillipeds can act as a single unit. [Synonymy: receptaculum].

Coxa refers to the first article of a thoracopod or second article of antennula and antenna. See also oostegite. [Plural: coxae].

Cuticular hair: see setule.

Dactylus is the seventh or distal segment of a pereopod, with distal claws. [Plural: dactyli].

Denticle is a short and pointed cuticular extension. It is never articulated and never flexible. Denticles may have one or more cusps and are more bulky than scales. Other than setae, they do not have a continuous lumen. [Synonymy: small spine, denticule, tooth; see also: seta].

Denticulate: see serrate.

Denticule: see denticle.

Denticulate seta refers to a seta with denticles. Often several denticles are organized in rows distally close to the setal tip [Synonymy: serrate seta].

Dorsum is the dorsal surface of the body.

Endopod is the medial or interior ramus of the biramous crustacean appendage arising from the basis. In Isopoda with their uniramous pereopods, this term is typically applied only for the inner ramus of the pleopods and uropods. [Synonymy: endopodite; see also: ramus].

Epipod refers to a laterally directed lobe of a coxa, e.g. in the maxilliped. [Synonymy: epipodite, exite].

Epipodite: see epipod.

Epistome: see clypeus.

Exite: see epipod.

Exopod is the lateral or exterior ramus of a biramous crustacean appendage arising from the basis. In Macrostylidae, exopods can be found only in the pleopods. [Synonymy: exopodite, outer ramus].

Exopodite: see exopod.

Fan seta is a specialized type of seta that can be found on the distal tip of the maxilliped endites. The cuticle is thin and transparent and the shape can be circumscribed as “hand-shaped”, “fan-shaped” or

“broadly lobate and serrate”. [See also: seta].

Flagellum. The long, tapering distal part of antenna I and antenna II, generally consisting of many articles but reduced in number in Macrostylidae. [Plural: flagella].

Fossosome refers to a tagma that is a subunit of the pereon and consisting of pereonites 1–3 in Macrostylidae. Together with various other unique features, for instance a spade-like head inserting flexibly into the first pereonite as well as the first three pairs of specialised pereopods, this apomorphy of the Macrostylidae is presumed to be an adaptation for burrowing (Thistle and Wilson 1987, 1996; Riehl *et al.* 2014). The fossosome is highly integrated, segments are not moveable against each other and segment borders of tergites and sternites are absent in some macrostylid species. [Synonymy: fossosome; see also: pereon, tagma].

Fringe-like describes an object as having a dense coat of setules distally on the shaft, as in fringe-like sensilla.

Frons refers generally in Isopoda to the anterior part of the cephalothorax bearing the clypeus, situated between the antennae I and II and below the rostrum or vertex. Due to fundamental transformations in the macrostylid head, the frons is located more centrally than anteriorly behind the clypeus and the frontal furrow (where present), and between the antennal sockets.

Frontal furrow is a suture line between frons and clypeus which is not in all species of macrostylids present. [Synonymy: frontal ridge (misconception of shape)].

Habitus refers to the general appearance of an animal [Plural: habitus].

Heterochrony comprises evolutionary changes in the timing and/or rates of ontogenetic development of morphological characters. This relative term requires a comparison between ancestral and descendant ontogenies. [See also: hypomorphosis, paedomorphosis].

Hypopharynx: see paragnaths.

Hypostome: see paragnaths.

Hypomorphosis describes heterochronic change between ancestral and descendant ontogenies where an early offset of the development of certain traits occurs. This term has been proposed to logically supersede the term “progenesis” which has accumulated (similar to “neoteny”) various ambiguous meanings (Reilly *et al.* 1997). Neoteny and progenesis are partly synonymous, depending on the definitions used. [Antonym: hypermorphosis; see also: heterochrony, paedomorphosis].

Imbricate ornamentation. A pattern of semicircular, roundish notches on the cuticle appear overlapping. These patterns may cover the whole cuticle of pereon and pleotelson or only certain areas of the macrostylid body. In some species these patterns are missing. [Synonymy: reticulate pattern, scale-like pattern, comb-like patten, honeycomb pattern.

Incisive process: see incisor process.

Incisor process is the distal-most of the functional regions of the mandible. It typically bears one or more cusps or teeth. On its medial side, it is associated with the *lacinia mobilis* and the remaining spine row [Synonymy: incisor, incisive process, pars incisivus].

Ischium refers to the third segment of a thoracic appendage. [Plural: ischia; see also: pereopod].

Labrum is an unpaired flap-shaped outgrowth of the clypeus, anteriorly and dorsally covering the mouth. [Synonymy: upper lip].

Lacinia mobilis is an enlarged, more or less articulated projection on the mandible located between spine row and incisor. In macrostylids, it is found on both mandibles asymmetrically. Often it is smaller on the right mandible. On both sides it may be reduced independently or at the same time and replaced by a large spine resembling the shape of the members of the spine row (Richter *et al.* 2002). [Synonymy: lacinia, movable tooth].

Lamellar describes a thin and flat shape.

Lobate describes a leaf-like shape.

Lower lip: see paragnaths.

Manca is the term used for the first three stages or instars of the postmarsupial life cycle of Cumacea, Isopoda, Tanaidacea, and some Thermosbaenacea wherein the seventh pereopod is absent or underdeveloped.

Mandible is the third cephalic and first mouthpart appendage of isopods. It generally has a lateral three-articulated palp, which is reduced in Macrostylidae. The following functional regions of the macrostylid mandible can be distinguished: incisor process, spine row, molar process, dorsal condyle, and posterior articulation.

Mandibular spine row is a functional region of the third cephalic appendage. It consists of a row of spines on the medial side of the mandible's incisor process. The *lacinia mobilis* may be an enlarged member of the spine row (Richter *et al.* 2002).

Marsupium in isopods is a ventral pereonal enclosure on brooding females for eggs and developing embryos. It is composed of oostegites projecting medially from the coxae of the anterior pereopods I–IV in asellote isopods). Some isopods have an additional small oostegite on the coxa of the maxilliped. In macrostylids, the oostegites got lost on pereopods I and II.

Maxillula is the second mouth part and fifth cephalic appendage. In the Janiroidea, it consists of two setose lobes: a large outer lobe bearing robust, tooth-like setae as well as smaller setae; and a smaller inner lobe with only small setae. [Synonymy: maxilla I, maxillule, first maxilla; plural: maxillae].

Maxilla is the third paired mouth part and fifth cephalic appendage. In Janiroidea (Asellota: Isopoda), it consists of a basal segment bearing three setose lobes. [Synonymy: maxilla II, second maxilla; plural: maxillae].

Maxilliped is a paired appendage on the posterior and ventral edge of the cephalothorax. It is the first thoracic appendage, and its body somite is fused with the cephalon. It consists of the following functional parts: coxa, basis bearing a flattened and setose endite, palp with 5 segments (ischium, merus, carpus, propodus, dactylus), and an epipod attached laterally to the coxa.

Merus refers to the fourth segment of a thoracic appendage. [Plural: meri; see also: pereopod].

Metastoma: see paragnaths.

Molar process is a medial process and one of the functional regions of the mandible. Plesiomorphically, it has a broad, distal, triturating surface with circumgnathal denticles, a posterior row of broad, setulate setae, and sensory pores on the distal surface. In Macrostylidae the molar process is reduced to a triangular lobe subacute and setiferous on the apex. [Synonymy: pars molaris].

Monoserrate seta is a seta with one row of denticles on its shaft. [Synonymy: one-sided serrate seta; see also: seta].

Neoteny: see hypomorphosis.

Non-ovigerous describes a female which is assumed to be in a pre-mating or mating condition, because it is similar in size to conspecifics bearing oostegites. This term may include preparatory females but the latter term is more exact and thus preferred when this condition can be unambiguously identified.

Oostegites are medial coxal cuticle processes that are lamellar and lobate and form a brood pouch under the ventral surface of the female anterior body by shingle-like overlapping. They may be seen in two forms of oostegite development can be found in Janiroidea: externally developing oostegites are small fat lobes that do not cross the ventral midline; on the other hand in Macrostylidae, Urstylidae

and potentially others have internally developing oostegites oostegites that can be seen through the translucent sternal cuticle using a light microscope.

One-sided serrate seta: see monoserrate seta.

Opercular refers to appendages or other body parts that form a covering.

Operculum is a covering of the branchial chamber of janiroidean isopods. In females, it is formed by the fused second pleopods and in the males by the first and second pleopods.

Ovigerous refers to females bearing developing eggs or embryos in the marsupium.

Paedomorphosis describes the preservation of ancestral juvenile characters or shapes by later ontogenetic stages of the descendants. Three separate processes may underly this phenomenon: deceleration, hypomorphosis, or post-displacement (Reilly *et al.* 1997). [See also: heterochrony, hypomorphosis]

Palp is a lateral appendage of the maxilliped or the mandible. The mandible palp is reduced in Macrostylidae.

Papilla is a small protuberance or nipplelike projection of the cuticle. [Plural: papillae].

Papillose refers to a surface covered with papillae.

Pappose describes a seta that has setules arranged loosely on the setal shaft and not in (opposite) rows. In macrostylids, pappose setae are typically found apically on the second and fourth pleopods and broom setae usually have a pappose arrangement of setules as well. However, setae may be pappose on many other macrostylid body parts and their presence and arrangement may be species specific. [See also: seta].

Paragnaths are a paired mouthpart that is not homologous to the appendages. Paragnaths are of a laminar form and in macrostylids consist of a larger outer lobe and a smaller inner lobe. Both lobes are setose. This lip-like structure is situated immediately posteriorly and ventrally to the mandibles. [Synonymy: hypopharynx, hypostome, lower lip, metastoma].

Pars incisivus: see incisor process.

Pars molaris: see molar process.

Pedestal seta is a seta that is raised above the dorsal surface of the body by a pedestal-like outpocketing

of the cuticle. [See also: seta].

Peduncle: see protopod.

Pereon is the intermediate body division in isopods between cephalothorax and pleotelson consisting of seven pereonites. [Synonymy: mesosome, peraeon].

Penicillate seta: see broom seta.

Pereonite is a segment of the pereon comprising thoracic segments 2–8, and bearing the locomotory appendages or pereopods. [Synonymy: peraeonite, pereomere, somite; see also: pleonite].

Pereopod refers to the 7 pereonal appendages. It consists of the following segments: coxa, basis, ischium, merus, carpus, propodus, dactylus. The coxae of ovigerous females bear oostegites. The distal five podomeres are homologous with the endopod of the more plesiomorphically biramous thoracic limb of other Crustacea. [Synonymy: peraeopod].

Pinnate seta was used by Birstein (1970) for the pappose setae e.g. apically on the operculum of *Macrostylis ovata*. [See pappose seta].

Pleon: see pleotelson.

Pleonite is a segment of the abdomen. Plesiomorphically in the Malacostraca, there are six free pleonites followed by the telson. In isopods, at least the sixth pleonite is fused to the telson to form a 'pleotelson' but there is considerable variation across the order. In most species of Macrostylidae, the other five segments are also fused with the pleotelson, thus forming a large pleotelson of compact shape. [See also: pleotelson].

Pleopod is one of the first 5 paired, plesiomorphically biramous, ventral limbs of the pleotelson. In unmodified form, it consists of a basal segment, the protopod, and 2 distal rami, the endopod and the exopod. The rami may be biarticulate. Female Asellota lack the first pleopods. In male Asellota, the first pleopods are present only as uniramous structures fused into a single elongate plate in the superfamily Janiroidea. The rami of the male second pleopod are modified as copulatory structures. Pleopods III–V have very thin cuticle and function as gills (branchiae).

Pleopodal cavity circumscribes the ventral surface of the pleotelson when it is deeply concave and encloses the pleopods dorsally and laterally (Wilson 1989). Since the more posterior pleopods function as gills, the pleopodal cavity can also be thought of as a 'branchial cavity' (Wilson 1989). [Synonymy: branchial cavity, branchial chamber].

Pleotelson is a highly integrated tagma resulting from fusion of up to all pleonites with the telson. In most macrostylid species, all pleonite tergites are fused with the telson but often the segment borders of the first pleonite are rudimentarily visible. So far, only in one species, *Macrostylis papillate* Riehl, Wilson and Hessler, 2012, the first pleonite is freely articulated dorsally. [Synonymy: abdomen, pleon].

Plumose refers to a seta with two opposing rows of setules on the shaft. Plumose setae in macrostylids are most prominently found along the pleopod III endopod distal margin. [Synonymy: feather-like seta].

Preanal trough is a cavity that posteriorly extends the pleopodal cavity to the pleotelson apex, resulting in the cavity to be open posteriorly. Its presence in Macrostylidae and Janirellidae is a homoplasy in the light of the latest analysis (Riehl *et al.* 2014). [Synonymy: longitudinal excavation (Wolff 1962)].

Preparatory female is a female with developing oostegites. This instar directly precedes the brooding condition (Wilson 1989). Instead of externally developing oostegites in buds, that are apparent in Munnopsidae and Desmosomatidae, macrostylids have internally-developing oostegites Riehl, unpubl. data. It is unclear, at what instar macrostylids enter the preparatory stage and whether multiple breeding cycles follow upon each other or not.

Progenesis: see hypomorphosis.

Propodus is the sixth segment of a thoracic appendage. [Plural: propodi; see also: pereopod].

Protopod is the basal segment of a crustacean appendage. Plesiomorphically, it consists of all basal articles up to and including the segment with the rami: precoxa, coxa and basis (Moore and McCormick 1969). In macrostylids and other Janiroidea, only the basal segment of the uropods and pleopods are referred to as protopods. [Synonymy: peduncle, protopodite, sympod, sympodite].

Protopodite: see protopod.

Pseudorostrum is a projection of the clypeus.

Quadrangular describes a structure as having a truncate distal margin at approximately right angles to the lateral sides, for example, the shape of the pleotelson of some macrostylid species. [Synonymy: quadrate].

Ramus is a branch of an appendage. The uropods of macrostylids, for instance, are uniramous, meaning they comprise only one branch, the endopod, as opposed to the plesiomorphically biramous appendages of crustaceans. [Plural: rami].

Receptaculum: see coupling hook.

Recurved describes a structure that is curved back on itself.

Scale describes a flattened denticle. [But see also: antenna].

Scaphocerite: see antennal scale.

Sclerite is a hardened and often calcified area of the arthropod cuticle and usually part of exoskeleton.

Sclerotized describes features, for example body parts or setae, with thick and sometimes calcified cuticle.

Sensillum is a modified seta and may generally describe all types of setae with assumed sensory function. In macrostylids, for example setae that are found along the ventral margins of the anterior pereopods, on the dactyli of all pereopods and on the maxilliped palp are specifically referred to as sensillae. Sensillae are often covered with many tiny setules (“fringe-like”; often only visible in a scanning electron micrograph (Riehl and Brandt 2010)). Terminal pores might be present. The name refers to assumed sensory functions of these setae that might not necessarily be identical or homologous. [Synonymy: sensory filament; sensory hair; plural: sensilla].

Sensory filament: see aesthetasc, sensilla.

Sensory hair: see sensilla.

Sensory spine: see seta, bifid seta.

Serrate describes an object, e.g. a seta, as having a row of short denticles or spines [Synonymy: denticulate].

Seta is a cuticular process with or without a clear articulation with the basal cuticle. Setae have a continuous lumen (which is not always visible in light microscopy) with sheath cells and sensory cilia (can never be identified by light microscopy). Setae develop during ontogeny from an invagination of the cuticle. This is the cause for the annulus, a ring structure, which is sometimes visible on the shaft but mostly disappears during intermoult. They may have a subterminal or terminal pore or show some perforation. Setae often bear diverse secondary or micro-structural outgrowths (i.e. substructures; see setule, denticle). Setae are mostly circular in cross-section, at least in the basal region but may have a flattened appearance as well and show high variability in form and function (see e.g. aesthetasc, broom Seta, retinaculum upon many more). Some papers in the isopod literature may use the term “spines” when heavily sclerotized setae are indicated. “Robust seta” or “spine-like seta” for such heavy setae is

more accurate. [Synonymy: bristle, sensilla; plural: setae; see also: spine].

Setule refers to a long, flexible and thin cuticular appendage. It commonly has a gradual transition to the cuticle but may be connected to a setal shaft via an articulation. On the general cuticle of tergites and sternites, it is referred to also as cuticular hair.

Slot-like apertures describes a pair of indentations posteriorly on the pleotelson tergite. These are assumed to be related to the statocysts. Potentially and analogous to statocysts in other crustaceans, they represent the cuticular opening through which the cuticular statocysts are shed. Not in all species of Macrostylidae this structure is clearly visible, sometimes it seems to be absent. Detailed anatomical studies remain to be conducted in order to clarify this organ's structure and function. [See also: statocyst].

Somite: see pereonite, pleonite.

Spine row: see mandibular spine row.

Spine is a more or less acute projection of the cuticle that is confluent with the cuticle at its base (never articulated). [See also: seta].

Squama: see antennal scale.

Statocyst is a small saclike sensory (equilibrium) organ, usually containing a granule, used to indicate its orientation to the animal. In Macrostylidae, a paired organ in the pleotelson interpreted as statocyst is an apomorphic character.

Sternite is a ventral sclerite of a crustacean body segment. Sternites are more or less strictly marked off from the tergite by lateral margins but may also blend seamlessly into it. [See also: tergite].

Sympod: see protopod.

Sympodite: see protopod.

Tagma is a section of the arthropod body consisting of one or more segments coherently derived in form and function. Tagmata may be a series of free segments similar in form and function (often with similar appendages) or comprise highly integrated to a functional unit [Plural: tagmata; see also cephalothorax, fossosome, pereon, pleotelson]

Tagmosis is the arrangement and composition of functional groupings of body segments into tagma. In all isopods the first thoracomere is integrated and fused with the cephalon to form a tagma called

cephalothorax. While in most Janiroidea the pereon is composed of an anterior tagma comprising pereomeres 1–4 and a posterior tagma comprising pereonites 5–7, there are various derived conditions. Some Nannoniscidae and Haploniscidae, for example, have variable numbers of posterior pereonites fused with the pleotelson. In Macrostylidae, the fourth pereonite is distinctly different from both anterior and posterior pereonal tagmata and thus constitutes a separate tagma.

Telson is the terminal segment of a crustacean body, bearing the anus. In isopods, the telson is fused to the anterior pleonite(s) forming a pleotelson.

Tergite is a dorsal sclerite of the exoskeleton of an arthropod's body segment. [See also: sternite].

Terminal male describes a fully mature male assuming it has reached the terminal stage of its lifecycle (Riehl *et al.* 2012). Since often data on the population structure and lifecycle of macrostylid species is not available, use of this term may be ambiguous. [Synonymy: adult male, copulatory male].

Tooth: see denticle.

Thoracopod is an appendage of the thorax. In Macrostylidae (and all other Malacostraca except Leptostraca), the first thoracomere is integrated with the cephalon to form the cephalothorax and the first thoracopod is hence called maxilliped. The subsequent thoracopods are referred to also as pereopods. [Synonymy: maxilliped, pereopod].

Two-sided serrate seta: see biserrate seta.

Unequally bifid seta refers to a type of seta that is often spine-like and has a smaller hair-like setule just proximal to its tip. The hair-like setule can be seen to have a nerve extending into the cuticle and is probably the external expression of a sensory nerve. [Synonymy: Sensory spine (Brandt 1988)].

Unguis: see claw.

Uniramous refers to appendages with only a single branch. [See also: ramus].

Uropod is the terminal appendage of the body, belonging to the sixth pleonite. It consists of a basal segment, the protopod, and plesiomorphically two uniarticulate rami, a larger endopod and a smaller exopod. In Macrostylidae, the uropods are always uniramous. [See also: ramus].

Whip seta describes a seta which is characterized by a relatively broad proximal part of the shaft that has a sudden transition to a more slender distal part. In some cases, whip setae have a sensory function and may be derived from the unequally bifid seta with the sensory hair situated at the distal tip.

References

- Birstein, Y. A. (1970) New Crustacea Isopoda from the Kurile-Kamchatka Trench area. In: Bogorov, V. G. (Ed.) *Fauna of the Kurile-Kamchatka Trench and its environment*. pp 308–356. Moscow: Academy of Sciences of the USSR. (Proceedings of the Shirshov Institute of Oceanology; 86).
- Brandt, A. (1988) Morphology and ultrastructure of the sensory spine, a presumed mechanoreceptor of *Sphaeroma hookeri* (Crustacea, Isopoda), and remarks on similar spines in other peracarids. *Journal of Morphology*, 198(2), 219–229.
- Brix, S. (2007) Four new species of Desmosomatidae Sars, 1897 (Crustacea: Isopoda) from the deep sea of the Angola Basin. *Marine Biology Research*, 3(4), 205–230.
- Cunha, M. R. and Wilson, G. D. F. (2006) The North Atlantic genus *Heteromesus* (Crustacea: Isopoda: Asellota: Ischnomesidae). *Zootaxa*, (1192), 1–76.
- Garm, A. (2004) Revising the definition of the crustacean seta and setal classification systems based on examinations of the mouthpart setae of seven species of decapods. *Zoological Journal of the Linnean Society*, 142(2), 233–252.
- Hansen, H. J. (1893) Zur Morphologie der Gliedmassen und Mundtheile bei Crustaceen und Insekten. *Zoologischer Anzeiger*, 16, 193–212.
- Hessler, R. R. (1970) *The Desmosomatidae (Isopoda, Asellota) of the Gay Head-Bermuda Transect* [online]. (Arrhebus, G. O. S., Cox, C. S., Fager, E. W., Hand, C. H., Newberry, T., and Schaefer, M. B., Eds.) Berkeley, Los Angeles, London: University of California Press. Available from: <http://escholarship.org/uc/item/1mn198vx>.
- Just, J. (2005) Xenosellidae, a new family of Janiroidea (Asellota: Isopoda: Crustacea), for *Xenosella coxospinosa* gen. nov., sp. nov., from the marine bathyal of eastern Australia. *Zootaxa*, 1085, 21–32.
- McLaughlin, P. A. (1980) *Comparative morphology of recent crustacea*. San Francisco: W. H. Freeman. ISBN 0716711214.
- Moore, R. C. and McCormick, L. (1969) General features of Crustacea. In: Moore, R. C. (Ed.) *Treatise on Invertebrate Paleontology, Part R, Arthropoda 4*. Lawrence: Geological Society of America and University of Kansas Press.
- Reilly, S. M., Wiley, E. O. and Meinhardt, D. J. (1997) An integrative approach to heterochrony: the distinction between interspecific and intraspecific phenomena. *Biological Journal of the Linnean Society*, 60(1), 119–143.
- Richter, S., Edgecombe, G. D. and Wilson, G. D. F. (2002) The *lacinia mobilis* and similar structures—a valuable character in arthropod phylogenetics? *Zoologischer Anzeiger—A Journal of Comparative Zoology*, 241(4), 339–361.
- Riehl, T. & Brandt, A. (2010) Descriptions of two new species in the genus *Macrostylis* Sars, 1864 (Isopoda, Asellota, Macrostylidae) from the Weddell Sea (Southern Ocean), with a synonymisation of the genus *Desmostylis* Brandt, 1992 with *Macrostylis*. *Zookeys*, 57, 9–49.
- Riehl, T. & Brandt, A. (2013) Southern Ocean Macrostylidae reviewed with a key to the species and new descriptions from Maud Rise. *Zootaxa*, 3692(1), 160–203.
- Riehl, T. & Kaiser, S. (2012) Conquered from the deep sea? A new deep-sea isopod species from the Antarctic shelf shows pattern of recent colonization. *PLoS ONE*, 7(11), e49354.
- Riehl, T., Wilson, G. D. F. & Hessler, R. R. (2012) New Macrostylidae Hansen, 1916 (Crustacea: Isopoda) from the Gay Head-Bermuda transect with special consideration of sexual dimorphism. *Zootaxa*, 3277, 1–26.
- Riehl, T., Wilson, G. D. F. & Malyutina, M. V. (2014) Urstylidae – A new family of deep-sea isopods and its phylogenetic implications. *Zoological Journal of the Linnean Society*, 170, 245–296.
- Thistle, D. & Wilson, G. D. F. (1987) A hydrodynamically modified, abyssal isopod fauna. *Deep-Sea Research. Part A. Oceanographic Research Papers*, 34(1), 73–87.
- Thistle, D. & Wilson, G. D. F. (1996) Is the HEBBLE isopod fauna hydrodynamically modified? A second test. *Deep-Sea*

- Watling, L. (1989) A classification system for crustacean setae based on the homology concept. *Functional morphology of feeding and grooming in Crustacea*, 6, 15–26.
- Wetzer, R. & Brusca, R. C. (1997) Guide to the coastal isopods of California. *Journal of Crustacean Biology*, 3, 1–9.
- Wilson, G. D. F. (1985) *The Systematic Position of the Ilyarachnoid Eurycopidae (Crustacea, Isopoda, Asellota)*. Diss. San Diego: University of California San Diego.
- Wilson, G. D. F. (1989) *A systematic revision of the deep-sea subfamily Lipomerinae of the isopod crustacean family Munnopsidae*. (Cox, C. S., Fleminger, A., Kooyman, G. L., & Rosenblatt, R. H., Eds.) Berkley, Los Angeles, London: University of California Press. (Bulletin of the Scripps Institution of Oceanography). ISBN 0-520-09745-9.
- Wilson, G. D. F. (2003) A new genus of Tainisopidae fam. nov. (Crustacea: Isopoda) from the Pilbara, Western Australia. *Zootaxa*, 245, 1–20.
- Wilson, G. D. F. (2009) The phylogenetic position of the Isopoda in the Peracarida (Crustacea: Malacostraca). *Arthropod Systematics & Phylogeny*, 67(2), 159–198.
- Wilson, G. D. F. *Glossary for anatomical terms of Asellota*. [online] (2013) (<http://www.scamit.org>). Available from: http://www.scamit.org/taxontools/toolbox-new/ARTHROPODA/Subphylum%20Crustacea/Class%20Malacostraca/Subclass%20Eumalacostraca/Superorder%20Peracarida/Order%20Isopoda/Suborder%20Asellota/-OTHER%20USEFUL%20TOOLS/Wilson_Asellota_Glossary_20130930.pdf. [Accessed 2013-10-23].
- Wilson, G. D. and Keable, S. J. (2002) New Phreatoicidea (Crustacea: Isopoda) from Grampians National Park, with revisions of Synamphisopus and Phreatoicopsis. *Memoirs of Museum Victoria*, 59(2), 457–529.
- Wolff, T. (1956) Isopoda from depths exceeding 6000 meters. *Galathea Report*, 2, 85–157.
- Wolff, T. (1962) The systematics and biology of bathyal and abyssal Isopoda Asellota. *Galathea Report*, 6(3), 1–320.
- Wägele, J.-W. (1983) On the homology of antennal articles in Isopoda. *Crustaceana*, 45(1), 31–37.
- Wägele, J.-W. (1992) Isopoda. In: Harrison, F. W. and Humes, A. G. (Eds.) *Crustacea*. pp 529–617. New York, Chichester, Brisbane, Toronto, Singapore: Wiley-Liss. (Microscopic Anatomy of Invertebrates). ISBN 0-471-56842-2.

Appendix 2

Adding depth to line-artwork by digital stippling – A step-by-step guide to the method

Published: Bober, S. & Riehl, T. (2014) Adding depth to line-artwork by digital stippling – A step-by-step guide to the method. *Organisms Diversity & Evolution*, DOI: 10.1007/s13127-014-0173-7.

Abstract

Vector-based software has revolutionized scientific illustrating and is well established in taxonomy. However, simple line drawings lack depth information. Shading techniques, such as stippling—the application of dots to generate shade—are the methods of choice for simulating shade, structure, shape, and texture. In this paper, a step-by-step guide for digital stippling is presented. Manual stippling offers great flexibility to achieve highly realistic results. A round brush is applied to the line art by tapping. To drastically reduce time consumption and generate homogeneous tinges, a semiautomation was developed: the smallest units of symmetric stippling patterns are stored in a brush library. Using macroinstructions (macros), such stored raw patterns are converted into symmetric repetitive patterns. This way, stippling can be applied quickly and evenly across large areas of the underlying line drawing. These methods come with all the advantages of vector illustrations, such as high scalability, reproducibility and easy correction of strokes that have turned out imperfect.

Keywords: systematics; taxonomic methods; stippling; shading; digital inking; illustration

Introduction

many organism groups, such as predominantly animal taxa (various groups of Arthropoda, but also Digenea, Gastrotricha, Kinorhyncha, Polychaeta, and Vertebrata among others) as well as fungi (Andres and Overstreet 2013; Barber and Keane 2007; Coleman and Sen-Dunlop 2013; Ivanova and Wilson 2009; Kieneke et al. 2008; Reuscher et al. 2009; Salles et al. 2011; Sørensen 2008; Weigmann et al. 2013). Digital illustration techniques have numerous advantages over traditional inking techniques (Bouck and Thistle 1999; Fisher and Dowling 2010). The easy and quick possibility to undo strokes that have turned out imperfect, for instance, is a major time-saving factor.

Vectorgraphics software allows manipulation of the actual drawing after the completion of the lines (Holzenthal 2008). It further permits compact data files and the possibility to scale an illustration without losing information or changing line weights, if unwanted. Manuals to the basically relevant scientific drawing techniques using a pen tablet and Adobe® Illustrator® (AI) are available (Barber and Keane 2007; Bouck and Thistle 1999; Coleman 2009; Holzenthal 2008). Through the application of macroinstructions (macros) and the brush tool, the illustration of frequently occurring features, such as setae, can be significantly sped up (Coleman 2009).

For transmitting a general impression of the shape and form of an organism or parts of the latter, line drawing is a powerful technique (Honomichl et al. 1982). There are instances where a purely line-based illustration providing a contour and certain important protruding features are fully sufficient. That is especially the case when the illustrated object is flat or has an otherwise even surface. However, a weakness of line drawings in general is the lack of depth.

Most biological objects comprise more than plain surfaces; edges, convex or concave areas, as well as form, and texture may be of significance (Dalby and Dalby 1980). To overcome this shortcoming and even emphasize certain features, shading techniques can be applied. They create the impression of three dimensionality (3D), texture, and to some degree even color (Dalby and Dalby 1980). Stippling is the method of choice to produce shaded line art in science (Briscoe 1996). It is achieved by producing dots into the line drawings and generates the illusion of greyscale within the preferable (Dalby and Dalby 1980) black-and-white (B/W) regime by varying densities of dots (Honomichl et al. 1982; Zweifel 1988). Stippling may be time consuming compared with plain line drawings, but it provides full control over the application of shading and highly realistic results are achievable (Sousa 2003). Stippling is therefore a widely applied method in biological sciences (e.g., Brandt and Wägele 1988; Meißner and Hutchings 2003; Kieneke et al. 2008; Miljutina and Miljutin 2012; Köhler and Criscione 2013; de Zeeuw et al. 2013; Moravec et al. 2014).

In this paper, we describe methods for vector-based stippling. These fulfill all requirements from scientific illustrations, such as reproducibility, clarity, and scalability. They allow shading without compromising the clarity, simplicity, and storage-saving advantages of B/W (e.g., bitmap) images. They are further advantageous over traditional stippling using ink because of the possibilities to electronically manipulate size and orientation. High flexibility in plate preparation as well as easy correction possibilities are further improvements (Bouck and Thistle 1999). Moreover, we describe a significantly time-saving automation technique.

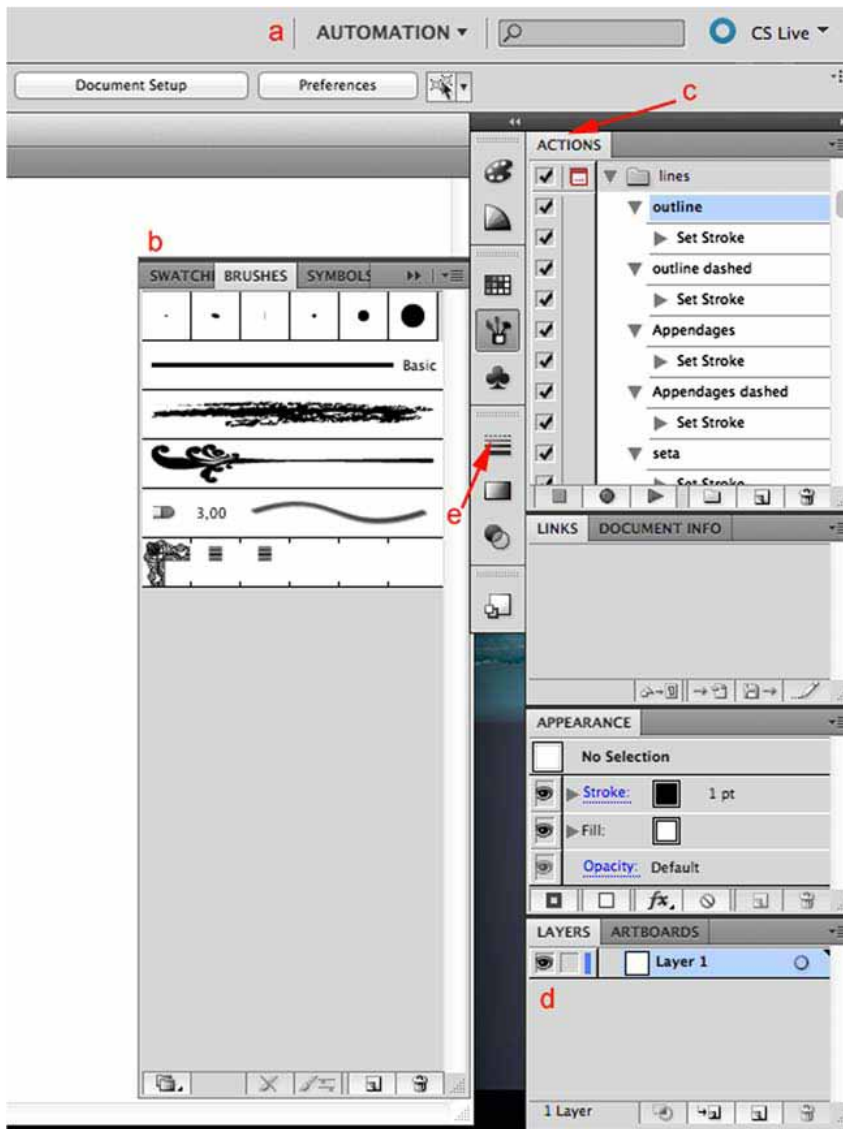


Figure 1. Overview over the AUTOMATION workspace in Adobe Illustrator. **a**, The workspace selection panel is located near the top right corner of the window. **b**, The *Brushes* menu. **c**, The *Actions* panel. **d**, The *Layers* menu. **e**, The *Stroke* panel.

Materials

Any computer with at least 1300 MHz processor, 1GB RAM and USB Port can be used. A second monitor is advisable. For this paper, both Apple and Windows operation systems in combination with Wacom Intuos pen tables (models 3 A4 (PTZ 930) and 4 A4 (PTK 840)) were used. The required hard- and software runs on any of the widely applied operation systems (Microsoft Windows, Macintosh OS, Linux). Throughout the guidelines, we provide keyboard shortcuts in brackets that are applicable for both Apple and Windows systems. The Apple-specific ⌘ key is used synonymously with the Windows Ctrl key. The Shift key is represented by ⇧.

The underlying scientific illustrations were created by following the methods described by Coleman (2003, 2009), and their creation is not part of this documentation. Adobe® Illustrator® (AI) CS5 (version 15.0.0 and 15.0.2) was used during the development of the methods. All methods described herein were successfully tested in the still widely applied AI CS 4 and the latest AI CS 6 version as well. We recommend to use the Automation workspace (Fig. 1a) because all necessary menus are found therein.

Manual Stippling

1. Open AI CS 5 and attach the drawing tablet.

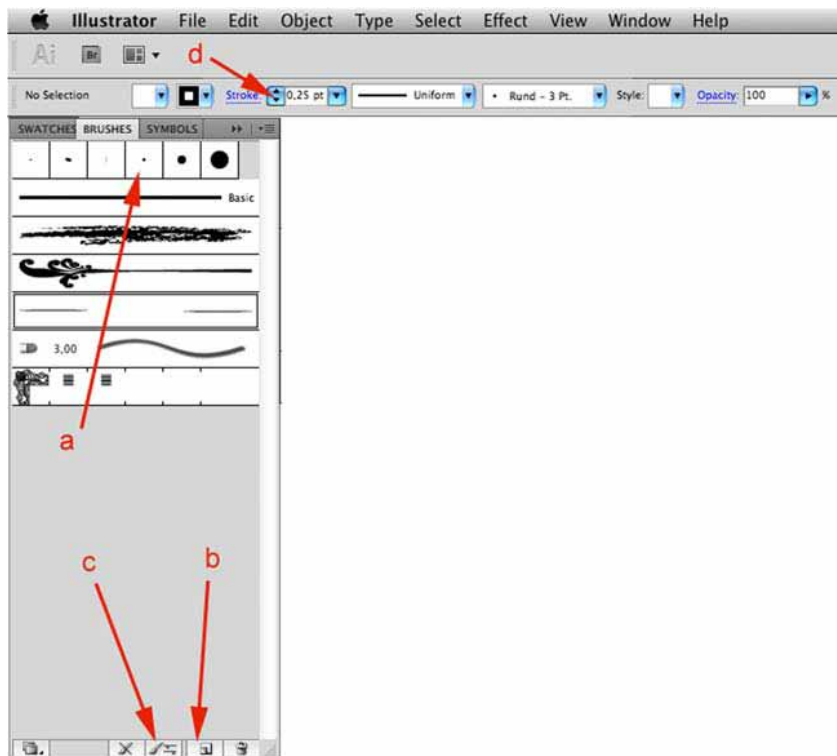


Figure 2. The *Brushes* panel. **a**, -3 pt. Round brush. **b**, Create New Brush. **c**, Selected Object Options. **d**, The suggested size for a single stipple is 0.25 pt.

2. Load a vector drawing, e.g. one prepared following the guidelines by Coleman (2003, 2009) (File → Open; or ⌘ O).
3. Open the *Brushes* panel (Fig. 1b) and select the 3 pt. Round brush (*Artistic_Caligraphic* library) (Fig. 2a). Adjust the stroke size to 0.25 pt. (Fig. 2d).
4. Add a row of dots by tapping on the tablet. The dots should evenly distributed (ca. 0.5 mm distance).
5. Add a second similar row of dots parallel and alternating to the first row.
6. Add a third row parallel and alternating to the second row.
7. Etc.

Following this pattern, the shade will look even without any gradation (Fig. 3a–c). If a desaturation is desired for this tone to receive a gradation, the next steps need to be followed (Fig. 3d–g).

8. Add another parallel row of dots with more distance to the previous row.
9. Use the same distance for one or more additional rows.

10. For a stronger desaturation effect, double the distance between the dots in another (set of) row(s) – alternating with every second dot in the previous row.
11. This can be deliberately expanded.

Automated Stippling

Stippling can be semi-automated through brushes and an appropriate macro (called “*Action*” in AI terminology). The latter method is described in the subsequent section *Automated Stippling*. We are providing exact values that lead to the example brushes in the electronic supplement.

Creating Stippling Brushes

1. Open a new document (⌘ N).
2. For easier navigation, activate the ruler (View → Ruler → Activate Ruler; or ⌘ R).
3. Use the *Brush* tool (b) and select the *Round -3 Pt* brush. Adjust the stroke size to 0.25 pt. (Fig. 2d).

Table 1. Exact coordinates that represent the fundamental stippling patterns discussed in and provided with the paper.

	1. Basic		2. Stretch		3. Standard		4. Standard 2		5. Wide		6. Wide 2		7. Concavity	
	X	Y	X	Y	X	Y	X	Y	X	Y	X	Y	X	Y
Dot 1	0	0.3	0	0.3	0	0.4	0	0.4	0	0.4	0	0.4	1.5	0
Dot 2	0,6	0	1.1	0	0.5	0	0.5	0	0.5	0	0.5	0	4.5	0
Dot 3					1.5	0	1.5	0	1.5	0	1.5	0	0	0.8
Dot 4					1	0.4	1	0.4	1	0.4	1	0.4	0	-0.8
Dot 5					0.5	0.8	0.5	0.8	0.5	0.8	0.5	0.8	3	0.8
Dot 6					1.5	0.8	1.5	0.8	1.5	0.8	1.5	0.8	3	-0.8
Dot 7							0	1.5	0	1.7	0	2	1.5	2.3
Dot 8							1	1.2	1	1.3	1	1.4	1.5	-2.3
Dot 9									1	2.1	1	2.6	4.5	2.3
Dot 10									0	2.9	0	3.6	4.5	-2.3
Dot 11											1	4.7	0	3.5
Dot 12													0	-3.5
Dot 13													3	5
Dot 14													3	-5
Dot 15													0	8
Dot 16													0	-8
Dot 17													3	12
Dot 18													3	-12

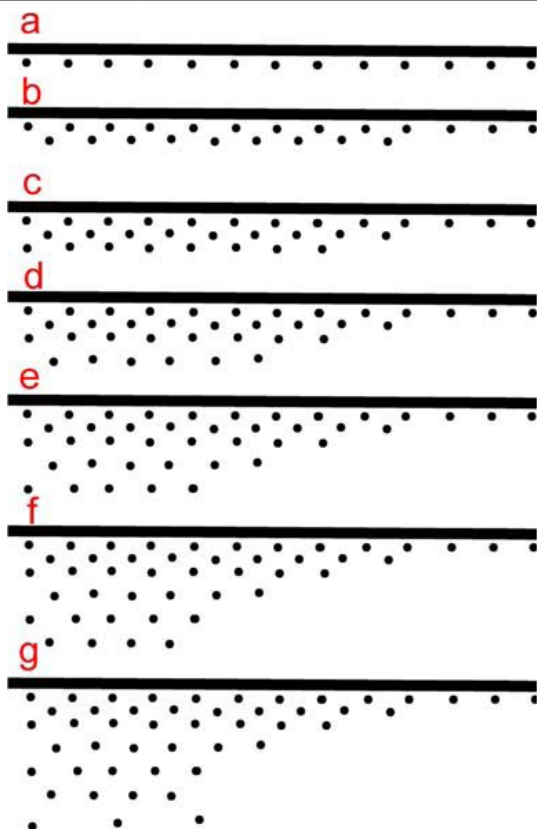


Figure 3. Example of how to build up shading through manual stippling. **a**, Start with one row of equally-spaced dots. **b–c**, Add second and third rows alternating to the previous row. **d–g** For a desaturation effect, add more rows but with increased distance between them. For a stronger desaturation, double the spacing between the dots in another (set of) row(s) - alternating with every second dot in the previous row. This pattern can be deliberately expanded.

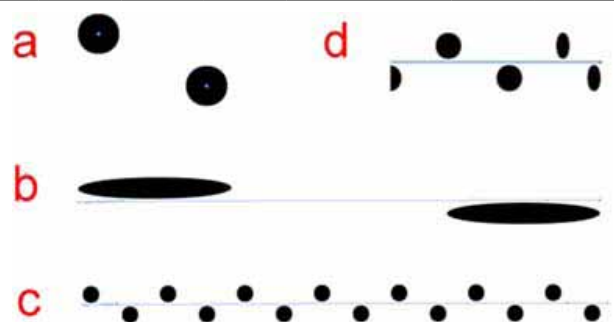


Figure 4. Steps for creating semi-automated stippling (not to scale). **a**, Two stipples are the basis for a simple repetitive pattern, *Stippling Basic*. **b**, When the stippling brush is applied without using the proper type of dashed line, a stretched stippling brush appears. **c**, After application of the corresponding action, the stretched brush is turned into a symmetric, repetitive pattern. **d**, The end of the stroke may be distorted. This can be adjusted by extending or shortening the vector at the terminal anchor point.

4. Create a random dot by tapping on the pen tablet and a second one 0.6 mm to the right and 0.7 mm below (Fig. 4a; this is the fundamental fragment of the simplest stippling pattern).
5. Select the pattern by either using the *Direct Selection* tool (A) or the *Lasso* tool (Q).

Table 2. Stroke settings fitting for the stippling patterns discussed in and provided with the paper.

	1. Stippling Basic	2. Stippling Standard	3. Stippling Stretch	4. Concavity
Function Key	[F9 + SHIFT]	[F10 + SHIFT]	[F11 + SHIFT]	[F12 + SHIFT]
Dash Length	2,5 pt	5 pt	4 pt	14 pt
Gap Length	0,5 pt	0,5 pt	2,5 pt	4 pt

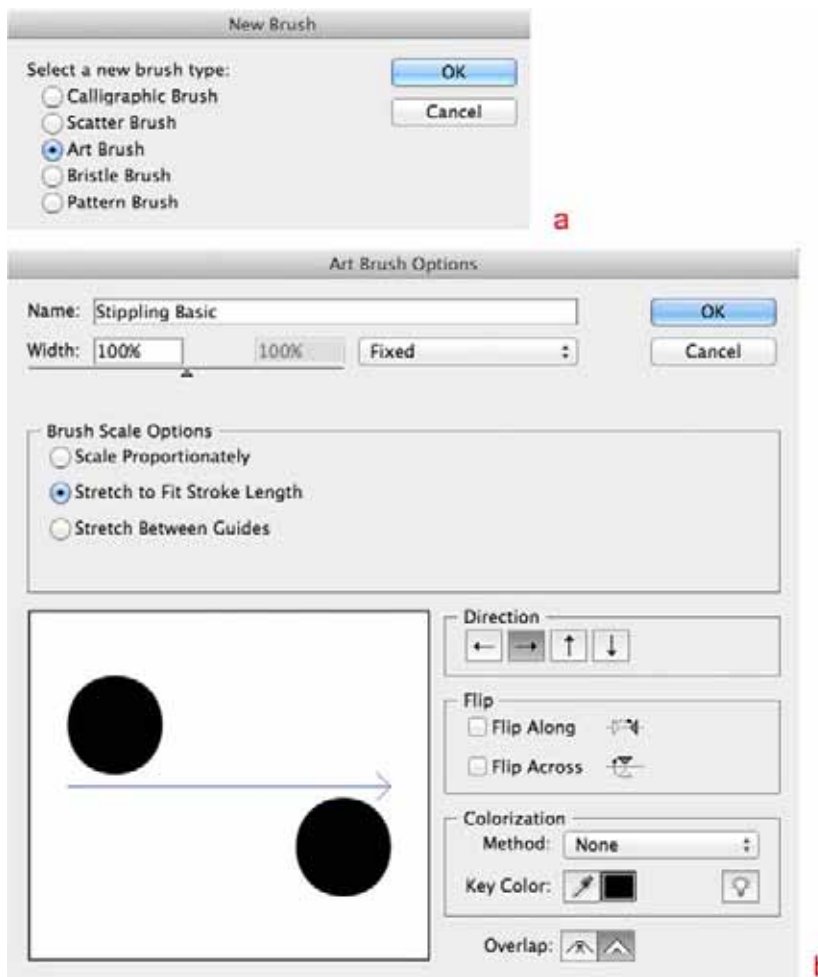


Figure 5. How to create a brush. **a**, The pattern is saved as *Art Brush*. **b**, The options *Stretch to Fit Stroke Length* and the brush *Direction* are set in the *Art Brush Options* window.

- Open the *Brushes* panel (Fig. 1b) and add a new brush by clicking the *New Brush* button on the bottom of the panel next to the *Bin* button (Fig. 2b). Select the *Art Brush* type (Fig. 5a) and name the brush (in this case, *Stippling basic*). The *Brush Scale Options* should be set to *Stretch to Fit Stroke Length* (Fig. 5b).

Make sure the stroke direction is correct and press *OK* (Fig. 5b).

Following the guideline above produces a rather simple stippling pattern. It is suitable, for example, for slight shadings or to pronounce layer separation (see, e.g., antennae and uropods in Fig. 6b).

This pattern can become more complex by adding more rows of dots and gradients. Once a pattern is established (e.g. by following steps 1–6 above, this pattern can be used as template to easily produce derivatives. Copies can be made and transformed by up- or down scaling with or without keeping the aspect ratio. A large library of stippling brushes can thus be generated quickly.

We recommend preparing a set of at least four to six stippling brushes. In Tab. 1, coordinates for six further stippling patterns are presented. Pattern no. 7 (*Concavity*) is different to all other patterns in that this special pattern is simulating a concavity (Fig. 6c).

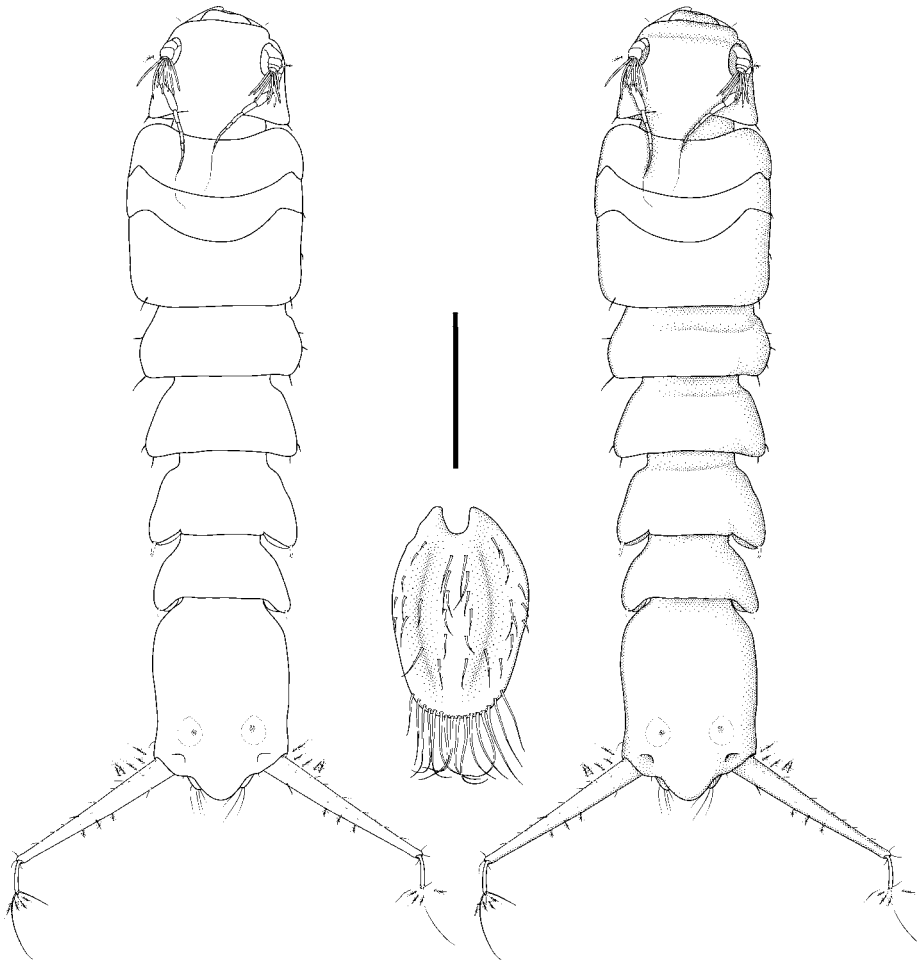


Figure 6. Plain versus stippled vector illustrations exemplified by the isopod (Crustacea) species *Macrostylis scotti* Riehl & Brandt, 2013. **a**, Plain illustration without any shading. **b**, Same illustration as **a** but with stippling added. Various types of brushed stiplings as well as manual stippling were applied. **c**, The second female pleopods (operculum) with concavities (stippling pattern no. 7) on the surface.

Once a brush library is generated, it can be saved (Fig. 7a) and is then available for further illustrations (Fig. 7b). An exemplary brush library containing those brushes presented here is provided in the electronic supplement.

Creating a Stippling Action

Stippling brushes have a certain length defined by its underlying pattern fragment. Longer homogeneous stippling is produced by using the *Dashed Line* function which produces repetition of the pattern fragment. The *Dash* length has to be set to equal the length of the pattern fragment and the *gap* length has to correspond to the necessary distance between two such fragments. *Actions* allow quick adjustments of these pattern-specific parameters so the generated stippling pattern is homogeneous. *Actions* are AI-specific macros. Once a brush is saved to the brush library, it is recommended to

program a corresponding *Action*.

1. In *Actions* panel (Fig. 1c), create a *New Set* and name it '*Stippling*' (Fig. 8a).
2. Create a *New Action* within this set and name it '*Stippling Basic*' (Fig. 8b). Assign the *Function Key* [\uparrow F9]. Click *Record* (Fig. 8b).
3. Open the *Stroke* panel (Fig. 1e). Set *Weight* to 1 pt. and check the *Dashed Line* box (Fig. 9a). To the right of this box, check *Preserves exact dash and gap lengths* (Fig. 9b).
Set the dash length to 2.5 pt. and the gap length to 0.5 pt. (Fig. 9c).
4. Stop recording by clicking the *Stop* button (Fig. 8c) next to the red *Record* button on the bottom of the *Actions* panel.
5. Use the *Brush Tool* (B), select the brush *Stippling Basic* and draw a line; the dots

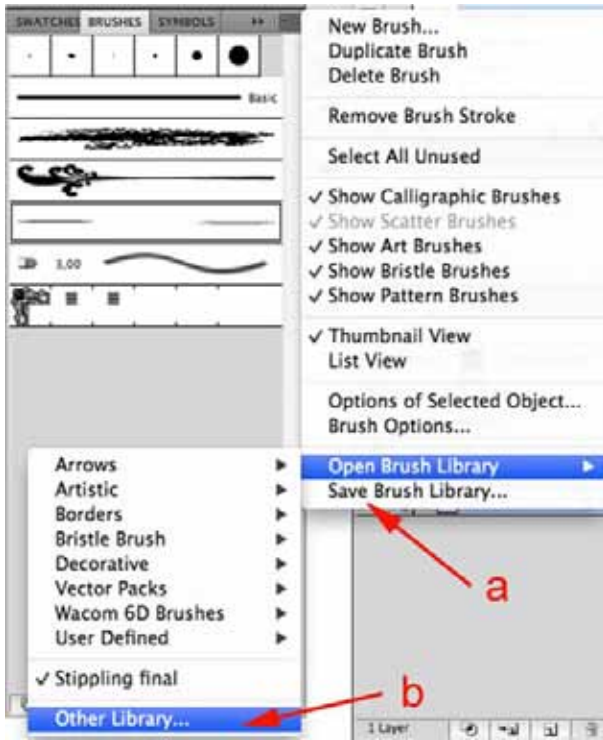


Figure 7. How to save and load a brush library. A click on the upper right corner of the *Brushes* panel opens a drop-down menu. **a**, *Save Brush Library* opens an explorer window to select the proper location for storing the library. **b**, Custom-made libraries can be loaded by clicking on *Other Library*.

appear stretched (Fig. 4b).

6. Press [\hat{u} •F9] and the stretched line are converted into a repetitive pattern (Fig. 4c).
7. The end of the stippling turns out squeezed

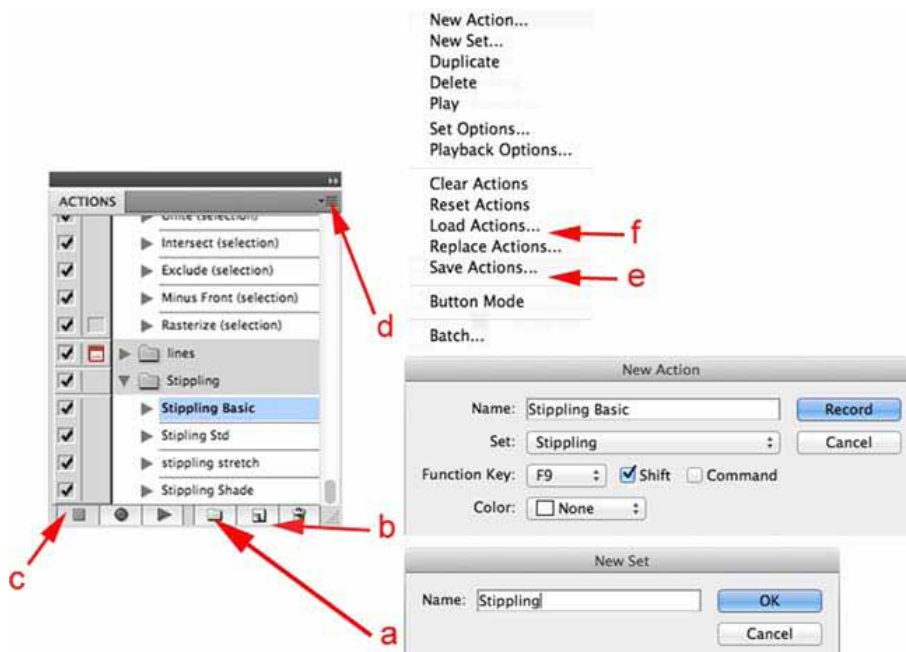


Figure 8. Every type of stippling brush needs a corresponding Action. **a**, *Actions* are saved to a *New Set* which can be called *Stippling*. **b**, For every *New Action* that is recorded, a unique name and *Function Key* should be assigned. **c**, To stop recording, press the *Stop* button. **d**, To save or load an *Action*, open the *Actions Options*. **e**, Then press *Save Actions* or **f**, *Load Action*.

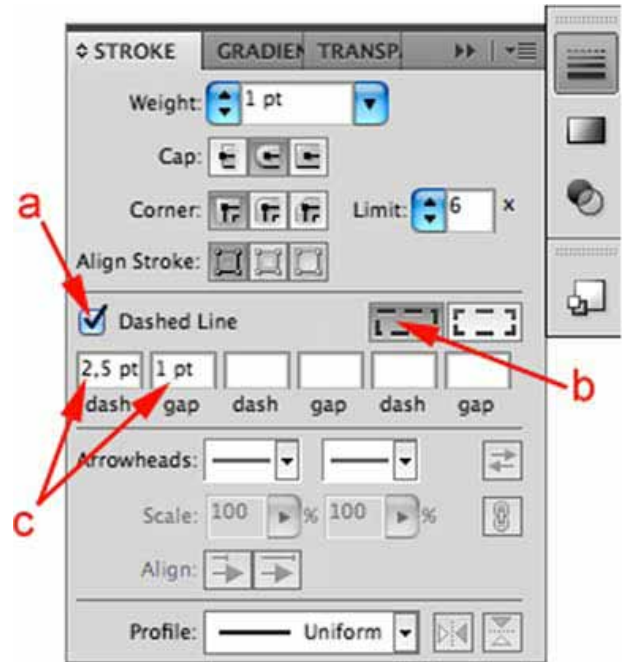


Figure 9. The Stroke panel. **a**, Checking this box change a line into a dashed line. **b**, For stippling brushes it is recommended to check *Preserves exact dash and gap lengths*. **c**, The dash and gap distance is manually adjustable and proper values depend on the underlying stippling pattern.

when the length of the underlying vector does not exactly equal a multiple of the fragment length (Fig. 4d). If this is the case, the length of the vector should be altered by moving the last *Anchor* point.

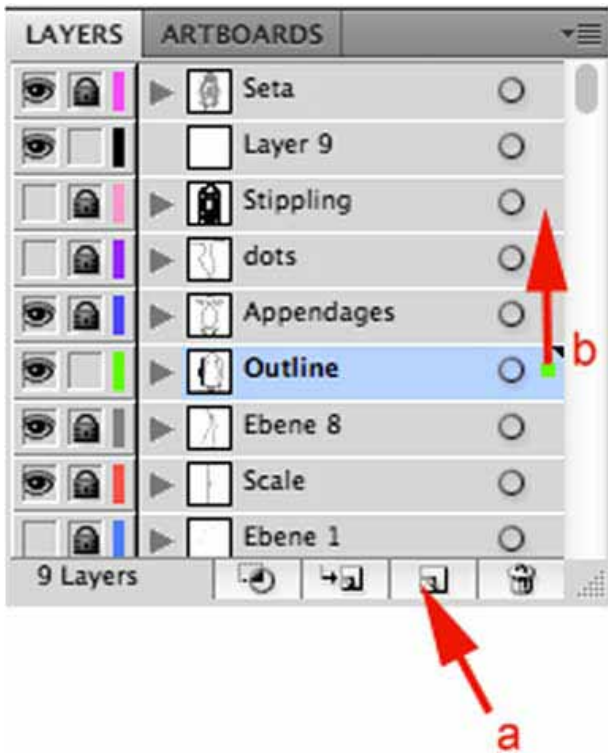


Figure 10. The *Layers* menu. **a**, Create a *New Layer*. **b** Selected paths can be moved to different layers.

Once the *Action Set* is generated, it can be saved and is available for further illustrations (Fig. 8d–f). This *Action* corresponds only to the stippling-brush

pattern described above as well as derivatives with similar fragment length and spacing between dots. We recommend to prepare *Actions* corresponding to each individual stippling type (Tab. 2). The *Actions* presented here are available as electronic supplement.

Adding stippling to a drawing

1. Open AI CS 5 and attach the pen tablet.
2. Load a vector drawing prepared following the guidelines by Coleman (2003, 2009) (File → Open; or ⌘ O).
3. Create a new *Layer* in the *Layer* panel by clicking *Create New Layer* next to the *Bin* symbol and name it (e.g., *Stippling*; Fig. 10a). Working with layers has many advantages. First of all, it helps to organise the document properly. Then, the order of the layers represents an object hierarchy (stacking order). Furthermore, layers can be selectively locked, masked out and

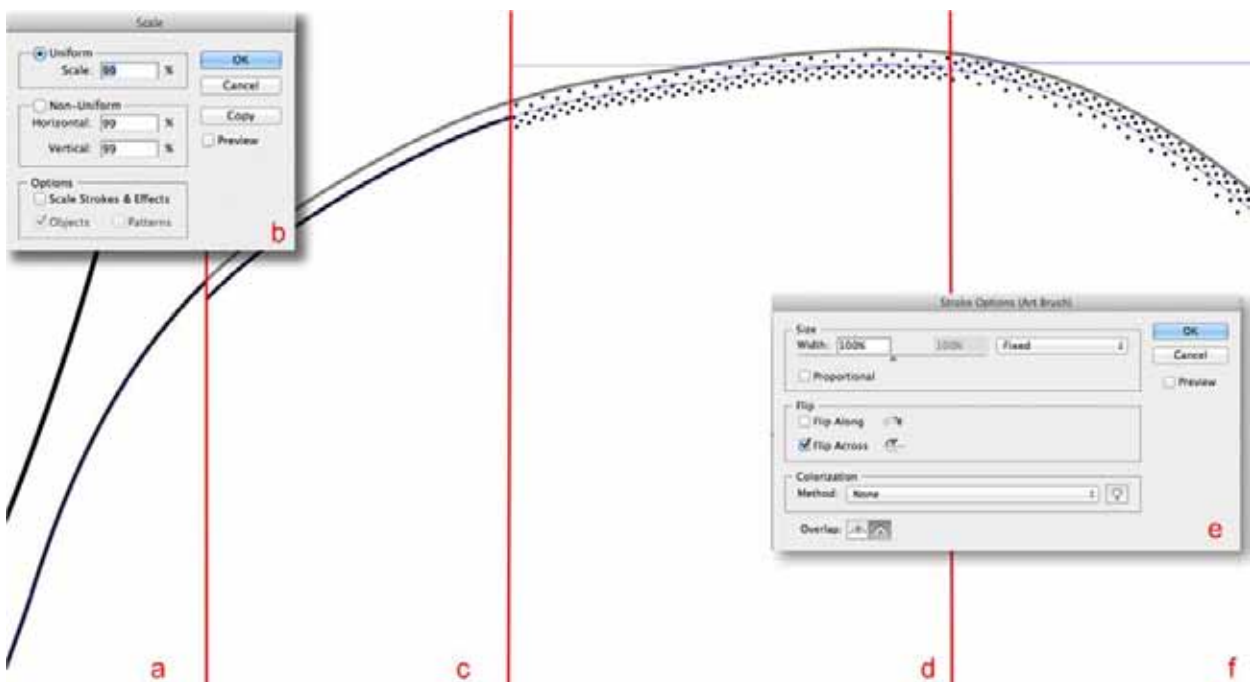


Figure 11. Excerpt of a round closed line that is supposed to get a stippling. **a**, Select a path, create a copy behind the template. **b**, Scale selected path to 99% of its original size. **c**, The path should now lie within the round structure. **d**, Convert path into a stippling brush by selecting an appropriate pattern from the brushes library. **e**, To flip over the stippling brush when it has turned out upside down, check the *Flip Across* box in the *Stroke Options* window. **f**, The ready stippling.

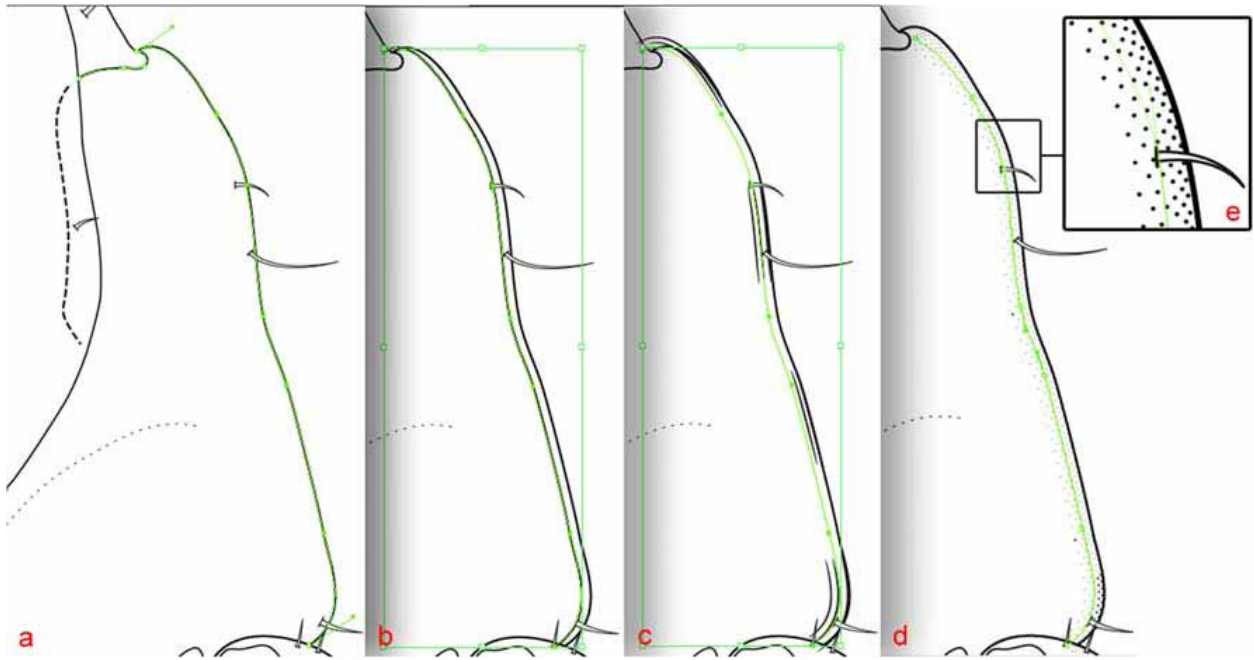


Figure 12. Automated stippling exemplified on a ventral head drawing of a macrostyloid isopod. **a**, Select a path. **b**, Copy the selected path behind the original template. **c**, Move the copied path to be parallel to the template. **c** Convert line into a stippling brush by selecting the desired pattern from the brush library. **d**, After applying the corresponding action command this stippling is adjusted. **e**, Magnification from d.

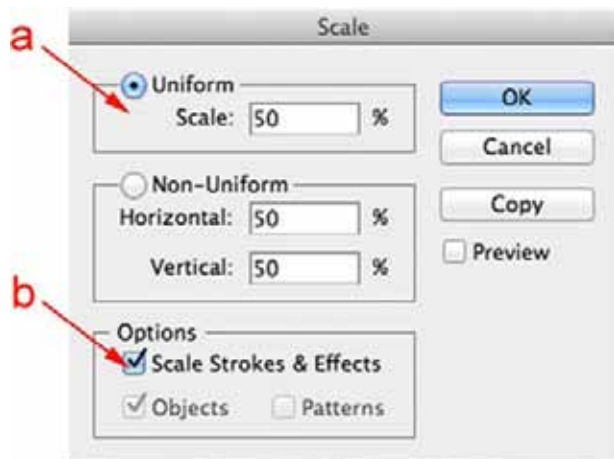


Fig. 13 How to scale vector illustrations that contain stippling patterns. **a**, Uniform scaling is required to keep length-width ratios of the illustration. **b**, The box *Scale Strokes & Effects* should be checked when lines and brushes are supposed to change their appearance equivalently to the overall drawing.

dimmed (amongst many other attributes) to provide great working comfort.

4. Use the *Brush Tool* (B) and select one of the previously prepared stippling brushes.
5. Activate the corresponding *Action*.
6. Trace those lines that need stippling.
7. If the stippling pattern is upside down (Fig. 11d) you can either draw the line in

the other direction, or preferably open the *Options for Selected Object* window (Fig. 3c) by clicking the button on the left to the *Create New Brush* button. Choose *Flip Across* (Fig. 11e).

8. Adjust the *Anchor* points for optimal coverage and avoiding a compressed end of the vector.

Line-parallel stippling over large areas

In cases where a large area that is parallel to a line needs homogeneous stippling, it may be easier to copy this line and transform it into a stippling pattern.

1. Select the whole line or parts that need stippling with either the *Selection tool* (V) or the *Lasso tool* (Q) (Fig. 12a).
2. Copy this line (⌘ C) and paste it behind the original line (⌘ B).
3. Use the *Selection Tool* (V) and move the copied line in the preferred position next to the original line (Fig. 12b).

4. Open the *Brushes* menu and choose one of the previously prepared stippling brushes (Fig. 12c).
5. Make adjustments if needed (Fig. 12c).
6. Apply the proper *Action* [⌘ F9].
7. Go to the *Layers* menu and drag the selection to the stippling layer (Fig. 10b).

Stippling within a closed line

Where roundish structures that are represented in a drawing by closed lines, such as any form of operculum (Fig. 1b) or micro-fungal conidia (Barber and Keane 2007), stippling may be used to simulate bulge form. To achieve this, parallel stippling on the inside of the closed line is required.

1. Select the whole line with either the *Selection* tool (V) or the *Lasso* tool (Q) (Fig. 11a).
2. Copy this line (⌘ C) and paste it behind the first (⌘ B).
3. Scale the selection (*Object* → *Transform* → *Scale*) to ≤ 99% depending on the used stippling brush (Fig. 11b) and diameter of the closed line.
4. Open the *Brushes* menu and transform the line into a stippling brush (Fig. 11d).
5. Make adjustments if needed (Fig. 11b,d,e).
6. Go to the *Layers* menu and drag the selection to the stippling layer (Fig. 10b).

Scaling of Stippled Illustrations

The final size of the illustration can be adjusted without compromising the quality even after the actual drawing is completed (*Object* → *Transform* → *Scale*; Fig. 13a). There is a high flexibility with regard to adjusting line weights etc. in the process of plate arrangement. Moreover, scaling may change the appearance of the illustration, if desired, by selectively excluding strokes

and brushes from the scaling process. When the box *Scale Strokes & Effects* in the *Scaling* panel is checked (Fig. 13b), lines and brushes change their appearance equivalently to the overall scaling. Thus, when the drawing size is reduced to 50%, a 1 pt. line becomes 0.5 pt. When the box *Scale Strokes & Effects* is unchecked, lines do not change their weight and brushes do not change their appearance during scaling. In the above-mentioned case, the line weight would double relative to the size of the drawing. This is also relevant for stippling, because manually applied dots and stippling brushes may behave differently depending on the applied settings. However, we present three ways of scaling artwork that contains stippling:

First of all, checking the box *Scale Strokes & Effects* allows for a straight-forward scaling approach where all relative values remain constant. Using this method, manual and brushed stipples are equally affected.

At the same time, AI provides a tool to change the relative dimensions of the stipples, without changing their relative positions while the overall size of the drawing is altered. The *Expand Appearance* function (*Object* → *Expand Appearance*) converts the stippling brushes as well as manually applied dots into circular paths filled with black colour. So, the dimensions of the black dots are not defined by a stroke anymore but by the diameter of the circular vector. Because during scaling the relative positions of the paths and anchor points always stay identical, downscaling in this case means downsizing the stipples and vice versa. This implies that as long as the box *Scale Strokes & Effects* remains unchecked, any scaling changes the appearance of the individual dots. Coming back to the previous example of the drawing that is scaled down to 50%: a 1 pt. outline retains its weight; the dots of the stippling, however, are reduced to 50% of their original diameter.

Since AI may automatically group dots of the brushed stipplings when the *Expand Appearance* function is applied, scaling may cause distortion of the stipple positions. To counteract this, select all stippling patterns (lock all layers, except the stippling layer; then press ⌘ A) and ungroup (*Object* → *Ungroup*; or ⌘ ⇧ G) the selection. To ensure that also groups nested within groups have ungrouped, the ungrouping may need to be repeated.

Finally, the *Transform Each Tool* (*Object* → *Transform* → *Transform Each*; or ⌘ ⇧ D) allows altering the intensity of the shading by scaling the selected dots individually. As a prerequisite for this approach, it is necessary to convert all stippling brushes to circular paths beforehand using the *Expand Appearance* tool.

Discussion

Line drawings involve selectiveness and emphasis to certain aspects of the illustrated objects (Dalby and Dalby 1980). Stippling is a method that allows emphasising structures interpreted as relevant by the scientist. It provides a high degree of freedom and adaptability. By applying a digital approach to stippling (Riehl and Brandt 2013; Riehl *et al.* 2012; 2014), this technique has been brought up to date concordant with widely applied digital line-drawing methods (Bouck and Thistle 1999; Coleman 2003, 2009).

Manual stippling can be relatively time consuming and to create homogeneous tinges over large areas can be difficult (Honomichl *et al.* 1982). We hence developed a method that allows relatively straight contours to be shaded reasonably quick. The automated stippling, however, fails to produce satisfactory results where the path underlying the stippling is heavily curved. In particu-

lar in broad stippling brushes, the dots of the outer rows may get distorted. To a certain degree, this might be tolerable, but it could cause accentuating effects that are not desirable. In curved regions it is thus recommended to link straight sections produced by the automated method with manually applied stipples.

We provide a general introduction to our new approach and any values provided here can be changed to fit the individual requirements. The method is an alternative to a recently described method (Barber and Keane 2007) that applies filters in Adobe® Photoshop® to automatically generate stippling. One disadvantage of the latter method, in contrast to our approach, lies in the computer-generated dot distribution that produces randomly variable distances and often overlapping of the individual dots which is generally not desirable (Sousa 2003). The method described herein allows full control over dot distribution. Likewise, their pixel-based approach does not provide the reproducibility and scalability inherent in vector drawings.

It should be noted that the freely available software Inkscape (<http://www.inkscape.org>; amongst others; see e.g. Barber and Keane (2007) and references therein) offers a suitable alternative to AI with regard to the manual stippling approach (see Riehl *et al.* 2014) and digital illustrations in general (see e.g., Wilson 2008). However, the methodology differs regarding the tools and settings, and possibilities to automate stippling need yet to be explored.

Acknowledgements

We are thankful for the support of A. Brandt and the helpful and friendly working environment at the Zoological Museum Hamburg. N. Heitland

practically tested the methods described in this paper. J. Ruch kindly provided comments on an earlier version which improved this paper. This paper benefitted from discussions about the topic with G.D.F. Wilson. During preparation of this manuscript, TR received funding from the German National Academic Foundation (Studienstiftung des deutschen Volkes).

References

- Barber, P. A., & Keane, P. J. (2007). A novel method of illustrating microfungi. *Fungal Diversity*, 27(1), 1–10.
- Bouck, L., & Thistle, D. (1999). A computer-assisted method for producing illustrations for taxonomic descriptions. *Vie et milieu*, 49(2-3), 101–105.
- Brandt, A., & Wägele, J.-W. (1988). *Antarcturus bovinus* n. sp., a new Weddell-Sea Isopod of the family arcturidae (Isopoda: Valvifera). *Polar Biology*, 8(6), 411–419.
- Briscoe, M. H. (1996). *Preparing scientific illustrations: a guide to better posters, presentations, and publications* (2nd ed.). New York: Springer.
- Coleman, C. O. (2003). “Digital inking”: how to make perfect line drawings on computers. *Organisms Diversity & Evolution*, 3(4), 303–304. doi:10.1078/1439-6092-00081
- Coleman, C. O. (2009). Drawing setae the digital way. *Zoosystematics and Evolution*, 85(2), 305–310. doi:10.1002/zoos.200900008
- Coleman, C. O., & Sen-Dunlop, Y. (2013). *Iphinotus lisae* n. sp. (Crustacea, Amphipoda, Phliantidae) from Western Australia. *Zoosystematics and Evolution*, 89(1), 5–11. doi:10.1002/zoos.201300001
- Dalby, C., & Dalby, D. H. (1980). Biological illustration: a guide to drawing for reproduction. *Field studies*, 5, 307–321.
- De Zeeuw, M., Westbroek, I., van Oijen, M., & Witte, F. (2013). Two new species of zooplanktivorous haplochromine cichlids from Lake Victoria, Tanzania. *ZooKeys*, 256(0), 1–34. doi:10.3897/zookeys.256.3871
- Holzenthal, R. W. (2008). Digital illustration of insects. *American Entomologist*, 54(4), 218.
- Honomichl, K., Risler, H., & Rupperecht, R. (1982). *Wissenschaftliches Zeichnen in der Biologie und verwandten Disziplinen*. Stuttgart: G. Fischer.
- Ivanova, E. S., & Wilson, M. J. (2009). Two new species of *Angiostoma* Dujardin, 1845 (Nematoda: Angiostomatidae) from British terrestrial molluscs. *Systematic Parasitology*, 74(2), 113–124. doi:10.1007/s11230-009-9200-z
- Kieneke, A., Arbizu, P. M., & Ahlrichs, W. H. (2008). Anatomy and ultrastructure of the reproductive organs in *Dactylopodola typhle* (Gastrotricha: Macrodasysida) and their possible functions in sperm transfer. *Invertebrate Biology*, 127(1), 12–32. doi:10.1111/j.1744-7410.2007.00111.x
- Köhler, F., & Criscione, F. (2013). Small snails in a big place: a radiation in the semi-arid rangelands in northern Australia (Eupulmonata, Camaenidae, *Nanotrachia* gen. nov.). *Zoological Journal of the Linnean Society*, 169(1), 103–123. doi:10.1111/zoj.12051
- Meißner, K., & Hutchings, P. A. (2003). *Spiophanes* species (Polychaeta: Spionidae) from Eastern Australia with descriptions of new species, new records and an emended generic diagnosis. *Records of the Australian Museum*, 55(2), 117–140.
- Miljutina, M. A., & Miljutin, D. M. (2012). Seven new and four known species of the genus *Acantholaimus* (Nematoda: Chromadoridae) from the abyssal manganese nodule field (Clarion-Clipperton Fracture Zone, North-Eastern Tropical Pacific). *Helgoland Marine Research*, 66(3), 413–462. doi:10.1007/s10152-011-0282-z
- Moravec, J., Lehr, E., Cusi, J. C., Cordova, J., & Gvozdk, V. (2014). A new species of the *Rhinella margaritifera* species group (Anura, Bufonidae) from the montane forest of the Selva Central, Peru. *ZooKeys*, 371, 35–56. doi:10.3897/zookeys.371.6580
- Riehl, T., & Brandt, A. (2013). Southern Ocean Macrostylidae reviewed with a key to the species and new descriptions from Maud Rise. *Zootaxa*, 3692(1), 160–203. doi:http://dx.doi.org/10.11646/zootaxa.3692.1.10
- Riehl, T., Wilson, G. D. F., & Hessler, R. R. (2012). New Macrostylidae Hansen, 1916 (Crustacea: Isopoda) from the Gay Head-Bermuda transect with special consideration of sexual dimorphism. *Zootaxa*, 3277, 1–26.
- Riehl, T., Wilson, G. D. F., & Malyutina, M. V. (2014). Urstylidae – A new family of deep-sea isopods and its phylogenetic implications. *Zoological Journal of the Linnean Society*, 170, 245–296. doi:10.1111/zoj.12104
- Sørensen, M. V. (2008). A new kinorhynch genus from the Antarctic deep sea and a new species of *Cephalorhyncha* from Hawaii (Kinorhyncha: Cyclorhagida: Echinoderidae). *Organisms Diversity & Evolution*, 8(3), 230.e1–230.e18. doi:10.1016/j.ode.2007.11.003
- Sousa, M. C. (2003). Scientific Illustration→ Part1: Traditional Techniques and NPR Approaches. *Theory and Practice of Non-Photorealistic Graphics: Algorithms, Methods, and Production Systems*, 10. <http://sites.google.com/site/>

Wilson, G. D. F. (2008). A review of taxonomic concepts in the Nannoniscidae (Isopoda, Asellota), with a key to the genera and a description of *Nannoniscus oblongus* Sars. *Zootaxa*, 1680, 1–24.

Zweifel, F. W. (1988). *A Handbook of Biological Illustration* (2nd ed.). Chicago and London: The University of Chicago Press.

Author contributions

The idea for this paper is by myself. I developed the manual stippling method and S. Bober developed the methods for automated stippling. The paper was written by myself and S. Bober to equal parts. S. Bober developed the method descriptions and created the figures.

Appendix 3

Field and laboratory methods for DNA studies on deep-sea isopod crustaceans

Published as: Riehl, T., Brenke, N., Brix, S., Driskell, A., Kaiser, S. & Brandt, A. (2014) Field and laboratory methods for DNA barcoding and molecular-systematic studies on deep-sea isopod crustaceans. *Polish Polar Research*, 25, 2, DOI: 10.2478/popore-2014-0018.

Abstract

Field and laboratory protocols that originally led to the success of published studies have previously been only briefly laid out in the methods sections of scientific publications. For the sake of repeatability, we regard the details of the methodology that allowed broad-range DNA studies on deep-sea isopods too valuable to be neglected. Here, a comprehensive summary of protocols for the retrieval of the samples, fixation on board research vessels, PCR amplification and cycle sequencing of altogether six loci (three mitochondrial and three nuclear) is provided. These were adapted from previous protocols and developed especially for asellote Isopoda from deep-sea samples but have been successfully used in some other peracarids as well. In total, about 2300 specimens of isopods, 100 amphipods and 300 tanaids were sequenced mainly for COI and 16S and partly for the other markers. Although we did not set up an experimental design, we were able to analyze amplification and sequencing success of different methods on 16S and compare success rates for COI and 16S. The primer pair 16S SF/SR was generally reliable and led to better results than universal primers in all studied Janiroidea except Munnopsidae and Dendrotonidae. The widely applied universal primers for the barcoding region of COI are problematic to use in deep-sea isopods with a success rate of 45-79% varying with family. To improve this, we recommend the development of taxon-specific primers.

Keywords

PCR, DNA sequencing, Barcoding Deep-sea Isopoda project, Janiroidea, benthos, abyssal, bathyal

Abbreviations

12S, mitochondrial small subunit (mtSSU) rRNA gene; 16S, mitochondrial large subunit (mtLSU) rRNA gene; 18S, nuclear small subunit (nSSU) rRNA gene; 28S, nuclear large subunit (nLSU) rRNA gene; CCDB, Canadian Centre of DNA Barcoding; COI, cytochrome-c-oxidase subunit 1; dNTP, deoxynucleotide triphosphates; LAB, Laboratories of Analytical Biology, Smithsonian National Museum of Natural History; PCR, polymerase chain reaction.

Introduction

The deep sea harbors an enormous number of species, and it was estimated that the majority is yet undescribed (Mora *et al.* 2011). Isopods are among the most diverse taxa, but also represent one of the better known groups inhabiting the deep sea (Rex & Etter 2010). Their correct classification is important for evolutionary, ecological, and biogeographic studies but also for conservation issues because as industrial pressures on the deep-sea environment grow (Glasby 2002, Hoagland *et al.* 2010, Barbier *et al.* 2014). Consequently, there is an urgency to establish standard methods for relatively fast and accurate species identification.

However, the tremendous isopod diversity and the high rate (>90%) of new species discoveries (Hessler *et al.* 1979, Gage 2004, Brandt *et al.* 2007, Wilson 2008) makes their description and classification challenging. Taxonomists working on deep-sea isopods classically (even though usually not explicitly stating so) apply the morphological (genotypic) cluster concept (Mallet 1995) when delimitating and describing new taxa using purely morphological data under the assumption that between-species variability is greater than within-species variability (Sites & Marshall 2004). This operational criterion can be inferred from most of the species concepts (Hausdorf 2011), for example, such as the biological species concept (Mayr 1942, 2000). Comprehending the deep-sea isopod diversity is further impaired because in

several groups morphologically highly similar or even almost identical – so called ‘cryptic’ – species are being increasingly discovered (Wilson 1982, 1983, Raupach & Wägele 2006, Raupach *et al.* 2007, Brökeland 2010, Riehl & Brandt 2010). In these cases, the (perceived) lack of morphological difference between lineages may disguise true (e.g. genetic) diversity.

Alternatively, strong dimorphisms hinder allocation of conspecific males and females, for instance where males undergo a metamorphosis during which their appearance is altered beyond variation that is commonly observed in the respective higher taxa (e.g. Riehl *et al.* 2012). Testing for the biological species concept is usually impractical because as live observations are impractical generally not feasible as a standard tool and the function of genital copulation structures are not well enough understood (but see Wilson 1986, 1991) to recognize potential “lock-and-key” patterns.

During the last decade, DNA barcoding and integrative approaches to systematic questions have become standard (Hebert *et al.* 2003, Gibbs 2009, Allcock *et al.* 2011, Schwentner *et al.* 2011, Havermans *et al.* 2013). Various species concepts can be applied when molecular data are applied used in addition to (sparse) morphological information (Schwentner *et al.* 2011). Although molecular methods have been used occasionally for deep-sea isopods (Raupach & Wägele 2006, Raupach *et al.* 2007, Brökeland & Raupach 2008),

Table 1. Number of sequences and DNA loci of *Asellota* present on GenBank (last date accessed: 26. November 2013) sorted by family and publication. Only those families are shown that show a partial or exclusive deep-sea distribution. New data presented in this volume are not yet considered.

	COI		12S		16S		18S		28S D1-3		28S D6-8	
Acanthaspidiidae	N/A	N/A	N/A	36 (Raupach & Wägele 2006)	5 (Raupach <i>et al.</i> 2004) 5 (Raupach <i>et al.</i> 2009)	N/A	N/A	10 (Raupach <i>et al.</i> 2009)				
Dendrotonidae	N/A	N/A	N/A	N/A	1 (Raupach <i>et al.</i> 2004) 2 (Raupach <i>et al.</i> 2009)	N/A	N/A	3 (Raupach <i>et al.</i> 2009)				
Desmosomatidae	2 (Schnurr & Brix 2012) 16 (Brix <i>et al.</i> in press)	N/A	N/A	1 (Schnurr & Brix 2012) 12 (Brix <i>et al.</i> in press)	4 (Raupach <i>et al.</i> 2004) 9 (Brix <i>et al.</i> in press)	N/A	N/A	4 (Raupach <i>et al.</i> 2009)				
Echinothambematidae	N/A	N/A	N/A	N/A	N/A	N/A	N/A	N/A				
Haplomunidae	N/A	N/A	N/A	N/A	1 (Raupach <i>et al.</i> 2004) 2 (Raupach <i>et al.</i> 2009)	N/A	N/A	2 (Raupach <i>et al.</i> 2009)				
Haplomiscidae	30 (Brix <i>et al.</i> 2011)	N/A	N/A	25 (Brökeland & Raupach 2008)	5 (Raupach <i>et al.</i> 2004) 3 (Brökeland & Raupach 2008) 9 (Raupach <i>et al.</i> 2009) 2 (Asmyhr & Cooper 2012)	N/A	N/A	12 (Raupach <i>et al.</i> 2009)				
Xostylus (ins. sed.)	N/A	N/A	N/A	N/A	1 (Raupach <i>et al.</i> 2009)	N/A	N/A	1 (Raupach <i>et al.</i> 2009)				
Ischnomesitidae	N/A	N/A	N/A	N/A	4 (Raupach <i>et al.</i> 2004) 1 (Osborn 2009) 2 (Raupach <i>et al.</i> 2009)	N/A	N/A	4 (Raupach <i>et al.</i> 2009)				
Janirellidae	N/A	N/A	N/A	N/A	1 (Raupach <i>et al.</i> 2004)	N/A	N/A	1 (Raupach <i>et al.</i> 2009)				
Janiridae	2 (Wetzer 2001) 1 (Osborn 2009) 1 (Radulovici <i>et al.</i> 2009) 1 (Kilpert <i>et al.</i> 2012)	2 (Michel-Salzat & Bouchon 2000) 2 (Wetzer 2001) 1 (Kilpert <i>et al.</i> 2012)	1 (Kilpert <i>et al.</i> 2012)	1 (Dreyer & Wägele 2001) 3 (Dreyer & Wägele 2002) 1 (Raupach <i>et al.</i> 2004) 1 (Osborn 2009) 4 (Raupach <i>et al.</i> 2009) 1 (Wägele <i>et al.</i> unpubl. data)	1 (Osborn 2009)	4 (Raupach <i>et al.</i> 2009)						
Joeropsididae	1 (Wetzer 2001)	1 (Wetzer 2001)	N/A	N/A	1 (Dreyer & Wägele 2002) 1 (Raupach <i>et al.</i> 2009)	N/A	N/A	1 (Raupach <i>et al.</i> 2009)				
Katianiridae	N/A	N/A	N/A	N/A	N/A	N/A	N/A	N/A				
Macrostylidae	21 (Riehl & Kaiser 2012)	39 (Riehl & Kaiser 2012) 10 (Riehl & Brandt 2013)	35 (Riehl & Kaiser 2012) 23 (Riehl & Brandt 2013)	2 (Raupach <i>et al.</i> 2004) 1 (Raupach <i>et al.</i> 2009) 3 (Riehl & Kaiser 2012)	N/A	N/A	2 (Raupach <i>et al.</i> 2009)					
Mesosignidae	N/A	N/A	N/A	N/A	1 (Raupach <i>et al.</i> 2004) 2 (Raupach <i>et al.</i> 2009)	N/A	N/A	2 (Raupach <i>et al.</i> 2009)				
Munnidae	1 (Fraser <i>et al.</i> 2011)	N/A	N/A	N/A	N/A	N/A	N/A	N/A				

Table1 continued.

	COI	12S	16S	18S	28S DI-3	28S D6-8
Munnopsidae	34 (Osborn 2009)	51 (Raupach <i>et al.</i> 2007)	N/A	1 (Dreyer & Wägele 2002) 4 (Wägele <i>et al.</i> 2003) 4 (Raupach <i>et al.</i> 2004) 8 (Raupach <i>et al.</i> 2007) 42 (Osborn 2009) 24 (Raupach <i>et al.</i> 2009) 2 (Wägele <i>et al.</i> unpubl. data)	37 (Osborn 2009)	4 (Raupach <i>et al.</i> 2007) 26 (Raupach <i>et al.</i> 2009)
Nannoniscidae	N/A	N/A	N/A	2 (Raupach <i>et al.</i> 2009)	N/A	2 (Raupach <i>et al.</i> 2009)
Paramunnidae	N/A	N/A	N/A	N/A	N/A	N/A
Steneriidae	N/A	N/A	N/A	1 (Raupach <i>et al.</i> 2004) 2 (Raupach <i>et al.</i> 2009)	N/A	2 (Raupach <i>et al.</i> 2009)
Thambematidae	N/A	N/A	N/A	N/A	N/A	N/A
Urstyliidae	N/A	N/A	N/A	N/A	N/A	N/A

they are still underdeveloped and lack standardized application, especially in taxonomy. The project *Barcoding Deep-sea Isopoda* (<http://www.cedamar.org/en/dna-barcoding.html>) was founded to implement such methods.

To date, molecular studies on deep-sea isopods are often not directly comparable because different DNA fragments were used. GenBank (Benson *et al.* 2008) queries for deep-sea isopods (using Isopoda as well as the respective family names as search terms) revealed relatively small numbers of sequences (Table 1) when compared to terrestrial or shallow-water crustaceans. The janiroid isopod family Munnopsidae is by far the most extensively studied group from the molecular perspective, followed by Macrostylidae, Haploniscidae and Desmosomatidae. For all these taxa, at least four loci have been studied. However, the majority of these data originate from only a few exemplary studies (altogether 18, and some based on shallow-water samples), covering a small range of species; for all other families, molecular data are almost or completely absent (Table 1).

The question is, why are there so few molecular studies on deep-sea isopods? One major problem might be the difficulty of obtaining fresh material containing intact DNA due to the remoteness of the habitat and related aspects of sampling. Protocols have been developed for DNA extraction from old and formalin-fixed collections (e.g. Schander & Halanych 2003; Boyle *et al.*

2004), but these produce only short DNA fragments (usually <200bp) and require large quantities of tissue as well as an enormous expenditure in terms of time and finances expense when compared to standard methods. Furthermore, problems with extraction or amplification of DNA from even “fresh” tissue have been frequently reported (Held 2000, Raupach *et al.* 2004, Raupach & Wägele 2006, Brix *et al.* 2011). Raupach *et al.* (2004) and Raupach & Wägele (2006) mention highly active nucleases that may quickly digest DNA, with reference to Dreyer & Wägele (2001, 2002). The latter however, only stated that material “fixed during field trips in warm ethanol yielded less DNA of high quality” compared to specimens that were fixed in ice-cold ethanol. However, finding the exact reason for the patterns observed by Dreyer & Wägele (2001, 2002) as well as the authors of the present paper and others (F. Leese, M. R. Raupach, W. Goodall-Copestake, pers. comm.) is beyond the scope of this article.

Nevertheless, the field and laboratory methods set the base line for any empirical study. In scientific publishing authors are usually encouraged to provide only short methodological protocols and important details may be omitted. In this paper, we provide a comprehensive description of our general methods. The markers employed here are suitable for a wide range of applications as they have strongly contrasting evolutionary rates and comprise mitochondrial as well as nuclear

fragments. Detailed descriptions of each relevant step from the collection and fixation of the samples to the cleanup of the PCR product and sequencing allow full reproducibility. We intend to push forward the integrative approach to isopod taxonomy and DNA barcoding in the remote and inaccessible deep-sea ecosystem.

Methods

Protocols for the widely-established markers COI, 16S and 18S are presented in detail. Furthermore, protocols are outlined for markers that have only rarely been used in deep-sea isopod systematics because they promise to be of value for taxonomy and systematics: 12S, and two fragments of the nuclear large subunit ribosomal RNA (28SD1–3 and 28SD6–8).

Our molecular methods presented here are not the result of any particular experimental design but rather a trial-and-error approach, and we thus cannot compare many alternative approaches in order to determine specific factors that may have an effect on the outcome of attempts to amplify and sequence DNA. Nevertheless, we are able to compare alternative universal primers for amplification success for the 16S marker.

The described methods were developed and tested during several deep-sea expeditions on the German research vessels (R/V) METEOR (M79/1, DIVA 3, and M85/3, IceAGE), POLAR-



Figure 1. The thermo boxes on the Camera Epibenthic Sledge (C-EBS; Brandt *et al.* 2013) are able to reduce warming of the samples during retrieval through the water column. A.) While the C-EBS is veered and heaved through the water column, the lever is extended (a). The thermo boxes (b) are closed. B.) When the C-EBS is at the bottom, the lever is pushed in and the thermo boxes are thus open (c) to reduce dynamic pressure.

STERN (ANTXXIV-1, ANDEEP-SYSTCO); and SONNE (SO223, KuramBio) to the North Atlantic, South-West Atlantic, North Pacific and Southern Ocean respectively. Subsequent laboratory studies were conducted at the Zoological Museum Hamburg (ZMH), at the Canadian Center for DNA

Barcoding (CCDB) and the Smithsonian Laboratories for Analytical Biology (LAB) as well as in the commercial LGC (Laboratory of the Government Chemist) genomics laboratories. General protocols, guidelines and recommendations for DNA Barcoding (Weigt *et al.* 2012) were followed. High-throughput methods were employed at LAB as well as in commercial laboratories. Based on Dreyer and Wägele's (2001, 2002) assumption (see above) and the unsuccessful DNA extractions during initial expeditions (DIVA-1), an undisturbed "cooling chain" was made first priority.

Sampling

Samples were collected by means of epibenthic sledges (EBS) as designed by Brenke (2005) and Brandt *et al.* (2013). Both models were equipped with thermally insulated boxes that enclose the cod ends of the nets as well as a spring-lever system that mechanically controls doors at the mouth of the sledge and allows for selectively collecting endo- and suprabenthic organisms only (Fig. 1) (Kaiser & Brenke in press). These are designed to have a minimal impact on dynamic pressures of the nets during trawling. During retrieval of the sledge from the ocean bottom, a closing mechanism that is connected to the spring-lever system of the sledges seals off the boxes. Water of the sampling depth is thus locked in and has an insulating effect on the cod ends of the nets. The cod ends themselves are

net buckets equipped with an optional rubber flap. The latter is designed to passively seal off the net bucket at its anterior end (opening) whenever the water current is directed against the trawling direction. While the gear with the samples is heaved through potentially warmer water layers, the samples are thus kept at the temperature of their origin (that is usually between -1.8°C and $+4^{\circ}\text{C}$), which should reduce the risk of DNA degradation within the samples. The flaps protect the samples from warm-water inflow as well as from being washed out by up-and-down movement of the ship in heavy sea conditions.

Fixation and preservation.

After retrieval of the sample from the gear (e.g. net bucket of EBS), samples were sieved ($300\ \mu\text{m}$) using chilled seawater (if required in a cooling room at approx. 2°C) and bulk-fixed in chilled (-30°C to -20°C) 96% ethanol (or higher; preferably non-denatured). Special care was taken care to minimize the amount of residual water in the sediment to be fixed, e.g. by washing the sample from the sieve into a bucket using pre-cooled ethanol instead of water in the last sieving step. Sample containers were used such that a minimum 5:1 ratio of container volume to sample volume was maintained. Jars of up to 5 L volume were used because larger containers have proven to be difficult to handle during later-on steps of the process. Jars were topped up with ethanol and then stored at -20°C to -30°C . During the first 24 h, the jars were carefully rolled



Figure 2. “Sorting on ice” set-up. Keeping the samples cool throughout the whole range of processes, from sampling until the extraction, seems to be beneficial for generating high-quality DNA sequences. A.) Ice dish used to cool the samples (not shown here) during the sorting process. B.) Ice bath with metal racks holding taxon vials.

every three to five hours in order to guarantee penetration of the ethanol through the sediment and to avoid separation of a water phase from the ethanol and subsequent freezing of that water phase. After 24 h, the fixation medium was decanted through a $300\ \mu\text{m}$ sieve and exchanged for new 96% non-denatured ethanol. Ethanol concentration in the samples was measured and a concentration of at least 70% was intended.

Sample sorting and determination

The subset of the samples to be used for DNA extraction was sorted directly onboard the research vessels. The EBS models used (Brenke 2005, Brandt *et al.* 2013) contain two separate samplers which are arranged on top of each other. The upper (supra) net was usually best suited because it has proven to be frequently the cleanest and thus fastest to sort. Other fractions of the samples were either fixed in formaldehyde and preserved in 80%

Table 2. 12S, 16S and COI primers used for amplification and sequencing of deep-sea isopod DNA.

Primer name	Sequence [5' – 3']	Reference
16S AR	CGCCTGTTTATCAAAAACAT	(Palumbi <i>et al.</i> 1991)
16S BR	CCGGTCTGAACTCAGATCACG	(Palumbi <i>et al.</i> 1991)
16S SF	GACCGTGCTAAGGTAGCATAATC	(L. M. Tsang, pers. comm.)
16S SR	CCGGTCTGAACTCAAATCGTG	(Tsang <i>et al.</i> 2009)
H13842-12S	TGTGCCAGCASCTGCGGTTAKAC	(Ryuji Machida, pers. comm.)
L13337-12S	YCTWTGYTACGACTTATCTC	(Ryuji Machida, pers. comm.)
dgLCO1490 (COI)	GGTCAACAAATCATAAAGAYATYGG	(Meyer <i>et al.</i> 2005)
dgHCO2198 (COI)	TAAACTTCAGGGTGACCAAAARAAYCA	(Meyer <i>et al.</i> 2005)
LCO1490 (COI)	TCAACAAATCATAAAGATATTGG	(Folmer <i>et al.</i> 1994)
HCO2198 (COI)	TAAACTTCAGGGTGACCAAAAAATCA	(Folmer <i>et al.</i> 1994)
CrustCOIF (COI)	TCAACAAATCAYAAAGAYATTGG	(Teske <i>et al.</i> 2006)
DecapCOIR (COI)	AATTAATAATRTAWACTTCTGG	(Teske <i>et al.</i> 2006)

denatured ethanol or fixed and preserved in 70–96% denatured ethanol. Sample sorting started after 48 hours of fixation. Stereo microscopes were used for sorting, which was conducted at room temperature. However, all jars, vials and sorting dishes as well as squeeze bottles with extra ethanol were kept on ice at all times using ice baths, chilled metal racks and the like (Fig. 2).

Isopods were identified to species level whenever possible using original scientific literature, identification keys and expert knowledge (family level minimum). They were individually separated as vouchers to allow for more exact determination in the lab. Individual numbers allow tracing each DNA sequence back to the specimen it originated from. Specimens are deposited and stored in freezers at the Senckenberg German Center for Marine Biodiversity Research (Deutsches Zentrum für Marine Biodiversitätsforschung, DZMB) in Hamburg and given DZMB numbers using the local Access 2010 database (Brix *et al.* 2012) or at

the ZMH

Tissue dissection

Tissue was dissected under sterile conditions and on ice. This was conducted on board immediately after sorting and identification, whenever ship time and sea state allowed. Otherwise, this step was conducted in the home laboratory. To minimize the morphological damage, only small amounts of limb tissue were dissected (one to three walking legs from one side from janiroidean isopods, depending on the size of the specimen). Otherwise, specimens were kept intact for vouchering and to allow further morphological studies and identification. Tissue was preserved until extraction in a minimal volume of ethanol (one drop from a 20 µL pipette) or extraction buffer (15 µL) and kept frozen (–20°C) whenever possible.

Transport and shipping

Samples and tissue were transported under cold conditions whenever possible. For domestic land-

Table 3. 18S sequencing primers used for deep-sea isopods.

Primer name	Sequence [5' – 3']	Reference
Forward		
18A1mod	CTGGTTGATCCTGCCAGTCATATGC	(Raupach <i>et al.</i> 2009)
A700Fmod	GCCGCGGTAATTCCAGC	(Raupach <i>et al.</i> 2009)
1155F	GTGAAACTTAAAGGAATTGACGG	(Dreyer & Wägele 2001)
1250FNmod	GGCCGTTCTTAGTTGGTGGAG	(Raupach <i>et al.</i> 2009)
Reverse		
1800mod	GATCCTTCCGCAGGTTACCTACG	(Raupach <i>et al.</i> 2009)
700R	CGCGGCTGCTGGCACCAGAC	(Dreyer & Wägele 2001)
1155R	CCGTCAATTCCTTTAAGTTTCAG	(Dreyer & Wägele 2001)
1500mod	CATCTAGGGCATCACAGACC	(Raupach <i>et al.</i> 2009)
Previous studies:		
1000F	CGATCAGATACCGCCCTAGTTC	(Dreyer & Wägele 2001)

based transport, dry ice was preferred. International sea-shipping was conducted using freezing containers. For international priority air shipping of the tissue, Styrofoam boxes and cooling packs were used that guaranteed 4°C or less for more than 48 h (tested in laboratory).

Total DNA extraction.

Residual ethanol was removed from the tissue by evaporation at room temperature. At LAB, extractions were done on an AutoGenPrep 965 following the manufacturer's protocol for animal tissue. Tissue digestion was performed overnight in a shaking bath at 56°C and 50 rpm using the AutoGen buffers and proteinase K. The suspension volume of extracted total DNA was 50 µL.

At LGC Genomics, the samples were homogenized with steel beads and extracted using the sbeadex forensic kit according to the manufacturer's protocol.

PCR at LGC Genomics

The complete 18S sequence as well as fragments of 16S and COI were separately amplified respectively using a 20 µL reaction volumes containing 1.0 µL DNA, 2 µL 5xBiostab PCR Optimizer, 4 µL Reaction Buffer (MyTaq Bioline 5x, containing dNTP and MgCl₂), 0.2 µL MyTaq Polymerase (5 µ/µL), 1 µL of each primer (5 pmol/µL), and 10.8 µL nuclease-free H₂O.

COI. For COI, the universal primers of Folmer *et al.* (1994) were used (LCO1490/HCO2198, Table 1). The PCR temperature profile consisted of an initial denaturation at 94°C (10 min), followed by 5 cycles of denaturation at 96°C (1 min), annealing at 45°C (45 s) and extension at 72°C (1 min). These cycles were followed by another 35 cycles of denaturation at 93°C (1 min), annealing at 50°C (45 s) and extension at 72°C (1 min) followed by a final extension at 72°C (5 min). Cycle sequencing was performed using the same primers as used for PCR.

Table 4. 28S D1-3 PCR and cycle-sequencing (CS) primers used for deep-sea isopods.

Primer name	Sequence [5' – 3']	Reference
Forward		
LSUD1F	ACCCGCTGAATTTAAGCATA	(Lenaers <i>et al.</i> 1989)
Reverse		
D3AR	ACGAACGATTTGCACGTCAG	(Lenaers <i>et al.</i> 1989)

16S. For 16S, the SF/SR primer pair was employed (Tsang *et al.* 2009). The PCR temperature profile consisted of an initial denaturation at 95°C (10 min), followed by 36 cycles of denaturation at 95°C (30 s), annealing at 48°C (30 s) and extension at 72°C (45 s). These cycles were followed by a final extension at 72°C (5 min). Cycle sequencing was performed using the same primers as used for PCR (Table 1).

18S. 18S was amplified in partially overlapping fragments using three primer pairs (18 A1 & 700 R; 400 F & 1155 R; 1000 F & 1800). The PCR profile comprised an initial denaturation at 95°C (10 min), followed by 36 cycles of denaturation at 94°C (30 s), annealing at 54°C (45 s) and extension at 72°C (3 min 12 s) followed by a final extension at 72°C (10 min). Cycle sequencing was performed using the same primers as used for PCR (Table 2).

PCR at LAB

Amplification and cycle sequencing reactions were mostly carried out on Peltier PTC200 and PTC225 Thermal Cyclers (MJ Research) and 2720 Thermal Cyclers (Applied Biosystems).

Mitochondrial genes. Three mitochondrial genes were partially amplified and sequenced.

The approximately 450–500 bp fragment of 16S rRNA, an approximately 650 bp fragment of COI and an approximately 550 bp fragment of 12S were amplified separately using reaction volumes of respectively 10 µL containing 0.25 µL BSA, 0.5 µL dNTP [2.5 mM each], 1 µL Bioline 10xNH4 reaction buffer, 0.3 µL of each primer [10 µM], 0.5 µL Biolase MgCl₂ [50 mM], 0.1 µL Biolase DNA Pol [5 u/µL], 2 µL of template DNA and nuclease-free H₂O. For 16S and 12S, the same primers were used for PCR amplification and cycle sequencing. Primers are listed in Table 2.

In most cases for COI, PCR amplification was carried using the primers dgLCO1490/dgHCO2198 which had been tagged with M13 primers. In these cases, M13 primers were then used for subsequent cycle sequencing. For several specimens, the primer pair LCO1490/HCO2198 were successfully used to amplify COI where dgLCO1490/dgHCO2198 failed. The PCR temperature profile in both cases for both sets of primers consisted of an initial denaturation at 95°C (5 min), followed by 34–36 cycles of denaturation at 95°C (30 s), annealing at 48°C (30 s) and extension at 72°C (45 s) followed by a final extension at 72°C (5 min). Sequencing and PCR primers were iden-

tical for specimens amplified with LCO1490. For cycle sequencing 30 cycles of 95°C (30 s), 48°C (30 s) and 60°C (4 min) were employed.

18S. At LAB, the complete 18S gene was amplified in a 20 µL reaction volume containing 0.5 µL BSA, 1.0 µL dNTP [2.5 mM each], 2.0 µL Bioline 10xNH4 reaction buffer, 0.6 µL of each primer [10 µM], 1.0 µL Biolase MgCl₂ [50 mM], 0.2 µL Biolase DNA Pol [5 u/ µL], 4.0 µL of template DNA and nuclease-free H₂O. PCR primers used were 18SA1mod/1800mod (Table 3). The PCR temperature profile consisted of an initial denaturation at 95°C (5 min), followed by 34 cycles of denaturation at 95°C (1 min), annealing at 55°C (1 min) and extension at 72°C (3 min), and a final extension at 72°C (7 min). Cycle sequencing was performed using the PCR primers plus additional primers (altogether five forward and five reverse; Table 3). For cycle sequencing, 30 cycles of 95°C (30 s), 50°C (30 s) and 60°C (4 min) were employed. This protocol is based Raupach *et al.* (2009).

28S. The 28S D1-D3 fragment was amplified in a 10 µL reaction volume containing 0.13 µL BSA, 0.5 µL dNTP [2.5mM each], 1 µL Bioline 10xNH4 reaction buffer, 0.3 µL of each primer [10µM], 0.5 µL Biolase MgCl₂ [50 mM], 0.1 µL Biolase DNA Pol [5 u/µL], 2 µL of template DNA and nuclease-free H₂O. PCR and cycle sequencing primers used were LSUD1F/D3AR (Table 3). Amplification and cycle sequencing reactions were mostly carried out on Peltier Thermal Cyclers

PTC200 and PTC225 (MJ Research) and 2720 Thermal Cyclers (Applied Biosystems). The PCR temperature profile consisted of an initial denaturation at 95°C (5 min), followed by 40 cycles of denaturation at 95°C (1 min), annealing at 60°C (1 min) and extension at 72°C (3 min), and a final extension at 72°C (7 min). Cycle sequencing was performed using the same primers as used for PCR. For cycle sequencing 30 cycles of 95°C (30 s), 50°C (30 s) and 60°C (4 min) were employed. This protocol was adapted from Osborn (2009) and primers are listed in Table 3.

The 28S D6-D8 fragment was amplified in a 10 µL reaction volume containing 0.13 µL BSA, 0.5 µL dNTP [2.5 mM each], 1 µL Bioline 10xNH4 reaction buffer, 0.3 µL of each primer [10 µM], 0.5 µL Biolase MgCl₂ [50 mM], 0.1 µL Biolase DNA Pol [5 u/µL], 2 µL of template DNA and nuclease-free H₂O. PCR and cycle sequencing primers used were 28EE/D8R (Tab 3). Amplification and cycle sequencing reactions were mostly carried out on Peltier PTC200 and PTC225 Thermal Cyclers (MJ Research) and 2720 Thermal Cyclers (Applied Biosystems). The PCR temperature profile consisted of an initial denaturation at 95°C (5 min), followed by 35 cycles of denaturation at 95°C (1 min), annealing at 55°C (1 min) and extension at 72°C (2 min), and a final extension at 72°C (7 min). Cycle sequencing was performed using the primers listed in Table 3. For cycle sequencing 30 cycles of 95°C (30 s), 50°C (30 s) and 60°C (4 min) were

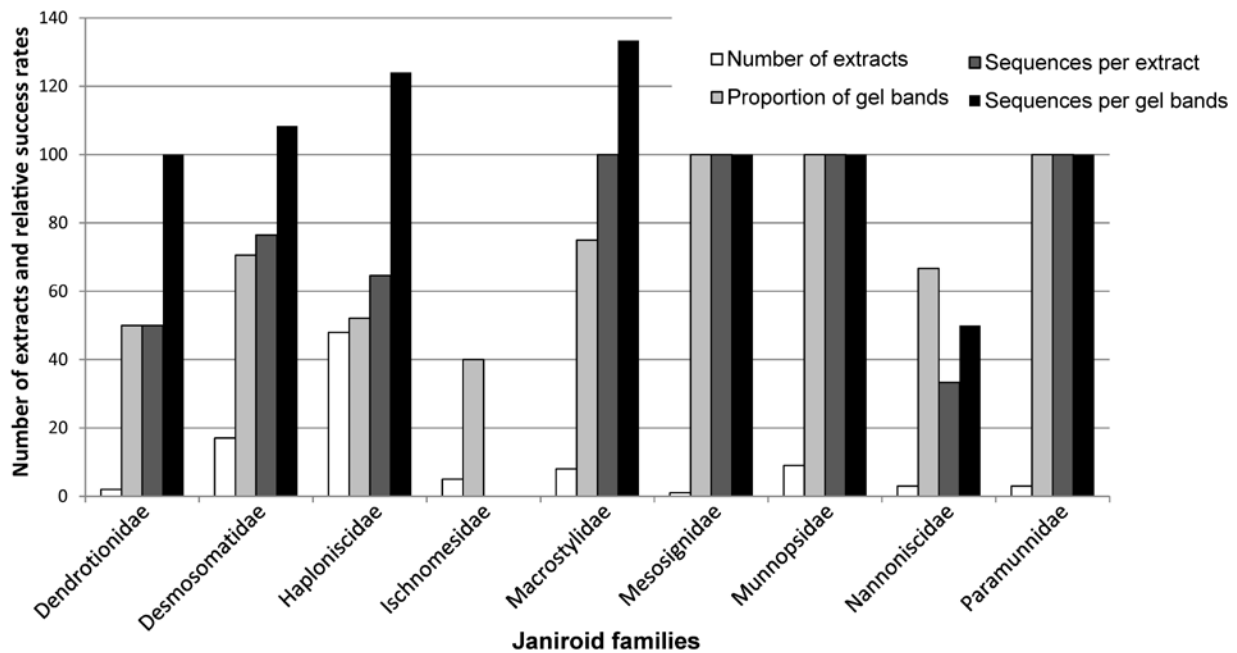


Figure 3. Success rates of amplification and sequencing using the universal 16S AR/BR primer pair. The success rates beyond 100% in case of the number of sequences per gel band can be explained by low diagnostic power of the gel bands. PCR products might contain too low concentrations of DNA to show up on an ethidium-bromide stained agarose gel. It might still contain sufficient DNA for successful sequencing. The graph shown is based on 96 samples belonging to nine janiroid (Isopoda: Asellota) families. Samples were collected during the expedition DIVA-3 with research vessel Meteor in the South Atlantic.

applied. This protocol was adapted from Raupach *et al.* (2009) and primers are listed in Table 4.

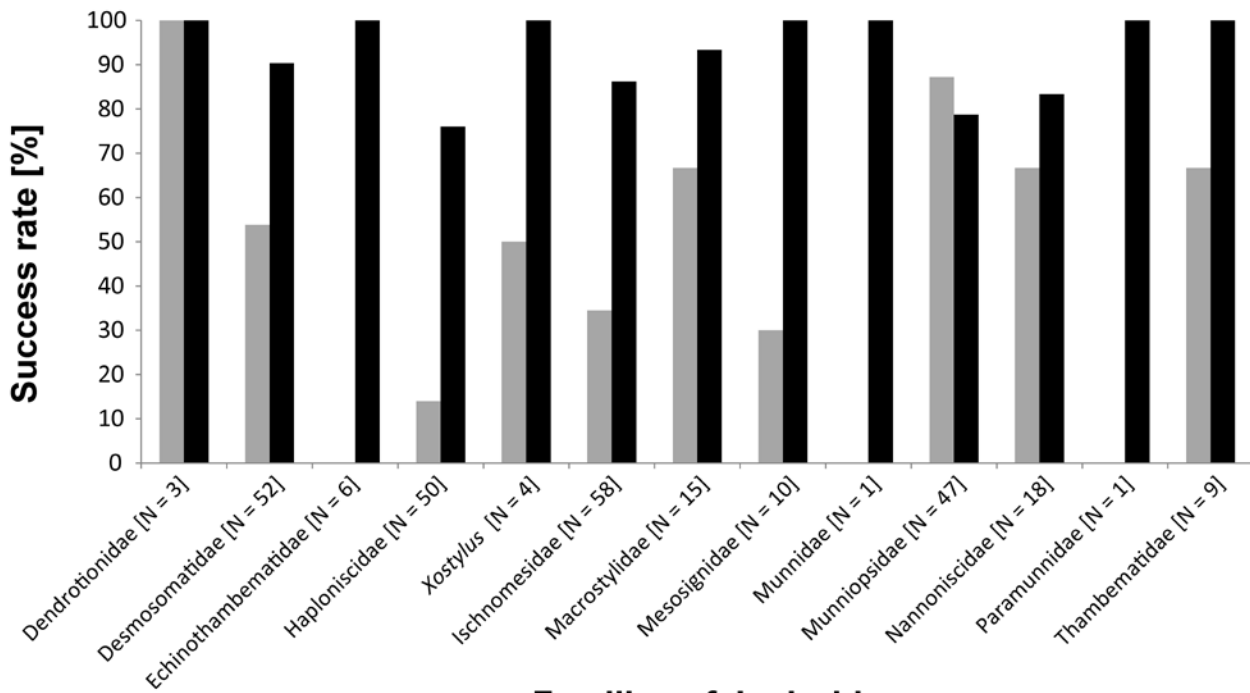
For cycle sequencing, 2.0 μ L of PCR product was analyzed for purity and size conformity by electrophoresis in a 1.5% agarose gel with ethidium bromide. The remaining PCR product was purified using ExoSap-IT (USB). A 5x dilution of the enzyme was used and 2 μ L of that solution were added to 8 μ L PCR product (or 4 μ L were added to 18 μ L PCR product). Samples were incubated for at 37°C (30 min) and the enzyme was deactivated at 80°C (20 min). Cycle sequencing was performed in 10 μ L volume containing 1 μ L purified PCR product, 0.5 μ L BigDye Terminator, 1.75 μ L Big Dye Terminator reaction buffer, 0.5 μ L primer and nuclease-free water. Cycle sequencing products

were cleaned up with the Sephadex G-50 (Sigma S-5897) method, dried and stored at -20°C until run on a 3730xl DNA Analyzer.

Multiple sequence alignment was conducted to analyze divergence within and between taxa. The widely applied alignment programs ClustalW (Thompson *et al.* 1994) and MAFFT (Katoh *et al.* 2002) were used and subsequently alignments were checked and corrected by hand where necessary.

Results

Our first attempts to extract DNA from deep-sea isopods were performed in the year 2000 with the beginning of the DIVA project (*Latitudinal Gradients of deep-sea BioDiversity in the Atlantic*



Families of Janiroidea

Figure 4. Amplification success using the universal primer pairs 16S AR/BR versus 16S SF/SR sorted by family of Janiroidea (Isopoda). The graph is based upon a dataset comprising 13 janiroid families and altogether 274 species. The same extracts were used as templates for both PCRs. Samples were collected during the DIVA-3 expedition on RV Meteor. Lab work took place at the Smithsonian Laboratories of Analytical Biology. Except for Dendrotoniidae and Munnopsidae, the 16S SF/SR primer pair consistently provided higher success rates compared to the 16S AR/BR primer pair.

Ocean) and the initial expedition DIVA-1 (M48-1) to the Southeast Atlantic Ocean. Unfortunately, all extractions were unsuccessful (Brix *et al.* 2014). Based on the observations of Dreyer and Wägele (2001, 2002) an undisturbed “cooling chain” was made our first priority during subsequent expeditions. While DIVA-2 (M63-2, 2005) was a first attempt and resulted in sample-by-sample extractions of about 280 single isopod specimens, during DIVA-3 (M79-1, 2009), standardized protocols as described above were applied. As these seemed to increase the success rate from around 40–60% (DIVA-2) to over 70%, this approach was followed further with additional stepwise modifications.

Through the above-mentioned protocols,

we were able to obtain sequences for 15 families of Janiroidea (Dendrotoniidae, Desmosomatidae, Echinothambematidae, Haplomunnidae, Haplomniscidae, Ischnomesidae, Joeropsidae, Katianiridae, Macrostylidae, Munnidae, Munnopsidae, Nannomniscidae, Paramunnidae, Stenetriidae, Thambematidae) and *Xostylus (insertae sedis)*. Furthermore, sequences could be obtained for Valvifera (Arcuridae and Idoteidae), Cymothoidea (Cirolanidae, Gnathiidae, Leptanthuridae), Sphaeromatidea (Serolidae, Brandt *et al.* in press) which are rather rare in the deep sea and thus limited in numbers in our samples. The first pioneer studies on Desmosomatidae (Brix *et al.* in press, 2014, Schnurr & Brix 2012), Haplomniscidae (Brix *et al.* 2011) and Mac-

rostylidae (Riehl & Kaiser 2012, Riehl & Brandt 2013) have been published and other taxonomic and phylogenetic studies are in progress.

Due to financial restrictions, we concentrated on COI and 16S. For these markers, in total about 2300 specimens of isopods, 100 amphipods and 300 tanaids were amplified and sequenced. The other markers were sequenced for only a subset of the samples. We failed to find a set of primers for the mitochondrial markers used that would consistently amplify DNA from all isopod taxa. Variability in success was apparent even within families. PCR were conducted in 96-well plates and whenever at least 50% of the wells showed distinct gel bands, the whole 96-well plate was carried further for cycle sequencing.

Due to this approach, we observed that even when the amplification product was too low in concentration to be detected on an agarose gel, it often was a suitable template for cycle sequencing (Fig. 3). Regarding 16S, the 16S SR/16S SF primers generally led to better amplification success than the universal primers 16S AR/BR (Fig. 3). Application of 16S AR in combination with 16S SR was also successful and led to a slightly longer fragment. We observed that universal primers for COI (Folmer *et al.* 1994) were for some taxa not as reliable as primers for 16S (Tsang *et al.* 2009) resulting in incomplete datasets (Fig. 4).

Discussion

During the last decade and in the context of the *Barcoding Deep-sea Isopoda* project, the protocols presented in this paper have been evolving gradually and were applied to a wide range of isopods as well as other peracarids (Amphipoda and Tanaidacea). Due to space restrictions, only the state of the art is presented in this paper but the yield of high-quality sequences grew from around 40% to substantially more than 80% in certain taxa (see Fig.4). Despite the apparent usefulness of genetic data to address systematic questions in biological studies (Hebert *et al.* 2003, Pons *et al.* 2006), these data have rarely been applied for deep-sea Isopoda so far. By closing a methodological information gap that might be partly responsible for this situation, the present paper aims to promote the application of standardized and field-tested molecular methods on deep-sea isopods.

Since the start of the *Barcoding Deep-sea Isopoda* project, the focus lay on gathering samples as well as developing and testing molecular methods. As a next step, reference databases need to be filled with quality-tested data. We are using the *Barcode of Life Database* (BoLD) for data storage and projects will soon be made publicly available with continuing publication of our research.

One major problem that we face at the current stage is stems from the lack of similar sequences on GenBank (Benson *et al.* 2008). Another major

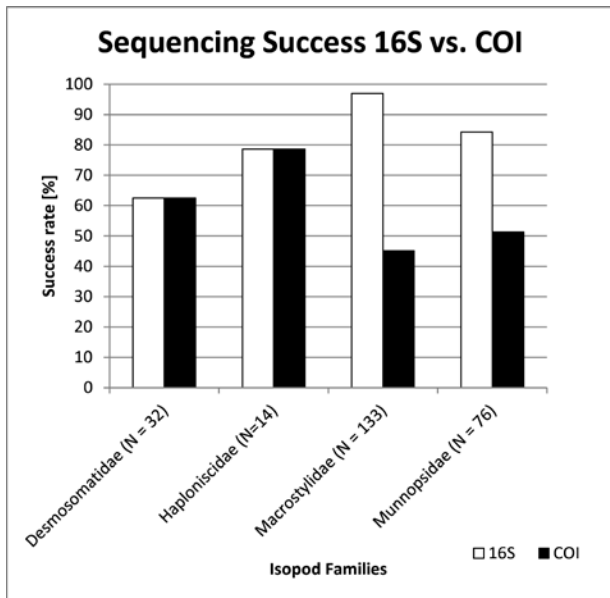


Figure 5. Success rates compared for sequencing cytochrome-c-oxidase subunit I (COI) and the mitochondrial large ribosomal RNA subunit (16S). Data for only those isopod families are shown were predominantly used for tissue dissection during the KuramBio expedition. Success rates for Desmosomatidae and Haplomiscidae were similar (below 80%) for both markers. For Macrostylidae and Munnopsidae, 16S could be sequenced much more reliably (96% and 84% success) using universal primers than COI (45% and 51% success).

concern is potentially related to primer mismatches. It is due to the pioneering nature of current molecular investigations on deep-sea isopods that a publicly available database does not exist to compare the new results against. Already within deep-sea isopod families, such as Macrostylidae (Riehl & Brandt 2013), Desmosomatidae (Brix *et al.* 2014), Haplomiscidae (Brix *et al.* 2011) or Munnopsidae (Osborn 2009), relatively fast-evolving markers, such as COI and 16S show variation clearly above 20% uncorrected p-distance (Brix *et al.* in press, 2011, Riehl & Brandt 2013). These values reach levels that are strongly influenced by saturation effects. Consequently, within families sequence di-

vergence can be similar to that between any isopod and other peracarid crustaceans or even hexapods. As a result, using the megablast search (Altschul *et al.* 1990, Zhang *et al.* 2000) in the context of contamination checking, the most frequent results comprise insects. The risk of missing contaminations, especially those caused by other deep-sea crustaceans for example during the sample handling, is consequently relatively high. By continuously publishing new data, we are working to overcome this situation.

While the methods described in this article are specifically designed to work on deep-sea isopods, Asellota in particular, to some extent they provide a first step for molecular research on other peracarid groups as well. The methods for COI have been tested extensively and successfully on Amphipoda (Havermans *et al.* 2013) and Tanaidacea (Błażewicz-Paszkowycz *et al.* in press). Most effort was spent on developing the protocols for the faster evolving DNA markers (COI, 16S, 12S) and especially the first two were most widely applied. However, due to their slower evolutionary rates and consequently more conserved priming regions, the 18S and 28S protocols can likely be regarded as more universal.

The statement that nucleases in isopods are particularly active cannot be substantiated here. However, our experience shows that an immediate transfer of the sample upon arrival on deck into cold (-20°C) conditions is preferable. This is in

accordance with previous assumptions (Dreyer & Wägele 2002, Raupach *et al.* 2004). We therefore suggest that in cases where the sample retrieved from the gear contains only negligible amounts of sediment, it should be fixed with chilled high-grade ethanol immediately and without sieving.

We further recommend dissecting tissue for DNA extraction directly on board and after an over-all fixation period of 48 hours. Although we cannot prove this statistically, the cooling chain and fresh tissue may be regarded as essential for a high success rate. However, there is evidence (not shown here) suggesting that acceptable results might be possible even after two years of storage as long as the samples were constantly kept in chilled conditions as recommended for various other taxa (Quicke *et al.* 1999, Gemeinholzer *et al.* 2010, Nagy 2010).

Recommended next steps

The protocols presented in this paper allowed sequencing of about 2300 specimens of isopods, 100 amphipods, and 300 tanaids and provide the first large-scale approach to sequencing DNA from deep-sea isopods. We were able to make family-specific suggestions regarding 16S primer choice. However, our results indicate that further optimization is required: Sequencing the barcoding marker COI was prone to a high rate of contamination and failed sequencing runs compared to e.g. 16S (Fig. 5). The alignments across families revealed variability beyond 30% uncorrected p-distance and only a very limited number of conserved sites. We

assume that the primer region might be variable in other Janiroidea as well. may Taxon-specific primers may need to be created in order to achieve a higher yield (compare, Derycke *et al.* 2010, Zeale *et al.* 2011).

The methods presented here were not tested using an experimental design. To further and more qualitatively evaluate the effects that sampling devices, storage and fixation temperature, working speed and laboratory methods have on the quality of the DNA, we recommend a thoroughly designed experimental setup. Too many variables might have influenced DNA degradation for us to distinguish the most crucial variables at the present time.

References

- Allcock, A. L., Barratt, I., Eléaume, M., Linse, K., Norman, M. D., Smith, P. J., Steinke, D., Stevens, D. W. & Strugnell, J. M. (2011) Cryptic speciation and the circumpolarity debate: A case study on endemic Southern Ocean octopuses using the COI barcode of life. *Deep Sea Research Part II: Topical Studies in Oceanography*, 58(1-2), 242–249.
- Altschul, S. F., Gish, W., Miller, W., Myers, E. W. & Lipman, D. J. (1990) Basic local alignment search tool. *Journal of molecular biology*, 215(3), 403–410.
- Asmyhr, M. G. & Cooper, S. J. B. (2012) Difficulties barcoding in the dark: the case of crustacean stygofauna from eastern Australia. *Invertebrate Systematics*, 26(6), 583–591.
- Barbier, E. B., Moreno-Mateos, D., Rogers, A. D., Aronson, J., Pendleton, L., Danovaro, R., Henry, L. A., Morato, T., Ardrón, J. & Van Dover, C. L. (2014) Protect the deep sea. *Nature*, 505(7484), 475–477.
- Benson, D. A., Karsch-Mizrachi, I., Lipman, D. J., Ostell, J. & Wheeler, D. L. (2008) GenBank. *Nucleic Acids Research*, 36(Database issue), D25–30.
- Błazewicz-Paszkowycz, M., Jennings, R. M., Jeskulke, K. & Brix, S. (in press) Discovery of ‘swimming’ males of Paratanaoidea (Tanaidacea). *Polish Polar Research*, 35(2).

- Boyle, E. E., Zardus, J. D., Chase, M. R., Etter, R. J. & Rex, M. A. (2004) Strategies for molecular genetic studies of preserved deep-sea macrofauna. *Deep-Sea Research Part I*, 51(10), 1319–1336.
- Brandt, A., Brix, S., Held, C. & Kihara, T.-C. (in press) Rare in the deep- enigmatic species of the Serolidae Dana, 1853 (Crustacea: Isopoda) revisited. Description of a new species of *Glabroserolis* and redescription of *Atlantoserolis vema* Menzies, 1962. *Zoological Journal of the Linnean Society*.
- Brandt, A., Elsner, N., Brenke, N., Golovan, O., Malyutina, M. V., Riehl, T., Schwabe, E. & Würzberg, L. (2013) Epifauna of the Sea of Japan collected via a new epibenthic sledge equipped with camera and environmental sensor systems. *Deep Sea Research Part II: Topical Studies in Oceanography*, 86-87, 43–55.
- Brandt, A., Gooday, A. J., Brandao, S. N., Brix, S., Brökeland, W., Cedhagen, T., Choudhury, M., Cornelius, N., Danis, B., de Mesel, I., Diaz, R. J., Gillan, D. C., Ebbe, B., Howe, J. A., Janussen, D., Kaiser, S., Linse, K., Malyutina, M. V., Pawlowski, J., Raupach, M. J. & Vanreusel, A. (2007) First insights into the biodiversity and biogeography of the Southern Ocean deep sea. *Nature*, 447(7142), 307–311.
- Brenke, N. (2005) An epibenthic sledge for operations on marine soft bottom and bedrock. *Marine Technology Society Journal*, 39(2), 10–21.
- Brix, S., Bauernfeind, W., Brenke, N., Blazewicz-Paszkowycz, M., Borges, V., Buldt, K., Cannon, J., Díaz Agras, G., Fiege, D., Fiorentino, D., Haraldsdóttir, S., Hoffmann, S., Holst, S., Hüttmann, F., Jeskulke, K., Jennings, R. M., Kocot, K., Khodami, S., Lucas Rodriguez, Y., Martinez Arbizu, P., Meißner, K., Mikkelsen, N., Miller, M., Murray, A., Neumann, H., Ostman, A., Riehl, T., Schnurr, S., Svavarsson, J. & Yasuhara, M. (2012) IceAGE - Icelandic marine Animals: Genetics and Ecology [online]. Hamburg: Senatskommission für Ozeanographie der Deutschen Forschungsgemeinschaft MARUM – Zentrum für Marine Umweltwissenschaften der Universität Bremen Leitstelle Deutsche Forschungsschiffe Institut für Meereskunde der Universität Hamburg. (METEOR Reports; 85-3).
- Brix, S., Leese, F., Riehl, T. & Kihara, T. C. (2014) A new genus and new species of Desmosomatidae Sars, 1897 (Isopoda) from the eastern South Atlantic abyss described by means of integrative taxonomy. *Marine Biodiversity*, [online]. Available from: <http://link.springer.com/10.1007/s12526-014-0218-3>. [Accessed 2014-05-06].
- Brix, S., Riehl, T. & Leese, F. (2011) First genetic data for *Haploniscus rostratus* and *Haploniscus unicornis* from neighbouring deep-sea basins in the South Atlantic. *Zootaxa*, 2838, 79–84.
- Brix, S., Svavarsson, J., Martinez Arbizu, P. & Leese, F. (in press) A multi-gene analysis reveals overlooked species with different bathymetric preferences inside the isopod *Chelator insignis* (Hansen, 1916) south of Iceland. *Polish Polar Research*, 35(2).
- Brökeland, W. (2010) Description of four new species from the *Haploniscus unicornis* Menzies, 1956 complex (Isopoda: Asellota: Haploniscidae). *Zootaxa*, 2536, 1–35.
- Brökeland, W. & Raupach, M. J. (2008) A species complex within the isopod genus *Haploniscus* (Crustacea: Malacostraca: Peracarida) from the Southern Ocean deep sea: a morphological and molecular approach. *Zoological Journal of the Linnean Society*, 152(4), 655–706.
- Derycke, S., Vanaverbeke, J., Rigaux, A., Backeljau, T. & Moens, T. (2010) Exploring the use of cytochrome oxidase c subunit 1 (COI) for DNA barcoding of free-living marine nematodes. *PLoS ONE*, 5(10), e13716.
- Dreyer, H. & Wägele, J.-W. (2001) Parasites of crustaceans (Isopoda: Bopyridae) evolved from fish parasites: Molecular and morphological evidence. *Zoology*, 103, 157–178.
- Dreyer, H. & Wägele, J.-W. (2002) The Scutocoxifera tax. nov. and the information content of nuclear ssu rDNA sequences for reconstruction of isopod phylogeny (Peracarida: Isopoda). *Journal of Crustacean Biology*, 22(2), 217–234.
- Folmer, O., Black, M., Hoeh, W., Lutz, R. & Vrijenhoek, R. (1994) DNA primers for amplification of mitochondrial cytochrome c oxidase subunit I from diverse metazoan invertebrates. *Molecular Marine Biology and Biotechnology*, 3(5), 294–299.
- Fraser, C. I., Nikula, R. & Waters, J. M. (2011) Oceanic rafting by a coastal community. *Proceedings of the Royal Society B: Biological Sciences*, 278(1706), 649–655.
- Gage, J. D. (2004) Diversity in deep-sea benthic macrofauna: the importance of local ecology, the larger scale, history and the Antarctic. *Deep Sea Research Part II: Topical Studies in Oceanography*, 51(14-16), 1689–1708.
- Gemeinholzer, B., Rey, I., Weising, K., Grundmann, M., Muellner, A. M., Zetzsche, H., Droege, G., Seberg, O., Petersen, G., Rawson, D. & Weigt, L. A. (2010) Organizing specimen and tissue preservation in the field for subsequent molecular analyses. In: Eymann, J., Degrege, J., Häuser, C., Monje, J. C., Samyn, Y., & Vanden Spiegel, D. (Eds.) *Manual of Field Recording Techniques and Protocols for All Taxa Biodiversity Inventories*. pp 129–157.
- Gibbs, J. (2009) Integrative taxonomy identifies new (and old) species in the *Lasioglossum (Dialictus) tegulare* (Robertson) species group (Hymenoptera, Halictidae). *Zootaxa*, 2032, 1–38.
- Glasby, G. P. (2002) Deep seabed mining: past failures and future prospects. *Marine Georesources and Geotechnology*, 20(2), 161–176.
- Hausdorf, B. (2011) Progress toward a general species concept. *Evolution*, 65(4), 923–931.
- Havermans, C., Sonet, G., d’Udekem d’Acoz, C., Nagy, Z. T.,

- Martin, P., Brix, S., Riehl, T., Agrawal, S. & Held, C. (2013) Genetic and morphological divergences in the cosmopolitan deep-sea amphipod *Eurythenes gryllus* reveal a diverse abyss and a bipolar species. *PLoS ONE*, 8(9), e74218.
- Hebert, P. D. N., Cywinska, A., Ball, S. L. & deWaard, J. R. (2003) Biological identifications through DNA barcodes. *Proceedings of the Royal Society of London, Series B: Biological Sciences*, 270(1512), 313–321.
- Held, C. (2000) Phylogeny and biogeography of serolid isopods (Crustacea, Isopoda, Serolidae) and the use of ribosomal expansion segments in molecular systematics. *Molecular Phylogenetics and Evolution*, 15(2), 165–178.
- Hessler, R. R., Wilson, G. D. F. & Thistle, D. (1979) The deep-sea isopods: a biogeographic and phylogenetic overview. *Sarsia*, 64(1-2), 67–75.
- Hillis, D. M. & Dixon, M. T. (1991) Ribosomal DNA: molecular evolution and phylogenetic inference. *The Quarterly Review of Biology*, 66(4), 411–453.
- Hoagland, P., Beaulieu, S., Tivey, M. A., Eggert, R. G., German, C., Glowka, L. & Lin, J. (2010) Deep-sea mining of seafloor massive sulfides. *Marine Policy*, 34(3), 728–732.
- Kaiser, S. & Brenke, N. (in press) Epibenthic sledges. In: Clark, M. R., Consalvey, M., & Rowden, A. A. (Eds.) *Biological Sampling in the Deep Sea*. Wiley-Blackwell.
- Katoh, K., Misawa, K., Kuma, K. & Miyata, T. (2002) MAFFT: a novel method for rapid multiple sequence alignment based on fast Fourier transform. *Nucleic Acids Research*, 30(14), 3059–3066.
- Kilpert, F., Held, C. & Podsiadlowski, L. (2012) Multiple rearrangements in mitochondrial genomes of Isopoda and phylogenetic implications. *Molecular Phylogenetics and Evolution*, 64(1), 106–117.
- Lenaers, G., Maroteaux, L., Michot, B. & Herzog, M. (1989) Dinoflagellates in evolution. A molecular phylogenetic analysis of large subunit ribosomal RNA. *Journal of Molecular Evolution*, 29(1), 40–51.
- Linse, K., Jackson, J. A., Malyutina, M. V. & Brandt, A. (2014) Shallow-water northern hemisphere *Jaera* (Crustacea, Isopoda, Janiridae) found on whale bones in the Southern Ocean deep sea: ecology and description of *Jaera tyleri* sp. nov. *PLoS ONE*, 9(3), e93018.
- Mallet, J. (1995) A species definition for the modern synthesis. *Trends in Ecology & Evolution*, 10(7), 294–299.
- Mayr, E. (1942) *Systematics and the Origin of Species: From the Viewpoint of a Zoologist* [online]. New York: Columbia University Press. Available from: http://books.google.de/books?hl=de&lr=&id=mAljnLp6r_MC&oi=fnd&pg=PR9&dq=Systematics+and+the+origin+of+species+from+the+viewpoint+of+a+zoologist.&ots=TRLvEmBeXI&sig=99HkqgciclyjCm_5QlaLgLITVKow. [Accessed 2013-11-14].
- Mayr, E. (2000) The Biological Species Concept. In: Wheeler, Q. D. & Platnick, N. I. (Eds.) *Species concepts and phylogenetic theory: a debate*. pp 17–29. New York: Columbia University Press. ISBN 0-231-10142-2.
- Meyer, C. P., Geller, J. B. & Paulay, G. (2005) Fine scale endemism on coral reefs: archipelagic differentiation in turbid gastropods. *Evolution*, 59(1), 113–125.
- Michel-Salzat, A. & Bouchon, D. (2000) Phylogenetic analysis of mitochondrial LSU rRNA in oniscids. *Comptes Rendus de l'Academie des Sciences Series III Sciences de la Vie*, 323(9), 827–837.
- Mora, C., Tittensor, D. P., Adl, S., Simpson, A. G. B. & Worm, B. (2011) How many species are there on Earth and in the ocean? *PLoS Biology*, 9(8), e1001127.
- Nagy, Z. T. (2010) A hands-on overview of tissue preservation methods for molecular genetic analyses. *Organisms Diversity & Evolution*, 10(1), 91–105.
- Omilian, A. R. & Taylor, D. J. (2001) Rate acceleration and long-branch attraction in a conserved gene of cryptic daphniid (Crustacea) species. *Molecular Biology and Evolution*, 18(12), 2201–2212.
- Osborn, K. J. (2009) Relationships within the Munnopsidae (Crustacea, Isopoda, Asellota) based on three genes. *Zoologica Scripta*, 38(6), 617–635.
- Palumbi, S. R., Martin, A., Romano, S., McMillan, W. O., Stice, L. & Grabowski, G. (1991) *The simple fool's guide to PCR*, Version 2. Honolulu: University of Hawaii Press.
- Pons, J., Barraclough, T. G., Gomez-Zurita, J., Cardoso, A., Duran, D. P., Hazell, S., Kamoun, S., Sumlin, W. D. & Vogler, A. P. (2006) Sequence-based species delimitation for the DNA taxonomy of undescribed insects. *Systematic Biology*, 55(4), 595–609.
- Quicke, D. L. J., Lopez-Vaamonde, C. & Belshaw, R. (1999) Preservation of hymenopteran specimens for subsequent molecular and morphological study. *Zoologica Scripta*, 28(1-2), 261–267.
- Radulovici, A. E., Bernard, S.-M. & Dufresne, F. (2009) DNA barcoding of marine crustaceans from the Estuary and Gulf of St Lawrence: a regional-scale approach. *Molecular Ecology Resources*, 9(s1), 181–187 (Barcoding Arthropods).
- Raupach, M. J., Held, C. & Wägele, J.-W. (2004) Multiple colonization of the deep sea by the Asellota (Crustacea: Peracarida: Isopoda). *Deep Sea Research Part II: Topical Studies in Oceanography*, 51, 1787–1795.
- Raupach, M. J., Malyutina, M. V., Brandt, A. & Wägele, J.-W. (2007) Molecular data reveal a highly diverse species flock within the munnopsoid deep-sea isopod *Betamorpha*

- fusiformis* (Barnard, 1920) (Crustacea: Isopoda: Asellota) in the Southern Ocean. Deep Sea Research Part II: Topical Studies in Oceanography, 54(16-17), 1820–1830.
- Raupach, M. J., Mayer, C., Malyutina, M. V. & Wägele, J.-W. (2009) Multiple origins of deep-sea Asellota (Crustacea: Isopoda) from shallow waters revealed by molecular data. Proceedings of the Royal Society B: Biological Sciences, 276, 799–808.
- Raupach, M. J. & Wägele, J.-W. (2006) Distinguishing cryptic species in Antarctic Asellota (Crustacea: Isopoda)-a preliminary study of mitochondrial DNA in *Acanthaspidia drygalskii*. Antarctic Science, 18(02), 191–198.
- Rex, M. A. & Etter, R. J. (2010) Deep-sea Biodiversity: Pattern and Scale. Cambridge, MA; London: Harvard University Press. ISBN 0674036077.
- Riehl, T. & Brandt, A. (2010) Descriptions of two new species in the genus *Macrostylis* Sars, 1864 (Isopoda, Asellota, Macrostylidae) from the Weddell Sea (Southern Ocean), with a synonymisation of the genus *Desmostylis* Brandt, 1992 with *Macrostylis*. Zookeys, 57, 9–49.
- Riehl, T. & Brandt, A. (2013) Southern Ocean Macrostylidae reviewed with a key to the species and new descriptions from Maud Rise. Zootaxa, 3692(1), 160–203.
- Riehl, T. & Kaiser, S. (2012) Conquered from the deep sea? A new deep-sea isopod species from the Antarctic shelf shows pattern of recent colonization. PLoS ONE, 7(11), e49354.
- Riehl, T., Wilson, G. D. F. & Hessler, R. R. (2012) New Macrostylidae Hansen, 1916 (Crustacea: Isopoda) from the Gay Head-Bermuda transect with special consideration of sexual dimorphism. Zootaxa, 3277, 1–26.
- Schander, C. & Halanych, K. M. (2003) DNA, PCR and formalized animal tissue - a short review and protocols. Organisms Diversity & Evolution, 3(3), 195–205.
- Schnurr, S. & Brix, S. (2012) *Eugerdella huberti* sp. nov. - a new species of Desmosomatidae Sars, 1897 (Crustacea, Isopoda) from the deep-sea of the South Atlantic Ocean. Marine Biodiversity, 42(1), 13–24.
- Schwentner, M., Timms, B. V. & Richter, S. (2011) An integrative approach to species delineation incorporating different species concepts: a case study of *Limnadopsis* (Branchiopoda: Spinicaudata). Biological Journal of the Linnean Society, 104(3), 575–599.
- Sites, J. W. & Marshall, J. C. (2004) Operational criteria for delimiting species. Annual Review of Ecology, Evolution and Systematics, 35, 199–227.
- Teske, P. R., McQuaid, C. D., Froneman, P. W. & Barker, N. P. (2006) Impacts of marine biogeographic boundaries on phylogeographic patterns of three South African estuarine crustaceans. Marine Ecology-Progress Series, 314, 283–293.
- Thompson, J. D., Higgins, D. G. & Gibson, T. J. (1994) CLUSTAL W: improving the sensitivity of progressive multiple sequence alignment through sequence weighting, position-specific gap penalties and weight matrix choice. Nucleic acids research, 22(22), 4673–4680.
- Tsang, L. M., Chan, B. K. K., Shih, F.-L., Chu, K. H. & Allen Chen, C. (2009) Host-associated speciation in the coral barnacle *Wanella milleporae* (Cirripedia: Pyrgomatidae) inhabiting the *Millepora* coral. Molecular Ecology, 18(7), 1463–1475.
- Weigt, L. A., Driskell, A. C., Ormos, A., Meyer, C. & Collins, A. (2012) Introduction to Animal DNA Barcoding Protocols. In: Kress, W. J. & Erickson, D. L. (Eds.) DNA Barcodes. pp 11–16. Humana Press. (858). ISBN 978-1-61779-590-9, 978-1-61779-591-6.
- Wetzer, R. (2001) Hierarchical analysis of mtDNA variation and the use of mtDNA for isopod (Crustacea: Peracarida: Isopoda) systematics. Contributions to Zoology, [online], 70(1). Available from: <http://dpc.uba.uva.nl/ctz/vol70/nr01/art02>.
- Wilson, G. D. F. (1982) Systematics of a species complex in the deep-sea genus *Eurycope*, with a revision of six previously described species (Crustacea, Isopoda, Eurycopidae). Berkeley, Los Angeles, London: University of California Press. (Bulletin of the Scripps Institution of Oceanography). ISBN 0-520-0968-9.
- Wilson, G. D. F. (1983) Variation in the deep-sea isopod *Eurycope ipthima* (Asellota, Eurycopidae): depth related clines in rostral morphology and in population structure. Journal of Crustacean Biology, 3(1), 127–140.
- Wilson, G. D. F. (1986) Evolution of the female cuticular organ in the Asellota (Crustacea, Isopoda). Journal of Morphology, 190(3), 297–305.
- Wilson, G. D. F. (1991) Functional morphology and evolution of isopod genitalia. In: Bauer, R. T. & Martin, J. W. (Eds.) Crustacean Sexual Biology. pp 228–245. New York: Columbia University Press.
- Wilson, G. D. F. (2008) Local and regional species diversity of benthic Isopoda (Crustacea) in the deep Gulf of Mexico. Deep-Sea Research Part II: Topological Studies in Oceanography, 55(24-26), 2634–2649.
- Wägele, J.-W., Holland, B., Dreyer, H. & Hackethal, B. (2003) Searching factors causing implausible non-monophyly: ssu rDNA phylogeny of Isopoda Asellota (Crustacea: Peracarida) and faster evolution in marine than in freshwater habitats. Molecular Phylogenetics and Evolution, 28(3), 536–551.
- Zeale, M. R. K., Butlin, R. K., Barker, G. L. A., Lees, D. C. & Jones, G. (2011) Taxon-specific PCR for DNA barcoding arthropod prey in bat faeces. Molecular Ecology Resources, 11(2), 236–244.

Zhang, Z., Schwartz, S., Wagner, L. & Miller, W. (2000) A greedy algorithm for aligning DNA sequences. *Journal of Computational biology*, 7(1-2), 203–214.

experience in the laboratory. All people involved in developing and distributing www.ZOTERO.org for free are thanked for their effort. The constructive criticism provided by two anonymous reviewers considerably helped to improve this article.

Acknowledgements

We thank all helping hands on board and in the lab, the crews, captains and chief scientists involved in the sampling, especially L. Kramer, K. Jeskulke and A. Ormos. L. M. Tsang and R. Machida are thanked for providing information on 12S and 16S primers. W. Wägele, M. Raupach and C. Held introduced SB into the DNA-lab methods applied on asellote isopods from the deep sea. P. Martinez always supported our work pushing the DNA barcoding approach forward in the Census of the Diversity of Abyssal Marine Life (CeDAMar). Two LAB visits of TR were funded by the CeDAMar taxonomic exchange fellowship and the Stiftung Universität Hamburg. The German National Academic Foundation (Studienstiftung des deutschen Volkes) funded TR's work during the writing of the manuscript. SB received funding from the German Science Foundation (DFG) during the first steps developing these protocols under contract No. Br 1121/28-1. D. Steinke and C. Steinke of the CCDB helped with establishing the isopod project in the Barcode of Life Database (BoLD). A. Braband of LGC Genomics kindly shared her knowledge and